JPL Publication 97-4

Chemical Kinetics and Photochemical Data for Use in Stratospheric Modeling

Evaluation Number 12

NASA Panel for Data Evaluation:

W. B. DeMore
S. P. Sander
Jet Propulsion Laboratory

D. M. Golden
SRI International

R. F. Hampson
M. J. Kurylo
National Institute of Standards and Technology

C. J. Howard
A. R. Ravishankara
NOAA Environmental Research Laboratory

C. E. Kolb
Aerodyne Research Inc.

M. J. Molina
Massachusetts Institute of Technology

January 15, 1997

National Aeronautics and
Space Administration

Jet Propulsion Laboratory
California Institute of Technology
Pasadena, California

The research described in this publication was carried out by the Jet Propulsion Laboratory, California Institute of Technology, under a contract with the National Aeronautics and Space Administration.

ABSTRACT

This is the twelfth in a series of evaluated sets of rate constants and photochemical cross sections compiled by the NASA Panel for Data Evaluation. The primary application of the data is in the modeling of stratospheric processes, with particular emphasis on the ozone layer and its possible perturbation by anthropogenic and natural phenomena. Copies of this evaluation are available from the Jet Propulsion Laboratory, California Institute of Technology, Document Distribution, MS 512-110, 4800 Oak Grove Drive, Pasadena, California, 91109.

Page intentionally left blank

TABLE OF CONTENTS

LIST OF TABLES

LIST OF FIGURES

CHEMICAL KINETICS AND PHOTOCHEMICAL DATA

FOR USE IN STRATOSPHERIC MODELING

INTRODUCTION

The present compilation of kinetic and photochemical data represents the 12th evaluation prepared by the NASA Panel for Data Evaluation. The Panel was established in 1977 by the NASA Upper Atmosphere Research Program Office for the purpose of providing a critical tabulation of the latest kinetic and photochemical data for use by modelers in computer simulations of stratospheric chemistry. The previous publications appeared as follows:

Evaluation		Reference
1	NASA RP 1010, Chapter 1	(Hudson [1])
2	JPL Publication 79-27	(DeMore et al. [12])
3	NASA RP 1049, Chapter 1	(Hudson and Reed [2])
4	JPL Publication 81-3	(DeMore et al. [11])
5	JPL Publication 82-57	(DeMore et al. [9])
6	JPL Publication 83-62	(DeMore et al. [10])
7	JPL Publication 85-37	(DeMore et al. [4])
8	JPL Publication 87-41	(DeMore et al. [5])
9	JPL Publication 90-1	(DeMore et al. [6])
10	JPL Publication 92-20	(DeMore et al. [7])
11	JPL Publication 94-26	(DeMore et al. [8])

The present composition of the Panel and the major responsibilities of each member are listed below:

W. B. DeMore, Chairman

D. M. Golden (three-body reactions, equilibrium constants)

R. F. Hampson (halogen chemistry)

C. J. Howard (HO_x chemistry, $O(^1D)$ reactions, singlet O_2, metal chemistry, profiles)

C. E. Kolb (heterogeneous chemistry)

M. J. Kurylo (SO_x chemistry)

M. J. Molina (photochemical data)

A. R. Ravishankara (oxidation of organic compounds)

S. P. Sander (NO_x chemistry, photochemical data)

As shown above, each Panel member concentrates his effort on a given area or type of data. Nevertheless, the final recommendations of the Panel represent a consensus of the entire Panel. Each member reviews the basis for all recommendations, and is cognizant of the final decision in every case. Communications regarding particular reactions may be addressed to the appropriate panel member.

W. B. DeMore
S. P. Sander
Jet Propulsion Laboratory
183-301
4800 Oak Grove Drive
Pasadena, CA 91109
wdemore@ftuvs.jpl.nasa.gov
ssander@ftuvs.jpl.nasa.gov

D. M. Golden
PS-031
SRI International
333 Ravenswood Ave.
Menlo Park, CA 94025
golden@cplvax.sri.com

R. F. Hampson
M. J. Kurylo
National Institute of Standards and Technology
Physical and Chemical Properties Division
Gaithersburg, MD 20899
hampson@enh.nist.gov
mkurylo@hq.nasa.gov

C. J. Howard
A. R. Ravishankara
NOAA-ERL, R/E/AL2
325 Broadway
Boulder, CO 80303
howard@al.noaa.gov
ravi@al.noaa.gov

C. E. Kolb
Aerodyne Research Inc.
45 Manning Rd.
Billerica, MA 01821
kolb@aerodyne.com

M. J. Molina
Department of Earth, Atmospheric, and Planetary Sciences
and Department of Chemistry
Massachusetts Institute of Technology
Cambridge, MA 02139
mmolina@athena.mit.edu

Copies of this evaluation may be obtained by requesting JPL Publication 97-04 from:

Jet Propulsion Laboratory
California Institute of Technology
Secondary Distribution, MS 512-110
4800 Oak Grove Drive
Pasadena, CA 91109
Telephone: (818) 397-7952

BASIS OF THE RECOMMENDATIONS

The recommended rate data and cross sections are based on laboratory measurements. In order to provide recommendations that are as up-to-date as possible, preprints and written private communications are accepted, but only when it is expected that they will appear as published journal articles. Under no circumstances are rate constants adjusted to fit observations of stratospheric concentrations. The Panel considers the question of consistency of data with expectations based on the theory of reaction kinetics, and when a discrepancy appears to exist this fact is pointed out in the accompanying note. The major use of theoretical extrapolation of data is in connection with three-body reactions, in which the required pressure or temperature dependence is sometimes unavailable from laboratory measurements, and can be estimated by use of appropriate theoretical treatment. In the case of important rate constants for which no experimental data are available, the panel may provide estimates of rate constant parameters based on analogy to similar reactions for which data are available.

RECENT CHANGES AND CURRENT NEEDS OF LABORATORY KINETICS

Format of the Evaluation

Changes or additions to the tables of data are indicated by shading. A new entry is completely shaded, whereas a changed entry is shaded only where the change was made. In some cases only the note has been changed, in which case the corresponding note number in the table is shaded. In the Photochemistry section, changed notes are indicated by shading of the note heading.

Each edition of the evaluation is self-contained, and it is not necessary to refer to earlier editions to obtain a complete set of data.

Appendix 1, listing heats of formation of many atmospheric species, has been updated and expanded. A new entry, Appendix 2, tabulates entropy data for most of these same species. Appendix 3 includes solar flux data as well as model-generated concentration profiles and J-values for important species in the upper atmosphere.

Computer Access

The contents of the evaluation (exclusive of the figures) are available in computer-readable formats. (In the near future, electronic versions of the figures will be available.) To maximize transferability to different personal computer and workstation/main frame environments, the evaluation will be made available in several different formats, including Microsoft Word, Rich Text Format (RTF), Postscript, and Adobe Acrobat files. Further details are provided in a 'Readme' file.

Files may be downloaded from *http://remus.jpl.nasa.gov/jpl97/* or may be copied via 'ftp' from the Internet host remus.jpl.nasa.gov. The username is *anonymous* and the password is the electronic address of the user logging in. The files are to be found in the */pub/jpl97* subdirectory just below the root directory.

Individuals who want to receive notices when the web page and/or ftp archive are revised should send email to *Majordomo@remus.jpl.nasa.gov*, with the first line of the message being *subscribe jpl97-announce*.

Questions may be addressed to Mark Allen (Mark.Allen@jpl.nasa.gov).

O_x Reactions

The kinetics of the O, O_2, and O_3 system are relatively well-established. However, the $O + O_2 + M$ reaction remains of fundamental importance in atmospheric chemistry. This is because the extent of ozone destruction is determined by the relative rates of competing reactions such as $O + O_3$, $O + NO_2$, O + OH, and O + ClO. Additional studies of the ozone-forming reaction, or its relative rate compared to the competing reactions, would be useful, especially at very low temperatures.

Reactions of Singlet Oxygen

$O(^1D)$ Reactions

The recommended rate coefficients for the $O(^1D)$ reactions correspond to the rate of removal of $O(^1D)$, which includes both chemical reactions and physical quenching of the excited O atoms. Details on the branching ratios and products are given in the notes.

The kinetic energy or hot atom effects of photolytically generated $O(^1D)$ are probably not important in the atmosphere, although the literature is rich with studies of these processes and with studies of the dynamics of many $O(^1D)$ reactions. The important atmospheric reactions of $O(^1D)$ include: (1) deactivation by major gases, N_2 and O_2, which limit the $O(^1D)$ steady-state concentrations; (2) reaction with trace gases, e.g., H_2O, CH_4, and N_2O, which generate radicals; and (3) reaction with long-lived trace gases, e.g., HCN, which have relatively slow atmospheric degradation rates. There are no data for the $O(^1D)$ + HCN reaction.

O_2 ($^1\Delta$ and $^1\Sigma$)

Fourteen reactions of the ($a^1\Delta_g$) and ($b^1\Sigma^+_g$) excited states of molecular oxygen are reviewed. These states are populated via photochemical processes, mainly the UV photolysis of ozone, and the reaction of $O(^1D)$ with O_2. Over the years they have been proposed as contributors to various reaction schemes in the atmosphere, but as yet no significant role in the chemistry of the stratosphere has been demonstrated. The fate of most of these excited species is physical quenching by means of energy transfer processes. In the few cases where chemical reaction occurs, it is indicated in the corresponding note.

HO_x Reactions

There have been no changes in the database for HO_x chemistry since the last evaluation. The $HO_2 + O_3$ reaction rate coefficient remains one of the most significant uncertainties in the HO_x system. High quality data at low temperatures are needed for this key reaction.

NO_x Reactions

There are no significant changes to the recommendations on NOx reactions. The recommendation for the HO_2 + NO reaction has been changed and the uncertainty factor reduced to reflect a new direct study of this reaction in the high pressure (several hundred torr) regime. The NH_2 + NO and NO + O_3 reactions have been re-evaluated, resulting in a significant reduction in the uncertainty factors of both reactions.

Oxidation of Organic Compounds

The major update in this evaluation is the inclusion of the reactions of acetone and alkyl nitrates. In addition, several changes to the recommended values have been made in light of recent data.

The rate coefficient for the reaction of OH with CH_4 has been revised very slightly, based on recent work at temperatures close to 200 K. Even though the recommendation is in the form of an Arrhenius expression, the three parameter expression given in the note may better represent the data and may be preferred in some cases.

There have been direct measurements of the rate coefficients for the reactions of many peroxy radicals with NO, and this data base has been significantly improved. The current recommendations reflect the better database on peroxy radical reactions. The rate coefficient for the reaction of $CH_3C(O)O_2$ with NO has been measured directly and is now recommended. This recommended value also leads to a consistency, which was previously absent, in the ratio of the rate coefficients for the reactions of $CH_3C(O)O_2$ with NO and NO_2. Even though there have been many studies of the reactions between peroxy radicals, the use of only UV absorption to measure the rate coefficients is still a limiting factor. All peroxy radicals have similar absorption spectra and cross sections. Therefore, deconvolution of the measured absorbances into changes in concentrations of individual reactants is not unambiguous. Use of peroxy radical detection by methods other than UV absorption would be very beneficial.

The reactions of OH with CH_3CN and HCN still require further study, because both the rates and mechanisms are uncertain. Studies of larger (>C3) hydrocarbons, especially those containing oxygen, will be of interest in elucidating the hydrocarbon chemistry in the upper troposphere and the lower stratosphere. Such information is needed to assess the effects of aircraft emissions on ozone and climate as well as the general state of the upper troposphere.

Halogen Reactions

The kinetics database for homogeneous reactions of halogen species has been expanded since the previous evaluation. Rate coefficients for the reaction of OH with sixteen HFCs, HFOCs, and HCFCs have been added, increasing to forty-nine the number of potential alternatives to the fully halogenated CFCs for which rate data for reaction with OH are now included. Rate coefficients for the reaction of chlorine atoms with many of these species are also included. Rate coefficient data for the reactions of these species with $O(^1D)$ are included in the $O(^1D)$ section of Table 1. More information on halocarbon degradation mechanisms in the atmosphere can be found in Francisco and Maricq [13], Wallington et al. [19], and WMO [20]. There have been some changes in the recommendations for reactions included in the previous evaluation, in particular for reactions of OH with HFCs and HCFCs.

SO_x Reactions

The database on gas phase atmospheric sulfur chemistry has seen only minor changes in the recommendations for the reactions that were included in the previous evaluation. Minor expansion of this section continues in the area of reactions important in the atmospheric oxidation of reduced sulfur compounds of natural and anthropogenic origin. The database also continues to expand as more information becomes available on halogen atom and halogen oxide radical reactions with a number of the reduced sulfur compounds. Some of these reactions are considered to be important in boundary layer chemistry affecting tropospheric polar ozone. Further mechanistic information can be obtained from other reviews such as Tyndall and Ravishankara [18].

Metal Chemistry

Sodium is deposited in the upper atmosphere by meteors along with larger amounts of silicon, magnesium, and iron; comparable amounts of aluminum, nickel, and calcium; and smaller amounts of potassium, chromium, manganese, and other elements. The interest is greatest in the alkali metals because they form the least stable oxides and thus free atoms can be regenerated through photolysis and reactions with O and O_3. The other meteoric elements are expected to form more stable oxides. A review by Plane [15] describes many aspects of atmospheric metal chemistry.

The total flux of alkali metals through the atmosphere is relatively small, e.g., one or two orders of magnitude less than CFCs. Therefore, extremely efficient catalytic cycles are required in order for Na to have a significant effect on stratospheric chemistry. There are no measurements of metals or metal compounds in the stratosphere which indicate a significant role.

It has been proposed that the highly polar metal compounds may polymerize to form clusters and that the stratospheric concentrations of free metal compounds are too small to play a significant role in the chemistry.

Some studies have shown that the polar species NaO and NaOH associate with abundant gases such as O_2 and CO_2 with very fast rates in the atmosphere. It has been proposed that reactions of this type will lead to the production of clusters with many molecules attached to the sodium compounds. In most cases thermal dissociation is slow, and photolysis competes with the association reactions and limits the cluster concentrations in daylight. If atmospheric sodium does form large clusters, it is unlikely that Na species can have a significant role in stratospheric ozone chemistry. In order to assess the importance of these processes, data are needed on the association rates and the photolysis rates involving the cluster species.

Photochemical Data

The recommendation for the quantum yield values for production of $O(^1D)$ in the photolysis of ozone around 300 nm (i.e., in the Huggins bands) has been modified to take into account recent work that corroborates the presence of the "tail" that had been observed in earlier laser experiments. The change incorporates the larger quantum yield values (0.2 - 0.3). Additional measurements for this quantum yield should be carried out as a function of temperature. For Cl_2O_2, the small absorption cross sections beyond 320 nm are potentially very important for photodissociation in the polar stratosphere, and need to be further studied. In addition, the photodissociation quantum yields for $ClONO_2$ at longer wavelengths (around 350 nm) should be further investigated.

There are new entries for HOBr and $CH_3C(O)O_2NO_2$ (PAN, peroxyacetyl nitrate) and significant new work has been published on the O_2 Herzberg continuum, ClOOCl, Cl_2O_3, and $BrONO_2$. Recent work on ClOOCl has

suggested that cross sections in the long-wavelength tail, where most of the photolysis occurs in the lower stratosphere, may be significantly smaller than previously thought. Spectral artificats arising from trace impurities are especially difficult to identify in this system, leading to large uncertainties in the cross sections in this spectral region. The situation is similar for HOBr, where a photodissociation study and one spectroscopic study indicate the presence of absorption features extending well into the visible region, but other spectroscopic studies see no absorption beyond 400 nm.

Heterogeneous Chemistry

There is no question that heterogeneous processes on the surfaces of polar stratospheric cloud particles play a critical role in the chemistry of the winter and spring polar stratospheres. Furthermore, there is a great deal of observational and modeling evidence that heterogeneous reactions on background sulfuric acid aerosols play a very important role in stratospheric processes at both polar and mid-latitudes, particularly when stratospheric sulfate levels are elevated by major volcanic eruptions.

Polar heterogeneous chemical processes identified to date have a tendency to enhance the destruction of stratospheric ozone, primarily by converting relatively inactive "reservoir" species HCl and $ClONO_2$ to more active Cl_2 and HOCl, which are easily photolyzed to Cl and ClO. In some scenarios the heterogeneous reaction of HOCl and N_2O_5 with HCl may also play an important role in promoting the production of more easily photolyzed species. In addition, interaction with PSC surfaces can remove N_2O_5 and HNO_3 vapor from the polar stratosphere, sequestering nitrogen oxides in the form of condensed phase nitric acid and, thus, reducing the normal mitigating effect gaseous NO_x can have on ClO_x-catalyzed ozone destruction. The net effect of these processes is a major buildup of ClO_x radicals in PSC-processed polar stratospheric air masses and, particularly over the Antarctic, a massive springtime destruction of stratospheric ozone.

The reaction of stratospheric N_2O_5 with liquid water in sulfuric acid aerosols to form HNO_3 can have a significant impact on NO_x/HNO_3 ratios in the lower mid-latitude stratosphere, bringing measured mid-latitude ozone losses into better agreement with observations. Models suggest that at current mid-latitude ratios of NO_x/ClO_x this process increases ozone loss by lowering NO_x levels and thus reducing the scavenging of ClO by $ClONO_2$ formation. The reactions of $ClONO_2$ and $BrONO_2$ with sulfuric acid aerosol may also play a role in denitrification, the release of photolyzable halogen species, and the perturbation of HO_x radical levels.

The stratosphere also contains carbonaceous soot from aircraft and rocket exhausts, alumina and other metal oxides from solid propellant rocket exhaust and spacecraft debris, and, possibly, sodium chloride from some volcanic eruptions. There is increasing interest in determining if and when heterogeneous processes on these relatively minor surfaces can influence stratospheric chemistry.

Heterogeneous processes involving the liquid water droplets and ice crystals found in tropospheric clouds and aircraft contrails and/or the sulfate aerosols found in the free troposphere may have a significant effect on the flux into the stratosphere of reactive species from partially oxidized hydrohalocarbons or aircraft exhaust. Proper modeling of these processes will be necessary to assess the atmospheric impact of reducing the use of partially chlorinated hydrocarbon solvents, replacing CFCs with HCFCs and HFCs, and the evolution of the civil aviation industry.

The laboratory study of heterogeneous processes relevant to the stratosphere is an immature field in comparison with the measurement of gas phase kinetic and photodissociation parameters. Heterogeneous experimental techniques are not yet as well developed, and the interpretation of experimental data is significantly more complex. Nonetheless, over the past several years, a number of experimental groups have made very significant progress and data from complementary techniques are increasingly available to help determine when the quantification of heterogeneous kinetic processes has been successfully distinguished from complicating mass transport and surface saturation processes.

However, it is well to remember that quantitative application of laboratory results on heterogeneous processes to the stratosphere is not straightforward. First, there is still a significant level of uncertainty in both the detailed chemical and physical characteristics of the droplet and particle surfaces present in the stratosphere and in how faithful the laboratory simulation of these surfaces in various experimental configurations may be. Secondly, the proper incorporation of heterogeneous processes into models of stratospheric and upper tropospheric chemistry is very difficult, and no current models incorporate formation of and reaction on droplet/particle surfaces in a fully coupled and self-consistent way. A great deal of effort will have to be expended before the modeling community is

as adept at incorporating heterogeneous effects as they are in representing gas phase kinetic and photochemical processes.

Gas Phase Enthalpy Data (Appendix 1)

This table lists $\Delta H_f(298)$ values for a number of atmospheric species. Most of the heat of formation data are taken from the IUPAC Evaluation (Atkinson et al. [3]) or the NIST Standard Database 25 [16]. However, some of the values may be different from those quoted in these sources, reflecting recent studies that have not yet been accepted and incorporated into those publications.

Entropy Data (Appendix 2)

Values for $S^o(298K)$ are taken mainly from the NIST Standard Database 25 [16], although in a few cases estimates based on structural similarity are included and are identified as such by enclosure in parentheses.

The listings of both enthalpy and entropy data are presented for utility only, and the present evaluation should not be cited as a primary literature reference for thermochemical data.

Solar Flux and Species Profiles (Appendix 3)

A set of two figures representing solar fluxes are included in this evaluation. One figure gives the solar flux from 110 to 600 nm above the atmosphere and the second gives the actinic flux from 180 to 400 nm at five altitudes from the surface to 50 km.

A set of nine figures presenting model-calculated altitude profiles for stratospheric temperature, trace species concentrations, and photolysis rate coefficients is given. Some details of the model used to generate the profiles are given at the beginning of Appendix 2. The efforts of Peter S. Connell and other members of the LLNL are gratefully acknowledged for providing these profiles.

The data in the eleven figures are presented to provide "order of magnitude" values of important parameters for the purpose of evaluating stratospheric kinetics and photochemical processes. Since the profiles are sensitive to variations in season, hour of the day, latitude, and aerosol density, some care must be taken in how they are applied to specific problems. They are not intended to be standards.

DATA FORMATS

In Table 1 (Rate Constants for Second Order Reactions) the reactions are grouped into the classes O_x, $O(^1D)$, Singlet O_2, HO_x, NO_x, Hydrocarbon Reactions, FO_x, ClO_x, BrO_x, IO_x, SO_x, and metal reactions. The data in Table 2 (Rate Constants for Association Reactions) are presented in the same order as the bimolecular reactions. The presentation of photochemical cross section data follows the same sequence.

Bimolecular Reactions

Some of the reactions in Table 1 are actually more complex than simple two-body reactions. To explain the pressure and temperature dependences occasionally seen in reactions of this type, it is necessary to consider the bimolecular class of reactions in terms of two subcategories, direct (concerted) and indirect (nonconcerted) reactions.

A direct or concerted bimolecular reaction is one in which the reactants A and B proceed to products C and D without the intermediate formation of an AB adduct that has appreciable bonding, i.e., no stable A-B molecule exists, and there is no reaction intermediate other than the transition state of the reaction, $(AB)^{\neq}$.

$$A + B \rightarrow (AB)^{\neq} \rightarrow C + D$$

The reaction of OH with CH_4 forming $H_2O + CH_3$ is an example of a reaction of this class.

Very useful correlations between the expected structure of the transition state $[AB]^{\neq}$ and the A-Factor of the reaction rate constant can be made, especially in reactions that are constrained to follow a well-defined approach of the two reactants in order to minimize energy requirements in the making and breaking of bonds. The rate constants

for these reactions are well represented by the Arrhenius expression k = A exp(-E/RT) in the 200-300 K temperature range. These rate constants are not pressure dependent.

The indirect or nonconcerted class of bimolecular reactions is characterized by a more complex reaction path involving a potential well between reactants and products, leading to a bound adduct (or reaction complex) formed between the reactants A and B:

$$A + B \leftrightarrow [AB]^* \rightarrow C + D$$

The intermediate [AB]* is different from the transition state $[AB]^{\neq}$, in that it is a bound molecule which can, in principle, be isolated. (Of course, transition states are involved in all of the above reactions, both forward and backward, but are not explicitly shown.) An example of this reaction type is ClO + NO, which normally produces Cl + NO_2. Reactions of the nonconcerted type can have a more complex temperature dependence and can exhibit a pressure dependence if the lifetime of [AB]* is comparable to the rate of collisional deactivation of [AB]*. This arises because the relative rate at which [AB]* goes to products C + D vs. reactants A + B is a sensitive function of its excitation energy. Thus, in reactions of this type, the distinction between the bimolecular and termolecular classification becomes less meaningful, and it is especially necessary to study such reactions under the temperature and pressure conditions in which they are to be used in model calculation, or, alternatively, to develop a reliable theoretical basis for extrapolation of data.

The rate constant tabulation for second-order reactions (Table 1) is given in Arrhenius form: k(T) = A exp ((-E/R)(1/T)) and contains the following information:

1. Reaction stoichiometry and products (if known). The pressure dependences are included, where appropriate.
2. Arrhenius A-factor.
3. Temperature dependence and associated uncertainty ("activation temperature" E/R±ΔE/R).
4. Rate constant at 298 K.
5. Uncertainty factor at 298 K.
6. Note giving basis of recommendation and any other pertinent information.

Termolecular Reactions

Rate constants for third order reactions (Table 2) of the type $A + B \leftrightarrow [AB]^* \xrightarrow{M} AB$ are given in the form

$$k_o(T) = k_o^{300}(T/300)^{-n} \text{ cm}^6 \text{ molecule}^{-2} \text{ s}^{-1},$$

(where k_o^{300} has been adjusted for air as the third body), together with a recommended value of n. Where pressure fall-off corrections are necessary, an additional entry gives the limiting high-pressure rate constant in a similar form:

$$k_\infty(T) = k_\infty^{300}(T/300)^{-m} \text{ cm}^3 \text{ molecule}^{-1} \text{ s}^{-1}.$$

To obtain the effective second-order rate constant for a given condition of temperature and pressure (altitude), the following formula is used:

$$k(Z) = k(M,T) = \left(\frac{k_o(T)[M]}{1 + (k_o(T)[M]/k_\infty(T))}\right) 0.6^{\{1 + [\log_{10}(k_o(T)[M]/k_\infty(T))]^2\}^{-1}}$$

The fixed value 0.6 that appears in this formula fits the data for all listed reactions adequately, although in principle this quantity may be different for each reaction, and also temperature dependent.

Thus, a compilation of rate constants of this type requires the stipulation of the four parameters, $k_0(300)$, n, $k_\infty(300)$, and m. These can be found in Table 2. The discussion that follows outlines the general methods we have used in establishing this table, and the notes to the table discuss specific data sources.

Low-Pressure Limiting Rate Constant [$k_0^x(T)$]

Troe [17] has described a simple method for obtaining low-pressure limiting rate constants. In essence this method depends on the definition:

$$k_0^x(T) \equiv \beta_x k_{0,sc}^x(T)$$

Here sc signifies "strong" collisions, x denotes the bath gas, and β_x is an efficiency parameter ($0 < \beta < 1$), which provides a measure of energy transfer.

The coefficient β_x is related to the average energy transferred in a collision with gas x, $\langle\Delta E\rangle_x$, via:

$$\frac{\beta_x}{1-\beta_x^{1/2}} = \frac{\langle\Delta E\rangle_x}{F_E\, kT}$$

Notice that $\langle\Delta E\rangle$ is quite sensitive to β. F_E is the correction factor of the energy dependence of the density of states (a quantity of the order of 1.1 for most species of stratospheric interest).

For some of the reactions of possible stratospheric interest reviewed here, there exist data in the low-pressure limit (or very close thereto), and we have chosen to evaluate and unify this data by calculating $k_{0,sc}^x(T)$ for the appropriate bath gas x and computing the value of β_x corresponding to the experimental value [Troe [17]]. A compilation (Patrick and Golden [14]) gives details for many of the reactions considered here.

From the β_x values (most of which are for N_2, i.e., β_{N2}), we compute $\langle\Delta E\rangle_x$ according to the above equation. Values of $\langle\Delta E\rangle_{N2}$ of approximately 0.3-1 kcal $mole^{-1}$ are generally expected. If multiple data exist, we average the values of $\langle\Delta E\rangle_{N2}$ and recommend a rate constant corresponding to the β_{N2} computed in the equation above.

Where no data exist we have sometimes estimated the low-pressure rate constant by taking $\beta_{N2} = 0.3$ at T = 300 K, a value based on those cases where data exist.

Temperature Dependence of Low-Pressure Limiting Rate Constants: T^n

The value of n recommended here comes from measurements or, in some cases, a calculation of $\langle\Delta E\rangle_{N2}$ from the data at 300 K, and a computation of β_{N2} (200 K) assuming that $\langle\Delta E\rangle_{N2}$ is independent of temperature in this range. This β_{N2} (200 K) value is combined with the computed value of k_0^{sc} (200 K) to give the expected value of the actual rate constant at 200 K. This latter, in combination with the value at 300 K, yields the value of n.

This procedure can be directly compared with measured values of k_0 (200 K) when those exist. Unfortunately, very few values at 200 K are available. There are often temperature-dependent studies, but some ambiguity exists when one attempts to extrapolate these down to 200 K. If data are to be extrapolated beyond the measured temperature range, a choice must be made as to the functional form of the temperature dependence. There are two general ways of expressing the temperature dependence of rate constants. Either the Arrhenius expression $k_0(T) = A\exp(-E/RT)$ or the form $k_0(T) = A' T^{-n}$ is employed. Since neither of these extrapolation techniques is soundly based, and since they often yield values that differ substantially, we have used the method explained earlier as the basis of our recommendations.

High-Pressure Limit Rate Constants [$k_\infty(T)$]

High-pressure rate constants can often be obtained experimentally, but those for the relatively small species of atmospheric importance usually reach the high-pressure limit at inaccessibly high pressures. This leaves two sources of these numbers, the first being guesses based upon some model, and the second being extrapolation of fall-off data up to higher pressures. Stratospheric conditions generally render reactions of interest much closer to the low-pressure limit and thus are fairly insensitive to the high-pressure value. This means that while the extrapolation is long, and the value of $k_\infty(T)$ not very accurate, a "reasonable guess" of $k_\infty(T)$ will then suffice. In some cases we have declined to guess since the low-pressure limit is effective over the entire range of stratospheric conditions.

Temperature Dependence of High-Pressure Limit Rate Constants: T^m

There are very few data upon which to base a recommendation for values of m. Values in Table 2 are often estimated, based on models for the transition state of bond association reactions and whatever data are available.

Uncertainty Estimates

For second-order rate constants in Table 1, an estimate of the uncertainty at any given temperature may be obtained from the following expression:

$$f(T) = f(298) \exp\left| \frac{\Delta E}{R}\left(\frac{1}{T} - \frac{1}{298}\right)\right|$$

Note that the exponent is an absolute value. An upper or lower bound (corresponding approximately to one standard deviation) of the rate constant at any temperature T can be obtained by multiplying or dividing the value of the rate constant at that temperature by the factor f(T). The quantities f(298) and $\Delta E/R$ are, respectively, the uncertainty in the rate constant at 298 K and in the Arrhenius temperature coefficient, as listed in Table 1. This approach is based on the fact that rate constants are almost always known with minimum uncertainty at room temperature. The overall uncertainty normally increases at other temperatures, because there are usually fewer data and it is almost always more difficult to make measurements at other temperatures. It is important to note that the uncertainty at a temperature T cannot be calculated from the expression $\exp(\Delta E/RT)$. The above expression for f(T) must be used to obtain the correct result.

The uncertainty represented by f(T) is normally symmetric; i.e., the rate constant may be greater than or less than the central value, k(T), by the factor f(T). In a few cases in Table 1 asymmetric uncertainties are given in the temperature coefficient. For these cases, the factors by which a rate constant is to be multiplied or divided to obtain, respectively, the upper and lower limits are not equal, except at 298 K where the factor is simply f(298 K). Explicit equations are given below for the case where the temperature dependence is (E/R +a, -b):

For T > 298 K, multiply by the factor

$$f(298\ K)e^{[a(1/298-1/T)]}$$

and divide by the factor

$$f(298\ K)e^{[b(1/298-1/T)]}$$

For T < 298 K, multiply by the factor

$$f(298\ K)e^{[b(1/T-1/298)]}$$

and divide by the factor

$$f(298\ K)e^{[a(1/T-1/298)]}$$

Examples of symmetric and asymmetric error limits are shown in Figure 1.

For three-body reactions (Table 2) a somewhat analogous procedure is used. Uncertainties expressed as increments to k_0 and k_∞ are given for these rate constants at room temperature. The additional uncertainty arising from the temperature extrapolation is expressed as an uncertainty in the temperature coefficients n and m.

The assigned uncertainties represent the subjective judgment of the Panel. They are not determined by a rigorous, statistical analysis of the database, which generally is too limited to permit such an analysis. Rather, the uncertainties are based on a knowledge of the techniques, the difficulties of the experiments, and the potential for systematic errors. There is obviously no way to quantify these "unknown" errors. The spread in results among different techniques for a given reaction may provide some basis for an uncertainty, but the possibility of the same, or compensating, systematic errors in all the studies must be recognized. Furthermore, the probability distribution may not follow the normal Gaussian form. For measurements subject to large systematic errors, the true rate constant may be much further from the recommended value than would be expected based on a Gaussian distribution with the stated uncertainty. As an example, the recommended rate constants for the reactions HO_2 + NO and Cl + $ClONO_2$ have changed by factors of 30-50. These changes could not have been allowed for with any reasonable values of σ in a Gaussian distribution.

Units

The rate constants are given in units of concentration expressed as molecules per cubic centimeter and time in seconds. Thus, for first-, second-, and third-order reactions the units of k are s^{-1}, cm^3 $molecule^{-1}$ s^{-1}, and cm^6 $molecule^{-2}$ s^{-1}, respectively. Cross sections are expressed as cm^2 $molecule^{-1}$, base e.

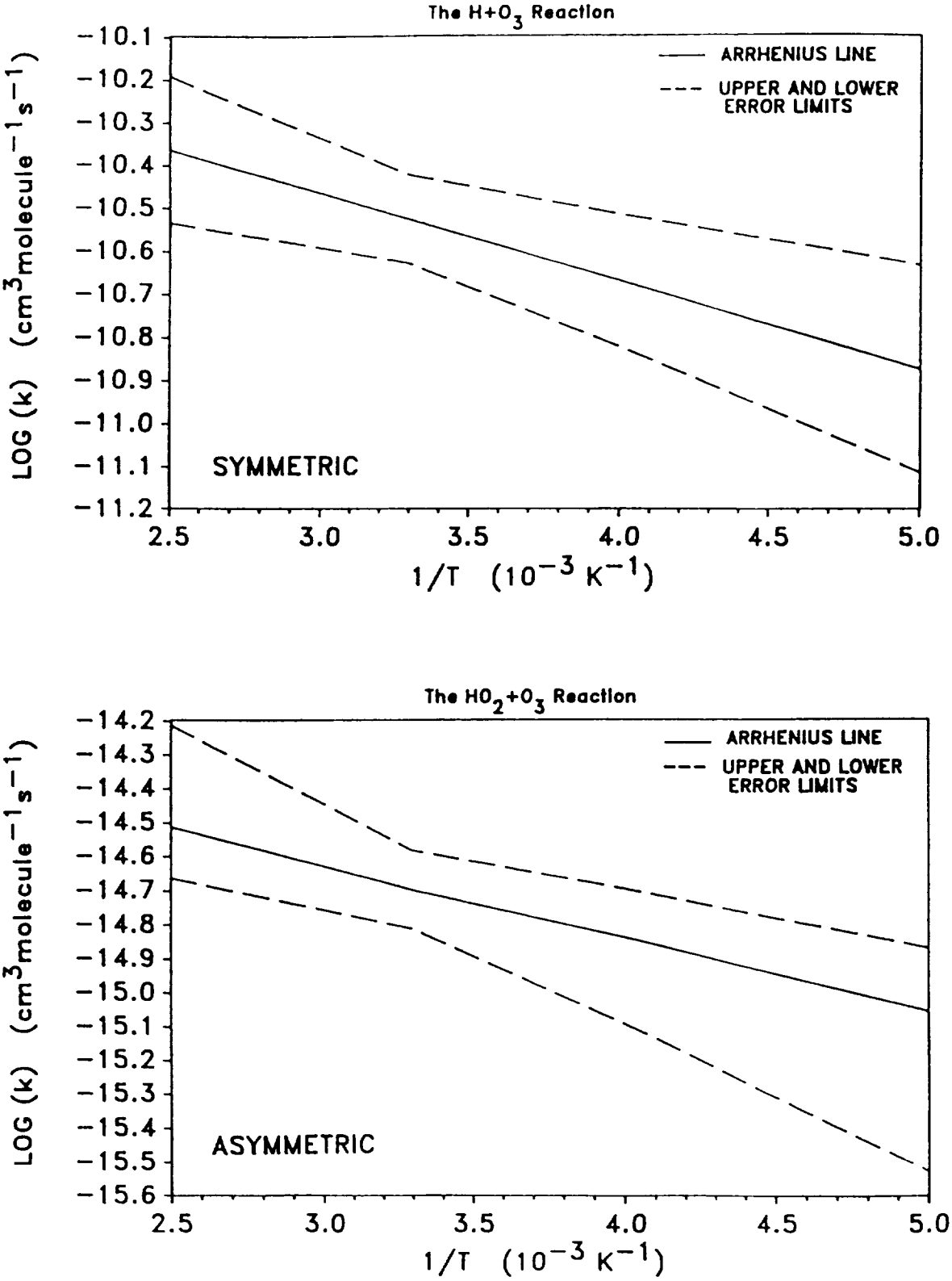

Figure 1. Symmetric and Asymmetric Error Limits

References for the Introduction

1. 1977, "Chlorofluoromethanes and the Stratosphere," NASA Reference Publication 1010, R.D. Hudson, Editor, NASA, Washington, D.C.
2. 1979, "The Stratosphere: Present and Future," NASA Reference Publication 1049, R.D. Hudson and E.I. Reed, Editors, NASA, Washington, D.C.
3. Atkinson, R., D.L. Baulch, R.A. Cox, R.F. Hampson, J.A. Kerr, and J. Troe, 1992, J. Phys. Chem. Ref. Data, **21**, 1125-1568.
4. DeMore, W.B., D.M. Golden, R.F. Hampson, C.J. Howard, M.J. Kurylo, J.J. Margitan, M.J. Molina, A.R. Ravishankara, and R.T. Watson, 1985, JPL Publication 85-37, Jet Propulsion Laboratory, California Institute of Technology, Pasadena, CA.
5. DeMore, W.B., D.M. Golden, R.F. Hampson, C.J. Howard, M.J. Kurylo, M.J. Molina, A.R. Ravishankara, and S.P. Sander, 1987, JPL Publication 87-41, Jet Propulsion Laboratory, California Institute of Technology, Pasadena, CA.
6. DeMore, W.B., D.M. Golden, R.F. Hampson, C.J. Howard, M.J. Kurylo, M.J. Molina, A.R. Ravishankara, and S.P. Sander, 1990, JPL Publication 90-1, Jet Propulsion Laboratory, California Institute of Technology, Pasadena, CA.
7. DeMore, W.B., D.M. Golden, R.F. Hampson, C.J. Howard, M.J. Kurylo, M.J. Molina, A.R. Ravishankara, and S.P. Sander, 1992, JPL Publication 92-20, 10, Jet Propulsion Laboratory, Calif. Inst. of Technology, Pasadena, CA.
8. DeMore, W.B., D.M. Golden, R.F. Hampson, C.J. Howard, M.J. Kurylo, M.J. Molina, A.R. Ravishankara, and S.P. Sander, 1994, JPL Publication 94-26, 11, Jet Propulsion Laboratory, Calif. Inst. of Technology, Pasadena, CA.
9. DeMore, W.B., D.M. Golden, R.F. Hampson, C.J. Howard, M.J. Kurylo, M.J. Molina, A.R. Ravishankara, and R.T. Watson, 1982, JPL Publication 82-57, Jet Propulsion Laboratory, California Institute of Technology, Pasadena, CA.
10. DeMore, W.B., D.M. Golden, R.F. Hampson, C.J. Howard, M.J. Kurylo, M.J. Molina, A.R. Ravishankara, and R.T. Watson, 1983, JPL Publication 83-62, Jet Propulsion Laboratory, California Institute of Technology, Pasadena, CA.
11. DeMore, W.B., D.M. Golden, R.F. Hampson, M.J. Kurylo, J.J. Margitan, M.J. Molina, L.J. Stief, and R.T. Watson, 1981, JPL Publication 81-3, Jet Propulsion Laboratory, California Institute of Technology, Pasadena, CA.
12. DeMore, W.B., L.J. Stief, F. Kaufman, D.M. Golden, R.F. Hampson, M.J. Kurylo, J.J. Margitan, M.J. Molina, and R.T. Watson, 1979, JPL Publication 79-27, Jet Propulsion Laboratory, California Institute of Technology, Pasadena, CA.
13. Francisco, J.S. and M.M. Maricq, 1995, Advances in Photochemistry, 20, John Wiley, New York, pp. 79-163.
14. Patrick, R. and D.M. Golden, 1983, Int. J. Chem. Kinet., **15**, 1189-1227.
15. Plane, J.M.C., 1991, Int. Rev. Phys. Chem., **10**, 55-106.
16. Stein, S.E., J.M. Rukkers, and R.L. Brown, 1991, "NIST Standard Reference Database 25," National Institute of Standards and Technology, Gaithersburg, MD.
17. Troe, J., 1977, J. Chem. Phys., **66**, 4745.
18. Tyndall, G.S. and A.R. Ravishankara, 1991, Int. J. Chem. Kinet., **23**, 483-527.
19. Wallington, T.J., W.F. Schneider, D.R. Worsnop, O.J. Nielsen, J. Sehested, W.J. DeBruyn, and J.A. Shorter, 1994, Environ. Sci. Technol., **28**, 320A-326A.
20. WMO, Scientific Assessment of Ozone Depletion: 1994, World Meteorological Organization Global Ozone Research and Monitoring Project, Report No. 37, 1994, Geneva: National Aeronautics and Space Administration.

Table 1. Rate Constants for Second Order Reactions

Reaction	A-Factor[a]	E/R±ΔE/R	k(298 K)[a]	f(298)[b]	Notes
O_x Reactions					
$O + O_2 \xrightarrow{M} O_3$	(See Table 2)				
$O + O_3 \rightarrow O_2 + O_2$	8.0×10^{-12}	2060±250	8.0×10^{-15}	1.15	A1
$O(^1D)$ Reactions					
$O(^1D) + O_2 \rightarrow O + O_2$	3.2×10^{-11}	-(70±100)	4.0×10^{-11}	1.2	A2,A3
$O(^1D) + O_3 \rightarrow O_2 + O_2$	1.2×10^{-10}	0±100	1.2×10^{-10}	1.3	A2, A4
$\rightarrow O_2 + O + O$	1.2×10^{-10}	0±100	1.2×10^{-10}	1.3	A2, A4
$O(^1D) + H_2 \rightarrow OH + H$	1.1×10^{-10}	0±100	1.1×10^{-10}	1.1	A2, A5
$O(^1D) + H_2O \rightarrow OH + OH$	2.2×10^{-10}	0±100	2.2×10^{-10}	1.2	A2 A6
$O(^1D) + N_2 \rightarrow O + N_2$	1.8×10^{-11}	-(110±100)	2.6×10^{-11}	1.2	A2
$O(^1D) + N_2 \xrightarrow{M} N_2O$	(See Table 2)				
$O(^1D) + N_2O \rightarrow N_2 + O_2$	4.9×10^{-11}	0±100	4.9×10^{-11}	1.3	A2 A7
$\rightarrow NO + NO$	6.7×10^{-11}	0±100	6.7×10^{-11}	1.3	A2 A7
$O(^1D) + NH_3 \rightarrow OH + NH_2$	2.5×10^{-10}	0±100	2.5×10^{-10}	1.3	A2, A8
$O(^1D) + CO_2 \rightarrow O + CO_2$	7.4×10^{-11}	-(120±100)	1.1×10^{-10}	1.2	A2
$O(^1D) + CH_4 \rightarrow$ products	1.5×10^{-10}	0±100	1.5×10^{-10}	1.2	A2 A9
$O(^1D) + HCl \rightarrow$ products	1.5×10^{-10}	0±100	1.5×10^{-10}	1.2	A10
$O(^1D) + HF \rightarrow OH + F$	1.4×10^{-10}	0±100	1.4×10^{-10}	2.0	A11
$O(^1D) + HBr \rightarrow$ products	1.5×10^{-10}	0±100	1.5×10^{-10}	2.0	A12
$O(^1D) + Cl_2 \rightarrow$ products	2.8×10^{-10}	0±100	2.8×10^{-10}	2.0	A13
$O(^1D) + CCl_2O \rightarrow$ products	3.6×10^{-10}	0±100	3.6×10^{-10}	2.0	A2, A14
$O(^1D) + CClFO \rightarrow$ products	1.9×10^{-10}	0±100	1.9×10^{-10}	2.0	A2, A14
$O(^1D) + CF_2O \rightarrow$ products	7.4×10^{-11}	0±100	7.4×10^{-11}	2.0	A2, A14

Table 1. (Continued)

Reaction	A-Factor[a]	E/R±(ΔE/R)	k(298 K)[a]	f(298)[b]	Notes
$O(^1D) + CCl_4 \rightarrow$ products (CFC-10)	3.3×10^{-10}	0±100	3.3×10^{-10}	1.2	A2, **A15**
$O(^1D) + CH_3Br \rightarrow$ products	1.8×10^{-10}	0±100	1.8×10^{-10}	1.3	A15, A16
$O(^1D) + CH_2Br_2 \rightarrow$ products	2.7×10^{-10}	0±100	2.7×10^{-10}	1.3	A15, A17
$O(^1D) + CHBr_3 \rightarrow$ products	6.6×10^{-10}	0±100	6.6×10^{-10}	1.5	A15, A18
$O(^1D) + CH_3F \rightarrow$ products (HFC-41)	1.5×10^{-10}	0±100	1.5×10^{-10}	1.2	A15 **A19**
$O(^1D) + CH_2F_2 \rightarrow$ products (HFC-32)	5.1×10^{-11}	0±100	5.1×10^{-11}	1.3	A15, A20
$O(^1D) + CHF_3 \rightarrow$ products (HFC-23)	9.1×10^{-12}	0±100	9.1×10^{-12}	1.2	A15, A21
$O(^1D) + CHCl_2F \rightarrow$ products (HCFC-21)	1.9×10^{-10}	0±100	1.9×10^{-10}	1.3	A15 **A22**
$O(^1D) + CHClF_2 \rightarrow$ products (HCFC-22)	1.0×10^{-10}	0±100	1.0×10^{-10}	1.2	A15,A23
$O(^1D) + CCl_3F \rightarrow$ products (CFC-11)	2.3×10^{-10}	0±100	2.3×10^{-10}	1.2	A2 **A15**
$O(^1D) + CCl_2F_2 \rightarrow$ products (CFC-12)	1.4×10^{-10}	0±100	1.4×10^{-10}	1.3	A2 **A15**
$O(^1D) + CClF_3 \rightarrow$ products (CFC-13)	8.7×10^{-11}	0±100	8.7×10^{-11}	1.3	A15 **A24**
$O(^1D) + CClBrF_2 \rightarrow$ products (Halon-1211)	1.5×10^{-10}	0±100	1.5×10^{-10}	1.3	A15,A25
$O(^1D) + CBr_2F_2 \rightarrow$ products (Halon-1202)	2.2×10^{-10}	0±100	2.2×10^{-10}	1.3	A15,A26
$O(^1D) + CBrF_3 \rightarrow$ products (Halon-1301)	1.0×10^{-10}	0±100	1.0×10^{-10}	1.3	A15 **A27**
$O(^1D) + CF_4 \rightarrow CF_4 + O$ (CFC-14)	-	-	2.0×10^{-14}	1.5	A15,A28
$O(^1D) + CH_3CH_2F \rightarrow$ products (HFC-161)	2.6×10^{-10}	0±100	2.6×10^{-10}	1.3	A15,A29
$O(^1D) + CH_3CHF_2 \rightarrow$ products (HFC-152a)	2.0×10^{-10}	0±100	2.0×10^{-10}	1.3	A15,A30

Table 1. (Continued)

Reaction	A-Factor[a]	E/R±(ΔE/R)	k(298 K)[a]	f(298)[b]	Notes
$O(^1D) + CH_3CCl_2F \rightarrow$ products (HCFC-141b)	$2.6x10^{-10}$	0±100	$2.6x10^{-10}$	1.3	A15,A31
$O(^1D) + CH_3CClF_2 \rightarrow$ products (HCFC-142b)	$2.2x10^{-10}$	0±100	$2.2x10^{-10}$	1.3	A15,A32
$O(^1D) + CH_3CF_3 \rightarrow$ products (HFC-143a)	$1.0x10^{-10}$	0±100	$1.0x10^{-10}$	3.0	A15,A33
$O(^1D) + CH_2ClCClF_2 \rightarrow$ products (HCFC-132b)	$1.6x10^{-10}$	0±100	$1.6x10^{-10}$	2.0	A15,A34
$O(^1D) + CH_2ClCF_3 \rightarrow$ products (HCFC-133a)	$1.2x10^{-10}$	0±100	$1.2x10^{-10}$	1.3	A15,A35
$O(^1D) + CH_2FCF_3 \rightarrow$ products (HFC-134a)	$4.9x10^{-11}$	0±100	$4.9x10^{-11}$	1.3	A15,A36
$O(^1D) + CHCl_2CF_3 \rightarrow$ products (HCFC-123)	$2.0x10^{-10}$	0±100	$2.0x10^{-10}$	1.3	A15,A37
$O(^1D) + CHClFCF_3 \rightarrow$ products (HCFC-124)	$8.6x10^{-11}$	0±100	$8.6x10^{-11}$	1.3	A15,A38
$O(^1D) + CHF_2CF_3 \rightarrow$ products (HFC-125)	$1.2x10^{-10}$	0±100	$1.2x10^{-10}$	2.0	A15,A39
$O(^1D) + CCl_3CF_3 \rightarrow$ products (CFC-113a)	$2x10^{-10}$	0±100	$2x10^{-10}$	2.0	A15,A40
$O(^1D) + CCl_2FCClF_2 \rightarrow$ products (CFC-113)	$2x10^{-10}$	0±100	$2x10^{-10}$	2.0	A15,A41
$O(^1D) + CCl_2FCF_3 \rightarrow$ products (CFC-114a)	$1x10^{-10}$	0±100	$1x10^{-10}$	2.0	A15,A42
$O(^1D) + CClF_2CClF_2 \rightarrow$ products (CFC-114)	$1.3x10^{-10}$	0±100	$1.3x10^{-10}$	1.3	A15,A43
$O(^1D) + CClF_2CF_3 \rightarrow$ products (CFC-115)	$5x10^{-11}$	0±100	$5x10^{-11}$	1.3	A15,A44
$O(^1D) + CBrF_2CBrF_2 \rightarrow$ products (Halon-2402)	$1.6x10^{-10}$	0±100	$1.6x10^{-10}$	1.3	A15 A45
$O(^1D) + CF_3CF_3 \rightarrow O + CF_3CF_3$ (CFC-116)	-	-	$1.5x10^{-13}$	1.5	A15,A46
$O(^1D) + CHF_2CF_2CF_2CHF_2 \rightarrow$ products (HFC-338pcc)	$1.8x10^{-11}$	0±100	$1.8x10^{-11}$	1.5	A15,A47
$O(^1D) + c\text{-}C_4F_8 \rightarrow$ products	-	-	$8x10^{-13}$	1.3	A15,A48

Table 1. (Continued)

Reaction	A-Factor[a]	E/R±(ΔE/R)	k(298 K)[a]	f(298)[b]	Notes
$O(^1D) + CF_3CHFCHFCF_2CF_3 \rightarrow$ products (HFC-43-10mee)	$2.1x10^{-10}$	0±100	$2.1x10^{-10}$	4	A15,A49
$O(^1D) + C_5F_{12} \rightarrow$ products (CFC-41-12)	-	-	$3.9x10^{-13}$	2	A15,A50
$O(^1D) + C_6F_{14} \rightarrow$ products (CFC-51-14)	-	-	$1x10^{-12}$	2	A15,A51
$O(^1D) + 1,2\text{-}(CF_3)_2c\text{-}C_4F_6 \rightarrow$ products	-	-	$2.8x10^{-13}$	2	A15,A52
$O(^1D) + SF_6 \rightarrow$ products	-	-	$1.8x10^{-14}$	1.5	A53
Singlet O_2 Reactions					
$O_2(^1\Delta) + O \rightarrow$ products	-	-	$<2x10^{-16}$	-	A54
$O_2(^1\Delta) + O_2 \rightarrow$ products	$3.6x10^{-18}$	220±100	$1.7x10^{-18}$	1.2	A55
$O_2(^1\Delta) + O_3 \rightarrow O + 2O_2$	$5.2x10^{-11}$	2840±500	$3.8x10^{-15}$	1.2	A56
$O_2(^1\Delta) + H_2O \rightarrow$ products	-	-	$4.8x10^{-18}$	1.5	A57
$O_2(^1\Delta) + N \rightarrow NO + O$	-	-	$<9x10^{-17}$	-	A58
$O_2(^1\Delta) + N_2 \rightarrow$ products	-	-	$<10^{-20}$	-	A59
$O_2(^1\Delta) + CO_2 \rightarrow$ products	-	-	$<2x10^{-20}$	-	A60
$O_2(^1\Sigma) + O \rightarrow$ products	-	-	$8x10^{-14}$	5.0	A61
$O_2(^1\Sigma) + O_2 \rightarrow$ products	-	-	$3.9x10^{-17}$	1.5	A62
$O_2(^1\Sigma) + O_3 \rightarrow$ products	$2.2x10^{-11}$	0±200	$2.2x10^{-11}$	1.2	A63
$O_2(^1\Sigma) + H_2O \rightarrow$ products	-	-	$5.4x10^{-12}$	1.3	A64
$O_2(^1\Sigma) + N \rightarrow$ products	-	-	$<10^{-13}$	-	A65
$O_2(^1\Sigma) + N_2 \rightarrow$ products	$2.1x10^{-15}$	0±200	$2.1x10^{-15}$	1.2	A66
$O_2(^1\Sigma) + CO_2 \rightarrow$ products	$4.2x10^{-13}$	0±200	$4.2x10^{-13}$	1.2	A67
HO_x Reactions					
$O + OH \rightarrow O_2 + H$	$2.2x10^{-11}$	-(120±100)	$3.3x10^{-11}$	1.2	B 1
$O + HO_2 \rightarrow OH + O_2$	$3.0x10^{-11}$	-(200±100)	$5.9x10^{-11}$	1.2	B 2
$O + H_2O_2 \rightarrow OH + HO_2$	$1.4x10^{-12}$	2000±1000	$1.7x10^{-15}$	2.0	B 3

Table 1. (Continued)

Reaction	A-Factor[a]	E/R±(ΔE/R)	k(298 K)[a]	f(298)[b]	Notes
$H + O_2 \xrightarrow{M} HO_2$	(See Table 2)				
$H + O_3 \rightarrow OH + O_2$	1.4×10^{-10}	470±200	2.9×10^{-11}	1.25	B 4
$H + HO_2 \rightarrow$ products	8.1×10^{-11}	0±100	8.1×10^{-11}	1.3	B 5
$OH + O_3 \rightarrow HO_2 + O_2$	1.6×10^{-12}	940±300	6.8×10^{-14}	1.3	B 6
$OH + H_2 \rightarrow H_2O + H$	5.5×10^{-12}	2000±100	6.7×10^{-15}	1.1	B 7
$OH + HD \rightarrow$ products	5.0×10^{-12}	2130±200	4.0×10^{-15}	1.2	B 8
$OH + OH \rightarrow H_2O + O$	4.2×10^{-12}	240±240	1.9×10^{-12}	1.4	B 9
$\xrightarrow{M} H_2O_2$	(See Table 2)				
$OH + HO_2 \rightarrow H_2O + O_2$	4.8×10^{-11}	-(250±200)	1.1×10^{-10}	1.3	B10
$OH + H_2O_2 \rightarrow H_2O + HO_2$	2.9×10^{-12}	160±100	1.7×10^{-12}	1.2	B11
$HO_2 + O_3 \rightarrow OH + 2O_2$	1.1×10^{-14}	$500\pm^{500}_{100}$	2.0×10^{-15}	1.3	B12
$HO_2 + HO_2 \rightarrow H_2O_2 + O_2$	2.3×10^{-13}	-(600±200)	1.7×10^{-12}	1.3	B13
$\xrightarrow{M} H_2O_2 + O_2$	1.7×10^{-33}[M]	-(1000±400)	4.9×10^{-32}[M]	1.3	B13
NO_x Reactions					
$O + NO \xrightarrow{M} NO_2$	(See Table 2)				
$O + NO_2 \rightarrow NO + O_2$	6.5×10^{-12}	-(120±120)	9.7×10^{-12}	1.1	C 1
$O + NO_2 \xrightarrow{M} NO_3$	(See Table 2)				
$O + NO_3 \rightarrow O_2 + NO_2$	1.0×10^{-11}	0±150	1.0×10^{-11}	1.5	C 2
$O + N_2O_5 \rightarrow$ products			$<3.0\times10^{-16}$		C 3
$O + HNO_3 \rightarrow OH + NO_3$			$<3.0\times10^{-17}$		C 4
$O + HO_2NO_2 \rightarrow$ products	7.8×10^{-11}	3400±750	8.6×10^{-16}	3.0	C 5
$H + NO_2 \rightarrow OH + NO$	4.0×10^{-10}	340±300	1.3×10^{-10}	1.3	C 6
$OH + NO \xrightarrow{M} HONO$	(See Table 2)				
$OH + NO_2 \xrightarrow{M} HNO_3$	(See Table 2)				
$OH + NO_3 \rightarrow$ products			2.2×10^{-11}	1.5	C 7

Table 1. (Continued)

Reaction	A-Factor[a]	E/R±(ΔE/R)	k(298 K)[a]	f(298)[b]	Notes
$OH + HONO \rightarrow H_2O + NO_2$	1.8×10^{-11}	$390\pm\frac{200}{500}$	4.5×10^{-12}	1.5	C 8
$OH + HNO_3 \rightarrow H_2O + NO_3$	(See Note)			1.3	C 9
$OH + HO_2NO_2 \rightarrow$ products	1.3×10^{-12}	$-(380\pm\frac{270}{500})$	4.6×10^{-12}	1.5	C10
$OH + NH_3 \rightarrow H_2O + NH_2$	1.7×10^{-12}	710±200	1.6×10^{-13}	1.2	C11
$HO_2 + NO \rightarrow NO_2 + OH$	3.5×10^{-12}	-(250±50)	8.1×10^{-12}	1.15	C12
$HO_2 + NO_2 \overset{M}{\rightarrow} HO_2NO_2$	(See Table 2)				
$HO_2 + NO_2 \rightarrow HONO + O_2$	(See Note)				C13
$HO_2 + NO_3 \rightarrow$ products			3.5×10^{-12}	1.5	C14
$HO_2 + NH_2 \rightarrow$ products			3.4×10^{-11}	2.0	C15
$N + O_2 \rightarrow NO + O$	1.5×10^{-11}	3600±400	8.5×10^{-17}	1.25	C16
$N + O_3 \rightarrow NO + O_2$			$<2.0\times10^{-16}$		C17
$N + NO \rightarrow N_2 + O$	2.1×10^{-11}	-(100±100)	3.0×10^{-11}	1.3	C18
$N + NO_2 \rightarrow N_2O + O$	5.8×10^{-12}	-(220±100)	1.2×10^{-11}	1.5	C19
$NO + O_3 \rightarrow NO_2 + O_2$	2.0×10^{-12}	1400±200	1.8×10^{-14}	1.1	C20
$NO + NO_3 \rightarrow 2NO_2$	1.5×10^{-11}	-(170±100)	2.6×10^{-11}	1.3	C21
$NO_2 + O_3 \rightarrow NO_3 + O_2$	1.2×10^{-13}	2450±150	3.2×10^{-17}	1.15	C22
$NO_2 + NO_3 \rightarrow NO + NO_2 + O_2$	(See Note)				C23
$NO_2 + NO_3 \overset{M}{\rightarrow} N_2O_5$	(See Table 2)				
$NO_3 + NO_3 \rightarrow 2NO_2 + O_2$	8.5×10^{-13}	2450±500	2.3×10^{-16}	1.5	C24
$NH_2 + O_2 \rightarrow$ products			$<6.0\times10^{-21}$		C25
$NH_2 + O_3 \rightarrow$ products	4.3×10^{-12}	930±500	1.9×10^{-13}	3.0	C26
$NH_2 + NO \rightarrow$ products	4.0×10^{-12}	-(450±150)	1.8×10^{-11}	1.3	C27
$NH_2 + NO_2 \rightarrow$ products	2.1×10^{-12}	-(650±250)	1.9×10^{-11}	3.0	C28
$NH + NO \rightarrow$ products	4.9×10^{-11}	0±300	4.9×10^{-11}	1.5	C29
$NH + NO_2 \rightarrow$ products	3.5×10^{-13}	-(1140±500)	1.6×10^{-11}	2.0	C30

Table 1. (Continued)

Reaction	A-Factor[a]	E/R±(ΔE/R)	k(298 K)[a]	f(298)[b]	Notes
$O_3 + HNO_2 \rightarrow O_2 + HNO_3$			$<5.0\times10^{-19}$		C31
$N_2O_5 + H_2O \rightarrow 2HNO_3$			$<2.0\times10^{-21}$		C32
$N_2(A,v) + O_2 \rightarrow$ products			2.5×10^{-12}, v=0	1.5	C33
$N_2(A,v) + O_3 \rightarrow$ products			4.1×10^{-11}, v=0	2.0	C34
Reactions of Organic Compounds					
$O + CH_3 \rightarrow$ products	1.1×10^{-10}	0±250	1.1×10^{-10}	1.3	D1
$O + HCN \rightarrow$ products	1.0×10^{-11}	4000±1000	1.5×10^{-17}	10	D2
$O + C_2H_2 \rightarrow$ products	3.0×10^{-11}	1600±250	1.4×10^{-13}	1.3	D3
$O + H_2CO \rightarrow$ products	3.4×10^{-11}	1600±250	1.6×10^{-13}	1.25	D4
$O + CH_3CHO \rightarrow CH_3CO + OH$	1.8×10^{-11}	1100±200	4.5×10^{-13}	1.25	D5
$O_3 + C_2H_2 \rightarrow$ products	1.0×10^{-14}	4100±500	1.0×10^{-20}	3	D6
$O_3 + C_2H_4 \rightarrow$ products	1.2×10^{-14}	2630±100	1.7×10^{-18}	1.25	D7
$O_3 + C_3H_6 \rightarrow$ products	6.5×10^{-15}	1900±200	1.1×10^{-17}	1.2	D8
OH + CO → Products	1.5×10^{-13} x $(1+0.6P_{atm})$	0±300	1.5×10^{-13} x $(1+0.6P_{atm})$	1.3	D9
$OH + CH_4 \rightarrow CH_3 + H_2O$	2.45×10^{-12}	1775±100	6.3×10^{-15}	1.1	D10
$OH + {}^{13}CH_4 \rightarrow {}^{13}CH_3 + H_2O$	(See Note)				D11
$OH + CH_3D \rightarrow$ products	3.5×10^{-12}	1950 ± 200	5.0×10^{-15}	1.15	D12
$OH + H_2CO \rightarrow H_2O + HCO$	1.0×10^{-11}	0±200	1.0×10^{-11}	1.25	D13
$OH + CH_3OH \rightarrow$ products	6.7×10^{-12}	600±300	8.9×10^{-13}	1.2	D14
$OH + CH_3OOH \rightarrow$ Products	3.8×10^{-12}	-(200±200)	7.4×10^{-12}	1.5	D15
$OH + HC(O)OH \rightarrow$ products	4.0×10^{-13}	0±200	4.0×10^{-13}	1.3	D16
$OH + HCN \rightarrow$ products	1.2×10^{-13}	400±150	3.1×10^{-14}	3	D17
$OH + C_2H_2 \xrightarrow{M}$ products	(See Table 2)				
$OH + C_2H_4 \xrightarrow{M}$ products	(See Table 2)				
$OH + C_2H_6 \rightarrow H_2O + C_2H_5$	8.7×10^{-12}	1070±100	2.4×10^{-13}	1.1	D18
$OH + C_3H_8 \rightarrow H_2O + C_3H_7$	1.0×10^{-11}	660±100	1.1×10^{-12}	1.2	D19
$OH + CH_3CHO \rightarrow CH_3CO + H_2O$	5.6×10^{-12}	-(270±200)	1.4×10^{-11}	1.2	D20

Table 1. (Continued)

Reaction	A-Factor[a]	E/R±(ΔE/R)	k(298 K)[a]	f(298)[b]	Notes
$OH + C_2H_5OH \rightarrow$ products	7.0×10^{-12}	235±100	3.2×10^{-12}	1.3	D21
$OH + CH_3C(O)OH \rightarrow$ products	4.0×10^{-13}	-200±400	8.0×10^{-13}	1.3	D22
$OH + CH_3C(O)CH_3 \rightarrow CH_3C(O)CH_2 + H_2O$	2.2×10^{-12}	685±100	2.2×10^{-13}	1.15	D23
$OH + CH_3CN \rightarrow$ products	7.8×10^{-13}	1050±200	2.3×10^{-14}	1.5	D24
$OH + CH_3ONO_2 \rightarrow$ products	5.0×10^{-13}	890±500	2.4×10^{-14}	3	D25
$OH + CH_3C(O)O_2NO_2$ (PAN)$\rightarrow$ products			$<4\times10^{-14}$		D26
$OH + C_2H_5ONO_2 \rightarrow$ products	8.2×10^{-13}	450±300	1.8×10^{-13}	3	D27
$HO_2 + CH_2O \rightarrow$ adduct	6.7×10^{-15}	-(600±600)	5.0×10^{-14}	5	D28
$HO_2 + CH_3O_2 \rightarrow CH_3OOH + O_2$	3.8×10^{-13}	-(800±400)	5.6×10^{-12}	2	D29
$HO_2 + C_2H_5O_2 \rightarrow C_2H_5OOH + O_2$	7.5×10^{-13}	-(700±250)	8.0×10^{-12}	1.5	D30
$HO_2 + CH_3C(O)O_2 \rightarrow$ products	4.5×10^{-13}	-(1000±600)	1.3×10^{-11}	2	D31
$NO_3 + CO \rightarrow$ products			$<4.0\times10^{-19}$		D32
$NO_3 + CH_2O \rightarrow$ products			5.8×10^{-16}	1.3	D33
$NO_3 + CH_3CHO \rightarrow$ products	1.4×10^{-12}	1900±300	2.4×10^{-15}	1.3	D34
$CH_3 + O_2 \rightarrow$ products			$<3.0\times10^{-16}$		D35
$CH_3 + O_2 \xrightarrow{M} CH_3O_2$	(See Table 2)				
$CH_3 + O_3 \rightarrow$ products	5.4×10^{-12}	220±150	2.6×10^{-12}	2	D36
$HCO + O_2 \rightarrow CO + HO_2$	3.5×10^{-12}	-(140±140)	5.5×10^{-12}	1.3	D37
$CH_2OH + O_2 \rightarrow CH_2O + HO_2$	9.1×10^{-12}	0±200	9.1×10^{-12}	1.3	D38
$CH_3O + O_2 \rightarrow CH_2O + HO_2$	3.9×10^{-14}	900±300	1.9×10^{-15}	1.5	D39
$CH_3O + NO \rightarrow CH_2O + HNO$	(See Note)				D40
$CH_3O + NO \xrightarrow{M} CH_3ONO$	(See Table 2)				
$CH_3O + NO_2 \rightarrow CH_2O + HONO$	1.1×10^{-11}	1200±600	2.0×10^{-13}	5	D41
$CH_3O + NO_2 \xrightarrow{M} CH_3ONO_2$	(See Table 2)				
$CH_3O_2 + O_3 \rightarrow$ products			$<3.0\times10^{-17}$		D42
$CH_3O_2 + CH_3O_2 \rightarrow$ products	2.5×10^{-13}	-(190±190)	4.7×10^{-13}	1.5	D43
$CH_3O_2 + NO \rightarrow CH_3O + NO_2$	3.0×10^{-12}	-(280±60)	7.7×10^{-12}	1.15	D44
$CH_3O_2 + NO_2 \xrightarrow{M} CH_3O_2NO_2$	(See Table 2)				

Table 1. (Continued)

Reaction	A-Factor[a]	E/R±(ΔE/R)	k(298 K)[a]	f(298)[b]	Notes
$CH_3O_2 + CH_3C(O)O_2 \rightarrow$ products	$1.3x10^{-12}$	-(640±200)	$1.1x10^{-11}$	1.5	D45
$C_2H_5 + O_2 \rightarrow C_2H_4 + HO_2$			$<2.0x10^{-14}$		D46
$C_2H_5 + O_2 \xrightarrow{M} C_2H_5O_2$	(See Table 2)				
$C_2H_5O + O_2 \rightarrow CH_3CHO + HO_2$	6.3×10^{-14}	550±200	$1.0x10^{-14}$	1.5	D47
$C_2H_5O + NO \xrightarrow{M}$ products	(See Table 2)				
$C_2H_5O + NO_2 \xrightarrow{M}$ products	(See Table 2)				
$C_2H_5O_2 + C_2H_5O_2 \rightarrow$ products	$6.8x10^{-14}$	0±300	$6.8x10^{-14}$	2	D48
$C_2H_5O_2 + NO \rightarrow$ products	$2.6x10^{-12}$	-365±150	$8.7x10^{-12}$	1.2	D49
$CH_3C(O)O_2 + CH_3C(O)O_2 \rightarrow$ products	$2.9x10^{-12}$	-(500±150)	$1.5x10^{-11}$	1.5	D50
$CH_3C(O)O_2 + NO \rightarrow$ products	$5.3x10^{-12}$	-360±150	$1.8x10^{-11}$	1.4	D51
$CH_3C(O)O_2 + NO_2 \xrightarrow{M}$ products	(See Table 2)				
<u>FO_x Reactions</u>					
$O + FO \rightarrow F + O_2$	$2.7x10^{-11}$	0±250	$2.7x10^{-11}$	3.0	E 1
$O + FO_2 \rightarrow FO + O_2$	$5.0x10^{-11}$	0±250	$5.0x10^{-11}$	5.0	E 2
$OH + CH_3F \rightarrow CH_2F + H_2O$ (HFC-41)	$3.0x10^{-12}$	1500±300	$2.0x10^{-14}$	1.1	E 3
$OH + CH_2F_2 \rightarrow CHF_2 + H_2O$ (HFC-32)	$1.9x10^{-12}$	1550±200	$1.0x10^{-14}$	1.2	E 4
$OH + CHF_3 \rightarrow CF_3 + H_2O$ (HFC-23)	$1.0x10^{-12}$	2440±200	$2.8x10^{-16}$	1.3	E 5
$OH + CF_3OH \rightarrow CF_3O + H_2O$			$<2x10^{-17}$		E6
$OH + CH_3CH_2F \rightarrow$ products (HFC-161)	$7.0x10^{-12}$	1100±300	$1.7x10^{-13}$	1.4	E 7
$OH + CH_3CHF_2 \rightarrow$ products (HFC-152a)	$2.4x10^{-12}$	1260±200	$3.5x10^{-14}$	1.2	E 8
$OH + CH_2FCH_2F \rightarrow CHFCH_2F + H_2O$ (HFC-152)	$1.7x10^{-11}$	1500±500	$1.1x10^{-13}$	2.0	E 9
$OH + CH_3CF_3 \rightarrow CH_2CF_3 + H_2O$ (HFC-143a)	$1.8x10^{-12}$	2170±150	$1.2x10^{-15}$	1.1	E 10
$OH + CH_2FCHF_2 \rightarrow$ products (HFC-143)	$4.0x10^{-12}$	1650±300	$1.6x10^{-14}$	1.5	E11

Table 1. (Continued)

Reaction	A-Factor[a]	E/R±(ΔE/R)	k(298 K)[a]	f(298)[b]	Notes
OH + CH_2FCF_3 → $CHFCF_3$ + H_2O (HFC-134a)	$1.5x10^{-12}$	1750±200	$4.2x10^{-15}$	1.1	E12
OH + CHF_2CHF_2 → CF_2CHF_2 (HFC-134) + H_2O	$1.6x10^{-12}$	1680±300	$5.7x10^{-15}$	2.0	E13
OH + CHF_2CF_3 → CF_2CF_3 + H_2O (HFC-125)	$5.6x10^{-13}$	1700±300	$1.9x10^{-15}$	1.3	E14
OH + CH_3OCHF_2 → products (HFOC-152a)	$6.0x10^{-12}$	1530±150	$3.5x10^{-14}$	1.2	E15
OH + CF_3OCH_3 → CF_3OCH_2 + H_2O (HFOC-143a)	$1.5x10^{-12}$	1450±150	$1.2x10^{-14}$	1.1	E16
OH + CF_2HOCF_2H → CF_2OCF_2H (HFOC-134) + H_2O	$1.9x10^{-12}$	2000±150	$2.3x10^{-15}$	1.2	E17
OH + CF_3OCHF_2 → CF_3OCF_2 + H_2O (HFOC-125)	$4.7x10^{-13}$	2100±300	$4.1x10^{-16}$	1.2	E18
OH + $CF_3CH_2CH_3$ → products (HFC-263fb)	-	-	$4.2x10^{-14}$	1.5	E19
OH + $CH_2FCF_2CHF_2$ → products (HFC-245ca)	$2.4x10^{-12}$	1660±150	$9.1x10^{-15}$	1.3	E20
OH + $CHF_2CHFCHF_2$ → products (HFC-245ea)	-	-	$1.6x10^{-14}$	2.0	E21
OH + CF_3CHFCH_2F → products (HFC-245eb)	-	-	$1.5x10^{-14}$	2.0	E22
OH + $CHF_2CH_2CF_3$ → products (HFC-245fa)	$6.1x10^{-13}$	1330±150	$7.0x10^{-15}$	1.2	E23
OH + $CF_3CF_2CH_2F$ → CF_3CF_2CHF (HFC-236cb) +H_2O	$1.5x10^{-12}$	1750±500	$4.2x10^{-15}$	2.0	E24
OH + $CF_3CHFCHF_2$ → products (HFC-236ea)	$1.1x10^{-12}$	1590±150	$5.3x10^{-15}$	1.1	E25
OH + $CF_3CH_2CF_3$ → CF_3CHCF_3 (HFC-236fa) +H_2O	$1.3x10^{-12}$	2480±150	$3.2x10^{-16}$	1.1	E26
OH + CF_3CHFCF_3 → CF_3CFCF_3+H_2O (HFC-227ea)	$5.0x10^{-13}$	1700±300	$1.7x10^{-15}$	1.1	E27
OH + $CHF_2OCH_2CF_3$ → products (HFOC-245fa)	$2.6x10^{-12}$	1610±150	$1.2x10^{-14}$	2.0	E28
OH + $CF_3CH_2CF_2CH_3$ → products (HFC-365mfc)	$2.0x10^{-12}$	1750±200	$5.7x10^{-15}$	1.3	E29

Table 1. (Continued)

Reaction	A-Factor[a]	E/R±(ΔE/R)	k(298 K)[a]	f(298)[b]	Notes
OH + $CF_3CH_2CH_2CF_3$ → products (HFC-356mff)	3.0×10^{-12}	1800±300	7.1×10^{-15}	1.3	E30
OH + $CF_3CF_2CH_2CH_2F$ → products (HFC-356mcf)	1.7×10^{-12}	1110±200	4.2×10^{-14}	2.0	E31
OH + $CHF_2CF_2CF_2CF_2H$ → products (HFC-338pcc)	7.8×10^{-13}	1530±200	4.6×10^{-15}	1.5	E32
OH + $CF_3CH_2CF_2CH_2CF_3$ → products (HFC-458mfcf)	1.2×10^{-12}	1830±200	2.6×10^{-15}	2.0	E33
OH + $CF_3CHFCHFCF_2CF_3$ → products (HFC-43-10mee)	5.2×10^{-13}	1500±300	3.4×10^{-15}	1.3	E34
OH + $CF_3CF_2CH_2CH_2CF_2CF_3$ → (HFC-55-10-mcff) products	-	-	8.3×10^{-15}	1.5	E35
F + $O_2 \xrightarrow{M} FO_2$	(See Table 2)				
F + O_3 → FO + O_2	2.2×10^{-11}	230±200	1.0×10^{-11}	1.5	E36
F + H_2 → HF + H	1.4×10^{-10}	500±200	2.6×10^{-11}	1.2	E37
F + H_2O → HF + OH	1.4×10^{-11}	0±200	1.4×10^{-11}	1.3	E38
F + NO $\xrightarrow{M}$ FNO	(See Table 2)				
F + $NO_2 \xrightarrow{M} FNO_2$	(See Table 2)				
F + HNO_3 → HF + NO_3	6.0×10^{-12}	-(400±200)	2.3×10^{-11}	1.3	E39
F + CH_4 → HF + CH_3	1.6×10^{-10}	260±200	6.7×10^{-11}	1.4	E40
FO + O_3 → products			$<1\times10^{-14}$		E41
FO + NO → NO_2 + F	8.2×10^{-12}	-(300±200)	2.2×10^{-11}	1.5	E42
FO + $NO_2 \xrightarrow{M} FONO_2$	(See Table 2)				
FO + FO → 2 F + O_2	1.0×10^{-11}	0±250	1.0×10^{-11}	1.5	E43
FO_2 + O_3 → products			$<3.4\times10^{-16}$		E44
FO_2 + NO → FNO + O_2	7.5×10^{-12}	690±400	7.5×10^{-13}	2.0	E45
FO_2 + NO_2 → products	3.8×10^{-11}	2040±500	4.0×10^{-14}	2.0	E46
FO_2 + CO → products			$<5.1\times10^{-16}$		E47
FO_2 + CH_4 → products			$<2\times10^{-16}$		E48
CF_3 + $O_2 \xrightarrow{M} CF_3O_2$	(See Table 2)				

Table 1. (Continued)

Reaction	A-Factor[a]	E/R±(ΔE/R)	k(298 K)[a]	f(298)[b]	Notes
$CF_3O + M \rightarrow F + CF_2O + M$	(See Table 2)				
$CF_3O + O_2 \rightarrow FO_2 + CF_2O$	$<3 \times 10^{-11}$	5000	$<1.5 \times 10^{-18}$		E49
$CF_3O + O_3 \rightarrow CF_3O_2 + O_2$	2×10^{-12}	1400±600	1.8×10^{-14}	1.3	E50
$CF_3O + H_2O \rightarrow OH + CF_3OH$	3×10^{-12}	>3600	$<2 \times 10^{-17}$		E51
$CF_3O + NO \rightarrow CF_2O + FNO$	3.7×10^{-11}	(-110±70)	5.4×10^{-11}	1.2	E52
$CF_3O + NO_2 \rightarrow$ products	(See Note)				E53
$\xrightarrow{M} CF_3ONO_2$	(See Table 2)				
$CF_3O + CO \rightarrow$ products			$<2 \times 10^{-15}$		E54
$\xrightarrow{M} CF_3OCO$	(See Table 2)				
$CF_3O + CH_4 \rightarrow CH_3 + CF_3OH$	2.6×10^{-12}	1420±200	2.2×10^{-14}	1.1	E55
$CF_3O + C_2H_6 \rightarrow C_2H_5 + CF_3OH$	4.9×10^{-12}	400±100	1.3×10^{-12}	1.2	E56
$CF_3O_2 + O_3 \rightarrow CF_3O + 2O_2$			$<3 \times 10^{-15}$		E57
$CF_3O_2 + CO \rightarrow CF_3O + CO_2$			$<5 \times 10^{-16}$		E58
$CF_3O_2 + NO \rightarrow CF_3O + NO_2$	5.4×10^{-12}	(-320±150)	1.6×10^{-11}	1.1	E59
$CF_3O_2 + NO_2 \xrightarrow{M} CF_3O_2NO_2$	(See Table 2)				
<u>ClO_X Reactions</u>					
$O + ClO \rightarrow Cl + O_2$	3.0×10^{-11}	-(70±70)	3.8×10^{-11}	1.2	F 1
$O + OClO \rightarrow ClO + O_2$	2.4×10^{-12}	960±300	1.0×10^{-13}	2.0	F 2
$O + OClO \xrightarrow{M} ClO_3$	(See Table 2)				
$O + Cl_2O \rightarrow ClO + ClO$	2.7×10^{-11}	530±150	4.5×10^{-12}	1.3	F 3
$O + HCl \rightarrow OH + Cl$	1.0×10^{-11}	3300±350	1.5×10^{-16}	2.0	F 4
$O + HOCl \rightarrow OH + ClO$	1.7×10^{-13}	0±300	1.7×10^{-13}	3.0	F 5
$O + ClONO_2 \rightarrow$ products	2.9×10^{-12}	800±200	2.0×10^{-13}	1.5	F 6
$O_3 + OClO \rightarrow$ products	2.1×10^{-12}	4700±1000	3.0×10^{-19}	2.5	F 7
$O_3 + Cl_2O_2 \rightarrow$ products	-	-	$<1.0 \times 10^{-19}$	-	F 8
$OH + Cl_2 \rightarrow HOCl + Cl$	1.4×10^{-12}	900±400	6.7×10^{-14}	1.2	F 9

Table 1. (Continued)

Reaction	A-Factor[a]	E/R±(ΔE/R)	k(298 K)[a]	f(298)[b]	Notes
$OH + ClO \rightarrow$ products	$1.1x10^{-11}$	-(120±150)	$1.7x10^{-11}$	1.5	F10
$OH + OClO \rightarrow HOCl + O_2$	$4.5x10^{-13}$	-(800±200)	$6.8x10^{-12}$	2.0	F11
$OH + HCl \rightarrow H_2O + Cl$	$2.6x10^{-12}$	350±100	$8.0x10^{-13}$	1.2	F12
$OH + HOCl \rightarrow H_2O + ClO$	$3.0x10^{-12}$	500±500	$5.0x10^{-13}$	3.0	F13
$OH + ClNO_2 \rightarrow HOCl + NO_2$	$2.4x10^{-12}$	1250±300	$3.6x10^{-14}$	2.0	F14
$OH + ClONO_2 \rightarrow$ products	$1.2x10^{-12}$	330±200	$3.9x10^{-13}$	1.5	F15
$OH + CH_3Cl \rightarrow CH_2Cl + H_2O$	$4.0x10^{-12}$	1400±250	$3.6x10^{-14}$	1.2	F16
$OH + CH_2Cl_2 \rightarrow CHCl_2 + H_2O$	$3.8x10^{-12}$	1050±150	$1.1x10^{-13}$	1.4	F17
$OH + CHCl_3 \rightarrow CCl_3 + H_2O$	$2.0x10^{-12}$	900±150	$1.0x10^{-13}$	1.2	F18
$OH + CCl_4 \rightarrow$ products	$\sim 1.0x10^{-12}$	>2300	$<5.0x10^{-16}$	-	F19
$OH + CFCl_3 \rightarrow$ products (CFC-11)	$\sim 1.0x10^{-12}$	>3700	$<5.0x10^{-18}$	-	F20
$OH + CF_2Cl_2 \rightarrow$ products (CFC-12)	$\sim 1.0x10^{-12}$	>3600	$<6.0x10^{-18}$	-	F21
$OH + CH_2ClF \rightarrow CHClF + H_2O$ (HCFC-31)	$2.8x10^{-12}$	1270±200	$3.9x10^{-14}$	1.2	F22
$OH + CHFCl_2 \rightarrow CFCl_2 + H_2O$ (HCFC-21)	$1.7x10^{-12}$	1250±150	$2.6x10^{-14}$	1.2	F23
$OH + CHF_2Cl \rightarrow CF_2Cl + H_2O$ (HCFC-22)	$1.0x10^{-12}$	1600±150	$4.7x10^{-15}$	1.1	F24
$OH + CH_3OCl \rightarrow$ products	$2.4x10^{-12}$	360±200	$7.2x10^{-13}$	3.0	F25
$OH + CH_3CCl_3 \rightarrow CH_2CCl_3 + H_2O$ (HCC-140)	$1.8x10^{-12}$	1550±150	$1.0x10^{-14}$	1.1	F26
$OH + C_2HCl_3 \rightarrow$ products	$4.9x10^{-13}$	-(450±200)	$2.2x10^{-12}$	1.25	F27
$OH + C_2Cl_4 \rightarrow$ products	$9.4x10^{-12}$	1200±200	$1.7x10^{-13}$	1.25	F28
$OH + CCl_3CHO \rightarrow H_2O + CCl_3CO$	$8.2x10^{-12}$	600±300	$1.1x10^{-12}$	1.5	F29
$OH + CH_3CFCl_2 \rightarrow CH_2CFCl_2 + H_2O$ (HCFC-141b)	$1.7x10^{-12}$	1700±150	$5.7x10^{-15}$	1.2	F30
$OH + CH_3CF_2Cl \rightarrow CH_2CF_2Cl + H_2O$ (HCFC-142b)	$1.3x10^{-12}$	1800±150	$3.1x10^{-15}$	1.2	F31
$OH + CH_2ClCF_2Cl \rightarrow CHClCF_2Cl + H_2O$ (HCFC-132b)	$3.6x10^{-12}$	1600±400	$1.7x10^{-14}$	2.0	F32

Table 1. (Continued)

Reaction	A-Factor[a]	E/R±(ΔE/R)	k(298 K)[a]	f(298)[b]	Notes
$OH + CHCl_2CF_2Cl \rightarrow CCl_2CF_2Cl + H_2O$ (HCFC-122)	1.0×10^{-12}	900±150	4.9×10^{-14}	1.2	F33
$OH + CHFClCFCl_2 \rightarrow CFClCFCl_2 + H_2O$ (HCFC-122a)	1.0×10^{-12}	1250±150	1.5×10^{-14}	1.1	F34
$OH + CH_2ClCF_3 \rightarrow CHClCF_3 + H_2O$ (HCFC-133a)	5.2×10^{-13}	1100±300	1.3×10^{-14}	1.3	F35
$OH + CHCl_2CF_3 \rightarrow CCl_2CF_3 + H_2O$ (HCFC-123)	7.0×10^{-13}	900±150	3.4×10^{-14}	1.2	F36
$OH + CHFClCF_2Cl \rightarrow CFClCF_2Cl + H2O$ (HCFC-123a)	9.2×10^{-13}	1280±150	1.3×10^{-14}	1.2	F37
$OH + CHFClCF_3 \rightarrow CFClCF_3 + H_2O$ (HCFC-124)	8.0×10^{-13}	1350±150	8.6×10^{-15}	1.2	F38
$OH + CH_3CF_2CFCl_2 \rightarrow$ products (HCFC-243cc)	7.7×10^{-13}	1700±300	2.6×10^{-15}	2.0	F39
$OH + CF_3CF_2CHCl_2 \rightarrow$ products (HCFC-225ca)	1.0×10^{-12}	1100±200	2.5×10^{-14}	1.3	F40
$OH + CF_2ClCF_2CHFCl \rightarrow$ products (HCFC-225cb)	5.5×10^{-13}	1250±200	8.3×10^{-15}	1.3	F41
$HO_2 + Cl \rightarrow HCl + O_2$	1.8×10^{-11}	-(170±200)	3.2×10^{-11}	1.5	F42
$\rightarrow OH + ClO$	4.1×10^{-11}	450±200	9.1×10^{-12}	2.0	F42
$HO_2 + ClO \rightarrow HOCl + O_2$	4.8×10^{-13}	$-(700\pm{}^{250}_{700})$	5.0×10^{-12}	1.4	F43
$H_2O + ClONO_2 \rightarrow$ products	-	-	$<2.0\times10^{-21}$	-	F44
$NO + OClO \rightarrow NO_2 + ClO$	2.5×10^{-12}	600±300	3.4×10^{-13}	2.0	F45
$NO + Cl_2O_2 \rightarrow$ products	-	-	$<2.0\times10^{-14}$	-	F46
$NO_3 + OClO \xrightarrow{M} O_2ClONO_2$	(See Table 2)				
$NO_3 + HCl \rightarrow HNO_3 + Cl$	-	-	$<5.0\times10^{-17}$	-	F47
$HO_2NO_2 + HCl \rightarrow$ products	-	-	$<1.0\times10^{-21}$	-	F48
$Cl + O_2 \xrightarrow{M} ClOO$	(See Table 2)				
$Cl + O_3 \rightarrow ClO + O_2$	2.9×10^{-11}	260±100	1.2×10^{-11}	1.15	F49
$Cl + H_2 \rightarrow HCl + H$	3.7×10^{-11}	2300±200	1.6×10^{-14}	1.25	F50
$Cl + H_2O_2 \rightarrow HCl + HO_2$	1.1×10^{-11}	980±500	4.1×10^{-13}	1.5	F51

Table 1. (Continued)

Reaction	A-Factor[a]	E/R±(ΔE/R)	k(298 K)[a]	f(298)[b]	Notes
$Cl + NO \xrightarrow{M} NOCl$	(See Table 2)				
$Cl + NO_2 \xrightarrow{M} ClONO\ (ClNO_2)$	(See Table 2)				
$Cl + NO_3 \rightarrow ClO + NO_2$	$2.4x10^{-11}$	0±400	$2.4x10^{-11}$	1.5	F52
$Cl + N_2O \rightarrow ClO + N_2$	(See Note)				F53
$Cl + HNO_3 \rightarrow$ products	-	-	$<2.0x10^{-16}$	-	F54
$Cl + CO \xrightarrow{M} ClCO$	(See Table 2)				
$Cl + CH_4 \rightarrow HCl + CH_3$	$1.1x10^{-11}$	1400±150	$1.0x10^{-13}$	1.1	F55
$Cl + CH_3D \rightarrow$ products	-	-	$7.4x10^{-14}$	2.0	F56
$Cl + H_2CO \rightarrow HCl + HCO$	$8.1x10^{-11}$	30±100	$7.3x10^{-11}$	1.15	F57
$Cl + CH_3O_2 \rightarrow$ products	-	-	$1.6x10^{-10}$	1.5	F58
$Cl + CH_3OH \rightarrow CH_2OH + HCl$	$5.4x10^{-11}$	0±250	$5.4x10^{-11}$	1.5	F59
$Cl + C_2H_2 \xrightarrow{M} ClC_2H_2$	(See Table 2)				
$Cl + C_2H_4 \xrightarrow{M} ClC_2H_4$	(See Table 2)				
$Cl + C_2H_6 \rightarrow HCl + C_2H_5$	$7.7x10^{-11}$	90±90	$5.7x10^{-11}$	1.1	F60
$Cl + C_2H_5O_2 \rightarrow ClO + C_2H_5O$	-	-	$7.4x10^{-11}$	2.0	F61
$\rightarrow HCl + C_2H_4O_2$	-	-	$7.7x10^{-11}$	2.0	F61
$Cl + CH_3CN \rightarrow$ products	$1.6x10^{-11}$	2140±300	$1.2x10^{-14}$	2.0	F62
$Cl + CH_3CO_3NO_2 \rightarrow$ products	-	-	$<1x10^{-14}$		F63
$Cl + C_3H_8 \rightarrow HCl + C_3H_7$	$1.2x10^{-10}$	-(40±250)	$1.4x10^{-10}$	1.3	F64
$Cl + OClO \rightarrow ClO + ClO$	$3.4x10^{-11}$	-(160±200)	$5.8x10^{-11}$	1.25	F65
$Cl + ClOO \rightarrow Cl_2 + O_2$	$2.3x10^{-10}$	0±250	$2.3x10^{-10}$	3.0	F66
$\rightarrow ClO + ClO$	$1.2x10^{-11}$	0±250	$1.2x10^{-11}$	3.0	F66
$Cl + Cl_2O \rightarrow Cl_2 + ClO$	$6.2x10^{-11}$	-(130±130)	$9.6x10^{-11}$	1.2	F67
$Cl + Cl_2O_2 \rightarrow$ products	-	-	$1.0x10^{-10}$	2.0	F68
$Cl + HOCl \rightarrow$ products	$2.5x10^{-12}$	130±250	$1.6x10^{-12}$	1.5	F69
$Cl + ClNO \rightarrow NO + Cl_2$	$5.8x10^{-11}$	-(100±200)	$8.1x10^{-11}$	1.5	F70
$Cl + ClONO_2 \rightarrow$ products	$6.5x10^{-12}$	-(135±50)	$1.0x10^{-11}$	1.2	F71

Table 1. (Continued)

Reaction	A-Factor[a]	E/R±(ΔE/R)	k(298 K)[a]	f(298)[b]	Notes
$Cl + CH_3Cl \rightarrow CH_2Cl + HCl$	$3.2x10^{-11}$	1250±200	$4.8x10^{-13}$	1.2	F72
$Cl + CH_2Cl_2 \rightarrow HCl + CHCl_2$	$3.1x10^{-11}$	1350±500	$3.3x10^{-13}$	1.5	F73
$Cl + CHCl_3 \rightarrow HCl + CCl_3$	$8.2x10^{-12}$	1325±300	$9.6x10^{-14}$	1.3	F74
$Cl + CH_3F \rightarrow HCl + CH_2F$ (HFC-41)	$2.0x10^{-11}$	1200±500	$3.5x10^{-13}$	1.3	F75
$Cl + CH_2F_2 \rightarrow HCl + CHF_2$ (HFC-32)	$1.2x10^{-11}$	1630±500	$5.0x10^{-14}$	1.5	F76
$Cl + CF_3H \rightarrow HCl + CF_3$ (HFC-23)	-	-	$3.0x10^{-18}$	5.0	F77
$Cl + CH_2FCl \rightarrow HCl + CHFCl$ (HCFC-31)	$1.2x10^{-11}$	1390±500	$1.1x10^{-13}$	2.0	F78
$Cl + CHFCl_2 \rightarrow HCl + CFCl_2$ (HCFC-21)	$5.5x10^{-12}$	1675±200	$2.0x10^{-14}$	1.3	F79
$Cl + CHF_2Cl \rightarrow HCl + CF_2Cl$ (HCFC-22)	$5.9x10^{-12}$	2430±200	$1.7x10^{-15}$	1.3	F80
$Cl + CH_3CCl_3 \rightarrow CH_2CCl_3 + HCl$	$2.8x10^{-12}$	1790±400	$7.0x10^{-15}$	2.0	F81
$Cl + CH_3CH_2F \rightarrow HCl + CH_3CHF$ (HFC-161)	$1.8x10^{-11}$	290±500	$6.8x10^{-12}$	3.0	F82
$\rightarrow HCl + CH_2CH_2F$	$1.4x10^{-11}$	880±500	$7.3x10^{-13}$	3.0	F82
$Cl + CH_3CHF_2 \rightarrow HCl + CH_3CF_2$ (HFC-152a)	$6.4x10^{-12}$	950±500	$2.6x10^{-13}$	1.3	F83
$\rightarrow HCl + CH_2CHF_2$	$7.2x10^{-12}$	2390±500	$2.4x10^{-15}$	3.0	F83
$Cl + CH_2FCH_2F \rightarrow HCl + CHFCH_2F$ (HFC-152)	$2.6x10^{-11}$	1060±500	$7.5x10^{-13}$	3.0	F84
$Cl + CH_3CFCl_2 \rightarrow HCl + CH_2CFCl_2$ (HCFC-141b)	$1.8x10^{-12}$	2000±300	$2.2x10^{-15}$	1.2	F85
$Cl + CH_3CF_2Cl \rightarrow HCl + CH_2CF_2Cl$ (HCFC-142b)	$1.4x10^{-12}$	2420±500	$4.2x10^{-16}$	1.2	F86
$Cl + CH_3CF_3 \rightarrow HCl + CH_2CF_3$ (HFC-143a)	$1.2x10^{-11}$	3880±500	$2.6x10^{-17}$	5.0	F87
$Cl + CH_2FCHF_2 \rightarrow HCl + CH_2FCF_2$ (HFC-143)	$5.5x10^{-12}$	1610±500	$2.5x10^{-14}$	3.0	F88
$\rightarrow HCl + CHFCHF_2$	$7.7x10^{-12}$	1720±500	$2.4x10^{-14}$	3.0	F88
$Cl + CH_2ClCF_3 \rightarrow HCl + CHClCF_3$ (HCFC-133a)	$1.8x10^{-12}$	1710±500	$5.9x10^{-15}$	3.0	F89
$Cl + CH_2FCF_3 \rightarrow HCl + CHFCF_3$ (HFC-134a)	-	-	$1.5x10^{-15}$	1.2	F90

Table 1. (Continued)

Reaction	A-Factor[a]	E/R±(ΔE/R)	k(298 K)[a]	f(298)[b]	Notes
$Cl + CHF_2CHF_2 \rightarrow HCl + CF_2CHF_2$ (HCF-134)	$7.5x10^{-12}$	2430±500	$2.2x10^{-15}$	1.5	F91
$Cl + CHCl_2CF_3 \rightarrow HCl + CCl_2CF_3$ (HCFC-123)	$4.4x10^{-12}$	1750±500	$1.2x10^{-14}$	1.3	F92
$Cl + CHFClCF_3 \rightarrow HCl + CFClCF_3$ (HCFC-124)	$1.1x10^{-12}$	1800±500	$2.7x10^{-15}$	1.3	F93
$Cl + CHF_2CF_3 \rightarrow HCl + CF_2CF_3$ (HFC-125)	-	-	$2.4x10^{-16}$	1.3	F94
$Cl + C_2Cl_4 \xrightarrow{M} C_2Cl_5$	(See Table 2)				
$ClO + O_3 \rightarrow ClOO + O_2$	-	-	$<1.4x10^{-17}$	-	F95
$\rightarrow OClO + O_2$	$1.0x10^{-12}$	>4000	$<1.0x10^{-18}$	-	F95
$ClO + H_2 \rightarrow$ products	$\sim 1.0x10^{-12}$	>4800	$<1.0x10^{-19}$	-	F96
$ClO + NO \rightarrow NO_2 + Cl$	$6.4x10^{-12}$	-(290±100)	$1.7x10^{-11}$	1.15	F97
$ClO + NO_2 \xrightarrow{M} ClONO_2$	(See Table 2)				
$ClO + NO_3 \rightarrow ClOO + NO_2$	$4.7x10^{-13}$	0±400	$4.7x10^{-13}$	1.5	F98
$ClO + N_2O \rightarrow$ products	$\sim 1.0x10^{-12}$	>4300	$<6.0x10^{-19}$	-	F99
$ClO + CO \rightarrow$ products	$\sim 1.0x10^{-12}$	>3700	$<4.0x10^{-18}$	-	F100
$ClO + CH_4 \rightarrow$ products	$\sim 1.0x10^{-12}$	>3700	$<4.0x10^{-18}$	-	F101
$ClO + H_2CO \rightarrow$ products	$\sim 1.0x10^{-12}$	>2100	$<1.0x10^{-15}$	-	F102
$ClO + CH_3O_2 \rightarrow$ products	$3.3x10^{-12}$	115±115	$2.2x10^{-12}$	1.5	F103
$ClO + ClO \rightarrow Cl_2 + O_2$	$1.0x10^{-12}$	1590±300	$4.8x10^{-15}$	1.5	F104
$\rightarrow ClOO + Cl$	$3.0x10^{-11}$	2450±500	$8.0x10^{-15}$	1.5	F104
$\rightarrow OClO + Cl$	$3.5x10^{-13}$	1370±300	$3.5x10^{-15}$	1.5	F104
$ClO + ClO \xrightarrow{M} Cl_2O_2$	(See Table 2)				
$ClO + OClO \xrightarrow{M} Cl_2O_3$	(See Table 2)				
$HCl + ClONO_2 \rightarrow$ products	-	-	$<1.0x10^{-20}$	-	F105
$CH_2Cl + O_2 \xrightarrow{M} CH_2ClO_2$	(See Table 2)				
$CHCl_2 + O_2 \xrightarrow{M} CHCl_2O_2$	(See Table 2)				
$CCl_3 + O_2 \xrightarrow{M} CCl_3O_2$	(See Table 2)				

Table 1. (Continued)

Reaction	A-Factor[a]	E/R±(ΔE/R)	k(298 K)[a]	f(298)[b]	Notes
$CFCl_2 + O_2 \xrightarrow{M} CFCl_2O_2$	(See Table 2)				
$CF_2Cl + O_2 \xrightarrow{M} CF_2ClO_2$	(See Table 2)				
$CCl_3O_2 + NO_2 \xrightarrow{M} CCl_3O_2NO_2$	(See Table 2)				
$CFCl_2O_2 + NO_2 \xrightarrow{M} CFCl_2O_2NO_2$	(See Table 2)				
$CF_2ClO_2 + NO_2 \xrightarrow{M} CF_2ClO_2NO_2$	(See Table 2)				
$CH_2ClO + O_2 \rightarrow CHClO + HO_2$	-	-	6×10^{-14}	5	F106
$CH_2ClO_2 + HO_2 \rightarrow CH_2ClO_2H + O_2$	3.3×10^{-13}	-(820±200)	5.2×10^{-12}	1.5	F107
$CH_2ClO_2 + NO \rightarrow CH_2ClO + NO_2$	7×10^{-12}	-(300±200)	1.9×10^{-11}	1.5	F108
$CCl_3O_2 + NO \rightarrow CCl_2O + NO_2 + Cl$	7.3×10^{-12}	-(270±200)	1.8×10^{-11}	1.3	F109
$CCl_2FO_2 + NO \rightarrow CClFO + NO_2 + Cl$	4.5×10^{-12}	-(350±200)	1.5×10^{-11}	1.3	F110
$CClF_2O_2 + NO \rightarrow CF_2O + NO_2 + Cl$	3.8×10^{-12}	-(400±200)	1.5×10^{-11}	1.2	F111
<u>BrO_x Reactions</u>					
$O + BrO \rightarrow Br + O_2$	1.9×10^{-11}	-(230±150)	4.1×10^{-11}	1.5	G 1
$O + HBr \rightarrow OH + Br$	5.8×10^{-12}	1500±200	3.8×10^{-14}	1.3	G 2
$O + HOBr \rightarrow OH + BrO$	1.2×10^{-10}	430±300	2.8×10^{-11}	3.0	G 3
$OH + Br_2 \rightarrow HOBr + Br$	4.2×10^{-11}	0±600	4.2×10^{-11}	1.3	G 4
$OH + BrO \rightarrow$ products	-	-	7.5×10^{-11}	3.0	G 5
$OH + HBr \rightarrow H_2O + Br$	1.1×10^{-11}	0±250	1.1×10^{-11}	1.2	G 6
$OH + CH_3Br \rightarrow CH_2Br + H_2O$	4.0×10^{-12}	1470±150	2.9×10^{-14}	1.1	G 7
$OH + CH_2Br_2 \rightarrow CHBr_2 + H_2O$	2.4×10^{-12}	900±300	1.2×10^{-13}	1.1	G 8
$OH + CHBr_3 \rightarrow CBr_3 + H_2O$	1.6×10^{-12}	710±200	1.5×10^{-13}	2.0	G 9
$OH + CHF_2Br \rightarrow CF_2Br + H_2O$	1.1×10^{-12}	1400±200	1.0×10^{-14}	1.1	G10
$OH + CH_2ClBr \rightarrow CHClBr + H_2O$	2.3×10^{-12}	930±150	1.0×10^{-13}	1.2	G11
$OH + CF_2ClBr \rightarrow$ products	-	-	$<1.5 \times 10^{-16}$	-	G12
$OH + CF_2Br_2 \rightarrow$ products	-	-	$<5.0 \times 10^{-16}$	-	G13
$OH + CF_3Br \rightarrow$ products	-	-	$<1.2 \times 10^{-16}$	-	G14

Table 1. (Continued)

Reaction	A-Factor[a]	E/R±(ΔE/R)	k(298 K)[a]	f(298)[b]	Notes
$OH + CH_2BrCF_3 \rightarrow CHBrCF_3 + H_2O$	1.4×10^{-12}	1340±200	1.6×10^{-14}	1.3	G15
$OH + CHFBrCF_3 \rightarrow CFBrCF_3$	7.2×10^{-13}	1110±150	1.8×10^{-14}	1.5	G16
$OH + CHClBrCF_3 \rightarrow CClBrCF_3 + H_2O$	1.3×10^{-12}	995±150	4.5×10^{-14}	1.5	G17
$OH + CF_2BrCHFCl \rightarrow CF_2BrCFCl + H_2O$	9.3×10^{-13}	1250±150	1.4×10^{-14}	1.5	G18
$OH + CF_2BrCF_2Br \rightarrow$ products	-	-	$<1.5\times10^{-16}$	-	G19
$HO_2 + Br \rightarrow HBr + O_2$	1.5×10^{-11}	600±600	2.0×10^{-12}	2.0	G20
$HO_2 + BrO \rightarrow$ products	3.4×10^{-12}	-(540±200)	2.1×10^{-11}	1.5	G21
$NO_3 + HBr \rightarrow HNO_3 + Br$	-	-	$<1.0\times10^{-16}$	-	G22
$Cl + CH_2ClBr \rightarrow HCl + CHClBr$	4.3×10^{-11}	1370±500	4.3×10^{-13}	3.0	G23
$Cl + CH_3Br \rightarrow HCl + CH_2Br$	1.5×10^{-11}	1060±100	4.3×10^{-13}	1.2	G24
$Cl + CH_2Br_2 \rightarrow HCl + CHBr_2$	6.4×10^{-12}	810±100	4.2×10^{-13}	1.2	G25
$Br + O_3 \rightarrow BrO + O_2$	1.7×10^{-11}	800±200	1.2×10^{-12}	1.2	G26
$Br + H_2O_2 \rightarrow HBr + HO_2$	1.0×10^{-11}	>3000	$<5.0\times10^{-16}$	-	G27
$Br + NO_2 \xrightarrow{M} BrNO_2$	(See Table 2)				
$Br + NO_3 \rightarrow BrO + NO_2$	-	-	1.6×10^{-11}	2.0	G28
$Br + H_2CO \rightarrow HBr + HCO$	1.7×10^{-11}	800±200	1.1×10^{-12}	1.3	G29
$Br + OClO \rightarrow BrO + ClO$	2.6×10^{-11}	1300±300	3.4×10^{-13}	2.0	G30
$Br + Cl_2O \rightarrow BrCl + ClO$	2.1×10^{-11}	470±150	4.3×10^{-12}	1.3	G31
$Br + Cl_2O_2 \rightarrow$ products	-	-	3.0×10^{-12}	2.0	G32
$BrO + O_3 \rightarrow$ products	$\sim1.0\times10^{-12}$	>3200	$<2.0\times10^{-17}$	-	G33
$BrO + NO \rightarrow NO_2 + Br$	8.8×10^{-12}	-(260±130)	2.1×10^{-11}	1.15	G34
$BrO + NO_2 \xrightarrow{M} BrONO_2$	(See Table 2)				
$BrO + NO_3 \rightarrow$ products	-	-	1.0×10^{-12}	3.0	G35
$BrO + ClO \rightarrow Br + OClO$	1.6×10^{-12}	-(430±200)	6.8×10^{-12}	1.25	G36
$\rightarrow Br + ClOO$	2.9×10^{-12}	-(220±200)	6.1×10^{-12}	1.25	G36
$\rightarrow BrCl + O_2$	5.8×10^{-13}	-(170±200)	1.0×10^{-12}	1.25	G36
$BrO + BrO \rightarrow$ products	1.5×10^{-12}	-(230±150)	3.2×10^{-12}	1.15	G37

Table 1. (Continued)

Reaction	A-Factor[a]	E/R±(ΔE/R)	k(298 K)[a]	f(298)[b]	Notes
$CH_2BrO_2 + NO \rightarrow CH_2O + NO_2 + Br$	$4x10^{-12}$	-(300±200)	1.1×10^{-11}	1.5	G38
IO_x Reactions					
$O + I_2 \rightarrow IO + I$	$1.4x10^{-10}$	0±250	$1.4x10^{-10}$	1.4	H 1
$O + IO \rightarrow O_2 + I$			$1.2x10^{-10}$	2.0	H 2
$OH + I_2 \rightarrow HOI + I$			$1.8x10^{-10}$	2.0	H 3
$OH + HI \rightarrow H_2O + I$			$3.0x10^{-11}$	2.0	H 4
$OH + CH_3I \rightarrow H_2O + CH_2I$	$3.1x10^{-12}$	1120±500	$7.2x10^{-14}$	3.0	H 5
$OH + CF_3I \rightarrow HOI + CF_3$			$3.1x10^{-14}$	5.0	H 6
$HO_2 + I \rightarrow HI + O_2$	$1.5x10^{-11}$	1090±500	$3.8x10^{-13}$	2.0	H 7
$HO_2 + IO \rightarrow HOI + O_2$			$8.4x10^{-11}$	1.5	H 8
$NO_3 + HI \rightarrow HNO_3 + I$	(See Note)				H 9
$I + O_3 \rightarrow IO + O_2$	$2.3x10^{-11}$	870±200	$1.2x10^{-12}$	1.2	H10
$I + NO \xrightarrow{M} INO$	(See Table 2)				
$I + NO_2 \xrightarrow{M} INO_2$	(See Table 2)				
$I + BrO \rightarrow IO + Br$	-	-	$1.2x10^{-11}$	2.0	H11
$IO + NO \rightarrow I + NO_2$	$9.1x10^{-12}$	-(240±150)	$2.0x10^{-11}$	1.2	H12
$IO + NO_2 \xrightarrow{M} IONO_2$	(See Table 2)				
$IO + ClO \rightarrow$ products	$5.1x10^{-12}$	-(280±200)	$1.3x10^{-11}$	2.0	H13
$IO + BrO \rightarrow$ products	-	-	$6.9x10^{-11}$	1.5	H14
$IO + IO \rightarrow$ products	$1.5x10^{-11}$	-(500±500)	$8.0x10^{-11}$	1.5	H15
$INO + INO \rightarrow I_2 + 2NO$	$8.4x10^{-11}$	2620±600	$1.3x10^{-14}$	2.5	H16
$INO_2 + INO_2 \rightarrow I_2 + 2NO_2$	$2.9x10^{-11}$	2600±1000	$4.7x10^{-15}$	3.0	H17
SO_x Reactions					
$O + SH \rightarrow SO + H$	-	-	$1.6x10^{-10}$	5.0	I1
$O + CS \rightarrow CO + S$	$2.7x10^{-10}$	760±250	$2.1x10^{-11}$	1.1	I2
$O + H_2S \rightarrow OH + SH$	$9.2x10^{-12}$	1800±550	$2.2x10^{-14}$	1.7	I3

Table 1. (Continued)

Reaction	A-Factor[a]	E/R±(ΔE/R)	k(298 K)[a]	f(298)[b]	Notes
$O + OCS \rightarrow CO + SO$	$2.1x10^{-11}$	2200±150	$1.3x10^{-14}$	1.2	I4
$O + CS_2 \rightarrow CS + SO$	$3.2x10^{-11}$	650±150	$3.6x10^{-12}$	1.2	I5
$O + SO_2 \xrightarrow{M} SO_3$	(See Table 2)				
$O + CH_3SCH_3 \rightarrow CH_3SO + CH_3$	$1.3x10^{-11}$	-(410±100)	$5.0x10^{-11}$	1.1	I6
$O + CH_3SSCH_3 \rightarrow CH_3SO + CH_3S$	$5.5x10^{-11}$	-(250±100)	$1.3x10^{-10}$	1.3	I7
$O_3 + H_2S \rightarrow$ products	-	-	$<2.0x10^{-20}$	-	I8
$O_3 + CH_3SCH_3 \rightarrow$ products	-	-	$<1.0x10^{-18}$	-	I9
$O_3 + SO_2 \rightarrow SO_3 + O_2$	$3.0x10^{-12}$	>7000	$<2.0x10^{-22}$	-	I10
$OH + H_2S \rightarrow SH + H_2O$	$6.0x10^{-12}$	75±75	$4.7x10^{-12}$	1.2	I11
$OH + OCS \rightarrow$ products	$1.1x10^{-13}$	1200±500	$1.9x10^{-15}$	2.0	I12
$OH + CS_2 \rightarrow$ products	(See Note)	-	-	-	I13
$OH + CH_3SH \rightarrow CH_3S + H_2O$	$9.9x10^{-12}$	-(360±100)	$3.3x10^{-11}$	1.2	I14
$OH + CH_3SCH_3 \rightarrow H_2O + CH_2SCH_3$	$1.2x10^{-11}$	260±100	$5.0x10^{-12}$	1.15	I15
$OH + CH_3SSCH_3 \rightarrow$ products	$6.0x10^{-11}$	-(400±200)	$2.3x10^{-10}$	1.2	I16
$OH + S \rightarrow H + SO$	-	-	$6.6x10^{-11}$	3.0	I17
$OH + SO \rightarrow H + SO_2$	-	-	$8.6x10^{-11}$	2.0	I18
$OH + SO_2 \xrightarrow{M} HOSO_2$	(See Table 2)				
$HO_2 + H_2S \rightarrow$ products	-	-	$<3.0x10^{-15}$	-	I19
$HO_2 + CH_3SH \rightarrow$ products	-	-	$<4.0x10^{-15}$	-	I19
$HO_2 + CH_3SCH_3 \rightarrow$ products	-	-	$<5.0x10^{-15}$	-	I19
$HO_2 + SO_2 \rightarrow$ products	-	-	$<1.0x10^{-18}$	-	I20
$NO_2 + SO_2 \rightarrow$ products	-	-	$<2.0x10^{-26}$	-	I21
$NO_3 + H_2S \rightarrow$ products	-	-	$<8.0x10^{-16}$	-	I22
$NO_3 + OCS \rightarrow$ products	-	-	$<1.0x10^{-16}$	-	I23
$NO_3 + CS_2 \rightarrow$ products	-	-	$<4.0x10^{-16}$	-	I24
$NO_3 + CH_3SH \rightarrow$ products	$4.4x10^{-13}$	-(210±210)	$8.9x10^{-13}$	1.25	I25
$NO_3 + CH_3SCH_3 \rightarrow CH_3SCH_2 + HNO_3$	$1.9x10^{-13}$	-(500±200)	$1.0x10^{-12}$	1.2	I26

Table 1. (Continued)

Reaction	A-Factor[a]	E/R±(ΔE/R)	k(298 K)[a]	f(298)[b]	Notes
$NO_3 + CH_3SSCH_3 \rightarrow$ products	$1.3x10^{-12}$	270±270	$5.3x10^{-13}$	1.4	I27
$NO_3 + SO_2 \rightarrow$ products	-	-	$<7.0x10^{-21}$	-	I28
$N_2O_5 + CH_3SCH_3 \rightarrow$ products	-	-	$<1.0x10^{-17}$	-	I29
$CH_3O_2 + SO_2 \rightarrow$ products	-	-	$<5.0x10^{-17}$	-	I30
$F + CH_3SCH_3 \rightarrow$ products	-	-	$2.4.x10^{-10}$	2.0	I31
$Cl + H_2S \rightarrow HCl + SH$	$3.7x10^{-11}$	-(210±100)	$7.4x10^{-11}$	1.25	I32
$Cl + OCS \rightarrow$ products	-	-	$<1.0x10^{-16}$	-	I33
$Cl + CS_2 \rightarrow$ products	-	-	$<4.0x10^{-15}$	-	I34
$Cl + CH_3SH \rightarrow CH_3S + HCl$	$1.2x10^{-10}$	-(150±50)	$2.0x10^{-10}$	1.25	I35
$Cl + CH_3SCH_3 \rightarrow$ products	(See Note)	-	-	-	I36
$ClO + OCS \rightarrow$ products	-	-	$<2.0x10^{-16}$	-	I37
$ClO + CH_3SCH_3 \rightarrow$ products	-	-	$9.5x10^{-15}$	2.0	I38
$ClO + SO \rightarrow Cl + SO_2$	$2.8x10^{-11}$	0±50	$2.8x10^{-11}$	1.3	I39
$ClO + SO_2 \rightarrow Cl + SO_3$	-	-	$<4.0x10^{-18}$	-	I37
$Br + H_2S \rightarrow HBr + SH$	$1.4x10^{-11}$	2750±300	$1.4x10^{-15}$	2.0	I40
$Br + CH_3SH \rightarrow CH_3S + HBr$	$9.2x10^{-12}$	390±100	$2.5x10^{-12}$	2.0	I40
$Br + CH_3SCH_3 \rightarrow$ products	(See Note)				I41
$BrO + CH_3SCH_3 \rightarrow$ products	$1.5x10^{-14}$	-(850±200)	$2.6x10^{-13}$	1.3	I42
$BrO + SO \rightarrow Br + SO_2$			$5.7x10^{-11}$	1.4	I43
$IO + CH_3SH \rightarrow$ products			$6.6x10^{-16}$	2.0	I44
$IO + CH_3SCH_3 \rightarrow$ products			$1.2x10^{-14}$	1.5	I45
$S + O_2 \rightarrow SO + O$	$2.3x10^{-12}$	0±200	$2.3x10^{-12}$	1.2	I46
$S + O_3 \rightarrow SO + O_2$			$1.2x10^{-11}$	2.0	I47
$SO + O_2 \rightarrow SO_2 + O$	$2.6x10^{-13}$	2400±500	$8.4x10^{-17}$	2.0	I48
$SO + O_3 \rightarrow SO_2 + O_2$	$3.6x10^{-12}$	1100±200	$9.0x10^{-14}$	1.2	I49
$SO + NO_2 \rightarrow SO_2 + NO$	$1.4x10^{-11}$	0±50	$1.4x10^{-11}$	1.2	I50
$SO + OClO \rightarrow SO_2 + ClO$			$1.9x10^{-12}$	3.0	I51
$SO_3 + H_2O \rightarrow$ products	(See Note)		-	-	I52

Table 1. (Continued)

Reaction	A-Factor[a]	E/R±(ΔE/R)	k(298 K)[a]	f(298)[b]	Notes
$SO_3 + NH_3 \rightarrow$ products	(See Table 2)		-	-	
$SO_3 + NO_2 \rightarrow$ products			1.0×10^{-19}	10.0	I53
$SH + O_2 \rightarrow OH + SO$			$<4.0 \times 10^{-19}$	-	I54
$SH + O_3 \rightarrow HSO + O_2$	9.0×10^{-12}	280±200	3.5×10^{-12}	1.3	I55
$SH + H_2O_2 \rightarrow$ products			$<5.0 \times 10^{-15}$	-	I56
$SH + NO \xrightarrow{M} HSNO$	(See Table 2)				
$SH + NO_2 \rightarrow HSO + NO$	2.9×10^{-11}	-(240±50)	6.5×10^{-11}	1.2	I57
$SH + Cl_2 \rightarrow ClSH + Cl$	1.7×10^{-11}	690±200	1.7×10^{-12}	2.0	I58
$SH + BrCl \rightarrow$ products	2.3×10^{-11}	-(350±200)	7.4×10^{-11}	2.0	I58
$SH + Br_2 \rightarrow BrSH + Br$	6.0×10^{-11}	-(160±160)	1.0×10^{-10}	2.0	I58
$SH + F_2 \rightarrow FSH + F$	4.3×10^{-11}	1390±200	4.0×10^{-13}	2.0	I58
$HSO + O_2 \rightarrow$ products			$<2.0 \times 10^{-17}$	-	I59
$HSO + O_3 \rightarrow$ products			1.0×10^{-13}	1.3	I60
$HSO + NO \rightarrow$ products			$<1.0 \times 10^{-15}$	-	I61
$HSO + NO_2 \rightarrow HSO_2 + NO$			9.6×10^{-12}	2.0	I61
$HSO_2 + O_2 \rightarrow HO_2 + SO_2$			3.0×10^{-13}	3.0	I62
$HOSO_2 + O_2 \rightarrow HO_2 + SO_3$	1.3×10^{-12}	330±200	4.4×10^{-13}	1.2	I63
$CS + O_2 \rightarrow OCS + O$			2.9×10^{-19}	2.0	I64
$CS + O_3 \rightarrow OCS + O_2$			3.0×10^{-16}	3.0	I65
$CS + NO_2 \rightarrow OCS + NO$			7.6×10^{-17}	3.0	I65
$CH_3S + O_2 \rightarrow$ products			$<3.0 \times 10^{-18}$	-	I66
$CH_3S + O_3 \rightarrow$ products	2.0×10^{-12}	-(290±100)	5.3×10^{-12}	1.15	I67
$CH_3S + NO \rightarrow$ products			$<1.0 \times 10^{-13}$	-	I68
$CH_3S + NO \xrightarrow{M}$ products	(See Table 2)				
$CH_3S + NO_2 \rightarrow CH_3SO + NO$	2.1×10^{-11}	-(320±100)	6.1×10^{-11}	1.15	I69
$CH_2SH + O_2 \rightarrow$ products			6.5×10^{-12}	2.0	I70
$CH_2SH + O_3 \rightarrow$ products			3.5×10^{-11}	2.0	I71

Table 1. (Continued)

Reaction	A-Factor[a]	E/R±(ΔE/R)	k(298 K)[a]	f(298)[b]	Notes
$CH_2SH + NO \rightarrow$ products			$1.9x10^{-11}$	2.0	I72
$CH_2SH + NO_2 \rightarrow$ products			$5.2x10^{-11}$	2.0	I73
$CH_3SO + O_3 \rightarrow$ products			$6.0x10^{-13}$	1.5	I74
$CH_3SO + NO_2 \rightarrow CH_3SO_2 + NO$			$1.2x10^{-11}$	1.4	I75
$CH_3SOO + O_3 \rightarrow$ products			$<8.0x10^{-13}$	-	I76
$CH_3SOO + NO \rightarrow$ products	$1.1x10^{-11}$	0±100	$1.1x10^{-11}$	2.0	I76
$CH_3SO_2 + NO_2 \rightarrow$ products	$2.2x10^{-11}$	0±100	$2.2x10^{-11}$	2.0	I77
$CH_3SCH_2 + O_2 \overset{M}{\rightarrow} CH_3SCH_2O_2$	(See Table 2)				
$CH_3SCH_2 + NO_3 \rightarrow$ products			3.0×10^{-10}	2.0	I78
$CH_3SCH_2O_2 + NO \rightarrow CH_3SCH_2O + NO_2$			1.9×10^{-11}	2.0	I79
$CH_3SS + O_3 \rightarrow$ products			$4.6x10^{-13}$	2.0	I80
$CH_3SS + NO_2 \rightarrow$ products			$1.8x10^{-11}$	2.0	I81
$CH_3SSO + NO_2 \rightarrow$ products			$4.5x10^{-12}$	2.0	I81
Metal Reactions					
$Na + O_2 \overset{M}{\rightarrow} NaO_2$	(See Table 2)				
$Na + O_3 \rightarrow NaO + O_2$	$1.0x10^{-9}$	95±50	$7.3x10^{-10}$	1.2	J 1
$\rightarrow NaO_2 + O$	-	-	$<4.0x10^{-11}$	-	J 1
$Na + N_2O \rightarrow NaO + N_2$	$2.8x10^{-10}$	1600±400	$1.3x10^{-12}$	1.2	J 2
$Na + Cl_2 \rightarrow NaCl + Cl$	$7.3x10^{-10}$	0±200	$7.3x10^{-10}$	1.3	J 3
$NaO + O \rightarrow Na + O_2$	$3.7x10^{-10}$	0±400	$3.7x10^{-10}$	3.0	J 4
$NaO + O_2 \overset{M}{\rightarrow} NaO_3$	(See Table 2)				
$NaO + O_3 \rightarrow NaO_2 + O_2$	$1.1x10^{-9}$	570±300	$1.6x10^{-10}$	1.5	J 5
$\rightarrow Na + 2O_2$	$6.0x10^{-11}$	0±800	$6.0x10^{-11}$	3.0	J 5
$NaO + H_2 \rightarrow NaOH + H$	$2.6x10^{-11}$	0±600	$2.6x10^{-11}$	2.0	J 6
$NaO + H_2O \rightarrow NaOH + OH$	$2.2x10^{-10}$	0±400	$2.2x10^{-10}$	2.0	J 7
$NaO + NO \rightarrow Na + NO_2$	$1.5x10^{-10}$	0±400	$1.5x10^{-10}$	4.0	J 8

Table 1. (Continued)

Reaction	A-Factor[a]	E/R±(ΔE/R)	k(298 K)[a]	f(298)[b]	Notes
$NaO + CO_2 \xrightarrow{M} NaCO_3$	(See Table 2)				
$NaO + HCl \rightarrow$ products	2.8×10^{-10}	0±400	2.8×10^{-10}	3.0	J 9
$NaO_2 + O \rightarrow NaO + O_2$	2.2×10^{-11}	0±600	2.2×10^{-11}	5.0	J10
$NaO_2 + NO \rightarrow NaO + NO_2$	-	-	$<10^{-14}$	-	J11
$NaO_2 + HCl \rightarrow$ products	2.3×10^{-10}	0±400	2.3×10^{-10}	3.0	J12
$NaOH + HCl \rightarrow NaCl + H_2O$	2.8×10^{-10}	0±400	2.8×10^{-10}	3.0	J13
$NaOH + CO_2 \xrightarrow{M} NaHCO_3$	(See Table 2)				

Shaded areas indicate changes or additions since JPL 94-26.

a Units are cm^3/molecule-s.

b f(298) is the uncertainty factor at 298 K. To calculate the uncertainty at other temperatures, use the expression:

$$f(T) = f(298) \exp \left| \frac{\Delta E}{R} \left(\frac{1}{T} - \frac{1}{298} \right) \right|$$

Note that the exponent is absolute value.

Notes to Table 1

A1. $O + O_3$. The recommended rate expression is from Wine et al. [1260] and is a linear least squares fit of all data (unweighted) from Davis et al. [313], McCrumb and Kaufman [772], West et al. [1239], Arnold and Comes [29], and Wine et al. [1260].

A2. $O(^1D)$ Reactions. The rate constants are for the disappearance of $O(^1D)$, which includes physical quenching or deactivation. Where information is available, product yields are given. The rate constant recommendations are based on averages of the absolute rate constant measurements reported by Streit et al. [1088], Davidson et al. [306] and Davidson et al. [305] for N_2O, H_2O, CH_4, H_2, N_2, O_2, O_3, CCl_4, $CFCl_3$, CF_2Cl_2, NH_3, and CO_2; by Amimoto et al. [17], Amimoto et al. [16], and Force and Wiesenfeld [392, 393] for N_2O, H_2O, CH_4, N_2, H_2, O_2, O_3, CO_2, CCl_4, $CFCl_3$, CF_2Cl_2, and CF_4; by Wine and Ravishankara [1261-1263] for N_2O, H_2O, N_2, H_2, O_3, CO_2 and CF_2O; by Brock and Watson (private communication, 1980) for N_2, O_2 and CO_2; by Lee and Slanger [677, 678] for H_2O and O_2; by Gericke and Comes [414] for H_2O; and by Shi and Barker [1020] for N_2 and CO_2, and Talukdar and Ravishankara [1120] for H_2. The weight of the evidence from these studies indicates that the results of Heidner and Husain [475], Heidner et al. [476] and Fletcher and Husain [386, 387] contain a systematic error. For the critical atmospheric reactants, such as N_2O, H_2O, and CH_4, the recommended absolute rate constants are in good agreement with the previous relative measurements when compared with N_2 as the reference reactant. A similar comparison with O_2 as the reference reactant gives somewhat poorer agreement.

A3. $O(^1D) + O_2$. The deactivation of $O(^1D)$ by O_2 leads to the production of $O_2(^1\Sigma)$ with an efficiency of 80±20%: Noxon [873], Biedenkapp and Bair [112], Snelling [1061], and Lee and Slanger [677]. The $O_2(^1\Sigma)$ is produced in the v=0, 1, and 2 vibrational levels in the amounts 60%, 40%, and <3%, Gauthier and Snelling [411] and Lee and Slanger [677].

A4. $O(^1D) + O_3$. The branching result for reaction of $O(^1D)$ with O_3 to give $O_2 + O_2$ or $O_2 + O + O$ is from Davenport et al. [300]. This is supported by measurements of Amimoto et al. [17] who reported that on average one ground state O is produced per $O(^1D)$ reaction with O_3. It seems unlikely that this could result from 100% quenching of the $O(^1D)$ by O_3.

A5. $O(^1D) + H_2$. Wine and Ravishankara [1262] have determined the yield of $O(^3P)$ is <4.9%. The major products are H + OH. Koppe et al. [628] report a 2.7 times larger rate coefficient at a kinetic energy of 0.12eV. This does not agree with the observations of Davidson et al. [306], who reported that k is independent of temperature (200-350K) and Matsumi et al. [767] who report no change in k when hot $O(^1D)$ is moderated with Ar.

A6. $O(^1D) + H_2O$. Measurements of the $O_2 + H_2$ product yield were made by Zellner et al. [1301] (1 +0.5 or -1)% and by Glinski and Birks [428] (0.6 +0.7 or -0.6)%. That the yield of $O(^3P)$ from $O(^1D) + H_2O$ is reported to be <(4.9±3.2)% by Wine and Ravishankara [1722] and (2±1)% by Takahashi et al. [1109].

A7. $O(^1D) + N_2O$. The branching ratio for the reaction of $O(^1D)$ with N_2O to give $N_2 + O_2$ or NO + NO is an average of the values reported by Davidson et al. [303]; Volltrauer et al. [1185]; Marx et al. [765] and Lam et al. [654], with a spread in R=k(NO + NO)/k(Total) = 0.52 - 0.62. Cantrell et al. [185] reported a measurement of R=0.57 and an analysis of all measurements from 1957-1994 leads them to recommend a value of R=0.61±0.06, where the uncertainty indicates their 95% confidence interval. The recommended branching ratio agrees well with earlier measurements of the quantum yield from N_2O photolysis (Calvert and Pitts [177]). The $O(^1D)$ translational energy and temperature dependence effects are not clearly resolved. Wine and Ravishankara [1262] have determined that the yield of $O(^3P)$ from $O(^1D) + N_2O$ is <4.0%. The uncertainty for this reaction includes factors for both the overall rate coefficient and the branching ratio. A direct measurement by Greenblatt and Ravishankara [437] of the NO yield from the $O(^1D) + N_2O$ reaction in the presence of airlike mixtures agrees very well with the value predicted using the recommended $O(^1D)$ rate constants for N_2, O_2, and N_2O and the $O(^1D) + N_2O$ product branching ratio. These authors suggest that their results support the recommendations and reduce the uncertainty in the collected rate parameters by over a factor of two.

A8. $O(^1D) + NH_3$. Sanders et al. [991] have detected the products $NH(a^1\Delta)$ and OH formed in the reaction. They report that the yield of $NH(a^1\Delta)$ is in the range 3-15% of the amount of OH detected.

A9. $O(^1D) + CH_4$. The reaction products are (a) $CH_3 + OH$, (b) CH_3O or $CH_2OH + H$ and (c) $CH_2O + H_2$. Lin and DeMore [718] analyzed the final products of N_2O/CH_4 photolysis mixtures and concluded that (a) accounted for about 90% and that CH_2O and H_2 (c) accounted for about 9%. Addison et al. [8] reported an OH yield of 80%. Casavecchia et al. [189] used a molecular beam experiment to observe H and CH_3O (or CH_2OH) products. They reported that the yield of H_2 was <25% of the yield of H from (b). Satyapal et al. [996] observed the production of H atoms in a pulsed laser experiment and reported a yield of H of (25±8)%. Matsumi et al. [767] measured the yields of H and $O(^3P)$ in low pressure gas mixtures and reported the yield of H was (15±3)% and the yield of $O(^3P)$ was <5%. Wine and Ravishankara [1262] reported that the yield of $O(^3P)$ was <4.3%. Takahashi et al. [1109] reported that the $O(^3P)$ yield is <1%. We recommend the following branching ratios: (a) (75±15)%, (b) (20±7)%, (c) (5±5)%.

A10. $O(^1D) + HCl$. The recommendation is the average of measurements by Davidson et al. [306] and Wine et al. [1270]. Product studies by the latter indicate: $O(^3P) + HCl$ (9±5)%; $H + ClO$ (24±5)%; and $OH + Cl$ (67±10)%. Takahashi et al. [1109] report the $O(^3P)$ yield is (15±4)%.

A11. $O(^1D) + HF$. Rate coefficient and product yield measured by Wine et al. (1984, private communication). The $O(^3P)$ yield is less than 4%.

A12. $O(^1D) + HBr$. Rate coefficient and products measured by Wine et al. [1270]. Product yields: $HBr + O(^3P)$ (20±7)%, $H + BrO$ <4.5%, and $OH + Br$ (80±12)%.

A13. $O(^1D) + Cl_2$. Rate coefficient and $O(^3P)$ product were measured by Wine et al. [1258], who reported $Cl_2 + O(^3P)$ (25±10)%. Takahashi et al. [1109] reported that the ClO yield is (74±15)%, in excellent agreement. An indirect study by Freudenstein and Biedenkapp [396] is in reasonable agreement on the yield of ClO.

A14. $O(^1D) + COCl_2$, COClF and COF_2. For the reactions of $O(^1D)$ with $COCl_2$ and COClF the recommended rate constants are derived from data of Fletcher and Husain [388]. For consistency, the recommended values for these rate constants were derived using a scaling factor (0.5) which corrects for the difference between rate constants from the Husain laboratory and the recommendations for other $O(^1D)$ rate constants in this table. The recommendation for COF_2 is from the data of Wine and Ravishankara [1263]. Their result is preferred over the value of Fletcher and Husain [388] because it appears to follow the pattern of decreased reactivity with increased fluorine substitution observed for other halocarbons. These reactions have been studied only at 298 K. Based on consideration of similar $O(^1D)$ reactions, it is assumed that E/R equals zero, and therefore the value shown for the A-factor has been set equal to k(298 K).

A15. $O(^1D)$ + halocarbons. The halocarbon rate constants are for the total disappearance of $O(^1D)$ and probably include physical quenching. Products of the reactive channels may include $CX_3O + X$, $CX_2O + X_2$ (or 2X), and $CX_3 + XO$, where X = H, F, Cl, or Br in various combinations. Bromine, chlorine and hydrogen are more easily displaced than fluorine from halocarbons. Some values have been reported for the fractions of the total rate of disappearance of $O(^1D)$ proceeding through physical quenching and reactive channels. For CCl_4: quenching = (14±6)% and reaction = (86±6)% (Force and Wiesenfeld [393]), ClO yield = (90±19)% (Takahashi et al. [1109]; for $CFCl_3$: quenching = (25±10)%, ClO formation = (60±15)% (Donovan, private communication, 1980), ClO yield = (88±18)% (Takahashi et al.); for CF_2Cl_2: quenching = (14±7)% and reaction = (86±14)% (Force and Wiesenfeld [393]), quenching = (20±10)%, ClO formation = (55±15)% (Donovan), quenching =(19±5)% and ClO formation =(87±18%) (Takahashi et al.)

A16. $O(^1D) + CH_3Br$. The recommendation is based on data from Thompson and Ravishankara [1127]. They report that the yield of $O(^3P)$ from physical quenching is 0±7%.

A17. $O(^1D) + CH_2Br_2$. The recommendation is based on data from Thompson and Ravishankara [1127]. They report that the yield of $O(^3P)$ from physical quenching is (5±7)%.

A18. $O(^1D) + CHBr_3$. The recommendation is based on data from Thompson and Ravishankara [1127]. The rate coefficient is somewhat large compared to analogous compounds. They report that the yield of $O(^3P)$ from physical quenching is (32±8)%.

A19. $O(^1D) + CH_3F$ (HFC-41). The recommendation is the average of measurements of Force and Wiesenfeld [393] and Schmoltner et al. [1005]. The $O(^3P)$ product yield was reported to be (25±3)% by Force and Wiesenfeld, (11±5)% by Schmoltner et al., and (19±5)% by Takahashi et al. [1109]. Burks and Lin [163] reported observing vibrationally excited HF as a product. Park and Wiesenfeld [895] observed OH.

A20. $O(^1D) + CH_2F_2$ (HFC-32). The recommendation is based upon the measurement of Schmoltner et al. [1005], who reported that the yield of $O(^3P)$ is (70±11)%. Green and Wayne [435] measured the loss of CH_2F_2 relative to the loss of N_2O. Their value when combined with our recommendation for $O(^1D) + N_2O$ yields a rate coefficient for reactive loss of CH_2F_2 that is about three times the result of Schmoltner et al. Burks and Lin [163] reported observing vibrationally excited HF as a product.

A21. $O(^1D) + CHF_3$ (HFC-23). The recommendation is the average of measurements of Force and Wiesenfeld [393] and Schmoltner et al. [1005]. The $O(^3P)$ product yield was reported to be (77±15)% by Force and Wiesenfeld and (102±3)% by Schmoltner et al. Although physical quenching is the dominant process, detectable yields of vibrationally excited HF have been reported by Burks and Lin [163] and Aker et al. [14], which indicate the formation of $HF + CF_2O$ products.

A22. $O(^1D) + CHCl_2F$ (HCFC-21). The recommendation is based upon the measurement by Davidson et al. [305] of the total rate coefficient (physical quenching and reaction). Takahashi et al. [1109] report the yield of ClO is (74±15)%.

A23. $O(^1D) + CHClF_2$ (HCFC-22). The recommendation is based upon the measurements by Davidson et al. [305] and Warren et al. [1222] of the total rate coefficient. A measurement of the rate of reaction (halocarbon removal) relative to the rate of reaction with N_2O by Green and Wayne [435] agrees very well with this value when the $O(^1D) + N_2O$ recommendation is used to obtain an absolute value. A relative measurement by Atkinson et al. [39] gives a rate coefficient about a factor of two higher. Addison et al. [8] reported the following product yields: ClO (55±10)%, CF_2 (45±10)%, $O(^3P)$ (28 +10 or -15)%, and OH 5%, where the $O(^3P)$ comes from a branch yielding CF_2 and HCl. Warren et al. [1222] also report a yield of $O(^3P)$ of (28±6)%, which they interpret as the product of physical quenching.

A24. $O(^1D) + CClF_3$ (CFC-13). The recommendation is based on the measurement by Ravishankara et al.[951] who report (31±10)% physical quenching. Takahashi et al. [1109] report the yields of $O(^3P)$ (16±5)% and ClO (85±18)%.

A25. $O(^1D) + CClBrF_2$ (Halon 1211). The recommendation is based on data from Thompson and Ravishankara [1127]. They report that the yield of $O(^3P)$ from physical quenching is (36±4)%.

A26. $O(^1D) + CBr_2F_2$ (Halon 1202). The recommendation is based on data from Thompson and Ravishankara [1127]. They report that the yield of $O(^3P)$ from physical quenching is (54±6)%.

A27. $O(^1D) + CBrF_3$ (Halon 1301). The recommendation is based on data from Thompson and Ravishankara [1127]. They report that the yield of $O(^3P)$ from physical quenching is (59±8)%. Lorenzen-Schmidt et al. [728] measured the Halon removal rate relative to the N_2O removal rate and report that the rate coefficient for the Halon destruction path is $(4.0\pm0.4)\times10^{-11}$, which is in excellent agreement with Thompson and Ravishankara.

A28. $O(^1D) + CF_4$ (CFC-14). The recommendation is based upon the measurement by Ravishankara et al. [951], who report (92±8)% physical quenching. Force and Wiesenfeld [393] measured a quenching rate coefficient about 10 times larger. Shi and Barker [1020] report an upper limit that is consistent with the recommendation. The small rate coefficient for this reaction makes it vulnerable to interference from reactant impurities. For this reason the recommendation should probably be considered an upper limit.

A29. $O(^1D) + CH_3CH_2F$ (HFC 161). The recommendation is based on data from Schmoltner et al. [1005]. They report that the yield of $O(^3P)$ from physical quenching is (18±5)%.

A30. $O(^1D) + CH_3CHF_2$ (HFC-152a). The recommendation is based on the measurements of Warren et al. [1222], who report (54±7)% physical quenching.

A31. $O(^1D) + CH_3CCl_2F$ (HCFC-141b). The recommendation is based upon the measurement of Warren et al. [1222], who report (31±5)% physical quenching.

A32. $O(^1D) + CH_3CClF_2$ (HCFC-142b). The recommendation is based upon the measurement of Warren et al. [1222], who report (26±5)% physical quenching. This agrees very well with Green and Wayne [435], who measured the loss of CH_3CF_2Cl relative to the loss of N_2O, when the recommendation for N_2O is used.

A33. $O(^1D) + CH_3CF_3$ (HFC-143a). The recommendation is based upon the relative rate measurement of Green and Wayne [435], who measured the loss of CH_3CF_3 relative to the loss of N_2O. The recommendation for N_2O is used to obtain the value given. It is assumed that there is no physical quenching, although the reported physical quenching by CH_2FCF_3 and CH_3CHF_2 suggests some quenching is possible.

A34. $O(^1D) + CH_2ClCClF_2$ (HCFC-132b). The recommendation is based upon the relative rate measurement of Green and Wayne [435], who measured the loss of CH_2ClCF_2Cl relative to the loss of N_2O. The recommendation for N_2O is used to obtain the value given. It is assumed that there is no physical quenching.

A35. $O(^1D) + CH_2ClCF_3$ (HCFC-133a). The recommendation is based upon the measurement of Warren et al. [1222], who report (20±5)% physical quenching. This agrees with Green and Wayne [435] who measured the loss of CH_2ClCF_3 relative to the loss of N_2O, when the recommendation for N_2O is used.

A36. $O(^1D) + CH_2FCF_3$ (HFC-134a). The recommendation is based on the measurement of Warren et al. [1222] who report (94+6/-1)% physical quenching. The predominance of physical quenching is surprising, considering the presence of C-H bonds, which are usually reactive toward $O(^1D)$.

A37. $O(^1D) + CHCl_2CF_3$ (HCFC-123). The recommendation is based upon measurements by Warren et al. [1222]. The relative rate measurement of Green and Wayne [435], who measured the loss of $CHCl_2CF_3$ relative to the loss of N_2O, agrees well with the recommendation when the recommendation for N_2O is used. Warren et al. report (21±8)% physical quenching.

A38. $O(^1D) + CHClFCF_3$ (HCFC-124). The recommendation is based upon the measurement of Warren et al. [1222], who report (31±10)% physical quenching.

A39. $O(^1D) + CHF_2CF_3$ (HFC-125). The recommendation is based upon the measurement of Warren et al. [1222], who report (85+15/-22)% physical quenching. Green and Wayne [435] measured the loss of CHF_2CF_3 relative to the loss of N_2O and report a loss corresponding to about 40% of the recommended rate coefficient. This reaction is much faster than one would predict by analogy to similar compounds, such as CH_2FCF_3.

A40. $O(^1D) + CCl_3CF_3$ (CFC-113a). The recommendation is an estimate based on analogy to similar compounds.

A41. $O(^1D) + CCl_2FCClF_2$ (CFC-113). The recommendation is an estimate based on analogy to similar compounds.

A42. $O(^1D) + CCl_2FCF_3$ (CFC-114a). The recommendation is an estimate based on analogy to similar compounds.

A43. $O(^1D) + CClF_2CClF_2$ (CFC-114). The recommendation is based on the measurement by Ravishankara et al. [951], who report (25±9)% physical quenching.

A44. $O(^1D) + CClF_2CF_3$ (CFC-115). The recommendation is based on the measurement by Ravishankara et al.[951], who report (70±7)% physical quenching.

A45. $O(^1D) + CBrF_2CBrF_2$ (Halon 2402). The recommendation is based on data from Thompson and Ravishankara [1127]. They report that the yield of $O(^3P)$ from physical quenching is (25±7)%. Lorenzen-Schmidt et al. [728] measured the Halon removal rate relative to the N_2O removal rate and report that the rate coefficient for the Halon destruction path is $(8.8\pm1.2)\times10^{-11}$, in fair agreement with the result of Thompson and Ravishankara.

A46. $O(^1D) + C_2F_6$ (CFC-116). The recommendation is based on a measurement by Ravishankara et al. [951], who report (85±15)% physical quenching. The small rate coefficient for this reaction makes it vulnerable to interference from reactant impurities. For this reason the recommendation should probably be considered an upper limit.

A47. $O(^1D) + CHF_2CF_2CF_2CHF_2$ (HFC 338 pcc). The recommendation is based on data from Schmoltner et al. [1005]. They report that the yield of $O(^3P)$ from physical quenching is (97±9)%.

A48. $O(^1D) + c\text{-}C_4F_8$. The recommendation for perfluorocyclobutane is based upon the measurement by Ravishankara et al. [951], who report (100+0/-15)% physical quenching. The small rate coefficient for this reaction makes it vulnerable to interference from reactant impurities. For this reason the recommendation should probably be considered an upper limit.

A49. $O(^1D) + CF_3CHFCHFCF_2CF_3$ (HFC 43-10 mee). The recommendation is based on data from Schmoltner et al. [1005]. The rate coefficients for this compound and CHF_2CF_3 do not follow the reactivity trend of other HFCs. Schmoltner et al. report that the yield of $O(^3P)$ from physical quenching is (91±4)%.

A50. $O(^1D) + C_5F_{12}$ (CFC 41-12). The recommendation is based on data from Ravishankara et al. [951]. They report that the yield of $O(^3P)$ from physical quenching is (79±12)%.

A51. $O(^1D) + C_6F_{14}$ (CFC 51-14). The recommendation is based on data from Ravishankara et al. [951]. They report that the yield of $O(^3P)$ from physical quenching is (75±9)%.

A52. $O(^1D) + 1,2\text{-}(CF_3)_2c\text{-}C_4F_6$. The recommendation is based on data from Ravishankara et al. [951]. They report that the yield of $O(^3P)$ from physical quenching is (84±16)%.

A53. $O(^1D) + SF_6$. The recommendation is based upon measurements by Ravishankara et al. [951] who report (32±10)% physical quenching. The small rate coefficient for this reaction makes it vulnerable to interference from reactant impurities. For this reason the recommendation should probably be considered an upper limit.

A54. $O_2(^1\Delta) + O$. The recommendation is based on the upper limit reported by Clark and Wayne [219].

A55. $O_2(^1\Delta) + O_2$. The recommendation is the average of eight room temperature measurements: Steer et al. [1073], Findlay and Snelling [379], Borrell et al. [131], Leiss et al. [682], Tachibana and Phelps [1103], Billington and Borrell [118], Raja et al. [942], and Wildt et al. [1251]. The temperature dependence is derived from the data of Findlay and Snelling and Billington and Borrell. Several other less direct measurements of the rate coefficient agree with the recommendation, including Clark and Wayne [218], Findlay et al. [378], and McLaren et al. [774]. Wildt et al. [1252] report observations of weak emissions in the near IR due to collision-induced radiation. Wildt et al. [1253] give rate coefficients for this process.

A56. $O_2(^1\Delta) + O_3$. The recommendation is the average of the room temperature measurements of Clark et al. [217], Findlay and Snelling [380], Becker et al. [92], and Collins et al. [256]. Several less direct measurements agree well with the recommendation (McNeal and Cook [775], Wayne and Pitts [1235], and Arnold and Comes [30]). The temperature dependence is from Findlay and Snelling and Becker et al., who agree very well, although both covered a relatively small temperature range. An earlier study by Clark et al. covered a much larger range, and found a much smaller temperature coefficient. The reason for this discrepancy is not clear. The yield of $O + 2O_2$ products appears to be close to unity, based on many studies of the quantum yield of O_3 destruction near the peak of the Hartley band. For example, measurements of the number of O_3 molecules destroyed per photon absorbed: Von Ellenrieder et al. [1186], Ravishankara et al. [957], Lissi and Heicklen [722], and references cited therein and measurements of O_3 loss and O atom temporal profiles in pulsed experiments Klais et al. [614] and Arnold and Comes [30]. Anderson et al. [26] report that the rate coefficient for atom exchange between $O_2(^1\Delta)$ and O_3 is $< 5x10^{-16}$ at 300K.

A57. $O_2(^1\Delta) + H_2O$. The recommendation is the average of the measurements reported by Becker et al. [91] and Findlay and Snelling [379]. An earlier study by Clark and Wayne [218] reported a value about three times larger.

A58. $O_2(^1\Delta) + N$. The recommendation is an upper limit based upon the measurement reported by Westenberg et al. [1246], who used ESR to detect $O_2(X^3\Sigma$ and $a^1\Delta)$, $O(^3P)$ and $N(^4S)$ with a discharge flow reactor. They used an excess of $O_2(^1\Delta)$ and measured the decay of N and the appearance of O at 195 and 300 K. They observed that the reaction of N with $O_2(^1\Delta)$ is somewhat slower than its reaction with $O_2(^3\Sigma)$. The recommended rate constant value for the latter provides the basis for the recommendation. Clark and Wayne [219, 220] and Schmidt and Schiff [1002] reported observations of an $O_2(^1\Delta)$ reaction with N that is about 30 times faster than the recommended limit. Schmidt and Schiff attribute the observed loss of $O_2(^1\Delta)$ in excess N to a rapid energy exchange with some constituent in discharged nitrogen, other than N.

A59. $O_2(^1\Delta) + N_2$. The recommendation is based upon the measurements by Findlay et al. [378] and Becker et al. [91]. Other studies obtained higher values for an upper limit: Clark and Wayne [218] and Steer et al. [1073].

A60. $O_2(^1\Delta) + CO_2$. The recommendation is based on the measurements reported by Findlay and Snelling [379] and Leiss et al. [682]. Upper limit rate coefficients reported by Becker et al. [91], McLaren et al. [774], and Singh et al. [1039] are consistent with the recommendation.

A61. $O_2(^1\Sigma) + O$. The recommendation is based on the measurement reported by Slanger and Black [1053].

A62. $O_2(^1\Sigma) + O_2$. The recommendation is the average of values reported by Martin et al. [763], Lawton et al. [664], and Lawton and Phelps [665], who are in excellent agreement. Measurements by Thomas and Thrush [1126], Chatha et al. [202], and Knickelbein et al. [620] are in reasonable agreement with the recommendation. Knickelbein et al. report an approximate unit yield of $O_2(^1\Delta)$ product.

A63. $O_2(^1\Sigma) + O_3$. The recommendation is based upon the room temperature measurements of Gilpin et al. [422], Slanger and Black [1053], Choo and Leu [215], and Shi and Barker [1020]. Measurements by Snelling [1061], Amimoto and Wiesenfeld [18], Ogren et al. [875], and Turnipseed et al. [1163] are in very good agreement with the recommendation. The temperature dependence is derived from the results of Choo and Leu. The yield of $O + 2O_2$ products is reported to be (70±20)% by Slanger and Black and Amimoto and Wiesenfeld.

A64. $O_2(^1\Sigma) + H_2O$. The recommendation is the average of room temperature measurements reported by Stuhl and Niki [1092], Filseth et al. [377], Wildt et al. [1251], and Shi and Barker [1020]. These data cover a range of about a factor of two. Measurements reported by O'Brien and Myers [874], Derwent and Thrush [334], and Thomas and Thrush [1126] are in good agreement with the recommendation. Wildt et al. [1251] report that the yield of $O_2(^1\Delta) \geq 90\%$.

A65. $O_2(^1\Sigma) + N$. The recommendation is based on the limit reported by Slanger and Black [1053].

A66. $O_2(^1\Sigma) + N_2$. The recommendation is the average of measurements reported by Izod and Wayne [546], Stuhl and Welge [1095], Filseth et al. [377], Martin et al. [763], Kohse-Höinghaus and Stuhl [625], Choo and Leu [215], Wildt et al. [1251], and Shi and Barker [1020]. Less direct measurements reported by Noxon [873], Myers and O'Brien [821], and Chatha et al. [202] are consistent with the recommendation. Kohse-Höinghaus and Stuhl observed no significant temperature dependence over the range 203-349 K.

A67. $O_2(^1\Sigma) + CO_2$. The recommendation is the average of measurements reported by Filseth et al. [377], Davidson et al. [304], Avilés et al. [49], Muller and Houston [818], Choo and Leu [215], Wildt et al. [1251], and Shi and Barker [1020] at room temperature. The temperature dependence is from the work of Choo and Leu. Muller and Houston and Singh and Setser [1040] give evidence that $O_2(^1\Delta)$ is a product. Wildt et al. report that the yield of $O_2(^1\Delta) \geq 90\%$.

B1. O + OH. The rate constant for O + OH is a fit to three temperature dependence studies: Westenberg et al. [1245], Lewis and Watson [703], and Howard and Smith [514]. This recommendation is consistent with earlier work near room temperature as reviewed by Lewis and Watson [703] and with the measurements of Brune et al. [148]. The ratio $k(O + HO_2)/k(O + OH)$ measured by Keyser [600] agrees with the rate constants recommended here.

B2. $O + HO_2$. The recommendation for the $O + HO_2$ reaction rate constant is the average of five studies at room temperature (Keyser [599], Sridharan et al. [1064], Ravishankara et al. [957], Brune et al. [148] and Nicovich and Wine [848]) fitted to the temperature dependence given by Keyser [599] and Nicovich and Wine [848]. Earlier studies by Hack et al. [449] and Burrows et al. [164, 167] are not considered, because the $OH + H_2O_2$ reaction was important in these studies and the value used for its rate constant in their analyses has been shown to be in error. Data from Lii et al. [713] are not used, because they are based on only four experiments and involve a curve fitting procedure that appears to be insensitive to the desired rate constant. Data from Ravishankara et al. [957] at 298 K show no dependence on pressure between 10 and 500 torr N_2. The ratio $k(O + HO_2)/k(O + OH)$ measured by Keyser [600] agrees with the rate constants recommended here. Sridharan et al. [1062] showed that the reaction products correspond to abstraction of an oxygen atom from HO_2 by the O reactant. Keyser et al. [604] reported <1% O_2 ($b^1\Sigma$) yield.

B3. $O + H_2O_2$. There are two direct studies of the $O + H_2O_2$ reaction: Davis et al. [314] and Wine et al. [1260]. The recommended value is a fit to the combined data. Wine et al. suggest that the earlier measurements may be too high because of secondary chemistry. The A-factor for both data sets is quite low compared to similar atom-molecule reactions. An indirect measurement of the E/R by Roscoe [972] is consistent with the recommendation.

B4. $H + O_3$. The recommendation is an average of the results of Lee et al. [670] and Keyser [595], which are in excellent agreement over the 200-400 K range. An earlier study by Clyne and Monkhouse [238] is in very good agreement on the T dependence in the range 300-560 K but lies about 60% below the recommended values. Although we have no reason not to believe the Clyne and Monkhouse values, we prefer the two studies that are in excellent agreement, especially since they were carried out over the T range of interest. Results by Finlayson-Pitts and Kleindienst [384] agree well with the present recommendations. Reports of a channel forming $HO_2 + O$ (Finlayson-Pitts and Kleindienst [384]: ~25%, and Force and Wiesenfeld [392]: ~40%) have been contradicted by other studies (Howard and Finlayson-Pitts [513]: <3%; Washida et al. [1225]: <6%; Finlayson-Pitts et al. [385]: <2%; and Dodonov et al. [348]: <0.3%). Secondary chemistry is believed to be responsible for the observed O-atoms in this system. Washida et al. [1226] measured a low limit (<0.1%) for the production of singlet molecular oxygen in the reaction $H + O_3$.

B5. $H + HO_2$. There are five studies of this reaction: Hack et al. [453], Hack et al. [451], Thrush and Wilkinson [1133], Sridharan et al. [1064] and Keyser [602]. Related early work and combustion studies are referenced in the Sridharan et al. paper. All five studies used discharge flow systems. It is difficult to obtain a direct measurement of the rate constant for this reaction because both reactants are radicals and the products OH and O are very reactive toward the HO_2 reactant. The recommendation is based on the data of Sridharan et al. and Keyser because their measurements were the most direct and required the fewest corrections. The other measurements, $(5.0\pm1.3) \times 10^{-11}$ cm^3 molecule^{-1} s^{-1} by Thrush and Wilkinson [1133] and $(4.65\pm1)\times 10^{-11}$ by Hack et al. [451] are in reasonable agreement with the recommended value. Three of the studies reported

the product channels: (a) 2OH, (b) H_2O + O, and (c) H_2 + O_2. Hack et al. [453] k_a/k = 0.69, k_b/k = 0.02, and k_c/k = 0.29; Sridharan et al. [1064] k_a/k = 0.87±0.04, k_b/k = 0.02±0.02, k_c/k = 0.09±.045; and Keyser [602] k_a/k = 0.90±0.04, k_b/k = 0.02±0.02, and k_c/k = 0.08±0.04. Hislop and Wayne [491], Keyser et al. [604], and Michelangeli et al. [801] reported on the yield of O_2 ($b^1\Sigma$) formed in channel (c) as (2.8±1.3) x 10^{-4}, <8 x 10^{-3}, and <2.1 x 10^{-2} respectively of the total reactions. Keyser found the rate coefficient and product yields to be independent of temperature for 245 < T < 300 K.

B6. OH + O_3. The recommendation for the OH + O_3 rate constant is based on the room temperature measurements of Kurylo [636] and Zahniser and Howard [1292] and the temperature dependence studies of Anderson and Kaufman [23], Ravishankara et al. [955] and Smith et al. [1056]. Kurylo's value was adjusted by -8% to correct for an error in the ozone concentration measurement (Hampson and Garvin [460]). The Anderson and Kaufman rate constants were normalized to k = 6.2 x 10^{-14} cm^3 $molecule^{-1}$ s^{-1} at 295 K as suggested by Chang and Kaufman [198].

B7. OH + H_2. The OH + H_2 reaction has been the subject of numerous studies (see Ravishankara et al. [949] for a review of experimental and theoretical work). The recommendation is fixed to the average of nine studies at 298 K: Greiner [439], Stuhl and Niki [1094], Westenberg and de Haas [1242], Smith and Zellner [1058], Atkinson et al. [41], Overend et al. [890], Tully and Ravishankara [1153], Zellner and Steinert [1300], and Ravishankara et al. [949]. Results reported by Talukdar et al. [1116] are in excellect agreement.

B8. OH + HD. The recommendation is based on direct measurements made by Talukdar et al. [1116] using pulsed photolysis-laser induced fluorescence over the temperature range 248-418K. The recommendation is in excellent agreement with the ratio k(OH + H_2)/k(OH + HD) = 1.65±0.05 at 298K reported by Ehhalt et al. [363] when combined with the recommended k(OH + H_2).

B9. OH + OH. The recommendation for the OH + OH reaction is the average of six measurements near 298 K: Westenberg and de Haas [1243], McKenzie et al. [773], Clyne and Down [227], Trainor and von Rosenberg [1140], Farquharson and Smith [371], and Wagner and Zellner [1188]. The rate constants for these studies all fall between (1.4 and 2.3) x 10^{-12} cm^3 $molecule^{-1}$ s^{-1}. The temperature dependence is from Wagner and Zellner, who reported rate constants for the range T = 250-580 K.

B10. OH + HO_2. A study by Keyser [603] appears to resolve a discrepancy between low-pressure discharge flow experiments that all gave rate coefficients near 7 x 10^{-11} cm^3 $molecule^{-1}$ s^{-1} : Keyser [598], Thrush and Wilkinson [1132], Sridharan et al. [1063, 1065], Temps and Wagner [1123], and Rozenshtein et al. [976], and atmospheric pressure studies that gave rate coefficients near 11 x 10^{-11}: Lii et al. [712], Hochanadel et al. [498], DeMore [323], Cox et al. [268], Burrows et al. [166], and Kurylo et al. [644]. Laboratory measurements using a discharge flow experiment and a chemical model analysis of the results by Keyser [603] demonstrate that the previous discharge flow measurements were probably subject to interference from small amounts of O and H. In the presence of excess HO_2 these atoms generate OH and result in a rate coefficient measurement that falls below the true value. The temperature dependence is from Keyser [603], who covered the range 254 to 382 K. A flow tube study by Schwab et al. [1009] reported k = (8.0 +3/-4) x 10^{-11}, in agreement with the recommendation. These workers measured the concentrations of HO_2, OH, O, and H and used a computer model of the relevant reactions to test for interference. A flow tube study by Dransfeld and Wagner [355] employing an isotope labelled ^{18}OH reactant obtained k = (11±2) x 10^{-11} in good agreement with the recommendation. They attributed about half of the reactive events to isotope scrambling because control experiments with ^{16} OH gave k = 6 x 10^{-11}. It should be noted that their control experiments were subject to the errors described by Keyser [603] due to the presence of small amounts of H and O, whereas their ^{18}OH measurements were not. Kurylo et al. [644] found no evidence of significant scrambling in isotope studies of the OH and HO_2 reaction. An additional careful study of the reaction temperature dependence would be useful. Hippler and Troe [489] have analysed data for this reaction at temperatures up to 1250K.

B11. OH + H_2O_2. The recommendation is a fit to the temperature dependence studies of Keyser [596], Sridharan et al. [1066], Wine et al. [1265], Kurylo et al. [648], and Vaghjiani et al. [1174]. The data from these studies have been revised to account for the H_2O_2 UV absorption cross section recommendations in this evaluation. The first two references contain a discussion of some possible reasons for the discrepancies with earlier work and an assessment of the impact of the new value on other kinetic studies. All of these measurements agree quite well and overlap one another. Measurements by Lamb et al. [655] agree at room temperature but

indicate a quite different temperature dependence with k increasing slightly with decreasing temperature. Their data were not incorporated in the fit. A measurement at room temperature by Marinelli and Johnston [757] agrees well with the recommendation. Hippler and Troe [489] have analysed data for this reaction at temperatures up to 1250K.

B12. $HO_2 + O_3$. There are four studies of this reaction using flow tube reactors: Zahniser and Howard [1292] at 245 to 365 K, Manzanares et al. [747] at 298 K, Sinha et al. [1049] at 243 to 413 K, and Wang et al. [1220] at 233 to 400 K. The data of Sinha et al. were given somewhat greater weight in the evaluation because this study did not employ an OH radical scavenger. The other studies fall close to the recommendation. All of the temperature dependence studies show some curvature in the Arrhenius plot with the E/R decreasing at lower temperature. The recommendation incorporates only data at temperatures less than 300 K; it is not valid for T > 300 K and is uncertain at T < 230 K, where there are no data. Zahniser and Nelson (private communication, 1991) observe curvature in the Arrhenius plot at low temperatures. High-quality low temperature data are needed for this reaction. Early studies using the $HO_2 + HO_2$ reaction as a reference (Simonaitis and Heicklen [1033]; DeMore and Tschuikow-Roux [332]) give results that fall below the recommendation by factors of about 2 and 1.5, respectively. The more recent study by DeMore [321] agrees with the recommendation. The mechanism of the reaction has been studied using ^{18}O labelled HO_2 by Sinha et al. [1049], who reported that the reaction occurs 75±10% via H atom transfer at 297K and by Nelson and Zahniser [828], who reported branching ratios for H transfer vs O transfer over the range 226-355K. They report that the H atom transfer decreases from 94±5% at 226±11K to 88±5% at 355±8K.

B13. $HO_2 + HO_2$. Two separate expressions are given for the rate constant for the $HO_2 + HO_2$ reaction. The effective rate constant is given by the sum of these two equations. This reaction has been shown to have a pressure-independent bimolecular component and a pressure-dependent termolecular component. Both components have negative temperature coefficients. The bimolecular expression is obtained from data of Cox and Burrows [267], Thrush and Tyndall [1129, 1130], Kircher and Sander [607], Takacs and Howard [1107, 1108], Sander [982] and Kurylo et al. [650]. Data of Rozenshtein et al. [976] are consistent with the low pressure recommendation, but they report no change in k with pressure up to 1 atm. Results of Thrush and Wilkinson [1131] and Dobis and Benson [346] are inconsistent with the recommendation. The termolecular expression is obtained from data of Sander et al. [986], Simonaitis and Heicklen [1037], and Kurylo et al. [650] at room temperature and Kircher and Sander [607] for the temperature dependence. This equation applies to M = air. On this reaction system there is general agreement among investigators on the following aspects of the reaction at high pressure (P ~1 atm): (a) the HO_2 UV absorption cross section: Paukert and Johnston [902], Cox and Burrows [267], Hochanadel et al. [498], Sander et al. [986], Kurylo et al. [652], and Crowley et al. [288]; (b) the rate constant at 300K: Paukert and Johnston [902], Hamilton and Lii [458], Cox and Burrows [267], Lii et al. [711], Tsuchiya and Nakamura [1145], Sander et al. [986], Simonaitis and Heicklen [1037], Kurylo et al. [650], Andersson et al. [27], and Crowley et al. [288] (all values fall in the range (2.5 to 4.7) x 10^{-12} cm^3 $molecule^{-1}$ s^{-1}); (c) the rate constant temperature dependence: Cox and Burrows [267], Lii et al. [711], and Kircher and Sander [607]; (d) the rate constant water vapor dependence: Hamilton [457], Hochanadel et al. [497], Hamilton and Lii [458], Cox and Burrows [267], DeMore [321], Lii et al. [714], Sander et al. [986], and Andersson et al. [27]; (e) the H/D isotope effect: Hamilton and Lii [458] and Sander et al. [986]; and (f) the formation $H_2O_2 + O_2$ as the major products at 300 K: Su et al. [1098], Niki et al. [865], Sander et al. [986], and Simonaitis and Heicklen [1037]. Sahetchian et al. [980, 981] give evidence for the formation of a small amount of H_2 (~10%) at temperatures near 500 K, but Baldwin et al. [55] and Ingold [541] give evidence that the yield must be much less. Glinski and Birks [428] report an upper limit of 1% H_2 yield at a total pressure of about 50 torr and 298 K, but their experiment may have interference from wall reactions. A smaller limit to H_2 production (0.01%) was later determined in the same laboratory (Stephens et al. [1077]). For systems containing water vapor, the multiplicative factor given by Lii et al. [714] and Kircher and Sander [607] can be used: $1 + 1.4 \times 10^{-21}$ $[H_2O]$ $\exp(2200/T)$. Lightfoot et al. [709] reported atmospheric pressure measurements over the temperature range 298-777 K that are in agreement with the recommended value at room temperature but indicate an upward curvature in the Arrhenius plot at elevated temperature. A high temperature study by Hippler et al. [490] confirms the strong curvature.

C1. $O + NO_2$. k(298 K) is based on the results of Davis et al. [309], Slanger et al. [1054], Bemand et al. [105], Ongstad and Birks [880] and Geers-Muller and Stuhl [412]. The recommendation for E/R is from Davis et al., Ongstad and Birks, and Geers-Muller and Stuhl with the A-factor adjusted to give the recommended k(298) value.

C2. $O + NO_3$. Based on the study of Graham and Johnston [433] at 298 K and 329 K. While limited in temperature range, the data indicate no temperature dependence. Furthermore, by analogy with the reaction of O with NO_2, it is assumed that this rate constant is independent of temperature. Clearly, temperature-dependence studies are needed.

C3. $O + N_2O_5$. Based on Kaiser and Japar [582].

C4. $O + HNO_3$. The upper limit reported by Chapman and Wayne [200] is accepted.

C5. $O + HO_2NO_2$. The recommended value is based on the study of Chang et al. [199]. The large uncertainty in E/R and k at 298 K are due to the fact that the recommendation is based on a single study.

C6. $H + NO_2$. The recommended value of k_{298} is derived from the studies of Wagner et al. [1190], Bemand and Clyne [103], Clyne and Monkhouse [238], Michael et al. [796] and Ko and Fontijn [624]. The temperature dependence is from the studies of Wagner et al. and Ko and Fontijn. The data from Wategaonkar and Setser [1229] and Agrawalla et al. [13] were not considered.

C7. $OH + NO_3$. The recommendation is derived from an average of the results of Boodaghians et al. [128], Mellouki et al. [782], Becker et al. [88] and Mellouki et al. [785]. There are no temperature dependence data. The reaction products are probably $HO_2 + NO_2$.

C8. OH + HONO. The recommended rate expression is derived from the work of Jenkin and Cox [557], which supersedes the earlier room temperature study of Cox et al. [275]. Recent results from the Ravishankara group [161] suggest that the reaction may have a small negative temperature dependence.

C9. $OH + HNO_3$. The intensive study of this reaction over the past few years has significantly reduced many of the apparent discrepancies among (a) the early studies yielding a low, temperature-independent rate constant (Smith and Zellner [1059] and Margitan et al. [751]); (b) more recent work (mostly flash photolysis) with a k(298) approximately 40% larger, and a strong negative T dependence below room temperature (Wine et al. [1264]; Kurylo et al. [642]; Margitan and Watson [752]; Marinelli and Johnston [757]; Ravishankara et al. [946]; Jourdain et al. [579]; C. A. Smith et al. [1056]; Jolly et al. [573] (298 K); Stachnik et al. [1068]); and (c) recent discharge low studies yielding the lower value for k(298 K) but showing substantial negative T dependence (Devolder et al. [335]; Connell and Howard [260]). Major features of the data are (1) a strong negative T dependence below room temperature, (2) a much weaker temperature dependence above room temperature, possibly leveling off around 500 K, and (3) small, measurable pressure dependence which becomes greater at low temperature. The pressure dependence has been determined by Margitan and Watson [752] over the ranges 20-100 torr and 225-298 K and by Stachnik et al. [1068] at pressures of 10, 60, and 730 torr at 298 K. The two studies are in excellent agreement. Their "low pressure limit" agrees well with the average k(298 K) = 1.0×10^{-13} cm^3 $molec^{-1}$ s^{-1} derived from the four low pressure discharge flow studies. The value measured for pressures typical of the other flash photolysis studies (20-50 torr) also agrees well. The two pressure-dependence studies indicate that the high pressure limit is approximately 50% greater than the low pressure limit at 298 K, and about a factor of 2 greater at 240 K. Thus, over the narrow pressure ranges explored in most flash photolysis studies, the P dependence can be represented by combining a low pressure (bimolecular) limit, k_o, with a Lindemann-Hinshelwood expression for the P dependence:

$$k(M,T) = k_o + \frac{k_3[M]}{1 + \frac{k_3[M]}{k_2}} \quad \text{with} \quad \begin{cases} k_0 = 7.2\times10^{-15} \exp(785/T) \\ k_2 = 4.1\times10^{-16} \exp(1440/T) \\ k_3 = 1.9\times10^{-33} \exp(725/T) \end{cases}$$

The coefficients k_3 and k_2 are the termolecular and high pressure limits for the "association" channel. The value of k at high pressures is the sum $k_o + k_2$. The weak pressure dependence and weak T dependence above 300 K explain many of the apparent discrepancies for all the data (including the 1975 studies), except for a few minor features which are probably due to the normally encountered experimental scatter. The Smith and Zellner flash photolysis values are low compared to other flash systems (closer to the flow studies), although the difference is not unusual (~30%). Conversely, the Jourdain et al. flow study is high relative to the other ones. The Connell and Howard T dependence (below 300 K) is significantly weaker than the other studies. The failure of Smith et al. to observe a pressure effect between 50 and 760 torr, even at 240 K, is in sharp

conflict with the effect seen by Stachnik et al. over the same range in a much more detailed study. Jolly et al. also could not detect a pressure dependence between 1 torr (M = HNO_3) and 600 torr (M = SF_6) at 298 K. Nelson et al. [833], Jourdain et al. and Ravishankara et al. have all shown that within experimental error the yield of NO_3 (per OH removed) is unity at 298 K, with similar results at 250 K (Ravishankara et al.).

C10. OH + HO_2NO_2. The recommendation for both k at 298 K and the Arrhenius expression is based upon the data of Trevor et al. [1141], Barnes et al. [61], C. A. Smith et al. [1056] and Barnes et al. [63]. Trevor et al. studied this reaction over the temperature range 246-324 K and reported a temperature invariant value of 4.0 x 10^{-12} cm^3 $molecule^{-1}$ s^{-1}, although a weighted least squares fit to their data yields an Arrhenius expression with an E/R value of (193±193) K. In contrast, Smith et al. studied the reaction over the temperature range 240-300 K and observed a negative temperature dependence with an E/R value of -(650±30) K. The early Barnes et al. study [61] was carried out only at room temperature and 1 torr total pressure while their most recent study was performed in the pressure range 1-300 torr N_2 and temperature range 268-295 K with no rate constant variation being observed. In addition, k_{298} derived in Barnes et al. [61] was revised upward in the later study from 4.1 x 10^{-12} to 5.0 x 10^{-12} due to a change in the rate constant for the reference reaction. The values of k at 298 K from the four studies are in excellent agreement. An unweighted least squares fit to the data from the above-mentioned studies yields the recommended Arrhenius expression. The less precise value for k at 298 K reported by Littlejohn and Johnston [723] is in fair agreement with the recommended value. The error limits on the recommended E/R are sufficient to encompass the results of both Trevor et al. and Smith et al. It should be noted that the values of k at 220 K deduced from the two studies differ by a factor of 2. Clearly, additional studies of k as a function of temperature and the identification of the reaction products are needed.

C11. OH + NH_3. The recommended value at 298 K is the average of the values reported by Stuhl [1090], Smith and Zellner [1059], Perry et al. [909], Silver and Kolb [1024], Stephens [1076] and Diau et al. [338]. The values reported by Pagsberg et al. [891] and Cox et al. [274] were not considered because these studies involved the analysis of a complex mechanism and the results are well outside the error limits implied by the above six direct studies. The results of Kurylo [636] and Hack et al. [447] were not considered because of their large discrepancies with the other direct studies (factors of 3.9 and 1.6 at room temperature, respectively). Because the Arrhenius plot displays considerable curvature, the temperature dependence is based only on the data below 300 K, i.e., the studies of Smith and Zellner [1059] and Diau et al. [338], and the A-factor has been selected to fit the recommended room temperature value.

C12. HO_2 +NO. The recommendation for HO_2 + NO is based on the average of eight measurements of the rate constant at room temperature and below: Howard and Evenson [512], Leu [689], Howard [509], Glaschick-Schimpf et al. [423], Hack et al. [450], Thrush and Wilkinson [1132] and Jemi-Alade Thrush [554], and Seeley et al. [1012]. All of these are in quite good agreement. The results of Imamura and Washida [540] were not considered due to the relatively large uncertainty limits reported in this study. An earlier study, Burrows et al. [164] has been disregarded because of an error in the reference rate constant, k(OH + H_2O_2). The room temperature study of Rozenshtein et al. [976] has also been disregarded due to an inadequate treatment of possible secondary reactions. The recommended Arrhenius parameters are obtained from a fit to all the data. The recommended value of k(298) is obtained from the Arrhenius line.

C13. HO_2 + NO_2 . Tyndall et al. [1165] obtained an upper limit to the rate coefficient of 5x10^{-16} cm^3 $molecule^{-1}$ s^{-1} based on static photolysis experiments with FTIR analysis at 296 K and 760 Torr of N_2.

C14. HO_2 + NO_3. The recommendation for k_{298} is based on a weighted average of the data of Hall et al. [455], Mellouki et al. [782], Becker et al. [88] and Mellouki et al. [785]. There are insufficient data on which to base the temperature dependence of the rate coefficient. The measured branching ratios for the OH + NO_2 + O_2 channel range from 0.57 to 1.0. The most direct measurement is derived from the study of Mellouki et al. [785], which obtained a value of 1.0 $^{+0.0}/_{-0.3}$ at 298 K.

C15. HO_2 + NH_2. There is a fairly good agreement on the value of k at 298 K between the direct study of Kurasawa and Lesclaux [634] and the relative studies of Cheskis and Sarkisov [212] and Pagsberg et al. [891]. The recommended value is the average of the values reported in these three studies. The identity of the

products is not known; however, Kurasawa and Lesclaux suggest that the most probable reaction channels give either $NH_3 + O_2$ or $HNO + H_2O$ as products.

C16. $N + O_2$. The recommended expression is derived from a least squares fit to the data of Kistiakowsky and Volpi [610], Wilson [1254], Becker et al. [90], Westenberg et al. [1246], Clark and Wayne [220], Winkler et al. [1273] and Barnett et al. [71]. k(298 K) is derived from the Arrhenius expression and is in excellent agreement with the average of all of the room temperature determinations.

C17. $N + O_3$. The recommendation is based on the results of Barnett et al. [71]. The value of $(1.0\pm0.2) \times 10^{-16}$ cm^3 $molecule^{-1}$ s^{-1} reported by Barnett et al. should probably be considered an upper limit rather than a determination. The low values reported by Barnett et al., Stief et al. [1086] and Garvin and Broida [410] cast doubt on the much faster rates reported by Phillips and Schiff [914], and Chen and Taylor [208].

C18. N + NO. The recommended temperature dependence is based on the discharge flow-resonance fluorescence studies of Wennberg and Anderson [1238], and the discharge flow-resonance fluorescence and flash photolysis-resonance fluorescence studies of Lee et al. [671]. There is relatively poor agreement between these studies and the results of Clyne and McDermid [235], Kistiakowsky and Volpi [611], Herron [482], Phillips and Schiff [914], Lin et al. [716], Ishikawa et al. [543], Sugawara et al. [1099], Cheah and Clyne [203], Husain and Slater [530], Clyne and Ono [242], Brunning and Clyne [149] and Jeoung et al. [568].

C19. $N + NO_2$. The recommendation for k_{298} is from the discharge flow-resonance fluorescence study of Wennberg and Anderson [1238]. The latter study had significantly better sensitivity for $N(^4S)$ than the discharge flow-resonance fluorescence study of Clyne and Ono [242], which obtained a value about four times smaller. The results of Husain and Slater [530] and Clyne and McDermid [235] are not considered. The temperature dependence is obtained from the study of Wennberg and Anderson. In the latter study, atomic oxygen was shown to be the principal reaction product, in agreement with Clyne and McDermid. A recent study by Iwata et al. [544] suggested an upper limit of 3.3×10^{-13} cm^3 $molecule^{-1}$ s^{-1} for the corresponding reaction involving $N(^2D)$ and $N(^2P)$ atoms (sum of all reaction channels).

C20. $NO + O_3$. The recommended Arrhenius expression is a least squares fit to the data reported by Birks et al. [120], Lippmann et al. [721], Ray and Watson [963], Michael et al. [790] and Borders and Birks [130] at and below room temperature, with the data at closely spaced temperatures reported in Lippmann et al. and Borders and Birks being grouped together so that these five studies are weighted equally. This expression fits all the data within the temperature range 195-304 K reported in these five studies to within 20%. Only the data between 195 and 304 K were used to derive the recommended Arrhenius expression, due to the observed non-linear Arrhenius behavior (Clyne et al. [244], Clough and Thrush [223], Birks et al., Michael et al. and Borders and Birks). Clough and Thrush, Birks et al., Schurath et al. [1008], and Michael et al. have all reported individual Arrhenius parameters for each of the two primary reaction channels. The range of values for k at stratospheric temperatures is somewhat larger than would be expected for such an easy reaction to study. The measurements of Stedman and Niki [1071] and Bemand et al. [105] at 298 K are in excellent agreement with the recommended value of k at 298 K.

C21. $NO + NO_3$. The recommendation is based on the studies of Hammer et al. [459], Sander and Kircher [985] and Tyndall et al. [1166], which are in excellent agreement.

C22. $NO_2 + O_3$. The recommended expression is derived from a least squares fit to the data of Davis et al. [312], Graham and Johnston [432], Huie and Herron [524], and Cox and Coker [269]. The data of Verhees and Adema [1177] and Stedman and Niki [1071] were not considered because of systematic discrepancies with the other studies.

C23. $NO_2 + NO_3$. The existence of the reaction channel forming $NO + NO_2 + O_2$ has not been firmly established. However, studies of N_2O_5 thermal decomposition that monitor NO_2 (Daniels and Johnston [298]; Johnston and Tao [571]; Cantrell et al. [183]) and NO (Hjorth et al. [492], and Cantrell et al. [186]) require reaction(s) that decompose NO_3 into $NO = O_2$. The rate constant from the first three studies is obtained from the product kK_{eq}, where K_{eq} is the equilibrium constant for $NO_2 + NO_3 = N_2O_5$, while for the

latter two studies the rate constant is obtained from the ratio k/k(NO + NO_3), where k(NO + NO_3) is the rate constant for the reaction NO + $NO_3 \rightarrow 2NO_2$. Using K_{eq} and k(NO + NO_3) from this evaluation, the rate expression that best fits the data from all five studies is 4.5×10^{-14} exp (-1260/T) cm^3 $molecule^{-1}$ s^{-1} with an overall uncertainty factor of 2.

C24. $NO_3 + NO_3$. . The recommendation for k(298) is from the studies of Graham and Johnston [433] and Biggs et al. [116]. The temperature dependence is from Graham and Johnston.

C25. $NH_2 + O_2$. This reaction has several product channels which are energetically possible, including NO + H_2O and HNO + OH. With the exception of the studies of Hack et al. [446] and Jayanty et al. [552] and several studies at high temperature, there is no evidence for a reaction. The following upper limits have been measured (cm^3 $molecule^{-1}$ s^{-1}): 3×10^{-18} (Lesclaux and Demissy [684]), 8×10^{-15} (Pagsberg et al. [891]), 1.5×10^{-17} (Cheskis and Sarkisov [212]), 3×10^{-18} (Lozovsky et al. [735]), 1×10^{-17} (Patrick and Golden [901]) and 7.7×10^{-18} (Michael et al. [792]) and 6×10^{-21} (Tyndall et al. [1167]). The recommendation is based on the study of Tyndall et al., which was sensitive to reaction paths leading to the products NO, NO_2 and N_2O. The reaction forming NH_2O_2 cannot be ruled out, but is apparently not important in the atmosphere.

C26. $NH_2 + O_3$. There is poor agreement among the recent studies of Cheskis et al. [211], k(298) = 1.5×10^{-13} cm^3 s^{-1}, Patrick and Golden [901], k(298) = 3.25×10^{-13} cm^3 s^{--1}, Hack et al. [445], 1.84×10^{-13} cm^3 s^{-1}, Bulatov et al. [154], 1.2×10^{-13} cm^3 s^{-1}, and Kurasawa and Lesclaux [635], 0.63×10^{-13} cm^3 s^{-1}. The very low value of Kurasawa and Lesclaux may be due to regeneration of NH_2 from secondary reactions (see Patrick and Golden), and it is disregarded here. The discharge flow value of Hack et al. is nearly a factor of two less than the recent Patrick and Golden flash photolysis value. The large discrepancy between Bulatov et al. and Patrick and Golden eludes explanation. The recommendation is the k(298) average of these four studies, and E/R is an average of Patrick and Golden (1151 K) with Hack et al. (710 K).

C27. NH_2 + NO. The recommended value for k at 298 K is the average of the values reported by Lesclaux et al. [686], Hancock et al. [461], Sarkisov et al. [995], Stief et al. [1084], Andresen et al. [28] Whyte and Phillips [1247], Dreier and Wolfrum [357], Atakan et al. [33], Wolf et al. [1274], Diau et al. [336] and Imamura and Washida [540]. The results of Gordon et al. [429], Gehring et al. [413], Hack et al. [452] and Silver and Kolb [1025] were not considered because they lie at least 2 standard deviations from the average of the previous group. The results tend to separate into two groups. The flash photolysis results average 1.8×10^{-11} cm^3 $molecule^{-1}$ s^{-1} (except for the pulse radiolysis study of Gordon et al.), while those obtained using the discharge flow technique average 0.9×10^{-11} cm^3 $molecule^{-1}$ s^{-1}. The apparent discrepancy cannot be due simply to a pressure effect as the pressure ranges of the flash photolysis and discharge flow studies overlapped and none of the studies observed a pressure dependence for k. Whyte and Phillips have suggested that the difference may be due to decomposition of the adduct NH_2NO, which occurs on the timescale of the flow experiments, but not the flash experiments. There have been many studies of the temperature dependence but most have investigated the regime of interest to combustion and only two have gone below room temperature (Hack et al. from 209-505 K and Stief et al. from 216-480 K. Each study reported k to decrease with increasing temperature The recommended temperature dependence is taken from a fit of to the Stief et al. data at room temperature and below. The reaction proceeds along a complex potential energy surface, which results in product branching ratios that are strongly dependent on temperature. *Ab initio* calculations by Walch [1193] show the existence of four saddle points in the potential surface leading to $N_2 + H_2O$ without a reaction barrier. Elimination to form OH + HN_2 can occur at any point along the surface. While results from early studies on the branching ratio for OH formation different significantly, the most recent studies (Hall et al., Dolson [350], Silver and Kolb [1028], Atakan et al., Stephens et al. [1075], Park and Lin [896]) agree on a value around 0.1 at 300 K, with N_2+H_2O making up the balance.

C28. $NH_2 + NO_2$. There have been four studies of this reaction (Hack et al. [452]; Kurasawa and Lesclaux [633]; Whyte and Phillips [1247]; and Xiang et al. [1282]). There is very poor agreement among these studies both for k at 298 K (factor of 2.3) and for the temperature dependence of k ($T^{-3.0}$ and $T^{-1.3}$). The recommended values of k at 298 K and the temperature dependence of k are averages of the results reported in these four

studies. Hack et al. have shown that the predominant reaction channel (>95%) produces $N_2O + H_2O$. Just as for the $NH_2 + NO$ reaction, the data for this reaction seem to indicate a factor of two discrepancy between flow and flash techniques, although the data base is much smaller.

C29. NH + NO. The recommendation is derived from the room temperature results of Hansen et al. [464], Cox et al. [264] and Harrison et al. [466]. The temperature dependence is from Harrison et al.

C30. $NH + NO_2$. The recommendation is derived from the temperature-dependence study of Harrison et al. [466].

C31. $O_3 + HNO_2$. Based on Kaiser and Japar [581] and Streit et al. [1089].

C32. $N_2O_5 + H_2O$. The recommended value at 298 K is based on the studies of Tuazon et al. [1148], Atkinson et al. [47] and Hjorth et al. [493]. Sverdrup et al. [1101] obtained an upper limit that is a factor of four smaller than that obtained in the other studies, but the higher upper limit is recommended because of the difficulty of distinguishing between homogeneous and heterogeneous processes in the experiment. See Table 59 for heterogeneous rate data for this reaction.

C33. $N_2(A,v) + O_2$. . Rate constants for the overall reaction for the v=0, 1 and 2 vibrational levels of $N_2(A)$ have been made by Dreyer et al. [358], Zipf [1312], Piper et al. [915], Iannuzzi and Kaufman [538], Thomas and Kaufman [1125] and De Sousa et al. [318]. The results of these studies are in relatively good agreement. The recommended values are (2.5±0.4), (4.0±0.6) and (4.5±0.6) ($x10^{-12}$ cm^3 $molecule^{-1}$ s^{-1}), from the work of De Sousa et al. The only temperature dependence data are from De Sousa et al., who obtained $k(T,v)=k(v,298K)(T/300)^{0.55}$ for v=0,1,2. The observation of high N_2O production initially reported by Zipf [1312] has not been reproduced by other groups, and the branching ratio for this channel is probably less than 0.02 (Iannuzzi et al. [537], Black et al. [123], De Sousa et al. [318], Fraser and Piper [394]). The branching ratios for the other channels are poorly established, although there is strong evidence for the formation of both $O(^3P)$ and $O_2(B^3\Sigma_u^-)$.

C34. $N_2(A,v) + O_3$. . The only study is that of Bohmer and Hack [127], who obtained 298K rate constants of 4.1±1.0, 4.1±1.2, 8.0±2.3, and 10±3.0 ($x10^{-11}$ cm^3 $molecule^{-1}$ s^{-1}) for the v=0-3 vibrational levels of $N_2(A)$, respectively. This study determined that the NO channel accounts for about 20% of the reaction products.

D1. $O + CH_3$. The recommended k(298 K) is the weighted average of three measurements by Washida and Bayes [1227], Washida [1224], and Plumb and Ryan [920]. The E/R value is based on the results of Washida and Bayes [1227], who found k to be independent of temperature between 259 and 341 K.

D2. O + HCN. Because it is a very slow reaction, there are no studies of this reaction below 450 K. Davies and Thrush [307] studied this reaction between 469 and 574 K while Perry and Melius [911] studied it between 540 and 900 K. Results of Perry and Melius are in agreement with those of Davies and Thrush. Our recommendation is based on these two studies. The higher-temperature (T>1000 K) combustion-related studies [Roth et al. [973], Szekely et al. [1102], and Louge and Hanson [729]] have not been considered. This reaction has two reaction pathways: $O + HCN \rightarrow H + NCO$, ΔH = -2 kcal/mol (k_a); and $O + HCN \rightarrow CO + NH$ (k_b), ΔH = -36 kcal/mol. The branching ratio k_a/k_b for these two channels has been measured to be ~2 at T = 860 K. The branching ratio at lower temperatures, which is likely to vary significantly with temperature, is unknown.

D3. $O + C_2H_2$. The value at 298 K is an average of ten measurements [Arrington et al. [31], Sullivan and Warneck [1100], Brown and Thrush [146], Hoyermann et al. [515, 516], Westenberg and deHaas [1240], James and Glass [549], Stuhl and Niki [1093], Westenberg and deHaas [1244], and Aleksandrov et al. [15]]. There is reasonably good agreement among these studies. Arrington et al. [31] did not observe a temperature dependence, an observation that was later shown to be erroneous by Westenberg and deHaas [1240]. Westenberg and deHaas [1240], Hoyermann et al. [516] and Aleksandrov et al. [15] are the only authors, who have measured the temperature dependence below 500 K. Westenberg and deHaas observed a curved Arrhenius plot at temperatures higher than 450 K. In the range 194-450 K, Arrhenius behavior provides an adequate description and the E/R obtained by a fit of the data from these three groups in this temperature range is

recommended. The A-factor was calculated to reproduce k(298 K). This reaction can have two sets of products, i.e., C_2HO + H or CH_2 + CO. Under molecular beam conditions C_2HO has been shown to be the major product. The study by Aleksandrov et al. using a discharge flow-resonance fluorescence method (under undefined pressure conditions) indicates that the C_2HO + H channel contributes no more than 7% to the net reaction at 298 K, while a similar study by Vinckier et al. [1183] suggests that both CH_2 and C_2HO are formed.

D4. $O + H_2CO$. The recommended values for A, E/R and k(298 K) are the averages of those determined by Klemm [616] (250 to 498 K) using flash photolysis-resonance fluorescence, by Klemm et al. [617] (298 to 748 K) using discharge flow-resonance fluorescence, and Chang and Barker [195] (296 to 436 K) using discharge flow-mass spectrometry techniques. All three studies are in good agreement. The k(298 K) value is also consistent with the results of Niki et al. [861], Herron and Penzhorn [484], and Mack and Thrush [737]. Although the mechanism for $O + H_2CO$ has been considered to be the abstraction reaction yielding OH + HCO, Chang and Barker suggest that an additional channel yielding $H + HCO_2$ may be occurring to the extent of 30% of the total reaction. This conclusion is based on an observation of CO_2 as a product of the reaction under conditions where reactions such as $O + HCO \rightarrow H + CO_2$ and $O + HCO \rightarrow OH + CO$ apparently do not occur. This interesting suggestion needs independent confirmation.

D5. $O + CH_3CHO$. The recommended k(298 K) is the average of three measurements by Cadle and Powers [173], Mack and Thrush [738], and Singleton et al. [1043], which are in good agreement. Cadle and Powers and Singleton et al. studied this reaction as a function of temperature between 298 and 475 K and obtained very similar Arrhenius parameters. The recommended E/R value was obtained by considering both sets of data. This reaction is known to proceed via H-atom abstraction [Mack and Thrush [738], Avery and Cvetanovic [48], and Singleton et al. [1043]].

D6. $O_3 + C_2H_2$. The database for this reaction is not well established. Room temperature measurements (Cadle and Schadt [174]; DeMore [319]; DeMore [320]; Stedman and Niki [1070]; Pate et al. [899]; and Atkinson and Aschmann [34]) disagree by as much as an order of magnitude. It is probable that secondary reactions involving destruction of ozone by radical products resulted in erroneously high values for the rate constants in several of the previous measurements. The present recommendation for k(298 K) is based on the room temperature value of Atkinson and Aschmann [34], which is the lowest value obtained and therefore perhaps the most accurate. The temperature dependence is estimated, based on an assumed A-factor of 1.0×10^{-14} $cm^3\ s^{-1}$ similar to that for the $O_3 + C_2H_4$ reaction and corresponding to the expected 5-membered ring structure for the transition state (DeMore [319, 320]). Further studies, particularly of the temperature dependence, are needed. Major products in the gas phase reaction are CO, CO_2, and HCOOH, and chemically-activated formic anhydride has been proposed as an intermediate of the reaction (DeMore [320], and DeMore and Lin [330]). The anhydride intermediates in several alkyne ozonations have been isolated in low temperature solvent experiments (DeMore and Lin [330]).

D7. $O_3 + C_2H_4$. The rate constant of this reaction is well established over a large temperature range, 178 to 360 K. Our recommendation is based on the data of DeMore [319], Stedman et al. [1072], Herron and Huie [483], Japar et al. [550, 551], Toby et al. [1135], Su et al. [1097], Adeniji et al. [9], Kan et al. [587], Atkinson et al. [36], and Bahta et al. [52].

D8. $O_3 + C_3H_6$. The rate constant of this reaction is well established over the temperature range 185 to 360 K. The present recommendation is based largely on the data of Herron and Huie [483], in the temperature range 235-362 K. (Note that a typographical error in Table 2 of that paper improperly lists the lowest temperature as 250 K, rather than the correct value, 235 K.) The recommended Arrhenius expression agrees within 25% with the low temperature (185-195 K) data of DeMore [319], and is consistent with, but slightly lower (about 40%) than the data of Adeniji et al. [9] in the temperature range 260-294 K. Room temperature measurements of Cox and Penkett [281], Stedman et al. [1072], Japar et al. [550, 551], and Atkinson et al. [36] are in good agreement (10% or better) with the recommendation.

D9. OH + CO. The recommendation allows for an increase in k with pressure. The zero pressure value was derived by averaging direct low pressure determinations [those listed in Baulch et al. [86] and the values reported by Dreier and Wolfrum [356], Husain et al. [528], Ravishankara and Thompson [952], Paraskevopoulos and Irwin [893], Hofzumahaus and Stuhl [499]. The results of Jonah et al. [574] are too high and were not included. An increase in k with pressure has been observed by a large number of

investigators [Overend and Paraskevopoulos [889], Perry et al. [910], Chan et al. [194], Biermann et al. [114], Cox et al. [275], Butler et al. [172], Paraskevopoulos and Irwin [892, 893], DeMore [324], Hofzumahaus and Stuhl [499], Hynes et al. [535]. In addition, Niki et al. [869] have measured k relative to OH + C_2H_4 in one atmosphere of air by following CO_2 production using FTIR. The recommended 298 K value was obtained by using a weighted nonlinear least squares analysis of all pressure-dependent data in N_2 [Paraskevopoulos and Irwin [893], DeMore [324], Hofzumahaus and Stuhl [499], and Hynes et al. [535]] as well as those in air [Niki et al. [870], Hynes et al. [535], to the form k = (A+BP)/(C+DP), where P is pressure in atmospheres. The data were best fit with D = 0 and therefore a linear form is recommended. Previous controversy regarding the effect of small amounts of O_2 (Biermann et al. [114]) has been resolved and is attributed to secondary reactions [DeMore [324], Hofzumahaus and Stuhl [499]]. The results of Butler et al. [172] have to be re-evaluated in the light of refinements in the rate coefficient for the OH + H_2O_2 reaction. The corrected rate coefficient is in approximate agreement with the recommended value. Currently, there are no indications to suggest that the presence of O_2 has any effect on the rate coefficient other than as a third body. The E/R value in the pressure range 50-760 torr has been shown to be essentially zero between 220 and 298 K by Hynes et al. [535]. Further substantiation of the temperature independence of k at 1 atm. may be worthwhile. Beno et al. [106] observe an enhancement of k with water vapor, which is in conflict with the flash photolysis studies; e.g., Ravishankara and Thompson [952], Paraskevopoulos and Irwin [893], and Hynes et al. [535]. The uncertainty factor is for 1 atm. of air.

The bimolecular channel yields H + CO_2 while the addition leads to HOCO. In the presence of O_2, the HOCO intermediate is converted to HO_2 + CO_2 (DeMore [324], Miyoshi et al. [803]). Miyoshi et al. report a rate constant for the reaction of HOCO with O_2 of ~1.5 x 10^{-12} cm^3 $molecule^{-1}$ s^{-1} at 298 K). Therefore, for atmospheric purposes, the products can be taken to be HO_2 and CO_2.

D10. OH + CH_4. This reaction has been extensively studied. The most recent data are from Vaghjiani and Ravishankara [1173], Saunders et al. [997], Finlayson-Pitts et al. [383], Dunlop and Tully [360], Mellouki et al. [788], and Gierczak et al. [419], who measured the absolute rate coefficients for this reaction using discharge flow and pulsed photolysis techniques. Sharkey and Smith [1019] have reported a high value (7.7 x 10^{-15} cm^3 $molecule^{-1}$ s^{-1}) for k(298 K), and this value has not been considered here. The current recommendation for k(298) was derived from the results of Vaghjiani and Ravishankara, Dunlop and Tully, Saunders et al., Mellouki et al., Finlayson-Pitts et al., and Gierczak et al. The temperature dependence of this rate coefficient has been measured by Vaghjiani and Ravishankara (223-420 K), Dunlop and Tully (above 298 K), Finlayson-Pitts et al. (278-378 K), and Mellouki et al. (233-343 K). Gierczak et al have extended the measurements of k to 195 K, and it appears that the rate coefficient does not strictly follow an Arrhenius expression. The recommended E/R was obtained from these results using data below 300 K. A more accurate representation of the rate constant as a function of temperature is obtained by using the three-parameter expression: $k = 2.80 \times 10^{-14} T^{0.667} \exp(-1575/T)$. This three-parameter fit may be preferred for lower stratosphere and upper troposphere calculations.

D11. OH + $^{13}CH_4$. This reaction has been studied relative to the OH + CH_4 reaction, since the ratio of the rate coefficients is the quantity needed for quantifying methane sources. Rust and Stevens [977], Davidson et al. [302], and Cantrell et al. [187] have measured k_{12}/k_{13} at 298 K to be 1.003, 1.010, and 1.0055, respectively. Cantrell et al.'s data supersede the results of Davidson et al. The recommended value of 1.005 ± 0.002 is based on the results of Rust and Stevens and Cantrell et al. Cantrell et al. find k_{12}/k_{13} to be independent of temperature between 273 and 353 K.

D12. OH + CH_3D. The rate coefficient for this reaction has been measured between 249 and 422 K using a pulsed laser photolysis-laser induced fluorescence system by Gierczak et al. [418]. The recommended values of k (298) and E/R are from this study. The recommendation agrees within about 10% at 298 K with the rate constant measured by DeMore [328] in a relative rate study over the temperature range 298 - 360 K. The difference, while small in an absolute sense, is nevertheless significant for the isotopic fractionation of atmospheric CH_3D and CH_4 by OH. An earlier result of Gordon and Mulac at 416 K [430] is in good agreement with the extrapolated data of both of these determinations. However, that measurement has not been explicitly included in this recommendation because the experiments were carried out at higher temperatures and therefore are less applicable to the atmosphere. The rate coefficients for the reactions of OH with other deuterated methanes have also been measured. (Dunlop and Tully [360], Gierczak et al. [1116], Gordon and Mulac [430]).

D13. $OH + H_2CO$. The value for k(298 K) is the average of those determined by Atkinson and Pitts [44], Stief et al. [1085], Temps and Wagner [1124], and Zabarnick et al. [1286]. The value reported by Morris and Niki [814] agrees within the stated uncertainty. There are two relative values that are not in agreement with the recommendations. The value of Niki et al. [863] relative to $OH + C_2H_4$ is higher, while the value of Smith [1060] relative to OH + OH is lower. The latter data are also at variance with the negligible temperature dependence observed in the two flash photolysis studies. The combined data set suggests E/R = 0. The abstraction reaction shown in the table is the major channel [Temps and Wagner [1124], Niki et al. [869]]; other channels may contribute to a small extent (Horowitz et al. [507]).

D14. $OH + CH_3OH$. The recommended value for k(298 K) is the average of seven direct studies [Overend and Paraskevopoulos [888], Ravishankara and Davis [944], Hagele et al. [454], Meier et al. [776], Greenhill and O'Grady [438], Wallington and Kurylo [1211], and Hess and Tully [486]]. Indirect measurements by Campbell et al. [178], Barnes et al. [62], Tuazon et al. [1149] and Klopffer et al. [619] are in good agreement with the recommended value. The temperature dependence of k has been measured by Hagele et al., Meier et al., Greenhill and O'Grady, Wallington and Kurylo, and Hess and Tully. The recommended value of E/R was calculated using the results obtained in the temperature range of 240 to 400 K by Greenhill and O'Grady [438] and Wallington and Kurylo [1211], the only investigators who have measured k below 298 K. Hess and Tully report a curved Arrhenius plot over the temperature range 298 - 1000 K, while Meier et al. do not observe such a curvature. This reaction has two pathways: abstraction of the H-atom from the methyl group or from the OH group. The results of Hagele et al., Meier et al., and Hess and Tully suggest that H abstraction from the methyl group is the dominant channel below room temperature.

D15. $OH + CH_3OOH$. The recommended value for k(298 K) is the average of the rate coefficients measured by Niki et al. [868] and Vaghjiani and Ravishankara [1172], which differ by nearly a factor of two. Niki et al. measured the rate coefficient relative to that for OH with C_2H_4 ($= 8.0 \times 10^{-12}$ cm^3 $molecule^{-1}$ s^{-1}) by monitoring CH_3OOH disappearance using an FTIR system. Vaghjiani and Ravishankara monitored the disappearance of OH, OD, and ^{18}OH in excess CH_3OOH in a pulsed photolysis-LIF system. They measured k between 203 and 423 K and report a negative activation energy with E/R = -190 K; the recommended E/R is based on their results. The reaction of OH with CH_3OOH occurs via abstraction of H from the oxygen end to produce the CH_3OO radical and from the CH_3 group to produce the CH_2OOH radical, as originally proposed by Niki et al. and confirmed by Vaghjiani and Ravishankara. CH_2OOH is unstable and falls apart to CH_2O and OH within a few microseconds. The possible reaction of CH_2OOH with O_2 is unimportant under atmospheric conditions (Vaghjiani and Ravishankara). The recommended branching ratios are,

$$OH + CH_3OOH \rightarrow CH_3O_2 + H_2O \quad (a) \quad 70\%$$

$$OH + CH_3OOH \rightarrow CH_2OOH + H_2O \quad (b) \quad 30\%,$$

(from Vaghjiani and Ravishankara) and are nearly independent of temperature.

D16. $OH + HC(O)OH$. The recommended value of k(298 K) is the average of those measured by Zetzsch and Stuhl [1303], Wine et al. [1255], Jolly et al. [572], Dagaut et al. [297], and Singleton et al. [1048]. The temperature dependence of k has been studied by Wine et al., who observed a very small negative activation energy and by Singleton et al., who observed k to be essentially independent of T. The recommended temperature dependence is based on these two studies.

Wine et al. found the rate coefficient for the OH + HC(O)OH reaction to be the same as that for OH + DC(O)OH reaction. Jolly et al. found the formic acid dimer to be unreactive toward OH, i.e., abstraction of the H atom attached to C was not the major pathway for the reaction. A comprehensive study of Singleton et al. showed that reactivity of HC(O)OH is essentially the same as that of DC(O)OH, but DC(O)OD reacts much slower than HC(O)OH and DC(O)OH. These observations show that the reaction proceeds via abstraction of the acidic H atom. Wine et al. and Jolly et al. also found that H atoms are produced in the reaction, which is consistent with the formation of HC(O)O, which would rapidly fall apart to CO_2 and H. End product studies are also consistent with the formation of CO_2 and H_2O in this reaction (Singleton et al. [1048]). The products of this reaction would be mostly HC(O)O and H_2O. The fate of HC(O)O in the atmosphere will be to give HO_2 either directly via reaction with O_2 or via thermal decomposition to H atom, which adds to O_2.

Wine et al. have suggested that, in the atmosphere, the formic acid could be hydrogen bonded to a water molecule and its reactivity with OH could be lowered because the hydrogen bonded water would obstruct the abstraction of the H atom. This suggestion needs to be checked.

D17. OH + HCN. This reaction is pressure dependent. The recommended value is the high pressure limit measured by Fritz et al. [401] using a laser photolysis-resonance fluorescence apparatus. Phillips [913] studied this reaction using a discharge flow apparatus at low pressures and found the rate coefficient to have reached the high pressure limit at ~10 torr at 298 K. Fritz et al.'s results contradict this finding. They agree with Phillip's measured value, within a factor of two, at 7 torr, but they find k to increase further with pressure. The products of the reaction are unknown.

D18. OH + C_2H_6. There are nineteen studies of this reaction at 298 K [Greiner [440], Howard and Evenson [510], Overend et al. [890], Lee and Tang [673], Leu [689], Tully et al. [1154], Jeong et al. [565], Tully et al. [1152], Nielsen et al. [856], Zabarnick et al. [1286], Wallington et al. [1213], Smith et al. [1056], Baulch et al. [85], Bourmada et al. [135], Abbatt et al. [1], Schiffman et al. [999], Talukdar et al. [1118], Sharkey and Smith [1019] and Anderson and Stephens [24]]. The recommended value is obtained by averaging the results of the recent investigations by Tully et al., Wallington et al., Abbatt et al., Schiffman et al., Talukdar et al. and Anderson and Stephens. The results of Sharkey and Smith are approximately 20% higher than those recommended here. When the measurements were not carried out at exactly 298 K, we have recalculated k using an E/R of 1070 K. The temperature dependence of the rate coefficient below 298 K has been measured only by Jeong et al., Wallington et al., Talukdar et al. and Anderson and Stephens. The last three studies are in good agreement. The recommended E/R is obtained from an analysis of the data of these three studies. The ratio of the rate coefficients for OH reactions with C_2H_6 and C_3H_8 has been measured by Finlayson-Pitts [383]. Our recommendations are in reasonable agreement with this ratio. Crowley et al. [287] have measured k at 247, 294, and 303 K, and the results are in agreement with the recommendations.

D19. OH + C_3H_8. There are many measurements of the rate coefficients at 298 K. In this evaluation we have considered only the direct measurements [Greiner [440], Tully et al. [1154], Droege and Tully [359], Schmidt et al. [1003], Baulch et al. [85], Bradley et al. [138], Abbatt et al. [1], Schiffman et al. [999], Talukdar et al. [1118], Anderson and Stephens [24] and Mellouki et al. [788]]. The 298 K value is the average of these ten studies. Greiner, Tully et al. [1151], Droege and Tully, Talukdar et al. and Mellouki et al. have measured the temperature dependence of this reaction. The recommended E/R was obtained from a linear least squares analysis of the data of Droege and Tully below 400 K and the data of Talukdar et al., Anderson and Stephens, and Mellouki et al. The A-factor was adjusted to reproduce k(298 K). This reaction has two possible channels, i.e., abstraction of the primary and the secondary H-atom. Therefore, non-Arrhenius behavior is exhibited over a wide temperature range, as shown by Tully et al. and Droege and Tully. The branching ratios were estimated from the latter study:

$$k_{primary} = 6.3 \times 10^{-12} \exp(-1050/T) \text{ cm}^3 \text{ molecule}^{-1} \text{ s}^{-1}$$
$$k_{secondary} = 6.3 \times 10^{-12} \exp(-580/T) \text{ cm}^3 \text{ molecule}^{-1} \text{ s}^{-1}$$

These numbers are in reasonable agreement with the older data of Greiner. The ratio of the rate coefficients for OH reactions with C_2H_6 and C_3H_8 has been measured by Finlayson-Pitts et al. [383]. Our recommendations are in reasonable agreement with this ratio.

D20. OH + CH_3CHO. There are six measurements of this rate coefficient at 298 K [Morris et al. [816], Niki et al. [863], Atkinson and Pitts [44], Kerr and Sheppard [592], Semmes et al. [1018], and Michael et al. [791]]. The recommended value of k(298 K) is the average of these measurements. Atkinson and Pitts, Semmes et al., and Michael et al. measured the temperature dependence of this rate coefficient and found it to exhibit a negative temperature dependence. The recommended E/R is the average value of these studies. The A-factor has been adjusted to yield the recommended value of k(298 K).

D21. OH + C_2H_5OH. The recommended value for k(298 K) is the average of those reported by Campbell et al. [178], Overend and Paraskevopoulos [888], Ravishankara and Davis [944], Cox and Goldstone [279], Kerr and Stocker [593], Wallington and Kurylo [1211], and Hess and Tully [485]. The value reported by Meier et al. is nearly a factor of two lower than that recommended here. The recommended value of E/R was obtained by using the data of Wallington and Kurylo, and Hess and Tully. The A-factor has been adjusted to yield the recommended value of k(298 K). At atmospheric temperatures, H-atom abstraction from the CH_2 group is the dominant channel [Meier et al. [777], Hess and Tully [485]], leading to CH_3CHO and HO_2.

D22. OH + $CH_3C(O)OH$. The recommended k(298K) is the average of the values obtained by Dagaut et al. [297] and Singleton et al. [1047]. The earlier results of Zetzsch and Stuhl [1303] are lower than these values, but within the uncertainty of the recommended value. The temperature dependence has been studied by Dagaut et al., who observe a very slight increase in k with temperature between 298 and 440 K and by Singleton et al., who observe a significant decrease with increase in temperature between 298 and 446 K. Further, Singleton et al. observe that the Arrhenius plot is curved. While Dagaut et al. observed that the acetic acid dimer reacts twice as fast as the monomer, Singleton et al. found the dimer to be essentially unreactive toward OH! The latter observations are consistent with the mechanism for the OH + HC(O)OH reaction, which is discussed in the note for that reaction. It is also consistent with the decrease in reactivity upon D substitution on the carboxylic site and no change upon substitution on the methyl group (Singleton et al. [1047]. Thus, there is some uncertainty as to the T dependence and the reaction mechanism. Here we recommend a slightly negative T dependence, but with an uncertainty that encompasses both the studies. The A factor and E/R suggest that this reaction may not be a simple metathesis reaction. Based on the analogy with OH + HC(O)OH reaction and the evidence of Singleton et al., the products are expected to be mostly $CH_3C(O)O + H_2O$. In the atmosphere, $CH_3C(O)O$ is expected to give $CH_3 + CO_2$.

D23. OH + $CH_3C(O)CH_3$. The rate coefficient for this reaction has been measured at temperatures close to 298 K by Cox et al. [277], Zetzsch [1302], Chiorboli et al. [214], Kerr and Stocker [593], Wallington and Kurylo [1212], and Bauerle et al.[84] The 298 K value was derived from the results of Zetzsch, Kerr and Stocker, Wallington and Kurylo, and Bauerle et al. Cox reported only an upper limit of $<5 \times 10^{-13}$ cm^3 $molecule^{-1}$ s^{-1}, which is consistent with this recommendation. The primary aim of Chiorboli et al. was to examine the atmospheric degradation of styrene, which produces acetone. They employed a relative rate measurement and reported a value of k(298 K) that is almost 3 times faster than the recommended value. Because of possible complications in their system, we have not included their results in arriving at the recommended value. Only Wallington and Kurylo and Bauerle et al. have reported k as a function of temperature; both these studies directly measured the rate constant using the pulsed photolysis method. Their results are in good agreement, and the recommended temperature dependence is based on these two studies.

D24. OH + CH_3CN. This rate coefficient has been measured as a function of temperature by Harris et al. [465] between 298 and 424 K, Kurylo and Knable [645] between 250 and 363 K, Rhasa [968] between 295 and 520 K, and Hynes and Wine [533] between 256 and 388 K. In addition, the 298 K value has been measured by Poulet et al. [927]. The 298 K results of Harris et al. are in disagreement with all other measurements and therefore have not been included. The recommended 298 K value is a weighted average of all other studies. The temperature dependence was computed using the results of Kurylo and Knable, the lower temperature values (i.e., 295-391 K) of Rhasa, and the data of Hynes and Wine. Three points are worth noting: (a) Rhasa observed a curved Arrhenius plot even in the temperature range of 295 to 520 K, and therefore extrapolation of the recommended expression could lead to large errors; (b) Hynes and Wine observed a pressure dependent increase of k(298 K) that levels off at about 1 atmosphere, and this observation is contradictory to the results of other investigations; (c) Hynes and Wine have carried out extensive pressure, temperature, O_2 concentration, and isotope variations in this reaction. Hynes and Wine postulate that the reaction proceeds via addition as well as abstraction pathways. They observe OH regeneration in the presence of O_2. The recommended k(298 K) and E/R are applicable for only lower tropospheric conditions. Because of the unresolved questions of pressure dependence and reaction mechanism, the recommended value may not be applicable under upper tropospheric and stratospheric conditions.

D25. OH + CH_3ONO_2. The rate coefficient for this reaction at 298 K has been measured by Kerr and Stocker [593], Nielsen et al. [858], Gaffney et al. [404], and Talukdar et al. [1117]. Nielsen et al. used both a relative rate technique and a direct method (the pulsed radiolysis-UV absorption method) to measure this rate constant, while Kerr used only a relative rate method. The results of Kerr and Stocker and of Nielsen et al. are a factor of ten higher than those of Gaffney et al. and Talukdar et al. Gaffney et al. carried out a flow tube measurement while Talukdar et al. used the pulsed photolysis method. There are no obvious reasons for the reported differences. Talukdar et al. have carried out a large number of checks to see if the difference could be due to the regeneration of OH via secondary reactions, effects of bath gas pressure, and formation of an adduct that could undergo further reaction in the presence of oxygen. They concluded that none of these factors affected their measured value. The lower value of Talukdar et al. could not be due to the presence of reactive impurities. Further, their measured temperature dependence of the rate constant, variation of the rate constant with the length of the hydrocarbon chain (i.e., in CH_3ONO_2, $C_2H_5ONO_2$, and $C_3H_7ONO_2$), variation with

isotopic substitution in the hydroxyl radical (OH, ^{18}OH and OD) and methyl nitrate (CH_3ONO_2 and CD_3ONO_2) are all consistent with this reaction proceeding via an H-atom abstraction pathway. Lastly, the values measured by Talukdar et al. and Gaffney et al. are consistent with the predictions of Atkinson and Aschmann[1989], who assumed an H-atom abstraction pathway. However, it is very puzzling that the relative rate measurements of both Kerr and Stocker and of Nielsen et al. are so different; the large uncertainty reflects this concern. Measurements of this rate constant will be very beneficial.

The temperature dependence of the rate coefficient has been measured by Nielsen et al, and by Talukdar et al. While Nielsen et al. report a negative activation energy, Talukdar et al. report a positive value. Because of the extensive tests carried out by Talukdar et al., as noted above, the temperature dependence measured by them are recommended here, with a large uncertainty. A thorough investigation of the temperature dependence of this reaction and the identification of the products of the reaction are needed.

D26. OH + $CH_3C(O)O_2NO_2$ (PAN). This reaction has been studied by four groups, Winer et al. [1271], Wallington et al. [1198], Tsalkani et al. [1142], and Talukdar et al. [1115]. Winer et al. obtained only an upper limit for the rate coefficient. Tsalkani et al. noted that their system was very ill-behaved and obtained a value of k(298 K) that is a factor of ~2 lower than that obtained by Wallington et al. The pulsed photolysis study of Wallington et al. yielded consistent results, but PAN was not directly measured and photodissociation of H_2O in the vacuum UV, where PAN absorbs strongly, was used as the OH source. The recent study of Talukdar et al. [1115] yielded much lower rate coefficients. These investigators measured the PAN concentration directly in their system, minimized secondary reactions due to the photodissociation of PAN, and carried out extensive tests for decomposition of PAN, impurities, and secondary reactions. The recommended upper limit is a factor two higher than the highest value measured by Talukdar et al. at 298 K and at 272 K. The quoted upper limit is expected to be valid at all atmospheric temperatures. The products of the reaction are not known. Further measurements of the rate coefficients and information on the reaction pathways are needed.

D27. OH + $C_2H_5ONO_2$. The rate constant for this reaction at 298 K has been measured by Kerr and Stocker [593], Nielsen et al. [858], and Talukdar et al. [1117]. As in the case of the reaction of OH with CH_3ONO_2, the results of Kerr and Stocker and of Nielsen et al. are larger (by a factor of 3) than those of Talukdar et al. The reasons for the differences are not clear. Because of the exhaustive tests carried out (see the note for the OH + CH_3ONO_2 reaction), the values of Talukdar et al. are recommended, with a large uncertainty. Nielsen et al. and Talukdar et al. have measured the rate constant as a function of temperature. While Talukdar et al. observe a small positive activation energy, Nielsen et al. report a negative activation energy. Talukdar et al. note that the rate coefficient for this reaction does not strictly follow Arrhenius behavior, consistent with the abstraction of both the primary and the secondary H atoms. The recommended value was obtained by fitting the rate coefficients measured by Talukdar et al. at $T \leq 298$ K. The large uncertainty reflects the discrepancies between the results of Talukdar et al. and of Nielsen et al. A thorough investigation of this reaction is needed.

D28. HO_2 + CH_2O. There is sufficient evidence to suggest that HO_2 adds to CH_2O [Su et al. [1096, 1098], Veyret et al. [1180], Zabel et al. [1288], Barnes et al. [67], and Veyret et al. [1179]]. The recommended k(298 K) is the average of values obtained by Su et al. [1096], Veyret et al. [1180], and Veyret et al. [1179]. The temperature dependence observed by Veyret et al. [1179] is recommended. The value reported by Barnes et al. at 273 K is consistent with this recommendation. The adduct HO_2•CH_2O seems to isomerize to $HOCH_2OO$ reasonably rapidly and reversibly. There is a great deal of discrepancy between measured values of the equilibrium constants for this reaction.

D29. HO_2 + CH_3O_2. The rate coefficient at 298 K has been measured by Cox and Tyndall [285, 286], Moortgat et al. [810], McAdam et al. [770], Kurylo et al. [643], Jenkin et al. [559], and Lightfoot et al. [710]. In all the studies, except that of Jenkin et al., both CH_3O_2 and HO_2 have been monitored via UV absorption. Jenkin et al. used IR absorption of HO_2 and UV absorption of CH_3O_2 to obtain the rate constants. Because of overlapping absorption spectra of CH_3O_2 and HO_2 and the unavoidable occurrence of the CH_3O_2 + CH_3O_2 and HO_2 + HO_2 reactions along with the CH_3O_2 + HO_2 reaction, the extraction of the rate coefficient requires modelling of the system and reliance on the UV cross sections of both CH_3O_2 and HO_2. The agreement among the values of k obtained by all these groups is not very good. Part of the difference is definitely due to different values of the UV cross sections used in various studies. Contribution from secondary reactions may also be partly responsible for the differences. Unfortunately, it is not feasible to correct the reported values to a common set of cross sections. Therefore, the average of rate coefficients from

Cox and Tyndall, Moortgat et al., McAdam et al., Kurylo and Wallington, Jenkin et al., and Lightfoot et al. are used to obtain the recommended value. Cox and Tyndall, Dagaut et al. [296], and Lightfoot et al. have measured the temperature dependence of this rate coefficient. The recommended E/R was obtained by plotting ln ($k_{(T)}/k_{298}$) vs 1/T from these studies. This method looks for only the E/R value in each data set. The A-factor was calculated to reproduce k(298 K). The studies by the above groups have indicated that this reaction is not affected by pressure or nature of the buffer gas. Jenkin et al. suggest that a substantial fraction of the reaction may yield $H_2O + CH_2O + O_2$ rather than $CH_3OOH + O_2$. The lower value of k measured by monitoring CH_3OOH formation by Moortgat et al. and Kan et al. [586] is consistent with the occurrence of the second channel and the lower value of k measured when CH_3OOH product yield is monitored. However, the recent work of Wallington [1194] indicates that CH_3OOH is the dominant (>92%), if not the only, product. Further work on measurement of k without reliance on UV absorption cross sections and branching ratios where CH_2O is monitored is needed.

D30. $HO_2 + C_2H_5O_2$. The recommended value is the weighted average of those measured by Cattell et al. [192], Dagaut et al. [295], Fenter et al. [376], and Maricq and Szente [754]. In all experiments the rate coefficient was obtained by modeling the reaction system. Also, the calculated rate coefficients depended on the UV absorption cross sections of both $C_2H_5O_2$ and HO_2. The absorption cross section of $C_2H_5O_2$ is not well-defined. The value reported by Dagaut et al. would be ~30% higher if the cross sections used by Maricq and Szente were used. The recommended E/R is that measured by Dagaut et al., Fenter et al., and Maricq and Szente. Wallington and Japar [1210] have shown that $C_2H_5O_2H$ and O_2 are the only products of this reaction.

D31. $HO_2 + CH_3C(O)O_2$. The recommendation is based on Moortgat et al. [812], the only measurement of this rate coefficient. They measured UV absorption at 210 and 260 nm as a function of time in a flash photolysis system and fitted the observed 210 and 260 nm absorption temporal profiles to a set of reactions involving $CH_3C(O)O_2$, CH_3O_2, and HO_2. The recommended temperature dependence is also from this study. The rate coefficient obtained in such a measurement is dependent on the UV absorption cross sections of all the absorbers and all their reactions. Hence, any change in these parameters can change the calculated rate coefficient. The recommended k and E/R are consistent with those for similar peroxy radical reactions. Moortgat et al. report two possible channels for this reaction:

$$CH_3C(O)O_2 + HO_2 \rightarrow CH_3C(O)OOH + O_2 \qquad (a)$$

$$CH_3C(O)O_2 + HO_2 \rightarrow CH_3C(O)OH + O_3 \qquad (b)$$

At 298 K, Niki et al. [870] measured k_b/k to be 0.25 which agrees reasonably with 0.33 measured by Moortgat et al. Horie and Moortgat [504] report the temperature dependence of the branching ratio to be $k_a/k_b = 330 \exp(-1430/T)$.

D32. $NO_3 + CO$. The upper limit is based on the results of Hjorth et al. [494], who monitored isotopically labeled CO loss in the presence of NO_3 by FTIR. Burrows et al. [168] obtained an upper limit of 4×10^{-16} cm^3 $molecule^{-1}$ s^{-1}, which is consistent with the Hjorth et al. study. Products are expected to be $NO_2 + CO_2$, if the reaction occurs.

D33. $NO_3 + CH_2O$. There are three measurements of this rate coefficient at 298 K: Atkinson et al. [46], Cantrell et al. [188], and Hjorth et al. [495]. The value reported by Atkinson et al. [46], $k = (3.23 \pm 0.26) \times 10^{-16}$ cm^3 $molecule^{-1}$ s^{-1}, is corrected to 5.8×10^{-16} cm^3 $molecule^{-1}$ s^{-1} to account for the different value of the equilibrium constant for the $NO_3 + NO_2 \leftrightarrow N_2O_5$ reaction that was measured subsequent to this study by the same group using the same apparatus. This correction is in accordance with their suggestion [Tuazon et al. [1150]]. The values reported by Cantrell et al. and Hjorth et al., $k = 6.3 \times 10^{-16}$ cm^3 $molecule^{-1}$ s^{-1} and $(5.4 \pm 1.1) \times 10^{-16}$ cm^3 $molecule^{-1}$ s^{-1}, respectively, are in good agreement with the corrected value of Atkinson et al. The recommended value is the average of these three studies. Cantrell et al. have good evidence to suggest that HNO_3 and CHO are the products of this reaction. The temperature dependence of this rate coefficient is unknown, but comparison with the analogous $NO_3 + CH_3CHO$ reaction suggests a large E/R.

D34. $NO_3 + CH_3CHO$. There are four measurements of this rate constant: Morris and Niki [815], Atkinson et al. [46], Cantrell et al. [182], and Dlugokencky and Howard [341]. The value reported by Atkinson et al. [46], k = (1.34±0.28) x 10^{-15} cm^3 $molecule^{-1}$ s^{-1}, is corrected to 2.4 x 10^{-15} cm^3 $molecule^{-1}$ s^{-1} as discussed for the $NO_3 + H_2CO$ reaction above and as suggested by Tuazon et al. [1150]. The recommended value is the average of the values obtained by Atkinson et al., Cantrell et al., and Dlugokencky and Howard. The results of Morris and Niki agree with the recommended value when their original data is re-analyzed using a more recent value for the equilibrium constant for the reaction $NO_2 + NO_3 \leftrightarrow N_2O_5$ as shown by Dlugokencky and Howard. Dlugokencky and Howard have studied the temperature dependence of this reaction. Their measured value of E/R is recommended. The A-factor has been calculated to yield the k(298K) recommended here. Morris and Niki, and Cantrell et al. observed the formation of HNO_3 and PAN in their studies, which strongly suggests that HNO_3 and CH_3CO are the products of this reaction.

D35. $CH_3 + O_2$. This bimolecular reaction is not expected to be important based on the results of Baldwin and Golden [54], who found k < 5 x 10^{-17} cm^3 $molecule^{-1}$ s^{-1} for temperatures up to 1200 K. Klais et al. [613] failed to detect OH (via $CH_3 + O_2 \rightarrow CH_2O + OH$) at 368 K and placed an upper limit of 3 x 10^{-16} cm^3 $molecule^{-1}$ s^{-1} for this rate coefficient. Bhaskaran et al. [109] measured k = 1x10^{-11} exp (-12,900/T) cm^3 $molecule^{-1}$ s^{-1} for 1800 < T < 2200 K. The latter two studies thus support the results of Baldwin and Golden. Studies by Selzer and Bayes [1017] and Plumb and Ryan [920] confirm the low value for this rate coefficient. Previous studies of Washida and Bayes [1227] are superseded by those of Selzer and Bayes. Plumb and Ryan have placed an upper limit of 3 x 10^{-16} cm^3 $molecule^{-1}$ s^{-1} based on their inability to find HCHO in their experiments. A study by Zellner and Ewig [1298] suggests that this reaction is important at combustion temperature but is unimportant for the atmosphere.

D36. $CH_3 + O_3$. The recommended A-factor and E/R are those obtained from the results of Ogryzlo et al. [876]. The results of Simonaitis and Heicklen [1034], based on an analysis of a complex system, are not used. Washida et al. [1226] used $O + C_2H_4$ as the source of CH_3. Studies on $O + C_2H_4$ reaction (Schmoltner et al. [1004], Kleinermanns and Luntz [615], Hunziker et al. [525], and Inoue and Akimoto [542]) have shown this reaction to be a poor source of CH_3. Therefore, the results of Washida et al. are also not used.

D37. $HCO + O_2$. The value of k(298 K) is the average of the determinations by Washida et al. [1228], Shibuya et al. [1022], Veyret and Lesclaux [1178], and Langford and Moore [659]. There are three measurements of k where HCO was monitored via the intracavity dye laser absorption technique (Reilly et al. [964], Nadtochenko et al. [822], and Gill et al. [420]). Even though there is excellent agreement between these three studies, they yield consistently lower values than those obtained by other techniques. There are several possible reasons for this discrepancy: (a) The relationship between HCO concentration and laser attenuation in an intracavity absorption experiment might not be linear, (b) there could have been depletion of O_2 in the static systems that were used (as suggested by Veyret and Lesclaux), and (c) these experiments were designed more for the study of photochemistry than kinetics. Therefore, these values are not included in obtaining the recommended value. The recommended temperature dependence is essentially identical to that measured by Veyret and Lesclaux. We have expressed the temperature dependence in an Arrhenius form even though Veyret and Lesclaux preferred a T^n form (k = 5.5 x 10^{-11} $T^{-(0.4\pm0.3)}$ cm^3 $molecule^{-1}$ s^{-1}).

D38. $CH_2OH + O_2$. The rate coefficient was first measured directly by Radford [938] by detecting the HO_2 product in a laser magnetic resonance spectrometer. The wall loss of CH_2OH could have introduced a large error in this measurement. Radford also showed that the previous measurement of Avramenko and Kolesnikova [50] was in error. Wang et al. [1218] measured a value of 1.4 x 10^{-12} cm^3 $molecule^{-1}$ s^{-1} by detecting the HO_2 product. Recently, Dobe et al. [344], Grotheer et al. [442], Payne et al. [904], Grotheer et al. [443] and Nesbitt et al. [840] have measured k(298 K) to be close to 1.0 x 10^{-11} cm^3 $molecule^{-1}$ s^{-1} under conditions where wall losses are small. This reaction appears to exhibit a very complex temperature dependence. Based on the recent data of Grotheer et al. [443] and Nesbitt et al. [840], k appears to increase from 200 K to approximately 250 K in an Arrhenius fashion, levels off at approximately 300 K, decreases from 300 to 500 K, and finally increases as temperature is increased. This complex temperature dependence is believed to be due to the formation of a $CH_2(OH)•O_2$ adduct which can isomerize to $CH_2O•HO_2$ or decompose to reactants. The $CH_2O•HO_2$ isomer can also decompose to CH_2O and HO_2 or reform the original adduct. At temperatures less than 250 K, the data of Nesbitt et al. suggests an E/R value of ~1700 K. For atmospheric purposes, the value E/R = 0 is appropriate.

D39. $CH_3O + O_2$. The recommended value for k(298 K) is the average of those reported by Lorenz et al. [727] and Wantuck et al. [1221]. The recommended E/R was obtained using the results of Gutman et al. [444] (413 to 608 K), Lorenz et al. [727] (298 to 450 K), and Wantuck et al. [1221] (298 to 498 K). These investigators have measured k directly under pseudo-first order conditions by following CH_3O via laser induced fluorescence. Wantuck et al. measured k up to 973 K and found the Arrhenius plot to be curved; only their lower temperature data are used in the fit to obtain E/R. The A factor has been adjusted to reproduce the recommended k(298 K). The previous high temperature measurements [Barker et al. [58] and Batt and Robinson [82]] are in reasonable agreement with the derived expression. This value is consistent with the 298 K results of Cox et al. [276], obtained from an end product analysis study, and with the upper limit measured by Sanders et al. [992]. The A-factor appears low for a hydrogen atom transfer reaction. The reaction may be more complicated than a simple abstraction. At 298 K, the products of this reaction are HO_2 and CH_2O, as shown by Niki et al. [866].

D40. $CH_3O + NO$. The reaction of CH_3O with NO proceeds mainly via addition to form CH_3ONO (Batt et al. [81], Wiebe and Heicklen [1250], Frost and Smith [402], and Ohmori et al. [877]). However, a fraction of the energized CH_3ONO adducts decompose to $CH_2O + HNO$, and appear to be a bimolecular channel. This reaction has been investigated recently by direct detection of CH_3O via laser-induced fluorescence [Zellner [1296]; Frost and Smith [402]; Ohmori et al. [877]]. The previous end-product studies (Batt et al. [81], Wiebe and Heicklen [1250]) are generally consistent with this conclusion. Since the fraction of the CH_3ONO adduct that falls apart to $CH_2O + HNO$ decreases with increases in pressure and decreases in temperature, it is not possible to derive a "bimolecular" rate coefficient. A value of $k < 8 \times 10^{-12}$ cm^3 $molecule^{-1}$ s^{-1} can be deduced from the work of Frost and Smith [402] and Ohmori et al.[877] for lower atmospheric conditions.

D41. $CH_3O + NO_2$. The reaction of CH_3O with NO_2 proceeds mainly via the formation of CH_3ONO_2. However, a fraction of the energized adducts fall apart to yield $CH_2O + HNO_2$. The bimolecular rate coefficient reported here is for the fraction of the reaction that yields CH_2O and HNO_2. It is not meant to represent a bimolecular metathesis reaction. The recommended value was derived from the study of McCaulley et al.[771] and is discussed in the section on association reactions.

D42. $CH_3O_2 + O_3$. There are no direct laboratory studies of this reaction. The quoted upper limit is based on the evidence obtained by Simonaitis and Heicklen [1034]. A much lower upper limit has been deduced by Monks et al. [808] by observing the decay of the peroxy radical in a remote clean troposphere at night.

D43. $CH_3O_2 + CH_3O_2$. This reaction has been studied at 298 K by Hochanadel et al. [496], Parkes [897], Anastasi et al. [21], Kan et al. [588], Sanhueza et al. [994], Cox and Tyndall [286], Sander and Watson [988], Basco and Parmar [80], McAdam et al. [770], Kurylo and Wallington [651], Jenkin et al. [559], Lightfoot et al. [708], and Simon et al. [1030]. All the above determinations used UV absorption techniques to monitor CH_3O_2 and hence measured k/σ, where σ is the absorption cross section for CH_3O_2 at the monitored wavelength. Therefore, the derived value of k critically depends on the value of σ that is used. Even though there is good agreement among the measured values of k/σ, there are large discrepancies (approximately a factor of 2) among the values of σ measured by Hochanadel et al., Parkes, Sander and Watson, Adachi et al. [6], McAdam et al., Kurylo et al. [652], and Simon et al. To obtain the recommended k value at 298 K, an average value of σ at 250 nm, 4.0×10^{-18} cm^2 (obtained by averaging the results of Sander and Watson, Kurylo and Wallington as amended in Dagaut and Kurylo [294], Lightfoot et al., and Jenkin et al.) was chosen. The value of k(298 K) was derived using this value of σ and the weighted average value of k/σ at 250 nm measured by Cox and Tyndall, Jenkin et al., Sander and Watson, McAdam et al., Kurylo and Wallington, Lightfoot et al., and Simon et al. The recommended temperature dependence was calculated by using the results of Sander and Watson, Kurylo and Wallington, Lightfoot et al. (at temperatures between 228 and 420 K), and Jenkin and Cox [558], using a value of σ independent of T. It has been recently shown by Lightfoot and Jemi-Alade [707] that σ is essentially invariant with temperature. It is not clear whether the above procedure of recalculating k using an average value of σ is valid. Therefore, the quoted error limits encompass the values of k calculated by various authors. This reaction has four possible sets of products, i.e.,

$CH_3O_2 + CH_3O_2 \rightarrow 2CH_3O + O_2$	k_a ; $k_a/k = 0.3$ at 298 K
$CH_3O_2 + CH_3O_2 \rightarrow CH_2O + CH_3OH + O_2$	k_b ; $k_b/k = 0.6$ at 298 K
$CH_3O_2 + CH_3O_2 \rightarrow CH_3OOCH_3 + O_2$	k_c ; $k_c/k = 0.1$ at 298 K
$CH_3O_2 + CH_3O_2 \rightarrow CH_3OOH + CH_2O_2$	k_d ; $k_d/k = 0.0$ at 298 K

FTIR studies by Kan et al. [586] and Niki et al. [866] are in reasonable agreement on the branching ratios at 298 K; $k_a/k \sim 0.35$, $k_b/k \sim 0.55$. The recent study by Lightfoot et al. also yields $k_a/k \cong 0.35$ while Horie et al. [503] obtain 0.30. The last two groups see a large decrease of k_a/k with decreasing temperature, which may be expressed as $(k_a/k) = 1/[1 + \{\exp(1130/T)\}/19]$. The results of Ballod et al. [57] are in fair agreement with this trend. Channel (d) was suggested by Nangia and Benson [824], but there are no experimental data to suggest its occurrence [Khursan et al. [605]]. Because of the existence of multiple pathways, the temperature dependence of k may be complex. Further work is required on both the temperature dependence and the variation of branching ratios with temperature. It should be noted that the recommended value of k depends on the branching ratios used for correcting for secondary reactions.

D44. $CH_3O_2 + NO$. The value of k(298 K) was derived from the results of Sander and Watson [987], Ravishankara et al. [949], Cox and Tyndall [286], Plumb et al. [923], Simonaitis and Heicklen [1036], Zellner et al. [1299] and Villalta et al. [1181]. Values lower by more than a factor of two have been reported by Adachi and Basco [4] and Simonaitis and Heicklen [1035]. The former direct study was probably in error because of interference by CH_3ONO formation. The results of Simonaitis and Heicklen [1035] and Plumb et al. [922] are assumed to be superseded by their more recent values. Masaki et al. [766]report a value of $(1.12\pm0.14) \times 10^{-11}$, which was measured using a flow tube equipped with a photoionization mass spectrometer. They encountered complications due to detection of other products and deduced that the lower limit for the rate constant was 9.8×10^{-12}. Even though this lower limit overlaps the recommended value, it was not used in deriving the recommendation. Ravishankara et al., Simonaitis and Heicklen, and Villalta et al. have measured the temperature dependence of k over limited temperature ranges. The recommended A-factor and E/R were obtained by a weighted least squares analysis of the data from these three studies. Ravishankara et al. find that the reaction channel leading to NO_2 accounts for at least 80% of the reaction. Zellner et al. have measured the yield of CH_3O to be 1.0 ± 0.2. These results, in conjunction with the indirect evidence obtained by Pate et al. [900], confirm that NO_2 formation is the major reaction path, at least at low pressures.

D45. $CH_3O_2 + CH_3C(O)O_2$. The reaction has been investigated by Addison et al. [7], Moortgat et al. [810], and Moortgat et al. [811] and Maricq and Szente [755] using UV absorption in conjunction with investigations of the $CH_3C(O)O_2$ self-reaction. The rate coefficient obtained by Addison et al. is a factor of ~5 lower than those measured by Moortgat et al. [810]. It is believed that this lower value is due to the use of low UV absorption cross sections, which were poorly known at the time of this study [Moortgat et al. [811]]. The recommended value is derived from Moortgat et al. and Maricq and Szente. The temperature dependence of k has been studied by Moortgat et al. [811] and more extensively by Maricq and Szente. The recommended value is derived from these studies.

The reaction has two pathways:

$$CH_3C(O)O_2 + CH_3O_2 \rightarrow CH_3C(O)O + CH_3O + O_2 \qquad \text{(a)}$$

$$\rightarrow CH_3C(O)OH + CH_2O + O_2 \qquad \text{(b)}$$

Horie and Moortgat [504] have measured the branching between these two channels to be $k_a/k_b = 2.2 \times 10^6 \exp(-3820/T)$. This report is expected to supersede the earlier branching ratio given by Moortgat et al. [811]. Roehl et al. [971] report that $k_a/k_b = 0.9$ at 298 K. However, Maricq and Szente show evidence that only channel b is operative below 298 K. Further work on the branching ratios for the products are needed.

D46. $C_2H_5 + O_2$. This is a complex reaction that involves the formation of an $C_2H_5O_2$ adduct, which can either be stabilized by collisions or fall apart to HO_2 and C_2H_4 (Wagner et al. [1187], Bozzelli and Dean [137], and Kaiser et al. [583]). The fraction of the energized adducts that fall apart to give HO_2 and C_2H_4 will decrease with increasing pressure and decreasing temperature, i.e., as the $C_2H_5O_2$ formation increases. The C_2H_4 formation channel cannot be separated from the addition reaction. Yet, we recommend a conservative upper limit as a guide to the extent of this reaction. This upper limit is applicable only for lower atmospheric pressure and temperature conditions.

D47. $C_2H_5O + O_2$. The recommendation is based on the pulsed laser photolysis studies of Gutman et al. [444] and Hartmann et al. [467]. In both these studies, removal of C_2H_5O in an excess of O_2 was directly monitored via laser induced fluorescence. Gutman et al. measured k at only two temperatures, while Hartmann et al. measured k at 5 temperatures between 295 and 411 K. The E/R is from Hartmann et al. The 298 K value deduced from an indirect study by Zabarnick and Heicklen [1285] is in reasonable agreement with the recommended value.

D48. $C_2H_5O_2 + C_2H_5O_2$. k(298 K) has been studied by Adachi et al. [5], Anastasi et al. [22], Munk et al. [819], Cattell et al. [192], Anastasi et al. [20], Wallington et al. [1204], Bauer et al. [83], and Fenter et al. [376]. All the above determinations used only UV absorption to monitor $C_2H_5O_2$ and hence measured k/σ, where σ is the absorption cross section of $C_2H_5O_2$ at the monitoring wavelength. These investigators also measured the σ that was used in evaluating the rate coefficient. There are large discrepancies in the measured values of σ. For this evaluation, we have used the cross sections recommended here and recalculated the values of k from each investigation. The recommended k is based on the results of Cattell et al., Wallington et al., Bauer et al., and Fenter et al. In all these experiments the observed rate coefficient is higher than the true rate coefficient because of secondary reactions involving HO_2. HO_2 is formed by the reaction of CH_3CH_2O with O_2 and it reacts with $C_2H_5O_2$ to enhance the observed rate coefficient (see Wallington et al. [1205] or Lightfoot et al. [706] for further discussion). Based on product branching ratios discussed below, which determine the magnitude of the necessary correction, the recommended rate coefficient is 0.6 times the average observed rate coefficient. The recommended value of E/R was obtained from the results of Anastasi et al., Wallington et al., Anastasi et al., Cattell et al., Bauer et al. and Fenter et al. The observed products (Niki et al. [867]), suggest that at 298K the channel to yield 2 $C_2H_5O + O_2$ accounts for about 60% of the reaction; the channel to yield $CH_3CHO + C_2H_5OH + O_2$ accounts for about 40% of the reaction; and the channel to yield $C_2H_5O_2C_2H_5 + O_2$ accounts for less than 5% of the reaction. These branching ratios were used above to obtain the true rate coefficient from the observed rate coefficient.

D49. $C_2H_5O_2 + NO$. The recommended k(298) is obtained from the results of Plumb et al. [924], Sehested et al. [1015], Daele et al. [293], Eberhard and Howard [361], and Maricq and Szente [755]. The value reported by Adachi and Basco [4], which is a factor of three lower than the recommended value, was not used. The rate coefficient for the $CH_3O_2 + NO$ reaction measured by Basco and co-workers [Adachi et al. [5]], using the same apparatus, is also much lower than the value recommended here. The recommended temperature dependence is derived from Eberhardt and Howard and Maricq and Szente, which are in good agreement.

D50. $CH_3C(O)O_2 + CH_3C(O)O_2$. This reaction has been studied by Addison et al. [7], Basco and Parmar [80], Moortgat et al. [811] Maricq and Szente [755], and Roehl et al. [971], using UV absorption techniques. The recommended value is obtained from the data of Moortgat et al., Maricq and Szente, and Roehl et al. As pointed out by Moortgat et al., the six times lower value of k obtained by Addison et al. is likely due to the use of incorrect UV absorption cross sections for the peroxyradical. The k obtained by Basco and Parmar is ~2 times lower than the recommended value. This discrepancy is possibly due to neglecting the UV absorption of CH_3O_2 and other stable products in their data analysis [Moortgat et al., Maricq and Szente]. The recommended temperature dependence was calculated from the data of Moortgat et al. and Maricq and Szente. Addison et al. reported the formation of O_3, which was attributed to the reaction channel which produces $CH_3C(O)OCH_3C(O) + O_3$. Moortgat et al. place an upper limit of 2% for this channel. The main products of this reaction appear to be $CH_3C(O)O + O_2$. The $CH_3C(O)O$ radicals rapidly decompose to give CH_3 and CO_2.

D51. $CH_3C(O)O_2 + NO$. This rate coefficient has been directly measured as a function of temperature by Villalta etal. [1182] and Maricq and Szente [755], using flow tube-chemical ionization mass spectrometry and laser photolysis-UV/IR absorption spectroscopy, respectively. The agreement between the two groups is reasonable. The precision of the data of Villalta et al was excellent. The k(298) and the Arrhenius parameters were derived from these two studies. The earlier investigations of this reaction were relative to that for the addition reaction of $CH_3C(O)O_2$ with NO_2 [Cox et al. [270], Cox and Roffey [282] , Hendry and Kenley [480], Kirchner et al. [608], and Tuazon et al. [1146]]. The current recommendations for the reactions of $CH_3C(O)O_2$ with NO and NO_2 are consistent with the ratio of these two rate constants measured by Zabel et al. [1287]. Hence, our recommendations are consistent with the rate coefficient for the thermal decomposition of PAN as recommended here. The products of the reaction are probably $CH_3C(O)O$ and NO_2.

E1. O + FO. The recommended value is based on results of the room temperature study of Bedzhanyan et al. [101] The temperature dependence of the rate constant is expected to be small, as it is for the analogous ClO reaction.

E2. O + FO_2. No experimental data. The rate constant for such a radical-atom process is expected to approach the gas collision frequency, and is not expected to exhibit a strong temperature dependence.

E3. OH + CH_3F (HFC-41). Relative rate data of DeMore [329] are in good agreement with the JPL 94-26 recommendation, which is based on results of Hsu and DeMore [519], Schmoltner et al. [1005], Nip et al [872], and Howard and Evenson [511].

E4. OH + CH_2F_2 (HFC-32). The preferred rate expression is derived from the results of Schmoltner et al. [1005] and Hsu and DeMore [519] and from the data of Jeong and Kaufman [567], Talukdar et al. [1114] below 400 K and the room temperature data of Howard and Evenson [511] and Nip et al. [872].

E5. OH + CHF_3 (HFC-23). The recommended value is based on the absolute rate measurements by Schmoltner et al. [1005] , the relative rate measurements of Hsu and DeMore [519], the room temperature points of Howard and Evenson [511], and the 387 K and 410 K points of Jeong and Kaufman [567].

E6. OH + CF_3OH. New Entry. There are no measurements of the rate coefficient of this reaction. The recommendation is based upon the recommended limit for the reverse reaction rate coefficient and an estimated equilibrium constant. The thermochemistry of CF_3O and CF_3OH are taken from *ab initio* calculations (Montgomery et al. [809] and Schneider and Wallington [1006]) and laboratory measurements (Huey et al. [523]) to estimate ΔG°_{298} (OH + $CF_3OH \leftrightarrow CF_3O + H_2O$) to be about (+2±4) kcal mol^{-1}. In considering the large uncertainty in the free energy change, the estimated rate coefficient limit is based on the assumption that the reaction is approximately thermoneutral.

E7. OH + CH_3CH_2F (HFC-161). The recommended value is based on a fit to the temperature dependent data of Hsu and DeMore [519] and Schmoltner et al. [1005] and the room temperature result of Nip et al. [872]. Singleton et al. [1045] determined that 85 ± 3% of the abstraction by OH is from the fluorine substituted methyl group.

E8. OH + CH_3CHF_2 (HFC-152a). The relative rate data of Hsu and DeMore [519] agree with previous absolute data at high temperatures, but at lower temperatures fall below those data. However, Zellner (private communication, 1993) reports an absolute value for k (293 K) that is in good agreement with the relative rate data at that temperature. The recommended temperature dependence is from Hsu and DeMore. Room temperature value averages these new results with those of Nielsen [852], Gierczak et al. [416], Liu et al. [724], Howard and Evenson [510], Handwerk and Zellner [463], and Nip et al. [872].

E9. OH + CH_2FCH_2F (HFC-152). The preferred rate expression is derived by fitting an estimated temperature dependence to the room temperature data of Martin and Paraskevopoulos [762].

E10. OH + CH_3CF_3 (HFC-143a). The recommended rate expression is based on temperature-dependent data from Hsu and DeMore [519], Orkin et al. [881], and Talukdar et al. [1114], all of which are in good agreement.

E11. OH + CH_2FCHF_2 (HFC-143). The preferred rate expression is based on results of the relative rate study of Barry et al. [76] normalized to the value of the rate constant for the reference reaction (OH + CH_3CCl_3) recommended in this evaluation. The room temperature value of Martin and Paraskevopoulos [762] is in good agreement. The significantly higher values reported by Clyne and Holt [231] were not considered.

E12. OH + CH_2FCF_3 (HFC-134a). Absolute rate constant measurements by Orkin and Khamaganov [883] are in good agreement with previous data such as that of Gierczak et al. [416] and Liu et al. [724]. Relative rate measurements of DeMore [327], referenced to CH_4, CH_3CCl_3, and HFC-125, yield a rate constant that is slightly lower (10-20%) than these absolute measurements, but with approximately the same temperature dependence. Leu and Lee [687] report absolute rate constant measurements that are in excellent agreement with the relative rate measurements. The recommended value averages results of the new studies with those of earlier studies of Gierczak et al. [416] above 243 K, Liu et al. [724], the 270 K data of Zhang et al. [1304] and the room temperature data of Martin and Paraskevopoulos [762]. The data of Jeong et al. [565], Brown et al.

[144], and Clyne and Holt [231] were not considered. Data of Bednarek et al. [96] at 298 K are in good agreement with the recommendation.

E13. OH + CHF_2CHF_2 (HFC-134). The preferred rate expression is based on results of the relative rate study of DeMore [327]. The room temperature value of Clyne and Holt [231] is in good agreement.

E14. OH + CHF_2CF_3 (HFC-125). The preferred rate expression is derived from the temperature dependence data of Talukdar et al. [1114] and the room temperature data of Martin and Paraskevopoulos [762] and DeMore [327].

E15. OH + CH_3OCHF_2 (HFOC-152a). Based on data of Orkin et al. [884].

E16. OH + CF_3OCH_3 (HFOC-143a). Based on data of Hsu and DeMore [520] and Orkin et al. [884], which are in excellent agreement.

E17. OH + CF_2HOCF_2H (HFOC-134). Temperature-dependent expression based on the results of Hsu and DeMore [520]. The significantly higher measurements of Garland et al. [407] were not used in derivation of the preferred value.

E18. OH + CF_3OCF_2H (HFOC-125). Recommended value is based on results of the relative rate study of Hsu and DeMore [520]. The room temperature result of Zhang et al. [1308] is significantly higher.

E19. OH + $CF_3CH_2CH_3$ (HFC-263fb). Based on room temperature measurement of Nelson et al. [831].

E20. OH + $CHF_2CF_2CH_2F$ (HFC-245ca). The absolute rate constant results of Zhang et al. [1306] are about 40% higher at 298 K than the relative rate data (Hsu and DeMore [519]) but show a similar T-dependence. The recommended value averages results of these studies.

E21. OH + $CHF_2CHFCHF_2$ (HFC-245ea). Based on room temperature measurement of Nelson et al. [831].

E22. OH + CF_3CHFCH_2F (HFC-245eb). Based on room temperature measurement of Nelson et al. [831].

E23. OH + $CHF_2CH_2CF_3$ (HFC-245fa). The recommended room temperature value is the mean of the values reported by Orkin et al. [881] and Nelson et al. [831], which are in good agreement. The temperature dependence is from Orkin et al. The A-factor from that study has been adjusted to fit the recommended room temperature value.

E24. OH + $CF_3CF_2CH_2F$ (HFC-236cb). The preferred rate expression given is that for the reaction of OH with CF_3CH_2F (HFC-134a). These reactions are expected to have very similar Arrhenius parameters. This estimate is preferred over the results reported by Garland et al. [407], the only published experimental study. The A-factor reported in that study is much lower than expected.

E25. OH + $CF_3CHFCHF_2$ (HFC-236ea). Recommended value is based on the temperature-dependence data of Hsu and DeMore [519] by the relative rate method and the absolute study of Nelson et al. [831] at room temperature, which are in good agreement. The significantly higher values of Garland et al. [407] and Zhang et al. [1306] were not used.

E26. OH + $CF_3CH_2CF_3$ (HFC-236fa). Recommended value is based on results of the relative rate study of Hsu and DeMore [519] and the absolute rate study of Gierczak et al. [417]. The significantly higher results of Nelson et al. [831] and of Garland and Nelson [408], which superseded the earlier results of Garland et al. [408], were not used.

E27. OH + CF_3CHFCF_3 (HFC-227ea). Data of Nelson et al. [830], Zellner et al. [1297], and Zhang et al. [1306] are in good agreement for this compound. Relative rate studies of Hsu and DeMore [519] are in good agreement with the absolute studies. Recommended value is an average.

E28. OH + $CHF_2OCH_2CF_3$ (HFOC-245fa). Based on data of Orkin et al. [884].

E29. OH + $CF_3CH_2CF_2CH_3$ (HFC-365-mfc). There are data for this reaction by Mellouki et al. [789] and Barry et al. [74]. The recommended Arrhenius expression is from the relative rate study of Barry et al., normalized to the reference rate constant (OH + CH_3CCl_3) recommended in this evaluation.

E30. OH + $CF_3CH_2CH_2CF_3$ (HFC-356mff). Recommended value is based on the room temperature measurement of Nelson et al.[831], and the temperature-dependent data of Zhang et al. [1306].

E31. OH + $CF_3CF_2CH_2CH_2F$ (HFC-356mcf). Based on Nelson et al. [831].

E32. OH + $CHF_2CF_2CF_2CF_2H$ (HFC-338pcc). Recommended value is based on results of Schmoltner et al. [1005] and Zhang et al. [1307].

E33. OH + $CF_3CH_2CF_2CH_2CF_3$ (HFC-458mfcf). Based on Nelson et al. [831].

E34. OH + $CF_3CHFCHFCF_2CF_3$. (HFC-43-10mee). Data of Schmoltner et al. [1005] and Zhang et al. [1307] are in reasonable agreement at 298 K and show similar Arrhenius parameters. Recommended value average results of these studies.

E35. OH + $CF_3CF_2CH_2CH_2CF_2CF_3$ (HFC-55-10mcff). Based on Nelson et al. [831]. As expected, the rate constant is similar to that for $CF_3CH_2CH_2CF_3$.

E36. F + O_3. The recommended value is based on results of the room temperature study of Bedzhanyan et al. [100] and the temperature-dependent study of Wagner et al. [1191]. The value appears to be quite reasonable in view of the well-known reactivity of atomic chlorine with O_3.

E37. F + H_2. The value of k at 298 K seems to be well established with the results reported by Zhitneva and Pshezhetskii [1311], Heidner et al. [473, 474], Wurzberg and Houston [1281], Dodonov et al. [347], Clyne et al. [236], Bozzelli [136], Igoshin et al. [539], Clyne and Hodgson [229] and Stevens et al. [1080] being in excellent agreement (range of k being 2.3-3.0 x 10^{-11} cm^3 $molecule^{-1}$ s^{-1}). The preferred value at 298 K is taken to be the mean of the values reported in these references. Values of E/R range from 433-595 K (Heidner et al.; Wurzberg and Houston; Igoshin et al.; and Stevens et al.). The preferred value of E/R is derived from a fit to the data in these studies. The A-factor was chosen to fit the recommended room temperature value.

E38. F + H_2O. The recommended temperature-independent value is based on results reported in the study by Stevens et al. [1080] over the temperature range 240-373 K using a discharge flow system with chemical conversion of fluorine atoms to deuterium atoms and detection of the latter by resonanace fluorescence. This value is in excellent agreement with the room temperature results of Frost et al. [403] and Walther and Wagner [1215]. The latter authors in a limited temperature-dependent study reported an E/R value of 400 K. Although these data have not been included in the derivation of the preferred value, with the exception of the one low temperature data point, they are encompassed within the indicated uncertainty limits.

E39. F + HNO_3. The recommendation is based on results of the temperature-dependent study of Wine et al. [1269] and the room temperature results of Mellouki et al. [781], Rahman et al. [940] and Becker et al. [87]. The values at room temperature are in good agreement. The study of Wine et al. [1269] was over the temperature range 260-373 K. Below 320 K the data were fitted with the Arrhenius expression recommended here, whereas at higher temperatures a temperature-independent value was found, suggesting the occurrence of different mechanisms in the two temperature regimes.

E40. F + CH_4. The recommended room temperature value is the mean of the results of Wagner et al. [1189], Clyne et al. [236], Kompa and Wanner [627], Foon and Reid [391], Fasano and Nogar [373], and Persky et al. [912]. The temperature dependence is that reported by Persky et al. in a competitive study using the reaction F + D_2 as the reference reaction. These results are preferred over the temperature dependences reported in the earlier studies of Wagner et al. and Foon and Reid.

E41. FO + O_3. Recommended upper limit is based on the results of Li et al. [704] in a study using a discharge flow-mass spectrometric technique. FO was produced in the reaction of F atoms with excess O_3. No appreciable decay of FO, and only a small increase in FO_2, was detected, allowing an upper limit to the rate constant of 1 x 10^{-14} cm^3 $molecule^{-1}s^{-1}$ to be derived. A two orders of magnitude higher upper limit was

derived by Sehested et al. [1016]. A lower value of the upper limit was derived by Colussi and Grela [258] from a re-analysis of data on the quantum yields for ozone destruction in F_2/O_3 mixtures reported by Starrico et al. [1069]. The results of the recent, more direct, study of Li et al. [704] are preferred over the earlier results of Starrico et al. There are two possible pathways which are exothermic, resulting in the production of $F + 2O_2$ or $FO_2 + O_2$.

E42. FO + NO. The recommended value is based on results of the temperature-dependent study of Bedzhanyan et al. [99] and the value reported by Ray and Watson [962] for k at 298 K using the discharge flow-mass spectrometric technique.

E43. FO + FO. The recommended value is based on the results of Bedzhanyan et al. [98] and Clyne and Watson [248]. Wagner et al. [1191], in a less direct study, report a higher value. The results of Bedzhanyan et al. indicate the predominant reaction channel is that to produce $2F + O_2$.

E44. $FO_2 + O_3$. Recommended value is based on results of Sehested et al. [1016]. A higher upper limit has been reported by Li et al. [704].

E45. FO_2 + NO. Recommended values are based on results of Li et al. [704], the only temperature-dependent study. The room temperature value is nearly a factor of 2 less than the previous recommendation, which was based on the results of Sehested et al. [1016].

E46. $FO_2 + NO_2$. Recommended values are based on results of Li et al. [704], the only temperature-dependent study. The room temperature value is a factor of 2.5 less than the previous recommendation, which was based on the results of Sehested et al. [1016]. This discrepancy might be attributable to a small NO impurity in the NO_2 sample used in the Sehested et al. study.

E47. FO_2 + CO. Recommended value is based on results of Sehested et al. [1016], the only published study of this reaction.

E48. $FO_2 + CH_4$. Recommended value is based on results of Li et al. [704]. This upper limit is a factor of 20 less than the previously recommended upper limit, which was based on the results of Sehested et al. [1016].

E49. $CF_3O + O_2$. The recommendation is based upon the results of Turnipseed et al. [1157] who reported $k(373K) \leq 4 \times 10^{-17}$. Assuming an E/R of 5000K, which is equal to the reaction endothermicity, yields the recommended A and k(298) limits. By comparison to other reactions involving abstraction by O_2 the A factor is likely to be much smaller.

E50. $CF_3O + O_3$. The recommendation is based on the average of room temperature measurements reported by Turnipseed et al. [1157], Wallington and Ball [1201] , and Bourbon et al. [132]. Turnipseed et al. and Bourbon et al. made direct measurements using LIF detection of CF_3O with pulsed photolysis and flow tube reactors, respectively. Wallington and Ball used a competetive reaction scheme with IR absorption detection and $CF_3O + CH_4$ as the reference reaction. The recommended A factor is estimated by comparison to other CF_3O reactions, and the E/R is calculated to give the recommended k(298). Upper limits reported by Maricq and Szente [753], Nielsen and Sehested [857], and Wallington et al. [1208] are consistent with the k(298) recommendation. Measurements reported by Fockenberg et al. [389] and Meller and Moortgat [778] gave rate coefficients about an order of magnitude less than the recommended value. Although the reason for this discrepancy is not known, both studies appear to have the possibility of significant secondary chemistry. The reaction products have not been observed.

E51. $CF_3O + H_2O$. The recommendation is based upon the measurement $k(381) \leq 2 \times 10^{-16}$ reported by Turnipseed et al. [1155]. The A factor is estimated and the E/R is calculated to fit k(381). The limits $k = (0.2\text{-}40) \times 10^{-17}$ at 296±2K given by Wallington et al. [1209] are consistent with the recommendation.

E52. CF_3O + NO. The recommendation is based upon the room temperature rate coefficients reported by Sehested and Nielsen [1014], Turnipseed et al. [1157], and Jensen et al. [562] which are in very good agreement. An earlier low value given by Bevilacqua et al. [108] is superseded by Jensen et al. The temperature-dependence is derived from measurements by Turnipseed (233-360K) and Jensen et al. (231-393K). Room temperature results from Bourbon et al. [133] and Bhatnagar and Carr [110] and a temperature dependence study by Dibble

et al. [339] are in good agreement with the recommendation. The reaction products have been reported by Chen et al. [206] Bevilacqua et al. [108], Bhatnagar and Carr and Dibble et al.

E53. $CF_3O + NO_2$. There are no published measurements of the rate coefficient for this reaction. The reaction products have been reported by Chen et al. [205] who used photolysis of CF_3NO to prepare CF_3O_2 and subsequently CF_3O in 700 torr of air at 297±2K. They considered two product channels: (a) CF_3ONO_2 obtained via three-body recombination and (b) $CF_2O + FNO_2$ obtained via fluorine transfer. Products from both channels were observed and found to be thermally stable in their reactor. They report $k_a/(k_a + k_b) \geq 90\%$ and $k_b/(k_a + k_b) \leq 10\%$, thus the formation of CF_3ONO_2 is the dominant channel at 700 torr and 297K.

E54. $CF_3O + CO$. The kinetics of this reaction were studied by Turnipseed et al. [1155], who used pulsed laser photolysis with pulsed laser-induced fluorescence detection and a flow tube reactor with chemical ionization detection to obtain data at temperatures from 233 to 332 K and at pressures from 0.8 to about 300 torr in He and at about 300 torr in SF_6. The reaction was found to be predominantly a three-body recombination, presumably producing CF_3OCO as described in Table 2. The bimolecular reaction has at least two product channels: (a) $CF_2O + CFO$ and (b) $CF_3 + CO_2$. The recommended bimolecular rate coefficient limit is derived from the low pressure results of Turnipseed et al., where the reaction was in the fall-off region. Their low pressure data indicate that $k_b < 4 \times 10^{-16}$ cm^3 molecule^{-1} s^{-1} at 298K. The fate of the CF_3OCO adduct is uncertain, and it may lead to the regeneration of CF_3 or CF_3O radicals in the atmosphere. Wallington and Ball [1202] report a yield of (96±8)% CO_2 at one atmosphere and (296±2)K.

E55. $CF_3O + CH_4$. The absolute rate coefficients reported by Saathoff and Zellner [979], Barone et al. [72], Jensen et al. [562], Bourbon et al. [134], and Bednarek et al. [97] at room temperature are in excellent agreement. Kelly et al. [590] used a relative method with FTIR detection to determine the ratio $k(CF_3O + CH_4)/k(CF_3O + C_2H_6) = R = 0.01\pm0.001$ at 298±2K. This does not agree with the ratio of our recommended values, which is 0.017. A relative rate measurement reported by Chen et al. [207] using FTIR methods also gives a low result for the rate coefficient. A relative rate measurement reported by Wallington and Ball [1202], R = 0.0152±0.0023 at 296K, is in good agreement with the recommended rate coefficients. The temperature dependence is from the data of Barone et al. (247-360K), Jensen et al. (231-385 K), and Bednarek et al. (235-401K), who agree very well. Measurements at higher temperatures by Bourbon et al. (296-573K) gave a higher E/R (1606K). The k(298) is the average of the three absolute studies. The CF_3OH product was observed by Jensen et al. and Bevilacqua et al. [108].

E56. $CF_3O + C_2H_6$. The room temperature recommendation is based on results reported by Saathoff and Zellner [979], Barone et al. [72], and Bourbon et al. [134]. These workers are in excellent agreement. Chen et al. [207] measured the rate coefficient relative to that for the $CF_3O + NO$ reaction in 700 torr of air at 297 K. Their ratio is in good agreement with the values recommended in this evaluation. Kelly et al. [590] used a relative method with FTIR detection to determine the ratio $k(CF_3O + CH_4)/k(CF_3O + C_2H_6) = 0.01\pm0.001$ at 298±2K. This does not agree with the ratio of our recommended values, which is 0.017. A relative rate measurement reported by Wallington and Ball [1202], R = 0.0152±0.0023 at 296k is in good agreement with the recommended rate coefficients. The temperature dependence is from the work of Barone et al., who studied the reaction over the temperature range from 233 to 360 K. Measurements by Bourbon et al. (295-573k) gave a higher E/R (642K). The products are inferred by analogy to other reactions of CF_3O with organic compounds.

E57. $CF_3O_2 + O_3$. The recommended upper limit is given by the measurements reported by Ravishankara et al. [953] who used chemical ionization detection of CF_3O_2 with a flow tube reactor. No measurable reaction was observed in their study. The less direct studies of Nielsen and Sehested [857], Maricq and Szente [753] and Turnipseed et al. [1157] all report somewhat larger upper limits to the rate coefficient. An observable reaction was reported in an indirect measurement by Meller and Moortgat [778]. Their result for the $CF_3O + O_3$ reaction is not consistent with the value recommended above. Their study may have interference from unknown reactions. The products are assumed to be $CF_3O + 2O_2$.

E58. $CF_3O_2 + CO$. The recommended upper limit is reported by Turnipseed et al. [1155] who used chemical ionization mass spectrometric detection of CF_3OO with a flow tube reactor at 296K. This result is at odds with an earlier study by Czarnowski and Schumacher [291], who deduced a "fast reaction" when they observed

the thermal decomposition of CF_3OOOCF_3 to accelerate in the presence of CO at 315-343K. It is possible that the reaction of CF_3O with CO could account for their observations.

E59. $CF_3O_2 + NO$. The recommendation is an average of the room temperature rate coefficients reported by Plumb and Ryan [921], Dognon et al. [349], Peeters et al. [906], Bevilacqua et al. [108], Sehested and Nielsen [1014], Turnipseed et al. [1157], Bourbon et al. [133], and Bhatnagar and Carr [110], all of whom are in excellent agreement. The temperature dependence is derived from the results of Dognon et al. Several studies have confirmed the identity of the products.

F1. $O + ClO$. Recently there have been five studies of this rate constant over an extended temperature range using a variety of techniques: Leu [692]; Margitan [749]; Schwab et al. [1010]; Ongstad and Birks [880]; and Nicovich et al. [850]. The recommended value is based on a least squares fit to the data reported in these studies and in the earlier studies of Zahniser and Kaufman [1293] and Ongstad and Birks [879]. Values reported in the early studies of Bemand et al. [104] and Clyne and Nip [240] are significantly higher and were not used in deriving the recommended value. Leu and Yung [701] were unable to detect $O_2(^1\Sigma)$ or $O_2(^1\Delta)$ and set upper limits to the branching ratios for their production of 4.4×10^{-4} and 2.5×10^{-2} respectively.

F2. $O + OClO$. The recommended value is based on results of the DF-RF study of Gleason et al. [426]. Over the temperature range from 400 K down to 240 K their data are well fitted by this Arrhenius expression, but at lower temperatures down to 200 K their data show an abrupt change to a negative temperature dependence. At 200 K the value measured is a factor of 3 higher than that calculated from the Arrhenius expression. Similar results were obtained in a recent study (Toohey, Avallone, and Anderson, private communication). Over the temperature range 413 - 273 K their data showed a temperature dependence very similar to that reported by Gleason et al. over the same temperature range. Moreover, as the temperature was lowered further their rate constant values also levelled off and then increased at the lowest temperature. Their rate constant values were nearly 50% lower than the values of Gleason et al. from 400 K down to 273 K and 30% lower at 253 K. Colussi [257], using a laser flash photolysis - resonance fluorescence technique over an extended pressure range, reported a value of the bimolecular rate coefficient at room temperature 50% higher than the recommended value. Colussi et al. [259] extended these measurements down to 248 K; in contrast to the positive temperature dependence over this temperature range reported by Gleason et al., these authors report a negative temperature dependence. The bimolecular rate constants reported by Colussi et al. are not directly measured but are derived quantities which are consistent with fall-off curves fitted to the experimental data over the pressure range 20 - 600 torr. It appears that the experiments of Bemand et al. [104], were complicated by secondary chemistry. The results of Colussi and Colussi et al. over an extended pressure range demonstrate the importance of the termolecular reaction $O + OClO + M \rightarrow ClO_3 + M$ (see entry for this reaction in Table 2). It should be noted that the termolecular rate constants derived by Gleason et al. on the basis of their low temperature data are not consistent with the termolecular rate constant expression recommended in this evaluation (factor of 3 difference). The recommended expression is based on the results of Colussi [257] and Colussi et al. [259].

F3. $O + Cl_2O$. Recommended value is based on the results of Stevens and Anderson [1079] and Miziolek and Molina [804], which are in good agreement. The significantly lower values of Wecker et al. [1236] are not included, nor are earlier results by Basco and Dogra [79] and Freeman and Phillips [395] due to data analysis difficulties in both studies.

F4. $O + HCl$. Fair agreement exists between the results of Brown and Smith [147], Wong and Belles [1275], Ravishankara et al. [950], Hack et al. [448] and Singleton and Cvetanovic [1042] at 300 K (some of the values for k(300 K) were obtained by extrapolation of the experimentally determined Arrhenius expressions), but these are a factor of ~7 lower than that of Balakhnin et al. [53]. Unfortunately, the values reported for E/R are in complete disagreement, ranging from 2260-3755 K. The preferred value was based on the results reported by Brown and Smith, Wong and Belles, Ravishankara et al., Hack et al. and Singleton and Cvetanovic, but not on those reported by Balakhnin et al.

F5. $O + HOCl$. Recommended value is based on results of Schindler et al. [1001]. In this study the rate constant was found to be practically independent of temperature in the range 213-298 K. Product analysis indicated that Cl atom abstraction is the predominant primary reaction channel.

F6. $O + ClONO_2$. The results reported by Molina et al. [806] and Kurylo [637] are in good agreement, and these data have been used to derive the preferred Arrhenius expression. The value reported by Ravishankara et al.

[945] at 245 K is a factor of 2 greater than those from the other studies, and this may possibly be attributed to (a) secondary kinetic complications, (b) the presence of NO_2 as a reactive impurity in the $ClONO_2$, or (c) formation of reactive photolytic products. None of the studies reported identification of the reaction products. The room temperature result of Adler-Golden and Wiesenfeld [10] is in good agreement with the recommended value.

F7. $O_3 + OClO$. The recommended value is based on results over the temperature range 262-296 K reported by Wongdontri-Stuper et al. [1276]. Within the indicated uncertainty limits it also encompasses the somewhat lower room temperature result of Birks et al. [119].

F8. $O_3 + Cl_2O_2$. The recommended upper limit is that determined by DeMore and Tschuikow-Roux [333]. It refers to a temperature of 195 K, and while the reaction possibly could be faster at higher temperatures, the value of the rate at the higher temperatures would be of no significance because of the thermal decomposition of the dimer.

F9. $OH + Cl_2$. The recommended room temperature value is the average of the results reported by Boodaghians et al. [129], Loewenstein and Anderson [725], Ravishankara et al. [947], and Leu and Lin [697]. The temperature dependence is from Boodaghians et al. Loewenstein and Anderson determined that the exclusive products are Cl + HOCl.

F10. OH + ClO. The recommended value is based on a fit to the 219-373 K data of Hills and Howard [488], the 243-298 K data of Burrows et al. [169], and the 298 K data of Poulet et al. [931]. Data reported in the studies of Ravishankara et al. [947], and Leu and Lin [697] were not used in deriving the recommended value because in these studies the concentration of ClO was not determined directly. The results of Burrows et al. are temperature-independent, while those of Hills and Howard show a slight negative temperature dependence. The fraction of total reaction yielding HO_2 + Cl as products has been determined by Leu and Lin (>0.65); Burrows et al. (0.85±0.2); Hills and Howard (0.86±0.14); and Poulet et al. (0.98±0.12). The latest study gives an upper limit of 0.14 for the branching ratio to give HCl + O_2 as products. Even though uncertainties in all studies allow for the HCl yield to be zero, none of the current measurements can exclude a small, but atmospherically significant, yield of HCl. Quantification of the HCl yield, especially at temperatures close to 200 K, is needed.

F11. OH + OClO. The recommended value is that reported by Poulet et al. [935], the only reported study of this rate constant, using a discharge flow system in which OH decay was measured by LIF or EPR over the temperature range 293-473 K. Product HOCl was detected by modulated molecular beam mass spectrometry. The branching ratio for the channel to produce HOCl + O_2 was determined to be close to unity, but experimental uncertainty would allow it to be as low as 0.80.

F12. OH + HCl. The recommended value is based on a least squares fit to the data reported in the studies by Molina et al. [807], Keyser [601], and Ravishankara et al. [959]. In these studies particular attention was paid to the determination of the absolute concentration of HCl by UV and IR spectrophotometry. Earlier studies by Takacs and Glass [1106], Zahniser et al. [1294], Smith and Zellner [1058], Ravishankara et al. [950], Hack et al. [448], Husain et al. [528], Cannon et al. [179], Husain et al. [529], and Smith and Williams [1057] had reported somewhat lower room temperature values. Results of a low temperature study by Sharkey and Smith [1019] are in good agreement with this recommendation down to 216 K but are significantly higher at 178 K and 138 K.

F13. OH + HOCl. In the only reported study of this system Ennis and Birks [367] reported the value of this rate constant at room temperature to lie in the range (1.7 - 9.5) x 10^{-13} cm^3 $molecule^{-1}$ s^{-1}. A temperature-dependent expression has been estimated by choosing a pre-exponential factor by analogy with the OH + H_2O_2 reaction and selecting the midpoint of the experimental range for the room temperature rate constant. The large uncertainty factor is needed to encompass the entire range.

F14. OH + $ClNO_2$. The recommended value is based on results of the direct study of Ganske et al. [405, 406] using the discharge flow-resonance fluorescence technique. Mass spectrometric studies showed HOCl to be the major chlorine-containing product, with no evidence for a channel to produce $HONO_2$ + Cl.

F15. OH + $ClONO_2$. The results reported by Zahniser et al. [1291] and Ravishankara et al. [945] are in good agreement at ~245 K (within 25%), considering the difficulties associated with handling $ClONO_2$. The preferred value is that of Zahniser et al. Neither study reported any data on the reaction products.

F16. OH + CH_3Cl. The recommended expression averages the relative rate data of Hsu and DeMore with the absolute rate data below 400 K from the studies of Taylor et al. [1122], Jeong and Kaufman [567], Davis et al. [311], Perry et al. [908] and the room temperature data of Howard and Evenson [511] and Paraskevopoulos et al. [894].

F17. OH + CH_2Cl_2. The relative rate data of Hsu and DeMore [518] lie below the data from absolute rate studies, although only slightly below that of Davis et al. [311]. The recommended expression averages this relative rate data with the absolute rate data below 400 K from the studies of Taylor et al. [1122], Davis et al. [311], and Jeong and Kaufman [567], and the room temperature data of Perry et al. [908] and Howard and Evenson [511].

F18. OH + $CHCl_3$. There have been two recent studies of this reaction rate - the relative rate study of Hsu and DeMore [518] and the absolute rate study of Taylor et al. [1122], which superseded Taylor et al. [1121]. Both studies report a lower activation energy than that reported in the earlier studies. The new data reconcile the problem with respect to transition state theory pointed out by Cohen and Benson [254] and Cohen and Westberg [255] for the previous data for this reaction (Davis et al. [311], Jeong and Kaufman [567], and Taylor et al. [1121]). The recommended expression averages the relative rate data of Hsu and DeMore with the absolute rate data below 400 K from the studies of Taylor et al. [1122], Jeong and Kaufman [567] and Davis et al. [311], and the room temperature data of Howard and Evenson [511].

F19. OH + CCl_4. The recommended upper limit at room temperature is based on the upper limit reported in the competitive study by Cox et al. [272]. The value given there has been increased by a factor of four to allow for uncertainties in the number of NO molecules oxidized. The recommendation is compatible with the less sensitive upper limits reported by Howard and Evenson [511] and Clyne and Holt [230]. None of these investigators reported any evidence for reaction between these species. The A-factor was estimated and a lower limit for E/R was derived.

F20. OH + $CFCl_3$. The A-factor was estimated, and a lower limit was derived for E/R by using the upper limit reported for the rate constant by Chang and Kaufman [196] at about 480 K. This expression is quite compatible with the upper limits reported by Atkinson et al. [41], Howard and Evenson [511], Cox et al. [272] and Clyne and Holt [230]. None of the investigators reported any evidence for reaction.

F21. OH + CF_2Cl_2. The A-factor was estimated, and a lower limit was derived for E/R by using the upper limit reported for the rate constant by Chang and Kaufman [196] at about 480 K. This expression is quite compatible with the upper limits reported by Atkinson et al. [41], Howard and Evenson [511], Cox et al. [272] and Clyne and Holt [230]. None of the investigators reported any evidence for reaction.

F22. OH + CH_2FCl (HCFC-31). The recommended Arrhenius expression includes the data of DeMore [329] along with the room temperature data of Howard and Evenson [511] and Paraskevopoulos et al. [894], and the temperature dependence data of Watson et al. [1231], Handwerk and Zellner [463] and Jeong and Kaufman [567] below 400 K.

F23. OH + $CHFCl_2$ (HCFC-21). Absolute rate coefficient data for this reaction have been reported by Howard and Evenson [511], Perry et al. [908], Watson et al. [1231], Chang and Kaufman [197], Clyne and Holt [231], Paraskevopoulos et al. [894] and Jeong and Kaufman [567]. New data are now available from Fang et al. [370] and DeMore (1997, to be published). The preferred Arrhenius expression fits the latter two sets of data.

F24. OH + CHF_2Cl (HCFC-22). Results for this compound show very good agreement among both absolute and relative rate constant measurements. The recommended Arrhenius expression fits the results of Orkin and Khamaganov [883], Hsu and DeMore [519], and Fang et al. [370] along with the earlier results reported by Howard and Evenson [511], Atkinson et al. [41], Watson et al. [1231], Chang and Kaufman [197], Handwerk and Zellner [463], Paraskevopoulos et al. [894] and Jeong and Kaufman [567].

F25. OH + CH_3OCl. Recommended value is based on results of Crowley et al. [287], the only reported study of this reaction.

F26. OH + CH_3CCl_3. The k(298K) recommendation is based on absolute rate studies of Talukdar et al. [1119] and Finlayson-Pitts et al. [382], and a relative rate study (CH_4 as reference) of DeMore [326]. The temperature dependence is that of Talukdar et al. [1119]. These studies indicate both a lower k(298K) and E/R than was reported in earlier studies: Nelson et al. [835], Jeong and Kaufman [566], and Kurylo et al. [640]. Recent measurements by Jiang et al. [569] and Lancar et al. [657] yield rate constants that are slightly higher at 298 K than this recommendation.

F27. OH + C_2HCl_3. The preferred value at 298 K is a mean of the values reported by Howard [508] and Chang and Kaufman [197]. The value derived from a relative rate coefficient study by Winer et al. [1272] is a factor of ~2 greater than the other values and is not considered in deriving the preferred value at 298 K. The Arrhenius parameters are based on those reported by Chang and Kaufman (the A-factor is reduced to yield the preferred value at 298 K). Kirchner et al. [609] report a room temperature rate constant and Arrhenius parameters in reasonable agreement with the recommended values.

F28. OH + C_2Cl_4. The preferred value at 298 K is a mean of the value reported by Howard [508] and Chang and Kaufman [197]. The value reported by Winer et al. [1272], which is more than a factor of 10 greater, is rejected. The preferred Arrhenius parameters are those of Chang and Kaufman. Kirchner et al. [609] report a room temperature rate constant in good agreement with the recommended value and Arrhenius parameters in reasonable agreement with the recommended values.

F29. OH + CCl_3CHO. The recommended room temperature value is that reported by Barry et al. [75] in a comprehensive study using three independent techniques. The temperature dependence is that reported by Dobe et al. [342].

F30. OH + CH_3CFCl_2 (HCFC-141b). Both absolute and relative rate measurements are in excellent agreement for this compound, and the data are linear over a wide temperature range. The recommended value averages results of the studies of Huder and DeMore [522] and Lancar et al. [657] with those of the earlier studies of Zhang et al. [1304], Liu et al. [724] at 330 K and above, and Talukdar et al. [1114] above 253 K. The temperature-dependence data of Brown et al. [144] were not considered because the relatively large rate constants and Arrhenius curvature are suggestive of sample impurities.

F31. OH + CH_3CF_2Cl (HCFC-142b). The recommended rate expression is derived from a fit to the temperature-dependence data of Gierczak et al. [416], Liu et al. [724], Watson et al. [1231], Handwerk and Zellner [463], the 270 K data of Zhang et al. [1304] and the room temperature data of Howard and Evenson [510], Paraskevopoulos et al. [894] and Mors et al. [817]. The data from Brown et al. [144] and Clyne and Holt [231] were not included in the fit.

F32. OH + CH_2ClCF_2Cl (HCFC-132b). The recommended rate expression was derived from the data of Watson et al. [1233], which were corrected by these authors for the presence of alkene impurities. The data of Jeong et al. [565], indicating substantially faster rate constants, may have been affected by such impurities; hence they were not included in deriving the recommendation.

F33. OH + $CHCl_2CF_2Cl$ (HCFC-122). Based on the data of Orkin and Khamaganov [883] and DeMore [329], which are in good agreement.

F34. OH + $CHFClCFCl_2$ (HCFC-122a). Fit to data of Hsu and DeMore [519] and Orkin (private communication), which are in good agreement.

F35. OH + CH_2ClCF_3 (HCFC-133a). The temperature dependence of the preferred rate expression was derived from the data of Handwerk and Zellner [463]. The recommended value of k_{298} is the average of the values of Howard and Evenson [510] and Handwerk and Zellner [463] adjusted to 298 K.

F36. OH + $CHCl_2CF_3$ (HCFC-123). The relative rate constant measurements of Hsu and DeMore [519], using HFC-152a as a reference compound, are in good agreement with the Zellner (private communication, 1993) value, but somewhat lower than most of the previous absolute data. The recommended value averages results

of the new studies with the earlier temperature-dependence data below 400 K of Nielsen [852], Gierczak et al. [416], Liu et al. [724], Watson et al. [1233], and the room temperature data of Howard and Evenson [510].

F37. OH + $CHFClCF_2Cl$ (HCFC-123a). Based on the data of Orkin and Khamaganov [883].

F38. OH + $CHFClCF_3$ (HCFC-124). The relative rate measurements of Hsu and DeMore [519], using both HFC-134 and CH_4 as reference compounds, are somewhat lower (about 30% at 298 K) than the absolute measurements, with a slightly greater temperature dependence. The recommended rate expression averages results of this new study with those of the earlier studies of Gierczak et al. [416], Watson et al. [1233], and the room temperature data of Howard and Evenson [510].

F39. OH + $CH_3CF_2CFCl_2$ (HCFC-243cc). The preferred rate expression is derived from the temperature-dependence data of Nelson et al. [829]. The recommended value of k_{298} is obtained from the temperature dependence expression.

F40. OH + $CF_3CF_2CHCl_2$ (HCFC-225ca). The preferred rate expression is derived from reanalysis of the final published temperature-dependence data of Nelson et al. [829] and Zhang et al. [1305].

F41. OH + CF_2ClCF_2CHFCl (HCFC-225cb). The preferred rate expression is derived from the temperature-dependence data of Nelson et al. [829] and Zhang et al. [1305].

F42. HO_2 + Cl. The recommendations for the two reaction channels are based upon the results by Lee and Howard [679] using a discharge flow system with laser magnetic resonance detection of HO_2, OH, and ClO. The total rate constant is temperature independent with a value of $(4.2\pm0.7) \times 10^{-11}$ cm^3 $molecule^{-1}$ s^{-1} over the temperature range 250-420 K. This value for the total rate constant is in agreement with the results of indirect studies relative to Cl + H_2O_2 [Leu and DeMore [693], Poulet et al. [933], Burrows et al. [164]] or to Cl + H_2 [Cox [265]]. The contribution of the reaction channel producing OH + ClO (21% at room temperature) is much higher than the upper limit reported by Burrows et al. (1% of total reaction). Cattell and Cox [193], using a molecular modulation-UV absorption technique over the pressure range 50-760 torr, report results in good agreement with those of Lee and Howard both for the overall rate constant and for the relative contribution of the two reaction channels. A study by Dobis and Benson [346] reports a total rate constant in good agreement with this recommendation but a much lower contribution (5±3%) of the channel producing OH + ClO. The rate constant for the channel producing ClO + OH can be combined with that for the reaction ClO + OH > Cl + HO_2 to give an equilibrium constant from which a value of the heat of formation of HO_2 at 298 K of 3.0 kcal/mol can be derived.

F43. HO_2 + ClO. There have now been five studies of this rate constant. Three were low pressure discharge flow studies, each using a different experimental detection technique (Reimann and Kaufman, [965]; Stimpfle et al. [1087]; Leck et al. [668]), and two were molecular modulation studies; at one atmosphere (Burrows and Cox [165]), and over the pressure range 50-760 torr (Cattell and Cox [193]). The 298 K values reported, in units of 10^{-12} cm^3 $molecule^{-1}$ s^{-1}, are: 3.8±0.5 (Reimann and Kaufman), 6.3±1.3 (Stimpfle et al.), 4.5±0.9 (Leck et al.), 5.4 (Burrows and Cox), and 6.2±1.5 (Cattell and Cox). The recommended value is the mean of these values. The study of Cattell and Cox over an extended pressure range, when combined with results of the low pressure discharge flow studies, seems to indicate that this reaction exhibits no pressure dependence at room temperature. The only temperature-dependence study (Stimpfle et al.) resulted in a nonlinear Arrhenius behavior. The data were best described by a four parameter equation of the form $k = Ae^{-B/T} + CT^n$, possibly suggesting that two different mechanisms may be occurring. The expression forwarded by Stimpfle et al. was $3.3 \times 10^{-11} \exp(-850/T) + 4.5 \times 10^{-12} (T/300)^{-3.7}$. Two possible preferred values can be suggested for the temperature dependence of k: (a) an expression of the form suggested by Stimpfle et al., but where the values of A and C are adjusted to yield a value of 5.0×10^{-12} at 298 K, or (b) a simple Arrhenius expression which fits the data obtained at and below 300 K (normalized to 5.0×10^{-12} at 298 K). The latter form is preferred. The two most probable pairs of reaction products are, (1) HOCl + O_2 and (2) HCl + O_3. Leu [691] and Leck et al. used mass spectrometric detection of ozone to place upper limits of 1.5% (298 K) and 3.0% (248 K); and 2.0% (298 K), respectively, on k_2/k. Burrows and Cox report an upper limit of 0.3% for k_2/k at 300 K. Finkbeiner et al. [381], using matrix-isolation/FTIR spectroscopy, studied product formation between 210 and 300 K at 700 Torr. HOCl was observed as the dominant product (> 95%

at all temperatures). The branching ratio values for k_2/k were determined to be <1% at 300 K and 270 K. 2±1% at 240 K, and 5±2% at 210 K. No evidence for any other product channel was found.

F44. $H_2O + ClONO_2$. This recommendation is based on the upper limits to the homogeneous bimolecular rate constant reported by Atkinson et al. [47], and by Hatakeyama and Leu [470, 471]. Atkinson et al. observed by FTIR analysis the decay of $ClONO_2$ in the presence of H_2O in large-volume (2500 and 5800 liters) Teflon or Teflon-coated chambers. Their observed decay rate gives an upper limit to the homogeneous gas phase rate constant, and they conclude that the decay observed is due to heterogeneous processes. Hatakeyama and Leu, using a static photolysis system with FTIR analysis, derive a similar upper limit. Rowland et al. [974] concluded that the decay they observed resulted from rapid heterogeneous processes. The homogeneous reaction is too slow to have any significant effect on atmospheric chemistry.

F45. NO + OClO. The Arrhenius expression was estimated based on 298 K data reported by Bemand, Clyne and Watson [104].

F46. $NO + Cl_2O_2$. The recommended upper limit is that determined by Friedl (private communication) in a study using a DF-MS technique.

F47. $NO_3 + HCl$. The recommended upper limit is that reported by Mellouki et al. [783] in a study using DF-EPR techniques. This upper limit shows that this reaction is of negligible importance in stratospheric chemistry. Somewhat lower upper limits have been reported by Cantrell et al. [184] and Canosa-Mas et al. [181]; the latter study also reports Arrhenius parameters at higher temperatures (333-473 K).

F48. $HO_2NO_2 + HCl$. This upper limit is based on results of static photolysis-FTIR experiments reported by Leu et al. [696].

F49. $Cl + O_3$. The results reported for k(298 K) by Watson et al. [1232], Zahniser et al. [1295], Kurylo and Braun [641] and Clyne and Nip [241] are in good agreement, and have been used to determine the preferred value at this temperature. The values reported by Leu and DeMore [693] (due to the wide error limits) and Clyne and Watson [247] (the value is inexplicably high) are not considered. The four Arrhenius expressions are in fair agreement within the temperature range 205-300 K. In this temperature range, the rate constants at any particular temperature agree to within 30-40%. Although the values of the activation energy obtained by Watson et al. and Kurylo and Braun are in excellent agreement, the value of k in the study of Kurylo and Braun is consistently (~17%) lower than that of Watson et al. This may suggest a systematic underestimate of the rate constant, as the values from the other three agree so well at 298 K. A more disturbing difference is the scatter in the values reported for the activation energy (338-831 cal/mol). However, there is no reason to prefer any one set of data to any other; therefore, the preferred Arrhenius expression shown above was obtained by computing the mean of the four results between 205 and 298 K. Inclusion of higher temperature (466 K) experimental data would yield the following Arrhenius expression: $k = (3.4\pm1.0) \times 10^{-11} \exp(-310\pm76/T)$. Results of the study by Nicovich et al. [845] show non-Arrhenius behavior over the temperature range 189-385 K. These results are in good agreement with the present recommendation above about 250 K, but at lower temperatures they are faster than the recommendation, although still within its stated uncertainty down to about 220 K. Results of Seeley et al. [1011] using the turbulent flow tube technique are in excellent agreement with the recommendation at room temperature but 20% higher than the recommendation at 220 K. DeMore [325] directly determined the ratio $k(Cl + O_3)/k(Cl + CH_4)$ at 197-217 K to be within 15% of that calculated from the absolute rate constant values recommended here.

Vanderzanden and Birks [1176] have interpreted their observation of oxygen atoms in this system as evidence for some production (0.1-0.5%) of O_2 ($^1\Sigma_g^+$) in this reaction. The possible production of singlet molecular oxygen in this reaction has also been discussed by DeMore [322], in connection with the Cl_2 photosensitized decomposition of ozone. However Choo and Leu [216] were unable to detect $O_2(^1\Sigma)$ or $O_2(^1\Delta)$ in the $Cl + O_3$ system and set upper limits to the branching ratios for their production of 5×10^{-4} and 2.5×10^{-2}, respectively. They suggested two possible mechanisms for the observed production of oxygen atoms, involving reactions of vibrationally excited ClO radicals with O_3 or with Cl atoms, respectively. Burkholder et al. [160], in a study of infrared line intensities of the ClO radical, present evidence in support of the second mechanism. In their experiments with excess Cl atoms, the vibrationally excited ClO radicals produced in the $Cl + O_3$ reaction can react with Cl atoms to give Cl_2 and oxygen atoms, which can then remove additional ClO radicals. These authors point out the possibility for systematic error from assuming a 1:1

stoichiometry for [Cl)]:[O_3]$_0$ when using the Cl + O_3 reaction as a quantitative source of ClO radicals for kinetic and spectroscopic studies.

F50. Cl + H_2. This Arrhenius expression is based on the data below 300 K reported by Watson et al. [1230], Lee et al. [669], Miller and Gordon [802], and Kita and Stedman [612]. The results of these studies are in excellent agreement below 300 K; the data at higher temperatures are in somewhat poorer agreement. The results of Watson et al., Miller and Gordon, and Kita and Stedman agree well (after extrapolation) with the results of Benson et al. [107] and Steiner and Rideal [1074] at higher temperatures. For a discussion of the large body of rate data at high temperatures, see the review by Baulch et al. [86]. The room temperature value of Kumaran et al. [632], in a study primarily at high temperatures, is in excellent agreement with this recommendation. Miller and Gordon and Kita and Stedman also measured the rate of the reverse reaction, and found the ratio to be in good agreement with equilibrium constant data.

F51. Cl + H_2O_2. The absolute rate coefficients determined at ~298 K by Watson et al. [1232], Leu and DeMore [693], Michael et al. [800], Poulet et al. [933] and Keyser [597] range in value from (3.6-6.2) x 10^{-13}. The studies of Michael et al., Keyser, and Poulet et al. are presently considered to be the most reliable. The preferred value for the Arrhenius expression is taken to be that reported by Keyser. The A-factor reported by Michael et al. is considerably lower than that expected from theoretical considerations and may possibly be attributed to decomposition of H_2O_2 at temperatures above 300 K. The data of Michael et al. at and below 300 K are in good agreement with the Arrhenius expression reported by Keyser. More data are required before the Arrhenius parameters can be considered to be well-established. Heneghan and Benson [481], using mass spectrometry, confirmed that this reaction proceeds only by the abstraction mechanism giving HCl and HO_2 as products.

F52. Cl + NO_3. The recommended value at room temperature is based on the discharge flow-EPR study of Mellouki et al. [781] and the discharge flow-mass spectrometric study of Becker et al. [89]. The results of these direct absolute rate studies are preferred over results of the earlier relative rate studies of Cox et al. [266], Burrows et al. [168], and Cox et al. [278], in all of which NO_3 was monitored in the photolysis of Cl_2-$ClONO_2$-N_2 mixtures. Complications in the chemistry of the earlier systems probably contributed to the spread in reported values. This radical-radical reaction is expected to have negligible temperature dependence, which is consistent with the results from the study of Cox et al. [278] in which the complications must have been temperature independent.

F53. Cl + N_2O. This rate coefficient has been determined in a study of the halogen-catalyzed decomposition of nitrous oxide at about 1000 K by Kaufman et al. [589]. The largest value reported was 10^{-17} cm^3 $molecule^{-1}$ s^{-1}, with an activation energy of 34 kcal/mol. Extrapolation of these results to low temperature shows that this reaction cannot be of any significance in atmospheric chemistry.

F54. Cl + HNO_3. The recommended upper limit at room temperature is that reported in the study of Wine et al. [1269], in which long-path laser absorption spectroscopy was used to look for the appearance of NO_3 following the pulsed laser photolysis of Cl_2-HNO_3 mixtures with no evidence for NO_3 production was observed. In the same study a less sensitive upper limit was derived from monitoring Cl atom decay by resonance fluorescence. A less sensitive upper limit was also found in the discharge flow-EPR study of Zagogianni et al. [1289]. Higher values obtained in earlier studies [Leu and DeMore [693], Kurylo et al. [649], and Clark et al. [221]] as well as the higher temperature results of Poulet et al. [933] are not used.

F55. Cl + CH_4. The values reported from the thirteen absolute rate coefficient studies for k at 298 K fall in the range (0.99 to 1.48) x 10^{-13}, with a mean value of 1.15 x 10^{-13}. However, based upon the stated confidence limits reported in each study, the range of values far exceeds that to be expected. A preferred average value of 1.0 x 10^{-13} can be determined from the absolute rate coefficient studies for k at 298 K by giving equal weight to the values reported in Lin et al. [719], Watson et al. [1232], Manning and Kurylo [745]; Whytock et al. [1248], Zahniser et al. [1290], Michael and Lee [793], Keyser [594], and Ravishankara and Wine [954]. The values derived for k at 298 K from the competitive chlorination studies of Pritchard et al. [936], Knox [621], Pritchard et al. [937], Knox and Nelson [623], and Lin et al. [719] range from (0.95-1.13) x 10^{-13}, with an average value of 1.02 x 10^{-13}. The preferred value of 1.0 x 10^{-13} was obtained by taking a mean value from the most reliable absolute and relative rate coefficient studies.

There have been nine absolute studies of the temperature dependence of k. In general, the agreement between most of these studies can be considered to be quite good. However, for a meaningful analysis of the reported studies it is best to discuss them in terms of two distinct temperature regions: (a) below 300 K, and (b) above 300 K. Three resonance fluorescence studies have been performed over the temperature range 200 to 500 K [Whytock et al. [1248], Zahniser et al. [1290] and Keyser [594]], and in each case a strong nonlinear Arrhenius behavior was observed. Ravishankara and Wine [954] also noted nonlinear Arrhenius behavior over a more limited temperature range. This behavior tends to explain partially the large variance in the values of E/R reported between those other investigators who mainly studied this reaction below 300 K [Watson et al. [1232] and Manning and Kurylo [745]] and those who only studied it above 300 K [Clyne and Walker [246], Poulet et al. [932], and Lin et al. [719]]. The agreement between all studies below 300 K is good, with values of (a) E/R ranging from 1229-1320 K, and (b) k(230 K) ranging from (2.64-3.32) x 10^{-14}. The mean of the two discharge flow values [Zahniser et al. [1290] and Keyser [594]] is 2.67 x 10^{-14}, while the mean of the flash photolysis values [Watson et al. [1232], Manning and Kurylo [745], Whytock et al. [1248], and Ravishankara and Wine [954]] is 3.22 x 10^{-14} at 230 K. There have not been any absolute studies at stratospheric temperatures other than those which utilized the resonance fluorescence technique. Ravishankara and Wine [954] have suggested that the results obtained using the discharge flow and competitive chlorination techniques may be in error at the lower temperatures (<240 K) due to a non-equilibration of the $^2P_{1/2}$ and $^2P_{3/2}$ states of atomic chlorine. Ravishankara and Wine observed that at temperatures below 240 K the apparent bimolecular rate constant was dependent upon the chemical composition of the reaction mixture; i.e., if the mixture did not contain an efficient spin equilibrator, e.g., Ar or CCl_4, the bimolecular rate constant decreased at high CH_4 concentrations. The chemical composition in each of the flash photolysis studies contained an efficient spin equilibrator, whereas this was not the case in the discharge flow studies. However, the reactor walls in the discharge flow studies could have been expected to have acted as an efficient spin equilibrator. Consequently, until the hypothesis of Ravishankara and Wine is proven it is assumed that the discharge flow and competitive chlorination results are reliable.

Above 300 K the three resonance fluorescence studies reported (a) "averaged" values of E/R ranging from 1530-1623 K, and (b) values for k(500 K) ranging from (7.74-8.76) x 10^{-13}. Three mass spectrometric studies have been performed above 300 K with E/R values ranging from 1409-1790 K. The data of Poulet et al. [932] are sparse and scattered; those of Clyne and Walker [246] show too strong a temperature dependence (compared to all other absolute and competitive studies) and k(298 K) is ~20% higher than the preferred value at 298 K. The data of Lin et al. [719] are in fair agreement with the resonance fluorescence results.

The competitive chlorination results differ from those obtained from the absolute studies in that linear Arrhenius behavior is observed. This difference is the major discrepancy between the two types of experiments. The values of E/R range from 1503 to 1530 K, and k(230 K) from (2.11-2.54) x 10^{-14} with a mean value of 2.27 x 10^{-14}. It can be seen from the above discussion that the average values at 230 K are: 3.19 x 10^{-14} (flash photolysis), 2.67 x 10^{-14} (discharge flow), and 2.27 x 10^{-14} (competitive chlorination). These differences increase at lower temperatures. Until the hypothesis of Ravishankara and Wine [954] is re-examined, the preferred Arrhenius expression attempts to best fit the results obtained between 200 and 300 K from all sources. The average value of k at 298 K is 1.04 x 10^{-13}, and at 230 K is 2.71 x 10^{-14} (this is a simple mean of the three average values). The preferred Arrhenius expression yields values similar to those obtained in the discharge flow-resonance fluorescence studies. If only flash photolysis-resonance fluorescence results are used then an alternate expression of 6.4 x 10^{-12} (exp(-1200/T)) can be obtained (k(298 K) = 1.07 x 10^{-13}, and k(230 K) = 3.19 x 10^{-14}). The room temperature result of Beichert et al. [102] is in good agreement with the recommendation. The results of Seeley et al. [1011], using the turbulent flow tube technique, are in excellent agreement with the recommendation at room temperature but 20% higher than the recommendation at 200 K.

F56. $Cl + CH_3D$. Recommended value is based on results of Wallington and Hurley [1207].

F57. $Cl + H_2CO$. The results from five of the six published studies [Michael et al. [798], Anderson and Kurylo [25], Niki et al. [862], Fasano and Nogar [372] and Poulet et al. [928]] are in good agreement at ~298 K, but are ~50% greater than the value reported by Foon et al. [390]. The preferred value at 298 K was obtained by combining the absolute values reported by Michael et al., Anderson and Kurylo, and Fasano and Nogar, with the values obtained by combining the ratio of $k(Cl + H_2CO)/k(Cl + C_2H_6)$ reported by Niki et al. (1.3±0.1) and by Poulet et al. (1.16±0.12) with the preferred value of 5.7 x 10^{-11} for $k(Cl + C_2H_6)$ at 298 K. The

preferred value of E/R was obtained from a least squares fit to all the data reported in Michael et al. and in Anderson and Kurylo. The A-factor was adjusted to yield the preferred value at 298 K.

F58. $Cl + CH_3O_2$. Recommended value is based on results of Maricq et al. [756], Jungkamp et al. [580], and Daele and Poulet [292]. All three studies agree that this overall reaction is very fast. However, there is a discrepancy in the reported values of the branching ratios for the two pathways producing $ClO + CH_3O$ (a) and $HCl + CH_2O_2$ (b). The branching ratio for the reaction channels producing $HCl + CH_2O_2$ (b) has been reported to be 50% by both Maricq et al. [756] and Jungkamp et al., but has been reported to be 90% by Daele and Poulet. Because of this large discrepancy no branching ratios are recommended.

F59. $Cl + CH_3OH$. This recommendation is based on results of the absolute rate studies of Michael et al. [797] Payne et al. [904], Dobe et al. [343] and results obtained in the competitive chlorination studies of Wallington et al. [1214], Lightfoot et al. [710] and Nelson et al. [834]. The temperature independence of the rate constant was reported by Michael et al. and Lightfoot et al. Product analysis and isotopic substitution have established that the reaction mechanism consists of abstraction of a hydrogen atom from the methyl group rather than from the hydroxyl group. See Radford [938], Radford et al. [939], Meier et al. [776], and Payne et al. [904]. This reaction has been used as a source of CH_2OH and as a source of HO_2 by the reaction of CH_2OH with O_2.

F60. $Cl + C_2H_6$. The absolute rate coefficients reported in all four studies [Davis et al. [308], Manning and Kurylo [745], Lewis et al. [702], and Ray et al. [961]] are in good agreement at 298 K. The value reported by Davis et al. was probably overestimated by ~10% (the authors assumed that I_f was proportional to $[Cl]^{0.9}$, whereas a linear relationship between I_f and [Cl] probably held under their experimental conditions). The preferred value at 298 K was taken to be a simple mean of the four values (the value reported by Davis et al. was reduced by 10%), i.e., 5.7×10^{-11}. The two values reported for E/R are in good agreement; E/R = 61 K (Manning and Kurylo) and E/R = 130 K (Lewis et al.). A simple least squares fit to all the data would unfairly weight the data of Lewis et al. due to the larger temperature range covered. Therefore, the preferred value of 7.7×10^{-11} exp(-90/T) is an expression which best fits the data of Lewis et al. and Manning and Kurylo between 220 and 350 K. The recent temperature-dependent results of Dobis and Benson [345] and room temperature results of Kaiser et al. [584], Hooshiyar and Niki [502] and Beichert et al. [102] are in good agreement with the recommendation.

F61. $Cl + C_2H_5O_2$. Recommended value is based on results of Maricq et al. [756].

F62. $Cl + CH_3CN$. The recommendation is based on results of the study of Tyndall et al. [1168]. The results of this study, using both relative and absolute methods and measured over a wide range of experimental conditions are preferred over the results of earlier studies of Kurylo and Knable [645], Poulet et al. [927], and Olbregts et al. [878]. Product studies reported by Tyndall et al. show that reaction proceeds predominantly by hydrogen atom abstraction.

F63. $Cl + CH_3CO_3NO_2$ (PAN). The recommended value is based on results of the relative rate study of Wallington et al. [1195]. In this study no reaction of PAN was observed in the presence of Cl atoms. These results are preferred over the results of the direct study of Tsalkani et al. [1142] using a discharge flow system with EPR detection of Cl atom decay (in which study the authors reported a rate constant of $(3.7 \pm 1.7) \times 10^{-13}$ cm^3 $molecule^{-1}$ s^{-1}). In both studies the major impurity in the PAN samples would be the alkane solvent. The presence of 0.1% tridecane in the PAN sample used by Tsalkani et al. could account for the observed Cl atom decay; however, solvent impurities in the PAN sample would be of no consequence in the relative rate study of Wallington et al.

F64. $Cl + C_3H_8$. The recommended room temperature value is the mean of results of the competitive chlorination studies of Pritchard et al. [937], Knox and Nelson [623], Atkinson and Aschmann [35], Wallington et al. [1214], and Hooshiyar and Niki [502], and the absolute rate studies of Lewis et al. [702] and Beichert et al. [102]. The temperature dependence is from Lewis et al. The A-factor from that study has been adjusted slightly to fit the recommended room temperature value.

F65. $Cl + OClO$. The data of Toohey [1136] are in good agreement with the results of Bemand et al. [104] at room temperature, and the recommended value at room temperature is the mean of the values reported in

these two studies. The slight negative temperature dependence reported by Toohey [1136] is accepted but with error limits that encompass the temperature independence reported in the earlier study.

F66. Cl + ClOO. The recommended value is based on the results of studies by Mauldin et al. [768] and Baer et al. [51], in which ClOO was formed by the pulsed photolysis of Cl_2/O_2 mixtures and its overall loss rate was monitored by UV absorption. In both studies k was found to be independent of temperature. These results are preferred over the results of the earlier, indirect studies of Johnston et al. [570], Cox et al. [273], and Ashford et al. [32]. The earlier studies did show that the predominant reaction pathway is that yielding Cl_2 + O_2 as products. From the branching ratio data of Cox et al., Ashford et al., and Nicholas and Norrish [841], it can be estimated that this reaction channel constitutes 95% of the overall reaction with ClO + ClO the products of the minor (5%) reaction channel.

F67. Cl + Cl_2O. The preferred value was determined from results of the temperature-dependent study of Stevens and Anderson [1079] and the results of two independent absolute rate coefficient studies reported by Ray et al. [961], which used the discharge flow-resonance fluorescence and discharge flow-mass spectrometric techniques. This value has been confirmed by Burrows and Cox [165], who determined the ratio k(Cl + Cl_2O)/k(Cl + H_2) = 6900 in modulated photolysis experiments. The earlier value reported by Basco and Dogra [77] has been rejected.

F68. Cl + Cl_2O_2. The recommended value is that determined by Friedl (private communication) in a study using a DF-MS technique. It is in agreement with the value reported by Cox and Hayman [280] in a study using a static photolysis technique with photodiode array UV spectroscopy.

F69. Cl + HOCl. This recommendation is based on results over the temperature range 243-365 K reported by Cook et al. [261] and the room temperature result of Vogt and Schindler [1184]. There is a significant discrepancy in the reported values of the product branching ratios. Ennis and Birks [366] reported that the major reaction channel is that to give the products Cl_2 + OH with a yield of 91±6%, whereas Vogt and Schindler report this yield to be 24±11%, with the major reaction channel giving HCl + ClO as products.

F70. Cl + ClNO. The discharge flow-resonance fluorescence study of Abbatt et al. [3] provides the first reliable data on the temperature dependence. The laser photolysis-LMR study of Chasovnikov et al. [201] provides rate data for each Cl atom spin state, and they attribute the low value reported by Nelson and Johnston [832] in a laser flash photolysis-resonance fluorescence study to reaction of the Cl $^2P_{1/2}$ state. Adsorption and decomposition of ClNO on the walls of their static system may account for the very low value of Grimley and Houston [441]. The results of Clyne and Cruse [226] in a discharge flow-resonance fluorescence study are significantly lower than all recent results. The recommended value at room temperature is the mean of the values reported by Abbatt et al. [3], Chasovnikov et al. [201], Nesbitt et al. [839], and Kita and Stedman [612]. The recommended temperature dependence is from the study of Abbatt et al. [3].

F71. Cl + $ClONO_2$. Recommended value is based on the results of Yokelson et al. [1284] and those of Margitan [748]. These results are in excellent agreement; the slightly higher values of Kurylo et al. [646] are encompassed within the stated uncertainties. Yokelson et al. report that at 298 K, more than 95% of this reaction proceeds by the reaction channel giving Cl_2 + NO_3 as products.

F72. Cl + CH_3Cl. The recommended room temperature value is the mean of results of the absolute rate studies of Manning and Kurylo [745] and Beichert et al. [102] and the relative rate study of Wallington et al. [1195]. The temperature dependence is from Manning and Kurylo. The A-factor from that study has been adjusted slightly to fit the recommended room temperature value. The results reported by Clyne and Walker [246] and Manning and Kurylo [745] are in good agreement at 298 K. However, the value of the activation energy measured by Manning and Kurylo is significantly lower than that measured by Clyne and Walker. Both groups of workers measured the rate constant for the Cl + CH_4 and, similarly, the activation energy measured by Manning and Kurylo was significantly lower than that measured by Clyne and Walker. It is suggested that the discharge flow-mass spectrometric technique used by Clyne and Walker was in this case subject to a systematic error, and that the flash photolysis results of Manning and Kurylo provide the basis for the recommended rate constant.

F73. Cl + CH_2Cl_2. The recommended value is based on results of the relative rate study of Tschuikow-Roux et al. [1143] normalized to the value of the rate constant for the reference reaction (Cl + CH_4) recommended in this evaluation. The room temperature value is in good agreement with results of the relative rate study of

Niki et al. [864] and the absolute rate study of Beichert et al. [102]. The higher results of Clyne and Walker [246] were not used.

F74. $Cl + CHCl_3$. There have been three recent studies of this reaction. In the studies of Beichert et al. [102] by an absolute technique and Brahan et al. [139] by a relative technique, room temperature values about 50% greater than the previous recommendation, which was based on the relative study of Knox [622], were reported. Talhaoui et al. [1111] in a temperature-dependent absolute rate study by the discharge flow-mass spectrometric technique reported a room temperature value in excellent agreement with the previous recommendation. The recommended room temperature value is the mean of the values reported in the studies of Knox , Beichert et al. , Brahan et al. and Talhaoui et al. The temperature dependence is from Talhaoui et al. and Knox. The A-factor has been fitted to the recommended room temperature value.

F75. $Cl + CH_3F$ (HFC-41). The recommended value is based on results of the temperature-dependent relative rate study of Tschuikow-Roux et al. [1143] and the relative rate studies of Tuazon et al. [1147] and Wallington et al. [1203] at room temperature. The results of the absolute rate study of Manning and Kurylo [745] are in good agreement at room temperature but show a weaker temperature dependence, which is encompassed within the error limits.

F76. $Cl + CH_2F_2$ (HFC-32). The recommended room temperature value is the mean of results of the relative rate studies of Tschuikow-Roux et al. [1144] and of Nielsen et al. [853], both normalized to the value of the rate constant for the reference reaction ($Cl + CH_4$) recommended in this evaluation. The temperature dependence is from Tschuikow-Roux et al. The A-factor from that study has been adjusted to fit the recommended room temperature value.

F77. $Cl + CF_3H$ (HFC-23). Recommended value is based on results of Coomber and Whittle [262].

F78. $Cl + CH_2FCl$ (HCFC-31). The recommended value is based on the room temperature results of Tuazon et al. [1147] and the temperature dependence reported by Tschuikow-Roux et al. [1143], normalized to the value of the rate constant for the reference reaction ($Cl + CH_4$) recommended in this evaluation.

F79. $Cl + CHFCl_2$ (HCFC-21). The recommended room temperature value is the mean of results of the relative rate study of Tuazon et al. [1147] and the absolute rate study of Talhaoui et al. [1111]. The temperature dependence is from Talhaoui et al. The A-factor from that study has been adjusted to fit the recommended room temperature value. These results are preferred over the earlier results of Glavas and Heicklen [424].

F80. $Cl + CHF_2Cl$ (HCFC-22). The recommended room temperature value is the mean of results of the relative rate studies of Tuazon et al. [1147] and the absolute rate studies of Sawerysyn et al. [998] and Talhaoui et al. [1111]. The temperature dependence is from Talhaoui et al. The A-factor from that study has been adjusted to fit the recommended room temperature value.

F81. $Cl + CH_3CCl_3$. Recommended value is based on results of the absolute rate study of Talhaoui et al. [1112]. It is consistent with the previous recommendation, which was a much higher upper limit reported by Wine et al. [1266] in a study in which it was concluded that a reactive impurity accounted for a significant fraction of the Cl atom removal. The value reported by Platz et al. [919] is in agreement with the recommendation.

F82. $Cl + CH_3CH_2F$ (HFC-161). The recommended values for the two reaction channels are based on results of the relative rate study of Tschuikow-Roux et al. [1144], normalized to the value of the rate constant for the reference reaction ($Cl + CH_4$) recommended in this evaluation.

F83. $Cl + CH_3CHF_2$ (HFC-152a). The recommended values for the two reaction channels are based on results of the relative rate study of Yano and Tschuikow-Roux [1283], normalized to the value of the rate constant for the reference reaction ($Cl + C_2H_6$) recommended in this evaluation. The overall rate constant value is in good agreement with results of the room temperature relative rate studies of Wallington and Hurley [1207], and Tuazon et al. [1147].

F84. $Cl + CH_2FCH_2F$ (HFC-152). The recommended value is based on results of the relative rate study of Yano and Tschuikow-Roux [1283], normalized to the value of the rate constant for the reference reaction ($Cl + C_2H_6$) recommended in this evaluation.

F85. Cl + CH_3CFCl_2 (HCFC-141b). The recommended value is based on results of absolute rate studies of Talhaoui et al. [1112] by the discharge flow - mass spectrometric technique and Warren and Ravishankara [1223] by the pulsed photolysis-resonance fluorescence technique and the relative rate studies of Wallington and Hurley [1207] and Tuazon et al. [1147].

F86. Cl + CH_3CF_2Cl (HCFC-142b). The recommended room temperature value is based on results of the relative rate studies of Wallington and Hurley [1207], and Tuazon et al. [1147], and the absolute rate study of Talhaoui et al. [1112]. The temperature dependence is from Talhaoui et al. The A-factor from that study has been adjusted to fit the recommended room temperature value.

F87. Cl + CH_3CF_3 (HFC-143a). The recommended value is based on results of the relative rate study of Tschuikow-Roux et al. [1144], normalized to the value of the rate constant for the reference reaction (Cl + CH_4) recommended in this evaluation.

F88. Cl + CH_2FCHF_2 (HFC-143). The recommended values for the two reaction channels are based on results of the relative rate study of Tschuikow-Roux et al. [1144] normalized to the value of the rate constant for the reference reaction (Cl + CH_4) recommended in this evaluation.

F89. Cl + CH_2ClCF_3 (HCFC-133a). The recommended value is based on results of the direct study of Jourdain et al. [576] using the discharge flow-mass spectrometric technique to monitor the decay of the HCFC in the presence of a large excess of Cl atoms. The A-factor is lower than expected.

F90. Cl + CH_2FCF_3 (HFC-134a). The recommended value is based on results of the relative rate studies of Wallington and Hurley [1207], and Tuazon et al. [1147], and the absolute rate study of Sawerysyn et al. [998].

F91. Cl + CHF_2CHF_2 (HFC-134). The recommended value is based on results of the relative rate study of Nielsen et al. [854] and that of Yano and Tschuikow-Roux [1283], normalized to the value of the rate constant for the reference reaction (Cl + C_2H_6) recommended in this evaluation.

F92. Cl + $CHCl_2CF_3$ (HCFC-123). The recommended value is based on results of the temperature-dependent study of Warren and Ravishankara [1223] using the pulsed photolysis-resonance fluorescence technique, and the relative rate studies of Wallington and Hurley [1207] and Tuazon et al. [1147] at room temperature.

F93. Cl + $CHFClCF_3$ (HCFC-124). The recommended value is based on results of the temperature-dependent study of Warren and Ravishankara [1223] using the pulsed photolysis-resonance fluorescence technique and the relative rate study of Tuazon et al. [1147] at room temperature. The A-factor is lower than expected.

F94. Cl + CHF_2CF_3 (HFC-125). Recommended value is based on results of the relative rate studies of Tuazon et al. [1147] and Sehested et al. [1013].

F95. ClO + O_3. There are two possible channels for this reaction: ClO + $O_3 \rightarrow$ ClOO + O_2 (k_1); and ClO + $O_3 \rightarrow$ OClO + O_2 (k_2). The recommended upper limit for k_1 at 298 K is based on results of the recent study by Stevens and Anderson [1078]. These authors also report that $k_1 = (4\pm2) \times 10^{-16}$ cm^3 $molecule^{-1}$ s^{-1} at 413 K. These data can be combined to derive the Arrhenius parameters $A = 2 \times 10^{-12}$ cm^3 $molecule^{-1}$ s^{-1} and E/R > 3600 K. The upper limit for k_2 is based on results reported by DeMore et al. [331] and Wongdontri-Stuper et al. [1276]; the Arrhenius parameters for k_2 were estimated.

F96. ClO + H_2. The Arrhenius expression was estimated based on the ~600 K data of Walker (reported in Clyne and Watson [247]).

F97. ClO + NO. The absolute rate coefficients determined in the four discharge flow-mass spectrometric studies [Clyne and Watson [247], Leu and DeMore [695], Ray and Watson [962] and Clyne and MacRobert [232]] and the discharge flow laser magnetic resonance study of Lee et al. [680] are in excellent agreement at 298 K, and are averaged to yield the preferred value. The value reported by Zahniser and Kaufman [1293] from a competitive study is not used in the derivation of the preferred value as it is about 33% higher. The magnitudes of the temperature dependences reported by Leu and DeMore [695] and Lee et al. are in excellent agreement. Although the E/R value reported by Zahniser and Kaufman [1293] is in fair agreement with the

other values, it is not considered as it is dependent upon the E/R value assumed for the Cl + O_3 reaction. The Arrhenius expression was derived from a least squares fit to the data reported by Clyne and Watson, Leu and DeMore, Ray and Watson, Clyne and MacRobert, and Lee et al.

F98. ClO + NO_3. The recommended value is based on results reported by Cox et al. [266], Cox et al. [278] Biggs et al. [117], and Kukui et al. [629]. Biggs et al. report the rate constant to be independent of temperature, consistent with the results of Cox et al. [278]. This recent study of Kukui et al. supersedes the earlier study of Becker et al. [89] from the same laboratory, which had indicated the major products to be OClO + NO_2. There is now agreement among all studies that the major reaction channel forms ClOO + NO_2 (see Biggs et al. [117] Cox et al. [278], and Kukui et al. From a study of the OClO/NO_3 system Friedl et al. [400] conclude that at 220 K the formation of ClOO + NO_2 is favored.

F99. ClO + N_2O. The Arrhenius expression was estimated based on the ~600 K data of Walker (reported in Clyne and Watson [247]).

F100. ClO + CO. The Arrhenius expression was estimated based on the ~600 K data of Walker (reported in Clyne and Watson [247]).

F101. ClO + CH_4. The Arrhenius expression was estimated based on the ~600 K data of Walker (reported in Clyne and Watson [247]).

F102. ClO + H_2CO. Poulet et al. [934] have reported an upper limit of 10^{-15} cm^3 $molecule^{-1}$ s^{-1} for k at 298 K using the discharge flow-EPR technique.

F103. ClO + CH_3O_2. The recommended expressions for the overall rate constant is based on the results of Helleis et al. [477]. It is consistent with the room temperature measurements of Simon et al. [1031] and Kenner et al. [591]. The results of Kukui et al. [631] for the overall reaction are in agreement with the recommendation at room temperature, but these values show a slight negative temperature dependence in contrast with the slight positive temperature dependence recommended here. There is general agreement that the only important reaction channels are the two channels resulting in the production of ClOO + CH_3O (a) and CH_3OCl + O_2 (b). However, there is severe disagreement on their relative importance; at room temperature reaction channel (a) is reported to be the major channel by Helleis et al. [477], Simon et al. [1031], Kukui et al. and Helleis et al. [478] but it is reported to be the minor channel by Biggs et al. [115] and Daele and Poulet [292]. Because of this large discrepancy, no branching ratios are recommended. The branching ratio studies that go down to low temperatures (Helleis et al. [477], Kukui et al. , and Helleis et al. [478]) report that reaction channels (a) and (b) are both significant down to lower polar stratospheric temperatures.

F104. ClO + ClO. There are three bimolecular channels for this reaction: ClO + ClO $\rightarrow$ Cl_2 + O_2 (k_1); ClO + ClO $\rightarrow$ ClOO + Cl (k_2); and ClO + ClO $\rightarrow$ OClO + Cl (k_3). The recommended values for the individual reaction channels are from the study of Nickolaisen et al. [842]. This study, using a flash photolysis/long path ultraviolet absorption technique, is the most comprehensive study of this system, covering a wide range of temperature and pressure. These results are preferred over the results of earlier studies of the total bimolecular rate coefficient at low pressures by Clyne and Coxon [224], Clyne and White [251], and Clyne et al. [237], and those of other studies reported by Hayman et al. [472], Cox and Derwent [271], Simon et al. [1032], Horowitz et al. [505], and Horowitz et al. [506]. The room temperature branching ratio are k_1:k_2:k_3 = 0.29:0.50:0.21. The reaction exhibits both bimolecular and termolecular reaction channels (see entry in Table 2). The termolecular reaction dominates at pressures higher than about 10 torr. The equilibrium constant for formation of the Cl_2O_2 dimer is given in Table 3.

F105. HCl + $ClONO_2$. Results of four studies of the kinetics of this system have been published, in which the following upper limits to the homogeneous bimolecular rate constant were reported: 1 x 10^{-19} cm^3 $molecule^{-1}$ s^{-1} by a static wall-less long-path UV absorption technique and a steady-state flow FTIR technique (Molina et al. [805]); 5 x 10^{-18} using a flow reactor with FTIR analysis (Friedl et al. [398]); and 8.4 x 10^{-21} using a static photolysis system with FTIR analysis (Hatakeyama and Leu [470] and Leu et al. [696]), and 1.5 x 10^{-19} by FTIR analysis of the decay of $ClONO_2$ in the presence of HCl in large-volume (2500 and 5800 liters) Teflon or Teflon-coated chambers (Atkinson et al. [38]). Earlier, Birks et al. [119] had

reported a higher upper limit. All studies found this reaction to be catalyzed by surfaces. The differences in the reported upper limits can be accounted for in terms of the very different reactor characteristics and detection sensitivities of the various studies. The homogeneous reaction is too slow to have any significant effect on atmospheric chemistry.

F106. $CH_2ClO + O_2$. The CH_2ClO radical is reported to be resistant to unimolecular dissociation into Cl + CH_2O products, according to chain reaction/product analysis studies by Sanhueza and Heicklen [993] and Niki et al. [864] and kinetics studies by Catoire et al. [191]. The recommendation is based on the work of Kaiser and Wallington [585] who studied the competition between reaction with O_2 and HCl elimination in a complex photochemical reaction system using FTIR detection of stable products. The recommendation is a factor of 5 higher than estimated using the empirical relationship given by Atkinson and Carter [40]. The fate of CH_2ClO in the atmosphere is this reaction with O_2.

F107. $CH_2ClO_2 + HO_2$. The recommendation is based on the measurement reported by Catoire et al. [191], who used pulsed photolysis with UV absorption detection at 1 atm pressure and 251- 588 K.

F108. $CH_2ClO_2 + NO$. The recommendation is based on the value reported by Sehested et al. [1015], who used pulsed radiolysis and UV absorption detection of NO_2 to measure the rate coefficient. The temperature dependence is estimated by analogy to similar $RO_2 + NO$ reactions.

F109. $CCl_3O_2 + NO$. The recommendation is based upon the measurements of Ryan and Plumb [978] and Dognon et al. [349], who agree well at room temperature. The temperature dependence is derived from the data of Dognon et al., who covered the temperature range 228-413 K. The CCl_3O primary product of the reaction of CCl_3O_2 with NO decomposes rapidly to eliminate Cl, according to Lesclaux et al. [685].

F110. $CCl_2FO_2 + NO$. The recommendation is based on the measurements made by Dognon et al. [349] using pulsed photolysis with mass spectrometry detection at 1-10 torr and 228-413 K. These results supersede the earlier study of Lesclaux and Caralp [683]. The CCl_2FO radical primary product of the $CCl_2FO_2 + NO$ reaction is reported by Lesclaux et al.[685] and Wu and Carr [1280] to rapidly decompose to eliminate Cl and to give the products indicated.

F111. $CClF_2O_2 + NO$. The recommendation is based on the measurements made by Dognon et al. [349], who used pulsed photolysis with mass spectrometry detection at 1-10 torr and 228-413 K, and Sehested et al. [1015], who used pulsed radiolysis with UV absorption detection of the NO_2 product at one atm and 298K. Wu and Carr [1280] observed the $CClF_2O$ radical primary product to rapidly dissociate to CF_2O and Cl.

G1. O + BrO. The preferred value is based on the value reported by Thorn et al. [1128] using a dual laser flash photolysis/long path absorption/resonance fluorescence technique. Clyne et al. [239] reported a value approximately 40% lower.

G2. O + HBr. Results of the flash photolysis-resonance fluorescence study of Nava et al. [825] for 221-455 K and the laser flash photolysis-resonance fluorescence study of Nicovich and Wine [849] for 250-402 K provide the only data at stratospheric temperatures. Results reported include those of Singleton and Cvetanovic [1041] for 298-554 K by a phase-shift technique, and discharge flow results of Brown and Smith [147] for 267-430 K and Takacs and Glass [1104] at 298 K. The preferred value is based on the results of Nava et al., as well as those of Nicovich and Wine and those of Singleton and Cvetanovic over the same temperature range, since these results are less subject to complications due to secondary chemistry than are the results using discharge flow techniques. The uncertainty at 298 K has been set to encompass these latter results.

G3. O + HOBr. Recommended room temperature value is the mean of results of Monks et al. [1128] and Kukui et al. [630]. The temperature dependence is from Nesbitt et al. [838]. The A-factor from that study has been adjusted to fit the recommended room temperature value. Kukui et al. determined that the Br atom abstraction channel is the only pathway at room temperature.

G4. $OH + Br_2$. The recommended room temperature value is the average of the values reported by Boodaghians et al. [129], Loewenstein and Anderson [725], and Poulet et al. [929]. The temperature independence is from Boodaghians et al. Loewenstein and Anderson determined that the exclusive products are Br + HOBr.

G5. OH + BrO. Recommended room temperature value is that reported by Bogan et al. [126]. This study, using discharge flow reactor techniques and beam sampling mass spectrometry, is the only experimental measurement of this rate constant. Because of the difficulty of analyzing the data, we assign a large uncertainty factor. The authors suggest that the reaction proceeds by recombination to form vibrationally excited HOOBr that dissociates to Br + HO_2.

G6. OH + HBr. The preferred value at room temperature is the average of the values reported by Ravishankara et al. [956] using FP-RF, by Jourdain et al. [578] using DF-DPR, by Cannon et al. [179] using FP-LIF, and by Ravishankara et al. [958] using LFP-RF and LFP-LIF techniques. In this latest study the HBr concentration was directly measured in-situ in the slow flow system by UV absorption. The rate constant determined in this re-investigation is identical to the value recommended here. The data of Ravishankara et al. [956] show no dependence on temperature over the range 249-416 K. Values reported by Takacs and Glass [1105] and by Husain et al. [528] are a factor of 2 lower and were not included in the derivation of the preferred value. Data by Sims et al. [1038] are in good agreement with the reommendation at 298 K but show a negative temperature dependence at lower temperatures.

G7. OH + CH_3Br. The recommended value averages results of Hsu and DeMore [518], Chichinin et al. [213], Mellouki et al. [787] and Zhang et al. [1309]. The results of these extensive studies are in excellent agreement and are preferred over the higher values reported in the earlier studies of Davis et al. [311] and Howard and Evenson [511].

G8. OH + CH_2Br_2. Recommended value is based on results of Mellouki et al. [787], DeMore [329], and Orlando et al. [887], all of which are in excellent agreement.

G9. OH + $CHBr_3$. Arrhenius expression from DeMore [329]. Results of Orkin et al. [884] are higher by a factor of 2 but have a similar temperature dependence.

G10. OH + CHF_2Br. The recommended value is a fit to the data of Talukdar et al. [1113], Orkin and Khamaganov [882] and Hsu and DeMore [519], all of which are in excellent agreement. These data are preferred over the consistently higher results reported by Brown et al. [143].

G11. OH + CH_2ClBr. Arrhenius expression fit to data of DeMore [329] and Orkin et al. [885], which are in good agreement.

G12. OH + CF_2ClBr. The recommended upper limit at room temperature is the upper limit reported by Burkholder et al. [162] in a study using pulsed photolysis-LIF and DF-LMR techniques. A less sensitive upper limit was reported by Clyne and Holt [230].

G13. OH + CF_2Br_2. The recommended upper limit at room temperature is the upper limit reported by Burkholder et al. [162] in a study using pulsed photolysis-LIF and DF-LMR techniques.

G14. OH + CF_3Br. The recommended upper limit at room temperature is the upper limit reported by Burkholder et al. [162] in a study using pulsed photolysis-LIF and DF-LMR techniques. A less sensitive upper limit was reported by Le Bras and Combourieu [666]. The upper limit of Orkin and Khamaganov [882] is in agreement.

G15. OH + CH_2BrCF_3. Fit to the data of Nelson et al. [830] and Orkin and Khamaganov [882], which are in reasonable agreement.

G16. OH + $CHFBrCF_3$. Based on data of Orkin and Khamaganov [882].

G17. OH + $CHClBrCF_3$. Based on data of Orkin and Khamaganov [882].

G18. OH + $CF_2BrCHFCl$. Based on DeMore [329].

G19. OH + CF_2BrCF_2Br. The recommended upper limit at room temperature is the upper limit reported by Burkholder et al. [162] in a study using pulsed photolysis-LIF and DF-LMR techniques. The upper limit of Orkin and Khamaganov [882] is in agreement.

G20. HO_2 + Br. This recommendation is based on results obtained over the 260-390 K temperature range in the study by Toohey et al. [1138], using a discharge flow system with LMR detection of HO_2 decay in excess Br. The room temperature value reported in this study is a factor of 3 higher than that reported by Poulet et al. [930] using LIF and MS techniques and is an order of magnitude larger than the value of Posey et al. [925]. The uncertainty in E/R is set to encompass the value E/R = O, as it is for other radical-radical reactions. The value determined by Laverdet et al. [663] using DF-EPR techniques is in good agreement with this recommendation. The reactions of Br atoms with H_2O_2, HCHO, and HO_2 are all slower than the corresponding reactions of Cl atoms by one to two orders of magnitude.

G21. HO_2 + BrO. The recommendation is based on results of the temperature-dependent studies of Larichev et al. [660], Elrod et al. ([365], and Li et al. [705]. The studies of Larichev et al. and Elrod et al. were done under pseudo-first-order conditions with excess HO_2; the study of Li et al. was done under pseudo-first-order conditions with either HO_2 or BrO in excess. The recommended room temperature value is the mean of the values reported in these studies, with the values of Li et al. under both conditions included. These studies all report a similar negative temperature dependence. The room temperature value of Bridier et al. [142], which was not obtained under pseudo-first-order decay conditions, was not included in derivation of the recommendation. Larichev et al. have determined an upper limit of 1.5% for production of HBr and O_3. From a study of the reverse reaction above room temperature, Mellouki et al. [786] determined by extrapolation that the yield of HBr + O_3 is an insignificant fraction (<0.01%) of the total reaction down to 200 K.

G22. NO_3 + HBr. The recommended upper limit is the upper limit reported by Mellouki et al. [783] in a study using DF-EPR techniques. This upper limit shows that this reaction is of negligible importance in stratospheric chemistry. Canosa-Mas et al. [181] reported a value that is consistent, within experimental error, with the upper limit of Mellouki et al.

G23. Cl + CH_2ClBr. Recommended value is based on results of Tschuikow-Roux et al. [1143] normalized to the value of the rate constant for the reference reaction (Cl + CH_4) recommended in this evaluation.

G24. Cl + CH_3Br. Recommended value is based on results of the absolute rate studies of Gierczak et al. [415] and Orlando et al. [887]. Results of these studies are in excellent agreement. Results of the relative rate study Tschuikow-Roux et al. [1143] were not used in derivation of the recommended value.

G25. Cl + CH_2Br_2. Recommended value is based on results of the absolute rate studies of Gierczak et al. [415] and Orlando et al. [887]. Results of these studies are in excellent agreement. Results of the relative rate study of Tschuikow-Roux et al. [1143] were not used in derivation of the recommended value.

G26. Br + O_3. The results reported for k(298 K) by Clyne and Watson [249], Leu and DeMore [694], Michael et al. [794], Michael and Payne [799], and Toohey et al. [1139] are in excellent agreement. The preferred value at 298 K is derived by taking a simple mean of these five values. The temperature dependences reported for k by Leu and DeMore and by Toohey et al. are in good agreement, but they can only be considered to be in fair agreement with those reported by Michael et al. and Michael and Payne. The preferred value was synthesized to best fit all the data reported from these five studies. The results of Nicovich et al. [845] are in excellent agreement with this recommendation.

G27. Br + H_2O_2. The recommended upper limit to the value of the rate constant at room temperature is based on results reported in the study by Toohey et al. [1138] using a discharge flow-resonance fluorescence/laser magnetic resonance technique. Their upper limit determined over the temperature range 298-378 K is consistent with less sensitive upper limits determined by Leu [690] and Posey et al. [925] using the discharge flow-mass spectrometric technique. The much higher value reported by Heneghan and Benson [481] may result from the presence of excited Br atoms in the very low pressure reactor. The pre-exponential factor was chosen to be consistent with that for the Cl + H_2O_2 rate constant, and the E/R value was fitted to the upper limit at 298 K. Mellouki et al. [786] have measured the rate of the reverse reaction.

G28. Br + NO_3. The recommended value is that reported by Mellouki et al. [783] in a study using DF-DPR techniques.

G29. Br + H_2CO. There have been two studies of this rate constant as a function of temperature: Nava et al. [827], using the flash photolysis-resonance fluorescence technique, and Poulet et al. [928], using the discharge flow-mass spectrometric technique. These results are in reasonably good agreement. The Arrhenius expression was derived from a least squares fit to the data reported in these two studies. The higher room temperature value of Le Bras et al. [667], using the discharge flow-EPR technique, has been shown to be in error due to secondary chemistry (Poulet et al.).

G30. Br + OClO. The recommended value at room temperature is the mean of the values reported by Clyne and Watson [250] and Toohey [1136]. In the study of Clyne and Watson, correction for the effect of the rapid reverse reaction was required. The temperature dependence reported by Toohey [1136] is accepted but with increased error limits.

G31. Br + Cl_2O. The recommended value is based on results reported by Stevens and Anderson [1079] and by Sander and Friedl [984], which are in good agreement.

G32. Br + Cl_2O_2. The recommended value is that determined by Friedl (private communication) in a study using a DF-MS technique.

G33. BrO + O_3. There have been two recent studies of this reaction. Rattigan et al. [943] report an overall rate constant of $\sim 10^{-17}$ cm^3 $molecule^{-1}s^{-1}$ over the temperature range 318-343 K. Rowley et al. [975] report a room temperature upper limit of $2x10^{-17}$ cm^3 $molecule^{-1}s^{-1}$. Both papers report a value of $\sim 2x10^{-18}$ cm^3 $molecule^{-1}$ s^{-1} for the channel to produce OBrO + O_2. The recommended upper limit of 2×10^{-17} cm^3 $molecule^{-1}s^{-1}$ is a factor of 2.5 less than the previously recommended upper limit of 5×10^{-17}, which was based on Mauldin et al. [769]. The pre-exponential factor was estimated, and E/R was calculated.

G34. BrO + NO. The results of the three low pressure mass spectrometric studies (Clyne and Watson [249]; Ray and Watson [962]; Leu [688]) and the high pressure UV absorption study (Watson et al. [1234]), which all used pseudo first-order conditions, are in excellent agreement at 298 K and are thought to be much more reliable than the earlier low pressure UV absorption study (Clyne and Cruse [225]). The results of the two temperature-dependence studies are in good agreement and both show a small negative temperature dependence. The preferred Arrhenius expression was derived from a least squares fit to all the data reported in the four recent studies. By combining the data reported by Watson et al. with those from the three mass spectrometric studies, it can be shown that this reaction does not exhibit any observable pressure dependence between 1 and 700 torr total pressure. The temperature dependences of k for the analogous ClO and HO_2 reactions are also negative and are similar in magnitude.

G35. BrO + NO_3. The recommended value is the geometric mean of the lower and upper limits reported by Mellouki et al. [783] in a study using DF-DPR techniques. These reported limits are encompassed within the indicated uncertainty limits.

G36. BrO + ClO. Friedl and Sander [399], using DF/MS techniques, measured the overall rate constant over the temperature range 220-400 K and also over this temperature range determined directly branching ratios for the reaction channels producing BrCl and OClO. The same authors in a separate study using flash photolysis-ultraviolet absorption techniques (Sander and Friedl [984]) determined the overall rate constant over the temperature range 220-400 K and pressure range 50-750 torr and also determined at 220 K and 298 K the branching ratio for OClO production. The results by these two independent techniques are in excellent agreement, with the overall rate constant showing a negative temperature dependence. Toohey and Anderson [1137], using DF/RF/LMR techniques, reported room temperature values of the overall rate constant and the branching ratio for OClO production. They also found evidence for the direct production of BrCl in a vibrationally excited π state. Poulet et al. [926], using DF/MS techniques, reported room temperature values of the overall rate constant and branching ratios for OClO and BrCl production. Overall room temperature rate constant values reported also include those from the DF/MS study of Clyne and Watson [250] and the very low value derived in the flash photolysis study of Basco and Dogra [78] using a different interpretation of the reaction mechanism. The recommended Arrhenius expressions for the individual reaction channels are taken from the study of Friedl and Sander [399]. This study and the study of Turnipseed et al. [1160] contain the most comprehensive sets of rate constant and branching ratio data. The overall rate constants reported in these two studies are in good agreement (20%) at room temperature and in excellent agreement at stratospheric temperatures. Both studies report that OClO production by channel (1) accounts for 60% of the overall reaction at 200 K. Both studies report a BrCl yield by channel (3) of about 8%, relatively independent of

temperature. The recommended expressions are consistent with the body of data from all studies except those of Hills et al. [487] and Basco and Dogra [78].

G37. BrO + BrO. Measurements of the overall rate constant can be divided into categories - those in which BrO was monitored by UV absorption and those in which BrO was monitored by mass spectrometer. Gilles et al. [421] have re-analyzed the results of the UV absorption studies and scaled the reported values of the rate constant to the UV absorption cross sections reported in their paper. When scaled in this manner, the room temperature rate constant values reported in the UV absorption studies (Sander and Watson [990], Mauldin et al. [769], Bridier et al. [142], Rowley et al. [975], Laszlo et al. [661], and Gilles et al.) come into very good agreement among themselves and also with results of the mass spectrometric studies of Clyne and Watson [249] and Lancar et al. [656]. This provides the basis for the recommended room temperature value. The temperature dependence is based on results of Sander and Watson, Turnipseed et al. [1159] and Gilles et al.

There are two possible bimolecular channels for this reaction: BrO + BrO $\rightarrow$ 2Br + O_2 (k_1) and BrO + BrO $\rightarrow$ Br_2 + O_2 (k_2). The partitioning of the total rate constant into its two components, k_1 and k_2, has been measured at room temperature by Sander and Watson [990], Turnipseed et al. [1159] and Lancar et al. [656], by Jaffe and Mainquist [548] from 258 to 333 K, by Cox et al. [284] from 278 to 348 K and by Mauldin et al. [769] from 220 to 298 K. All are in agreement that $k_1/k = 0.85 \pm 0.03$ at 298 K. From the values of $k_1/k = 0.85$ at 298 K (all studies) and 0.68 at 220 K (Mauldin et al. and Cox et al. extrapolated), one can derive the temperature dependent expression $k_1/k = 1.60 \exp(-190/T)$. From the recommended Arrhenius expression for the overall rate constant $k = k_1 + k_2$ and the expression for the branching ratio k_1/k, one can derive the following Arrhenius expressions for the individual reaction channels: $k_1 = 2.4 \times 10^{-12} \exp(40/T)$ cm^3 molecule^{-1}s^{-1} and $k_2 = 2.8 \times 10^{-14} \exp(860/T)$ cm^3 molecule^{-1}s^{-1}.

G38. CH_2BrO_2 + NO. The recommendation is based on the 298 K measurement of Sehested et al. [1015], who used pulsed radiolysis with UV absorption detection of the NO_2 product formation rate. The temperature dependence is estimated based on analogy to similar RO_2 + NO reactions. The CH_2BrO product has been shown to undergo rapid unimolecular decomposition to yield CH_2O + Br by Chen et al. [204] and Orlando et al. [886] The domination of this channel over the reaction of CH_2BrO with O_2 is consistent with the fate of other alkoxy radicals (Chen et al. and Orlando et al.), but contradicts the easrlier result of Nielson et al. [855].

H1. O + I_2. Based on the room temperature data of Ray and Watson [962] and Laszlo et al. [662]. The molecular beam study of Parrish and Herschbach [898] suggests a zero activation energy, consistent with the near gas kinetic value of k at 298 K.

H2. O + IO. Based on results of Laszlo et al. [662], the only reported study of this rate constant. This value was derived from modeling a system in which the concentrations of I_2 and IO were monitored simultaneously. This rate constant is a factor of 4 greater than the values for the corresponding reactions of O with ClO and BrO.

H3. OH + I_2. Based on the data of Loewenstein and Anderson [726] and Jenkin et al. [555].

H4. OH + HI. Based on the data of Lancar et al. [658] and MacLeod et al. [740].

H5. OH + CH_3I. Based on the data of Brown et al. [145], the only reported study of this reaction.

H6. OH + CF_3I. The recommended value is based on results of the discharge flow/resonance fluorescence study of Brown et al. [145]. The value reported in this study is preferred over the much higher value (factor of 4) reported by Garraway and Donovan [409], using flash photolysis with time-resolved absorption photometry. The Garraway and Donovan value is encompassed within the stated uncertainty.

H7. HO_2 + I. Based on the data of Jenkin et al. [561], the only reported study of this reaction.

H8. HO_2 + IO. The recommended value is the average of the values reported by Jenkin et al. [560] and Maguin et al. [743].

H9. NO_3 + HI. No recommendation is given, based on the potential for severe complications resulting from secondary chemistry in the only reported study of the reaction (Lancar et al. [658]).

H10. $I + O_3$. Based on the room temperature data of Jenkin and Cox [556] and Sander [983], and the temperature dependent data of Buben et al. [152] and Turnipseed et al. [1162].

H11. $I + BrO$. Based on results of Laszlo et al. [661], the only reported study of this rate constant. This value was derived from modeling the simultaneous decay of BrO and IO in a $Br_2/I_2/N_2O$ system.

H12. $IO + NO$. Based on the data of Ray and Watson [962], Daykin and Wine [317], Buben et al. [153], and Turnipseed et al. [1162].

H13. $IO + ClO$. Based on results of Turnipseed et al. [1161], the only reported study of this reaction. These authors also reported the product yield for channel(s) yielding an I atom to be 0.8 ± 0.2.

H14. $IO + BrO$. Based primarily on results of Laszlo et al. [661]. Gilles et al. [421] reported the following Arrhenius expression for non-iodine atom producing channels: 2.5×10^{-11} exp (260/T) cm^3 $molecule^{-1}s^{-1}$. They also reported a branching ratio of <0.35 for channels producing I atoms. From their data they could constrain the value of the overall rate constant to be: $6 \times 10^{-11} < k < 10 \times 10^{-11}$ cm^3 $molecule^{-1}s^{-1}$, the range of which is consistent with the results of Laszlo et al.

H15. $IO + IO$. Changed from the previous recommendation, which was based on the results of Sander [983]. In that study, over the temperature range 250-373 K, a negative temperature dependence was reported for the overall rate constant and for the absorption cross section at 427.2 nm. In the recent study of Harwood et al. [468], the overall rate constant and the absorption cross section were found to be independent of temperature from 253 to 320 K. The recommended room temperature value is the average of the values reported by Sander, Harwood et al., and Laszlo et al. [662]. The recommended temperaure dependence is the average of the values reported by Sander and by Harwood et al., with an uncertainty sufficient to encompass the two reported values. The A-factor has been fitted to the recommended room temperature rate constant and the recommended temperature dependence. The overall rate constant for the decay of IO in the absence of ozone has been found to be independent of pressure by Sander, Laszlo et al., and Harwood et al. A comparison of the overall rate observed in excess ozone to that in the absence of ozone was interpreted by Sander and by Harwood et al. to imply that formation of the dimer I_2O_2 is the dominant reaction channel in the IO self-reaction.

H16. $INO + INO$. Based on the data of Van den Bergh and Troe [1175].

H17. $INO_2 + INO_2$. Based on the data of Van den Bergh and Troe [1175].

I1. $O + SH$. This recommendation accepts the results of Cupitt and Glass [289]. The large uncertainty reflects the absence of any confirming investigation.

I2. $O + CS$. The room temperature recommendation is an average of the rate constants determined by Slagle et al. [1052], Bida et al. [111], Lilenfeld and Richardson [715], and Hancock and Smith [462]. The temperature dependence is that of Lilenfeld and Richardson, with the A-factor adjusted to yield the recommended value of k(298 K).

I3. $O + H_2S$. This recommendation is derived from an unweighted least squares fit of the data of Singleton et al. [1044] and Whytock et al. [1249]. The results of Slagle et al. [1050] show very good agreement for E/R in the temperature region of overlap (300 - 500 K) but lie systematically higher at every temperature. The uncertainty factor at 298 K has been chosen to encompass the room temperature rate constant values of Slagle et al. [1050] and Hollinden et al. [500]. Other than the 263 K data point of Whytock et al. and the 281 K point of Slagle et al., the main body of rate constant data below 298 K comes from the study of Hollinden et al., which indicates a dramatic change in E/R in this temperature region. Thus, $\Delta E/R$ was set to account for these observations. Such a nonlinearity in the Arrhenius plot might indicate a change in the reaction mechanism from abstraction (as written) to addition. An addition channel (resulting in H atom displacement) has been proposed by Slagle et al. [1050], Singleton et al. [1044], and Singleton et al. [1046]. In the latter two studies, an upper limit of 20% was placed on the displacement channel. Direct observations of product HSO was made in the reactive scattering experiments of Clemo et al. [222] and Davidson et al. [301]. A threshold energy of 3.3 kcal/mole was observed (similar to the activation energy measured in earlier studies), suggesting the importance of this direct displacement channel. Addition products from this reaction have been seen in a matrix by Smardzewski and Lin [1055]. Further kinetic studies in the 200 - 300 K temperature

range, as well as quantitative direct mechanistic information, could clarify these issues. However, this reaction is thought to be of limited importance in stratospheric chemistry.

I4. $O + OCS$. The value of k(298 K) is the average of the determinations by Westenberg and de Haas [1241], Klemm and Stief [618], Wei and Timmons [1237], Manning et al. [746], and Breckenridge and Miller [141]. The recommended value of E/R is the average value taken from the first three listed studies. Hsu et al. [517] report that this reaction proceeds exclusively by a stripping mechanism. The vibrational and rotational state distributions in the SO and CO products have been reported by Chen et al. [209] and Nickolaisen et al. [843] respectively.

I5. $O + CS_2$. The value of k(298 K) is an average of the rate constants determined by Wei and Timmons [1237], Westenberg and de Haas [1241], Slagle et al. [1051], Callear and Smith [176], Callear and Hedges [175], Homann et al. [501], and Graham and Gutman [431]. The E/R value is an average of the determinations by Wei and Timmons and Graham and Gutman. The $\Delta E/R$ has been set to encompass the limited temperature data of Westenberg and de Haas. The principal reaction products are thought to be CS + SO. However, Hsu et al. [517] report that 1.4% of the reaction at 298 K proceeds through a channel yielding $CO + S_2$ and calculate a rate constant for the overall process in agreement with that recommended. Graham and Gutman [431] have found that 9.6% of the reaction proceeds to yield OCS + S at room temperature. Using time-resolved diode laser spectroscopy, Cooper and Hershberger [263] determined the branching ratios for the CO and OCS producing channels to be (3.0±1.0)% and (8.5±1.0)% respectively.

I6. $O + CH_3SCH_3$. This recommendation is based on a fit of the data from Nip et al. [871], Lee et al. [676], and Lee et al. [675]. Product studies by Cvetanovic et al. [290] indicate that the reaction proceeds almost entirely by addition followed by rapid fragmentation to the products as written. Pavanaja et al. [903] examined the pressure and reactant ratio dependencies of $OH(A^2\Sigma^+)$ and $SO_2(^3B, ^1B)$ emissions in this reaction system. Their observations are consistent with initial product formation as written, followed by secondary generation of both OH and SO_2.

I7. $O + CH_3SSCH_3$. This recommendation averages the 298 K rate constants of Nip et al. [871] and Lee et al. [672], which differ by nearly a factor of 2. The temperature dependence is that of Nip et al.; Lee et al. having reported no temperature dependence over the limited range of 270-329K. The A-factor has been adjusted to yield the recommended (averaged) value of k(298K). Product studies by Cvetanovic et al. [290] indicate that the reaction proceeds mainly by addition followed by rapid fragmentation to the products as written. Pavanaja et al. [903] examined the pressure and reactant ratio dependencies of $OH(A^2\Sigma^+)$ and $SO_2(^3B, ^1B)$ emissions in this reaction system. Their observations are consistent with initial product formation as written, followed by secondary generation of both OH and SO_2.

I8. $O_3 + H_2S$. This upper limit was determined by Becker et al. [93] from measurements of the rates of SO_2 production and O_3 consumption. The heterogeneous reaction between H_2S and O_3 is far more efficient in most laboratory systems.

I9. $O_3 + CH_3SCH_3$. This rate constant upper limit is based on the measurements of Martinez and Herron [764], which represent the only reported study of this reaction.

I10. $SO_2 + O_3$. This recommendation is based on the limited data of Davis et al. [312] at 300 K and 360 K in a stopped flow investigation using mass spectrometric and UV spectroscopic detection.

I11. $OH + H_2S$. The values of k(298 K) and E/R are derived from a composite unweighted least squares fit to the individual data points of Perry et al. [909], Cox and Sheppard [283], Wine et al. [1257], Leu and Smith [700], Michael et al. [795], Lin [717], Lin et al. [720], Barnes et al. [60], and Lafage et al. [653]. The studies of Leu and Smith [700], Lin et al. [720], Lin [717], and Lafage et al. [653] show a slight parabolic temperature dependence of k with a minimum occurring near room temperature. However, with the error limits stated in this evaluation, all data are fit reasonably well by an Arrhenius expression. Lafage et al. and Michael et al. discuss the results in terms of a two-channel reaction scheme involving direct H atom abstraction and complex (adduct) formation. Lafage et al. analyzed their results above room temperature to yield an apparent E/R = 400K for the abstraction channel, in good agreement with the E/R value determined above room temperature by Westenberg and de Haas [1243]. The results of these latter workers lie systematically higher (by about 70%), presumably due to secondary reactions. The room temperature value measured by Stuhl [1091] lies just outside the 2σ error limit set for k(298 K).

I12. OH + OCS. The value of k(298 K) is an average of the determinations by Wahner and Ravishankara [1192] and Cheng and Lee [210]. The room temperature rate constants from these studies are a factor of 3 higher than the earlier determination by Leu and Smith [698]. As discussed in the later studies, this difference may be due to an overcorrection of the Leu and Smith data to account for OH reaction with H_2S impurities and also to possible regeneration of OH. Nevertheless, the uncertainty factor at 298 K has been set to encompass the earlier study within 2σ. The work by Wahner and Ravishankara [1192] supersedes the study of Ravishankara et al. [948], which minimized complications due to secondary and/or excited state reactions that presumably were interfering with the experiments of Atkinson et al. [43] and of Kurylo [639]. The upper limit for k(298 K) reported by Cox and Sheppard [283] is too insensitive to permit comparison with the more recent studies. The room temperature measurements of Wahner and Ravishankara demonstrate the lack of an effect of total pressure (or O_2 partial pressure) on the rate constant and are supported by the more limited pressure and O_2 studies of Cheng and Lee. The recommendation for E/R is based on the study of Cheng and Lee who determined a value considerably lower than reported by Leu and Smith, although this difference may be due in part to the earlier mentioned overcorrection of the data by the latter authors.

Product observations by Leu and Smith indicate that SH is a primary product of this reaction and tentatively confirm the suggestion of Kurylo and Laufer [647] that the predominant reaction pathway is to produce SH + CO_2 through a complex (adduct) mechanism similar to that observed for the OH + CS_2 reaction. However, the absence of an O_2/pressure effect for OH + OCS is in marked contrast with the strong dependence seen in studies of OH + CS_2 (see note for the latter reaction).

Experiments by Greenblatt and Howard [436] have shown that oxygen atom exchange in the reaction of ^{18}OH with OCS is relatively unimportant, leading to an upper limit of 1×10^{-15} being set on the rate constant of the exchange reaction.

I13. OH + CS_2. There is a consensus of experimental evidence that this reaction proceeds very slowly as a direct bimolecular process. Wine et al. [1267] set an upper limit on k(298 K) of 1.5×10^{-15} cm^3 $molecule^{-1}$ s^{-1}. A consistent upper limit is also reported by Iyer and Rowland [545] for the rate of direct product of OCS, suggesting that OCS and SH are primary products of the bimolecular process. This mechanistic interpretation is further supported by the studies of Leu and Smith [699] and of Biermann et al. [113], which set somewhat higher upper limits on k(298 K). The more rapid reaction rates measured by Atkinson et al. [43], Kurylo [639], and Cox and Sheppard [283] may be attributable to severe complications arising from excited state and secondary chemistry in their photolytic systems. The Cox and Sheppard study in particular may have been affected by the reaction of electronically excited CS_2 (produced via the 350 nm photolysis) with O_2 (in the one-atmosphere synthetic air mixture) as well as by the accelerating effect of O_2 on the OH + CS_2 reaction itself, which has been observed by other workers as summarized below. The possible importance of electronically excited CS_2 reactions in the tropospheric oxidation of CS_2 to OCS has been discussed by Wine et al. [1256].

An accelerating effect of O_2 on the OH + CS_2 reaction rate has been observed by Jones et al. [575], Barnes et al. [66], and Hynes et al. [534], along with a near unity product yield for SO_2 and OCS. In the latter two studies the effective bimolecular rate constant was found to be a function of total pressure (O_2 + N_2), and exhibited an appreciably negative temperature dependence. These observations are consistent with the formation of a long-lived adduct as postulated by Kurylo [639] and Kurylo and Laufer [647], followed by its reaction with O_2:

$$OH + CS_2 + M \underset{k_b}{\overset{k_a}{\leftrightarrow}} HOCS_2 + M$$

$$HOCS_2 + O_2 \xrightarrow{k_c} \text{Products}$$

Hynes et al. [534], Murrells et al. [820], Becker et al. [94], and Bulatov et al. [155] directly observed the approach to equilibrium in this reversible adduct formation. In the Hynes et al. study, the equilibrium constant was measured as a function of temperature, and the heat of formation of $HOCS_2$ was calculated (-27.4 kcal/mole). A rearrangement of this adduct followed by dissociation into OCS and SH corresponds to

the bimolecular (low k) channel referred to earlier. Hynes et al. [534] measured the rate constant for this process in the absence of O_2 (at approximately one atmosphere of N_2) to be $< 8 \times 10^{-16}$ cm^3 $molecule^{-1}$ s^{-1}. Hynes et al. [534], Murrells et al. [820], and Diau and Lee [337] agree quite well on the value of k_c, with an average value of 2.9×10^{-14} being reported independent of temperature and pressure. Diau and Lee also report the rate constants for the reactions of the adduct (CS_2OH) with NO and NO_2 to be 7.3×10^{-13} and 4.2×10^{-11} respectively.

The effective second order rate constant for CS_2 or OH removal in the above reaction scheme can be expressed as

$$1/k_{eff} = (k_b/k_a k_c)(1/P_{O2}) + (1/k_a)(1/P_M)$$

where P_{O2} is the partial pressure of O_2 and P_M equals $P_{O2} + P_{N2}$. The validity of this expression requires that k_a and k_b are invariant with the P_{O2}/P_{N2} ratio. A 1/k vs $1/P_{O2}$ plot of the data of Jones et al. [575] taken at atmospheric pressure exhibits marked curvature, suggesting a more complex mechanistic involvement of O_2, whereas the data of Barnes et al. [66] and Hynes et al. [534] are more satisfactorily represented by this analytical expression. Nevertheless, while the qualitative features of the data from all three laboratories agree, there are some quantitative inconsistencies. First, under similar conditions of O_2 and N_2 pressures, the Barnes et al. rate constants lie approximately 60% higher than those of Jones et al. and up to a factor of 2 higher than those derived by Hynes et al. Secondly, two fits each of both the Barnes et al. and Hynes et al. data can be made: one at fixed P_M and varying P_{O2}, and the other at fixed P_{O2} and varying P_M (i.e., varying added N_2). Within each data set, rate constants calculated from both fits agree reasonably well for mole fractions of O_2 near 0.2 (equivalent to air) but disagree by more than a factor of 2 for measurements in a pure O_2 system. Finally, the temperature dependence (from 264 - 293 K) of the k_{eff} values from Barnes et al. varies systematically from an E/R of -1300 K for experiments in pure O_2 (at 700 torr total pressure) to -2900 K for experiments in a 50 torr O_2 plus 650 torr N_2 mixture. An Arrhenius fit of the Hynes et al. data (from 251 - 348 K) recorded in synthetic air at 690 torr yields an E/R = -3300 K, although the data show marked curvature over the temperature range of study. These observations suggest that k_a and k_b may not be independent of the identity of M. For this reason, we limit our recommendation to air mixtures (i.e., $P_{O2}/P_{N2} = 0.25$) at atmospheric pressure. Since most CS_2 is oxidized within the atmospheric boundary layer, such restriction does not limit the applicability of this recommendation in atmospheric modeling.

The present recommendation accepts the measurements of Hynes et al. [534], which appear to be the most sensitive of the three investigations. Thus, k(298 K) is derived from the Arrhenius fit of the data near room temperature.

$$k(298\ K) = 1.2 \times 10^{-12}\ cm^3\ molecule^{-1}\ s^{-1}$$

The uncertainty factor, f(298) = 1.5, encompasses the results of Barnes et al. [66] within 2σ. To compute values of k below 298 K, we have accepted the analysis of Hynes et al.

$$k(T) = \{1.25 \times 10^{-16} \exp(4550/T)\}/\{T + 1.81 \times 10^{-3} \exp(3400/T)\}$$

This recommendation is only valid for one atmosphere pressure of air. It is interesting to note that measurements by Hynes et al. [534] at approximately 250 K and 700 torr total pressure result in k_{eff} values that are independent of the amount of O_2 for partial pressures between 145 - 680 torr. This suggests that the adduct is quite stable with respect to dissociation into the reactants (OH + CS_2) at this low temperature and the that effective rate constant for reactant removal approaches the elementary rate constant for adduct formation.

From a mechanistic viewpoint, the primary products of reaction c determine the products of CS_2 oxidation in air. Lovejoy et al. [732] have shown that the yields of both HO_2 and SO_2 are equal and near unity. Together with the earlier mentioned unity yield of OCS, these observations suggest that the oxidation equation

$$OH + CS_2 + 2O_2 \rightarrow OCS + HO_2 + SO_2$$

describes this atmospheric system. Further insight is provided by the mechanistic study of Stickel et al. [1081], who observe OCS and CO product yields of (0.83±0.08) and (0.16±0.03) respectively. The results from this study are interpreted to imply that OCS and CO are formed either as primary products of the $CS_2OH + O_2$ reaction or as products of a secondary reaction between a primary product and O_2. These same authors report an SO_2 yield of (1.15±0.10), with the results suggesting that only about 75% of the SO_2 formed as a prompt product, with the remainder generated via a slow reaction of SO (generated as a prompt product of the $CS_2OH + O_2$ reaction) with O_2. Insight into the specific reaction pathways can be gleaned from the study of Lovejoy et al. [731] in which k_c for the reaction of $DOCS_2 + O_2$ was found to be the same as that for $HOCS_2$, indicating that simple H atom abstraction is not the likely process. Rather, HO_2 production most likely involves complex formation followed by HO_2 elimination. Lovejoy et al. [733] found that the ^{18}O atom in the ^{18}OH reactant is transferred predominantly (90 ± 20)% to the SO_2 product. These findings are consistent with an S-O bonded CS_2-OH adduct and preservation of the S-O bond in the steps leading to SO_2 formation. Additional work involving direct intermediate observations would be helpful in elucidating this reaction mechanism.

I14. $OH + CH_3SH$. This recommendation is based on a composite fit to the data of Atkinson et al. [42], Wine et al. [1257], Wine et al. [1268], and Hynes and Wine [532], which are in excellent agreement. The results from the relative rate study of Barnes et al. [60] are in agreement with this recommendation and indicate that the higher value of Cox and Sheppard [283] is due to complications resulting from the presence of O_2 and NO in their reaction system. MacLeod et al. [741, 742] and Lee and Tang [674] obtained rate constants at 298K approximately 50% lower than recommended here. These authors also obtained lower values for the ethanethiol reaction in comparison with results from studies upon which the methanethiol recommendation is made. Wine et al. [1268] present evidence that this reaction proceeds via adduct formation to produce a species that is thermally stable over the temperature range and time scales of the kinetic measurements. Tyndall and Ravishankara [1169] have determined the yield of CH_3S (via laser-induced fluorescence) to be unity, indicating that any adduct must be short lived (less than 100 μs). Longer lifetimes would have led to anomalies in the OH decay kinetics used for the rate constant determinations. Hynes and Wine [532] failed to observe any effect of O_2 on the rate constant.

I15. $OH + CH_3SCH_3$. This recommendation is based on the results of Hynes et al. [536], Wine et al. [1257], Hsu et al. [521], Abbatt et al. [2], and Barone et al.[73]. The earlier higher rate constant values of Atkinson et al. [43] and Kurylo [638] are presumably due to reactive impurities, while those of MacLeod et al. [742] were most likely overestimated because of heterogeneous reactions. Absolute determinations lower than those recommended were obtained by Martin et al. [760], Wallington et al. [1197], and Nielsen et al. [860]. While the reasons for these differences are not readily apparent, these results are encompassed within the 2σ error limits of the 298K recommendation. Hynes et al. have demonstrated the importance of a second reaction channel involving addition of OH to dimethyl sulfide (approximately 30% in 1 atmosphere of air at 298K). More recently, Hynes et al. and Barone et al. have examined the reaction mechanism in more detail using fully deuterated DMS. Both groups report similar rate constants for the bimolecular (non-adduct-forming) rate constant and adduct bond strengths (13.0 and 10.1 kcal/mole - Hynes et al.; 10.2 and 10.7 kcal/mole - Barone et al.) from second and third law calculations, respectively. Values of the rate constant for the reaction of the adduct with O_2 were also nearly identical (0.8×10^{-12} cm^3 $molec^{-1}$ s^{-1} from Hynes et al., and 1.0×10^{-12} cm^3 $molec^{-1}$ s^{-1} from Barone et al for both DMS and d^6-DMS) independent of pressure and temperature.

The recommendation given here is for the abstraction reaction only. Confirmation of the products as written is obtained from the study of Stickel et al. [1083] who determined an HDO product yield of (0.84±0.15) for the $OD + CH_3SCH_3$. Further mechanistic insight comes from the studies of Barnes et al. [69, 70] and Turnipseed et al. [1158] who find that the abstraction product, CH_3SCH_2, leads predominantly to CH_3S under atmospheric conditions. Barnes et al. measure a 0.7% yield of OCS under low NO_x conditions, which they attribute to further oxidation of CH_3S. Both Barnes et al. and Turnipseed et al. find a significant (20-30%) yield of dimethyl sulfoxide, apparently produced via the reaction of the DMS-OH adduct with O_2. Zhao et al. [1310] determined an upper yield of 0.07 for CH_3 elimination in the $OD + CH_3SCH_3$ reaction system.

Due to the rapid decomposition of a DMS-OH adduct, only the direct abstraction channel is measured in the absence of O_2. The reaction of the adduct with O_2, as quantified most recently by Hynes et al. and Barone et al., is responsible for the majority of the products formed in the atmospheric oxidation of DMS. An increase

in the observed rate constant (k_{obs}) with increasing O_2 concentration has clearly been observed by Hynes et al. [536], Wallington et al. [1197], Barnes et al. [59], Nielsen et al. [860], Barone et al. [73], and Hynes et al. [531]. This O_2 effect has been suggested as an explanation for the higher rate constants obtained in many of the earlier relative rate studies. Hynes et al. give the following expression for the observed rate constant in one atmosphere of air:

$$k_{obs} = \{T \exp(-234/T) + 8.46 \times 10^{-10} \exp(7230/T) + 2.68 \times 10^{-10} \exp(7810/T)\} / \{1.04 \times 10^{11} T + 88.1 \exp(7460/T)\}$$

This expression was derived empirically from the analysis of a complex data set, which also yielded a value of the rate constant for reaction of the adduct with O_2 that was a factor of 4 larger than the values derived by Hynes et al. [531] and Barone et al. [73] and appeared to be both pressure and temperature dependent. The effect of these revisions in the adduct + O_2 rate constant on the k_{obs} expression is not easily ascertained.

I16. $OH + CH_3SSCH_3$. This recommendation is based on the temperature-dependent studies of Wine et al. [1257] and Abbatt et al. [2] and the room temperature relative rate study of Cox and Sheppard [283]. Domine and Ravishankara [352] have observed both CH_3S (via laser-induced fluorescence) and CH_3SOH (via photoionization mass spectrometry) as products of this reaction. At 298 K, the yield of CH_3S alone was quantified at approximately 30%. An FTIR product study of the photooxidation of dimethyl disulfide by Barnes et al. [68] presents evidence that oxidation of the CH_3SOH product is the principal source of the methane sulfonic acid observed.

I17. OH + S. This recommendation is based on the study by Jourdain et al. [577]. Their measured value for k(298 K) compares favorably with the recommended value of k(O + OH) when one considers the slightly greater exothermicity of the present reaction.

I18. OH + SO. The value recommended for k(298 K) is an average of the determinations by Fair and Thrush [368] and Jourdain et al. [577]. Both sets of data have been corrected using the present recommendation for the O + OH reaction.

I19. $HO_2 + H_2S$, $HO_2 + CH_3SH$, $HO_2 + CH_3SCH_3$. These upper limits are taken from the discharge flow laser magnetic resonance study of Mellouki and Ravishankara [784]. The H_2S value disagrees with the rate constant reported by Bulatov et al. [159] by approximately three orders of magnitude. The reason for this difference is not readily apparent. However, the recommended upper limit is consistent with the values for CH_3SH and CH_3SCH_3, which respectively agree with upper limits from the work of Barnes et al. [60] and Niki (reported as a private communication in the Mellouki and Ravishankara paper).

I20. $HO_2 + SO_2$. This upper limit is based on the atmospheric pressure study of Graham et al. [434]. A low pressure laser magnetic resonance study by Burrows et al. [164] places a somewhat higher upper limit on k(298 K) of 4×10^{-17} (determined relative to $OH + H_2O_2$). Their limit is based on the assumption that the products are OH and SO_3. The weight of evidence from both studies suggests an error in the earlier determination by Payne et al. [905].

I21. $NO_2 + SO_2$. This recommendation is based on the study of Penzhorn and Canosa [907] using second derivative UV spectroscopy. While these authors actually report a measured value for k(298 K), their observations of strong heterogeneous and water vapor catalyzed effects prompt us to accept their measurement as an upper limit. This value is approximately two orders of magnitude lower than that for a dark reaction observed by Jaffe and Klein [547], much of which may have been due to heterogeneous processes. Penzhorn and Canosa suggest that the products of this reaction are $NO + SO_3$.

I22. $NO_3 + H_2S$. This recommendation accepts the upper limit set by Dlugokencky and Howard [340] based on experiments in which NO_3 loss was followed in the presence of large concentrations of H_2S. Less sensitive upper limits for the rate constant have been reported by Wallington et al. [1199] and Cantrell et al. [184].

I23. $NO_3 + OCS$. This upper limit is based on the relative rate data of MacLeod et al. [739].

I24. $NO_3 + CS_2$. This upper limit is based on the study of Burrows et al. [168]. A somewhat higher upper limit was derived in the relative rate data of MacLeod et al. [739].

I25. $NO_3 + CH_3SH$. The recommended values are derived from a composite fit to the data of Wallington et al. [1199], Rahman et al. [940], and Dlugokencky and Howard [340]. The room temperature rate constant derived in the relative rate experiments of MacLeod et al. [739] is in good agreement with the recommended value. The suite of investigations shows the rate constant to be pressure independent over the range 1 - 700 torr. Dlugokencky and Howard place an upper limit of 5% on the production of NO_2 via this reaction at low pressure. Based on the product distribution observed in their investigation, Jensen et al. [564] propose a reaction mechanism initiated by abstraction of the hydrogen atom from the SH group, possibly after formation of an initial adduct as suggested by Wallington et al. and Dlugokencky and Howard.

I26. $NO_3 + CH_3SCH_3$. The recommended values are derived from a composite fit to the data of Wallington et al. [1199], Tyndall et al. [1164], and Dlugokencky and Howard [340]. The relative rate study of Atkinson et al. [45] yields a rate constant at room temperature in good agreement with that recommended. The experimental data from all investigations demonstrate the pressure independence of the rate constant over the range 1 - 740 torr. Room temperature investigations by Daykin and Wine [316] and Wallington et al. [1200] are also in agreement with the recommended value. Jensen et al. [563] propose a mechanism that involves hydrogen abstraction as the first step to explain their observed product distribution. In a later study, Jensen et al. [564] measured a kinetic isotope effect for the rate constant for CH_3SCH_3 vs. that for CD_3SCD_3 of k_H/k_D = (3.8±0.6), providing further confirmation of such abstraction. Butkovskaya and Le Bras [170] utilized chemical titration of the primary radical produced from $NO_3 + CH_3SCH_3$ in a discharge flow mass spectrometer system to show that the reaction produces predominantly $CH_3SCH_2 + HNO_3$. An upper limit of 2% was placed on the reaction channel yielding $CH_3 + CH_3SONO_2$.

I27. $NO_3 + CH_3SSCH_3$. The recommended values were derived from a composite fit to the data of Wallington et al. [1199] and Dlugokencky and Howard [340]. The investigation by Atkinson et al. [37] indicates that the relative rate technique cannot be considered as yielding reliable rate data for this reaction due to chemical complexities. Thus, the much lower room temperature results from the study of MacLeod et al. [739] can be considered to be erroneous. Based on their observations of intermediate and end products, Jensen et al. [564] proposed a reaction mechanism in which the initial addition of NO_3 to one of the sulfur atoms results in formation of $CH_3S + CH_3SO + NO_2$.

I28. $NO_3 + SO_2$. This recommended upper limit for k(298 K) is based on the study by Daubendiek and Calvert [299]. Considerably higher upper limits have been derived by Burrows et al. [168], Wallington et al. [1199], Canosa-Mas et al. [180], and Dlugokencky and Howard [340].

I29. $N_2O_5 + CH_3SCH_3$. This recommendation is based on the value estimated by Tyndall and Ravishankara [1171] from the study by Atkinson et al. [45].

I30. $CH_3O_2 + SO_2$. This recommendation accepts the results from the study of Sander and Watson [989], which is believed to be the most appropriate for stratospheric modeling purposes. These authors conducted experiments using much lower CH_3O_2 concentrations than employed in the earlier investigations of Sanhueza et al. [994] and Kan et al. [588], both of which resulted in k(298 K) values approximately 100 times greater. A later report by Kan et al. [587] postulates that these differences are due to the reactive removal of the $CH_3O_2SO_2$ adduct at high CH_3O_2 concentrations prior to its reversible decomposition into CH_3O_2 and SO_2. They suggest that such behavior of $CH_3O_2SO_2$ or its equilibrated adduct with O_2 ($CH_3O_2SO_2O_2$) would be expected in the studies yielding high k values, while decomposition of $CH_3O_2SO_2$ into reactants would dominate in the Sander and Watson experiments. It does not appear likely that such secondary reactions involving CH_3O_2, NO, or other radical species would be rapid enough, if they occur under normal stratospheric conditions to compete with the adduct decomposition. This interpretation, unfortunately, does not explain the high rate constant derived by Cocks et al. [253] under conditions of low $[CH_3O_2]$.

I31. $F + CH_3SCH_3$. This recommendation is based on the discharge flow mass spectrometric study by Butkovskaya et al. [171]. The uncertainty placed on this recommendation has been increased over that estimated by the authors to reflect the lack of any confirming investigations. Titration of the primary organic radical products indicated that the reaction proceeds via two channels to produce $HF + CH_3SCH_2$ and $CH_3 + CH_3SF$ with a branching ratio of approximately 0.8/0.2 respectively.

I32. Cl + H_2S. This recommendation is based on the study by Nicovich et al. [847], who conducted an elaborate study with attention to sources of possible systematic error. The rate constant at 298K is in good agreement with that determined by Nesbitt and Leone [836], who refined the data of Braithwaite and Leone [140], but is significantly greater than the values reported by Clyne and Ono [243], Clyne et al. [234], and Nava et al. [826]. The small, but clearly observed, negative activation energy determined by Nicovich et al. contrasts with the lack of a temperature dependence observed by Nava et al.. In fact, at the lowest temperature of overlap, the results from these two studies differ by 50%. Nevertheless, the Nicovich et al. study yields consistent results for both H_2S and CH_3SH as well as for D_2S and CD_3SD. While the reason for these differences remains to be determined, the full range of reported values is encompassed within the 2σ error limits recommended. Lu et al. [736] also measured a temperature-independent rate constant but report a value at 298K, about 40% greater than that of Nicovich et al. However, the presence of 4000 torr of CF_3Cl bath gas in the Lu et al may suggest a slight pressure dependence of the reaction, although Nicovich et al. observed no pressure dependence for pressures ranging up to 600 torr with N_2.

I33. Cl + OCS. This upper limit is based on the minimum detectable decrease in atomic chlorine measured by Eibling and Kaufman [364]. Based on the observation of product SCl, these authors set a lower limit on k(298 K) of 10^{-18} for this reaction channel. Considerably higher upper limits on k(298 K) were determined in the studies of Clyne et al. [234] and Nava et al. [826].

I34. Cl + CS_2. This upper limit for the overall reaction is based on determinations by Nicovich et al. [846] and Wallington et al. [1196]. The first authors confirm that the reaction proceeds via reversible adduct formation as suggested by Martin et al. [758]. The much larger rate constant values determined by Martin et al. may possibly be attributed to reactive impurities in the CS_2 sample. Nicovich et al. set an upper limit on the rate constant for the adduct (CS_2Cl) reacting with O_2 of 2.5×10^{-16} at room temperature.

I35. Cl + CH_3SH. This recommendation is based on the results of Nicovich et al. [847], who used laser photolysis with resonance fluorescence detection to study the reactions of Cl with H_2S, D_2S, CH_3SH, and CD_3SD. The room temperature determination by Nesbitt and Leone [836] is in good agreement with the value recommended. The k(298K) value from the study by Mellouki et al. [780] is nearly a factor of 2 lower. However, the low sensitivity of EPR detection of Cl atoms did not permit these latter authors to conduct a precise determination of k under pseudo-first-order conditions, and a more complex analysis of experiments conducted under second-order conditions was required. Nesbitt and Leone [837] report that less than 2% of the reaction occurs via abstraction of an H atom from the CH_3 group.

I36. Cl + CH_3SCH_3. Stickel et al. [1082] have used laser photolysis resonance fluorescence to measure that rate constant between 240-421K, over the pressure range of 3-700 torr. The rate constant is near collisional but increases with increasing pressure from a low pressure limit of 1.8×10^{-10} to a value of 3.3×10^{-10} at 700 torr. The yield of HCl at 297K, measured by diode laser spectroscopy, decreased from near unity at low pressure to a value of approximately 0.5 at 203 torr, suggesting that stabilization of a $(CH_3)_2SCl$ adduct becomes competitive with hydrogen atom abstraction with increasing pressure. These investigators also observed a negative temperature dependence for the reaction. Butkovskaya et al. [171] conducted a discharge flow mass spectrometric study at 298K, in which they determined that the reaction proceeds to form HCl + CH_3SCH_2 almost exclusively at 1 torr total pressure. The sum of all other possible channels was estimated at less than 3%. Zhao et al. [1310] used laser photolysis coupled with CH_3 detection by time-resolved tunable diode laser absorption spectroscopy to determine an upper limit for CH_3 elimination at 298K and pressures between 10-30 torr. Room temperature measurements by Nielsen et al. [859] at 740 torr and Kinnison et al. [606] at 760 torr agree quite well with the results of Stickel et al. Kinnison et al. also observed the rate constant to increase from 3.6×10^{-10} to 4.2×10^{-10} cm^3 $molec^{-1}$ s^{-1} when the bath gas was changed from pure N_2 to synthetic air, suggesting that the $(CH_3)_2SCl$ adduct reacts with O_2.

I37. ClO + OCS; ClO + SO_2. These recommendations are based on the discharge flow mass spectrometric data of Eibling and Kaufman [364]. The upper limit on k(298 K) for ClO + OCS was set from the minimum detectable decrease in ClO. No products were observed. The upper limit on k(298 K) for ClO + SO_2 is based on the authors' estimate of their SO_3 detection limit. The upper limit for this same reaction based on the minimum detectable decrease in ClO was not used due to the potential problem of ClO reformation from the Cl + O_3 source reaction.

I38. $ClO + CH_3SCH_3$. This recommendation is based on the study by Barnes et al. [64] using discharge flow mass spectrometry. The authors prefer the present value of the rate constant to one a factor of 4 higher, which they determined in an earlier version of their apparatus. The uncertainty factor reflects the absence of any confirming investigations.

I39. ClO + SO. The value of k(298 K) is an average of the determinations by Clyne and MacRobert [233] and Brunning and Stief [150]. The temperature independence is taken from the latter study with the A-factor recalculated to fit the k(298 K) recommendation.

I40. $Br + H_2S$, $Br + CH_3SH$. These recommendations are based on the study by Nicovich et al. [844] who measured both the forward and reverse reactions by time-resolved resonance fluorescence detection of Br atoms. The uncertainties placed on these recommendations have been increased over those estimated by the authors to reflect the absence of any confirming investigations.

I41. $Br + CH_3SCH_3$. Wine et al. [1259] used laser photolysis resonance fluorescence to study reversible adduct formation in the $Br + CH_3SCH_3$ reaction system over the temperature range 260 - 310K from which they derive a $(CH_3)_2S$-Br bond strength of 14.5 ± 1.2 kcal $mole^{-1}$. Above 375K, adduct decomposition is so rapid that the addition channel is effectively negligible. Extrapolation of these data to conditions typical of the springtime Arctic boundary layer (760 torr, 230 - 270K) leads these authors to suggest that under such conditions, the addition of Br to CH_3SCH_3 proceeds with a rate constant of approximately 1.3×10^{-10} cm^3 $molecule^{-1}$ s^{-1}. Researchers from the same laboratory (Jefferson et al. [553]) studied the abstraction reaction over the temperature range 386 - 604K. These authors observed the reactants to be in equilibrium with the products $HBr + CH_3SCH_2$ and determined Arrhenius expressions for the forward and reverse reactions respectively of 9.0×10^{-11} $\exp(-2386/T)$ cm^3 $molec^{-1}$ s^{-1} and 8.6×10^{-13} $\exp(836/T)$ cm^3 $molec^{-1}$ s^{-1}. Analysis of the equilibrium data also permitted determination of the heat of formation of CH_3SCH_2 (see Appendix 1).

I42. $BrO + CH_3SCH_3$. This recommendation is based on the discharge flow mass spectrometric study by Bedjanian et al. [95], performed at 1 torr over the temperature range 233-320K. The rate constant at 298K is nearly identical to that derived by Barnes et al. [64], using a similar experimental system. Bedjanian et al. also determined a near unity yield for the production of dimethylsulfoxide and suggest that the reaction proceeds via production of an adduct that decomposes into the sulfoxide and bromine atoms.

I43. BrO + SO. This recommendation is based on the measurements of Brunning and Stief [151] performed under both excess BrO and excess SO conditions. The rate constant is supported by the lower limit assigned by Clyne and MacRobert [233] from measurements of SO_2 production.

I44. $IO + CH_3SH$. The value of k(298K) comes from the study by Maguin et al. [744] using discharge flow mass spectrometry. The investigators establish a branching ratio near unity for the production of HOI. The uncertainty factor reflects the absence of any confirming investigations.

I45. $IO + CH_3SCH_3$. This recommendation comes from the studies by Daykin and Wine [315] using laser photolysis absorption spectroscopy and by Maguin et al. [744] and Barnes et al. [64] using discharge flow mass spectroscopy. These groups obtained rate constants of $\leq 3.5 \times 10^{-14}$, 1.5×10^{-14}, and 8.8×10^{-15} respectively. The last two studies supersede earlier, less direct measurements by the same groups, which resulted in rate constants of 1.5×10^{-11} (Martin et al. [759]) and 3.0×10^{-11} (Barnes et al. [65]).

I46. $S + O_2$. This recommendation is based primarily on the study of Davis et al. [310]. Modest agreement at 298 K is found in the studies of Fair and Thrush [368], Fair et al. [369], Donovan and Little [354], and Clyne and Townsend [245]. The study by Clyne and Whitefield [252], which indicates a slightly negative E/R between 300 and 400 K, is encompassed by the assigned uncertainty limits.

I47. $S + O_3$. This recommendation accepts the only available experimental data of Clyne and Townsend [245]. In this study the authors measure a value of the rate constant for $S + O_2$ in reasonable agreement with that recommended above.

I48. $SO + O_2$. This recommendation is based on the low temperature measurements of Black et al. [124, 125]. The room temperature value accepts the results of the more recent paper as recommended by the authors. The uncertainties cited reflect the need for further confirmation and the fact that these results lie significantly higher than an extrapolation of the higher temperature data of Homann et al. [501]. A room temperature upper limit on k set by Breckenridge and Miller [141] is consistent with the Black et al. data.

I49. $SO + O_3$. The value of k(298 K) is an average of the determinations by Halstead and Thrush [456], Robertshaw and Smith [970], and Black et al. [124, 125] using widely different techniques. The value of E/R is an average of the values reported by Halstead and Thrush and Black et al. [124], with the A-factor recalculated to fit the recommendation for k(298 K).

I50. $SO + NO_2$. The value of k(298 K) is an average of the determinations by Clyne and MacRobert [232], Black et al. [125], and Brunning and Stief [150], which agree quite well with the rate constant calculated from the relative rate measurements of Clyne et al. [228]. The Arrhenius parameters are taken from Brunning and Stief.

I51. SO + OClO. This recommendation is based on the room temperature study by Clyne and MacRobert [233]. The uncertainty reflects the absence of any confirming investigation.

I52. $SO_3 + H_2O$. Several research groups have attempted to quantify the rate of sulfuric acid formation via this reaction in the gas phase. Reiner and Arnold [966] placed an upper limit of 2.4×10^{-15} cm^3 $molec^{-1}$ s^{-1} on the rate constant, slightly lower than that determined by Wang et al. [1219]. The inability to cite the results as other than an upper limit is due to the difficulty in excluding all heterogeneous effects from the experiments. The higher rate constant reported earlier by Castleman et al. [190] may have resulted from an underestimation of the effects of such heterogeneous reactions. Subsequently, Reiner and Arnold [967] sought to improve their rate constant determination by more detailed quantification of heterogeneous contributions. They derived a value of 1.2×10^{-15} cm^3 $molec^{-1}$ s^{-1}, independent of pressure (from 31-260 mbar of synthetic air). Evidence was also obtained that H_2SO_4 was, indeed, the product of the reaction.

Kolb et al. [626] attempted to measure the gas phase reaction using a turbulent flow reactor designed to minimize wall effects. Their results, when analyzed as representing a bimolecular reaction, support a rate constant between $(1 - 7) \times 10^{-15}$ cm^3 $molec^{-1}$ s^{-1}. However, a more considered analysis of the data indicated that the gas phase reaction was second order in water vapor. The reaction rate was also observed to increase as the temperature was lowered from 333K to 243K. These observations, together with calculations by Morokuma and Mugurama [813], led the latter authors to suggest that SO_3 consumption likely involved its reaction with the water dimer or the reaction of $SO_3 \cdot H_2O + H_2O$, leading to the formation of sulfuric acid.

A laminar flow reactor study by Lovejoy et al. [730] over the temperature range 256 - 360K also revealed SO_3 loss to be second order in water concentration and independent of pressure (from 20 to 80 torr of N_2 at 300K). These latter authors measured a strong negative temperature dependence for the rate constant and a significant kinetic isotope effect ($k_{H2O} \approx 2k_{D2O}$), leading them to describe the reaction as proceeding via the rapid association between SO_3 and H_2O followed by a slower reaction between the adduct and water to form sulfuric acid. Lovejoy at al.'s measurement of a -13 kcal mol^{-1} "activation" energy was viewed as energetically inconsistent with the SO_3 + water dimer reaction mechanism since it would require a large negative activation energy for the $SO_3 + (H_2O)_2$ step. The first order expression for SO_3 loss derived by these authors is 2.26×10^{-43} $T \exp(6544/T)$ $[H_2O]^2$ and is recommended here.

I53. $SO_3 + NO_2$. This recommendation is based on the study of Penzhorn and Canosa [907] using second derivative UV spectroscopy. These authors observe the production of a white aerosol, which they interpret to be the adduct NSO_5. This claim is supported by ESCA spectra.

I54. $SH + O_2$. This upper limit for k(298 K) is based on the study by Stachnik and Molina [1067] utilizing experiments sensitive to the production of OH. Somewhat higher upper limits of 1.0×10^{-17} and 1.5×10^{-17} were assigned by Friedl et al. [397] and Wang et al. [1217] respectively from the detection sensitivities for OH detection and SH decay respectively. An even higher upper limit by Black [121], based on the lack of

SH decay, may have been complicated by SH regeneration. Much less sensitive upper limits have been calculated by Tiee et al. [1134], Nielsen [851], and Cupitt and Glass [289]. Stachnik and Molina [1067] also report a somewhat higher upper limit (< 1.0×10^{-18}) for the rate constant for the sum of the two SH + O_2 reaction channels (producing OH + SO and H + SO_2).

I55. SH + O_3. The value for k(298 K) is an average of the determinations by Friedl et al. [397] (laser-induced fluorescence detection of SH), Schonle et al. [1007] (mass spectrometric detection of reactant SH and product HSO) as revised by Schindler and Benter [1000], and Wang and Howard [1216] (laser magnetic resonance detection of SH). The temperature dependence is from Wang and Howard with the A-factor calculated to agree with the recommended value for k(298 K). $\Delta E/R$ reflects the fact that the temperature dependence comes from measurements above room temperature and, thus, extrapolation to lower temperatures may be subject to additional uncertainties. Wang and Howard report observing a minor reaction channel that produces H + SO + O_2.

I56. SH + H_2O_2. This recommended upper limit for k(298 K) is based on the study of Friedl et al. [397]. Their value is calculated from the lack of SH decay (measured by laser-induced fluorescence) and the lack of OH production (measured by resonance fluorescence). The three possible product channels yield: H_2S + HO_2, HSOH + OH, and HSO + H_2O.

I57. SH + NO_2. This recommendation is based on the measurements of Wang et al. [1217]. These authors suggest that the lower values of k(298 K) reported by Black [121], Friedl et al. [397], and Bulatov et al. [156] are due to SH regeneration from the H_2S source compound. In the study by Stachnik and Molina [1067], attempts were made at minimizing such regeneration, and the reported value of k(298 K) was significantly higher than that from the earlier studies, but still 30% lower than that measured by Wang et al., who used two independent SH source reactions. A slightly higher rate constant measured by Schonle et al. [1007], as revised by Schindler and Benter [1000], has not been recommended due to the somewhat more limited database for their determination. The reaction as written represents the most exothermic channel. In fact, HSO has been detected as a product by Leu and Smith [700], Bulatov et al. [156], Schonle et al. [1007], and Wang et al. [1217]. The absence of a primary deuterium isotope effect, as observed by Wang et al. [1217], coupled with the large magnitude of the rate constant suggests that the (four-center intermediate) channels producing SO + HNO and OH + SNO are of minor importance. No evidence for a three-body combination reaction was found by either Black [121] or Friedl et al. [397]. Based on a pressure independence of the rate constant between 30 - 300 torr, Black set an upper limit of 7.0×10^{-31} for the termolecular rate constant. Similarly, Stachnik and Molina [1067] saw no change in decay rate between 100 and 730 torr with O_2 (although these O_2 experiments were designed primarily to limit SH regeneration). The recommendation given here is supported by the recent discharge flow laser-induced fluorescence study of the SD + NO_2 reaction by Fenter and Anderson [375]. These investigators report a rate constant at 298K of 6.8×10^{-11} cm^3 $molec^{-1}$ s^{-1}, which compares favorably with the value of 7.1×10^{-11} cm^3 $molec^{-1}$ s^{-1} determined in the Wang et al. of the same reaction. Fenter and Anderson also obtained an E/R value of -210 K, very similar to the -237 K value derived by Wang et al. for the SH reaction.

I58. SH + Cl_2; SH + BrCl; SH + Br_2; SH + F_2. The recommendations for these reactions are derived from the data of Fenter and Anderson [374] for the SD radical. The uncertainties have been increased over those estimated by the investigators to reflect the absence of any confirming investigations and the influence of the secondary isotope effect. For the BrCl reaction, the channel producing ClSD + Br was found to be described by the rate expression $k = 2.3 \times 10^{-11} \exp(100/T)$.

I59. HSO + O_2. This recommendation is based on the study by Lovejoy et al. [734], who employed laser magnetic resonance monitoring of HSO in a discharge flow system. The upper limit thus derived for k(298 K) is nearly two orders of magnitude lower than measured by Bulatov et al. [158].

I60. HSO + O_3. This recommendation is based on the determinations by Friedl et al. [397] and Wang and Howard [1216]. In the first study, performed at higher O_3 concentrations, greater quantities of HSO were produced in the flow tube and SH approached a steady state due to its generation via HSO + O_3. The rate constant for this reaction was thus determined relative to SH + O_3 from measurements of the steady state SH concentration as a function of the initial SH concentration. In the second study, the rate constant and its branching ratio were measured at two temperatures. At room temperature, the overall rate constant is in

excellent agreement with that of Friedl et al. More recently, Lee et al. [681] determined a room temperature rate constant of 4.7×10^{-14} for the sum of all reaction channels not producing HS. This value is approximately 30% greater than that measured by Wang and Howard for the same channels. Lee et al. derive an Arrhenius activation energy of 1120K for these channels from data between 273-423K, in agreement with the more limited temperature data of Wang and Howard.

The lack of an isotope effect when SD was employed in the Friedl et al. study suggests that the products of the HSO + O_3 reaction are SH + $2O_2$ (analogous to those for HO_2 + O_3). However, Wang and Howard found that only 70% of the reaction leads to HS formation. In addition, their observations of HO_2 production in the presence of O_2 suggests the existence of a reaction channel producing HSO_2 + O_2 followed by HSO_2 + $O_2 \rightarrow HO_2 + SO_2$. At the present time, no recommendation is given for the product channels. Further mechanistic work is suggested, since it is important to understand whether this reaction in the atmosphere leads to HS regeneration or to oxidation of the sulfur.

I61. HSO + NO; HSO + NO_2. The recommendations for these reactions are based on the study by Lovejoy et al. [734] in which laser magnetic resonance was used to monitor HSO in a discharge flow system. Their upper limit for the NO reaction is a factor of 25 lower than the rate constant measured by Bulatov et al. [157] using intracavity laser absorption at pressures between 10 and 100 torr. Since it is unlikely that this reaction rate undergoes a factor of 25 increase between 1 torr (the pressure of the Lovejoy et al. work) and 10 torr, the higher rate constant may be due to secondary chemistry associated with the HSO production methods employed.

The recommendation for the NO_2 reaction is a factor of 2 higher than the rate constant reported by Bulatov et al. [156]. Lovejoy et al. have attributed this difference to HSO regeneration under the experimental conditions used by Bulatov et al. [156]. The product assignment for this reaction is discussed in the note for the HSO_2 + O_2 reaction.

I62. HSO_2 + O_2. This recommendation is based on the rate of HO_2 formation measured by Lovejoy et al. [734] upon addition of O_2 to the HSO + NO_2 reaction system. While HSO_2 was not observed directly, a consideration of the mechanistic possibilities for HSO + NO_2, coupled with measurements of the HO_2 production rate at various O_2 pressures, led these authors to suggest that HSO_2 is both a major product of the HSO + NO_2 reaction and a precursor for HO_2 via reaction with O_2.

I63. $HOSO_2$ + O_2. This recommendation is based on the studies of Gleason et al. [427] and Gleason and Howard [425] in which the $HOSO_2$ reactant was monitored using a chemical ionization mass spectrometric technique. Gleason and Howard conducted their measurements over the 297-423 K temperature range in the only temperature dependence investigation. Thus, $\Delta E/R$ has been increased from their quoted limits to account for the potential uncertainties in extrapolating their data to sub-ambient temperatures. The value of k(298 K) derives further support from the studies of Margitan [750] and Martin et al. [761], both of whom used modeling fits of OH radical decays in the OH + SO_2 + M reaction system in the presence of O_2 and NO. In this latter analysis, the $HOSO_2$ reacts with O_2, yielding HO_2, which subsequently regenerates OH through its reaction with NO. The infrared spectrum of $HOSO_2$ has been recorded in low temperature matrix isolation experiments by Hashimoto et al. [469] and Nagase et al. [823]. Mass spectrometric detection of $HOSO_2$ in the gas phase has also been reported by Egsgaard et al. [362].

I64. CS + O_2. The recommendation given for k(298 K) is based on the work of Black et al. [123] using laser-induced fluorescence to monitor CS. This value agrees with the somewhat less precise determination by Richardson [969] using OCS formation rates. The latter author presents evidence that this reaction channel dominates over the one producing SO + CO by more than a factor of 10. Measurements by Richardson at 293 K and 495 K yield an E/R of 1860 K. However, use of this activation energy with the recommended value of k(298 K) results in an unusually low Arrhenius A-factor of 1.5×10^{-16}. In view of this, no recommendation is given for the temperature dependence.

I65. CS + O_3; CS + NO_2. The k(298 K) recommendations for both reactions accept the results of Black et al. [123], who used laser-induced fluorescence to monitor the CS reactant in a room temperature experiment. The uncertainty factors reflect the absence of any confirming measurements.

I66. $CH_3S + O_2$. This upper limit is based on the study by Tyndall and Ravishankara [1170]. Somewhat higher upper limits were derived in the earlier studies of Balla et al. [56] and Black and Jusinski [122].

I67. $CH_3S + O_3$. This recommendation is based on the temperature-dependent study of Turnipseed et al. [1156] and the room temperature determinations of Tyndall and Ravishankara [1169] and Domine et al. [353]. Domine et al. measured the yield of CH_3SO to be 15% at low pressure and used this value to revise the corrections applied in the Tyndall and Ravishankara investigation to account for CH_3S regeneration by $CH_3SO + O_3$. A failure to observe significant reaction in the study by Black and Jusinski [122] is interpreted as due to rapid regeneration of CH_3S in their system. The value of $\Delta E/R$ has been set larger than that derived by Turnipseed et al. to reflect the existence of only one temperature dependence investigation.

I68. $CH_3S + NO$. The upper limit for the bimolecular reaction between CH_3S and NO is based on estimates by Balla et al. [56], who conducted a temperature dependence study of the termolecular reaction.

I69. $CH_3S + NO_2$. This recommendation is based on the temperature dependent data of Turnipseed et al. [1156] and the room temperature results of Tyndall and Ravishankara [1170]. The room temperature value of Domine et al. [351] is encompassed by the recommended uncertainty factor. The value of $\Delta E/R$ has been set larger than that derived by Turnipseed et al. to reflect the existence of only one temperature dependence investigation. An earlier study by Balla et al. [56] yielded a room temperature rate constant nearly a factor of two higher than the present recommendation, which may be attributed to secondary reactions at higher radical concentrations. Tyndall and Ravishankara determined the NO yield to be $(80 \pm 20)\%$. Together with the unity yield of CH_3SO obtained by Domine et al., this implies that the primary reaction channel is as written.

I70. $CH_2SH + O_2$. This recommendation is the average of the rate constant obtained by Rahman et al. [941] in a fast flow mass spectrometer system and that from Anastasi et al. [19] using a pulse radiolysis kinetic absorption apparatus. The value of Anastasi et al. is nearly twice that of Rahman et al. It is difficult at present to indicate a preference for the results of one study over the other, and the value of f(298) has been chosen to reflect this uncertainty. Since this is a fast bimolecular reaction, one would expect the products to be $HO_2 + CH_2S$, by analogy with the reaction between CH_2OH and O_2.

I71. $CH_2SH + O_3$. The value of k(298K) comes from the study by Rahman et al. [941] using fast flow mass spectrometry. The uncertainty factor reflects the absence of any confirming investigations.

I72. $CH_2SH + NO$. The value of k(298K) comes from the study by Anastasi et al. [19] using a pulse radiolysis kinetic absorption apparatus. The uncertainty factor reflects the absence of any confirming investigations.

I73. $CH_2SH + NO_2$. This recommendation averages the rate constant obtained by Rahman et al. [941] in a fast flow mass spectrometer system with that from Anastasi et al. [19], using a pulse radiolysis kinetic absorption apparatus. The value of Rahman et al. is nearly twice that of Anastasi et al. It is difficult at present to indicate a preference for the results of one study over the other, and the value of f(298) has been chosen to reflect this uncertainty.

I74. $CH_3SO + O_3$. This recommendation is based on the study by Domine et al. [353]. It is supported by the study of Tyndall and Ravishankara [1169], in which the rate constant was derived from a complex analysis of the $CH_3S + O_3$ reaction system. Domine et al. place the direct yield of CH_2SO at approximately 10% and that of CH_3S at 13% at low pressure.

I75. $CH_3SO + NO_2$. This recommendation is based on the direct measurements of Domine et al. [351]. The results are supported by somewhat less direct measurements of Tyndall and Ravishankara [1170] and Mellouki et al. [779].

I76. $CH_3SOO + O_3$, $CH_3SOO + NO$, $CH_3SOO + NO_2$. These recommendations are based on the experiments of Turnipseed et al. [1156] in which CH_3S was monitored by LIF in equilibrium with CH_3SOO. The upper limit for the O_3 reaction was determined from experiments at 227K. The results for the NO and NO_2 reactions were independent of temperature over the ranges 227-256K and 227-246K, respectively. The uncertainties placed on these recommendations have been increased over those estimated by the authors to reflect the absence of any confirming investigations.

I77. $CH_3SO_2 + NO_2$. This recommendation is based on the study by Ray et al. [960] using a discharge flow reactor equipped with laser-induced fluorescence and mass spectrometric detection. The CH_3SO_2 was produced by the sequential oxidation of CH_3S and CH_3SO by NO_2 and is to be differentiated from the weakly bound adduct, CH_3SOO, formed by the reaction of CH_3S with O_2 at low temperature (Turnipseed et al [1156]). The uncertainty limit on the rate constant has been increased over that given by the authors to reflect the absence of any confirming investigation. However, some additional support for this recommendation does come from the study of the $CH_3S + NO_2$ reaction by Tyndall and Ravishankara [1170]. These authors observed fluorescence from a product species tentatively identified as CH_3SO_2, produced by the reaction of CH_3SO with NO_2. Computer simulation of the rise and fall of the fluorescence signal yielded an approximate rate constant value for the reaction $CH_3SO_2 + NO_2$ of 7.0×10^{-12} cm^3 $molec^{-1}$ s^{-1}. However, an unambiguous differentiation between the production and disappearance rate constants was not possible.

I78. $CH_3SCH_2 + NO_3$. This recommendation is based on the experiments of Butkovskaya and Le Bras [170]. The uncertainty factor reflects the absence of any confirming investigation.

I79. $CH_3SCH_2O_2 + NO$. This recommendation is based on the experiments of Wallington et al. [1206]. The uncertainty factor reflects the absence of any confirming investigation.

I80. $CH_3SS + O_3$. This recommendation is based on the discharge flow photoionization mass spectroscopy study by Domine et al. [353]. The uncertainty factor reflects the absence of any confirming investigations. The rate constant ratio for the reactions of CH_3SS with O_3 and NO_2 is consistent with the rate constant ration for the corresponding CH_3S reactions.

I81. $CH_3SS + NO_2$; $CH_3SSO + NO_2$. These recommendations are based on the discharge flow photoionization mass spectroscopy study by Domine et al. [351]. The rate constant ratio for these two reactions agrees with that observed for other RS/RSO radicals with NO_2. The assigned uncertainties reflect this agreement but acknowledge the absence of any confirming investigation. In the Domine et al. study, CH_3SSO was produced by reacting away all CH_3SS with high NO_2 concentrations. Thus, as expected, O atom transfer may be the primary channel in the CH_3SS reaction.

J1. $Na + O_3$. The recommendation is based on the measurements of Ager et al. [12], Worsnop et al. [1277] as corrected in Worsnop et al. [1278], and Plane et al. [917]. The data of Worsnop et al. supersede earlier work from that laboratory (Silver and Kolb [1026]). Measurements made by Husain et al. [527] at 500 K are somewhat lower, probably because they did not recognize that secondary chemistry, $NaO + O_3 \rightarrow Na + 2O_2$, interferes with the rate coefficient measurement. The temperature dependence is from results of Worsnop et al. [1278] (214-294 K) and Plane et al. [917] (208-377K). Ager et al. [12] estimate that the $NaO_2 + O$ product channel is $\leq 5\%$. Evidence that the NaO product is in the $^2\Sigma^+$ excited electronic state was reported by Shi et al. [1021] and Wright et al. [1279].

J2. $Na + N_2O$. The recommendation incorporates the data of Husain and Marshall [526], Ager et al. [12], Plane and Rajasekhar [918], and Worsnop et al. [1278]. Silver and Kolb [1026] measured a rate coefficient at 295 K that is lower and is superseded by Worsnop et al. [1278]. Helmer and Plane [479] report a measurement at 300K in excellent agreement with the recommendation. Earlier, less direct studies are discussed by Ager et al. [12]. The NaO product does not react significantly with N_2O at room temperature [k (for $Na + N_2 + O_2$ products) $\leq 10^{-16}$ and k (for $NaO_2 + N_2$ products) $\leq 2 \times 10^{-15}$ Ager et al.]. Wright et al. [1279] used UV photoelectron spectroscopy to determine the product NaO is formed predominantly in the excited $^2\Sigma^+$ state.

J3. $Na + Cl_2$. Two measurements of the rate coefficient for this reaction are in excellent agreement: Silver [1023] and Talcott et al. [1110]. The recommended value is the average of these room temperature results.

J4. NaO + O. The recommendation is based on a measurement at 573 K by Plane and Husain [916]. They reported that $\leq 1\%$ of the Na product is in the 3^2P excited state.

J5. $NaO + O_3$. This reaction was studied by Silver and Kolb [1026], Ager et al. [12], and Plane et al. [917], who agree on the rate coefficient and branching ratio. This agreement may be fortuitous because Silver and Kolb used an indirect method and an analysis based on their rate coefficient for the $Na + O_3$ reaction, which is about

1/2 of the recommended value. Ager et al. employed a somewhat more direct measurement, but the study is complicated by a chain reaction mechanism in the Na/O_3 system. Plane et al. reported rate coefficient measurements for the $NaO_2 + O_2$ product channel over the temperature range 207-377K using pulsed photolysis LIF methods. The recommendation for that channel is based on all three studies, and the recommendation for the $Na + 2O_2$ channel is based upon the results of Silver and Kolb and Ager et al. The latter reaction channel may also have a significant temperature dependence.

J6. $NaO + H_2$. The recommendation is based on a measurement by Ager and Howard [11]. They also reported a significant $Na + H_2O$ product channel and that a small fraction of the Na from this channel is in the 3^2P excited state.

J7. $NaO + H_2O$. The recommendation is based on a measurement by Ager and Howard [11].

J8. NaO + NO. The recommendation is based on an indirect measurement reported by Ager et al. [12].

J9. NaO + HCl. There is only one indirect measurement of the rate coefficient for this reaction, that from the study by Silver et al. [1029]. They indicate that the products are NaCl and OH, although some NaOH and Cl production is not ruled out.

J10. $NaO_2 + O$. The recommendation is based on a flow tube study at 300K by Helmer and Plane [479].

J11. $NaO_2 + NO$. This reaction is endothermic. The upper limit recommended is from an experimental study by Ager et al. [12].

J12. $NaO_2 + HCl$. The recommendation is based on a measurement reported by Silver and Kolb [1027]. They indicated that the products are $NaCl + HO_2$, but NaOOH + Cl may be possible products.

J13. NaOH + HCl. The recommendation is based on the study by Silver et al. [1029], which is the only published study of this reaction.

References for Table 1

1. Abbatt, J.P.D., K.L. Demerjian, and J.G. Anderson, 1990, J. Phys. Chem., **94**, 4566-4575.
2. Abbatt, J.P.D., F.F. Fentner, and J.G. Anderson, 1992, J. Phys. Chem., **96**, 1780-1785.
3. Abbatt, J.P.D., D.W. Toohey, F.F. Fenter, P.S. Stevens, W.H. Brune, and J.G. Anderson, 1989, J. Phys. Chem., **93**, 1022-1029.
4. Adachi, H. and N. Basco, 1979, Chem. Phys. Lett., **63**, 490.
5. Adachi, H., N. Basco, and D.G.L. James, 1979, Int. J. Chem. Kinet., **11**, 1211-1229.
6. Adachi, H., N. Basco, and D.G.L. James, 1980, Int. J. Chem. Kinet., **12**, 949.
7. Addison, M.C., J.P. Burrows, R.A. Cox, and R. Patrick, 1980, Chem. Phys. Lett., **73**, 283.
8. Addison, M.C., R.J. Donovan, and J. Garraway, 1979, J. Chem. Soc. Faraday Disc., **67**, 286-296.
9. Adeniji, S.A., J.A. Kerr, and M.R. Williams, 1981, Int. J. Chem. Kinet., **13**, 209.
10. Adler-Golden, S.M. and J.R. Wiesenfeld, 1981, Chem. Phys. Lett., **82**, 281.
11. Ager, J.W., III and C.J. Howard, 1987, J. Chem. Phys., **87**, 921-925.
12. Ager, J.W., III, C.L. Talcott, and C.J. Howard, 1986, J. Chem. Phys., **85**, 5584-5592.
13. Agrawalla, B.S., A.S. Manocha, and D.W. Setser, 1981, J. Phys. Chem., **85**, 2873-2877.
14. Aker, P.M., B.I. Niefer, J.J. Sloan, and H. Heydtmann, 1987, J. Chem. Phys., **87**, 203-209.
15. Aleksandrov, E.N., V.S. Arutyunov, and S.N. Kozlov, 1981, Kinetics and Catalysis, **22**, 391-394.
16. Amimoto, S.T., A.P. Force, R.G. Gulotty Jr., and J.R. Wiesenfeld, 1979, J. Chem. Phys., **71**, 3640-3647.
17. Amimoto, S.T., A.P. Force, and J.R. Wiesenfeld, 1978, Chem. Phys. Lett., **60**, 40-43.
18. Amimoto, S.T. and J.R. Wiesenfeld, 1980, J. Chem. Phys., **72**, 3899-3903.
19. Anastasi, C., M. Broomfield, O.J. Nielsen, and P. Pagsberg, 1992, J. Phys. Chem., **96**, 696-701.
20. Anastasi, C., M.J. Brown, D.B. Smith, and D.J. Waddington, paper presented at the Joint French and Italian sections of the Combustion Institute, 1987, Amalfi, Italy.
21. Anastasi, C., I.W.M. Smith, and D.A. Parkes, 1978, J. Chem. Soc. Faraday Trans. 1, **74**, 1693-1701.
22. Anastasi, C., D.J. Waddington, and A. Woolley, 1983, J. Chem. Soc. Faraday Trans., **79**, 505-516.
23. Anderson, J.G. and F. Kaufman, 1973, Chem. Phys. Lett., **19**, 483-486.
24. Anderson, L.G. and R.D. Stephens, 1994, personal communication.
25. Anderson, P.C. and M.J. Kurylo, 1979, J. Phys. Chem., **83**, 2055.
26. Anderson, S.M., J. Morton, K. Mauersberger, Y.L. Yung, and W.B. DeMore, 1992, Chem. Phys. Lett., **189**, 581-585.
27. Andersson, B.Y., R.A. Cox, and M.E. Jenkin, 1988, Int. J. Chem. Kinetics, **20**, 283-295.

28. Andresen, P., A. Jacobs, C. Kleinermanns, and J. Wolfrum, 1982, 19th Symp. (Intl.) Combustion, pp. 11.
29. Arnold, I. and F.J. Comes, 1979, Chem. Phys., **42**, 231.
30. Arnold, I. and F.J. Comes, 1980, Chem. Phys., **47**, 125-130.
31. Arrington, C.A., W. Brennen, G.P. Glass, J.V. Michael, and H. Niki, 1965, J. Chem. Phys., **43**, 525.
32. Ashford, R.D., N. Basco, and J.E. Hunt, 1978, Int. J. Chem. Kinet., **10**, 1233-1244.
33. Atakan, B.A. Jacobs, M. Wahl, R. Weller, and J. Wolfrum, 1989, Chem. Phys. Lett., **155**, 609-613.
34. Atkinson, R. and S.M. Aschmann, 1984, Int. J. Chem. Kinet., **16**, 259.
35. Atkinson, R. and S.M. Aschmann, 1985, Int. J. Chem. Kinet., **17**, 33-41.
36. Atkinson, R., S.M. Aschmann, D.R. Fitz, A.M. Winer, and J.N. Pitts Jr., 1982, Int. J. Chem. Kinet., **14**, 13.
37. Atkinson, R., S.M. Aschmann, and J.N. Pitts Jr., 1988, J. Geophys. Res., **93**, 7125-7126.
38. Atkinson, R., S.M. Aschmann, E.C. Tuazon, M.A. Goodman, and A.M. Winer, 1987, J. Atmos. Chem., **5**, 83-90.
39. Atkinson, R., G.M. Breuer, and J.N. Pitts Jr., 1976, J. Geophys. Res., **81**, 5765-5770.
40. Atkinson, R. and W.P.L. Carter, 1991, J. Atmos. Chem., **13**, 195-210.
41. Atkinson, R., D.A. Hansen, and J.N. Pitts Jr., 1975, J. Chem. Phys., **63**, 1703-1706.
42. Atkinson, R., R.A. Perry, and J.N. Pitts Jr., 1977, J. Chem. Phys., **66**, 1578.
43. Atkinson, R., R.A. Perry, and J.N. Pitts Jr., 1978, Chem. Phys. Lett., **54**, 14.
44. Atkinson, R. and J.N. Pitts Jr., 1978, J. Chem. Phys., **68**, 3581.
45. Atkinson, R., J.N. Pitts Jr., and S.M. Aschmann, 1984, J. Phys. Chem., **88**, 1584.
46. Atkinson, R., C.N. Plum, W.P.L. Carter, A.M. Winer, and J.N. Pitts Jr., 1984, J. Phys. Chem., **88**, 1210-1215.
47. Atkinson, R., R.C. Tuazon, H. Macleod, S.M. Aschmann, and A.M. Winer, 1986, Geophys. Res. Lett., **13**, 117-120.
48. Avery, H.E. and R.J. Cvetanovic, 1965, J. Chem. Phys., **43**, 3727-3733.
49. Aviles, R.G., D.F. Muller, and P.L. Houston, 1980, Appl. Phys. Lett., **37**, 358-360.
50. Avramenko, L.I. and R.V. Kolesnikova, 1961, Bull. Acad. Sci. USSR, Div. Chem. Sci., 545.
51. Baer, S., H. Hippler, R. Rahn, M. Siefke, N. Seitzinger, and J. Troe, 1991, J. Chem. Phys., **95**, 6463-6470.
52. Bahta, A., R. Simonaitis, and J. Heicklen, 1984, Int. J. Chem. Kinet., **16**, 1227.
53. Balakhnin, V.P., V.I. Egorov, and E.I. Intezarova, 1971, Kinetics and Catalysis , **12**, 299.
54. Baldwin, A.C. and D.M. Golden, 1978, Chem. Phys. Lett., **55**, 350.
55. Baldwin, R.R., C.E. Dean, M.R. Honeyman, and R.W. Walker, 1984, J. Chem. Soc. Faraday Trans. 1, **80**, 3187-3194.
56. Balla, R.J., H.H. Nelson, and J.R. McDonald, 1986, Chem. Phys., **109**, 101.
57. Ballod, A.P., A.I. Poroikova, T.A. Titarchuk, and V.N. Khabarov, 1989, Kinetics and Catalysis, **30**, 476-483.
58. Barker, J.R., S.W. Benson, and D.M. Golden, 1977, Int. J. Chem. Kinet., **9**, 31.
59. Barnes, I., V. Bastian, and K.H. Becker, 1988, Int. J. Chem. Kinet., **20**, 415-431.
60. Barnes, I., V. Bastian, K.H. Becker, E.H. Fink, and W. Nelsen, 1986, J. Atmos. Chem., **4**, 445-466.
61. Barnes, I., V. Bastian, K.H. Becker, E.H. Fink, and F. Zabel, 1981, Chem. Phys. Lett. , **83**, 459-464.
62. Barnes, I., V. Bastian, K.H. Becker, E.H. Fink, and F. Zabel, 1982, Atmos. Environ., **16**, 545.
63. Barnes, I., V. Bastian, K.H. Becker, E.H. Fink, and F. Zabel, 1986, Chem. Phys. Lett., **123**, 28-32.
64. Barnes, I., V. Bastian, K.H. Becker, and R.D. Overath, 1991, Int. J. Chem. Kinet., **23**, 579-591.
65. Barnes, I., K.H. Becker, P. Carlier, and G. Mouvier, 1987, Int. J. Chem. Kinet., **19**, 489-501.
66. Barnes, I., K.H. Becker, E.H. Fink, A. Reimer, F. Zabel, and H. Niki, 1983, Int. J. Chem. Kinet., **15**, 631-645.
67. Barnes, I., K.H. Becker, E.H. Fink, A. Reimer, F. Zabel, and H. Niki, 1985, Chem. Phys. Lett., **115**, 1.
68. Barnes, I., K.H. Becker, and N. Mihalopoulas, 1994, J. Atmos. Chem., **18**, 267-289.
69. Barnes, I., K.H. Becker, and I. Patroescu, 1994, Geophys. Res. Lett., **21**, 2389-2392.
70. Barnes, I., K.H. Becker, and I. Patroescu, 1996, Atmos. Environ., **30**, 1805-1814.
71. Barnett, A.J., G. Marston, and R.P. Wayne, 1987, J. Chem. Soc. Faraday Trans. 2, **83**, 1453-1463.
72. Barone, S.B., A.A. Turnipseed, and A.R. Ravishankara, 1994, J. Phys. Chem., **98**, 4602-4608.
73. Barone, S.B., A.A. Turnipseed, and A.R. Ravishankara, 1996, J. Phys. Chem., **100**, 14694-14702.
74. Barry, J., G. Locke, S. D., H. Sidebottom, J. Treacy, C. Clerbeaux, and R. Colin, 1996, to be published.
75. Barry, J., *et al.*, 1994, Chem. Phys. Lett., **221**, 353-358.
76. Barry, J., H. Sidebottom, J. Treacy, and J. Franklin, 1995, Int. J. Chem. Kinet., **27**, 27-36.
77. Basco, N. and S.K. Dogra, 1971, Proc. Roy. Soc. A., **323**, 401.
78. Basco, N. and S.K. Dogra, 1971, Proc. Roy. Soc. A., **323**, 417.
79. Basco, N. and S.K. Dogra, 1971, Proc. Roy. Soc. A., **323**, 29.
80. Basco, N. and S.S. Parmar, 1985, Int. J. Chem. Kinet., **17**, 891.
81. Batt, L., R.T. Milne, and R.D. McCulloch, 1977, Int. J. Chem. Kinet., **9**, 567-587.
82. Batt, L. and G.N. Robinson, 1979, Int. J. Chem. Kinet., **11**, 1045.
83. Bauer, D., J.N. Crowley, and G.K. Moortgat, 1992, J. Photochem and Photobiol., **A65**, 329-344.
84. Bauerle, S., F. Battin-LeClerc, T. Gierczak, and A.R. Ravishankara, 1997, Manuscript in preparation.
85. Baulch, D.L., I.M. Campbell, and S.M. Saunders, 1985, J. Chem. Soc. Faraday Trans. 1, **81**, 259-263.
86. Baulch, D.L., R.A. Cox, R.F. Hampson Jr., J.A. Kerr, J. Troe, and R.T. Watson, 1980, J. Phys. Chem. Ref. Data, **9**, 295-471.
87. Becker, E., T. Benter, R. Kampf, R.N. Schindler, and U. Wille, 1991, Ber. Bunsenges. Phys. Chem., **95**, 1168-1173.
88. Becker, E., M.M. Rahman, and R.N. Schindler, 1992, Ber. Bunsenges. Phys. Chem., **96**, 776-783.
89. Becker, E., U. Wille, M.M. Rahman, and R.H. Schindler, 1991, Ber. Bunsenges. Phys. Chem., **95**, 1173-1179.

90. Becker, K.H., W. Groth, and D. Kley, 1969, Z. Naturforsch, **A24**, 1280.
91. Becker, K.H., W. Groth, and U. Schurath, 1971, Chem. Phys. Lett., **8**, 259-262.
92. Becker, K.H., W. Groth, and U. Schurath, 1972, Chem. Phys. Lett., **14**, 489-492.
93. Becker, K.H., M.A. Inocencio, and U. Schurath, 1975, Int. J. Chem. Kinet., **Symp. No. 1**, 205-220.
94. Becker, K.H., W. Nelsen, Y. Su, and K. Wirtz, 1990, Chem. Phys. Lett., **168**, 559-563.
95. Bedjanian, Y., G. Poulet, and G. Le Bras, 1996, Int. J. Chem. Kinet, **28**, 383-389.
96. Bednarek, G., M. Breil, A. Hoffman, J.P. Kohlman, V. Mors, and R. Zellner, 1996, Ber. Bunsenges. Phys. Chem., **100**, 528-539.
97. Bednarek, G., J.P. Kohlmann, H. Saathoff, and R. Zellner, 1995, Z, Phys. Chem., **188**, 1-15.
98. Bedzhanyan, Y.R., E.M. Markin, and Y.M. Gershenzon, 1993, Kinetics and Catalysis, **33**, 601-606.
99. Bedzhanyan, Y.R., E.M. Markin, and Y.M. Gershenzon, 1993, Kinetics and Catalysis, **34**, 1-3.
100. Bedzhanyan, Y.R., E.M. Markin, and Y.M. Gershenzon, 1993, Kinetics and Catalysis, **33**, 594-601.
101. Bedzhanyan, Y.R., E.M. Markin, G.G. Politenkova, and Y.M. Gershenzon, 1993, Kinetics and Catalysis, **33**, 797-801.
102. Beichert, P., J.L. Wingen, R. Vogt, M.J. Ezell, M. Ragains, R. Neavyn, and B.J. Finlayson-Pitts, 1995, J. Phys. Chem., **99**, 13156-13162.
103. Bemand, P.P. and M.A.A. Clyne, 1977, J. Chem. Soc. Faraday Trans. 2, **73**, 394.
104. Bemand, P.P., M.A.A. Clyne, and R.T. Watson, 1973, J. Chem. Soc. Faraday Trans. 1, **69**, 1356.
105. Bemand, P.P., M.A.A. Clyne, and R.T. Watson, 1974, J. Chem. Soc. Faraday Trans. 2, **70**, 564.
106. Beno, M.F., C.D. Jonah, and W.A. Mulac, 1985, Int. J. Chem. Kinet., **17**, 1091-1101.
107. Benson, S.W., F.R. Cruickshank, and R. Shaw, 1969, Int. J. Chem. Kinet., **1**, 29.
108. Bevilacqua, T.J., D.R. Hanson, and C.J. Howard, 1993, J. Phys. Chem., **97**, 3750-3757.
109. Bhaskaran, K.A., P. Frank, and T. Just, 1979, 12th International Shock Tube Symposium, Jerusalem.
110. Bhatnagar, A. and R.W. Carr, 1994, Chem. Phys. Lett., **231**, 454-459.
111. Bida, G.T., W.H. Breckenridge, and W.S. Kolln, 1976, J. Chem. Phys., **64**, 3296.
112. Biedenkapp, D. and E.J. Bair, 1970, J. Chem. Phys., **52**, 6119-6125.
113. Biermann, H.W., G.W. Harris, and J.N. Pitts Jr., 1982, J. Phys. Chem., **86**, 2958-2964.
114. Biermann, H.W., C. Zetzsch, and F. Stuhl, 1978, Ber. Bunsenges Phys. Chem., **82**, 633.
115. Biggs, P., C.E. Canosa-Mas, J.-M. Fracheboud, D.E. Shallcross, and R.P. Wayne, 1995, Geophys. Res. Lett., **22**, 1221-1224.
116. Biggs, P., C.E. Canosa-Mas, P.S. Monks, R.P. Wayne, T. Benter, and R.N. Schindler, 1993, Int. J. Chem. Kinet., **25**, 805-817.
117. Biggs, P., M.H. Harwood, A.D. Parr, and R.P. Wayne, 1991, J. Phys. Chem., **97**, 7746-7751.
118. Billington, A.P. and P. Borrell, 1986, J. Chem. Soc. Faraday Trans. 2, **82**, 963-970.
119. Birks, J.W., B. Shoemaker, T.J. Leck, R.A. Borders, and L.J. Hart, 1977, J. Chem. Phys., **66**, 4591.
120. Birks, J.W., B. Shoemaker, T.J. Leck, and D.M. Hinton, 1976, J. Chem. Phys., **65**, 5181.
121. Black, G., 1984, J. Chem. Phys., **80**, 1103-1107.
122. Black, G. and L.E. Jusinski, 1986, J. Chem. Soc. Faraday Trans. 2, **86**, 2143.
123. Black, G., L.E. Jusinski, and T.G. Slanger, 1983, Chem. Phys. Lett., **102**, 64-68.
124. Black, G., R.L. Sharpless, and T.G. Slanger, 1982, Chem. Phys. Lett., **93**, 598-602.
125. Black, G., R.L. Sharpless, and T.G. Slanger, 1982, Chem. Phys. Lett., **90**, 55-58.
126. Bogan, D.J., R.P. Thorn, F.L. Nesbitt, and L.J. Stief, 1996, J. Phys. Chem., **100**, 14383-14389.
127. Bohmer, E. and W. Hack, 1991, Ber. Bunsenges. Phys. Chem., **95**, 1688-1690.
128. Boodaghians, R.B., C.E. Canosa-Mas, P.J. Carpenter, and R.P. Wayne, 1988, J. Chem. Soc. Faraday Trans. 2, **84**, 931-948.
129. Boodaghians, R.B., I.W. Hall, and R.P. Wayne, 1987, J. Chem. Soc. Faraday Trans. 2, **83**, 529-538.
130. Borders, R.A. and J.W. Birks, 1982, J. Phys. Chem., **86**, 3295-3302.
131. Borrell, P., P.M. Borrell, and M.D. Pedley, 1977, Chem. Phys. Lett., **51**, 300-302.
132. Bourbon, C., M. Brioukov, and P. Devolder, 1996, C.A. Acad. Sci. Paris, **322**, 181-188.
133. Bourbon, C., M. Brioukov, B. Hanoune, J.P. Sawerysyn, and P. Devolder, 1996, Chem. Phys. Lett., **254**, 203-212.
134. Bourbon, C., C. Fittschen, J.P. Sawerysyn, and P. Devolder, 1995, J. Phys. Chem., **99**, 15102-15107.
135. Bourmada, N., C. Lafage, and P. Devolder, 1987, Chem. Phys. Lett., **136**, 209-214.
136. Bozzelli, J.W., Ph.D. Thesis, 1973, Dept. of Chemistry, Princeton University, (Diss. Abstr. Int. B 34(2) 608).
137. Bozzelli, J.W. and A.M. Dean, 1990, J. Phys. Chem., **94**, 3313-3317.
138. Bradley, J.N., W. Hack, K. Hoyermann, and H.G. Wagner, 1973, J. Chem. Soc. Faraday Trans. 1, **69**, 1889.
139. Brahan, K.M., A.D. Hewitt, G.D. Boone, and S.A. Hewitt, 1996, Int. J. Chem. Kinet., **28**, 397-404.
140. Braithwaite, M. and S.R. Leone, 1978, J. Chem. Phys., **69**, 839-845.
141. Breckenridge, W.H. and T.A. Miller, 1972, J. Chem. Phys., **56**, 465.
142. Bridier, I., B. Veyret, and R. Lesclaux, 1993, Chem. Phys. Lett., **201**, 563-568.
143. Brown, A.C., C.E. Canosa-Mas, A.D. Parr, K. Rothwell, and R.P. Wayne, 1990, Nature, **347**, 541-543.
144. Brown, A.C., C.E. Canosa-Mas, A.D. Parr, and R.P. Wayne, 1990, Atmos. Environ., **24A**, 2499-2511.
145. Brown, A.C., C.E. Canosa-Mas, and R.P. Wayne, 1990, Atmos. Environ., **24A**, 361-367.
146. Brown, A.C. and B.A. Thrush, 1967, Trans. Faraday Soc., **63**, 630.
147. Brown, R.D. and I.W.M. Smith, 1975, Int. J. Chem. Kinet., **7**, 301.
148. Brune, W.H., J.J. Schwab, and J.G. Anderson, 1983, J. Phys. Chem., **87**, 4503-4514.
149. Brunning, J. and M.A.A. Clyne, 1984, J. Chem. Soc. Faraday Trans 2, **80**, 1001-1014.

150. Brunning, J. and L.J. Stief, 1986, J. Chem. Phys., **84**, 4371-4377.
151. Brunning, J. and L.J. Stief, 1986, J. Chem. Phys., **85**, 2591.
152. Buben, S.N., I.K. Larin, N.A. Messineva, and E.M. Trofimova, 1990, Khim. Fiz., **9**, 116-126.
153. Buben, S.N., I.K. Larin, N.A. Messineva, and E.M. Trofimova, 1991,
154. Bulatov, V.P., A.A. Buloyan, S.G. Cheskis, M.Z. Kozliner, O.M. Sarkisov, and A.I. Trostin, 1980, Chem. Phys. Lett., **74**, 288.
155. Bulatov, V.P., S.G. Cheskis, A.A. Iogensen, P.V. Kulakov, O.M. Sarkisov, and E. Hassinen, 1988, Chem. Phys. Lett., **153**, 258-262.
156. Bulatov, V.P., M.Z. Kozliner, and O.M. Sarkisov, 1984, Khim. Fiz., **3**, 1300-1305.
157. Bulatov, V.P., M.Z. Kozliner, and O.M. Sarkisov, 1985, Khimi Fiz., **4**, 1353.
158. Bulatov, V.P., O.M. Sarkisov, M.Z. Kozliner, and V.G. Ergorov, 1986, Khim. Fiz., **5**, 1031.
159. Bulatov, V.P., S.I. Vereschchuk, F.N. Dzegilenko, O.M. Sarkisov, and V.N. Khabarov, 1990, Khim. Fiz., **9**, 1214.
160. Burkholder, J.B., P.D. Hammer, C.J. Howard, and A. Goldman, 1989, J. Geophys. Res., **94**, 2225-2234.
161. Burkholder, J.B., A. Mellouki, R. Talukdar, and A.R. Ravishankara, 1994, Int. J. Chem. Kinet., **24**, 711-725.
162. Burkholder, J.B., R.R. Wilson, T. Gierczak, R. Talukdar, S.A. McKeen, J.J. Orlando, G.L. Vaghjiani, and A.R. Ravishankara, 1991, J. Geophys. Res., **96**, 5025-5043.
163. Burks, T.L. and M.C. Lin, 1981, Int. J. Chem. Kinet., **13**, 13977-13999.
164. Burrows, J.P., D.I. Cliff, G.W. Harris, B.A. Thrush, and J.P.T. Wilkinson, 1979, Proc. Roy. Soc. (London), **A368**, 463-481.
165. Burrows, J.P. and R.A. Cox, 1981, J. Chem. Soc. Faraday Trans. 1, **77**, 2465.
166. Burrows, J.P., R.A. Cox, and R.G. Derwent, 1981, J. Photochem., **16**, 147-168.
167. Burrows, J.P., G.W. Harris, and B.A. Thrush, 1977, Nature, **267**, 233-234.
168. Burrows, J.P., G.S. Tyndall, and G.K. Moortgat, 1985, J. Phys. Chem., **89**, 4848-4856.
169. Burrows, J.P., T.J. Wallington, and R.P. Wayne, 1984, J. Chem. Soc. Faraday Trans. 2, **80**, 957-971.
170. Butkovskaya, N.I. and G. Le Bras, 1994, J. Phys. Chem., **98**, 2582-2591.
171. Butkovskaya, N.I., G. Poulet, and G. Le Bras, 1995, J. Phys. Chem., **99**, 4536-4543.
172. Butler, R., I.J. Solomon, and A. Snelson, 1978, Chem. Phys. Lett., **54**, 19.
173. Cadle, R.D. and J.W. Powers, 1967, J. Phys. Chem., **71**, 1702-1706.
174. Cadle, R.D. and C. Schadt, 1953, J. Phys. Chem., **21**, 163.
175. Callear, A.B. and R.E.M. Hedges, 1970, Trans. Faraday Soc., **66**, 605.
176. Callear, A.B. and I.W.M. Smith, 1967, Nature, **213**, 382.
177. Calvert, J.G. and J.N. Pitts, 1966, Photochemistry, John Wiley & Sons, Inc., New York, pp. 783.
178. Campbell, I.M., D.F. McLaughlin, and B.J. Handy, 1976, Chem. Phys. Lett., **38**, 362-64.
179. Cannon, B.D., J.S. Robertshaw, I.W.M. Smith, and M.D. Williams, 1984, Chem. Phys. Lett., **105**, 380-385.
180. Canosa-Mas, C., S.J. Smith, S. Toby, and R.P. Wayne, 1988, J. Chem. Soc. Faraday Trans. 2, **84**, 247-262.
181. Canosa-Mas, C.E., S.J. Smith, S. Toby, and R.P. Wayne, 1989, J. Chem. Soc. Faraday Trans. 2, **85**, 709-725.
182. Cantrell, C.A., J.A. Davidson, K.L. Busarow, and J.G. Calvert, 1986, J. Geophys. Res., **91**, 5347-5353.
183. Cantrell, C.A., J.A. Davidson, A.H. McDaniel, R.E. Shetter, and J.G. Calvert, 1988, J. Chem. Phys., **88**, 4997-5006.
184. Cantrell, C.A., J.A. Davidson, R.E. Shetter, B.A. Anderson, and J.G. Calvert, 1987, J. Phys. Chem., **91**, 6017-6021.
185. Cantrell, C.A., R.E. Shetter, and J.G. Calvert, 1994, J. Geophys. Res., **99**, 3739-3743.
186. Cantrell, C.A., R.E. Shetter, A.H. McDaniel, and J.G. Calvert, 1990, J. Geophys. Res., **95**, 20531-20537.
187. Cantrell, C.A., R.E. Shetter, A.J. McDaniel, J.G. Calvert, J.A. Davidson, D.C. Lowe, S.C. Tyler, R.J. Cicerone, and J.P. Greenberg, 1990, J. Geophys. Res., **95**, 22455-22462.
188. Cantrell, C.A., W.R. Stockwell, L.G. Anderson, K.L. Busarow, D. Perner, A. Schmeltekopf, J.G. Calvert, and H.S. Johnston, 1985, J. Phys. Chem., **89**, 139-146.
189. Casavecchia, P., R.J. Buss, S.J. Sibener, and Y.T. Lee, 1980, J. Chem. Phys., **73**, 6351-6352.
190. Castleman, A.W., R.E. Davis, H.R. Munkelwitz, I.N. Tang, and W.P. Wood, 1975, Int. J. Chem. Kinet., **Symp. 1**, 629.
191. Catoire, V., R. Lesclaux, P.D. Lightfoot, and M.-T. Rayez, 1994, J. Phys. Chem., **98**, 2889-2898.
192. Cattell, F.C., J. Cavanagh, R.A. Cox, and M.E. Jenkin, 1986, J. Chem. Soc. Faraday Trans. 2, **82**, 1999-2018.
193. Cattell, F.C. and R.A. Cox, 1986, J. Chem. Soc. Faraday Trans. 2, **82**, 1413-1426.
194. Chan, W.H., W.M. Uselman, J.G. Calvert, and J.H. Shaw, 1977, Chem. Phys. Lett., **45**, 240.
195. Chang, J.S. and J.R. Barker, 1979, J. Phys. Chem., **83**, 3059.
196. Chang, J.S. and F. Kaufman, 1977, Geophys. Res. Lett., **4**, 192-194.
197. Chang, J.S. and F. Kaufman, 1977, J. Chem. Phys., **66**, 4989.
198. Chang, J.S. and F. Kaufman, 1978, J. Phys. Chem., **82**, 1683-1686.
199. Chang, J.S., P.L. Trevor, and J.R. Barker, 1981, Int. J. Chem. Kinet., **13**, 1151-1161.
200. Chapman, C.J. and R.P. Wayne, 1974, Int. J. Chem. Kinet., **6**, 617-630.
201. Chasovnikov, S.A., A.I. Chichinin, and L.N. Krasnoperov, 1987, Chem. Phys., **116**, 91-99.
202. Chatha, J.P.S., P.K. Arora, N. Raja, P.B. Kulkarni, and K.G. Vohra, 1979, Int. J. Chem. Kinetics, **11**, 175-185.
203. Cheah, C.T. and M.A.A. Clyne, 1980, J. Chem. Soc. Faraday Trans., **76**, 1543.
204. Chen, J., V. Catoire, and H. Niki, 1995, Chem. Phys. Lett, **245**, 519-528.
205. Chen, J., V. Young, T. Zhu, and H. Niki, 1993, J. Phys. Chem., **97**, 11696-11698.
206. Chen, J., T. Zhu, and H. Niki, 1992, J. Phys. Chem., **96**, 6115-6117.

207. Chen, J., T. Zhu, H. Niki, and G.J. Mains, 1992, Geophys. Res. Lett., **19**, 2215-2218.
208. Chen, M.C. and H.A. Taylor, 1961, J. Chem. Phys., **34**, 1344-1347.
209. Chen, X., F. Wu, and B.R. Weiner, 1995, Chem. Phys. Lett., **247**, 313-320.
210. Cheng, B.-M. and Y.-P. Lee, 1986, Int. J. Chem. Kinet., **18**, 1303-1314.
211. Cheskis, S.G., A.A. Iogansen, O.M. Sarkisov, and A.A. Titov, 1985, Chem. Phys. Lett., **120**, 45-49.
212. Cheskis, S.G. and O.M. Sarkisov, 1979, Chem. Phys. Lett., **62**, 72.
213. Chichinin, A., S. Teton, G. Le Bras, and G. Poulet, 1994, J. Atmos. Chem, **18**, 239-245.
214. Chiorboli, C., C.A. Bignozzi, A. Maldotti, P.F. Giardini, A. Rossi, and V. Carassiti, 1983, Int. J. Chem. Kinet., **15**, 579-586.
215. Choo, K.Y. and M.-T. Leu, 1985, Int. J. Chem. Kinetics, **17**, 1155-1167.
216. Choo, K.Y. and M.T. Leu, 1985, J. Phys. Chem., **89**, 4832-4837.
217. Clark, I.D., I.T.N. Jones, and R.P. Wayne, 1970, Proc. Roy. Soc. Lond. A., **317**, 407-416.
218. Clark, I.D. and R.P. Wayne, 1969, Proc. Roy. Soc. Lond. A., **314**, 111-127.
219. Clark, I.D. and R.P. Wayne, 1969, Chem. Phys. Lett., **3**, 405-407.
220. Clark, I.D. and R.P. Wayne, 1970, Proc. Roy. Soc. London. A., **316**, 539-550.
221. Clark, R.H., D. Husain, and J.Y. Jezequel, 1982, J. Photochem., **18**, 39-46.
222. Clemo, A.R., F.E. Davidson, G.L. Duncan, and R. Grice, 1981, Chem. Phys. Lett., **84**, 509-511.
223. Clough, P.N. and B.A. Thrush, 1967, Trans. Faraday Soc., **63**, 915.
224. Clyne, M.A.A. and J.A. Coxon, 1968, Proc. Roy. Soc. A, **303**, 207-231.
225. Clyne, M.A.A. and H.W. Cruse, 1970, Trans. Faraday Soc., **66**, 2227.
226. Clyne, M.A.A. and H.W. Cruse, 1972, J. Chem. Soc. Faraday Trans. 2, **68**, 1281.
227. Clyne, M.A.A. and S. Down, 1974, J. Chem. Soc. Faraday Trans. 2, **70**, 253-266.
228. Clyne, M.A.A., C.J. Halstead, and B.A. Thrush, 1966, Proc. Soc. London Ser. A., **295**, 355.
229. Clyne, M.A.A. and A. Hodgson, 1985, J. Chem. Soc. Faraday Trans. 2, **81**, 443-455.
230. Clyne, M.A.A. and P.M. Holt, 1979, J. Chem. Soc. Faraday Trans. 2, **75**, 569-581.
231. Clyne, M.A.A. and P.M. Holt, 1979, J. Chem. Soc. Faraday Trans. 2, **75**, 582-591.
232. Clyne, M.A.A. and A.J. MacRobert, 1980, Int. J. Chem. Kinet., **12**, 79-96.
233. Clyne, M.A.A. and A.J. MacRobert, 1981, Int. J. Chem. Kinet., **13**, 187-197.
234. Clyne, M.A.A., A.J. MacRobert, T.P. Murrells, and L.J. Stief, 1984, J. Chem. Soc. Faraday Trans. 2, **80**, 877-886.
235. Clyne, M.A.A. and I.S. McDermid, 1975, J. Chem. Soc. Faraday Trans. 1, **71**, 2189.
236. Clyne, M.A.A., D.J. McKenney, and R.F. Walker, 1973, Can. J. Chem., **51**, 3596.
237. Clyne, M.A.A., D.J. McKenney, and R.T. Watson, 1975, Chem. Soc. Faraday Trans. 1, **71**, 322-335.
238. Clyne, M.A.A. and P. Monkhouse, 1977, J. Chem. Soc. Faraday Trans. 2, **73**, 298-309.
239. Clyne, M.A.A., P.B. Monkhouse, and L.W. Townsend, 1976, Int. J. Chem. Kinet., **8**, 425.
240. Clyne, M.A.A. and W.S. Nip, 1976, J. Chem. Soc. Faraday Trans. 1, **72**, 2211.
241. Clyne, M.A.A. and W.S. Nip, 1976, J. Chem. Soc. Faraday Trans. 2, **72**, 838.
242. Clyne, M.A.A. and Y. Ono, 1982, Chem. Phys., **69**, 381-388.
243. Clyne, M.A.A. and Y. Ono, 1983, Chem. Phys. Lett., **94**, 597-602.
244. Clyne, M.A.A., B.A. Thrush, and R.P. Wayne, 1964, Trans. Faraday Soc., **60**, 359.
245. Clyne, M.A.A. and L.W. Townsend, 1975, Int. J. Chem. Kinet., **Symp. 1**, 73-84.
246. Clyne, M.A.A. and R.F. Walker, 1973, J. Chem. Soc. Faraday Trans. 1, **69**, 1547.
247. Clyne, M.A.A. and R.T. Watson, 1974, J. Chem. Soc. Faraday Trans. 1, **70**, 2250.
248. Clyne, M.A.A. and R.T. Watson, 1974, J. Chem. Soc. Faraday Trans. 1, **70**, 1109.
249. Clyne, M.A.A. and R.T. Watson, 1975, J. Chem. Soc. Faraday Trans. 1, **71**, 336.
250. Clyne, M.A.A. and R.T. Watson, 1977, J. Chem. Soc. Faraday Trans. 1, **73**, 1169.
251. Clyne, M.A.A. and I.F. White, 1971, Trans. Faraday Soc., **67**, 2068-2076.
252. Clyne, M.A.A. and P.D. Whitefield, 1979, J. Chem. Soc. Faraday Trans. 2, **75**, 1327.
253. Cocks, A.T., R.P. Fernanado, and I.S. Fletcher, 1986, Atmos. Environ., **20**, 2359-2366.
254. Cohen, N. and S.W. Benson, 1987, J. Phys. Chem., **91**, 162-170.
255. Cohen, N. and K.R. Westberg, 1991, J. Phys. Chem. Ref. Data , **20**, 1211-1311.
256. Collins, R.J., D. Husain, and R.J. Donovan, 1973, J. Chem. Soc. Faraday Trans. 2, **69**, 145-157.
257. Colussi, A.J., 1990, J. Phys. Chem., **94**, 8922-8926.
258. Colussi, A.J. and M.A. Grela, 1994, Chem. Phys. Lett., **229**, 134-138.
259. Colussi, A.J., S.P. Sander, and R.R. Friedl, 1992, J. Phys.Chem., **96**, 4442-4445.
260. Connell, P.S. and C.J. Howard, 1985, Int. J. Chem. Kinet., **17**, 17.
261. Cook, J.L., C.A. Ennis, T.J. Leck, and J.W. Birks, 1981, J. Chem. Phys., **74**, 545.
262. Coomber, J.W. and E. Whittle, 1966, Trans. Faraday Soc., **62**, 2183-2190.
263. Cooper, W.F. and J.F. Hershberger, 1992, J. Phys. Chem., **96**, 5405-5410.
264. Cox, J.W., H.H. Nelson, and J.R. McDonald, 1985, Chem. Phys., **96**, 175.
265. Cox, R.A., 1980, Int. J. Chem. Kinet., **12**, 649.
266. Cox, R.A., R.A. Barton, E. Ljungstrum, and D.W. Stocker, 1984, Chem. Phys. Lett., **108**, 228-232.
267. Cox, R.A. and J.P. Burrows, 1979, J. Phys. Chem., **83**, 2560-2568.
268. Cox, R.A., J.P. Burrows, and T.J. Wallington, 1981, Chem. Phys. Lett., **84**, 217-221.
269. Cox, R.A. and G.B. Coker, 1983, J. Atmos. Chem., **1**, 53.
270. Cox, R.A., R. Derwent, P.M. Holt, and J.A. Kerr, 1976, J. Chem. Soc. Faraday Trans I, **72**, 2061-2075.
271. Cox, R.A. and R.G. Derwent, 1979, J. Chem. Soc. Far. Trans. 1, **75**, 1635-1647.

272. Cox, R.A., R.G. Derwent, A.E.J. Eggleton, and J.E. Lovelock, 1976, Atmos. Environ., **10**, 305.
273. Cox, R.A., R.G. Derwent, A.E.J. Eggleton, and H.J. Read, 1979, J. Chem. Soc. Faraday Trans. I, **75**, 1648-1666.
274. Cox, R.A., R.G. Derwent, and P.M. Holt, 1975, Chemosphere, **4**, 201.
275. Cox, R.A., R.G. Derwent, and P.M. Holt, 1976, J. Chem. Soc. Faraday Trans. 1, **72**, 2031.
276. Cox, R.A., R.G. Derwent, S.V. Kearsey, L. Batt, and K.G. Patrick, 1980, J. Photochem., **13**, 149.
277. Cox, R.A., R.G. Derwent, and M.R. Williams, 1980, Environ. Sci. and Technol., **14**, 57-61.
278. Cox, R.A., M. Fowles, D. Moulton, and R.P. Wayne, 1987, J. Phys. Chem., **91**, 3361-3365.
279. Cox, R.A. and A. Goldstone, 1982, Proceedings of the 2nd European Symposium on the "Physico-Chemical Behaviour of the Atmospheric Pollutants", D. Reidel Publishing Co., Varese, Italy, pp. 112-119.
280. Cox, R.A. and G.D. Hayman, 1988, Nature, **332**, 796-800.
281. Cox, R.A. and S.A. Penkett, 1972, J. Chem. Soc., Faraday Trans. 1, **68**, 1735.
282. Cox, R.A. and J.J. Roffey, 1977, Environ. Sci. Technol., **11**, 900.
283. Cox, R.A. and D. Sheppard, 1980, Nature, **284**, 330-331.
284. Cox, R.A., D.W. Sheppard, and M.P. Stevens, 1982, J. Photochem., **19**, 189-207.
285. Cox, R.A. and G. Tyndall, 1979, Chem. Phys. Lett., **65**, 357.
286. Cox, R.A. and G.S. Tyndall, 1980, J. Chem. Soc. Faraday Trans. 2, **76**, 153.
287. Crowley, J.N., P. Campuzano-Jost, and G.K. Moortgat, 1996, J. Phys. Chem., **100**, 3601-3606.
288. Crowley, J.N., F.G. Simon, J.P. Burrows, G.K. Moortgat, M.E. Jenkin, and R.A. Cox, 1991, J. Photochem. and Photobiol. A: Chem., **60**, 1-10.
289. Cupitt, L.T. and G.P. Glass, 1975, Int. J. Chem. Kinet., **Symp. 1**, 39-50.
290. Cvetanovic, R.J., D.L. Singleton, and R.S. Irwin, 1981, J. Am. Chem. Soc., **103**, 3530.
291. Czarnowski, J. and H.J. Schumacher, 1981, Int. J. Chem. Kinet., **13**, 639-649.
292. Daele, V. and G. Poulet, 1996, J. Chim. Phys., **93**, 1081-1099.
293. Daele, V., A. Ray, I. Vassali, G. Poulet, and G. Le Bras, 1995, Int. J. Chem. Kinet., **27**, 1121-1133.
294. Dagaut, P. and M.J. Kurylo, 1990, J. Photochem. and Photobiol. A:Chem., **51**, 133.
295. Dagaut, P., T.J. Wallington, and M.J. Kurylo, 1988, J. Phys. Chem., **92**, 3836-3839.
296. Dagaut, P., T.J. Wallington, and M.J. Kurylo, 1988, J. Phys. Chem., **92**, 3833-3836.
297. Dagaut, P., T.J. Wallington, R. Liu, and M.J. Kurylo, 1988, Int. J. Chem. Kinet., **20**, 331-338.
298. Daniels, F. and E.H. Johnston, 1921, J. Am. Chem. Soc., **43**, 53.
299. Daubendiek, R.L. and J.G. Calvert, 1975, Environ. Lett., **8**, 103.
300. Davenport, J.E., B. Ridley, H.I. Schiff, and K.H. Welge, 1972, J. Chem. Soc. Faraday Discussion, **53**, 230-231.
301. Davidson, F.E., A.R. Clemo, G.L. Duncan, R.J. Browett, J.H. Hobson, and R. Grice, 1982, Molec. Phys., **46**, 33-40.
302. Davidson, J.A., C.A. Cantrell, S.C. Tyler, R.E. Shetter, R.J. Cicerone, and J.G. Calvert, 1987, J. Geophys. Res., **92**, 2195-2199.
303. Davidson, J.A., C.J. Howard, H.I. Schiff, and F.C. Fehsenfeld, 1979, J. Chem. Phys., **70**, 1697-1704.
304. Davidson, J.A., K.E. Kear, and E.W. Abrahamson, 1972/1973, J. Photochem., **1**, 307-316.
305. Davidson, J.A., H.I. Schiff, T.J. Brown, and C.J. Howard, 1978, J. Chem. Phys., **69**, 4277-4279.
306. Davidson, J.A., H.I. Schiff, G.E. Streit, J.R. McAfee, A.L. Schmeltekopf, and C.J. Howard, 1977, J. Chem. Phys., **67**, 5021-5025.
307. Davies, P.B. and B.A. Thrush, 1968, Trans. Far. Soc., **64**, 1836.
308. Davis, D.D., W. Braun, and A.M. Bass, 1970, Int. J. Chem. Kinet., **2**, 101.
309. Davis, D.D., J.T. Herron, and R.E. Huie, 1973, J. Chem. Phys., **58**, 530.
310. Davis, D.D., R.B. Klemm, and M. Pilling, 1972, Int. J. Chem. Kinet., **4**, 367-382.
311. Davis, D.D., G. Machado, B. Conaway, Y. Oh, and R.T. Watson, 1976, J. Chem. Phys., **65**, 1268.
312. Davis, D.D., J. Prusazcyk, M. Dwyer, and P. Kim, 1974, J. Phys. Chem., **78**, 1775-1779.
313. Davis, D.D., W. Wong, and J. Lephardt, 1973, Chem. Phys. Lett., **22**, 273-278.
314. Davis, D.D., W. Wong, and R. Schiff, 1974, J. Phys. Chem., **78**, 463-464.
315. Daykin, E.P. and P.H. Wine, 1990, J. Geophys. Res., **95**, 18547-18553.
316. Daykin, E.P. and P.H. Wine, 1990, Int. J. Chem. Kinet., **22**, 1083-1094.
317. Daykin, E.P. and P.H. Wine, 1990, J. Phys. Chem., **94**, 4528-4535.
318. De Sousa, A.R., M. Touzeau, and M. Petitdidier, 1985, Chem. Phys. Lett., **121**, 423-428.
319. DeMore, W.B., 1969, Int. J. Chem. Kinet., **1**, 209-220.
320. DeMore, W.B., 1971, Int. J. Chem. Kinet., **3**, 161-173.
321. DeMore, W.B., 1979, J. Phys. Chem., **83**, 1113-1118.
322. DeMore, W.B., paper presented at the 182nd National Meeting of the American Chemical Society, 1981, New York.
323. DeMore, W.B., 1982, J. Phys. Chem, **86**, 121-126.
324. DeMore, W.B., 1984, Int. J. Chem. Kinet., **16**, 1187-1200.
325. DeMore, W.B., 1991, J. Geophys. Res., **96**, 4995-5000.
326. DeMore, W.B., 1992, Geophys. Res. Lett., **19**, 1367-1370.
327. DeMore, W.B., 1993, Geophys. Res. Lett., **20**, 1359-1362.
328. DeMore, W.B., 1993, J. Phys. Chem., **97**, 8564-8566.
329. DeMore, W.B., 1996, J. Phys. Chem., **100**, 5813-5820.
330. DeMore, W.B. and C.L. Lin, 1973, J. Org. Chem., **38**, 985-989.

331. DeMore, W.B., C.L. Lin, and S. Jaffe, paper presented at the 12th Informal Conference on Photochemistry, 1976, NBS, 287-289.
332. DeMore, W.B. and E. Tschuikow-Roux, 1974, J. Phys. Chem., **78**, 1447-1451.
333. DeMore, W.B. and E. Tschuikow-Roux, 1990, J. Phys. Chem., **94**, 5856-5860.
334. Derwent, R.G. and B.A. Thrush, 1971, Trans. Faraday Soc., **67**, 2036-2043.
335. Devolder, P., M. Carlier, J.F. Pauwels, and L.R. Sochet, 1984, Chem. Phys. Lett., **111**, 94-99.
336. Diau, E.W., T. Yu, M.A.G. Wagner, and M.C. Lin, 1994, J. Phys. Chem., **98**, 4034-4042.
337. Diau, E.W.-G. and Y.-P. Lee, 1991, J. Phys. Chem., **95**, 7726-7732.
338. Diau, E.W.-G., T.-L. Tso, and Y.-P. Lee, 1990, J. Phys. Chem., **94**, 5261-5265.
339. Dibble, T.S., M.M. Maricq, J.J. Szente, and J.S. Francisco, 1995, J. Phys. Chem., **99**, 17394-17402.
340. Dlugokencky, E.J. and C.J. Howard, 1988, J. Phys. Chem., **92**, 1188-1193.
341. Dlugokencky, E.J. and C.J. Howard, 1989, J. Phys. Chem., **93**, 1091-1096.
342. Dobe, S., L.A. Khachatryan, and T. Berces, 1989, Ber. Bunsenges. Phys. Chem., **93**, 847-852.
343. Dobe, S., M. Otting, F. Temps, H.G. Wagner, and H. Ziemer, 1993, Ber. Bunsenges. Phys. Chem., **97**, 877-884.
344. Dobe, S., F. Temps, T. Bohland, and H.G. Wagner, 1985, Z. Naturforsch., **40a**, 1289-1298.
345. Dobis, O. and S.W. Benson, 1991, J. Am. Chem. Soc., **113**, 6377-6386.
346. Dobis, O. and S.W. Benson, 1993, J. Am. Chem. Soc., **115**, 8798-8809.
347. Dodonov, A.F., G.K. Lavrovskaya, I.I. Morozov, and V.L. Tal'rose, 1971, Dokl. Adak. Nauk USSR, 1971, Vol. 198, 622: Dokl. Phys. Chem. (Engl. Trans.), **198**, 440-442.
348. Dodonov, A.F., V.V. Zelenov, A.S. Kukui, and E.A.P.V.L. Tal'Rose, 1985, Khim. Fiz., **4**, 1335-1343.
349. Dognon, A.M., F. Caralp, and R. Lesclaux, 1985, J. Chim. Phys. Phys.-Chim. Biol., **82**, 349-352.
350. Dolson, D.A., 1986, J. Phys. Chem., **90**, 6714-6718.
351. Domine, F., T.P. Murrells, and C.J. Howard, 1990, J. Phys. Chem., **94**, 5839-5847.
352. Domine, F. and A.R. Ravishankara, 1992, Int. J. Chem. Kinet., **24**, 943-951.
353. Domine, F., A.R. Ravishankara, and C.J. Howard, 1992, J. Phys. Chem., **96**, 2171-2178.
354. Donovan, R.J. and D.J. Little, 1972, Chem. Phys. Lett., **13**, 488.
355. Dransfeld, P. and H.G. Wagner, 1986, Z. Naturforsch., **42a**, 471-476.
356. Dreier, T. and J. Wolfrum, 1980, 18th International Symposium on Combustion, The Combustion Institute, pp. 801-809.
357. Dreier, T. and J. Wolfrum, paper presented at the 20th International Symposium on Combustion, 1984, The Combustion Institute, 695-702.
358. Dreyer, J.W., D. Perner, and C.R. Roy, 1974, J. Chem. Phys., **61**, 3164.
359. Droege, A.T. and F.P. Tully, 1986, J. Phys. Chem., **90**, 1949-1954.
360. Dunlop, J.R. and F.P. Tully, 1993, J. Phys. Chem., **97**, 11148-11150.
361. Eberhard, J. and C.J. Howard, 1996, Int. J. Chem. Kinet., **28**, 731-740.
362. Egsgaard, H., L. Carlson, H. Florencio, T. Drewello, and H. Schwarz, 1988, Chem. Phys. Lett., **148**, 537-540.
363. Ehhalt, D.H., J.A. Davidson, C.A. Cantrell, I. Friedman, and S. Tyler, 1989, J. Geophys. Res., **94**, 9831-9836.
364. Eibling, R.E. and M. Kaufman, 1983, Atmos. Environ., **17**, 429-431.
365. Elrod, M.J., R.F. Meads, J.B. Lipson, J.V. Seeley, and M.J. Molina, 1996, J. Phys. Chem., **100**, 5808-5812.
366. Ennis, C.A. and J.W. Birks, 1985, J. Phys. Chem., **89**, 186-191.
367. Ennis, C.A. and J.W. Birks, 1988, J. Phys. Chem., **93**, 1119-1126.
368. Fair, R.W. and B.A. Thrush, 1969, Trans. Faraday Soc., **65**, 1557.
369. Fair, R.W., A. van Roodaelaar, and O.P. Strausz, 1971, Can. J. Chem., **49**, 1659.
370. Fang, T.D., P.H. Taylor, and B. Dellinger, 1996, J. Phys. Chem., **100**, 4048-4054.
371. Farquharson, G.K. and R.H. Smith, 1980, Aust. J. Chem., **33**, 1425-1435.
372. Fasano, D.M. and N.S. Nogar, 1981, Int. J. Chem. Kinet., **13**, 325.
373. Fasano, D.M. and N.S. Nogar, 1982, Chem. Phys. Lett., **92**, 411-414.
374. Fenter, F.F. and J.G. Anderson, 1991, J. Phys. Chem., **95**, 3172-3180.
375. Fenter, F.F. and J.G. Anderson, 1994, Int. J. Chem. Kinet., **26**, 801-812.
376. Fenter, F.F., V. Catoire, R. Lesclaux, and P.D. Lightfoot, 1993, J. Phys. Chem., **97**, 3530-3538.
377. Filseth, S.V., A. Zia, and K.H. Welge, 1970, J. Chem. Phys., **52**, 5502-5510.
378. Findlay, F.D., C.J. Fortin, and D.R. Snelling, 1969, Chem. Phys. Lett., **3**, 204-206.
379. Findlay, F.D. and D.R. Snelling, 1971, J. Chem. Phys., **55**, 545-551.
380. Findlay, F.D. and D.R. Snelling, 1971, J. Chem. Phys., **54**, 2750-2755.
381. Finkbeiner, M., J.N. Crowley, O. Horie, R. Muller, G.K. Moortgat, and P.J. Crutzen, 1995, J. Phys. Chem., **99**, 16264-16275.
382. Finlayson-Pitts, B.J., M.J. Ezell, T.M. Jayaweera, H.N. Berko, and C.C. Lai, 1992, Geophys. Res. Lett., **19**, 1371-1374.
383. Finlayson-Pitts, B.J., S.K. Hernandez, and H.N. Berko, 1993, J. Phys. Chem., **97**, 1172-1177.
384. Finlayson-Pitts, B.J. and T.E. Kleindienst, 1979, J. Chem. Phys., **70**, 4804-4806.
385. Finlayson-Pitts, B.J., T.E. Kleindienst, J.J. Ezell, and D.W. Toohey, 1981, J. Chem. Phys., **74**, 4533-4543.
386. Fletcher, I.S. and D. Husain, 1976, J. Phys. Chem., **80**, 1837-1840.
387. Fletcher, I.S. and D. Husain, 1976, Can. J. Chem., **54**, 1765-1770.
388. Fletcher, I.S. and D. Husain, 1978, J. Photochem., **8**, 355-361.
389. Fockenberg, C., H. Saathoff, and R. Zellner, 1994, Chem. Phys. Lett., **218**, 21-28.
390. Foon, R., G. Le Bras, and J. Combourieu, 1979, C.R. Acad. Sci. Paris, **Series C 288**, 241.

391. Foon, R. and G.P. Reid, 1971, Trans. Faraday Soc., **67**, 3513.
392. Force, A.P. and J.R. Wiesenfeld, 1981, J. Chem. Phys., **74**, 1718-1723.
393. Force, A.P. and J.R. Wiesenfeld, 1981, J. Phys. Chem., **85**, 782-785.
394. Fraser, M.E. and L.G. Piper, 1989, J. Phys. Chem., **93**, 1107-1111.
395. Freeman, C.G. and L.F. Phillips, 1968, J. Phys. Chem., **72**, 3025.
396. Freudenstein, K. and D. Biedenkapp, 1976, Ber. Bunsenges. Phys. Chem., **80**, 42-48.
397. Friedl, R.R., W.H. Brune, and J.G. Anderson, 1985, J. Phys. Chem., **89**, 5505-5510.
398. Friedl, R.R., J.H. Goble, and S.P. Sander, 1986, Geophys. Res. Lett., **13**, 1351-1354.
399. Friedl, R.R. and S.P. Sander, 1989, J. Phys. Chem., **93**, 4756-4764.
400. Friedl, R.R., S.P. Sander, and Y.L. Yung, 1992, J. Phys. Chem., **96**, 7490-7493.
401. Fritz, B., K. Lorenz, W. Steinert, and R. Zellner, 1984, Oxidation Communications, **6**, 363-370.
402. Frost, M.J. and I.W.M. Smith, 1990, J. Chem. Soc. Farad. Trans., **86**, 1757-1762.
403. Frost, R.J., D.S. Green, M.K. Osborn, and I.W.M. Smith, 1986, Int. J. Chem. Kinet., **18**, 885-898.
404. Gaffney, J.S., R. Fajer, G.I. Senum, and J.H. Lee, 1986, Int. J. Chem. Kinet., **18**, 399-407.
405. Ganske, J.A., H.N. Berko, M.J. Ezell, and B.J. Finlayson-Pitts, 1992, J. Phys. Chem., **96**, 2568-2572.
406. Ganske, J.A., M.J. Ezell, H.N. Berko, and B.J. Finlayson-Pitts, 1991, Chem. Phys. Lett., **179**, 204-210.
407. Garland, N.L., L.J. Medhurst, and H.H. Nelson, 1993, J. Geophys. Res. D., **98**, 23107-23111.
408. Garland, N.L. and H.H. Nelson, 1996, Chem. Phys. Lett., **248**, 296-300.
409. Garraway, J. and R.J. Donovan, 1979, J. Chem. Soc. Chem. Commun., 1108.
410. Garvin, D. and H.P. Broida, paper presented at the 9th Symposium on Combustion, 1963, The Combustion Institute, 678.
411. Gauthier, M.J.E. and D.R. Snelling, 1974, Can. J. Chem., **52**, 4007-4015.
412. Geers-Muller, R. and F. Stuhl, 1987, Chem. Phys. Lett., **135**, 263-268.
413. Gehring, M., K. Hoyermann, H. Sahaeke, and J. Wolfrum, paper presented at the 14th Int. Symposium on Combustion, 1973, The Combustion Institute, 99.
414. Gericke, K.-H. and F.J. Comes, 1981, Chem. Phys. Lett., **81**, 218-222.
415. Gierczak, T., L. Goldfarb, D. Sueper, and A.R. Ravishankara, 1994, Int. J. Chem. Kinet., **26**, 719-728.
416. Gierczak, T., R. Talukdar, G.L. Vaghjiani, E.R. Lovejoy, and A.R. Ravishankara, 1991, J. Geophys. Res., **96**, 5001-5011.
417. Gierczak, T., R.K. Talukdar, J.B. Burkholder, R.W. Portmann, J.S. Daniel, S. Solomon, and A.R. Ravishankara, 1996, J. Geophys. Res., **101**, 12905-12911.
418. Gierczak, T., R.K. Talukdar, and A.R. Ravishankara, 1997, J. Phys. Chem., in press.
419. Gierczak, T., S. Talukdar, S. Herndon, G.L. Vaghjiani, and A.R. Ravishankara, 1997, J. Phys. Chem., in press.
420. Gill, R.J., W.D. Johnson, and G.H. Atkinson, 1981, Chem. Phys., **58**, 29.
421. Gilles, M.K., A.A. Turnipseed, J.B. Burkholder, A.R. Ravishankara, and S. Solomon, 1996, manuscript.
422. Gilpin, R., H.I. Schiff, and K.H. Welge, 1971, J. Chem. Phys., **55**, 1087-1093.
423. Glaschick-Schimpf, I., A. Leiss, P.B. Monkhouse, U. Schurath, K.H. Becker, and E.H. Fink, 1979, Chem. Phys. Lett., **67**, 318-323.
424. Glavas, S. and J. Heicklen, 1985, J. Photochem., **31**, 21-28.
425. Gleason, J.F. and C.J. Howard, 1988, J. Phys. Chem., **92**, 3414-3417.
426. Gleason, J.F., F.L. Nesbitt, and L.J. Stief, 1994, J. Phys. Chem., **98**, 126-131.
427. Gleason, J.F., A. Sinha, and C.J. Howard, 1987, J. Phys. Chem., **91**, 719-724.
428. Glinski, R.J. and J.W. Birks, 1985, J. Phys. Chem., **89 90**, 3449-3453 342.
429. Gordon, S., W. Mulac, and P. Nangia, 1971, J. Phys. Chem., **75** , 2087.
430. Gordon, S. and W.A. Mulac, 1975, Int. J. Chem. Kinet., **Symp. 1**, 289-299.
431. Graham, R.A. and D.J. Gutman, 1977, J. Phys. Chem., **81**, 207.
432. Graham, R.A. and H.S. Johnston, 1974, J. Chem. Phys., **60**, 4628.
433. Graham, R.A. and H.S. Johnston, 1978, J. Phys. Chem., **82**, 254-268.
434. Graham, R.A., A.M. Winer, R. Atkinson, and J.N. Pitts Jr., 1979, J. Phys. Chem., **83**, 1563.
435. Green, R.G. and R.P. Wayne, 1976/77, J. Photochem., **6**, 371-374.
436. Greenblatt, G.D. and C.J. Howard, 1989, J. Phys. Chem., **93**, 1035-1042.
437. Greenblatt, G.D. and A.R. Ravishankara, 1990, J. Geophys. Res., **95**, 3539-3547.
438. Greenhill, P.G. and B.V. O'Grady, 1986, Aust. J. Chem., **39**, 1775-1787.
439. Greiner, N.R., 1969, J. Chem. Phys., **51**, 5049-5051.
440. Greiner, N.R., 1970, J. Chem. Phys., **53**, 1284-1285.
441. Grimley, A.J. and P.L. Houston, 1980, J. Chem. Phys., **72**, 1471-1475.
442. Grotheer, H.H., G. Riekert, U. Meier, and T. Just, 1985, Ber. Bunsenges. Phys. Chem., **89**, 187-191.
443. Grotheer, H.H., G. Riekert, D. Walter, and T. Just, 1988, J. Phys. Chem., **92**, 4028.
444. Gutman, D., N. Sanders, and J.E. Butler, 1982, J. Phys. Chem., **86**, 66.
445. Hack, W., O. Horie, and H.G. Wagner, 1981, Ber. Bunsenges. Phys. Chem., **85**, 72.
446. Hack, W., O. Horie, and H.G. Wagner, 1982, J. Phys. Chem., **86**, 765.
447. Hack, W., K. Hoyermann, and H.G. Wagner, 1974, Ber. Bunsenges. Phys. Chem., **78**, 386.
448. Hack, W., G. Mex, and H.G. Wagner, 1977, Ber. Bunsenges. Phys. Chem., **81**, 677-684.
449. Hack, W., A.W. Preuss, F. Temps, and H.G. Wagner, 1979, Ber. Bunsenges. Phys. Chem., **83**, 1275-1279.
450. Hack, W., A.W. Preuss, F. Temps, H.G. Wagner, and K. Hoyermann, 1980, Int. J. Chem. Kinet., **12**, 851-860.
451. Hack, W., A.W. Preuss, H.G. Wagner, and K. Hoyermann, 1979, Ber. Bunsenges. Phys. Chem., **83**, 212-217.

452. Hack, W., H. Schacke, M. Schroter, and H.G. Wagner, paper presented at the 17th International Symposium on Combustion, 1979.
453. Hack, W., H.G. Wagner, and K. Hoyermann, 1978, Ber. Bunsenges. Phys. Chem., **82**, 713-719.
454. Hagele, J., K. Lorenz, D. Rhasa, and R. Zellner, 1983, Ber. Bunsenges. Phys. Chem., **87**, 1023-1026.
455. Hall, I.W., R.P. Wayne, R.A. Cox, M.E. Jenkin, and G.D. Hayman, 1988, J. Phys. Chem., **92**, 5049-5054.
456. Halstead, C.J. and B.A. Thrush, 1966, Proc. Roy. Soc. London, **Ser. A 295**, 380.
457. Hamilton, E.J., Jr., 1975, J. Chem. Phys., **63**, 3682-3683.
458. Hamilton, E.J., Jr. and R.-R. Lii, 1977, Int. J. Chem. Kinet., **9**, 875-885.
459. Hammer, P.D., E.J. Dlugokencky, and C.J. Howard, 1986, J. Phys. Chem., **90**, 2491-2496.
460. Hampson, R.F., Jr. and D. Garvin, 1977, Reaction Rate and Photochemical Data for Atmospheric Chemistry, SP-513, National Bureau of Standards, Washington, D.C., pp. 33.
461. Hancock, G., W. Lange, M. Lenzi, and K.H. Welge, 1975, Chem. Phys. Lett., **33**, 168.
462. Hancock, G. and I.W.M. Smith, 1971, Trans. Faraday Soc., **67**, 2586.
463. Handwerk, V. and R. Zellner, 1978, Ber. Bunsenges. Phys. Chem., **82**, 1161-1166.
464. Hansen, I., K. Hoinghaus, C. Zetzsch, and F. Stuhl, 1976, Chem. Phys. Lett., **42**, 370-372.
465. Harris, G.W., T.E. Kleindienst, and J.N. Pitts Jr., 1981, Chem. Phys. Lett., **80**, 479-483.
466. Harrison, J.A., A.R. Whyte, and L.F. Phillips, 1986, Chem. Phys. Lett., **129**, 346-352.
467. Hartmann, D., J. Karthauser, J.P. Sawerysyn, and R. Zellner, 1990, Ber. Bunsenges. Phys. Chem., **94**, 639-645.
468. Harwood, M.H., J.B. Burkholder, M. Hunter, R.W. Fox, and A.R. Ravishankara, 1997, J. Phys. Chem. A, **101**, 853-863.
469. Hashimoto, S., G. Inoue, and H. Akimoto, 1984, Chem. Phys. Lett., **107**, 198-202.
470. Hatakeyama, S. and M.T. Leu, 1986, Geophys. Res. Lett., **13**, 1343-1346.
471. Hatakeyama, S. and M.T. Leu, 1989, J. Phys. Chem., **93**, 5784-5789.
472. Hayman, G.D., J.M. Davies, and R.A. Cox, 1986, Geophys. Res. Lett., **13**, 1347-1350.
473. Heidner, R.F., J.F. Bott, C.E. Gardner, and J.E. Melzer, 1979, J. Chem. Phys., **70**, 4509.
474. Heidner, R.F., J.F. Bott, C.E. Gardner, and J.E. Melzer, 1980, J. Chem. Phys., **72**, 4815.
475. Heidner, R.F., III and D. Husain, 1973, Int. J. Chem. Kinet., **5**, 819-831.
476. Heidner, R.F., III , D. Husain, and J.R. Weisenfeld, 1973, J. Chem. Soc. Faraday Trans. 2, **69**, 927-938.
477. Helleis, F., J.N. Crowley, and G.K. Moortgat, 1993, J. Phys. Chem., **97**, 11464-11473.
478. Helleis, F., J.N. Crowley, and G.K. Moortgat, 1994, Geophys. Res. Lett., **21**, 1795-1798.
479. Helmer, M. and J.M.C. Plane, 1993, J. Geophys. Res., **98**, 23207-23222.
480. Hendry, D.G. and R.A. Kenley, 1977, J. Amer. Chem. Soc., **99**, 3198-99.
481. Heneghan, S.P. and S.W. Benson, 1983, Int. J. Chem. Kinet., **15**, 1311-1319.
482. Herron, J.T., 1961, J. Chem. Phys., **35**, 1138.
483. Herron, J.T. and R.E. Huie, 1974, J. Phys. Chem., **78**, 2085.
484. Herron, J.T. and R.D. Penzhorn, 1969, J. Phys. Chem., **73**, 191.
485. Hess, W.P. and F.P. Tully, 1988, Chem. Phys. Lett., **152**, 183-189.
486. Hess, W.P. and F.P. Tully, 1989, J. Phys. Chem., **93**, 1944-1947.
487. Hills, A.J., R.J. Cicerone, J.G. Calvert, and J.W. Birks, 1988, J. Phys. Chem., **92**, 1853-1858.
488. Hills, A.J. and C.J. Howard, 1984, J. Chem. Phys., **81**, 4458-4465.
489. Hippler, H. and J. Troe, 1992, Chem. Phys. Lett., **192**, 333-337.
490. Hippler, H., J. Troe, and J. Willner, 1990, J. Chem. Phys., **93**, 1755-1760.
491. Hislop, J.R. and R.P. Wayne, 1977, J. Chem. Soc. Faraday Trans. 2, **73**, 506-516.
492. Hjorth, J., F. Cappellani, C.J. Nielsen, and G. Restelli, 1989, J. Phys. Chem., **93**, 5458-5461.
493. Hjorth, J., G. Ottobrini, F. Cappellani, and G. Restelli, 1987, J. Phys. Chem., **91**, 1565-1568.
494. Hjorth, J., G. Ottobrini, and G. Restelli, 1986, Int. J. Chem. Kinet., **18**, 819-828.
495. Hjorth, J., G. Ottobrini, and G. Restelli, 1988, J. Phys. Chem., **92**, 2669.
496. Hochanadel, C.J., J.A. Ghormley, J.W. Boyle, and P.J. Ogren, 1977, J. Phys. Chem., **81**, 3.
497. Hochanadel, C.J., J.A. Ghormley, and P.J. Ogren, 1972, J. Chem. Phys., **56**, 4426-4432.
498. Hochanadel, C.J., T.J. Sworski, and P.J. Ogren, 1980, J. Phys. Chem., **84**, 3274-3277.
499. Hofzumahaus, A. and F. Stuhl, 1984, Ber. Bunsenges Phys. Chem., **88**, 557-561.
500. Hollinden, G.A., M.J. Kurylo, and R.B. Timmons, 1970, J. Phys. Chem., **74**, 988-991.
501. Homann, K.H., G. Krome, and H.G. Wagner, 1968, Ber. Bunsenges. Phys. Chem., **72**, 998.
502. Hooshiyar, P.A. and H. Niki, 1995, Int. J. Chem. Kinet., **27**, 1197-1206.
503. Horie, O., J.N. Crowley, and G.K. Moortgat, 1990, J. Phys. Chem., **94**, 8198-8203.
504. Horie, O. and G.K. Moortgat, 1992, J. Chem. Soc. Faraday Trans., **88**, 3305-3312.
505. Horowitz, A., D. Bauer, J.N. Crowley, and G.K. Moortgat, 1993, Geophys. Res. Lett., **20**, 1423-1426.
506. Horowitz, A., J.N. Crowley, and G.K. Moortgat, 1994, J. Phys. Chem., **98**, 11924-11930.
507. Horowitz, A., F. Su, and J.G. Calvert, 1978, Int. J. Chem. Kinet., **10**, 1099.
508. Howard, C.J., 1976, J. Chem. Phys., **65**, 4771.
509. Howard, C.J., 1979, J. Chem. Phys., **71**, 2352-2359.
510. Howard, C.J. and K.M. Evenson, 1976, J. Chem. Phys., **64**, 4303.
511. Howard, C.J. and K.M. Evenson, 1976, J. Chem. Phys., **64**, 197.
512. Howard, C.J. and K.M. Evenson, 1977, Geophys. Res. Lett., **4**, 437-440.
513. Howard, C.J. and B.J. Finlayson-Pitts, 1980, J. Chem. Phys., **72**, 3842-3843.
514. Howard, M.J. and I.W.M. Smith, 1981, J. Chem. Soc. Faraday Trans. 2, **77**, 997-1008.

515. Hoyermann, K., H.G. Wagner, and J. Wolfrum, 1967, Z. Phys. Chem., **55**, 72.
516. Hoyermann, K., H.G. Wagner, and J. Wolfrum, 1969, Z. Phys. Chem., **63**, 193.
517. Hsu, D.S.Y., W.M. Shaub, T.L. Burks, and M.C. Lin, 1979, Chem Phys., **44**, 143-150.
518. Hsu, K.J. and W.B. DeMore, 1994, Geophys. Res. Lett., **21**, 805-808.
519. Hsu, K.J. and W.B. DeMore, 1995, J. Phys. Chem., **99**, 1235-1244.
520. Hsu, K.J. and W.B. DeMore, 1995, J. Phys. Chem., **99**, 11141-11930.
521. Hsu, Y.-C., D.-S. Chen, and Y.-P. Lee, 1987, Int. J. Chem. Kinet., **19** , 1073-1082.
522. Huder, K.J. and W.B. DeMore, 1993, Geophys. Res. Lett., **20**, 1575-1577.
523. Huey, L.G., E.J. Dunlea, and C.J. Howard, 1996, J. Phys. Chem, **100**, 6504-6508.
524. Huie, R.E. and J.T. Herron, 1974, Chem. Phys. Lett., **27**, 411.
525. Hunziker, H.E., H. Kneppe, and H.R. Wendt, 1981, J. Photochem., **17**, 377.
526. Husain, D. and P. Marshall, 1985, Combust. and Flame, **60**, 81-87.
527. Husain, D., P. Marshall, and J.M.C. Plane, 1985, J. Chem. Soc. Chem. Comm., 1216-1218.
528. Husain, D., J.M.C. Plane, and N.K.H. Slater, 1981, J. Chem. Soc. Faraday Trans. 2, **77**, 1949.
529. Husain, D., J.M.C. Plane, and C.C. Xiang, 1984, J. Chem. Soc. Faraday Trans. 2, **80**, 713-728.
530. Husain, D. and N.K.H. Slater, 1980, J. Chem. Soc. Faraday Trans. 2, **76**, 606-619.
531. Hynes, A.J., R.B. Stocker, A.J. Pounds, T. Mckay, J.D. Bradshaw, J.M. Nicovich, and P.H. Wine, 1995, J. Phys. Chem., **99**, 16967-16975.
532. Hynes, A.J. and P.H. Wine, 1987, J. Phys. Chem., **91**, 3672.
533. Hynes, A.J. and P.H. Wine, 1991, J. Phys. Chem., **95**, 1232-1240.
534. Hynes, A.J., P.H. Wine, and J.M. Nicovich, 1988, J. Phys. Chem., **92**, 3846-3852.
535. Hynes, A.J., P.H. Wine, and A.R. Ravishankara, 1986, J. Geophys. Res., **91**, 815-820.
536. Hynes, A.J., P.H. Wine, and D.H. Semmes, 1986, J. Phys. Chem., **90**, 4148-4156.
537. Iannuzzi, M.P., J.B. Jeffries, and F. Kaufman, 1982, Chem. Phys. Lett., **87**, 570-574.
538. Iannuzzi, M.P. and F. Kaufman, 1981, J. Phys. Chem., **85**, 2163.
539. Igoshin, V.I., L.V. Kulakov, and A.I. Nikitin, 1974, Sov. J. Quant. Electron., **3**, 306.
540. Imamura, T. and N. Washida, 1995, Laser Chem., **16**, 43-51.
541. Ingold, K.U., 1988, J. Phys. Chem., **92**, 4568-4569.
542. Inoue, G. and H. Akimoto, 1981, J. Chem. Phys., **84**, 425-433.
543. Ishikawa, Y., K. Sugawara, and S. Sato, Abstracts of Papers, Vol. 1. 1979, ACS/CSJ Chemical Congress.
544. Iwata, R., R.A. Ferrieri, and A.P. Wolf, 1986, J. Phys. Chem., **90**, 6722-6726.
545. Iyer, R.S. and F.S. Rowland, 1980, Geophys. Res. Lett., **7**, 797-800.
546. Izod, T.P.J. and R.P. Wayne, 1968 , Proc. Roy. Soc. A, **308**, 81-94.
547. Jaffe, S. and F.S. Klein, 1966, Trans. Faraday Soc., **62**, 2150-2157.
548. Jaffe, S. and W.K. Mainquist, 1980, J. Phys. Chem, **84**, 3277.
549. James, G.S. and G.P. Glass, 1970, J. Chem. Phys., **50**, 2268.
550. Japar, S.M., C.H. Wu, and H. Niki, 1974, J. Phys. Chem., **78**, 2318.
551. Japar, S.M., C.H. Wu, and H. Niki, 1976, J. Phys. Chem., **80**, 2057.
552. Jayanty, R.K.M., R. Simonaitis, and J. Heicklen, 1976, J. Phys. Chem., **80**, 443.
553. Jefferson, A., J.M. Nicovich, and P.H. Wine, 1994, J. Phys. Chem., **98**, 7128-7135.
554. Jemi-Alade, A.A. and B.A. Thrush, 1990, J. Chem. Soc. Faraday Trans. 2, **86**, 3355-3363.
555. Jenkin, M.E., K.C. Clemitshaw, and R.A. Cox, 1984, J. Chem. Soc. Faraday Trans. 2, **80**, 1633-1641.
556. Jenkin, M.E. and R.A. Cox, 1985, J. Phys. Chem., **89**, 192-199.
557. Jenkin, M.E. and R.A. Cox, 1987, Chem. Phys. Lett., **137**, 548-552.
558. Jenkin, M.E. and R.A. Cox, 1991, J. Phys. Chem., **95**, 3229.
559. Jenkin, M.E., R.A. Cox, G. Hayman, and L.J. Whyte, 1988, J. Chem. Soc. Faraday Trans. 2, **84**, 913.
560. Jenkin, M.E., R.A. Cox, and G.D. Hayman, 1991, Chem. Phys. Lett., **177**, 272-278.
561. Jenkin, M.E., R.A. Cox, A. Mellouki, G. Le Bras, and G. Poulet, 1990, J. Phys. Chem., **94**, 2927-2934.
562. Jensen, N.R., D.R. Hanson, and C.J. Howard, 1994, J. Phys. Chem., **98**, 8574-8579.
563. Jensen, N.R., J. Hjorth, C. Lohse, H. Skov, and G. Restelli, 1991, Atmos. Environ., **24A**, 1897-1904.
564. Jensen, N.R., J. Hjorth, C. Lohse, H. Skov, and G. Restelli, 1992, J. Atmos. Chem., **14**, 95-108.
565. Jeong, K.M., K.J. Hsu, J.B. Jeffries, and F. Kaufman, 1984, J. Phys. Chem., **88**, 1222-1226.
566. Jeong, K.M. and F. Kaufman, 1979, Geophys. Res. Lett., **6**, 757-759.
567. Jeong, K.M. and F. Kaufman, 1982, J. Phys. Chem., **86**, 1808-1815.
568. Jeoung, S.C., K.Y. Choo, and S.W. Benson, 1991, J. Phys. Chem., **95**, 7282-7290.
569. Jiang, Z., P.H. Taylor, and B. Dellinger, 1992, J. Phys. Chem., **96**, 8961-8964.
570. Johnston, H.S., E.D. Morris Jr., and J. Van den Bogaerde, 1969, J. Am. Chem. Soc., **91**, 7712.
571. Johnston, H.S. and Y.-S. Tao, 1951, J. Am. Chem Soc., **73**, 2948.
572. Jolly, G.S., D.J. McKenney, D.L. Singleton, G. Paraskevopoulos, and A.R. Bossard, 1986, J. Phys. Chem., **90**, 6557-6562.
573. Jolly, G.S., G. Paraskevopoulos, and D.L. Singleton, 1985, Chem. Phys. Lett., **117**, 132-137.
574. Jonah, C.D., W.A. Mulac, and P. Zeglinski, 1984, J. Phys. Chem., **88**, 4100-4104.
575. Jones, B.M.R., J.P. Burrows, R.A. Cox, and S.A. Penkett, 1982, Chem. Phys. Lett., **88**, 372-376.
576. Jourdain, J.L., G. Le Bras, and J. Combourieu, 1978, J. Chim. Phys., **75**, 318-323.
577. Jourdain, J.L., G. Le Bras, and J. Combourieu, 1979, Int. J. Chem. Kinet., **11**, 569-577.
578. Jourdain, J.L., G. Le Bras, and J. Combourieu, 1981, Chem. Phys. Lett., **78**, 483.

579. Jourdain, J.L., G. Poulet, and G. Le Bras, 1982, J. Chem. Phys., **76**, 5827-5833.
580. Jungkamp, T.P., A. Kukui, and R.N. Schindler, 1995, Ber. Bunsenges. Phys. Chem., **99**, 1057-1066.
581. Kaiser, E.W. and S.M. Japar, 1977, Chem. Phys. Lett., **52**, 121.
582. Kaiser, E.W. and S.M. Japar, 1978, Chem. Phys. Lett., **54**, 265.
583. Kaiser, E.W., I.M. Lorkovic, and T.J. Wallington, 1990, J. Phys. Chem., **94**, 3352-3354.
584. Kaiser, E.W., L. Rimai, E. Schwab, and E.C. Lim, 1992, J. Phys. Chem., **96**, 303-306.
585. Kaiser, E.W. and T.J. Wallington, 1994, J. Phys. Chem., **98**, 5679-5685.
586. Kan, C.S., J.G. Calvert, and J.H. Shaw, 1980, J. Phys. Chem., **84**, 3411.
587. Kan, C.S., J.G. Calvert, and J.H. Shaw, 1981, J. Phys. Chem., **85**, 1126-1132.
588. Kan, C.S., R.D. McQuigg, M.R. Whitbeck, and J.G. Calvert, 1979, Int. J. Chem. Kinet., **11**, 921.
589. Kaufman, F., N.J. Gerri, and D.A. Pascale, 1956, J. Chem. Phys., **24**, 32-34.
590. Kelly, C., J. Treacy, H.W. Sidebottom, and O.J. Nielsen, 1993, Chem. Phys. Lett., **207**, 498-503.
591. Kenner, R.D., K.R. Ryan, and I.C. Plumb, 1993, Geophys. Res. Lett., **20**, 1571-1574.
592. Kerr, J.A. and D.W. Sheppard, 1981, Environ. Sci. and Technol., **15**, 960.
593. Kerr, J.A. and D.W. Stocker, 1986, J. Atmos. Chem., **4**, 253-262.
594. Keyser, L.F., 1978, J. Chem. Phys., **69**, 214.
595. Keyser, L.F., 1979, J. Phys. Chem., **83**, 645-648.
596. Keyser, L.F., 1980, J. Phys. Chem., **84** , 1659-1663.
597. Keyser, L.F., 1980, J. Phys. Chem., **84**, 11-14.
598. Keyser, L.F., 1981, J. Phys. Chem., **85**, 3667-3673.
599. Keyser, L.F., 1982, J. Phys. Chem., **86**, 3439-3446.
600. Keyser, L.F., 1983, J. Phys. Chem., **87**, 837-841.
601. Keyser, L.F., 1984, J. Phys. Chem., **88**, 4750-4758.
602. Keyser, L.F., 1986, J. Phys. Chem., **90**, 2994-3003.
603. Keyser, L.F., 1988, J. Phys. Chem., **92**, 1193-1200.
604. Keyser, L.F., K.Y. Choo, and M.T. Leu, 1985, Int. J. Chem. Kinet., **17**, 1169-1185.
605. Khursan, S.L., V.S. Martem'yanov, and E.T. Denisov, 1990, Kinet. and Catal. (translation from Russian), **31**, 899-907.
606. Kinnison, D.J., W. Mengon, and J.A. Kerr, 1996, J. Chem. Soc. Faraday Trans., **92**, 369-372.
607. Kircher, C.C. and S.P. Sander, 1984, J. Phys. Chem., **88**, 2082-91.
608. Kirchner, F., F. Zabel, and K.H. Becker, 1990, Ber. Bunsenges. Phys. Chem., **94**, 1379-1382.
609. Kirchner, K., D. Helf, P. Ott, and S. Vogt, 1990, Ber. Bunsenges. Phys. Chem., **94**, 77-83.
610. Kistiakowsky, G.B. and G.G. Volpi, 1957, J. Chem. Phys., **27**, 1141-1149.
611. Kistiakowsky, G.B. and G.G. Volpi, 1958, J. Chem. Phys., **28**, 665.
612. Kita, D. and D.H. Stedman, 1982, J. Chem. Soc. Faraday Trans. 2, **78**, 1249-1259.
613. Klais, O., P.C. Anderson, A.H. Laufer, and M.J. Kurylo, 1979, Chem. Phys. Lett., **66**, 598.
614. Klais, O., A.H. Laufer, and M.J. Kurylo, 1980, J. Chem. Phys., **73**, 2696-2699.
615. Kleinermanns, K. and A.C. Luntz, 1981, J. Phys. Chem., **85**, 1966.
616. Klemm, R.B., 1979, J. Chem. Phys., **71**, 1987.
617. Klemm, R.B., E.G. Skolnik, and J.V. Michael, 1980, J. Chem. Phys., **72**, 1256.
618. Klemm, R.B. and L.J. Stief, 1974, J. Chem. Phys., **61**, 4900.
619. Klopffer, W., R. Frank, E.G. Kohl, and F. Haag, 1986, Chemiker-Zeitung, **110**, 57-61.
620. Knickelbein, M.B., K.L. Marsh, O.E. Ulrich, and G.E. Busch, 1987, J. Chem. Phys., **87**, 2392-2393.
621. Knox, J.H., 1955, Chemistry and Industry, 1631.
622. Knox, J.H., 1962, Trans. Faraday Soc., **58**, 275.
623. Knox, J.H. and R.L. Nelson, 1959, Trans. Far. Soc., **55**, 937.
624. Ko, T. and A. Fontijn, 1991, J. Phys. Chem., **95**, 3984-3987.
625. Kohse-Höinghaus, K. and F. Stuhl, 1980, J. Chem. Phys., **72**, 3720-3726.
626. Kolb, C.E., J.T. Jayne, D.R. Worsnop, M.J. Molina, R.F. Meads, and A.A. Viggiano, 1994, J. Am. Chem. Soc., **116**, 10314-10315.
627. Kompa, K.L. and J. Wanner, 1972, Chem. Phys. Lett., **12**, 560.
628. Koppe, S., T. Laurent, P.D. Naik, H.-R. Volpp, J. Wolfrum, T. Arusi-Parpar, I. Bar, and S. Rosenwaks, 1993, Chem. Phys. Lett., **214**, 546-552.
629. Kukui, A., T.P.W. Jungkamp, and R.N. Schindler, 1994, Ber. Bunsenges. Phys. Chem., **98**, 1619-1621.
630. Kukui, A., U. Kirchner, T. Benter, and R.N. Schindler, 1996, Ber. Bunsenges. Phys. Chem., **100**, 455-461.
631. Kukui, A.S., T.P.W. Jungkamp, and R.N. Schindler, 1994, Ber. Bunsenges. Phys. Chem., **98**, 1298-1302.
632. Kumaran, S.S., K.P. Lim, and J.V. Michael, 1994, J. Chem. Phys., **101**, 9487-9498.
633. Kurasawa, H. and R. Lesclaux, 1979, Chem. Phys. Lett., **66**, 602.
634. Kurasawa, H. and R. Lesclaux, paper presented at the 14th Informal Photochemistry Conference, 1980, Newport Beach, CA.
635. Kurasawa, H. and R. Lesclaux, 1980, Chem. Phys. Lett., **72**, 437.
636. Kurylo, M.J., 1973, Chem. Phys. Lett., **23**, 467-471.
637. Kurylo, M.J., 1977, Chem. Phys. Lett., **49**, 467.
638. Kurylo, M.J., 1978, Chem. Phys. Lett., **58**, 233.
639. Kurylo, M.J., 1978, Chem. Phys. Lett., **58**, 238-242.
640. Kurylo, M.J., P.C. Anderson, and O. Klais, 1979, Geophys. Res. Lett., **6**, 760-762.

641. Kurylo, M.J. and W. Braun, 1976, Chem. Phys. Lett., **37**, 232.
642. Kurylo, M.J., K.D. Cornett, and J.L. Murphy, 1982, J. Geophys. Res., **87**, 3081-3085.
643. Kurylo, M.J., P. Dagaut, T.J. Wallington, and D.M. Neuman, 1987, Chem. Phys. Lett., **139**, 513-518.
644. Kurylo, M.J., O. Klais, and A.H. Laufer, 1981, J. Phys. Chem., **85**, 3674-3678.
645. Kurylo, M.J. and G.L. Knable, 1984, J. Phys. Chem., **88**, 3305-3308.
646. Kurylo, M.J., G.L. Knable, and J.L. Murphy, 1983, Chem. Phys. Lett., **95**, 9-12.
647. Kurylo, M.J. and A.H. Laufer, 1979, J. Chem. Phys., **70**, 2032-2033.
648. Kurylo, M.J., J.L. Murphy, G.S. Haller, and K.D. Cornett, 1982, Int. J. Chem. Kinet, **14**, 1149-1161.
649. Kurylo, M.J., J.L. Murphy, and G.L. Knable, 1983, Chem. Phys. Lett., **94**, 281-284.
650. Kurylo, M.J., P.A. Ouellette, and A.H. Laufer, 1986, J. Phys. Chem., **90**, 437-440.
651. Kurylo, M.J. and T.J. Wallington, 1987, Chem. Phys. Lett., **138**, 543-547.
652. Kurylo, M.J., T.J. Wallington, and P.A. Ouellette, 1987, J. Photochem., **39**, 201-215.
653. Lafage, C., J.-F. Pauwels, M. Carlier, and P. Devolder, 1987, J. Chem. Soc. Faraday Trans. 2, **83**, 731-739.
654. Lam, L., D.R. Hastie, B.A. Ridley, and H.I. Schiff, 1981, J. Photochem., **15**, 119-130.
655. Lamb, J.J., L.T. Molina, C.A. Smith, and M.J. Molina, 1983, J. Phys. Chem., **87**, 4467-4470.
656. Lancar, I., G. Laverdet, G. Le Bras, and G. Poulet, 1991, Int. J. Chem. Kinet., **23**, 37-45.
657. Lancar, I., G. Le Bras, and G. Poulet, 1993, J. Chim. Physique, **90**, 1897-1908.
658. Lancar, I., A. Mellouki, and G. Poulet, 1991, Chem. Phys. Lett., **177**, 554-558.
659. Langford, A.O. and C.B. Moore, 1984, J. Chem. Phys., **80**, 4211-4221.
660. Larichev, M., F. Maguin, G. Le Bras, and G. Poulet, 1995, J. Phys. Chem., **99**, 15911-15918.
661. Laszlo, B., R.E. Huie, M.J. Kurylo, and A.W. Miziolek, 1997, J. Geophys. Res., **102**, 1523-1532.
662. Laszlo, B., M.J. Kurylo, and R.E. Huie, 1995, J. Phys. Chem., **99**, 11701-11707.
663. Laverdet, G., G. Le Bras, A. Mellouki, and G. Poulet, 1990, Chem. Phys. Lett., **172**, 430-434.
664. Lawton, S.A., S.E. Novick, H.P. Broida, and A.V. Phelps, 1977, J. Chem. Phys., **66**, 1381-1382.
665. Lawton, S.A. and A.V. Phelps, 1978, J. Chem. Phys., **69**, 1055-1068.
666. Le Bras, G. and J. Combourieu, 1978, Int. J. Chem. Kinet., **10**, 1205-1213.
667. Le Bras, G., R. Foon, and J. Combourieu, 1980, Chem. Phys. Lett., **73**, 357.
668. Leck, T.J., J.E. Cook, and J.W. Birks, 1980, J. Chem. Phys., **72**, 2364-2373.
669. Lee, J.H., J.V. Michael, W.A. Payne Jr., and L.J. Stief, 1977, J. Chem. Soc. Faraday Trans. 1, **73**, 1530-1536.
670. Lee, J.H., J.V. Michael, W.A. Payne Jr., and L.J. Stief, 1978, J. Chem. Phys., **69**, 350-353.
671. Lee, J.H., J.V. Michael, W.A. Payne Jr., and L.J. Stief, 1978, J. Chem. Phys., **69**, 3069-3076.
672. Lee, J.H. and I.N. Tang, 1980, J. Chem. Phys., **72**, 5718-5720.
673. Lee, J.H. and I.N. Tang, 1982, J. Chem. Phys., **77**, 4459-63.
674. Lee, J.H. and I.N. Tang, 1983, J. Chem. Phys., **78**, 6646.
675. Lee, J.H., I.N. Tang, and R.B. Klemm, 1980, J. Chem. Phys., **72**, 1793-1796.
676. Lee, J.H., R.B. Timmons, and L.J. Stief, 1976, J. Chem. Phys., **64**, 300-305.
677. Lee, L.C. and T.G. Slanger, 1978, J. Chem. Phys., **69**, 4053-4060.
678. Lee, L.C. and T.G. Slanger, 1979, Geophys. Res. Lett., **6**, 165-166.
679. Lee, Y.-P. and C.J. Howard, 1982, J. Chem. Phys., **77** , 756-763.
680. Lee, Y.-P., R.M. Stimpfle, R.A. Perry, J.A. Mucha, K.M. Evenson, D.A. Jennings, and C.J. Howard, 1982, Int. J. Chem. Kinet., **14**, 711-732.
681. Lee, Y.-Y., Y.-P. Lee, and N.S. Wang, 1994, J. Chem. Phys., **100**, 387-392.
682. Leiss, A., U. Schurath, K.H. Becker, and E.H. Fink, 1978, J. Photochem., **8**, 211-214.
683. Lesclaux, R. and F. Caralp, 1984, Int. J. Chem. Kinet., **16**, 1117-1128.
684. Lesclaux, R. and M. Demissy, 1977, Nouv. J. Chim., **1**, 443.
685. Lesclaux, R., A.M. Dognon, and F. Caralp, 1987, J. Photochem. and Photobiol., **A41**, 1-11.
686. Lesclaux, R., P.V. Khe, P. Dezauzier, and J.C. Soulignac, 1975, Chem. Phys. Lett., **35**, 493.
687. Leu, G.-H. and Y.-P. Lee, 1994, J. Chin. Chem. Soc., **41**, 645-649.
688. Leu, M.T., 1979, Chem. Phys. Lett., **61**, 275-279.
689. Leu, M.T., 1979, J. Chem. Phys., **70**, 1662-1666.
690. Leu, M.T., 1980, Chem. Phys. Lett., **69**, 37-39.
691. Leu, M.T., 1980, Geophys. Res. Lett., **7**, 173-175.
692. Leu, M.T., 1984, J. Phys. Chem., **88**, 1394-1398.
693. Leu, M.T. and W.B. DeMore, 1976, Chem. Phys. Lett., **41**, 121-124.
694. Leu, M.T. and W.B. DeMore, 1977, Chem. Phys. Lett., **48**, 317.
695. Leu, M.T. and W.B. DeMore, 1978, J. Phys. Chem., **82**, 2049.
696. Leu, M.T., S. Hatkeyama, and K.J. Hsu, 1989, J. Phys. Chem., **93**, 5778-5784.
697. Leu, M.T. and C.L. Lin, 1979, Geophys. Res. Lett., **6**, 425-428.
698. Leu, M.T. and R.H. Smith, 1981, J. Phys. Chem., **85**, 2570-2575.
699. Leu, M.T. and R.H. Smith, 1982, J. Phys. Chem., **86**, 958-961.
700. Leu, M.T. and R.H. Smith, 1982, J. Phys. Chem., **86**, 73-81.
701. Leu, M.T. and Y.L. Yung, 1987, Geophys. Res. Lett., **14**, 949-952.
702. Lewis, R.S., S.P. Sander, S. Wagner, and R.T. Watson, 1980, J. Phys. Chem., **84**, 2009-2015.
703. Lewis, R.S. and R.T. Watson, 1980, J. Phys. Chem., **84**, 3495-3503.
704. Li, Z., R.R. Friedl, and S.P. Sander, 1995, J. Phys. Chem., **99**, 13445-13451.
705. Li, Z., R.R. Friedl, and S.P. Sander, 1997, J. Chem. Soc. Farad. Trans., submitted.

706. Lightfoot, P.D., R.A. Cox, J.N. Crowley, M. Destriau, G.D. Hayman, M.E. Jenkin, G.K. Moortgat, and F. Zabel, 1992, Atmos. Environ., **26A**, 1805-1961.
707. Lightfoot, P.D. and A.A. Jemi-Alade, 1991, J.Photochem. and Photobiol. A: Chem., **59**, 1-10.
708. Lightfoot, P.D., R. Lesclaux, and B. Veyret, 1990, J. Phys. Chem., **94**, 700-707.
709. Lightfoot, P.D., B. Veyret, and R. Lesclaux, 1988, Chem. Phys. Lett., **150**, 120-126.
710. Lightfoot, P.D., B. Veyret, and R. Lesclaux, 1990, J. Phys. Chem., **94**, 708-714.
711. Lii, R.-R., R.A. Gorse Jr., M.C. Sauer Jr., and S. Gordon, 1979, J. Phys. Chem., **83**, 1803-1804.
712. Lii, R.-R., R.A. Gorse Jr., M.C. Sauer Jr., and S. Gordon, 1980, J. Phys. Chem., **84**, 819-821.
713. Lii, R.-R., M.C. Sauer Jr., and S. Gordon, 1980, J. Phys. Chem., **84**, 817-819.
714. Lii, R.-R., M.C. Sauer Jr., and S. Gordon, 1981, J. Phys. Chem., **85**, 2833-2834.
715. Lilenfeld, H.V. and R.J. Richardson, 1977, J. Chem. Phys., **67**, 3991.
716. Lin, C.-L., D.A. Parkes, and F. Kaufman, 1970, J. Chem. Phys., **53**, 3896-3900.
717. Lin, C.L., 1982, Int. J. Chem. Kinet., **14**, 593-598.
718. Lin, C.L. and W.B. DeMore, 1973, J. Phys. Chem., **77** , 863-869.
719. Lin, C.L., M.T. Leu, and W.B. DeMore, 1978, J. Phys. Chem., **82**, 1772.
720. Lin, Y.-L., N.-S. Wang, and Y.-P. Lee, 1985, Int. J. Chem. Kinet., **17**, 1201-1214.
721. Lippmann, H.H., B. Jesser, and U. Schurath, 1980, Int. J. Chem. Kinet., **12**, 547-554.
722. Lissi, E. and J. Heicklen, 1972, J. Photochem., **1**, 39-68.
723. Littlejohn, D. and H.S. Johnston, 1980, EOS, **61**, 966.
724. Liu, R., R.E. Huie, and M.J. Kurylo, 1990, J. Phys. Chem., **94**, 3247-3249.
725. Loewenstein, L.M. and J.G. Anderson, 1984, J. Phys. Chem., **88**, 6277-6286.
726. Loewenstein, L.M. and J.G. Anderson, 1985, J. Phys. Chem., **89**, 5371-5379.
727. Lorenz, K., D. Rhasa, R. Zellner, and B. Fritz, 1985, Ber. Bunsenges. Phys. Chem., **89**, 341-342.
728. Lorenzen-Schmidt, H., R. Weller, and O. Schrems, 1994, Ber. Bunsenges. Phys. Chem., **98**, 1622-1629.
729. Louge, M.Y. and R.K. Hanson, 1984, Twentieth Symposium (International) on Combustion, 665-672.
730. Lovejoy, E.R., D.R. Hanson, and L.G. Huey, 1996, J. Phys. Chem., **100**, 19911-19916.
731. Lovejoy, E.R., K.S. Kroeger, and A.R. Ravishankara, 1990, Chem. Phys. Lett., **167**, 183-187.
732. Lovejoy, E.R., T.P. Murrells, A.R. Ravishankara, and C.J. Howard, 1990, J. Phys. Chem., **94**, 2386-2393.
733. Lovejoy, E.R., A.R. Ravishankara, and C.J. Howard, 1994, Int. J. Chem. Kinet., **26**, 551-560.
734. Lovejoy, E.R., N.S. Wang, and C.J. Howard, 1987, J. Phys. Chem., **91**, 5749-5755.
735. Lozovsky, V.A., M.A. Ioffe, and O.M. Sarkisov, 1984, Chem. Phys. Lett., **110**, 651-654.
736. Lu, E.C.C., R.S. Iyer, and F.S. Rowland, 1986, J. Phys. Chem., **90**, 1988-1990.
737. Mack, G.P.R. and B. Thrush, 1973, J. Chem. Soc. Faraday Trans. 1, **69**, 208.
738. Mack, G.P.R. and B. Thrush, 1974, J. Chem. Soc. Faraday Trans. 1, **70**, 173-186.
739. MacLeod, H., S.M. Aschmann, R. Atkinson, E.C. Tuazon, J.A. Sweetman, A.M. Winer, and J.N. Pitts Jr., 1986, J. Geophys. Res., **91**, 5338.
740. MacLeod, H., C. Balestra, J.L. Jourdain, G. Laverdet, and G. Le Bras, 1990, Int. J. Chem. Kinet., **22**, 1167-1176.
741. MacLeod, H., J.L. Jourdain, G. Poulet, and G. Le Bras, 1984, Atmos. Environ., **18**, 2621.
742. MacLeod, H., G. Poulet, and G. Le Bras, 1983, J. Chim. Phys., **80**, 287.
743. Maguin, F., G. Laverdet, G. Le Bras, and G. Poulet, 1992, J. Phys. Chem., **96**, 1775-1780.
744. Maguin, F., A. Mellouki, G. Laverdet, G. Poulet, and G. Le Bras, 1991, Int. J. Chem. Kinet., **23**, 237-245.
745. Manning, R. and M.J. Kurylo, 1977, J. Phys. Chem., **81**, 291.
746. Manning, R.G., W. Braun, and M.J. Kurylo, 1976, J. Chem. Phys., **65**, 2609.
747. Manzanares, E.R., M. Suto, L.C. Lee, and D. Coffey, 1986, J. Chem. Phys., **85**, 5027-5034.
748. Margitan, J.J., 1983, J. Phys. Chem., **87**, 674-679.
749. Margitan, J.J., 1984, J. Phys. Chem., **88**, 3638-3643.
750. Margitan, J.J., 1984, J. Phys. Chem., **88**, 3314-3318.
751. Margitan, J.J., F. Kaufman, and J.G. Anderson, 1975, Int. J. Chem. Kinet., **Symp. No. 1**, 281.
752. Margitan, J.J. and R.T. Watson, 1982, J. Phys. Chem., **86**, 3819-3824.
753. Maricq, M.M. and J.J. Szente, 1993, Chem. Phys. Lett., **213**, 449-456.
754. Maricq, M.M. and J.J. Szente, 1994, J. Phys. Chem., **98**, 2078-2082.
755. Maricq, M.M. and J.J. Szente, 1996, J. Phys. Chem., **100**, 12374.
756. Maricq, M.M., J.J. Szente, E.W. Kaiser, and J. Shi, 1994, J. Phys. Chem., **98**, 2083-2089.
757. Marinelli, W.J. and H.S. Johnston, 1982, J. Chem. Phys., **77**, 1225-1234.
758. Martin, D., I. Barnes, and K.H. Becker, 1987, Chem. Phys. Lett., **140**, 195.
759. Martin, D., J.L. Jourdain, G. Laverdet, and G. Le Bras, 1987, Int. J. Chem. Kinet., **19**, 503-512.
760. Martin, D., J.L. Jourdain, and G. Le Bras, 1985, Int. J. Chem. Kinet., **17**, 1247.
761. Martin, D., J.L. Jourdain, and G. Le Bras, 1986, J. Phys. Chem., **90**, 4143-4147.
762. Martin, J.-P. and G. Paraskevopoulos, 1983, Can. J. Chem., **61**, 861-865.
763. Martin, L.R., R.B. Cohen, and J.F. Schatz, 1976, Chem. Phys. Lett., **41**, 394-396.
764. Martinez, R.I. and J.T. Herron, 1978, Int. J. Chem. Kinet., **10**, 433.
765. Marx, W., F. Bahe, and U. Schurath, 1979, Ber. Bunsenges. Phys. Chem., **83**, 225-230.
766. Masaki, A., N. Tsunashima, and N. Washida, 1994, Chem. Phys. Lett., **218**, 523-528.
767. Matsumi, Y., K. Tonokura, Y. Inagaki, and M. Kawasaki, 1993, J. Phys. Chem., **97**, 6816-6821.
768. Mauldin, R.L., III, J.B. Burkholder, and A.R. Ravishankara, 1992, J. Phys. Chem., **96**, 2582-2588.
769. Mauldin, R.L., III, A. Wahner, and A.R. Ravishankara, 1993, J. Phys. Chem., **97**, 7585-7596.

770. McAdam, K., B. Veyret, and R. Lesclaux, 1987, Chem. Phys. Lett., **133**, 39-44.
771. McCaulley, J.A., S.M. Anderson, J.B. Jeffries, and F. Kaufman, 1985, Chem Phys. Lett., **115**, 180.
772. McCrumb, J.L. and F. Kaufman, 1972, J. Chem. Phys., **57**, 1270-1276.
773. McKenzie, A., M.F.R. Mulcahy, and J.R. Steven, 1973, J. Chem. Phys., **59**, 3244-3254.
774. McLaren, I.A., N.W. Morris, and R.P. Wayne, 1981, J. Photochem., **16**, 311-319.
775. McNeal, R.J. and G.R. Cook, 1967, J. Chem. Phys., **47**, 5385-5389.
776. Meier, U., H.H. Grotheer, and T. Just, 1984, Chem. Phys. Lett., **106**, 97-101.
777. Meier, U., H.H. Grotheer, G. Riekert, and T. Just, 1985, Chem. Phys. Lett., **115**, 221-225.
778. Meller, R. and G.K. Moortgat, 1995, J. Photochem. Photobio. A: Chem., **86**, 15-25.
779. Mellouki, A., J.L. Jourdain, and G. Le Bras, 1988, Chem. Phys. Lett., **148**, 231-236.
780. Mellouki, A., G. Laverdet, L. Jourdain, and G. Poulet, 1989, Int. J. Chem. Kinet., **21**, 1161-1172.
781. Mellouki, A., G. Le Bras, and G. Poulet, 1987, J. Phys. Chem., **91**, 5760-5764.
782. Mellouki, A., G. Le Bras, and G. Poulet, 1988, J. Phys. Chem., **92**, 2229-2234.
783. Mellouki, A., G. Poulet, G. Le Bras, R. Singer, J.P. Burrows, and G.K. Moortgat, 1989, J. Phys. Chem., **93**, 8017-8021.
784. Mellouki, A. and A.R. Ravishankara, 1994, Int. J. Chem. Kinet., **26**, 355-365.
785. Mellouki, A., R.K. Talukdar, A.M.R.P. Bopegedera, and C.J. Howard, 1993, Int. J. Chem. Kinet., **25**, 25-39.
786. Mellouki, A., R.K. Talukdar, and C.J. Howard, 1994, J. Geophys. Res., **99**, 22949-22954.
787. Mellouki, A., R.K. Talukdar, A.-M. Schmoltner, T. Gierczak, M.J. Mills, S. Soloman, and A.R. Ravishankara, 1992, Geophys. Res. Lett., **19**, 2059-2062.
788. Mellouki, A., S. Teton, G. Laverdet, A. Quilgars, and G. Le Bras, 1994, J. Chem. Physique, **91**, 473-487.
789. Mellouki, A., S. Teton, and G. Le Bras, 1995, Geophys. Res. Lett., **22**, 389-392.
790. Michael, J.V., J.E. Allen Jr., and W.D. Brobst, 1981, J. Phys. Chem., **85**, 4109.
791. Michael, J.V., D.G. Keil, and R.B. Klemm, 1985, J. Chem. Phys., **83** , 1630-1636.
792. Michael, J.V., R.B. Klemm, W.D. Brobst, S.R. Bosco, and D.F. Nava, 1985, J. Phys. Chem., **89**, 3335-3337.
793. Michael, J.V. and J.H. Lee, 1977, Chem. Phys. Lett., **51**, 303.
794. Michael, J.V., J.H. Lee, W.A. Payne, and L.J. Stief, 1978, J. Chem. Phys., **68**, 4093.
795. Michael, J.V., D.F. Nava, W. Brobst, R.P. Borkowski, and L.J. Stief, 1982, J. Phys. Chem., **86**, 81-84.
796. Michael, J.V., D.F. Nava, W.A. Payne, J.H. Lee, and L.J. Stief, 1979, J. Phys. Chem., **83**, 2818.
797. Michael, J.V., D.F. Nava, W.A. Payne, and L.J. Stief, 1979, J. Chem. Phys., **70**, 3652.
798. Michael, J.V., D.F. Nava, W.A. Payne, and L.J. Stief, 1979, J. Chem. Phys., **70**, 1147.
799. Michael, J.V. and W.A. Payne, 1979, Int. J. Chem. Kinet., **11**, 799.
800. Michael, J.V., D.A. Whytock, J.H. Lee, W.A. Payne, and L.J. Stief, 1977, J. Chem. Phys., **67**, 3533.
801. Michelangeli, D.V., K.-Y. Choo, and M.T. Leu, 1988, Int. J. Chem. Kinet., **20**, 915-938.
802. Miller, J.C. and R.J. Gordon, 1981, J. Chem. Phys., **75**, 5305.
803. Miyoshi, A., H. Matsui, and N. Washida, 1994, J. Chem. Phys., **100**, 3532-3539.
804. Miziolek, A.W. and M.J. Molina, 1978, J. Phys. Chem., **82**, 1769.
805. Molina, L.T., M.J. Molina, R.A. Stachnik, and R.D. Tom, 1985, J. Phys. Chem., **89**, 3779-3781.
806. Molina, L.T., J.E. Spencer, and M.J. Molina, 1977, Chem. Phys. Lett., **45**, 158-162.
807. Molina, M.J., L.T. Molina, and C.A. Smith, 1984, Int. J. Chem. Kinet., **16**, 1151-1160.
808. Monks, P.S., L.J. Carpenter, S.A. Penkett, G. Ayers, and P. Gregory, 1996, Geophys. Res. Lett., **23**, 535.
809. Montgomery, J.A., H.H. Michels, and J.S. Francisco, 1994, Chem. Phys. Lett., **220**, 391-396.
810. Moortgat, G.K., J.P. Burrows, W. Schneider, G.S. Tyndall, and R.A. Cox, 1986, Proceedings of the 4th European Symposium on Physico-Chemical Behavior of Atmospheric Pollutants, Stresa, Sept. 23-25, 271-281.
811. Moortgat, G.K., B. Veyret, and R. Lesclaux, 1989, J. Phys. Chem., **93**, 2362-2368.
812. Moortgat, G.K., B. Veyret, and R. Lesclaux, 1989, Chem. Phys. Lett., **160**, 443-447.
813. Morokuma, K. and C. Mugurama, 1994, J. Am. Chem. Soc., **116**, 10316-10317.
814. Morris, E.D., Jr. and H. Niki, 1971, J. Chem. Phys., **55**, 1991-1992.
815. Morris, E.D. and H. Niki, 1974, J. Phys. Chem., **78**, 1337-1338.
816. Morris, E.D., D.H. Stedman, and H. Niki, 1971, J. Am. Chem. Soc., **93**, 3570.
817. Mors, V., A. Hoffman, W. Malms, and R. Zellner, 1996, Ber. Bunsenges, Phys. Chem., **100**, 540-552.
818. Muller, D.F. and P.L. Houston, 1981, J. Phys. Chem., **85**, 3563-3565.
819. Munk, J., P. Pagsberg, E. Ratajczak, and A. Sillesen, 1986, J. Phys. Chem., **90**, 2752-2757.
820. Murrells, T.P., E.R. Lovejoy, and A.R. Ravishankara, 1990, J. Phys. Chem., **94**, 2381-2386.
821. Myers, G.H. and R.J. O'Brien Jr., 1970, Ann. N.Y. Acad. Sci., **171**, 224-225.
822. Nadtochenko, V.A., O.M. Sarkisov, and V.I. Vedeneev, 1979, Doklady Akademii Nauk SSSR, **244**, 152.
823. Nagase, S., S. Hashimoto, and H. Akimoto, 1988, J. Phys. Chem., **92**, 641-644.
824. Nangia, P.S. and S.W. Benson, 1980, Int. J. Chem. Kinet., **12**, 43.
825. Nava, D.F., S.R. Bosco, and L.J. Stief, 1983, J. Chem. Phys., **78**, 2443-2448.
826. Nava, D.F., W.D. Brobst, and L.J. Stief, 1985, J. Phys. Chem., **89**, 4703-4707.
827. Nava, D.F., J.V. Michael, and L.J. Stief, 1981, J. Phys. Chem., **85**, 1896.
828. Nelson, D.D., Jr. and M.S. Zahniser, 1994, J. Phys. Chem., **98**, 2101-2104.
829. Nelson, D.D., Jr., M.S. Zahniser, and C.E. Kolb, 1992, J. Phys. Chem., **96**, 249-253.
830. Nelson, D.D., Jr., M.S. Zahniser, and C.E. Kolb, 1993, Geophys. Res. Lett., **20**, 197-200.
831. Nelson, D.D., M.S. Zahniser, C.E. Kolb, and H. Magid, 1995, J. Phys. Chem., **99**, 16301-16306.
832. Nelson, H.H. and H.S. Johnston, 1981, J. Phys. Chem., **85**, 3891.

833. Nelson, H.H., J. Marinelli, and H.S. Johnston, 1981, Chem. Phys. Lett., **78** , 495-499.
834. Nelson, L., O. Rattigan, R. Neavyn, H. Sidebottom, J. Treacy, and O.J. Nielsen, 1990, Int. J. Chem. Kinet., **22**, 1111-1126.
835. Nelson, L., I. Shanahan, H.W. Sidebottom, J. Treacy, and O.J. Nielsen, 1990, Int. J. Chem. Kinet., **22**, 577-590.
836. Nesbitt, D.J. and S.R. Leone, 1980, J. Chem. Phys., **72**, 1722-1732.
837. Nesbitt, D.J. and S.R. Leone, 1981, J. Chem. Phys., **75**, 4949.
838. Nesbitt, F.L., P.S. Monks, W.A. Payne, L.J. Stief, and R. Toumi, 1995, Geophys. Res. Lett., **22**, 827-830.
839. Nesbitt, F.L., D.F. Nava, W.A. Payne, and L.J. Stief, 1987, J. Phys. Chem., **91**, 5337-5340.
840. Nesbitt, F.L., W.A. Payne, and L.J. Stief, 1988, J. Phys. Chem., **92**, 4030-4032.
841. Nicholas, J.E. and R.G.W. Norrish, 1968, Proc. Roy. Soc. A, **307**, 391.
842. Nickolaisen, S.L., R.R. Friedl, and S.P. Sander, 1994, J. Phys. Chem., **98**, 155-169.
843. Nickolaisen, S.L., D.W. Veney, and H.E. Cartland, 1994, J. Chem. Phys., **100**, 4925-4931.
844. Nicovich, J.M., K.D. Kreutter, C.A. van Dijk, and P.H. Wine, 1992, J. Phys. Chem., **96**, 2518-2528.
845. Nicovich, J.M., K.D. Kreutter, and P.H. Wine, 1990, Int. J Chem. Kinet., **22**, 399-414.
846. Nicovich, J.M., C.J. Shackelford, and P.H. Wine, 1990, J. Phys. Chem., **94**, 2896-2903.
847. Nicovich, J.M., S. Wang, and P.H. Wine, 1995, Int. J. Chem. Kinet., **27**, 359-368.
848. Nicovich, J.M. and P.H. Wine, 1987, J. Phys. Chem., **91**, 5118-5123.
849. Nicovich, J.M. and P.H. Wine, 1990, Int. J. Chem. Kinet., **22**, 379-397.
850. Nicovich, J.M., P.H. Wine, and A.R. Ravishankara, 1988, J. Chem. Phys., **89**, 5670-5679.
851. Nielsen, O.J., 1979, "Chemical Kinetics in the Gas Phase Pulse Radiolysis of Hydrogen Sulfide Systems", No. Riso-M-2216, Riso National Laboratory.
852. Nielsen, O.J., 1991, Chem. Phys. Lett., **187**, 286-290.
853. Nielsen, O.J., T. Ellermann, E. Bartkiewicz, T.J. Wallington, and M.D. Hurley, 1992, Chem. Phys. Lett., **192**, 82-88.
854. Nielsen, O.J., T. Ellermann, J. Sehested, and T.J. Wallington, 1992, J. Phys. Chem., **96**, 10875-10879.
855. Nielsen, O.J., J. Munk, G. Locke, and T.J. Wallington, 1991, J. Phys. Chem., **95**, 8714-8719.
856. Nielsen, O.J., J. Munk, P. Pagsberg, and A. Sillesen, 1986, Chem. Phys. Lett., **128**, 168-171.
857. Nielsen, O.J. and J. Sehested, 1993, Chem. Phys. Lett., **213**, 433-441.
858. Nielsen, O.J., H.W. Sidebottom, M. Donlon, and J. Treacy, 1991, Chem. Phys. Lett., **178**, 163-170.
859. Nielsen, O.J., H.W. Sidebottom, L. Nelson, O. Rattigan, J.J. Treacy, and D.J. O'Farrell, 1990, Int. J. Chem. Kinet., **22**, 603-612.
860. Nielsen, O.J., H.W. Sidebottom, L. Nelson, J.J. Treacy, and D.J. O'Farrell, 1989, Int. J. Chem. Kinet., **21**, 1101-1112.
861. Niki, H., E.E. Daby, and B. Weinstock, 1969, Twelfth Symposium (International) on Combustion, The Combustion Institute, pp. 277.
862. Niki, H., P.D. Maker, L.P. Breitenbach, and C.M. Savage, 1978, Chem. Phys. Lett., **57**, 596.
863. Niki, H., P.D. Maker, C.M. Savage, and L.P. Breitenbach, 1978, J. Phys. Chem., **82**, 132.
864. Niki, H., P.D. Maker, C.M. Savage, and L.P. Breitenbach, 1980, Int. J. Chem. Kinet., **12**, 1001-1012.
865. Niki, H., P.D. Maker, C.M. Savage, and L.P. Breitenbach, 1980, Chem. Phys. Lett., **73**, 43-46.
866. Niki, H., P.D. Maker, C.M. Savage, and L.P. Breitenbach, 1981, J. Phys. Chem., **85**, 877.
867. Niki, H., P.D. Maker, C.M. Savage, and L.P. Breitenbach, 1982, J. Phys. Chem., **86**, 3825.
868. Niki, H., P.D. Maker, C.M. Savage, and L.P. Breitenbach, 1983, J. Phys. Chem., **87**, 2190-2193.
869. Niki, H., P.D. Maker, C.M. Savage, and L.P. Breitenbach, 1984, J. Phys. Chem., **88**, 2116-2119.
870. Niki, H., P.D. Maker, C.M. Savage, and L.P. Breitenbach, 1985, J. Phys. Chem., **89**, 588.
871. Nip, W.S., D.L. Singleton, and R.J. Cvetanovic, 1981, J. Am. Chem. Soc., **103**, 3526.
872. Nip, W.S., D.L. Singleton, R. Overend, and G. Paraskevopoulos, 1979, J. Phys. Chem., **83**, 2440-2443.
873. Noxon, J.F., 1970, J. Chem. Phys., **52**, 1852-1873.
874. O'Brien, R.J., Jr. and G.H. Myers, 1970, J. Chem. Phys., **53**, 3832-3835.
875. Ogren, P.J., T.J. Sworski, C.J. Hochanadel, and J.M. Cassel, 1982, J. Phys. Chem., **86**, 238-242.
876. Ogryzlo, E.A., R. Paltenghi, and K.D. Bayes, 1981, Int. J. Chem. Kinet., **13**, 667-675.
877. Ohmori, K., K. Yamasaki, and H. Matsui, 1993, Bull. Chem. Soc. Jpn., **66**, 51-56.
878. Olbregts, J., G. Brasseur, and E.J. Arijs, 1984, J. Photochem., **24**, 315-322.
879. Ongstad, A.P. and J.W. Birks, 1984, J. Chem. Phys., **81**, 3922-3930.
880. Ongstad, A.P. and J.W. Birks, 1986, J. Chem. Phys., **85**, 3359-3368.
881. Orkin, V.L., R.E. Huie, and M.J. Kurylo, 1996, J. Phys. Chem., **100**, 8907-8912.
882. Orkin, V.L. and V.G. Khamaganov, 1993, J. Atmos. Chem., **16**, 169-178.
883. Orkin, V.L. and V.G. Khamaganov, 1993, J. Atmos. Chem., **16**, 157-167.
884. Orkin, V.L., V.G. Khamaganov, A.G. Guschin, R.E. Huie, and M.J. Kurylo, paper presented at the International Symposium on Gas Kinetics, 1994, Dublin.
885. Orkin, V.L., V.G. Khamaganov, A.G. Guschin, R.E. Huie, and M.J. Kurylo, 1997, J. Phys. Chem. A, **101**, 174-178.
886. Orlando, J.J., G.S. Tyndall, and T.J. Wallington, 1996, J. Phys. Chem., **100**, 7026-7033.
887. Orlando, J.J., G.S. Tyndall, T.J. Wallington, and M. Dill, 1996, Int. J. Chem. Kinet., **28**, 433-442.
888. Overend, R. and G. Paraskevopoulos, 1978, J. Phys. Chem., **82**, 1329-1333.
889. Overend, R.P. and G. Paraskevopoulos, 1977, Chem. Phys. Lett., **49**, 109.
890. Overend, R.P., G. Paraskevopoulos, and R.J. Cvetanovic, 1975, Canad. J. Chem., **53**, 3374-3382.

891. Pagsberg, P.B., J. Erikson, and H.C. Christensen, 1979, J. Phys. Chem., **83**, 582.
892. Paraskevopoulos, G. and R.S. Irwin, paper presented at the XV Informal Conference on Photochemistry, 1982, Stanford, CA.
893. Paraskevopoulos, G. and R.S. Irwin, 1984, J. Chem. Phys., **80**, 259-266.
894. Paraskevopoulos, G., D.L. Singleton, and R.S. Irwin, 1981, J. Phys. Chem., **85**, 561.
895. Park, C.R. and J.R. Wiesenfeld, 1991, Chem. Phys. Lett., **186**, 170-176.
896. Park, J. and M.C. Lin, 1996, J. Phys. Chem., **100**, 3317-3319.
897. Parkes, D.A., 1977, Int. J. Chem. Kinet., **9**, 451.
898. Parrish, D.D. and D.R. Herschbach, 1973, J. Am. Chem. Soc., **95**, 6133.
899. Pate, C.T., R. Atkinson, and J.N. Pitts Jr., 1976, J. Environ. Sci. Health, **A11**, 1.
900. Pate, C.T., B.J. Finlayson, and J.N. Pitts Jr., 1974, J. Am. Chem. Soc., **96**, 6554.
901. Patrick, R. and D.M. Golden, 1984, J. Phys. Chem., **88**, 491-495.
902. Paukert, T.T. and H.S. Johnston, 1972, J. Chem. Phys., **56**, 2824-2838.
903. Pavanaja, U.B., H.P. Upadhyaya, A.V. Sapre, K.V.S.R. Rao, and J.P. Mittal, 1994, J. Chem. Soc. Faraday. Trans., **90**, 825-829.
904. Payne, W.A., J. Brunning, M.B. Mitchell, and L.J. Stief, 1988, Int. J. Chem. Kinet., **20**, 63-74.
905. Payne, W.A., L.J. Stief, and D.D. Davis, 1973, J. Am. Chem. Soc., **95**, 7614.
906. Peeters, J., J. Vertommen, and I. Langhans, 1992, Ber. Bunsenges. Phys. Chem., **96**, 431-436.
907. Penzhorn, R.D. and C.E. Canosa, 1983, Ber. Bunsenges. Phys. Chem., **87**, 648-654.
908. Perry, R.A., R. Atkinson, and J.N. Pitts Jr., 1976, J. Chem. Phys., **64**, 1618.
909. Perry, R.A., R. Atkinson, and J.N. Pitts Jr., 1976, J. Chem. Phys., **64**, 3237.
910. Perry, R.A., R. Atkinson, and J.N. Pitts Jr., 1977, J. Chem. Phys., **67**, 5577.
911. Perry, R.A. and C.F. Melius, 1984, Twentieth Symposium (International) on Combustion, The Combustion Institute, pp. 639-646.
912. Persky, A., 1996, J. Phys. Chem., **100**, 689-693.
913. Phillips, L.F., 1978, Chem. Phys. Lett., **57**, 538-539.
914. Phillips, L.F. and H.I. Schiff, 1962, J. Chem. Phys., **36**, 1509-1517.
915. Piper, L.G., G.E. Caledonia, and J.P. Konnealy, 1981, J. Chem. Phys., **74**, 2888.
916. Plane, J.M.C. and D. Husain, 1986, J. Chem. Soc. Faraday 2, **82**, 2047-2052.
917. Plane, J.M.C., C.-F. Nien, M.R. Allen, and M. Helmer, 1993, J. Phys. Chem., **97**, 4459-4467.
918. Plane, J.M.C. and B. Rajasekhar, 1989, J. Phys. Chem., **93**, 3135-3140.
919. Platz, J., O.J. Nielson, J. Sehested, and T.J. Wallington, 1995, J. Phys. Chem., **99**, 6570-6579.
920. Plumb, I.C. and K.R. Ryan, 1982, Int. J. Chem. Kinet., **14**, 861-874.
921. Plumb, I.C. and K.R. Ryan, 1982 , Chem. Phys. Lett., **92**, 236-238.
922. Plumb, I.C., K.R. Ryan, J.R. Steven, and M.F.R. Mulcahy, 1979, Chem. Phys. Lett., **63**, 255.
923. Plumb, I.C., K.R. Ryan, J.R. Steven, and M.F.R. Mulcahy, 1981, J. Phys. Chem., **85**, 3136.
924. Plumb, I.C., K.R. Ryan, J.R. Steven, and M.F.R. Mulcahy, 1982, Int. J. Chem. Kinet., **14**, 183.
925. Posey, J., J. Sherwell, and M. Kaufman, 1981, Chem. Phys. Lett., **77**, 476-479.
926. Poulet, G., I.T. Lancar, G. Laverdet, and G. Le Bras, 1990, J. Phys. Chem., **94**, 278-284.
927. Poulet, G., G. Laverdet, J.L. Jourdain, and G. Le Bras, 1984, J. Phys. Chem., **88**, 6259-6263.
928. Poulet, G., G. Laverdet, and G. Le Bras, 1981, J. Phys. Chem., **85**, 1892.
929. Poulet, G., G. Laverdet, and G. Le Bras, 1983, Chem. Phys. Lett., **94**, 129-132.
930. Poulet, G., G. Laverdet, and G. Le Bras, 1984, J. Chem. Phys., **80**, 1922-1928.
931. Poulet, G., G. Laverdet, and G. Le Bras, 1986, J. Phys. Chem., **90**, 159-165.
932. Poulet, G., G. Le Bras, and J. Combourieu, 1974, J. Chim. Physique, **71**, 101.
933. Poulet, G., G. Le Bras, and J. Combourieu, 1978, J. Chem. Phys., **69**, 767.
934. Poulet, G., G. Le Bras, and J. Combourieu, 1980, Geophys. Res. Lett., **7**, 413-414.
935. Poulet, G., H. Zagogianni, and G. Le Bras, 1986, Int. J. Chem. Kinet., **18**, 847-859.
936. Pritchard, H.O., J.B. Pyke, and A.F. Trotman-Dickenson, 1954, J. Amer. Chem. Soc., **76**, 1201.
937. Pritchard, H.O., J.B. Pyke, and A.F. Trotman-Dickenson, 1955, J. Amer. Chem. Soc., **77**, 2629.
938. Radford, H.E., 1980, Chem. Phys. Lett., **71**, 195.
939. Radford, H.E., K.M. Evenson, and D.A. Jennings, 1981, Chem. Phys. Lett., **78**, 589.
940. Rahman, M.M., E. Becker, T. Benter, and R.N. Schindler, 1988, Ber. Bunsenges. Phys. Chem., **92**, 91-100.
941. Rahman, M.M., E. Becker, U. Wille, and R.N. Schindler, 1992, Ber. Bunsenges. Phys. Chem., **96**, 783-787.
942. Raja, N., P.K. Arora, and J.P.S. Chatha, 1986, Int. J. Chem. Kinetics, **18**, 505-512.
943. Rattigan, O.V., R.A. Cox, and R.L. Jones, 1995, J. Chem. Soc. Faraday Soc. Trans., **91**, 4189-4197.
944. Ravishankara, A.R. and D.D. Davis, 1978, J. Phys. Chem., **82**, 2852-2853.
945. Ravishankara, A.R., D.D. Davis, G. Smith, G. Tesi, and J. Spencer, 1977, Geophys. Res. Lett., **4**, 7.
946. Ravishankara, A.R., F.L. Eisele, and P.H. Wine, 1982, J. Phys. Chem., **86**, 1854-1958.
947. Ravishankara, A.R., F.L. Eisele, and P.H. Wine, 1983, J. Chem. Phys., **78**, 1140-1144.
948. Ravishankara, A.R., N.M. Kreutter, R.C. Shah, and P.H. Wine, 1980, Geophys. Res. Lett., **7**, 861-864.
949. Ravishankara, A.R., J.M. Nicovich, R.L. Thompson, and F.P. Tully, 1981, J. Phys. Chem., **85**, 2498-2503.
950. Ravishankara, A.R., G.J. Smith, R.T. Watson, and D.D. Davis, 1977, J. Phys. Chem., **81**, 2220.
951. Ravishankara, A.R., S. Solomon, A.A. Turnipseed, and R.F. Warren, 1993, Science, **259**, 194-199.
952. Ravishankara, A.R. and R.L. Thompson, 1983, Chem. Phys. Lett., **99**, 377.

953. Ravishankara, A.R., A.A. Turnipseed, N.R. Jensen, S. Barone, M. Mills, C.J. Howard, and S. Solomon, 1994, Science, **263**, 71-75.
954. Ravishankara, A.R. and P.H. Wine, 1980, J. Chem. Phys., **72**, 25-30.
955. Ravishankara, A.R., P.H. Wine, and A.O. Langford, 1979, J. Chem. Phys., **70**, 984-989.
956. Ravishankara, A.R., P.H. Wine, and A.O. Langford, 1979, Chem. Phys. Lett., **63**, 479.
957. Ravishankara, A.R., P.H. Wine, and J.M. Nicovich, 1983, J. Chem. Phys., **78**, 6629-6639.
958. Ravishankara, A.R., P.H. Wine, and J.R. Wells, 1985, J. Chem. Phys., **83**, 447-448.
959. Ravishankara, A.R., P.H. Wine, J.R. Wells, and R.L. Thompson, 1985, Int. J. Chem. Kinet., **17**, 1281-1297.
960. Ray, A., I. Vassalli, G. Laverdet, and G. Le Bras, 1996, J. Phys. Chem., **100**, 8895-8900.
961. Ray, G.W., L.F. Keyser, and R.T. Watson, 1980, J. Phys. Chem., **84**, 1674-1681.
962. Ray, G.W. and R.T. Watson, 1981, J. Phys. Chem., **85**, 2955-2960.
963. Ray, G.W. and R.T. Watson, 1981, J. Phys. Chem., **85** , 1673-1676.
964. Reilly, J.D., J.H. Clark, C.B. Moore, and G.C. Pimentel, 1978, J. Chem. Phys., **69**, 4381.
965. Reimann, B. and F. Kaufman, 1978, J. Chem. Phys., **69**, 2925.
966. Reiner, T. and F. Arnold, 1993, Geophys. Res. Lett., **20**, 2659-2662.
967. Reiner, T. and F. Arnold, 1994, J. Chem. Phys., **101**, 7399-7407.
968. Rhasa, D., 1983, Diplomarbeit, Univ. of Gottingen, FRG.
969. Richardson, R.J., 1975, J. Phys. Chem., **79**, 1153-1158.
970. Robertshaw, J.S. and I.W.M. Smith, 1980, Int. J. Chem. Kinet., **12**, 729.
971. Roehl, C.M., D. Bauer, and G.K. Moortgat, 1996, J. Phys. Chem., **100**, 4038-4047.
972. Roscoe, J.M., 1982, Int. J. Chem. Kinet., **14**, 471-478.
973. Roth, P., R. Lohr, and H.D. Hermanns, 1980, Ber. Bunsenges. Phys. Chem., **84**, 835-840.
974. Rowland, F.S., H. Sato, H. Khwaja, and S.M. Elliott, 1986, J. Phys. Chem., **90**, 1985 -1988.
975. Rowley, D.M., M.H. Harwood, R.A. Freshwater, and R.L. Jones, 1996, J. Phys. Chem., **100**, 3020-3029.
976. Rozenshtein, V.B., Y.M. Gershenzon, S.O. Il'in, and O.P. Kishkovitch, 1984, Chem. Phys. Lett., **112**, 473-478.
977. Rust, F. and C.M. Stevens, 1980, Int. J. Chem. Kinet., **12**, 371-377.
978. Ryan, K.R. and I.C. Plumb, 1984, Int. J. Chem. Kinet., **16**, 591-602.
979. Saathoff, H. and R. Zellner, 1993, Chem. Phys. Lett., **206**, 349-354.
980. Sahetchian, K.A., A. Heiss, and R. Rigny, 1982, Can. J. Chem., **60**, 2896-2902.
981. Sahetchian, K.A., A. Heiss, and R. Rigny, 1987, J. Phys. Chem., **91**, 2382-2386.
982. Sander, S.P., 1984, J. Phys. Chem., **88**, 6018-6021.
983. Sander, S.P., 1986, J. Phys. Chem., **90**, 2194-2199.
984. Sander, S.P. and R.R. Friedl, 1989, J. Phys. Chem., **93**, 4764-4771.
985. Sander, S.P. and C.C. Kircher, 1986, Chem. Phys. Lett., **126**, 149-152.
986. Sander, S.P., M. Peterson, R.T. Watson, and R. Patrick, 1982, J. Phys. Chem., **86**, 1236-1240.
987. Sander, S.P. and R.T. Watson, 1980, J. Phys. Chem., **84**, 1664.
988. Sander, S.P. and R.T. Watson, 1981, J. Phys. Chem., **85**, 2960.
989. Sander, S.P. and R.T. Watson, 1981, Chem. Phys. Lett., **77**, 473-475.
990. Sander, S.P. and R.T. Watson, 1981, J. Phys. Chem., **85**, 4000.
991. Sanders, N.D., J.E. Butler, and J.R. McDonald, 1980, J. Chem. Phys., **73**, 5381-5383.
992. Sanders, N.D., J.E. Butler, L.R. Pasternack, and J.R. McDonald, 1980, Chem. Phys., **48**, 203.
993. Sanhueza, E. and J. Heicklen, 1975, J. Phys. Chem., **79**, 7-11.
994. Sanhueza, E., R. Simonaitis, and J. Heicklen, 1979, Int. J. Chem. Kinet., **11**, 907.
995. Sarkisov, O.M., S.G. Cheskis, and E.A. Sviridenkov, 1978, Bull. Acad. Sci. USSR Chem., **Ser. 27**, 2336.
996. Satyapal, S., J. Park, R. Bersohn, and B. Katz, 1989, J. Chem. Phys., **91**, 6873-6879.
997. Saunders, S.M., K.J. Hughes, M.J. Pilling, D.L. Baulch, and P.I. Smurthwaite, paper presented at the Optical Methods in Atmospheric Chemistry, 1992, **1715**, Berlin SPIE, 88-89.
998. Sawerysyn, J.P., A. Talhaoui, B. Meriaux, and P. Devolder, 1992, Chem. Phys. Lett., **198**, 197-199.
999. Schiffman, A., D.D. Nelson, M.S. Robinson, and D.J. Nesbitt, 1991, J. Phys. Chem., **95**, 2629-2636.
1000. Schindler, R.N. and T. Benter, 1988, Ber. Bunsenges. Phys. Chem., 92, 558.
1001. Schindler, R.N., J. Dethlefs, and M. Schmidt, 1996, Ber. Bunsenges. Phys. Chem., **100**, 1242-1249.
1002. Schmidt, C. and H.I. Schiff, 1973, Chem. Phys. Lett., **23**, 339-342.
1003. Schmidt, V., G.Y. Zhu, K.H. Becker, and E.H. Fink, 1985, Ber. Bunsenges. Phys. Chem., **89**, 321.
1004. Schmoltner, A.-M., P.M. Chu, R.J. Brudzynski, and Y.T. Lee, 1989, J. Chem. Phys., **91**, 6926-6936.
1005. Schmoltner, A.M., R.K. Talukdar, R.F. Warren, A. Mellouki, L. Goldfarb, T. Gierczak, S.A. McKeen, and A.R. Ravishankara, 1993, J. Phys. Chem., **97**, 8976-8982.
1006. Schneider, W.F. and T.J. Wallington, 1994, J. Phys. Chem., **98**, 7448-7451.
1007. Schonle, G., M.M. Rahman, and R.N. Schindler, 1987, Ber. Bunsenges. Phys. Chem., **91**, 66-75.
1008. Schurath, U., H.H. Lippmann, and B. Jesser, 1981, Ber. Bunsenges. Phys. Chem., **85**, 807-813.
1009. Schwab, J.J., W.H. Brune, and J.G. Anderson, 1989, J. Phys. Chem., **93**, 1030-1035.
1010. Schwab, J.J., D.W. Toohey, W.H. Brune, and J.G. Anderson, 1984, J. Geophys. Res., **89**, 9581-9587.
1011. Seeley, J.V., J.T. Jayne, and M.J. Molina, 1996, J. Phys. Chem., **100**, 4019-4025.
1012. Seeley, J.V., R.F. Meads, M.J. Elrod, and M.J. Molina, 1996, J. Phys. Chem., **100**, 4026-4031.
1013. Sehested, J., T. Ellermann, O.J. Nielsen, T.J. Wallington, and M.D. Hurley, 1993, Int. J. Chem. Kinet., **25**, 701-717.
1014. Sehested, J. and O.J. Nielsen, 1993, Chem. Phys. Lett., **206**, 369-375.

1015. Sehested, J., O.J. Nielsen, and T.J. Wallington, 1993, Chem. Phys. Lett., **213**, 457-464.
1016. Sehested, J., K. Sehested, O.J. Nielsen, and T.J. Wallington, 1994, J. Phys. Chem., **98**, 6731-6739.
1017. Selzer, E.A. and K.D. Bayes, 1983, J. Phys. Chem., **87**, 392-394.
1018. Semmes, D.H., A.R. Ravishankara, C.A. Gump-Perkins, and P.H. Wine, 1985, Int. J. Chem. Kinet., **17**, 303-313.
1019. Sharkey, P. and I.W.M. Smith, 1993, J. Chem. Soc. Faraday Trans., **89**, 631-638.
1020. Shi, J. and J.R. Barker, 1990, Int. J. Chem. Kinetics, **20**, 1283-1301.
1021. Shi, X., D.R. Herschbach, D.R. Worsnop, and C.E. Kolb, 1993, J. Phys. Chem., **97**, 2113-2122.
1022. Shibuya, K., T. Ebatu, K. Obi, and I. Tanaka, 1977, J. Phys. Chem., **81**, 2292.
1023. Silver, J.A., 1986, J. Chem. Phys., **84**, 4718-4720.
1024. Silver, J.A. and C.E. Kolb, 1980, Chem. Phys. Lett., **75**, 191.
1025. Silver, J.A. and C.E. Kolb, 1982, J. Phys. Chem., **86**, 3240-3246.
1026. Silver, J.A. and C.E. Kolb, 1986, J. Phys. Chem., **90**, 3263-3266.
1027. Silver, J.A. and C.E. Kolb, 1986, J. Phys. Chem., **90**, 3267-3269.
1028. Silver, J.A. and C.E. Kolb, 1987, J. Phys. Chem., **91**, 3713-3714.
1029. Silver, J.A., A.D. Stanton, M.S. Zahniser, and C.E. Kolb, 1984, J. Phys. Chem., **88**, 3123-3129.
1030. Simon, F.-G., W. Schneider, and G.K. Moortgat, 1990, Int. J. Chem. Kinet., **22**, 791-813.
1031. Simon, F.G., J.P. Burrows, W. Schneider, G.K. Moortgat, and P.J. Crutzen, 1989, J. Phys. Chem., **93**, 7807-7813.
1032. Simon, F.G., W. Schneider, G.K. Moortgat, and J.P. Burrows, 1990, J. Photochem. Photobiol., **A55**, 1-23.
1033. Simonaitis, R. and J. Heicklen, 1973, J. Phys. Chem, **77**, 1932-1935.
1034. Simonaitis, R. and J. Heicklen, 1975, J. Phys. Chem., **79**, 298.
1035. Simonaitis, R. and J. Heicklen, 1979, Chem. Phys. Lett., **65**, 361.
1036. Simonaitis, R. and J. Heicklen, 1981, J. Phys. Chem., **85** , 2946.
1037. Simonaitis, R. and J. Heicklen, 1982, J. Phys. Chem., **86**, 3416-3418.
1038. Sims, I.R., I.W.M. Smith, D.C. Clary, P. Bocherel, and B.R. Rowe, 1994, J. Chem. Phys., **101**, 1748-1751.
1039. Singh, J.P., J. Bachar, D.W. Setser, and S. Rosenwaks, 1985, J. Phys. Chem., **89**, 5347-5353.
1040. Singh, J.P. and D.W. Setser, 1985, J. Phys. Chem., **89**, 5353-5358.
1041. Singleton, D.L. and R.J. Cvetanovic, 1978, Can. J. Chem., **56**, 2934.
1042. Singleton, D.L. and R.J. Cvetanovic, 1981, Int. J. Chem. Kinet., **13**, 945.
1043. Singleton, D.L., R.S. Irwin, and R.J. Cvetanovic, 1977, Can. J. Chem., **55**, 3321-3327.
1044. Singleton, D.L., R.S. Irwin, W.S. Nip, and R.J. Cvetanovic, 1979, J. Phys. Chem., **83**, 2195-2200.
1045. Singleton, D.L., G. Paraskevopoulos, and R.S. Irwin, 1980, J. Phys. Chem., **84** , 2339-2343.
1046. Singleton, D.L., G. Paraskevopoulos, and R.S. Irwin, 1982, J. Phys. Chem., **86**, 2605-2609.
1047. Singleton, D.L., G. Paraskevopoulos, and R.S. Irwin, 1989, J. Am. Chem. Soc., **111**, 5248-5251.
1048. Singleton, D.L., G. Paraskevopoulos, R.S. Irwin, G.S. Jolly, and D.J. McKenney, 1988, J. Am. Chem. Soc., **110**, 7786-7790.
1049. Sinha, A., E.R. Lovejoy, and C.J. Howard, 1987, J. Chem. Phys., **87**, 2122-2128.
1050. Slagle, I.R., F. Baiocchi, and D. Gutman, 1978, J. Phys. Chem., **82** , 1333.
1051. Slagle, I.R., J.R. Gilbert, and D. Gutman, 1974, J. Chem. Phys., **61**, 704.
1052. Slagle, I.R., R.E. Graham, J.R. Gilbert, and D. Gutman, 1975, Chem. Phys. Lett., **32**, 184.
1053. Slanger, T.G. and G. Black, 1979, J. Chem. Phys., **70**, 3434-3438.
1054. Slanger, T.G., B.J. Wood, and G. Black, 1973, Int. J. Chem. Kinet., **5**, 615.
1055. Smardzewski, R.R. and M.C. Lin, 1977, J. Chem. Phys., **66**, 3197-3204.
1056. Smith, C.A., L.T. Molina, J.J. Lamb, and M.J. Molina, 1984, Int. J. Chem. Kinet., **16**, 41-45.
1057. Smith, I.W.M. and M.D. Williams, 1986, J. Chem. Soc. Faraday Trans. 2, **82**, 1043-1055.
1058. Smith, I.W.M. and R. Zellner, 1974, J. Chem. Soc. Faraday Trans. 2, **70**, 1045-1056.
1059. Smith, I.W.M. and R. Zellner, 1975, Int. J. Chem. Kinet., **Symp. 1**, 341.
1060. Smith, R.H., 1978, Int. J. Chem. Kinet., **10**, 519.
1061. Snelling, D.R., 1974, Can. J. Chem., **52**, 257-270.
1062. Sridharan, U.C., F.S. Klein, and F. Kaufman, 1985, J. Chem. Phys., **82**, 592-593.
1063. Sridharan, U.C., L.X. Qiu, and F. Kaufman, 1981, J. Phys. Chem., **85**, 3361-3363.
1064. Sridharan, U.C., L.X. Qiu, and F. Kaufman, 1982, J. Phys. Chem., **86**, 4569-4574.
1065. Sridharan, U.C., L.X. Qiu, and F. Kaufman, 1984, J. Phys. Chem., **88**, 1281-1282.
1066. Sridharan, U.C., B. Reimann, and F. Kaufman, 1980, J. Chem. Phys., **73** , 1286-1293.
1067. Stachnik, R.A. and M.J. Molina, 1987, J. Phys. Chem., **91**, 4603.
1068. Stachnik, R.A., M.J. Molina, and L.T. Molina, 1986, J. Phys. Chem., **90**, 2777-2780.
1069. Staricco, E.H., S.E. Sicre, and H.J. Schumacher, 1962, Z. Phys. Chem. N.F., **31**, 385.
1070. Stedman, D.H. and H. Niki, 1973, Environ. Lett., **4**, 303.
1071. Stedman, D.H. and H. Niki, 1973, J. Phys. Chem., **77**, 2604.
1072. Stedman, D.H., C.H. Wu, and H. Niki, 1973, J. Phys. Chem., **77**, 2511.
1073. Steer, R.P., R.A. Ackerman, and J.N. Pitts Jr., 1969, J. Chem. Phys., **51**, 843-844.
1074. Steiner, H. and E.K. Rideal, 1939, Proc. Roy. Soc. (London) Sec. A., **173**, 503.
1075. Stephens, J.W., C.L. Morter, S.K. Farhat, G.P. Glass, and R.F. Curl, 1993, J. Phys. Chem., **97**, 8944-8951.
1076. Stephens, R.D., 1984, J. Phys. Chem., **88**, 3308-3313.
1077. Stephens, S.L., J.W. Birks, and R.J. Glinski, 1989, J. Phys. Chem., **93**, 8384-8385.
1078. Stevens, P.S. and J.G. Anderson, 1990, Geophys. Res. Lett., **17**, 1287-1290.
1079. Stevens, P.S. and J.G. Anderson, 1992, J. Phys. Chem., **96**, 1708-1718.

1080. Stevens, P.S., W.H. Brune, and J.G. Anderson, 1989, J. Phys. Chem., **93**, 4068-4079.
1081. Stickel, R.E., M. Chin, E.P. Daykin, A.J. Hynes, P.H. Wine, and T.J. Wallington, 1993, J. Phys. Chem., **97**, 13653-13661.
1082. Stickel, R.E., J.M. Nicovich, S. Wang, Z. Zhao, and P.H. Wine, 1992, J. Phys. Chem., **96**, 9875-9883.
1083. Stickel, R.E., Z. Zhao, and P.H. Wine, 1993, Chem. Phys. Lett., **212**, 312-318.
1084. Stief, L.J., W.D. Brobst, D.F. Nava, R.P. Borkowski, and J.V. Michael, 1982, J. Chem. Soc. Faraday Trans. 2, **78**, 1391-1401.
1085. Stief, L.J., D.F. Nava, W.A. Payne, and J.V. Michael, 1980, J. Chem. Phys., **73**, 2254-2258.
1086. Stief, L.J., W.A. Payne, J.H. Lee, and J.V. Michael, 1979, J. Chem. Phys., **70**, 5241-5243.
1087. Stimpfle, R., R. Perry, and C.J. Howard, 1979, J. Chem. Phys., **71**, 5183-5190.
1088. Streit, G.E., C.J. Howard, A.L. Schmeltekopf, J.A. Davidson, and H.I. Schiff, 1976, J. Chem. Phys., **65**, 4761-4764.
1089. Streit, G.E., J.S. Wells, F.C. Fehsenfeld, and C.J. Howard, 1979, J. Chem. Phys., **70**, 3439-3443.
1090. Stuhl, F., 1973, J. Chem. Phys., **59**, 635.
1091. Stuhl, F., 1974, Ber. Bunsenges. Phys. Chem., **78**, 230.
1092. Stuhl, F. and H. Niki, 1970, Chem. Phys. Lett., **7**, 473-474.
1093. Stuhl, F. and H. Niki, 1971, J. Chem. Phys., **55**, 3954-3957.
1094. Stuhl, F. and H. Niki, 1972, J. Chem. Phys., **57**, 3671-3677.
1095. Stuhl, F. and K.H. Welge, 1969, Can. J. Chem., **47**, 1870-1871.
1096. Su, F., J.G. Calvert, and J.H. Shaw, 1979, J. Phys. Chem., **83**, 3185-3191.
1097. Su, F., J.G. Calvert, and J.H. Shaw, 1980, J. Phys. Chem., **84**, 239.
1098. Su, F., J.G. Calvert, J.H. Shaw, H. Niki, P.D. Maker, C.M. Savage, and L.D. Breitenbach, 1979, Chem. Phys. Lett., **65**, 221-225.
1099. Sugawara, K., Y. Ishikawa, and S. Sato, 1980, Bull. Chem. Soc. Japan, **53**, 3159.
1100. Sullivan, J.O. and P. Warneck, 1965, J. Phys. Chem., **69**, 1749.
1101. Sverdrup, G.M., C.W. Spicer, and G.F. Ward, 1987, Int. J. Chem. Kinet., **19**, 191-205.
1102. Szekely, A., R.K. Hanson, and C. Bowman, 1984, Twentieth Symposium (International) on Combustion, The Combustion Institute, pp. 647-654.
1103. Tachibana, K. and A.V. Phelps, 1981, J. Chem. Phys., **75**, 3315-3320.
1104. Takacs, G.A. and G.P. Glass, 1973, J. Phys. Chem., **77**, 1182.
1105. Takacs, G.A. and G.P. Glass, 1973, J. Phys. Chem., **77**, 1060.
1106. Takacs, G.A. and G.P. Glass, 1973, J. Phys. Chem., **77**, 1948.
1107. Takacs, G.A. and C.J. Howard, 1984, J. Phys. Chem., **88**, 2110.
1108. Takacs, G.A. and C.J. Howard, 1986, J. Phys. Chem., **90**, 687-690.
1109. Takahashi, K., R. Wada, Y. Matsumi, and M. Kawasaki, 1996, J. Phys. Chem., **100**, 10145-10149.
1110. Talcott, C.L., J.W. Ager III, and C.J. Howard, 1986, J. Chem. Phys., **84**, 6161-6169.
1111. Talhaoui, A., B. Louis, B. Meriaux, P. Devolder, and J.P. Sawerysyn, 1996, J. Phys. Chem., **100**, 2107-2113.
1112. Talhaoui, A., F. Louis, P. Devolder, B. Meriaux, J.P. Sawerysyn, M.T. Rayez, and J.C. Rayez, 1996, J. Phys. Chem., **100**, 13531-13538.
1113. Talukdar, R., A. Mellouki, T. Gierczak, J.B. Burkholder, S.A. McKeen, and A.R. Ravishankara, 1991, Science, **252**, 693-695.
1114. Talukdar, R., A. Mellouki, T. Gierczak, J.B. Burkholder, S.A. McKeen, and A.R. Ravishankara, 1991, J. Phys. Chem., **95**, 5815-5821.
1115. Talukdar, R.K., J.B. Burkholder, A.-M. Schmoltner, J.M. Roberts, R. Wilson, and A.R. Ravishankara, 1995, J. Geophys. Res., **100**, 14163-14173.
1116. Talukdar, R.K., T. Gierczak, L. Goldfarb, Y. Rudich, B.S. Madhava Rao, and A.R. Ravishankara, 1996, J. Phys. Chem., **100**, 3037-3043.
1117. Talukdar, R.K., S. Herndon, J.B. Burkholder, J.M. Roberts, and A.R. Ravishankara, 1997, Trans. Faraday. Soc., manuscript in preparation.
1118. Talukdar, R.K., A. Mellouki, T. Gierczak, S. Barone, S.-Y. Chiang, and A.R. Ravishankara, 1994, Int. J. Chem. Kinet., **26**, 973-990.
1119. Talukdar, R.K., A. Mellouki, A.-M. Schmoltner, T. Watson, S. Montzka, and A.R. Ravishankara, 1992, Science, **257**, 227-230.
1120. Talukdar, R.K. and A.R. Ravishankara, 1996, Chem. Phys. Lett., **253**, 177-183.
1121. Taylor, P.H., J.A. D'Angelo, M.C. Martin, J.H. Kasner, and B. Dellinger, 1989, Int. J. Chem. Kinet., **21**, 829-846.
1122. Taylor, P.H., Z. Jiang, and B. Dellinger, 1993, Int. J. Chem. Kinet., **25**, 9-23.
1123. Temps, F. and H.G. Wagner, 1982, Ber. Bunsenges. Phys. Chem., **86**, 119.
1124. Temps, F. and H.G. Wagner, 1984, Ber. Bunsenges Phys. Chem., **88**, 415.
1125. Thomas, J.W. and F. Kaufman, 1985, J. Chem. Phys., **83**, 2900-2903.
1126. Thomas, R.G.O. and B.A. Thrush, 1975, J. Chem. Soc. Faraday Trans. 2, **71**, 664-667.
1127. Thompson, J.E. and A.R. Ravishankara, 1993, Int. J. Chem. Kinet., **25**, 479-487.
1128. Thorn, R.P., J.M. Conkhite, J.M. Nicovich, and P.H. Wine, 1995, J. Chem. Phys., **102**, 4131-4142.
1129. Thrush, B.A. and G.S. Tyndall, 1982, J. Chem. Soc. Faraday 2, **78**, 1469-1475.
1130. Thrush, B.A. and G.S. Tyndall, 1982, Chem. Phys. Lett., **92**, 232-235.
1131. Thrush, B.A. and J.P.T. Wilkinson, 1979, Chem. Phys. Lett., **66**, 441-443.
1132. Thrush, B.A. and J.P.T. Wilkinson, 1981, Chem. Phys. Lett., **81**, 1-3.

1133. Thrush, B.A. and J.P.T. Wilkinson, 1981, Chem. Phys. Lett., **84**, 17-19.
1134. Tiee, J.J., F.B. Wampler, R.C. Oldenborg, and W.W. Rice, 1981, Chem. Phys. Lett., **82**, 80-84.
1135. Toby, F.S., S. Toby, and H.E. O'Neal, 1976, Int. J. Chem. Kinet., **8**, 25.
1136. Toohey, D.W., 1988, Ph. D. Thesis, "Kinetic and Mechanistic Studies of Reactions of Bromine and Chlorine Species Important in the Earth's Stratosphere", Harvard University.
1137. Toohey, D.W. and J.G. Anderson, 1988, J. Phys. Chem., **92**, 1705-1708.
1138. Toohey, D.W., W.H. Brune, and J.G. Anderson, 1987, J. Phys. Chem., **91**, 1215-1222.
1139. Toohey, D.W., W.H. Brune, and J.G. Anderson, 1988, Int. J. Chem. Kinet., **20**, 131-144.
1140. Trainor, D.W. and C.W. von Rosenberg Jr., 1974, J. Chem. Phys., **61**, 1010-1015.
1141. Trevor, P.L., G. Black, and J.R. Barker, 1982, J. Phys. Chem., **86**, 1661.
1142. Tsalkani, N., A. Mellouki, G. Poulet, G. Toupance, and G. Le Bras, 1988, J. Atmos. Chem., **7**, 409-419.
1143. Tschuikow-Roux, E., F. Faraji, S. Paddison, J. Niedzielski, and K. Miyokawa, 1988, J. Phys. Chem., **92**, 1488-1495.
1144. Tschuikow-Roux, E., T. Yano, and J. Niedzielski, 1985, J. Chem. Phys., **82** , 65-74.
1145. Tsuchiya, S. and T. Nakamura, 1979, Bull. Chem. Soc. Japan, **52**, 1527-1528.
1146. Tuazon, E., W.P.L. Carter, and R. Atkinson, 1991, J. Phys. Chem., **95**, 2434-2437.
1147. Tuazon, E.C., R. Atkinson, and S.B. Corchnoy, 1992, Int. J. Chem. Kinet., **24**, 639-648.
1148. Tuazon, E.C., R. Atkinson, C.N. Plum, A.M. Winer, and J.N. Pitts, 1983, Geophys. Res. Lett., **10**, 953-956.
1149. Tuazon, E.C., W.P.L. Carter, R. Atkinson, and J.N. Pitts Jr., 1983, Int. J. Chem. Kinet., **15**, 619-629.
1150. Tuazon, E.C., E. Sanhueza, R. Atkinson, W.P.L. Carter, A.M. Winer, and J.N. Pitts Jr., 1984, J. Phys. Chem., **88**, 3095-3098.
1151. Tully, F.P., 1983, Chem. Phys. Lett., **96**, 148-153.
1152. Tully, F.P., A, T. Droege, M.L. Koszykowski, and C.F. Melius, 1986, J. Phys. Chem., **90**, 691-698.
1153. Tully, F.P. and A.R. Ravishankara, 1980, J. Phys. Chem., **84**, 3126-3130.
1154. Tully, F.P., A.R. Ravishankara, and K. Carr, 1983, Inter. J. Chem. Kinet., **15**, 1111-1118.
1155. Turnipseed, A.A., S.B. Barone, N.R. Jensen, D.R. Hanson, C.J. Howard, and A.R. Ravishankara, 1995, J. Phys. Chem., **99**, 6000-6009.
1156. Turnipseed, A.A., S.B. Barone, and A.R. Ravishankara, 1993, J. Phys. Chem., **97**, 5926-5934.
1157. Turnipseed, A.A., S.B. Barone, and A.R. Ravishankara, 1994, J. Phys. Chem., **98**, 4594-4601.
1158. Turnipseed, A.A., S.B. Barone, and A.R. Ravishankara, 1996, J. Phys. Chem., **100**, 14703-14713.
1159. Turnipseed, A.A., J.W. Birks, and J.G. Calvert, 1990, J. Phys. Chem., **94**, 7477-7482.
1160. Turnipseed, A.A., J.W. Birks, and J.G. Calvert, 1991, J. Phys. Chem., **95**, 4356-4364.
1161. Turnipseed, A.A., M.K. Gilles, J.B. Burkholder, and A.R. Ravishankara, manuscript.
1162. Turnipseed, A.A., M.K. Gilles, J.B. Burkholder, and A.R. Ravishankara, 1995, Chem. Phys. Lett., **242**, 427-434.
1163. Turnipseed, A.A., G.L. Vaghjiani, T. Gierczak, J.E. Thompson, and A.R. Ravishankara, 1991, J. Chem. Phys., **95**, 3244-3251.
1164. Tyndall, G.S., J.P. Burrows, W. Schneider, and G.K. Moortgat, 1986, Chem. Phys. Lett., **130**, 463-466.
1165. Tyndall, G.S., J.J. Orlando, and J.G. Calvert, 1995, Environ. Sci. Technol., **29**, 202-206.
1166. Tyndall, G.S., J.J. Orlando, C.A. Cantrell, R.E. Shetter, and J.G. Calvert, 1991, J. Phys. Chem., **95**, 4381-4386.
1167. Tyndall, G.S., J.J. Orlando, K.E. Nickerson, C.A. Cantrell, and J.G. Calvert, 1991, J. Geophys. Res., **96**, 20761-20768.
1168. Tyndall, G.S., J.J. Orlando, T.J. Wallington, J. Sehested, and O.J. Nielsen, 1996, J. Phys. Chem., **100**, 660-668.
1169. Tyndall, G.S. and A.R. Ravishankara, 1989, J. Phys. Chem., **93**, 4707-4710.
1170. Tyndall, G.S. and A.R. Ravishankara, 1989, J. Phys. Chem., **93**, 2426-2435.
1171. Tyndall, G.S. and A.R. Ravishankara, 1991, Int. J. Chem. Kinet., **23**, 483-527.
1172. Vaghjiani, G.L. and A.R. Ravishankara, 1989, J. Phys. Chem., **93**, 1948.
1173. Vaghjiani, G.L. and A.R. Ravishankara, 1991, Nature, **350**, 406-409.
1174. Vaghjiani, G.L., A.R. Ravishankara, and N. Cohen, 1989, J. Phys. Chem., **93**, 7833-7837.
1175. Van den Bergh, H. and J. Troe, 1976, J. Chem. Phys., **64**, 736-742.
1176. Vanderzanden, J.W. and J.W. Birks, 1982, Chem. Phys. Lett., **88**, 109-114.
1177. Verhees, P.W.C. and E.H. Adema, 1985, J. Atmos. Chem., **2**, 387.
1178. Veyret, B. and R. Lesclaux, 1981, J. Phys. Chem., **85**, 1918.
1179. Veyret, B., R. Lesclaux, M.-T. Rayez, J.-C. Rayez, R.A. Cox, and G.K. Moortgat, 1989, J. Phys. Chem., **93**, 2368-2374.
1180. Veyret, B., J.C. Rayez, and R. Lesclaux, 1982, J. Phys. Chem., **86**, 3424-3430.
1181. Villalta, P.W., L.G. Huey, and C.J. Howard, 1995, J. Phys. Chem., **99**, 12829-12834.
1182. Villalta, P.W., E.R. Lovejoy, and D.R. Hanson, 1996, Geophys. Res. Lett., **23**, 1765-1768.
1183. Vinckier, C., M. Schaekers, and J. Peeters, 1985, J. Phys. Chem., **89**, 508-512.
1184. Vogt, R. and R.N. Schindler, 1993, Ber. Bunsenges. Phys. Chem., **97**, 819-829.
1185. Volltrauer, H.N., W. Felder, R.J. Pirkle, and A. Fontijn, 1979, J. Photochem., **11**, 173-181.
1186. Von Ellenrieder, G., E. Castellano, and H.J. Schumacher, 1971, Chem. Phys. Lett., **9**, 152-156.
1187. Wagner, A.F., I.R. Slagle, D. Sarzynski, and D. Gutman, 1990, J. Phys. Chem., **94**, 1853-1864.
1188. Wagner, G. and R. Zellner, 1981, Ber. Bunsenges. Phys. Chem., **85**, 1122-1128.
1189. Wagner, H.G., J. Warnatz, and C. Zetzsch, 1971, Anales Assoc. Quim. Argentina, **59**, 169-177.
1190. Wagner, H.G., U. Welzbacher, and R. Zellner, 1976, Ber Bunsenges. Phys. Chem., **80**, 1023-1027.
1191. Wagner, H.G., C. Zetzsch, and J. Warnatz, 1972, Ber. Bunsenges. Phys. Chem., **76**, 526.

1192. Wahner, A. and A.R. Ravishankara, 1987, J. Geophys. Res., **92**, 2189-2194.
1193. Walch, S.P., 1993, J. Chem. Phys., **99**, 5295-5300.
1194. Wallington, T.J., 1991, J. Chem. Soc. Faraday Trans., **87**, 2379-2382.
1195. Wallington, T.J., J.M. Andino, J.C. Ball, and S.M. Japar, 1990, J. Atmos. Chem., **10**, 301-313.
1196. Wallington, T.J., J.M. Andino, A.R. Potts, and P.H. Wine, 1991, Chem. Phys. Lett., **176**, 103-108.
1197. Wallington, T.J., R. Atkinson, E.C. Tuazon, and S.M. Aschmann, 1986, Int. J. Chem. Kinet., **18**, 837-846.
1198. Wallington, T.J., R. Atkinson, and A.M. Winer, 1984, Geophys. Res. Lett., **11**, 861-864.
1199. Wallington, T.J., R. Atkinson, A.M. Winer, and J.N. Pitts Jr., 1986, J. Phys. Chem., **90**, 5393-5396.
1200. Wallington, T.J., R. Atkinson, A.M. Winer, and J.N. Pitts Jr., 1986, J. Phys. Chem., **90**, 4640-4644.
1201. Wallington, T.J. and J.C. Ball, 1995, Chem. Phys. Lett., **234**, 187-194.
1202. Wallington, T.J. and J.C. Ball, 1995, J. Phys. Chem., **99**, 3201-3205.
1203. Wallington, T.J., J.C. Ball, O.J. Nielsen, and E. Bartkiewicz, 1992, J. Phys. Chem., **96**, 1241-1246.
1204. Wallington, T.J., P. Dagaut, and M.J. Kurylo, 1988, J. Photochem. Photobiol. A: Chemistry, **42**, 173-185.
1205. Wallington, T.J., P. Dagaut, and M.J. Kurylo, 1992, Chem. Rev., **92**, 667-710.
1206. Wallington, T.J., T. Ellermann, and O.J. Nielsen, 1993, J. Phys. Chem., **97**, 8442-8449.
1207. Wallington, T.J. and M.D. Hurley, 1992, Chem. Phys. Lett., **189**, 437-442.
1208. Wallington, T.J., M.D. Hurley, and W.F. Schneider, 1993, Chem. Phys. Lett., **213**, 442-448.
1209. Wallington, T.J., M.D. Hurley, W.F. Schneider, J. Sehested, and O.J. Nielsen, 1993, J. Phys. Chem., **97**, 7606-7611.
1210. Wallington, T.J. and S.M. Japar, 1990, Chem. Phys. Lett., **166**, 495-499.
1211. Wallington, T.J. and M.J. Kurylo, 1987, Int. J. Chem. Kinet., **19**, 1015-1023.
1212. Wallington, T.J. and M.J. Kurylo, 1987, J. Phys. Chem., **91**, 5050-5054.
1213. Wallington, T.J., D.M. Neuman, and M.J. Kurylo, 1987, Int. J. Chem. Kinet., **19**, 725-739.
1214. Wallington, T.J., L.M. Skewes, W.O. Siegl, C.H. Wu, and S.M. Japar, 1988, Int. J. Chem. Kinet., **20**, 867-875.
1215. Walther, C.-D. and H.G. Wagner, 1983, Ber. Bunsenges. Phys. Chem., **87**, 403-409.
1216. Wang, N.S. and C.J. Howard, 1990, J. Phys. Chem., **94**, 8787-8794.
1217. Wang, N.S., E.R. Lovejoy, and C.J. Howard, 1987, J. Phys. Chem., **91**, 5743-5749.
1218. Wang, W.C., M. Suto, and L.C. Lee, 1984, J. Chem. Phys., **81**, 3122-3126.
1219. Wang, X., Y.G. Jin, M. Suto, and L.C. Lee, 1988, J. Chem. Phys., **89**, 4853-4860.
1220. Wang, X., M. Suto, and L.C. Lee, 1988, J. Chem. Phys., **88** , 896-899.
1221. Wantuck, P.J., R.C. Oldenberg, S.L. Baughcum, and K.R. Winn, 1987, J. Phys. Chem., **91**, 4653.
1222. Warren, R., T. Gierczak, and A.R. Ravishankara, 1991, Chem. Phys. Lett., **183**, 403-409.
1223. Warren, R.F. and A.R. Ravishankara, 1993, Int. J. Chem. Kinet., **25**, 833-844.
1224. Washida, N., 1980, J. Chem. Phys., **73**, 1665.
1225. Washida, N., H. Akimoto, and M. Okuda, 1980, J. Chem. Phys., **72**, 5781-5783.
1226. Washida, N., H. Akimoto, and M. Okuda, 1980, Bull. Chem. Soc. Japan, **53**, 3496-3503.
1227. Washida, N. and K.D. Bayes, 1976, Int. J. Chem. Kinet., **8**, 777.
1228. Washida, N., R.J. Martinez, and K.D. Bayes, 1974, Z. Naturforsch., **29A**, 251.
1229. Wategaonkar, S.J. and D.W. Setser, 1989, J. Chem. Phys., **90**, 251-264.
1230. Watson, R.T., E.S. Machado, R.L. Schiff, S. Fischer, and D.D. Davis, 1975, Proceedings of the 4th CIAP Conference, DOT-TSC-OST-75-38, Dept. of Transportation Washington D.C, Cambridge, MA.
1231. Watson, R.T., G. Machado, B.C. Conaway, S. Wagner, and D.D. Davis, 1977, J. Phys. Chem., **81**, 256.
1232. Watson, R.T., G. Machado, S. Fischer, and D.D. Davis, 1976, J. Chem. Phys., **65**, 2126.
1233. Watson, R.T., A.R. Ravishankara, G. Machado, S. Wagner, and D.D. Davis, 1979, Int. J. Chem. Kinet., **11**, 187-197.
1234. Watson, R.T., S.P. Sander, and Y.L. Yung, 1979, J. Phys. Chem., **83**, 2936.
1235. Wayne, R.P. and J.N. Pitts Jr., 1969, J. Chem. Phys., **50**, 3644-3645.
1236. Wecker, D., R. Johanssen, and R.N. Schindler, 1982, Ber. Bunsenges. Phys. Chem., **86**, 532-538.
1237. Wei, C.N. and R.B. Timmons, 1975, J. Chem. Phys., **62**, 3240.
1238. Wennberg, P.O., J.G. Anderson, and D.K. Weisenstein, 1994, J. Geophys. Res., **99**, 18839-18846.
1239. West, G.A., R.E. Weston Jr., and G.W. Flynn, 1978, Chem. Phys. Lett., **56**, 429.
1240. Westenberg, A.A. and N. de Haas, 1969, J. Phys. Chem., **73**, 1181.
1241. Westenberg, A.A. and N. de Haas, 1969, J. Chem. Phys., **50**, 707-709.
1242. Westenberg, A.A. and N. de Haas, 1973, J. Chem. Phys., **58**, 4061-4065.
1243. Westenberg, A.A. and N. de Haas, 1973, J. Chem. Phys., **58**, 4066-4071.
1244. Westenberg, A.A. and N. de Haas, 1977, J. Chem. Phys., **66**, 4900.
1245. Westenberg, A.A., N. de Haas, and J.M. Roscoe, 1970, J. Phys. Chem., **74**, 3431.
1246. Westenberg, A.A., J.M. Roscoe, and N. de Haas, 1970, Chem. Phys. Lett., **7**, 597-599.
1247. Whyte, A.R. and L.F. Phillips, 1983, Chem. Phys. Lett., **102**, 451-454.
1248. Whytock, D.A., J.H. Lee, J.V. Michael, W.A. Payne, and L.J. Stief, 1977, J. Chem. Phys., **66**, 2690.
1249. Whytock, D.A., R.B. Timmons, J.H. Lee, J.V. Michael, W.A. Payne, and L.J. Stief, 1976, J. Chem. Phys., **65**, 2052-2055.
1250. Wiebe, H.A. and J. Heicklen, 1973, J. Am. Chem. Soc., **95**, 1-7.
1251. Wildt, J., G. Bednarek, E.H. Fink, and R.P. Wayne, 1988, Chem. Phys., **122**, 463-470.
1252. Wildt, J., E.H. Fink, P. Biggs, and R.P. Wayne, 1989, Chem. Phys., **139**, 401-407.
1253. Wildt, J., E.H. Fink, P. Biggs, R.P. Wayne, and A.F. Vilesov, 1992, Chem. Phys., **159**, 127-140.

1254. Wilson, W.E., 1967, J. Chem. Phys., **46**, 2017-2018.
1255. Wine, P.H., R.J. Astalos, and R.L. Mauldin III, 1985, J. Phys. Chem., **89**, 2620-2624.
1256. Wine, P.H., W.L. Chameides, and A.R. Ravishankara, 1981, Geophys. Res. Lett., **8** , 543-546.
1257. Wine, P.H., N.M. Kreutter, C.A. Gump, and A.R. Ravishankara, 1981, J. Phys. Chem., **85**, 2660-2665.
1258. Wine, P.H., J.M. Nicovich, and A.R. Ravishankara, 1985, J. Phys. Chem., **89**, 3914-3918.
1259. Wine, P.H., J.M. Nicovich, R.E. Stickel, Z. Zhao, C.J. Shackelford, K.D. Kreutter, E.P. Daykin, and S. Wang, The Tropospheric Chemistry of Ozone in the Polar Regions, NATO ASI, eds. H. Niki and K.H. Becker. Vol. 17. 1993, Berlin: Springer-Verlag. 385-395.
1260. Wine, P.H., J.M. Nicovich, R.J. Thompson, and A.R. Ravishankara, 1983, J. Phys. Chem., **87**, 3948-3954.
1261. Wine, P.H. and A.R. Ravishankara, 1981, Chem. Phys. Lett., **77**, 103-109.
1262. Wine, P.H. and A.R. Ravishankara, 1982, Chem. Phys., **69**, 365-373.
1263. Wine, P.H. and A.R. Ravishankara, 1983, Chem. Phys. Lett., **96**, 129-132.
1264. Wine, P.H., A.R. Ravishankara, N.M. Kreutter, R.C. Shah, J.M. Nicovich, R.L. Thompson, and D.J. Wuebbles, 1981, J. Geophys. Res., **86**, 1105-1112.
1265. Wine, P.H., D.H. Semmes, and A.R. Ravishankara, 1981, J. Chem. Phys., **75**, 4390-4395.
1266. Wine, P.H., D.H. Semmes, and A.R. Ravishankara, 1982, Chem. Phys. Lett., **90**, 128-132.
1267. Wine, P.H., R.C. Shah, and A.R. Ravishankara, 1980, J. Phys. Chem., **84**, 2499-2503.
1268. Wine, P.H., R.J. Thompson, and D.H. Semmes, 1984, Int. J. Chem. Kinet., **16**, 1623.
1269. Wine, P.H., J.R. Wells, and J.M. Nicovich, 1988, J. Phys. Chem., **92**, 2223-2228.
1270. Wine, P.H., J.R. Wells, and A.R. Ravishankara, 1986, J. Chem. Phys., **84**, 1349-1354.
1271. Winer, A.M., A.C. Lloyd, K.R. Darnall, R. Atkinson, and J.N. Pitts Jr., 1977, Chem. Phys. Lett., **51**, 221-226.
1272. Winer, A.M., A.C. Lloyd, K.R. Darnall, and J.N. Pitts Jr., 1976, J. Phys. Chem., **80**, 1635.
1273. Winkler, I.C., R.A. Stachnik, J.I. Steinfeld, and S.M. Miller, 1986, J. Chem. Phys., **85**, 890.
1274. Wolf, M., D.L. Yang, and J.L. Durant, 1994, J. Photochem. Photobiol. A: Chem., **80**, 85-93.
1275. Wong, E.L. and F.R. Belles, 1971, NASA TN D-6495, NASA, Washington, D. C.
1276. Wongdontri-Stuper, W., R.K.M. Jayanty, R. Simonaitis, and J. Heicklen, 1979, J. Photochem., **10**, 163.
1277. Worsnop, D.R., M.S. Zahniser, and C.E. Kolb, 1991, J. Phys. Chem., **95**, 3960-3964.
1278. Worsnop, D.R., M.S. Zahniser, and C.E. Kolb, 1992, J. Phys. Chem., **96**, 9088.
1279. Wright, T.G., A.M. Ellis, and J.M. Dyke, 1993, J. Chem. Phys., **98**, 2891-2907.
1280. Wu, F. and R.W. Carr, 1992, J. Phys. Chem., **96**, 1743-1748.
1281. Wurzburg, E. and P.L. Houston, 1980, J. Chem. Phys., **72**, 4811.
1282. Xiang, T., L. M, Torres, and W.A. Guillory, 1985, J. Chem. Phys., **83**, 1623-1629.
1283. Yano, T. and E. Tschuikow-Roux, 1986, J. Photochem., **32**, 25-37.
1284. Yokelson, R.J., J.B. Burkholder, L. Goldfarb, R.W. Fox, M.K. Gilles, and A.R. Ravishankara, 1995, J. Phys. Chem., **99**, 13976-13983.
1285. Zabarnick, S. and J. Heicklen, 1985, Int. J. Chem. Kinet., **17**, 455-476.
1286. Zabarnick, S., J. W, Fleming, and M.C. Lin, 1988, Int. J. Chem. Kinet., **20**, 117-129.
1287. Zabel, F., A. Reimer, K.H. Becker, and E.H. Fink, 1989, J. Phys. Chem., **93**, 5500-5507.
1288. Zabel, F., K.A. Sahetchian, and C. Chachaty, 1987, Chem. Phys. Lett., **134**, 433.
1289. Zagogianni, H., A. Mellouki, and G. Poulet, 1987, C. R. Acad. Sci. Paris, **Series II 304**, 573-578.
1290. Zahniser, M.S., B.M. Berquist, and F. Kaufman, 1978, Int. J. Chem. Kinet., **10**, 15.
1291. Zahniser, M.S., J. Chang, and F. Kaufman, 1977, J. Chem. Phys., **67**, 997.
1292. Zahniser, M.S. and C.J. Howard, 1980, J. Chem. Phys., **73**, 1620-1626.
1293. Zahniser, M.S. and F. Kaufman, 1977, J. Chem. Phys., **66**, 3673.
1294. Zahniser, M.S., F. Kaufman, and J.G. Anderson, 1974, Chem. Phys. Lett., **27**, 507.
1295. Zahniser, M.S., F. Kaufman, and J.G. Anderson, 1976, Chem. Phys. Lett., **37**, 226.
1296. Zellner, R., 1987, J. Chem. Phys., **84**, 403.
1297. Zellner, R., G. Bednarek, A. Hoffmann, J.P. Kohlmann, V. Mors, and H. Saathoff, 1994, Ber. Bunsenges. Phys. Chem., **98**, 141-146.
1298. Zellner, R. and F. Ewig, 1988, J. Phys Chem., **92**, 2971.
1299. Zellner, R., B. Fritz, and K. Lorenz, 1986, J. Atmos. Chem., **4**, 241-251.
1300. Zellner, R. and W. Steinert, 1981, Chem. Phys. Lett., **81**, 568-572.
1301. Zellner, R., G. Wagner, and B. Himme, 1980, J. Phys. Chem., **84**, 3196-3198.
1302. Zetzsch, C., paper presented at the 7th International Symposium on Gas Kinetics, 1982, Goettingen, Germany.
1303. Zetzsch, C. and F. Stuhl, 1982, Proceedings of the 2nd European Symposium on the Physico-Chemical Behaviour of Atmospheric Pollutants, D. Reidel Publishing Co., Dordrecht, Holland, pp. 129-137.
1304. Zhang, Z., R.E. Huie, and M.J. Kurylo, 1992, J. Phys. Chem., **96**, 1533-1535.
1305. Zhang, Z., R. Liu, R.E. Huie, and M.J. Kurylo, 1991, Geophys. Res. Lett., **18**, 5-7.
1306. Zhang, Z., S. Padmaja, R.D. Saini, R.E. Huie, and M.J. Kurylo, 1994, J. Phys. Chem., **98**, 4312-4315.
1307. Zhang, Z., R.D. Saini, M.J. Kurylo, and R.E. Huie, 1992, Chem. Phys. Lett., **200**, 230-234.
1308. Zhang, Z., R.D. Saini, M.J. Kurylo, and R.E. Huie, 1992, J. Phys. Chem., **96**, 9301-9304.
1309. Zhang, Z., R.D. Saini, M.J. Kurylo, and R.E. Huie, 1992, Geophys. Res. Lett., **19**, 2413-2416.
1310. Zhao, Z., R.E. Stickel, and P.H. Wine, 1996, Chem. Phys. Lett., **251**, 59-66.
1311. Zhitneva, G.P. and S.Y. Pshezhetskii, 1978, Kinetika i Kataliz, **19**, 296.
1312. Zipf, E.C., 1980, Nature (London), **287**, 523-525.

Table 2. Rate Constants for Association Reactions

Reaction	Low Pressure Limit[a] $k_o(T) = k_o^{300}(T/300)^{-n}$		High Pressure Limit[b] $k_\infty(T) = k_\infty^{300}(T/300)^{-m}$		Notes
	k_o^{300}	n	k_∞^{300}	m	
		O_x Reactions			
$O + O_2 \xrightarrow{M} O_3$	(6.0±0.5) (-34)	2.3±0.5	-	-	A1
		$O(^1D)$ Reactions			
$O(^1D) + N_2 \xrightarrow{M} N_2O$	(3.5±3.0) (-37)	$0.6\pm^{2.0}_{0.6}$	-	-	A2
		HO_x Reactions			
$H + O_2 \xrightarrow{M} HO_2$	(5.7±0.5) (-32)	1.6±0.5	(7.5±4.0) (-11)	0±1.0	B1
$OH + OH \xrightarrow{M} H_2O_2$	(6.2±1.2) (-31)	$1.0\pm^{2.0}_{1.0}$	(2.6±1.0) (-11)	0±0.5	B2
		NO_x Reactions			
$O + NO \xrightarrow{M} NO_2$	(9.0±2.0) (-32)	1.5±0.3	(3.0±1.0) (-11)	0±1.0	C1
$O + NO_2 \xrightarrow{M} NO_3$	(9.0±1.0) (-32)	2.0±1.0	(2.2±0.3) (-11)	0±1.0	C2
$OH + NO \xrightarrow{M} HONO$	(7.0±1.0) (-31)	2.6±0.3	(3.6±1.0) (-11)	0.1±0.5	C3
$OH + NO_2 \xrightarrow{M} HNO_3$ (See note)	(2.5±0.1) (-30)	4.4±0.3	(1.6±0.2) (-11)	1.7±0.2	C4
$HO_2 + NO_2 \xrightarrow{M} HO_2NO_2$	(1.8±0.3) (-31)	3.2±0.4	(4.7±1.0) (-12)	1.4±1.4	C5
$NO_2 + NO_3 \xrightarrow{M} N_2O_5$	(2.2±0.5) (-30)	3.9±1.0	(1.5±0.8) (-12)	0.7±0.4	C6
$NO_3 \xrightarrow{M} NO + O_2$	See Note				C7
		Hydrocarbon Reactions			
$CH_3 + O_2 \xrightarrow{M} CH_3O_2$	(4.5±1.5) (-31)	3.0±1.0	(1.8±0.2) (-12)	1.7±1.7	D1
$C_2H_5 + O_2 \xrightarrow{M} C_2H_5O_2$	(1.5±1.0) (-28)	3.0±1.0	(8.0±1.0) (-12)	0±1.0	D2
$OH + C_2H_2 \xrightarrow{M} HOCHCH$	(5.5±2.0) (-30)	0.0±0.2	(8.3±1.0) (-13)	$-2\pm^{2}_{1}$	D3
$OH + C_2H_4 \xrightarrow{M} HOCH_2CH_2$	(1.0±0.6) (-28)	0.8±2.0	(8.8±0.9) (-12)	$0\pm^{0}_{2}$	D4
$CH_3O + NO \xrightarrow{M} CH_3ONO$	(1.4±0.5) (-29)	3.8±1.0	(3.6±1.6) (-11)	0.6±1.0	D5
$CH_3O + NO_2 \xrightarrow{M} CH_3ONO_2$	(1.1±0.4) (-28)	4.0±2.0	(1.6±0.5) (-11)	1.0±1.0	D6
$C_2H_5O + NO \xrightarrow{M} C_2H_5ONO$	(2.8±1.0) (-27)	4.0±2.0	(5.0±1.0) (-11)	1.0±1.0	D7

Table 2. (Continued)

Reaction	Low Pressure Limit[a] $k_0(T) = k_0^{300}(T/300)^{-n}$ k_0^{300}	n	High Pressure Limit[b] $k_\infty(T) = k_\infty^{300}(T/300)^{-m}$ k_∞^{300}	m	Notes
$C_2H_5O + NO_2 \xrightarrow{M} C_2H_5ONO_2$	(2.0±1.0) (-27)	4.0±2.0	(2.8±0.4) (-11)	1.0±1.0	D8
$CH_3O_2 + NO_2 \xrightarrow{M} CH_3O_2NO_2$	(1.5±0.8) (-30)	4.0±2.0	(6.5±3.2) (-12)	2.0±2.0	D9
$CH_3C(O)O_2 + NO_2 \xrightarrow{M} CH_3C(O)O_2NO_2$	(9.7±3.8) (-29)	5.6±2.8	(9.3±0.4)(-12)	1.5±0.3	D10
	FO_x Reactions				
$F + O_2 \xrightarrow{M} FO_2$	(4.4±0.4) (-33)	1.2±0.5	-	-	E1
$F + NO \xrightarrow{M} FNO$	(1.8±0.3) (-31)	1.0±10	(2.8±1.4) (-10)	0.0±1.0	E2
$F + NO_2 \xrightarrow{M} FNO_2$	(6.3±3.0) (-32)	2.0±2.0	(2.6±1.3) (-10)	0.0±1.0	E3
$FO + NO_2 \xrightarrow{M} FONO_2$	(2.6±2.0) (-31)	1.3±1.3	(2.0±1.0) (-11)	1.5±1.5	E4
$CF_3 + O_2 \xrightarrow{M} CF_3O_2$	(3.0±0.3) (-29)	4.0±2.0	(4.0±1.0) (-12)	1.0±1.0	E5
$CF_3O + NO_2 \xrightarrow{M} CF_3ONO_2$	See Note				E6
$CF_3O_2 + NO_2 \xrightarrow{M} CF_3O_2NO_2$	(2.2±0.5) (-29)	5.0±1.0	(6.0±1.0) (-12)	2.5±1.0	E7
$CF_3O + CO \xrightarrow{M} CF_3OCO$	(2.5±0.2) (-31)	-	(6.8±0.4) (-14)	-1.2	E8
$CF_3O \xrightarrow{M} CF_2O + F$	See Note				E9
	ClO_x Reactions				
$Cl + O_2 \xrightarrow{M} ClOO$	(2.7±1.0) (-33)	1.5±0.5	-	-	F1
$Cl + NO \xrightarrow{M} ClNO$	(9.0±2.0) (-32)	1.6±0.5	-	-	F2
$Cl + NO_2 \xrightarrow{M} ClONO$	(1.3±0.2) (-30)	2.0±1.0	(1.0±0.5) (-10)	1.0±1.0	F3
$\xrightarrow{M} ClNO_2$	(1.8±0.3) (-31)	2.0±1.0	(1.0±0.5) (-10)	1.0±1.0	
$Cl + CO \xrightarrow{M} ClCO$	(1.3±0.5) (-33)	3.8±0.5	-	-	F4
$Cl + C_2H_2 \xrightarrow{M} ClC_2H_2$	((5.9±1.0) (-30)	2.1±1.0	(2.1±0.4) (-10)	1.0±0.5	F5
$Cl + C_2H_4 \xrightarrow{M} ClC_2H_4$	(1.6±1) (-29)	3.3±1.0	(3.1±2) (-10)	1.0±0.5	F6
$Cl + C_2Cl_4 \xrightarrow{M} C_2Cl_5$	(1.4±0.6) (-28)	8.5±1.0	(4.0±1.0) (-11)	1.2±0.5	F7

Table 2. (Continued)

Reaction	Low Pressure Limit[a] $k_0(T) = k_0^{300}(T/300)^{-n}$		High Pressure Limit[b] $k_\infty(T) = k_\infty^{300}(T/300)^{-m}$		Notes
	k_0^{300}	n	k_∞^{300}	m	
$ClO + NO_2 \xrightarrow{M} ClONO_2$	(1.8±0.3) (-31)	3.4±1.0	(1.5±0.7) (-11)	1.9±1.9	F8
$OClO + NO_3 \xrightarrow{M} O_2ClONO_2$	See Note				F9
$ClO + ClO \xrightarrow{M} Cl_2O_2$	(2.2±0.4) (-32)	3.1±0.5	(3.5±2) (-12)	1.0±1.0	F10
$ClO + OClO \xrightarrow{M} Cl_2O_3$	(6.2±1.0) (-32)	4.7±0.6	(2.4±1.2) (-11)	0±1.0	F11
$OClO + O \xrightarrow{M} ClO_3$	(1.9±0.5) (-31)	1.1±1.0	(3.1±0.8) (-11)	0±1.0	F12
$CH_2Cl + O_2 \xrightarrow{M} CH_2ClO_2$	(1.9±0.1) (-30)	3.2±0.2	(2.9±0.2) (-12)	1.2±0.6	F13
$CHCl_2 + O_2 \xrightarrow{M} CHCl_2O_2$	(1.3±0.1) (-30)	4.0±0.2	(2.8±0.2) (-12)	1.4±0.6	F14
$CCl_3 + O_2 \xrightarrow{M} CCl_3O_2$	(6.9±0.2) (-31)	6.4±0.3	(2.4±0.2) (-12)	2.1±0.6	F15
$CFCl_2 + O_2 \xrightarrow{M} CFCl_2O_2$	(5.0±0.8) (-30)	4.0±2.0	(6.0±1.0) (-12)	1.0±1.0	F16
$CF_2Cl + O_2 \xrightarrow{M} CF_2ClO_2$	(3.0±1.5) (-30)	4.0±2.0	(3±2) (-12)	1.0±1.0	F17
$CCl_3O_2 + NO_2 \xrightarrow{M} CCl_3O_2NO_2$	(5.0±1.0) (-29)	5.0±1.0	(6.0±1.0) (-12)	2.5±1.0	F18
$CFCl_2O_2 + NO_2 \xrightarrow{M} CFCl_2O_2NO_2$	(3.5±0.5) (-29)	5.0±1.0	(6.0±1.0) (-12)	2.5±1.0	F19
$CF_2ClO_2 + NO_2 \xrightarrow{M} CF_2ClO_2NO_2$	(3.3±0.7) (-29)	6.7±1.3	(4.1±1.9) (-12)	2.8±0.7	F20
	BrO_x Reactions				
$Br + NO_2 \xrightarrow{M} BrNO_2$	(4.2±0.8) (-31)	2.4±0.5	(2.7±0.5) (-11)	0±1.0	G1
$BrO + NO_2 \xrightarrow{M} BrONO_2$	(5.2±0.6) (-31)	3.2±0.8	(6.9±1.0) (-12)	2.9±1.0	G2
	IO_x Reactions				
$I + NO \xrightarrow{M} INO$	(1.8±0.5) (-32)	1.0±0.5	(1.7±1.0) (-11)	0±1.0	H1
$I + NO_2 \xrightarrow{M} INO_2$	(3.0±1.5) (-31)	1.0±1.0	(6.6±5.0) (-11)	0±1.0	H2
$IO + NO_2 \xrightarrow{M} IONO_2$	(5.9±2.0) (-31)	3.5±1.0	(9.0±1.0) (-12)	1.5±1.0	H3
	SO_x Reactions				
$HS + NO \xrightarrow{M} HSNO$	(2.4±0.4) (-31)	3.0±1.0	(2.7±0.5) (-11)	$0\pm^{0}_{2}$	I1
$CH_3S + NO \xrightarrow{M} CH_3SNO$	(3.2±0.4) (-29)	4.0±1.0	(3.9±0.6) (-11)	2.7±1.0	I2

Table 2. (Continued)

Reaction	Low Pressure Limit[a] $k_0(T) = k_0^{300}(T/300)^{-n}$ k_0^{300}	n	High Pressure Limit[b] $k_\infty(T) = k_\infty^{300}(T/300)^{-m}$ k_∞^{300}	m	Notes
$O + SO_2 \xrightarrow{M} SO_3$	$(1.3\pm^{1.3}_{0.7})(-33)$	-3.6±0.7			I3
$OH + SO_2 \xrightarrow{M} HOSO_2$	(3.0±1.0) (-31)	3.3±1.5	(1.5±0.5) (-12)	$0\pm^{0}_{2}$	I4
$CH_3SCH_2 + O_2 \xrightarrow{M} CH_3SCH_2O_2$	See Note				I5
$SO_3 + NH_3 \xrightarrow{M} H_3NSO_3$	(3.9±0.8) (-30)	3.0±3.0	(4.7±1.3) (-11)	0±1.0	I6
	Metal Reactions				
$Na + O_2 \xrightarrow{M} NaO_2$	(3.2±0.3) (-30)	1.4±0.3	(6.0±2.0) (-10)	0±1.0	J1
$NaO + O_2 \xrightarrow{M} NaO_3$	(3.5±0.7) (-30)	2.0±2.0	(5.7±3.0) (-10)	0±1.0	J2
$NaO + CO_2 \xrightarrow{M} NaCO_3$	(8.7±2.6) (-28)	2.0±2.0	(6.5±3.0) (-10)	0±1.0	J3
$NaOH + CO_2 \xrightarrow{M} NaHCO_3$	(1.3±0.3) (-28)	2.0±2.0	(6.8±4.0) (-10)	0±1.0	J4

Note: $k(Z) = k(M,T) = \left(\frac{k_0(T)[M]}{1 + (k_0(T)[M]/k_\infty(T))}\right) 0.6^{\{1 + [\log_{10}(k_0(T)[M]/k_\infty(T))]^2\}^{-1}}$

The values quoted are suitable for air as the third body, M.

a Units are $cm^6/molecule^2$-sec.

b Units are $cm^3/molecule$-sec.

Shaded areas indicate changes or additions since JPL 94-26.

Notes to Table 2

A1. $O + O_2$. Low pressure limit and T dependence are an average of Klais, Anderson, and Kurylo [119] and Lin and Leu [141]. The result is in agreement with most previous work (see references therein) and with the study of Hippler et al. [98]. Kaye [114] has calculated isotope effects for this reaction, using methods similar to those discussed in the Introduction; Troe [223], Patrick and Golden [178]. Croce de Cobos and Troe [63] are in agreement with earlier work. Rawlins et al. [190] report values in Ar between 80 and 150K that extrapolate to agreement with the recommended values.

A2. $O(^1D) + N_2$. Low pressure limit from Kajimoto and Cvetanovic [113]. The T dependence is obtained by assuming a constant β. The rate constant is extremely low in this special system due to electronic curve crossing. Maric and Burrows [148] extract $(8.8\pm3.3)\times10^{-37}$ cm^6s^{-1} from a study of the photolysis of synthetic air, in agreement with the recommended value within mutual error limits.

B1. $H + O_2$. Kurylo [125], Wong and Davis [250] and Hsu et al. [104] are averaged to obtain the low pressure limiting value at 300K. The first two studies include T dependence, as does a study by Hsu et al. [103]. The recommended value is chosen with constant $\langle\Delta E\rangle_{N2}$ ~.05 kcal mol^{-1}. This very low number reflects rotational effects. The high pressure limit is from Cobos et al. [51]. The temperature dependence is estimated. Cobos et al. [51] estimate m = -0.6, which is within our uncertainty. High temperature measurements in Ar by Pirraglia et al. [182] are in good agreement. Measurements in the range $298<T/K<750$ by Carleton et al. [44] agree within error limits.

B2. OH + OH. Recommended values are from fits of measurements by Zellner et al. [257] in N_2, and by Forster et al. [85] in 1-150 kbar He scaled to N_2. We find that these two data sets agree, in contrast to the conclusion of Forster et al., which is a result of not scaling their He data to correspond to N_2. A study by Fagerstrom et al. [81] in 85-1000 mbar SF_6 gives slightly different values. A pressure independent bimolecular channel to $H_2O + O$ with a rate 1.9×10^{-12} is observed (see Table 1). The temperature dependence of k_0 takes into account both Zellner et al. and Fagerstrom et al.. The unsymmetrical error limits in k_0 (298) take into account contributions from $H + OH \rightarrow H_2O$. Trainor and von Rosenberg [222] report a value at 300K that is lower by a factor of 2.7.

C1. O + NO. Low pressure limit and n from direct measurements of Schieferstein et al. [202] and their re-analysis of the data of Whytock et al. [246]. Error limits encompass other studies. High pressure limit and m from Baulch et al. [23] and Baulch et al. [22], slightly modified. Shock tube measurements by Yarwood et al. [253] in argon from 300-1300K are consistent with these values.

C2. $O + NO_2$. Values of rate constants and temperature dependences from the evaluation of Baulch et al. [23]. They use $F_c = 0.8$ to fit the measured data at 298 K, but our value of $F_c = 0.6$ gives a similar result. In a supplementary review, Baulch et al. [22] suggest a slight temperature dependence for F_c, which would cause their suggested value to rise to $F_c = 0.85$ at 200 K.

C3. OH + NO. The low pressure limit rate constant has been reported by Anderson and Kaufman [6], Stuhl and Niki [220], Morley and Smith [157], Westenberg and de Haas [245], Anderson et al. [7], Howard and Evenson [102], Harris and Wayne [95], Atkinson et al. [14], Overend et al. [170], Anastasi and Smith [5], Burrows et al. [39] and Atkinson and Smith [11]. The general agreement is good, and the recommended values of both the rate constant and the temperature dependence are weighted averages. Studies by Sharkey et al. [207] and Donahue et al. [78] in the transition regime between low and high pressure limits are in agreement and serve to reduce the uncertainty. These latter studies yield a value for the high pressure limiting rate constant in agreement with the results of Forster et al. [85], whose study reached pressures of 100 bar in He. The temperature dependence of the high pressure limiting rate constant is from the data of Anastasi and Smith [5] and Sharkey et al. (Both cis- and trans- HONO are expected to be formed.) A study by Zabarnick [254] is noted.

C4. $OH + NO_2$. Both the low pressure limit and the high pressure limiting rate constants are from a fit to the data (at effective nitrogen densities less than $5x10^{19}$ molecules/cm^3) of Anderson et al. [7], Howard and Evenson [102], Anastasi and Smith [4], Wine et al. [248], Burrows et al. [39], Robertshaw and Smith [193], Erler et al. [80] and Dohahue et al. [78]. Data of Forster et al [85] appear to be systematically too high. The Forster et al. results and those of Robertshaw and Smith [193], who have measured k in up to 8.6 atmospheres of CF_4, suggest that k_∞ might be higher than suggested here (~50%). This disagreement might also be due to other causes (i.e., the failure of the simplified fall-off expression as suggested by Donahue et al., isomer formation, or involvement of excited electronic states). Burkholder et al. [35] have shown that $HONO_2$ is the only isomer formed (yield - $.75\pm^{.25}_{.10}$) and the fit to the data used here assumes that only this isomer is formed. The temperature dependence of both limiting rate constants is from the data of Wine et al. [248] and Anastasi and Smith [4] and is consistent with Smith and Golden [215] and Patrick and Golden [178]. The recommendation here fits all data over the range of atmospheric interest.

C5. $HO_2 + NO_2$. Kurylo and Ouellette [126] have remeasured the 300K range constants. Kurylo and Ouellette [127] have also remeasured the temperature dependence. The recommended values are taken from this latter reference wherein their data were combined with that of Sander and Peterson [199]. The recommended k_0 (300K) is consistent with Howard [101]. Other studies by Simonaitis and Heicklen [210] and Cox and Patrick [61] are in reasonable agreement with the recommendation.

C6. $NO_2 + NO_3$. Data with N_2 as the bath gas from Kircher et al. [118], Smith et al. [213], Burrows et al. [38], and Wallington et al. [235] were used to obtain k_0^{300} and k_∞^{300}. A study by Orlando et al. [168] is in excellent agreement. The values of n and m are from Kircher et al. [118] and Orlando et al. [168]. Values from Croce de Cobos et al. [62] are excluded due to arguments given by Orlando et al. [168], who point out that a reanalysis of these data using better values for the rate constant for $NO_3 + NO \rightarrow 2NO_2$ yields a negative value for $NO_2 + NO_3 + M$. The study of Fowles et al. [86] is noted, but not used. Johnston et al. [106] have reviewed this reaction.

A study of the reverse reaction has been carried out by Cantrell et al. [40]. These data are in excellent agreement with those obtained by Connell and Johnston [54] and Viggiano et al. [230]. The equilibrium constant recommended in Table 3 is taken from Cantrell et al. [40], who computed it from the ratio of the rate constant of Orlando et al. [168] and their rate constants for the reverse reaction.

C7. $O_2 + NO_3$. Johnston et al. [106] and Davidson et al. [69] have suggested significant thermal decomposition of NO_3. This has been disputed by Russell et al. [194]. Davis et al. [71] claim that the barrier to thermal dissociation is 47.3 kcal mol^{-1}. This would seem to rule out such a process in the atmosphere.

D1. $CH_3 + O_2$. Low pressure limit from Selzer and Bayes [205]. (These workers determined the rate constants as a function of pressure in N_2, Ar, O_2, and He. Only the N_2 points were used directly in the evaluation, but the others are consistent.) Plumb and Ryan [184] report a value in He which is consistent within error limits with the work of Selzer and Bayes. Pilling and Smith [181] have measured this process in Ar (32-490 torr). Their low pressure limiting rate constant is consistent with this evaluation, but their high pressure value is a little low. Cobos et al. [50] have made measurements in Ar and N_2 from 0.25 to 150 atmospheres. They report parameters somewhat different than recommended here, but their data are reproduced well by the recommended values. The work of Laguna and Baughcum [128] seems to be in the fall-off region. Results of Pratt and Wood [186] in Ar are consistent with this recommendation, although the measurements are indirect. Their T dependence is within our estimate. As can be seen from Patrick and Golden [178], the above value leads to a very small β, ~.02, and thus temperature dependence is hard to calculate. The suggested value accommodates the values of Keiffer et al. [115], who measure the process in Ar between 20 and 600 torr and in the range $334 \leq T/K \leq 582$. Ryan and Plumb [197] suggest that the same type of calculation as employed by Patrick and Golden yields a reasonable value of β. We have not been able to reproduce their results. The high pressure rate constant fits the data of Cobos et al. [50]. The temperature dependence is an estimate. (Data of van den Bergh and Callear [229], Hochanadel et al. [99], Basco et al. [21], Washida and Bayes [244],

Laufer and Bass [130], and Washida [243] are also considered.) The fit to Keiffer et al. [115] is very good, suggesting that the temperature dependence for the high pressure limit is also reasonable. Kaiser [109] has determined values in reasonable agreement (±30%) with the recommended values.

D2. $C_2H_5 + O_2$. A relative rate study by Kaiser et al. [111] yields $k_\infty = (9.2 \pm 0.9) \times 10^{-12}$ cm^3 molecule^{-1}s^{-1} and $k_0 = (6.5 \pm 2.0) \times 10^{-29}$ cm^6 molecule^{-2}s^{-1} in He at 298K and pressures between 3 and 1500 torr. Their k_∞ agrees with the value calculated by Wagner et al. [232] ($k_\infty = 7 \times 10^{-12}$ cm^3 molecule^{-1}s^{-1}) using variational RRKM theory. The extrapolation to the low pressure limit is difficult due to the complex potential energy surface, but agrees with a Patrick and Golden-type calculation [178] using $\Delta H^o_o = 32.4$ kcal mol^{-1}. The recommended values use the calculated temperature dependence and a 2.5 times higher rate constant for air as the bath gas.

D3. $OH + C_2H_2$. The rate constant for this complex process has been re-examined by Smith et al. [214] in the temperature range from 228 to 1400 K, and in the pressure range 1 to 760 torr. Their analysis, which is cast in similar terms to those used here, is the source of the rate constants and temperature dependences at both limits. The negative value of m reflects the fact that their analysis includes a 1.2 kcal/mol barrier for the addition of OH to C_2H_2. The data analyzed include those of Pastrana and Carr [177], Perry et al. [179], Michael et al. [154], and Perry and Williamson [180]. Other data of Wilson and Westenberg [247], Breen and Glass [30], Smith and Zellner [218], and Davis et al. [70] were not included. Studies by Liu et al. [142] and Lai et al. [129] are in general agreement with the recommendation. Calculations of k_0 via the methods of Patrick and Golden [178] yield values compatible with those of Smith et al. [214].

D4. $OH + C_2H_4$. Experimental data of Tully [225], Davis et al. [70], Howard [100], Greiner [92], Morris et al. [158], and Overend and Paraskevopoulos [169] in helium, Atkinson et al. [15] in argon, and Lloyd et al. [143] and Cox [56] and Klein et al. [120] in nitrogen/oxygen mixtures, have been considered in the evaluation. This well-studied reaction is considerably more complex than most others in this table. The parameters recommended here fit exactly the same curve proposed by Klein et al. [120] at 298 K. An error in the k_0 value has been corrected from the previous evaluation. Discrepancies remain and the effect of multiple product channels is not well understood. Kuo and Lee [124] report very strong temperature dependence for the low pressure limit (n=4). Calculations of the type in Patrick and Golden [178] yield the recommended value. The high pressure limit temperature dependence has been determined by several workers. Almost all obtain negative activation energies, the Zellner and Lorenz [258] value being equivalent to m = +0.8 over the range ($296 < T/K < 524$) at about 1 atmosphere. Although this could theoretically arise as a result of reversibility, the equilibrium constant is too high for this possibility. If there is a product channel that proceeds with a low barrier via a tight transition state, a complex rate constant may yield the observed behavior. The actual addition process ($OH + C_2H_4$) may even have a small positive barrier. The recommended limits encompass the reported values. A new high temperature measurement has been reported by Diau and Lee [75].

D5. $CH_3O + NO$. The recommended values are taken from the results of Frost and Smith [88] in argon. Temperature dependences are from their higher temperature results. The low pressure rate constant is consistent with the measurement of McCaulley et al. [152] and Daele et al. [64] in helium and half the value from Troe-type calculations. A bimolecular (chemical activation) path also exists, forming $HNO + CH_2O$ (Frost and Smith [88]). Studies by Ohmori et al. [166] and Dobé et al. [77] are in general agreement with Frost and Smith with respect to both the addition and bimolecular pathways. (See the note in Table 1 for the bimolecular pathway.)

D6. $CH_3O + NO_2$. Recommended values at 298K from the study of Frost and Smith [89] in argon (corrected by Frost and Smith [90] and that of Biggs et al [25] in He. Low pressure results agree within a factor of two with the measurements of McCaulley et al. [151] in helium. A bimolecular (chemical activation) pathway is also observed. Temperature dependences are estimated.

D7 C_2H_5O + NO. High pressure data at 298K in Ar from Frost and Smith [88] and low pressure measurements in He by Daele et el. [65] are scaled to N_2 and fit with an expression summing the bimolecular and termolecular channels. The low pressure value agrees with theory. The bimolecular channel with an estimated rate of about 10^{-12} needs to be verified by direct studies. The temperature dependence is estimated.

D8. C_2H_5O + NO_2. High pressure rate constant at 298K from Frost and Smith [89]. Other values estimated from similar reactions.

D9. CH_3O_2 + NO_2. Parameters from a reasonable fit to the temperature- and pressure-dependent data in Sander and Watson [201] and Ravishankara et al. [187]. These references report $F_c = 0.4$, and their parameters are a somewhat better fit at all temperatures than those recommended here. We do not adopt them since they are not much better in the stratospheric range, and they would require both a change in our $F_c = 0.6$ format and the adoption of a quite large negative activation energy for k_∞. A study of the reverse reaction by Zabel et al. [255] also uses $F_c = 0.4$. The values recommended herein, taken with the value of the equilibrium constant in Table 3, fit the data in Zabel et al. [255] very well. Destriau and Troe [74] have fit the above data with k_∞ independent of temperature and $F_c = 0.36$. Bridier et al. [32] are in good agreement with this recommendation at one atmosphere and 298K.

D10. $CH_3C(O)O_2$ + NO_2. The recommended parameters are from the data of Bridier et al. [31], who report in the format represented here, but using $F_c = 0.3$. Their values are: $k_o^{300} = (2.7 \pm 1.5) \times 10^{-28}$, $k_\infty^{300} = (12.1 \pm 2.0) \times 10^{-12}$, with $n = 7.1 \pm 1.7$ and $m = 0.9 \pm 0.15$. Studies of the decomposition of $CH_3C(O)O_2NO_2$ [PAN] by Roberts and Bertman [192], Grosjean et al. [93], and Orlando et al. [167] are in accord with Bridier et al. [31]. In the former study it was shown that PAN decomposition yields only peroxyacetyl radical and NO_2; no methyl nitrate.

E1. F + O_2. A study by Pagsberg et al. [174] reports k_o in argon = 4.38×10^{-33} $(T/300)^{-1.2}$. This is in good agreement with earlier values of Smith and Wrigley [217], Smith and Wrigley [216], Shamonina and Kotov [206], Arutyunov et al. [9] and slightly lower than the values of Chen et al. [47] and Chegodaev et al. [46]. Wallington and Nielsen [241], Wallington et al. [240] and Ellerman et al. [79] confirm the value of Pagsberg et al. [174]. Lyman and Holland [145] report a slightly lower value in Ar at 298K. We assume that $\beta_{Ar} = \beta_{N2}$ at all temperatures. Pagsberg et al. [174], also determined the equilibrium constant and thus ΔH_f (FO_2). See F + O_2, Table 3. A calculation such as described in Patrick and Golden [178], using the new value yields: $k_o = 1.06 \times 10^{-33}$ $(T/300)^{-1.5}$ using $\beta_{N2} = 0.3$ (i.e., $\langle \Delta E \rangle = 2$kJ mol^{-1}). This is not good agreement.

E2. F + NO. A study by Pagsberg et al [172], taking into account data from Zetzsch [259], Skolnik et al. [211], Kim et al. [117], Pagsberg et al. [173] and Wallington et al. [238], reports rate constants for this reaction in several bath gases. Converting their values to the form used in this compilation yields the recommended parameters.

E3. F + NO_2. A study by Pagsberg et al. [171], taking into account the experimental data of Fasano and Nogar [82] and Zetzsch [259], was used to determine both the high and low pressure limits at 300 K. Converting their values to the form used in this compilation yields the recommended parameters. Treatment of the data for this system requires knowledge of the relative stabilities of FNO_2 and FONO. Patrick and Golden [178] assumed that the difference between these would be the same as between the $ClNO_2$ isomers. Theoretical work by Dixon and Christie [76], Lee and Rice [133] and Amos et al. [3] indicates that FNO_2 is 35-40 kcal mol^{-1} more stable than FONO, and therefore the measured rate refers to FNO_2 formation. The value of n = 2 is from Patrick and Golden, but consistent with Pagsberg et al.. The value of m is a rough estimate from similar reactions, but is also consistent with Pagsberg et al..

E4. FO + NO_2. Low pressure limit from strong collision calculation and $\beta = 0.33$. T dependence from resultant $\langle \Delta E \rangle = .523$ kcal mol^{-1}. High pressure limit and T dependence estimated. A theoretical study by Rayez

and Destriau [191] indicates that the product is the single isomer $FONO_2$. Bedzhanyan et al. [24] report a value extracted from a complex mixture of bath gases.

E5. $CF_3 + O_2$. Caralp et al. [42] have measured the rate constant in N_2 between 1 and 10 torr. This supplants the value from Caralp and Lesclaux [41]. Kaiser et al. [112] have extended the pressure range to 580 torr. They both recommend different parameters, but the data are well represented by the currently recommended values. Data of Ryan and Plumb [196] are in agreement.

E6. $CF_3O + NO_2$. There are no published measurements of the rate coefficient for this reaction. The reaction products have been reported by Chen et al. [48], who used photolysis of CF_3NO to prepare CF_3O_2 and subsequently CF_3O in 700 torr of air at 297 ± 2K. They considered two product channels: (a) CF_3ONO_2 obtained via three-body recombination and (b) $CF_2O + FNO_2$ obtained via fluorine transfer. Both products were observed and found to be thermally stable in their reactor. They report $k_a/(k_a+k_b) > 90\%$ and $k_b/(k_a+k_b) < 10\%$, thus the formation of CF_3ONO_2 is the dominant channel at 700 torr and 297 K.

E7. $CF_3O_2 + NO_2$. Based on experiments in O_2 of Caralp et al. [43], who suggest a somewhat different fitting procedure, but the values recommended here fit the data just as well. Destriau and Troe [74] use yet a different fitting procedure that does not represent the data quite as well as that recommended here. Reverse rate data are given by Köppenkastrop and Zabel [122].

E8. $CF_3O + CO$. Values taken from Turnipseed et al. [226]. The numbers were obtained for Ar as the bath gas and are assumed to hold for N_2 as well. The temperature dependence of the high pressure rate constant was determined over the range $233<T/K<332$ in SF_6. No temperature dependence of the low pressure limiting rate constant was reported. Wallington and Ball [236] report values in good agreement with Turnipseed et al.

E9. $CF_3O + M$. The activation energy for thermal decomposition of CF_3O to $CF_2O + F$ has been reported to be 31 kcal mol^{-1} by Kennedy and Levy [116]. Thermochemical data yield $\Delta H^o(298) = 23$ kcal mol^{-1}. This implies an intrinsic barrier of about 8 kcal mol^{-1} to elimination of F from CF_3O. Electronic structure calculations by Li and Francisco [140] support this observation. Adopting the A-factor for unimolecular dissociation, $A = 3 \times 10^{14} s^{-1}$ and E = 31 kcal mol^{-1} from Kennedy and Levy, $k_\infty(298)$ is about $6 \times 10^{-9} s^{-1}$. This corresponds to a lifetime of about 6 years; therefore, thermal decomposition of CF_3O is unimportant throughout the atmosphere.

F1. $Cl + O_2$. Nicovich et al. [161] measure $k=(9 \pm 3) \times 10^{-33}$ cm^6 $molecule^{-2} s^{-1}$ at $T = 187 \pm 6K$ in O_2. Using the methods described in Patrick and Golden [178], but adjusting the thermochemistry of ClO_2 such that $S^o_{298} = 64.3$ cal mol^{-1} K^{-1} and $\Delta H_{f,298} = 23.3 \pm 0.6$ kcal mol^{-1} ($Cl + O_2$, Table 3). We calculate 5.4×10^{-33} cm^6 $molecule^{-2}$ s^{-1} at T = 185K, with collisional efficiency of the bath gas taken from the formula $[\beta/(1-\beta^{1/2})] = \langle\Delta E\rangle/F_E kT$ and $\langle\Delta E\rangle \sim 0.5$ kcal mol^{-1} (i.e., $\beta_{185} = .42$ and $\beta_{300} = .30$). Since O_2 may be particularly efficient for this process, we use this calculation with broader error limits. The value from the calculation at 300K (i.e., 2.7×10^{-33} cm^6 $molec^{-2}$ s^{-1}) compares with an older value of Nicholas and Norrish [159] of 1.7×10^{-33} in an $N_2 + O_2$ mixture. The temperature dependence is from the calculation. Baer et al. [16] report a value at 298 K in good agreement with the value recommended here, but the temperature dependence is strikingly different, as noted by the authors.

F2. $Cl + NO$. Low pressure limit from Lee et al. [132], Clark et al. [49], Ashmore and Spencer [10], and Ravishankara et al. [188]. Temperature dependence from Lee et al. [132] and Clark et al. [49].

F3. $Cl + NO_2$. Low pressure limit and T dependence from Leu [138]. (Assuming similar T dependence in N_2 and He.) Leu [138] confirms the observation of Niki et al. [164] that both ClONO and $ClNO_2$ are formed, with the former dominating. This has been explained by Chang et al. [45], with detailed calculations in Patrick and Golden [178]. The temperature dependence is as predicted in Patrick and Golden [178]. Leu's

results are in excellent agreement with those reported in Ravishankara et al. [189]. The latter work extends to 200 torr, and the high pressure limit was chosen to fit these measurements. The temperature dependence of the high pressure limit is estimated. A turbulent flow study by Seeley et al. [204] that extends results to 250 torr of Ar is in agreement with earlier work.

F4. $Cl + CO$. From Nicovich et al. [162], who measured the process in N_2 for $185 \leq T/K \leq 260$.

F5. $Cl + C_2H_2$. The recommended values are taken from the work of Kaiser [108] and Kaiser and Wallington [110], which extends the pressure range to 0.3-6000 torr. The data are in reasonable agreement with earlier measurements of Brunning and Stief [33] and Wallington et al. [234], although the derived temperature dependence is much less than obtained by Brunning and Stief [33]. These values are compatible with earlier studies of Poulet et al. [185], Atkinson and Aschmann [12], Lee and Rowland [131] and Wallington et al. [242]. Using FTIR, Zhu et al. [260] reported branching of 16% and 84% to the trans and cis adduct isomers, respectively, at 700 torr N_2 and 295K.

F6. $Cl + C_2H_4$. Values at 300K are from Wallington et al. [234]. A study by Kaiser and Wallington [110] extends the pressure range to 0.3-6000 torr and is compatible with earlier studies. Temperature dependence is taken from Kaiser and Wallington. Values are in reasonable agreement with earlier studies.

F7 $Cl + C_2Cl_4$. New Entry. Recommendation is from the flash photolysis study of Nicovich et al. [163] done at 231-390 K in 3-700 torr N_2.

F8. $ClO + NO_2$. Several independent low pressure determinations (Zahniser et al. [256]; Birks et al. [27]; Leu et al. [139]; Lee et al. [135]) of the rate of ClO disappearance via the $ClO + NO_2 + M$ reaction are in excellent agreement and give an average $k_0(300)$ near 1.8×10^{-31} cm^6 s^{-1}. No product identification was carried out, and it was assumed that the reaction gave chlorine nitrate, $ClONO_2$. In contrast, direct measurements of the rate of thermal decomposition of $ClONO_2$ (Knauth [121]; Schonle et al. [203]; and Anderson and Fahey [8]), when combined with the accepted thermochemistry give a value lower by a factor of 3. It is concluded that earlier measurements of the heat of formation are incorrect,and so the value 5.5 kcal mol^{-1} evaluated from the kinetics by Anderson and Fahey [8] is accepted. Earlier explanations to the effect that the low pressure ClO disappearance studies measured not only a reaction forming $ClONO_2$, but also another channel forming an isomer, such as $OClNO_2$, ClOONO, or OClONO (Chang et al. [45]; Molina et al. [155]) are obviated by the above and the work of Margitan [146], Cox et al. [57], and Burrows et al. [37], which indicates that there are no isomers of $ClONO_2$ formed. Wallington and Cox [237] confirm current values but are unable to explain the effect of OClO observed by both Molina et al. [155] and themselves. A theoretical study by Rayez and Destriau [191] supports the idea of a single isomer being the product. The high pressure limit rate constants and their temperature dependence are from the model of Smith and Golden [215]. The recommended rate constants fit measured rate data for the disappearance of reactants (Cox and Lewis [60]; Dasch et al. [68]). Data from Handwerk and Zellner [94] indicate a slightly lower k_∞.

F9. $OClO + NO_3$. Friedl et al. [87], studied this system at $1 \leq P/torr \leq 5$ for Helium and $220 \leq T/K \leq 298$. They deduced values for the rate constant consistent with their data of $k_0 \sim 10^{-31}$ and $k_\infty \sim 10^{-11}$. They also suggest a value for the equilibrium constant: K/cm^3 $molecule^{-1} = 1 \times 10^{-28} \exp(9300/T)$. However, Boyd et al. [29] have raised the question of possible heterogeneous effects in this system, and further work is needed.

F10. $ClO + ClO$. The recommendation is based on data from Sander et al. (194 - 247 K) [198], Nickolaisen et al. (260 - 390 K) [160], and Trolier et al. (200 - 263 K) [224]. The latter data have been corrected for the effect of Cl_2 as third body, as suggested by Nickolaisen et al. With this adjustment all the data are in good agreement. The k_0 value for N_2 is not in accord with a Patrick and Golden-type calculation. This may be due to uncertainty in the ClOOCl thermochemistry, which is based on the equilibrium constants reported by Nickolaisen et al. and Cox and Hayman [59]. Other previous rate constant measurements, such as those of Hayman et al. [96], Cox and Derwent [58], Basco and Hunt [20], Walker [233], and Johnston et al. [107]. range from $1\text{-}5 \times 10^{-32}$ cm^6 s^{-1}, with N_2 or O_2 as third bodies. The major dimerization product is chlorine

peroxide (Birk et al. [26], DeMore and Tschuikow-Roux [73], Slanina and Uhlik [212], Stanton et al. [219] and Lee et al. [134]).

F11. $ClO + OClO$. Corrected from the entry in 94-26, which had an error in k_∞. Data are from Burkholder et al. [36], who measured the rate constant in N_2 at $200 \leq T/K \leq 260$ and densities from $(1.1\text{-}10.9) \times 10^{18}$ molecules cm^{-3}. They also measured the equilibrium constant. Parr et al. [176] also report a value for the rate constant in reasonable agreement with the recommendation.

F12. $O + OClO$. The recommendation is based on data of Colussi et al. [53] and Colussi [52], who measured the pressure dependence between 248 and 312K. Their results are consistent with calculations. A zero pressure rate constant of $(1.6 \pm 0.4) \times 10^{-13}$ cm^3 s^{-1} is reported for the chemical activation channel producing $ClO + O_2$, and their value of $\Delta H^o_f(ClO_3) = 52$ kcal mol^{-1} is derived at 298K. A low pressure study by Gleason et al. [91] suggests a direct abstraction as well. See Table 1.

F13. $CH_2Cl + O_2$. Measured by Fenter et al. [83] over the range $298 \leq T/K \leq 448$ and $1 \leq P/torr \leq 760$ in nitrogen. Two different techniques were employed: laser photolysis/photoionization mass spectrometry in the range 1-10 torr and laser photolysis/UV absorption for the range 20-760 torr.

F14. $CHCl_2 + O_2$. Measured by Fenter et al. [83] over the range $298 \leq T/K \leq 383$ and $1 \leq P/Torr \leq 760$ in nitrogen. Two different techniques were employed: laser photolysis/photoionization mass spectrometry in the range 1-10 torr and laser photolysis/UV absorption for the range 20-760 torr. A study by Nottingham et al. [165], in He, is in agreement.

F15. $CCl_3 + O_2$. Fenter et al. [84] present new data for this reaction. They combine these new data with those of Danis et al. [67] to determine the recommended rate parameters. Experimental data of Ryan and Plumb [197] have been considered in the evaluation. A study by Nottingham et al. [165], in He, is in agreement. A Patrick and Golden-type calculation using the thermochemistry of Russell et al. [195] yields $k_o^{300} = 1.5 \times 10^{-30}$, with $\beta = 0.3$. A value of $k_\infty^{300} = 5 \times 10^{-12}$ has been reported by Cooper et al. [55].

F16. $CFCl_2 + O_2$. Values for both low and high pressure limits at 300K are from Caralp and Lesclaux [41]. Temperature dependences are rough estimates based on calculations and similar reactions.

F17. $CF_2Cl + O_2$. Values estimated from other reactions in this series.

F18. $CCl_3O_2 + NO_2$. Based on experiments in O_2 of Caralp et al. [43], who suggest a somewhat different fitting procedure, but the values recommended here fit the data as well. Destriau and Troe [74] use yet a different fitting procedure that does not represent the data quite as well as that recommended herein. Reverse rate data are given by Köppenkastrop and Zabel [122].

F19. $CFCl_2O_2 + NO_2$. Based on experiments in O_2 of Caralp et al. [43], who suggest a somewhat different fitting procedure, but the values recommended here fit the data as well. Destriau and Troe [74] use yet a different fitting procedure that does not represent the data quite as well as that recommended herein. Reverse rate data are given by Köppenkastrop and Zabel [122].

F20. $CF_2ClO_2 + NO_2$. A study by Wu and Carr [251] supersedes the earlier work of Moore and Carr [156] and is recommended here. Reverse rate data are given by Köppenkastrop and Zabel [122] and Xiong and Carr [252].

G1. $Br+NO_2$. The recommended values are from a study by Kreutter et al. [123]. Their k_o value agrees with the measurement of Mellouki et al. [153] at 300K. A Patrick and Golden-type calculation using the known structure of the more stable $BrNO_2$ isomer and the measured equilibrium by Kreutter et al. [123] underpredicts

k_0 by an order of magnitude. Participation by other electronic states and isomers such as BrONO merits further consideration, in keeping with the chlorine analog.

G2. $BrO + NO_2$. Values from a study by Thorn et al. [221] that is in excellent agreement with Sander et al. [200] are recommended. Danis et al. [66] give slightly lower values for the low pressure limiting rate constant and a smaller temperature dependence as well. A theoretical study by Rayez and Destriau [191] suggests that the bond dissociation energy in $BrONO_2$ is higher than that in $ClONO_2$, thus rationalizing the relative values of the low pressure limiting rate constants for these two processes.

H1. I + NO. Evaluation taken from IUPAC [105]. The data is from van den Bergh et al. [227] and Basco and Hunt [19]. Although IUPAC recommends $F_c = 0.75$, any differences will be insignificant, since this reaction is in the low pressure limit under atmospheric conditions.

H2. $I + NO_2$. Evaluation taken from IUPAC [105]. The data is from van den Bergh et al. [227], Mellouki et al. [153], Buben et al. [34] and van den Bergh and Troe [228]. IUPAC uses $F_c = 0.63$, which is the same as the universal value adopted here of $F_c = 0.6$. (No evidence of possible isomers [INO_2 or IONO] is reported.)

H3. $IO + NO_2$. Data taken from Daykin and Wine [72]. They suggest $k_0 = 7.7 \times 10^{-31} (T/300)^{-5.0}$, $k_\infty = 1.5 \times 10^{-11}$ and $F_c = 0.4$. The values recommended here fit the data as well.

I1. HS + NO. Data and analysis are from the work of Black et al. [28]. The temperature dependence of k has been estimated.

I2. $CH_3S + NO$. The recommended values are from the study by Balla et al. [17] at 296K in nitrogen. Temperature dependences are derived from the higher temperature results of the same study.

I3 $O + SO_2$. New Entry. The recommendation is taken from Atkinson et al. [13] and was transformed to the format used herein.

I4. $OH + SO_2$. Values of the rate constant as a function of pressure at 298 K from Leu [137], Paraskevopoulos et al. [175], and Wine et al. [249]. The value of the low pressure limit is from Leu [137], corrected for fall-off. The high pressure limit is from a fit to all the data. The value of n comes from the above data combined with calculations such as those of Patrick and Golden [178], except that the heat of formation of $HOSO_2$ is raised by 4 kcal mol^{-1}, as suggested by the work of Margitan [147]. The value of m is estimated. This is not a radical-radical reaction and is unlikely to have a positive value of m. The limit of m = -2 corresponds to a real activation energy of ~1 kcal mol^{-1}. Earlier data listed in Baulch et al. [23] and Baulch et al. [22] are noted. Work of Martin et al. [150], Barnes et al. [18], and Lee et al. [136] confirm the current evaluation.

I5. $CH_3SCH_2 + O_2$. Wallington et al. [239] have employed a pulse radiolysis technique, allowing the derivation of $k = 5.7 \pm 0.4 \times 10^{-12}$ in 992 mbar of SF_6 at room temperature.

I6 $SO_3 + NH_3$. New Entry. (Moved from Table 1). Recommendation is from Lovejoy and Hanson [144], who studied this reaction from 10-400 torr N_2 at 295 K. They observe that the adduct isomerizes rapidly to sulfamic acid and clusters efficiently with itself and sulfuric acid. Observed sulfamic acid dimerization rate constant exceeds 5×10^{-11}. Measurements of Shen et al. [208] made at 1-2 torr He are much higher than those of Lovejoy and Hanson. Temperature dependences are rough estimates.

J1. $Na + O_2$. A study by Plane and Rajasekhar [183] finds $k_0 = (2.9 \pm 0.7) \times 10^{-30}$ at 300 K with $n = 1.30 \pm .04$. They also estimate k_∞ to be about 6×10^{-10}, with a small positive temperature dependence. Another study by Helmer and Plane [97] yields $k_0 = (3.1 \pm 0.2) \times 10^{-30}$ at 300K with $n = 1.52 \pm 0.27$. The recommended values are taken from these studies. They are consistent with values measured by Marshall et

al. [149] at 600K and those measured by Vinckier et al. [231] at higher temperature. The k_0 value is about 60% higher than that of Silver et al. [209].

J2. $NaO + O_2$. Ager and Howard [1] have measured the low pressure limit at room temperature in several bath gases. Their value in N_2 is used in the recommendation. They performed a Troe calculation, as per Patrick and Golden [178], to obtain collision efficiency and temperature dependence. They obtained a high pressure limit rate constant by use of a simple model. The temperature dependence is estimated.

J3. $NaO + CO_2$. Ager and Howard [1] have measured the rate constant for this process in the "fall-off" regime. Their lowest pressures are very close to the low pressure limit. The temperature dependence is an estimate. Ager and Howard calculate the high pressure rate constant from a simple model. The temperature dependence is an estimate.

J4. $NaOH + CO_2$. Ager and Howard [2] have measured the low pressure limiting rate constant. The temperature dependence is an estimate. Ager and Howard have calculated the high pressure limit using a simple model. The temperature dependence is an estimate.

References for Table 2

1. Ager, J.W., III and C.J. Howard, 1986, Geophys. Res. Lett., **13**, 1395-1398.
2. Ager, J.W., III and C.J. Howard, 1987, J. Geophys. Res., **92**, 6675-6678.
3. Amos, R.D., C.W. Murray, and N.C. Handy, 1993, Chem. Phys. Lett., **202**, 489-494.
4. Anastasi, C. and I.W.M. Smith, 1976, J. Chem. Soc. Faraday Trans. 2, **72**, 1459-1468.
5. Anastasi, C. and I.W.M. Smith, 1978, J. Chem. Soc. Faraday Trans. 2, **74**, 1056.
6. Anderson, J.G. and F. Kaufman, 1972, Chem. Phys. Lett., **16**, 375-379.
7. Anderson, J.G., J.J. Margitan, and F. Kaufman, 1974, J. Chem. Phys., **60**, 3310.
8. Anderson, L.C. and D.W. Fahey, 1990, J. Phys. Chem., **94**, 644-652.
9. Arutyunov, V.S., L.S. Popov, and A.M. Chaikin, 1976, Kinet. Katal., **17**, 286.
10. Ashmore, P.G. and M.S. Spencer, 1959, Trans. Faraday Soc., **55**, 1868.
11. Atkinson, D.B. and M.A. Smith, 1994, J. Phys. Chem., **98**, 5797-5800.
12. Atkinson, R. and S.M. Aschmann, 1985, Int. J. Chem. Kinet., **17**, 33-41.
13. Atkinson, R., D.L. Baulch, R.A. Cox, R.F. Hampson, J.A. Kerr, and J. Troe, 1992, J. Phys. Chem. Ref. Data, **21**, 1125-1568.
14. Atkinson, R., D.A. Hansen, and J.N. Pitts Jr., 1975, J. Chem. Phys., **62**, 3284-3288.
15. Atkinson, R., R.A. Perry, and J.N. Pitts Jr., 1977, J. Chem. Phys., **66**, 1197.
16. Baer, S., H. Hippler, R. Rahn, M. Siefke, N. Seitzinger, and J. Troe, 1991, J. Chem. Phys., **95**, 6463-6470.
17. Balla, R.J., H.H. Nelson, and J.R. McDonald, 1986, Chem. Phys., **109**, 101.
18. Barnes, I., V. Bastian, K.H. Becker, E.H. Fink, and W. Nelsen, 1986, J. Atmos. Chem., **4**, 445-466.
19. Basco, N. and J.E. Hunt, 1978, Int. J. Chem Kinet., **10**, 733-743.
20. Basco, N. and J.E. Hunt, 1979, Int. J. Chem. Kinet., **11**, 649.
21. Basco, N., D.G.L. James, and F.C. James, 1972, Int. J. Chem. Kinet. , **4**, 129.
22. Baulch, D.L., R.A. Cox, P.J. Crutzen, R.F. Hampson Jr., J.A. Kerr, J. Troe, and R.T. Watson, 1982, J. Phys. Chem. Ref. Data, **11**, 327-496.
23. Baulch, D.L., R.A. Cox, R.F. Hampson Jr., J.A. Kerr, J. Troe, and R.T. Watson, 1980, J. Phys. Chem. Ref. Data, **9**, 295-471.
24. Bedzhanyan, Y.R., E.M. Markin, and Y.M. Gershenzon, 1993, Kinetics and Catalysis, **34**, 190-193.
25. Biggs, P., C.E. Canosa-Mas, J.M. Fracheboud, D.E. Shallcross, R.P. Wayne, and F. Caralp, 1993, J. Chem. Soc. Faraday Trans., **89**, 4163-4169.
26. Birk, M., R.R. Friedl, E.A. Cohen, H.M. Pickett, and S.P. Sander, 1989, J. Chem. Phys., **91**, 6588-6597.
27. Birks, J.W., B. Shoemaker, T.J. Leck, R.A. Borders, and L.J. Hart, 1977, J. Chem. Phys., **66**, 4591.
28. Black, G., R. Patrick, L.E. Jusinski, and T.G. Slanger, 1984, J. Chem. Phys., **80**, 4065.
29. Boyd, A.A., G. Marston, and R.P. Wayne, 1996, J. Phys. Chem., **100**, 130-137.
30. Breen, J.E. and G.P. Glass, 1971, Int. J. Chem. Kinet., **3**, 145.

31. Bridier, I., F. Caralp, H. Loirat, R. Lesclaux, B. Veyret, K.H. Becker, A. Reimer, and F. Zabel, 1991, J. Phys. Chem., **95**, 3594-3600.
32. Bridier, I., R. Lesclaux, and B. Veyret, 1992, Chem. Phys. Lett., **191**, 259-263.
33. Brunning, J. and L.J. Stief, 1985, J. Chem. Phys., **83**, 1005-1009.
34. Buben, S.N., I.K. Larin, N.A. Messineva, and E.M. Trofimova, 1990, Kinetika i Kataliz, **31**, 973.
35. Burkholder, J.B., P.D. Hammer, and C.J. Howard, 1987, J. Phys. Chem., **91**, 2136-2144.
36. Burkholder, J.B., R.L. Mauldin, R.J. Yokelson, S. Solomon, and A.R. Ravishankara, 1993, J. Phys. Chem., **97**, 7597-7605.
37. Burrows, J.P., D.W.T. Griffith, G.K. Moortgat, and G.S. Tyndall, 1985, J. Phys. Chem., **89**, 266-271.
38. Burrows, J.P., G.S. Tyndall, and G.K. Moortgat, 1985, J. Phys. Chem., **89**, 4848-4856.
39. Burrows, J.P., T.J. Wallington, and R.P. Wayne, 1983, J. Chem. Soc. Faraday Trans. 2, **79**, 111-122.
40. Cantrell, C.A., R.E. Shetter, J.G. Calvert, G.S. Tyndall, and J.J. Orlando, 1993, J. Phys. Chem., **97**, 9141-9148.
41. Caralp, F. and R. Lesclaux, 1983, Chem. Phys. Lett., **102**, 54-58.
42. Caralp, F., R. Lesclaux, and A.M. Dognon, 1986, Chem. Phys. Lett., **129**, 433-438.
43. Caralp, F., R. Lesclaux, M.T. Rayez, J.-C. Rayez, and W. Forst, 1988, J. Chem. Soc. Faraday Trans. 2, **84**, 569-585.
44. Carleton, K.J., W.J. Kessler, and W.J. Marinelli, 1993, J. Phys. Chem., **97**, 6412-6417.
45. Chang, J.S., A.C. Baldwin, and D.M. Golden, 1979, Chem. Phys., **71**, 2021.
46. Chegodaev, P.P. and V.I. Tubikov, 1973, Dokl. Akad. Nauk. SSSR, **210**, 647.
47. Chen, H.L., D.W. Trainor, R.E. Center, and W.T. Fyfe, 1977, J. Chem. Phys., **66**, 5513.
48. Chen, J., V. Young, T. Zhu, and H. Niki, 1993, J. Phys. Chem., **97**, 11696-11698.
49. Clark, T.C., M.A.A. Clyne, and D.H. Stedman, 1966, Trans. Faraday Soc., **62**, 3354.
50. Cobos, C.J., H. Hippler, K. Luther, A.R. Ravishankara, and J. Troe, 1985, J. Phys. Chem., **89**, 4332-4338.
51. Cobos, C.J., H. Hippler, and J. Troe, 1985, J. Phys. Chem., **89**, 342-349.
52. Colussi, A.J., 1990, J. Phys. Chem., **94**, 8922-8926.
53. Colussi, A.J., S.P. Sander, and R.R. Friedl, 1992, J. Phys.Chem., **96**, 4442-4445.
54. Connell, P.S. and H.S. Johnston, 1979, Geophys. Res. Lett., **6**, 553.
55. Cooper, R., J.B. Cumming, S. Gordon, and W.A. Mulac, 1980, Radiat. Phys. Chem., **16**, 169.
56. Cox, R.A., 1975, Int. J. Chem. Kinet. Symp., **1**, 379.
57. Cox, R.A., J.P. Burrows, and G.B. Coker, 1984, Int. J. Chem. Kinet., **16**, 445-67.
58. Cox, R.A. and R.G. Derwent, 1979, J. Chem. Soc. Far. Trans. 1, **75**, 1635-1647.
59. Cox, R.A. and G.D. Hayman, 1988, Nature, **332**, 796-800.
60. Cox, R.A. and R. Lewis, 1979, J. Chem. Soc. Faraday Trans. 1, **75**, 2649.
61. Cox, R.A. and R. Patrick, 1979, Int. J. Chem. Kinet., **11**, 635.
62. Croce de Cobos, A.E., H. Hippler, and J. Troe, 1984, J. Phys. Chem., **88**, 5083-5086.
63. Croce de Cobos, A.E. and J. Troe, 1984, Int. J. Chem. Kinet., **16**, 1519-1530.
64. Daele, V., G. Laverdet, G. Le Bras, and G. Poulet, 1995, J. Phys. Chem., **99**, 1470-1477.
65. Daele, V., A. Ray, I. Vassali, G. Poulet, and G. Le Bras, 1995, Int. J. Chem. Kinet., **27**, 1121-1133.
66. Danis, F., F. Caralp, J. Masanet, and R. Lesclaux, 1990, Chem. Phys. Lett., **167**, 450.
67. Danis, F., F. Caralp, M. Rayez, and R. Lesclaux, 1991, J. Phys. Chem., **95**, 7300-7307.
68. Dasch, W., K.-H. Sternberg, and R.N. Schindler, 1981, Ber. Bunsenges. Phys. Chem., **85**, 611.
69. Davidson, J.A., C.A. Cantrell, R.E. Shetter, A.H. McDaniel, and J.G. Calvert, 1990, J. Geophys. Res., **95**, 13963-13969.
70. Davis, D.D., S. Fischer, R. Schiff, R.T. Watson, and W. Bollinger, 1975, J. Chem. Phys., **63**, 1707.
71. Davis, H.F., B. Kim, H.S. Johnston, and Y.T. Lee, 1993, J. Phys. Chem., **97**, 2172-2180.
72. Daykin, E.P. and P.H. Wine, 1990, J. Phys. Chem. , **94**, 4528-4535.
73. DeMore, W.B. and E. Tschuikow-Roux, 1990, J. Phys. Chem., **94**, 5856-5860.
74. Destriau, M. and J. Troe, 1990, Int. J. Chem. Kinet., **22**, 915-934.
75. Diau, E.W.-G. and Y.-P. Lee, 1992, J. Chem. Phys., **96**, 377-386.
76. Dixon, D.A. and K.O. Christie, 1992, J. Phys. Chem., **95**, 1018-1021.
77. Dobe, S., G. Lendvay, I. Szilagyi, and T. Berces, 1994, Int. J. Chem. Kinet., **26**, 887-901.
78. Donahue, N.M., M.K. Dubey, R. Mohrschladt, K. Demerjian, and J.G. Anderson, 1996, Accepted by J. Geophys. Res.
79. Ellerman, T., J. Sehested, O.J. Nielson, P. Pagsberg, and T.J. Wallington, 1994, Chem. Phys. Lett., **218**, 287-294.

80. Erler, K., D. Field, R. Zellner, and I.W.M. Smith, 1977, Ber. Bunsenges. Phys. Chem., **81**, 22.
81. Fagerstrom, K., A. Lund, G. Mahmound, J.T. Jodkowski, and E. Ratajczak, 1994, Chem. Phys. Lett., **224**, 43-50.
82. Fasano, D.M. and N.S. Nogar, 1983, J. Chem. Phys., **78**, 6688-6694.
83. Fenter, F.F., P.D. Lightfoot, F. Caralp, R. Lesclaux, J.T. Niranen, and D. Gutman, 1993, J. Phys. Chem., **97**, 4695-4703.
84. Fenter, F.F., P.D. Lightfoot, J.T. Niranen, and D. Gutman, 1993, J. Phys. Chem., **97**, 5313-5320.
85. Forster, R., M. Frost, H.F. Hamann, H. Hippler, Schlepegreli, and J. Troe, 1996, J. Chem. Phys., **103**, 2949-2958.
86. Fowles, M., D.N. Mitchell, J.W.L. Morgan, and R.P. Wayne, 1982, J. Chem. Soc. Faraday Trans. 2, **78**, 1239-1248.
87. Friedl, R.R., S.P. Sander, and Y.L. Yung, 1992, J. Phys. Chem., **96**, 7490-7493.
88. Frost, M.J. and I.W.M. Smith, 1990, J. Chem. Soc. Farad. Trans., **86**, 1757-1762.
89. Frost, M.J. and I.W.M. Smith, 1990, J. Chem. Soc. Farad. Trans., **86**, 1751-1756.
90. Frost, M.J. and I.W.M. Smith, 1993, J. Chem. Soc. Faraday Trans, **89**, 4251.
91. Gleason, J.F., F.L. Nesbitt, and L.J. Stief, 1994, J. Phys. Chem., **98**, 126-131.
92. Greiner, N.R., 1970, J. Chem. Phys., **53**, 1284-1285.
93. Grosjean, D., E. Grosjean, and E.L. Williams, 1994, J. Air and Waste Manage. Assoc., **44**, 391-396.
94. Handwerk, V. and R. Zellner, 1984, Ber. Bunsenges. Phys. Chem., **88**, 405.
95. Harris, G.W. and R.P. Wayne, 1975, J. Chem. Soc. Faraday Trans. 1, **71**, 610.
96. Hayman, G.D., J.M. Davies, and R.A. Cox, 1986, Geophys. Res. Lett., **13**, 1347-1350.
97. Helmer, M. and J.M.C. Plane, 1993, J. Geophys. Res., **98**, 23207-23222.
98. Hippler, H., R. Rahn, and J. Troe, 1990, J. Chem. Phys., **93**, 6560.
99. Hochanadel, C.J., J.A. Ghormley, J.W. Boyle, and P.J. Ogren, 1977, J. Phys. Chem., **81**, 3.
100. Howard, C.J., 1976, J. Chem. Phys., **65**, 4771.
101. Howard, C.J., 1977, J. Chem. Phys., **67**, 5258.
102. Howard, C.J. and K.M. Evenson, 1974, J. Chem. Phys., **61**, 1943.
103. Hsu, K.J., S.M. Anderson, J.L. Durant, and F. Kaufman, 1989, J. Phys. Chem., **93**, 1018.
104. Hsu, K.J., J.L. Durant, and F. Kaufman, 1987, J. Phys. Chem., **91**, 1895-1899.
105. IUPAC, 1992, J. Phys. Chem. Ref. Data, **21**, 1125-1568.
106. Johnston, H.S., C.A. Cantrell, and J.G. Calvert, 1986, J. Geophys. Res., **91**, 5159-5172.
107. Johnston, H.S., E.D. Morris Jr., and J. Van den Bogaerde, 1969, J. Am. Chem. Soc., **91**, 7712.
108. Kaiser, E.W., 1992, Int. J. Chem. Kinet., **24**, 179-189.
109. Kaiser, E.W., 1993, J. Phys. Chem., **97**, 11681-11688.
110. Kaiser, E.W. and T.J. Wallington, 1996, J. Phys. Chem., **100**, 4111-4119.
111. Kaiser, E.W., T.J. Wallington, and J.M. Andino, 1990, Chem. Phys. Lett., **168**, 309.
112. Kaiser, E.W., T.J. Wallington, and M.D. Hurley, 1995, Int. J. Chem. Kinet., **27**, 205-218.
113. Kajimoto, O. and R.J. Cvetanovic, 1976, J. Chem. Phys., **64**, 1005.
114. Kaye, J.A., 1986, J. Geophys. Res., **91**, 7865-7874.
115. Keiffer, M., M.J. Pilling, and M.J.C. Smith, 1987, J. Phys. Chem., **91**, 6028-6034.
116. Kennedy, R.C. and J.B. Levy, 1972, J. Phys. Chem., **76**, 3480-3488.
117. Kim, P., D.I. MacLean, and W.G. Valence, 1980, J. Phys. Chem., **84**, 1806.
118. Kircher, C.C., J.J. Margitan, and S.P. Sander, 1984, J. Phys. Chem., **88**, 4370-4375.
119. Klais, O., P.C. Anderson, and M.J. Kurylo, 1980, Int. J. Chem. Kinet., **12**, 469.
120. Klein, T., I. Barnes, K.H. Becker, E.H. Fink, and F. Zabel, 1984, J. Phys. Chem., **88**, 5020-5025.
121. Knauth, H.D., 1978, Ber. Bunsenges. Phys. Chem., **82**, 212.
122. Köppenkastrop, D. and F. Zabel, 1991, Int. J. Chem. Kinet., **23**, 1-15.
123. Kreutter, K.D., J.M. Nicovich, and P.H. Wine, 1991, J. Phys. Chem., **95**, 4020.
124. Kuo, C.H. and Y.P. Lee, 1991, J. Phys. Chem., **95**, 1253.
125. Kurylo, M.J., 1972, J. Phys. Chem., **76**, 3518.
126. Kurylo, M.J. and P.A. Ouellette, 1986, J. Phys. Chem., **90**, 441-444.
127. Kurylo, M.J. and P.A. Ouellette, 1987, J. Phys. Chem., **91**, 3365-3368.
128. Laguna, G.A. and S.L. Baughcum, 1982, Chem. Phys. Lett., **88**, 568-71.
129. Lai, L.-H., Y.-C. Hsu, and Y.-P. Lee, 1992, J. Chem. Phys., **97**, 3092-3099.
130. Laufer, A.H. and A.M. Bass, 1975, Int. J. Chem. Kinet., **7**, 639.
131. Lee, F.S.C. and F.S. Rowland, 1977, J. Phys. Chem., **81**, 684.

132. Lee, J.H., J.V. Michael, W.A. Payne Jr., and L.J. Stief, 1978, J. Chem. Phys., **68**, 5410-5413.
133. Lee, T.J. and J.E. Rice, 1992, J. Chem. Phys., **97**, 4223-4232.
134. Lee, T.J., C.M. Rohlfing, and J.E. Rice, 1992, J. Chem. Phys., **97**, 6593-6605.
135. Lee, Y.-P., R.M. Stimpfle, R.A. Perry, J.A. Mucha, K.M. Evenson, D.A. Jennings, and C.J. Howard, 1982, Int. J. Chem. Kinet., **14**, 711-732.
136. Lee, Y.-Y., W.C. Kao, and Y.-P. Lee, 1990, J. Phys. Chem., **94**, 4535.
137. Leu, M.T., 1982, J. Phys. Chem., **86**, 4558.
138. Leu, M.T., 1984, Int. J. Chem. Kinet., **16**, 1311-1320.
139. Leu, M.T., C.L. Lin, and W.B. DeMore, 1977, J. Phys. Chem., **81**, 190.
140. Li, Z. and J.S. Francisco, 1989, J. Am. Chem. Soc., **111**, 5660-5667.
141. Lin, C.L. and M.T. Leu, 1982, Int. J. Chem. Kinet., **14**, 417.
142. Liu, A., W.A. Mulac, and C.D. Jonah, 1988, J. Phys. Chem., **92**, 5942-5945.
143. Lloyd, A.C., K.R. Darnall, A.M. Winer, and J.N. Pitts Jr., 1976, J. Phys. Chem., **80**, 789.
144. Lovejoy, E.R. and D.R. Hanson, 1996, J. Phys. Chem., **100**, 4459-4465.
145. Lyman, J. and R. Holland, 1988, J. Phys. Chem., **92**, 7232-7241.
146. Margitan, J.J., 1983, J. Geophys. Res., **88**, 5416-5420.
147. Margitan, J.J., 1984, J. Phys. Chem., **88**, 3314-3318.
148. Maric, D. and J.P. Burrows, 1992, J.Photochem. Photobiol. A: Chem., **66**, 291-312.
149. Marshall, P., A.S. Narayan, and A. Fontijn, 1990, J. Phys. Chem., **94**, 2998.
150. Martin, D., J.L. Jourdain, and G. Le Bras, 1986, J. Phys. Chem., **90**, 4143-4147.
151. McCaulley, J.A., S.M. Anderson, J.B. Jeffries, and F. Kaufman, 1985, Chem Phys. Lett., **115**, 180.
152. McCaulley, J.A., A.M. Moyle, M.F. Golde, S.M. Anderson, and F. Kaufman, 1990, J. Chem Soc. Farad. Trans., **86**, 4001-4009.
153. Mellouki, A., G. Laverdet, J.L. Jourdain, and G. Poulet, 1989, Int. J. Chem. Kinet., **21**, 1161.
154. Michael, J.V., D.F. Nava, R.P. Borkowski, W.A. Payne, and L.J. Stief, 1980, J. Chem. Phys., **73**, 6108.
155. Molina, M.J., L.T. Molina, and T. Ishiwata, 1980, J. Phys. Chem., **84**, 3100.
156. Moore, S.B. and R.W. Carr, 1990, J. Phys. Chem., **94**, 1393.
157. Morley, C. and I.W.M. Smith, 1972, J. Chem. Soc. Faraday Trans., **68**, 1016.
158. Morris, E.D., D.H. Stedman, and H. Niki, 1971, J. Am. Chem. Soc., **93**, 3570.
159. Nicholas, J.E. and R.G.W. Norrish, 1968, Proc. Roy. Soc. A, **307**, 391.
160. Nickolaisen, S.L., R.R. Friedl, and S.P. Sander, 1994, J. Phys. Chem., **98**, 155-169.
161. Nicovich, J.M., K.D. Kreutter, C.J. Shackelford, and P.H. Wine, 1991, Chem. Phys. Lett., **179**, 367-373.
162. Nicovich, J.M., K.D. Kreutter, and P.H. Wine, 1990, J. Chem. Phys., **92**, 3539-3544.
163. Nicovoch, J.M., S. Wang, M.L. McKee, and P.H. Wine, 1996, J. Phys. Chem., **100**, 680-688.
164. Niki, H., P.D. Maker, C.M. Savage, and L.P. Breitenbach, 1978, Chem. Phys. Lett., **59**, 78.
165. Nottingham, W.C., R.N. Rudolph, K.P. Andrews, J.H. Moore, and J.A. Tossell, 1994, Int. J. Chem. Kinet., **26**, 749-756.
166. Ohmori, K., K. Yamasaki, and H. Matsui, 1993, Bull. Chem. Soc. Jpn., **66**, 51-56.
167. Orlando, J.J., G.S. Tyndall, and J.G. Calvert, 1992, Atmos. Environ., **26A**, 3111-3118.
168. Orlando, J.J., G.S. Tyndall, C.A. Cantrell, and J.G. Calvert, 1991, J. Chem. Soc. Far. Trans., **87**, 2345-2349.
169. Overend, R.P. and G. Paraskevopoulos, 1977, J. Chem. Phys., **67**, 674.
170. Overend, R.P., G. Paraskevopoulos, and C. Black, 1976, J. Chem. Phys., **64**, 4149.
171. Pagsberg, p., A. Sillesen, J.T. Jodowski, and E. Ratajczak, 1996, Chem. Phys. Lett., **252**, 165-171.
172. Pagsberg, P., A. Sillesen, J.T. Jodowski, and E. Ratajczak, 1996, Chem. Phys. Lett., **249**, 358-364.
173. Pagsberg, P., B. Sztuba, E. Ratajczak, and A. Sillesen, 1991, Acta Chem. Scand., **45**, 329.
174. Pagsberg, P.B., E. Ratajczak, A. Sillesen, and J.T. Jodkowski, 1987, Chem. Phys. Lett., **141**, 88-94.
175. Paraskevopoulos, G., D.L. Singleton, and R.S. Irwin, 1983, Chem. Phys. Lett., **100**, 83-87.
176. Parr, A.D., R.P. Wayne, G.D. Hayman, M.E. Jenkin, and R.A. Cox, 1990, Geophys. Res. Lett., **17**, 2357-2360.
177. Pastrana, A.V. and R.W. Carr Jr., 1974, Int. J. Chem. Kinet., **6**, 587.
178. Patrick, R. and D.M. Golden, 1983, Int. J. Chem. Kinet., **15**, 1189-1227.
179. Perry, R.A., R. Atkinson, and J.N. Pitts Jr., 1977, J. Chem. Phys., **67**, 5577.
180. Perry, R.A. and D. Williamson, 1982, Chem. Phys. Lett., **93**, 331-334.
181. Pilling, M.J. and M.J.C. Smith, 1985, J. Phys. Chem., **89**, 4713-4720.
182. Pirraglia, A.N., J.V. Michael, J.W. Sutherland, and R.B. Klemm, 1989, J. Phys. Chem., **93**, 282-291.

183. Plane, J.M.C. and B. Rajasekhar, 1989, J. Phys. Chem., **93**, 3135-3140.
184. Plumb, I.C. and K.R. Ryan, 1982, Int. J. Chem. Kinet., **14**, 861-874.
185. Poulet, G., J. Barassin, G. Le Bras, and J. Combourieu, 1973, Bull. Soc. Chim. Fr., **1**, 1.
186. Pratt, G.L. and S.W. Wood, 1984, J. Chem. Soc. Faraday Trans. 1, **80**, 3419-3427.
187. Ravishankara, A.R., F.L. Eisele, and P.H. Wine, 1980, J. Chem. Phys., **73**, 3743.
188. Ravishankara, A.R., G. Smith, and D.D. Davis, paper presented at the 13th Informal Photochemistry Conference, 1978, Clearwater Beach, Florida .
189. Ravishankara, A.R., G.J. Smith, and D.D. Davis, 1988, Int. J. Chem. Kinet., **20**, 811-814.
190. Rawlins, W.T., G.E. Caledonia, and R.A. Armstrong, 1987, J. Chem. Phys., **87**, 5209-5213.
191. Rayez, M.T. and M. Destriau, 1993, Chem. Phys. Lett., **206**, 278-284.
192. Roberts, J.M. and S.B. Bertman, 1992, Int. J. Chem. Kinet., **24**, 297-307.
193. Robertshaw, J.S. and I.W.M. Smith, 1982, J. Phys. Chem., **86**, 785.
194. Russell, A.G., G.R. Cass, and J.H. Seinfeld, 1986, Environ. Sci. Technol., **20**, 1167-1172.
195. Russell, J.J., J.A. Setula, D. Gutman, F. Danis, F.Caralp, P.D. Lightfoot, R. Lesclaux, C.F. Melius, and S.M. Senkan, 1990, J. Phys. Chem., **94**, 3277-3283.
196. Ryan, K.R. and I.C. Plumb, 1982, J. Phys. Chem., **86**, 4678-4683.
197. Ryan, K.R. and I.C. Plumb, 1984, Int. J. Chem. Kinet., **16**, 591-602.
198. Sander, S.P., R.P. Friedl, and Y.L. Yung, 1989, Science, **245**, 1095-1098.
199. Sander, S.P. and M. Peterson, 1984, J. Phys. Chem., **88**, 1566-1571.
200. Sander, S.P., G.W. Ray, and R.T. Watson, 1981, J. Phys. Chem., **85**, 199.
201. Sander, S.P. and R.T. Watson, 1980, J. Phys. Chem. , **84**, 1664.
202. Schieferstein, M., K. Kohse-Höinghaus, and F. Stuhl, 1983, Ber. Bunsenges. Phys. Chem., **87**, 361-366.
203. Schonle, G., H.D. Knauth, and R.N. Schindler, 1979, J. Phys. Chem., **83**, 3297.
204. Seeley, J.V., J.T. Jayne, and M.J. Molina, 1996, J. Phys. Chem., **100**, 4019-4025.
205. Selzer, E.A. and K.D. Bayes, 1983, J. Phys. Chem., **87**, 392-394.
206. Shamonina, N.F. and A.G. Kotov, 1979, Kinet. i Kataliz., **20**, 233.
207. Sharkey, P., I.R. Sims, I.W.M. Smith, P. Bocherl, and B.R. Rowe, 1994, J. Chem. Soc. Far. Trans., **90**, 3609-3616.
208. Shen, G., M. Suto, and L.C. Lee, 1990, J. Geophys. Res., **95**, 13981-13984.
209. Silver, J.A., M.S. Zahniser, A.C. Stanton, and C.E. Kolb, 1984, 20th International Symposium on Combustion, Pittsburgh, PA, pp. 605-612.
210. Simonaitis, R. and J. Heicklen, 1978, Int. J. Chem. Kinet., **10**, 67-87.
211. Skolnik, E.D., M.G. Veysey, M.G. Ahmed, and W.E. Jones, 1975, Can. J. Chem., **53**, 3188.
212. Slanina, Z. and F. Uhlik, 1991, Chem. Phys. Lett., **182**, 51-56.
213. Smith, C.A., A.R. Ravishankara, and P.H. Wine, 1985, J. Phys. Chem., **89**, 1423-1427.
214. Smith, G.P., P.W. Fairchild, and D.R. Crosley, 1984, J. Chem. Phys., **81**, 2667.
215. Smith, G.P. and D.M. Golden, 1978, Int. J. Chem. Kinet., **10**, 489.
216. Smith, I.W.M. and D.J. Wrigley, 1981, Chem. Phys., **63**, 321.
217. Smith, I.W.M. and D.J. Wrigley, 1980, Chem. Phys. Lett., **70**, 481.
218. Smith, I.W.M. and R. Zellner, 1973, J. Chem. Soc. Faraday Trans. 2, **69**, 1617.
219. Stanton, J.F., C.M.L. Rittby, R.J. Bartlett, and D.W. Toohey, 1991, J. Phys. Chem., **95**, 2107-2110.
220. Stuhl, F. and H. Niki, 1972, J. Chem. Phys., **57**, 3677-3679.
221. Thorn, R.P., E.P. Daykin, and P.H. Wine, 1993, Int J. Chem. Kinet., **25**, 521-537.
222. Trainor, D.W. and C.W. von Rosenberg Jr., 1974, J. Chem. Phys., **61**, 1010-1015.
223. Troe, J., 1977, J. Chem. Phys., **66**, 4745.
224. Trolier, M., R.L. Mauldin III, and A.R. Ravishankara, 1990, J. Phys. Chem., **94**, 4896-4907.
225. Tully, F.P., 1983, Chem. Phys. Lett., **96**, 148-153.
226. Turnipseed, A.A., S.B. Barone, N.R. Jensen, D.R. Hanson, C.J. Howard, and A.R. Ravishankara, 1995, J. Phys. Chem., **99**, 6000-6009.
227. Van den Bergh, H., N. Benoit-Guyot, and J. Troe, 1977, Int. J. Chem Kinet., **9**, 223-234.
228. Van den Bergh, H. and J. Troe, 1976, J. Chem. Phys., **64**, 736-742.
229. Van den Bergh, H.E. and A.B. Callear, 1971, Trans. Faraday Soc., **67**, 2017.
230. Viggiano, A.A., J.A. Davidson, F.C. Fehsenfeld, and E.E. Ferguson, 1981, J. Chem. Phys., **74**, 6113.
231. Vinckier, C., A. Dumoulin, and S. DeJaegere, 1991, J. Chem. Soc. Faraday Trans., **87**, 1075-1081.

232. Wagner, A.F., I.R. Slagle, D. Sarzynski, and D. Gutman, 1990, J. Phys. Chem., **94**, 1853-1864.
233. Walker, R.W., 1972, Ph.D. Thesis, Queen Mary College University of London.
234. Wallington, T.J., J.M. Andino, I.M. Lorkovic, E.W. Kaiser, and G. Marston, 1990, J. Phys. Chem., **94**, 3644-3648.
235. Wallington, T.J., R. Atkinson, A.M. Winer, and J.N. Pitts Jr., 1987, Int. J. Chem. Kinet., **19**, 243-249.
236. Wallington, T.J. and J.C. Ball, 1995, J. Phys. Chem., **99**, 3201-3205.
237. Wallington, T.J. and R.A. Cox, 1986, J. Chem. Soc. Faraday Trans. 2, **82**, 275-289.
238. Wallington, T.J., T. Ellerman, O.J. Nielsen, and J. Sehested, 1994, J. Phys. Chem., **98**, 2346.
239. Wallington, T.J., T. Ellermann, and O.J. Nielsen, 1993, J. Phys. Chem., **97**, 8442-8449.
240. Wallington, T.J., M.M. Mariq, T. Ellerman, and O.J. Nielsen, 1992, J. Phys. Chem., **96**, 982-986.
241. Wallington, T.J. and O.J. Nielsen, 1991, Int. J. Chem. Kinet., **23**, 785-798.
242. Wallington, T.J., L.M. Skewes, and W.O. Siegl, 1988, J. Photochem. Photobiol. A, **45**, 167.
243. Washida, N., 1980, J. Chem. Phys., **73**, 1665.
244. Washida, N. and K.D. Bayes, 1976, Int. J. Chem. Kinet., **8**, 777.
245. Westenberg, A.A. and N. de Haas, 1972, J. Chem. Phys., **57**, 5375-5378.
246. Whytock, D.A., J.V. Michael, and W.A. Payne, 1976, Chem. Phys. Lett., **42**, 466-471.
247. Wilson, W.E. and A.A. Westenberg, 1967, 11th Symposium on Combustion, The Combustion Institute, Pittsburgh, pp. 1143.
248. Wine, P.H., N.M. Kreutter, and A.R. Ravishankara, 1979, J. Phys. Chem., **83**, 3191.
249. Wine, P.H., R.J. Thompson, A.R. Ravishankara, D.H. Semmes, C.A. Gump, A. Torabi, and J.M. Nicovich, 1984, J. Phys. Chem., **88**, 2095.
250. Wong, W.D. and D. Davis, 1974, Int. J. Chem. Kinet., **6**, 401.
251. Wu, F. and R.W. Carr, 1991, Int. J. Chem. Kinet., **23**, 701-715.
252. Xiong, J.Q. and R.W. Carr, 1994, J. Phys. Chem., **98**, 9811-9822.
253. Yarwood, G., J.W. Sutherland, M.A. Wickramaaratchi, and R.B. Klemm, 1991, J. Phys. Chem., **95**, 8771-8775.
254. Zabarnick, S., 1993, Chem Phys., **171**, 265-273.
255. Zabel, F., A. Reimer, K.H. Becker, and E.H. Fink, 1989, J. Phys. Chem., **93**, 5500-5507.
256. Zahniser, M.S., J. Chang, and F. Kaufman, 1977, J. Chem. Phys., **67**, 997.
257. Zellner, R., F. Ewig, R. Paschke, and G. Wagner, 1988, J. Phys. Chem., **92**, 4184-4190.
258. Zellner, R. and K. Lorenz, 1984, J. Phys. Chem., **88**, 984-989.
259. Zetzsch, C., paper presented at the European Symposium on Combustion, 1973, Academic Press, 35.
260. Zhu, T., G. Yarwood, J. Chen, and H. Niki, 1994, J. Phys. Chem., **98**, 5065-5067.

EQUILIBRIUM CONSTANTS

Format

Some of the three-body reactions in Table 2 form products which are thermally unstable at atmospheric temperatures. In such cases the thermal decomposition reaction may compete with other loss processes, such as photodissociation or radical attack. Table 3 lists the equilibrium constants, K(T), for several reactions which may fall into this category. The table has three column entries, the first two being the parameters A and B which can be used to express K(T):

$$K(T)/cm^3\ molecule^{-1} = A \exp(B/T)\ (200 < T < 300\ K)$$

The third column entry in Table 3 is the calculated value of K at 298 K.

The data sources for K(T) are described in the individual notes to Table 3.

Definitions

When values of the heats of formation and entropies of all species are known at the temperature T, we note that:

$$\log_{10}[K(T)/cm^3 molecule^{-1}] = \frac{\Delta S_T^o}{2.303R} - \frac{\Delta H_T^o}{2.303RT} + \log_{10}(T) - 21.87$$

Where the superscript "o" refers to a standard state of one atmosphere. In some cases K values were calculated from this equation, using thermochemical data. In other cases the K values were calculated directly from kinetic data for the forward and reverse reactions. When available, JANAF values were used for the equilibrium constants. The following equations were then used to calculate the parameters A and B:

$$B/^oK = 2.303 \log_{10}(K_{200}/K_{300}) \times [(300 \times 200)/(300-200)]$$

$$B/^oK = 1382 \log_{10}(K_{200}/K_{300})$$

$$\log_{10} A = \log_{10} K(T) - B/2.303\ T$$

The relationships between the parameters A and B and the quantities $\Delta S^o(298K)$ and $\Delta H^o(298K)$ are as follows:

$$A = (eR'T/N_{av}) \exp(\Delta S^o/R) = 3.7 \times 10^{-22}\ T \exp(\Delta S^o/R)$$

$$B = -\Delta H^o/R - T(K)$$

Table 3. Equilibrium Constants

Reaction	A/cm^3 molecule^{-1}	B±ΔB/°K	K_{eq}(298 K)	f(298 K)[a]	Note
$HO_2 + NO_2 \rightarrow HO_2NO_2$	2.1×10^{-27}	10900±1000	1.6×10^{-11}	5	1
$NO + NO_2 \rightarrow N_2O_3$	3.3×10^{-27}	4667±100	2.1×10^{-20}	2	2
$NO_2 + NO_2 \rightarrow N_2O_4$	5.2×10^{-29}	6643±250	2.5×10^{-19}	2	3
$NO_2 + NO_3 \rightarrow N_2O_5$	2.7×10^{-27}	11000±500	2.9×10^{-11}	1.3	4
$CH_3O_2 + NO_2 \rightarrow CH_3O_2NO_2$	1.3×10^{-28}	11200±1000	2.7×10^{-12}	2	5
$CH_3C(O)O_2 + NO_2 \rightarrow CH_3C(O)O_2NO_2$	9.0×10^{-29}	14000±200	2.3×10^{-8}	2	6
$F + O_2 \rightarrow FOO$	3.2×10^{-25}	6100±1200	2.5×10^{-16}	10	7
$Cl + O_2 \rightarrow ClOO$	5.7×10^{-25}	2500±750	2.5×10^{-21}	2	8
$Cl + CO \rightarrow ClCO$	1.6×10^{-25}	4000±500	1.1×10^{-19}	5	9
$ClO + O_2 \rightarrow ClO{\cdot}O_2$	2.9×10^{-26}	<3700	$<7.2\times10^{-21}$	-	10
$ClO + ClO \rightarrow Cl_2O_2$	1.3×10^{-27}	8744±850	7.2×10^{-15}	1.5	11
$ClO + OClO \rightarrow Cl_2O_3$	1.1×10^{-24}	5455±300	9.8×10^{-17}	3	12
$OClO + NO_3 \rightarrow O_2ClONO_2$	1×10^{-28}	9300±1000	3.6×10^{-15}	5	13
$OH + CS_2 \rightarrow CS_2OH$	4.5×10^{-25}	5140±500	1.4×10^{-17}	1.4	14
$CH_3S + O_2 \rightarrow CH_3SO_2$	1.8×10^{-27}	5545±300	2.2×10^{-19}	1.4	15

K/cm^3 molecule^{-1} = A exp (B/T) [200 < T/K < 300]

[a] f(298) is the uncertainty factor at 298 K. To calculate the uncertainty at other temperatures, use the expression:

$$f(T) = f(298\ K) \exp\left[\Delta B \left(\frac{1}{T} - \frac{1}{298}\right)\right].$$

Shaded areas indicate changes or additions since JPL 94-26

Notes to Table 3

1. $HO_2 + NO_2$. The value was obtained by combining the data of Sander and Peterson [44] for the rate constant of the reaction as written and that of Graham et al. [24] for the reverse reaction. From the equilibrium constant, it may be inferred that the thermal decomposition of HO_2NO_2 is unimportant in the stratosphere, but it is important in the troposphere.

2. $NO + NO_2$. The data are from JANAF [30] and Chao et al. [17]. This process is included because a recent measurement of the rate constant by Smith and Yarwood [45] and Markwalder et al. [32] shows that it is too slow to be an important rate process, but there will be some equilibrium concentration present.

3. $NO_2 + NO_2$. The data are from JANAF [30] and Vosper [48], Chao et al. [18] and Amoruso et al. [1]. Rate data for this process are reported by Brunning et al. [11], Borrell et al. [8] Gozel et al. [23] and Markwalder et al. [31]. A direct study by Harwood and Jones [25] at low temperatures is in agreement with the recommendation.

4. $NO_2 + NO_3$. The recommendation is from Cantrell et al. [15]. They report rate constants for the decomposition reaction, which they combine with the rate constants of Orlando et al. [38] to obtain the equilibrium constant. Agreement is quite good with the data of Burrows et al. [13] and Cantrell et al. [14], and the room temperature data of Tuazon et al. [46], Perner et al. [40] and Hjorth et al. [27]. A recent evaluation by Pritchard [43] is also in excellent agreement with the recommendation.

5. $CH_3O_2 + NO_2$. Thermochemical values at 300 K for $CH_3O_2NO_2$ and CH_3O_2 are from Baldwin [6]. In the absence of data, $\Delta H°$ and $\Delta S°$ were assumed to be independent of temperature. Bahta et al. [5] have measured k(dissociation) at 263 K. Using the values of k(recombination) suggested in this evaluation, they compute $K(263) = (2.68 \pm 0.26) \times 10^{-10}$ cm^3. Our values predict 3.94×10^{-10} cm^3, in good agreement.

   Zabel et al. [49] have measured k(dissociation) as a function of pressure and temperature. ($CH_3O_2 + NO_2$, Table 2). Their values are in good agreement with Bahta et al. [5] and, taken together with k(recombination), would lead to $A = 5.2 \times 10^{-28}$ and B = 10,766. This is sufficiently close to the value in Table 3 to forgo any change in parameters, but the uncertainty has been reduced. Bridier et al. [10] measure an equilibrium constant in good agreement with this recommendation.

6. $CH_3C(O)O_2 + NO_2$. New Entry. From measurements of the rate constants in both directions by Bridier et al. [9].

7. $F + O_2$. Calculated from JANAF thermochemical values except for $\Delta H_{f,298}(FO_2) = 6.24 \pm 0.5$ kcal mol^{-1}. The latter was taken from Pagsberg et al. [39]. This direct measurement, which falls between the earlier disputed values, would seem to settle that controversy, but the calculated value of k_o is not in good agreement with the experiment (see $F + O_2$ of Table 2).

8. $Cl + O_2$. Baer et al. [4] determined K in the temperature range 180 to 300K. Their value at 185.4 K (5.23×10^{-19} cm^3 molecule^{-1}) compares well with the Nicovich et al. [36] measurement $K = 4.77 \times 10^{-19}$ cm^3 molecule^{-1}, and within error with the Mauldin et al. [33] value of 2.55×10^{-19} cm^3 molecule^{-1}. A different expression for K by Avallone et al. [3] gives $S°_{298}(ClOO) = 61.8$ cal K^{-1} mol^{-1} and $\Delta H°_{f,298}$ (ClOO) = 23.3 kcal mol^{-1}. Using known thermochemistry for Cl and O_2 and computed entropy values for ClOO, $\Delta H_{f,298}$ (ClOO) = 23.3 ±0.6 kcal mole^{-1} is obtained from the Nicovich et al. [36] data. The value of $S°_{298}$ (ClOO) = 64.3 cal mole^{-1} K^{-1} used is computed from a structure with a 105° bond angle and Cl-O and O-O bond lengths of 1.73 and 1.30 Å respectively. Frequencies of 1441, 407 and 373 cm^{-1} are from Arkell and Schwager [2]. Symmetry number is 1 and degeneracy is 2.

9. Cl + CO. From Nicovich et al. [37] who measured both k and K between 185 and 260K in N_2. They report $\Delta H_{f,298}$ (ClCO) = -5.2 ± 0.7 kcal mole^{-1}.

10. $ClO + O_2$. DeMore [20] reports $K < 4 \times 10^{-18}$ cm^3 molecule^{-1} at 197K. His temperature dependence of the equilibrium constant is estimated using $S°_{298}$ ($ClO·O_2$) = 73 cal mol^{-1}K^{-1} and $\Delta H°_{298} < 7.7$ kcal mol^{-1}. A higher value of K has been proposed by Prasad [41], but it requires $S°(ClO·O_2)$ to be about 83 cal mol^{-1} K^{-1}, which seems unreasonably high. Carter and Andrews [16] found no experimental evidence for $ClO·O_2$ in

matrix experiments. Prasad and Lee [42] discuss these issues and question the validity of the upper limit reported by DeMore.

11. ClO + ClO. The value is from a third-law calculation based on the data from Cox and Hayman [19] and Nickolaisen et al. [35]. The entropy of ClOOCl, the value of which is 72.2 cal mol^{-1} K^{-1} at 300K, is calculated from structural and spectroscopic data given by Birk et al. [7]. The heat of formation at 300K is $\Delta H^0_{f,300}$ = 30.8 kcal mol^{-1}. A study of branching ratios of ClO + ClO channels in $Cl_2/O_2/O_3$ mixtures by Horowitz et al.[28] also finds the equilibrium constant in O_2 at 285 K to be in agreement wih the recommendation.

12. ClO + OClO. The value in Table 3 is that of Burkholder et al. [12] who report a second law value combining their own data and those of Hayman and Cox [26] except for the lowest temperature point from the latter study. They deduce $\Delta H_f(Cl_2O_3) \approx 37$ kcal mol^{-1} and $S°(Cl_2O_3) \approx 95$ cal mol^{-1} $°K^{-1}$. The value from Hayman and Cox [26] is in agreement with entropy calculations based on molecular properties (3rd law). All calculations assume the chlorine chlorate structure ($ClOCl(O)_2$). The deviation that Burkholder et al. [12] observe from third law behavior may indicate that the reaction is more complex than written. Other structures might be stable at the lowest temperatures (i.e., ClOOClO, OClOClO, $OClCl(O)_2$?).

13. OClO + NO_3. Deduced by Friedl et al. [22].

14. OH + CS_2. Average of the concordant recent measurements of Murrells et al. [34] and Diau and Lee [21] between 249 and 298K. The measurements of Hynes et al. [29] indicate a less stable adduct, but agree within combined experimental error.

15. CH_3S + O_2. Turnipseed et al. [47] report the equilibrium constant for $216 \leq T/K \leq 258$. From a third law analysis using ΔS^o_{237} = -36.8 ±2.6 eu, they obtain ΔH^o_{237} = -11.5±0.9 kcal/mole.

References for Table 3

1. Amoruso, A., L. Crescentini, G. Fiocco, and M. Volpe, 1993, J. Geophys. Res., **98**, 16857-16863.
2. Arkell, A. and I. Schwager, 1967, J. Amer. Chem. Soc., **89**, 5999-6006.
3. Avallone, L.M., D.W. Toohey, and J.G. Anderson, 1991, personal communication.
4. Baer, S., H. Hippler, R. Rahn, M. Siefke, N. Seitzinger, and J. Troe, 1991, J. Chem. Phys., **95**, 6463-6470.
5. Bahta, A., R. Simonaitis, and J. Heicklen, 1982, J. Phys. Chem. , **86**, 1849.
6. Baldwin, A.C., 1982, "Thermochemistry of Peroxides," Chemistry of Functional Groups, S. Patai, Editor, John Wiley and Sons Inc., New York.
7. Birk, M., R.R. Friedl, E.A. Cohen, H.M. Pickett, and S.P. Sander, 1989, J. Chem. Phys., **91**, 6588-6597.
8. Borrell, P., C.J. Cobos, and K. Luther, 1988, J. Phys. Chem., **92**, 4377-4384.
9. Bridier, I., F. Caralp, H. Loirat, R. Lesclaux, B. Veyret, K.H. Becker, A. Reimer, and F. Zabel, 1991, J. Phys. Chem., **95**, 3594-3600.
10. Bridier, I., R. Lesclaux, and B. Veyret, 1992, Chem. Phys. Lett., **191**, 259-263.
11. Brunning, J., M.J. Frost, and I.W.M. Smith, 1988, Int. J. Chem. Kinetics, **20**, 957.
12. Burkholder, J.B., R.L. Mauldin, R.J. Yokelson, S. Solomon, and A.R. Ravishankara, 1993, J. Phys. Chem., **97**, 7597-7605.
13. Burrows, J.P., G.S. Tyndall, and G.K. Moortgat, 1985, Chem. Phys. Lett., **119**, 193-198.
14. Cantrell, C.A., J.A. Davidson, A.H. McDaniel, R.E. Shetter, and J.G. Calvert, 1988, J. Chem. Phys., **88**, 4997-5006.
15. Cantrell, C.A., R.E. Shetter, J.G. Calvert, G.S. Tyndall, and J.J. Orlando, 1993, J. Phys. Chem., **97**, 9141-9148.
16. Carter, R.O. and L. Andrews, 1981, J. Phys. Chem., **85**, 2351.
17. Chao, J., R.C. Wilhoit, and B.J. Zwolinski, 1974, Thermochim. Acta, **10**, 359-360.
18. Chao, J., R.C. Wilhoit, and B.J. Zwolinski, 1974, Thermochim. Acta, **10**, 361-371.
19. Cox, R.A. and G.D. Hayman, 1988, Nature, **332**, 796-800.
20. DeMore, W.B., 1990, Geophys. Res. Lett., **17**, 2353-2355.
21. Diau, E.W.-G. and Y.-P. Lee, 1991, J. Phys. Chem., **95**, 379.
22. Friedl, R.R., S.P. Sander, and Y.L. Yung, 1992, J. Phys. Chem., **96**, 7490-7493.
23. Gozel, P., B. Calpani, and H. van den Bergh, 1984, Isrl. J. Chem., **24**, 210.
24. Graham, R.A., A.M. Winer, and J.N. Pitts Jr., 1977, Chem. Phys. Lett., **51**, 215.

25. Harwood, M.H. and R.L. Jones, 1994, J. Geophys. Res., **99**, 22995-22964.
26. Hayman, G.D. and R.A. Cox, 1989, Chem. Phys. Lett., **155**, 1-7.
27. Hjorth, J., J. Nothholt, and G. Restelli, 1992, Int. J. Chem. Kinet., **24**, 51-65.
28. Horowitz, A., J.N. Crowley, and G.K. Moortgat, 1994, J. Phys. Chem., **98**, 11924-11930.
29. Hynes, A.J., P.H. Wine, and J.M. Nicovich, 1988, J. Phys. Chem., **92**, 3846-3852.
30. JANAF, JANAF Thermochemical Tables, Third ed. 1985, National Bureau of Standards.
31. Markwalder, B., P. Gozel, and H. van den Bergh, 1992, J. Chem. Phys., **97**, 5472-5479.
32. Markwalder, B., P. Gozel, and H. van den Bergh, 1993, J. Phys. Chem., **97**, 5260-5265.
33. Mauldin, R.L., III, J.B. Burkholder, and A.R. Ravishankara, 1992, J. Phys. Chem., **96**, 2582-2588.
34. Murrells, T.P., E.R. Lovejoy, and A.R. Ravishankara, 1990, J. Phys. Chem., **94**, 2381-2386.
35. Nickolaisen, S.L., R.R. Friedl, and S.P. Sander, 1994, J. Phys. Chem., **98**, 155-169.
36. Nicovich, J.M., K.D. Kreutter, C.J. Shackelford, and P.H. Wine, 1991, Chem. Phys. Lett., **179**, 367-373.
37. Nicovich, J.M., K.D. Kreutter, and P.H. Wine, 1990, J. Chem. Phys., **92**, 3539-3544.
38. Orlando, J.J., G.S. Tyndall, C.A. Cantrell, and J.G. Calvert, 1991, J. Chem. Soc. Far. Trans., **87**, 2345-2349.
39. Pagsberg, P.B., E. Ratajczak, A. Sillesen, and J.T. Jodkowski, 1987, Chem. Phys. Lett., **141**, 88-94.
40. Perner, D., A. Schmeltekopf, R.H. Winkler, H.S. Johnston, J.G. Calvert, C.A. Cantrell, and W.R. Stockwell, 1985, J. Geophys. Res., **90**, 3807-3812.
41. Prasad, S.S., 1980, Nature, **285**, 152.
42. Prasad, S.S. and T.J. Lee, 1994, J. Geophys. Res., **99**, 8225-8230.
43. Pritchard, H.O., 1994, Int. J. Chem. Kinet., **26**, 61-72.
44. Sander, S.P. and M. Peterson, 1984, J. Phys. Chem., **88**, 1566-1571.
45. Smith, I.W.M. and G. Yarwood, 1986, Chem. Phys. Lett., **130**, 24-28.
46. Tuazon, E.C., E. Sanhueza, R. Atkinson, W.P.L. Carter, A.M. Winer, and J.N. Pitts Jr., 1984, J. Phys. Chem., **88**, 3095-3098.
47. Turnipseed, A.A., S.B. Baron, and A.R. Ravishankara, 1992, J. Phys. Chem., **96**, 7502-7505.
48. Vosper, A.J., 1970, J. Chem. Soc. A, **1970**, 625.
49. Zabel, F., A. Reimer, K.H. Becker, and E.H. Fink, 1989, J. Phys. Chem., **93**, 5500-5507.

PHOTOCHEMICAL DATA

Discussion of Format and Error Estimates

In Table 4 we present a list of photochemical reactions considered to be of stratospheric interest. The absorption cross sections of O_2 and O_3 largely determine the extent of penetration of solar radiation into the stratosphere and troposphere. Some comments and references to these cross sections are presented in the text, but only a sample of the data is listed here. (See, for example, WMO Report No. 11 [1]; WMO Report No. 16 [330]) The photodissociation of NO in the O_2 Schumann-Runge band spectral range is another important process requiring special treatment and is not discussed in this evaluation (see, for example, Frederick and Hudson [92]; Allen and Frederick [3]; WMO Report No. 11 [1], and Minschwaner and Siskind [195]).

For some other species having highly structured spectra, such as CS_2 and SO_2, some comments are given in the text, but the photochemical data are not presented. The species CH_2O, NO_2, NO_3, ClO, BrO, and OClO also have complicated spectra, but in view of their importance for atmospheric chemistry a sample of the data is presented in the evaluation; for more detailed information on their high-resolution spectra and temperature dependence, the reader is referred to the original literature.

Table 5 gives recommended reliability factors for some of the more important photochemical reactions. These factors represent the combined uncertainty in cross sections and quantum yields, taking into consideration the atmospherically important wavelength regions, and they refer to the total dissociation rate regardless of product identity. The exception is $O(^1D)$ production from photolysis of O_3: the reliability factor applies to the quantum yield at the indicated wavelengths.

The error estimates are not rigorous numbers resulting from a detailed error propagation analysis of statistical manipulations of the different sets of literature values; they merely represent a consensus among the panel members as to the reliability of the data for atmospheric photodissociation calculations, taking into account the difficulty of the measurements, the agreement among the results reported by various groups, etc.

The absorption cross sections are defined by the following expression of Beer's Law:

$$I = I_0 \exp(-\sigma n l),$$

where I_0 and I are the incident and transmitted light intensity, respectively; σ is the absorption cross section in cm^2 $molecule^{-1}$; n is the concentration in molecule cm^{-3}; and l is the pathlength in cm. The cross sections are room temperature values at the specific wavelengths listed in the table, and the expected photodissociation quantum yields are unity, unless otherwise stated.

Table 4. Photochemical Reactions

&	$O_2 + h\nu \rightarrow O + O$	
&	$O_3 + h\nu \rightarrow O_2 + O$	
*	$O_3 + h\nu \rightarrow O_2 + O(^1D)$	
	$HO_2 + h\nu \rightarrow$ products	
	$H_2O + h\nu \rightarrow H + OH$	
	$H_2O_2 + h\nu \rightarrow OH + OH$	
	$NO + h\nu \rightarrow N + O$	
&	$NO_2 + h\nu \rightarrow NO + O$	
*	$NO_3 + h\nu \rightarrow$ products	
	$N_2O + h\nu \rightarrow N_2 + O(^1D)$	
	$N_2O_5 + h\nu \rightarrow$ products	
	$NH_3 + h\nu \rightarrow NH_2 + H$	(1)
	$HONO + h\nu \rightarrow OH + NO$	
*	$HNO_3 + h\nu \rightarrow OH + NO_2$	
	$HO_2NO_2 + h\nu \rightarrow$ products	
	$CO + h\nu \rightarrow C + O$	(1)
	$CO_2 + h\nu \rightarrow CO + O$	(1)
	$CH_4 + h\nu \rightarrow$ products	(2)
	$CH_2O \rightarrow$ products	
&	$CH_3O_2 + h\nu \rightarrow$ products	
&	$C_2H_5O_2 + h\nu \rightarrow$ products	
	$CH_3OOH + h\nu \rightarrow$ products	
#	$CH_3C(O)O_2NO_2 + h\nu \rightarrow$ products	
	$HCN + h\nu \rightarrow$ products	
	$CH_3CN + h\nu \rightarrow$ products	
	$Cl_2 + h\nu \rightarrow Cl + Cl$	
	$ClO + h\nu \rightarrow Cl + O$	
	$ClOO + h\nu \rightarrow$ products	
&	$OClO + h\nu \rightarrow O + ClO$	
&	$ClO_3 + h\nu \rightarrow$ products	
&	$Cl_2O + h\nu \rightarrow$ products	
&	$Cl_2O_2 + h\nu \rightarrow$ products	
*	$Cl_2O_3 + h\nu \rightarrow$ products	
	$Cl_2O_4 + h\nu \rightarrow$ products	
	$Cl_2O_6 + h\nu \rightarrow$ products	
	$HCl + + h\nu \rightarrow H + Cl$	
	$HF + h\nu \rightarrow H + F$	
&	$HOCl + h\nu \rightarrow OH + Cl$	
	$ClNO + h\nu \rightarrow Cl + NO$	
#	$FNO + h\nu \rightarrow F + NO$	
	$ClNO_2 + h\nu \rightarrow$ products	
	$ClONO + h\nu \rightarrow$ products	
*	$ClONO_2 + h\nu \rightarrow$ products	
	$CCl_4 + h\nu \rightarrow$ products	
	$CCl_3F + h\nu \rightarrow$ products	
	$CCl_2F_2 + h\nu \rightarrow$ products	
	$CF_2ClCFCl_2 + h\nu \rightarrow$ products	
	$CF_2ClCF_2Cl + h\nu \rightarrow$ products	
	$CF_3CF_2Cl + h\nu \rightarrow$ products	
	$CF_4 + h\nu \rightarrow$ products	
	$C_2F_6 + h\nu \rightarrow$ products	
	$CCl_2O + h\nu \rightarrow$ products	
	$CClFO + h\nu \rightarrow$ products	
	$CF_2O + h\nu \rightarrow$ products	
#	$CF_3OH + h\nu \rightarrow$ products	
	$CH_3Cl + h\nu \rightarrow$ products	
	$CH_3CCl_3 + h\nu \rightarrow$ products	
	$CHClF_2 + h\nu \rightarrow$ products	
	$CH_3CF_2Cl + h\nu \rightarrow$ products	
	$CF_3CHCl_2 + h\nu \rightarrow$ products	
	$CF_3CHFCl + h\nu \rightarrow$ products	
	$CH_3CFCl_2 + h\nu \rightarrow$ products	
	$CF_3CF_2CHCl_2 + h\nu \rightarrow$ products	
	$CF_2ClCF_2CHFCl + h\nu \rightarrow$ products	
#	$CH_3OCl + h\nu \rightarrow$ products	
	$BrO + h\nu \rightarrow$ products	
#	$HOBr + h\nu \rightarrow$ products	
*	$BrONO_2 + h\nu \rightarrow$ products	
#	$BrCl + h\nu \rightarrow Br + Cl$	
	$CH_3Br + h\nu \rightarrow$ products	
	$CHBr_3 + h\nu \rightarrow$ products	
&	$CF_3Br + h\nu \rightarrow$ products	
&	$CF_2Br_2 + h\nu \rightarrow$ products	
&	$CF_2BrCF_2Br + h\nu \rightarrow$ products	
&	$CF_2ClBr + h\nu \rightarrow$ products	
	$CF_3I + h\nu \rightarrow CF_3 + I$	
	$SO_2 + h\nu \rightarrow SO + O$	
	$H_2S + h\nu \rightarrow HS + H$	(1)
	$CS_2 + h\nu \rightarrow CS + S$	
	$OCS + h\nu \rightarrow CO + S$	
	$SF_6 + h\nu \rightarrow$ products	
	$NaOH + h\nu \rightarrow Na + OH$	
	$NaCl + h\nu \rightarrow Na + Cl$	

(1) Hudson and Kieffer [132].
(2) Turco [305].
\# New Entry.
* Indicates a change in the recommendation from the previous evaluation.
& Indicates a change in the note.

Table 5. Combined Uncertainties for Cross Sections and Quantum Yields

Species	Uncertainty	
O_2 (Schumann-Runge bands)	1.2	
O_2 (Continua)	1.2	
O_3 (Cross Sections Only)	1.1	
$O_3 \rightarrow O(^1D)$, $\lambda > 310$ nm	1.3	
$O_3 \rightarrow O(^1D)$, $290 < \lambda < 310$ nm	1.2	
H_2O_2	1.3	
NO_2	1.2	
NO_3	1.5	
N_2O	1.2	
N_2O_5	2.0	
HNO_3	1.3	
HO_2NO_2	2.0	
CH_2O	1.4	
CH_3OOH	1.5	
$CH_3C(O)O_2NO_2$	1.3	$\lambda < 300$ nm
$CH_3C(O)O_2NO_2$	2.0	$\lambda \geq 300$ nm
HCl	1.1	
HOCl	1.4	
ClOOCl	1.5	$\lambda < 300$ nm
ClOOCl	3.0	$\lambda \geq 300$ nm
Cl_2O_3	1.5	$\lambda < 300$ nm
Cl_2O_3	3.0	$\lambda \geq 300$ nm
$ClONO_2$	1.3	
CCl_4	1.1	
CCl_3F	1.1	
CCl_2F_2	1.1	
CH_3Cl	1.1	
CF_2O	2.0	
CF_3Br	1.3	
CF_2ClBr	2.0	
CF_2Br_2	2.0	
$C_2F_4Br_2$	2.0	
HOBr	2.0	$\lambda < 350$ nm
HOBr	10	$\lambda \geq 350$ nm
$BrONO_2$	1.4	

$O_2 + h\nu \rightarrow O + O$

The photodissociation of molecular oxygen in the stratosphere is due primarily to absorption of solar radiation in the 200-220 nm wavelength region, i.e., within the Herzberg continuum. The 185-200 nm region-the O_2 Schumann-Runge band spectral range-is also very important, since solar radiation penetrates efficiently into the stratosphere at those wavelengths.

Frederick and Mentall [93] Herman and Mentall [121] and Anderson and Hall [8, 9] estimated O_2 absorption cross sections from balloon measurements of solar irradiance in the stratosphere. These authors find the cross sections in the 200-210 nm range to be ~35% smaller than the smallest of the older laboratory results, which are those of Shardanand and Prasad Rao [279]. The more recent laboratory studies (Johnston et al. [144]; Cheung et al. [54, 55], Jenouvrier et al. [137]) confirm the lower values obtained from solar irradiance measurements. The recommended absorption cross section values between 205 and 240 nm are listed in Table 6; they are taken from Yoshino et al. [334] and are based on the latter set of laboratory measurements. Amoruso et al. [7] have also carried out cross section measurements in this wavelength range (the Herzberg continuum); their values are ~15% lower than those reported by Yoshino et al.

Table 6. Absorption Cross Sections of O_2 Between 205 and 240 nm

λ (nm)	$10^{24}\sigma$ (cm^2)	λ (nm)	$10^{24}\sigma$ (cm^2)
205	7.35	223	3.89
206	7.13	224	3.67
207	7.05	225	3.45
208	6.86	226	3.21
209	6.68	227	2.98
210	6.51	228	2.77
211	6.24	229	2.63
212	6.05	230	2.43
213	5.89	231	2.25
214	5.72	232	2.10
215	5.59	233	1.94
216	5.35	234	1.78
217	5.13	235	1.63
218	4.88	236	1.48
219	4.64	237	1.34
220	4.46	238	1.22
221	4.26	239	1.10
222	4.09	240	1.01

The studies of the penetration of solar radiation in the atmosphere in the Schumann-Runge wavelength region were based originally on laboratory measurements of cross sections that were affected by instrumental parameters due to insufficient spectral resolution. Yoshino et al. [342] reported high resolution O_2 cross section measurements at 300 K, between 179 and 202 nm, obtaining the first set of results which is independent of the instrument width. Additional studies at other temperatures, wavelengths, and isotopic compositions have been carried out by Yoshino et al. [336, 338-341], Lewis et al. [158, 159], Cheung et al. [53], and Chiu et al. [56]. More recently, Yoshino et al. [335] reported cross sections of the Schumann-Runge bands in the window region between the rotational lines for wavelengths between 180 and 195 nm; these measurements supersede their earlier ones. Minschwaner et al. [194] have fit temperature-dependent O_2 cross sections between 175 and 204 nm with polynomial expressions, providing accurate means of determining the Schumann-Runge band cross sections with a model that incorporates the most recent laboratory data. Coquart et al. [67] have reported Herzberg continuum absorption cross sections in the wavelength region 196-205 nm of the Schumann-Runge bands.

For parameterizations of the O_2 absorption in the Schumann-Runge bands used in atmospheric modeling calculations, see, e.g., the review in WMO Report No. 16 [330]. More recent work by Murtagh [220], Nicolet and Kennes, [229] and Minschwaner et al. [194] incorporates results of the later laboratory measurements into efficient schemes for computing broad-band transmission and photolysis rates. Transmission values obtained by Murtagh [220] agree well with the WMO [330] recommendations, although the high-resolution calculations of Minschwaner and Salawitch differ with the WMO values by as much as 10 - 20% at some wavelengths.

In view of the quality of the high-resolution laboratory measurements, the primary source of uncertainty in modeling O_2 photolysis in the Schumann-Runge bands (other than the issue of absolute solar irradiance) has shifted to the choice of broadband parameterization.

$O_3 + h\nu \rightarrow O + O_2$

The O_3 absorption cross sections and their temperature dependence have been measured by several groups. An earlier review is presented in WMO Report No. 16 [330]; this reference should be consulted to obtain data for atmospheric modeling calculations. Table 7 lists merely a sample of the data taken from this review, namely the 273 K cross section values averaged over the wavelength intervals commonly employed in modeling calculations, except for the wavelength range 185 to 225 nm, where the present recommendation incorporates the averaged values from the work of Molina and Molina [206]; the older values were based on the work of Inn and Tanaka [136]. More recently, Daumont et al. [79] and Brion et al. [30] reported ozone absorption cross section measurements between 195 and 345 nm, in the temperature range 200 - 300 K; and Yoshino et al. [337] measured the cross sections in the 185 to 254 nm wavelength range at 195, 228, and 295 K; the results of these studies yield values in very good agreement with those reported by Molina and Molina [206]. Cacciani et al. [46] reported measurements of the ozone cross sections in the wavelength range from 339 to 355 nm, in reasonable agreement with the present recommendation; the same group has measured also the cross sections in the 590-610 nm region, at 230 K and at 299 K (Amoruso et al. [5]). The temperature effect on the cross sections is negligible for wavelengths shorter than ~260 nm. Recent work by Mauersberger et al. [181, 182] yields a value of 1137×10^{-20} cm^2 for the cross section at 253.7 nm, the mercury line wavelength; it is about 1% smaller than the commonly accepted value of 1147×10^{-20} cm^2 reported by Hearn [119]; about 2% smaller than the value obtained by Molina and Molina [206], 1157×10^{-20} cm^2; and 0.5% larger than the value obtained by Daumont et al. [79]. The reason for the small discrepancy, which appears to be beyond experimental precision, is unclear.

Malicet et al. [170] report cross section measurements in the 195-345 nm range, at temperatures between 218 and 295 K, with a spectral bandwidth of 0.01-0.02 nm.; the results are in good agreement with the recommended values. Their data are presented in graphical form, and are also available on floppy disks.

Table 7 Absorption Cross Sections of O_3 at 273 K

λ (nm)	10^{20} σ(cm^2) average	λ (nm)	10^{20} σ(cm^2) average
175.439 - 176.991	81.1	238.095 - 240.964	797
176.991 - 178.571	79.9	240.964 - 243.902	900
178.571 - 180.180	78.6	243.902 - 246.914	1000
180.180 - 181.818	76.3	246.914 - 250.000	1080
181.818 - 183.486	72.9	250.000 - 253.165	1130
183.486 - 185.185	68.8	253.165 - 256.410	1150
185.185 - 186.916	62.2	256.410 - 259.740	1120
186.916 - 188.679	57.6	259.740 - 263.158	1060
188.679 - 190.476	52.6	263.158 - 266.667	965
190.476 - 192.308	47.6	266.667 - 270.270	834
192.308 - 194.175	42.8	270.270 - 273.973	692
194.175 - 196.078	38.3	273.973 - 277.778	542
196.078 - 198.020	34.7	277.778 - 281.690	402
198.020 - 200.000	32.3	281.690 - 285.714	277
200.000 - 202.020	31.4	285.714 - 289.855	179
202.020 - 204.082	32.6	289.855 - 294.118	109
204.082 - 206.186	36.4	294.118 - 298.507	62.4
206.186 - 208.333	43.4	298.507 - 303.030	34.3
208.333 - 210.526	54.2	303.030 - 307.692	18.5
210.526 - 212.766	69.9	307.692 - 312.5	9.80
212.766 - 215.054	92.1	312.5 - 317.5	5.01
215.054 - 217.391	119	317.5 - 322.5	2.49
217.391 - 219.780	155	322.5 - 327.5	1.20
219.780 - 222.222	199	327.5 - 332.5	0.617
222.222 - 224.719	256	332.5 - 337.5	0.274
224.719 - 227.273	323	337.5 - 342.5	0.117
227.273 - 229.885	400	342.5 - 347.5	0.0588
229.885 - 232.558	483	347.5 - 352.5	0.0266
232.558 - 235.294	579	352.5 - 357.5	0.0109
235.294 - 238.095	686	357.5 - 362.5	0.00549

The quantum yields for $O(^1D)$ production, $\Phi(O^1D)$, for wavelengths near 310 nm, i.e., the energetic threshold or fall-off region, have been measured mostly relative to quantum yields for wavelengths shorter than 300 nm, which were assumed to be unity. There are several studies that indicate that this assumption is not correct: Fairchild et al. [88] observed approximately 10% of the primary photolysis products in the ground state channel, that is $\Phi(O^3P)$ ~0.1, at 274 nm; Sparks et al. [289] also report $\Phi(O^3P)$ ~0.1, at 266 nm; according to Brock and Watson [32] $\Phi(O^1D) = 0.88$ at 266 nm; Amimoto et al. [4] report $\Phi(O^1D) = 0.85$ at 248 nm; and Wine and Ravishankara [328] measured directly $\Phi(O^1D) = 0.9$ at 248 nm. There are also some indications that $\Phi(O^1D)$ decreases slightly between 304 and 275 nm (see Brock and Watson [31, 32]). Turnipseed et al. [307] report $\Phi(O^1D) = 0.87 \pm 0.04$ at 222 nm and 0.46 ± 0.29 at 193 nm, and Cooper et al. [65] report values between 0.83 and 0.88 in the wavelength region 221 - 243.5 nm. The photochemistry of ozone has been reviewed by Wayne [325] and by Steinfeld et al. [293]. The recommended $\phi(O^1D)$ values in the fall-off range 305 to 325 nm (the Huggins bands) are presented in Table 8, which lists the parameters for a polynomial expression that yields $\phi(O^1D)$ as a function of temperature and wavelength. The expression was developed by Michelsen et al. [193] on the basis of a model that accounts for absorption by vibrationally and rotationally excited ozone. The parameters have been adjusted to yield a value of 0.95 at 305 nm.

Our earlier recommendation for $\phi(O^1D)$ in the fall-off wavelength range was to eliminate the "tail" seen in some of the laser experiments, because it was not reproduced in the monochromator experiments. The present recommendation is to use the larger quantum yields (0.2 - 0.3) at these wavelengths- i.e., not to eliminate the tail in question, in agreement with the high resolution data of Arnold et al. [10], Brock and Watson [32], and Trolier and

Wiesenfeld [304]; with the more recent work of Takahashi et al. [298], who carried out direct quantum yield measurements at room temperature; and with the work of Ball et al. [12, 13], who measured between 227 and 300 K the quantum yield for O_2 ($^1\Delta_g$), which correlates with that of $O(^1D)$, assuming spin forbidden processes do not occur. Additional experimental work is needed to establish the temperature dependency of the quantum yield in this fall-off wavelength region.

Note that the recommendation in Table 8 applies only for $\lambda > 290$ nm. For $220 < \lambda < 280$ nm the more recent quantum yield measurements yield values around 0.85-0.9; however, the contribution from these wavelengths to $O(^1D)$ production in the stratosphere and troposphere is not significant.

The uncertainty in the quantum yield values for atmospheric modeling purposes is estimated in Table 5 as 1.2 for $290 < \lambda < 305$ nm, and 1.3 for $\lambda > 305$ nm. Considering the importance of the process additional measurements should be carried out in the fall-off region (the Huggins bands) for quantum yields and their temperature dependence.

Table 8. Quantum Yields, Φ, for Production of $O(^1D)$ in the Photolysis of O_3

λ (nm)	A	B (K)
305	0.96	5.659
306	0.96	16.56
307	1.00	47.61
308	1.09	114.2
309	1.32	230.1
310	1.80	392.1
311	2.78	586.9
312	4.63	793.3
313	7.80	981.7
314	12.6	1139
315	16.7	1225
316	19.4	1300
317	17.1	1295
318	20.7	1365
319	17.2	1282
320	16.3	1534
321	7.59	1395
322	10.9	1728
323	13.6	1701
324	10.2	1657
325	11.2	2065

$\Phi(\lambda,T) = A \exp[-B/T]$

$185K < T < 320K$

for $290 \text{ nm} < \lambda < 305\text{nm}$, $\Phi(\lambda) = 0.95$

for $\lambda > 325$ nm, $\Phi(\lambda) = 0$

$HO_2 + h\nu \rightarrow OH + H$

The absorption cross sections of the hydroperoxyl radical, HO_2, in the 200-250 nm region have been measured at room temperature by Paukert and Johnston [242]; Hochanadel et al. [123]; Cox and Burrows [70]; McAdam et al. [186]; Kurylo et al. [153]; Moortgat et al. [217]; Dagaut and Kurylo [77]; Lightfoot and Jemi-Alade [162]; who measured the cross sections up to 777 K; Crowley et al. [76]; and Sander et al. [269] at 227.5 nm. There are significant discrepancies in the cross section values, particularly around 200 nm; no definitive explanation of the differences can be offered at present.

Table 9 lists the recommended cross sections, which are taken from the review by Wallington et al. [321]. Photolysis of HO_2 in the stratosphere and troposphere is slow and can be neglected, but the UV absorption cross sections are important in laboratory studies of reaction kinetics.

Lee [156] has detected $O(^1D)$ as a primary photodissociation product at 193 and at 248 nm, with a quantum yield that is about 15 times larger at the longer wavelength. The absolute quantum yield for $O(^1D)$ production has not been reported yet.

Table 9. Absorption Cross Sections of HO_2

λ(nm)	$10^{20}\sigma(cm^2)$
190	387
200	458
210	454
220	373
230	245
240	135
250	60

$H_2O + h\nu \rightarrow H + OH$

Water vapor has a continuum absorption spectrum at wavelengths longer than 145 nm, with a maximum around 165 nm, the cross sections falling off rapidly toward longer wavelengths; the photodissociation threshold occurs at 246 nm. Below 69 nm the spectrum is also a continuum, and between 69 and 145 nm it consists of diffuse bands. In the atmosphere water vapor is photodissociated mainly by the solar Lyman alpha line (121.6 nm).

The absorption cross sections and the photochemistry of water vapor have been reviewed, for example, by Hudson [130, 131], by Hudson and Kiefer [132], by Calvert and Pitts [47], and by Okabe [234].

The recommended absorption cross sections are taken from the review by Hudson and Kiefer [132] and are listed in Table 10 between 175 and 190 nm. At these wavelengths the quantum yield for production of H and OH is unity. At shorter wavelengths H_2 and O are also formed as primary products. Stief et al. [294] report a quantum yield of 0.11 for this process between 105 and 145 nm.

Table 10. Absorption Cross Sections of H_2O Vapor

λ(nm)	$10^{20}\sigma(cm^2)$
175.5	262.8
177.5	185.4
180.0	78.1
182.5	23.0
185.0	5.5
186.0	3.1
187.5	1.6
189.3	0.7

$H_2O_2 + h\nu \rightarrow OH + OH$

The recommended 298 K absorption cross section values, listed in Table 11, are the mean of the data of Lin et al. [164], Molina and Molina [203], Nicovich and Wine [230], and Vaghjiani and Ravishankara [310]. Molina and Molina [203] supersedes the earlier results of Molina et al. [209]. Nicovich and Wine measured the cross sections at $\lambda \pm 230$ relative to the values at 202.6, $\sigma = 4.32 \times 10^{-19}$ cm^2, and at 228.8 nm, $\sigma = 1.86 \times 10^{-19}$ cm^2. The values are within 2% of the recommended value.

Table 11. Absorption Cross Sections of H_2O_2 Vapor

λ(nm)	$10^{20}\sigma$(cm^2)		λ(nm)	$10^{20}\sigma$(cm^2)	
	298 K	355 K		298 K	355 K
190	67.2		270	3.3	3.5
195	56.4		275	2.6	2.8
200	47.5		280	2.0	2.2
205	40.8		285	1.5	1.6
210	35.7		290	1.2	1.3
215	30.7		295	0.90	1.0
220	25.8		300	0.68	0.79
225	21.7		305	0.51	0.58
230	18.2	18.4	310	0.39	0.46
235	15.0	15.2	315	0.29	0.36
240	12.4	12.6	320	0.22	0.27
245	10.2	10.8	325	0.16	0.21
250	8.3	8.5	330	0.13	0.17
255	6.7	6.9	335	0.10	0.13
260	5.3	5.5	340	0.07	0.10
265	4.2	4.4	345	0.05	0.06
			350	0.04	0.05

Nicovich and Wine have measured the temperature dependence of these cross sections. They expressed the measured cross sections as the sum of two components: σ_1, due to absorption from H_2O_2, which has the O-O stretch excited; and σ_0, due to absorption by ground state molecules. For atmospheric calculations the expression given in Table 12 may be used. The photodissociation quantum yield is believed to be unity. At and above 248 nm, the major photodissociation process is that leading to OH, i.e., the quantum yield for OH production is 2 (Vaghjiani and Ravishankara [311] and Vaghjiani et al. [312]). At 193 nm this quantum yield decreases to about 1.5 (Vaghjiani et al. [312]; Schiffman et al. [273]), and the quantum yield for O-atom production increases to about 0.16 (Vaghjiani et al. [312]).

Table 12. Mathematical Expression for Absorption Cross Sections of H_2O_2 as a Function of Temperature

$$10^{21}\ \sigma(\lambda,T) = \chi \sum_{n=0}^{7} A_n\ \lambda^n + (1-\chi) \sum_{n=0}^{4} B_n\ \lambda^n$$

Where T: temperature K; λ: nm; $\chi = [1 + \exp(-1265/T)]^{-1}$

$A_0 = 6.4761 \times 10^4$	$B_0 = 6.8123 \times 10^3$
$A_1 = -9.2170972 \times 10^2$	$B_1 = -5.1351 \times 10^1$
$A_2 = 4.535649$	$B_2 = 1.1522 \times 10^{-1}$
$A_3 = -4.4589016 \times 10^{-3}$	$B_3 = -3.0493 \times 10^{-5}$
$A_4 = -4.035101 \times 10^{-5}$	$B_4 = -1.0924 \times 10^{-7}$
$A_5 = 1.6878206 \times 10^{-7}$	
$A_6 = -2.652014 \times 10^{-10}$	
$A_7 = 1.5534675 \times 10^{-13}$	

Range 260-350 nm; 200-400 K

$NO_2 + h\nu \rightarrow NO + O$

Earlier recommendations for the absorption cross sections of nitrogen dioxide were taken from the work of Bass et al. [18]. More recent measurements have been reported by Schneider et al. [274], at 298 K, for the wavelength range from 200 to 700 nm, and by Davidson et al. [81], from 270 to 420 nm, in the 232-397 K temperature range. At room temperature the agreement between these three sets of measurements is good (within 5% between 305 and 345 nm and within 10% at the longer wavelengths). The agreement is poor below room temperature, as well as at the shorter wavelengths. A possible cause for the discrepancies is the presence of N_2O_4. The corrections needed to account for the presence of this species are largest around 200 nm, where it absorbs strongly. The corrections are also large at the lowest temperatures, because a significant fraction of the NO_2 forms N_2O_4. On the other hand, there is no error apparent in the corrections carried out by Bass et al., so that the reason for the discrepancy is not clear. Measurements of the absorption cross sections in the visible (440 to 460 nm), between 273 and 404 K, have been reported by Amoruso et al. [6], and Corcoran et al. [68] carried out high-resolution measurements at a few selected wavelength ranges between 470 and 616 nm, at 295, 573 and 673 K. Additional high-resolution studies of the cross sections, mainly aimed at improving the accuracy of atmospheric measurements, have been reported by Harwood and Jones [115], Coquart et al. [66], Mérienne et al. [192], Frost et al. [94], and Harder et al. [113].

Table 13 lists the recommended absorption cross sections, averaged over the wavelength intervals used for atmospheric photodissociation calculations. For the wavelength range from 200 to 274 nm the values are taken from Schneider et al. [274]; in this range the temperature effect is negligible. For the 274 to 420 nm region the temperature-dependent values are taken from Davidson et al. [81].

Table 13. Absorption Cross Sections of NO_2

λ (nm)	10^{20} σ, average at 25°C cm^2 $molecule^{-1}$	λ (nm)	10^{20} σ, average at 0°C (cm^2 $molecule^{-1}$)	10^{22} a* (cm^2 $molecule^{-1}$ $degree^{-1}$)
202.02 - 204.08	41.45	273.97 - 277.78	5.03	0.075
204.08 - 206.19	44.78	277.78 - 281.69	5.88	0.082
206.19 - 208.33	44.54	281.69 - 285.71	7.00	-0.053
208.33 - 210.53	46.41	285.71 - 289.85	8.15	-0.043
210.53 - 212.77	48.66	289.85 - 294.12	9.72	-0.031
212.77 - 215.06	48.18	294.12 - 298.51	11.54	-0.162
215.06 - 217.39	50.22	298.51 - 303.03	13.44	-0.284
217.39 - 219.78	44.41	303.03 - 307.69	15.89	-0.357
219.78 - 222.22	47.13	307.69 - 312.50	18.67	-0.536
222.22 - 224.72	37.72	312.5 - 317.5	21.53	-0.686
224.72 - 227.27	39.29	317.5 - 322.5	24.77	-0.786
227.27 - 229.89	27.40	322.5 - 327.5	28.07	-1.105
229.89 - 232.56	27.78	327.5 - 332.5	31.33	-1.355
232.56 - 235.29	16.89	332.5 - 337.5	34.25	-1.277
235.29 - 238.09	16.18	337.5 - 342.5	37.98	-1.612
238.09 - 240.96	8.812	342.5 - 347.5	40.65	-1.890
240.96 - 243.90	7.472	347.5 - 352.5	43.13	-1.219
243.90 - 246.91	3.909	352.5 - 357.5	47.17	-1.921
246.91 - 250.00	2.753	357.5 - 362.5	48.33	-1.095
250.00 - 253.17	2.007	362.5 - 367.5	51.66	-1.322
253.17 - 256.41	1.973	367.5 - 372.5	53.15	-1.102
256.41 - 259.74	2.111	372.5 - 377.5	55.08	-0.806
259.74 - 263.16	2.357	377.5 - 382.5	56.44	-0.867
263.16 - 266.67	2.698	382.5 - 387.5	57.57	-0.945
266.67 - 270.27	3.247	387.5 - 392.5	59.27	-0.923
270.27 - 273.97	3.785	392.5 - 397.5	58.45	-0.738
		397.5 - 402.5	60.21	-0.599
		402.5 - 407.5	57.81	-0.545
		407.5 - 412.5	59.99	-1.129
		412.5 - 417.5	56.51	0.001
		417.5 - 422.5	58.12	-1.208

* The quantity **a** is the temperature coefficient of σ as defined in the equation

$\sigma(t) = \sigma(0°) + \mathbf{a} \cdot \mathbf{t}$, where **t** is in degrees Celsius.

The earlier recommendation for quantum yields was based on the work of Harker et al. [114] and of Davenport [80] for the atmospherically important 375-470 nm region. The work by Gardner et al. [97] yields values that are in much better agreement with the values reported earlier by Jones and Bayes [147]. The recommended quantum yield values, listed in Table 14, are in agreement with the recommendation of Gardner et al. [97]; they are based on a smooth fit to the data of Gardner et al. [97] for the wavelength range from 334 to 404 nm; Harker et al. [114] for 397-420 nm (corrected for cross sections); Davenport [80] for 400-420 nm; and Jones and Bayes [147] for 297-412 nm. Direct measurements of the solar photodissociation rate of NO_2 in the troposphere by Parrish et al. [241] and by Shetter et al. [280] agree better with theoretical estimates based on this recommendation than with the earlier one.

Table 14. Quantum Yields for NO_2 Photolysis

λ, nm	Φ	λ, nm	Φ
< 285	1.000	393	0.953
290	0.999	394	0.950
295	0.998	395	0.942
300	0.997	396	0.922
305	0.996	397	0.870
310	0.995	398	0.820
315	0.994	399	0.760
320	0.993	400	0.695
325	0.992	401	0.635
330	0.991	402	0.560
335	0.990	403	0.485
340	0.989	404	0.425
345	0.988	405	0.350
350	0.987	406	0.290
355	0.986	407	0.225
360	0.984	408	0.185
365	0.983	409	0.153
370	0.981	410	0.130
375	0.979	411	0.110
380	0.975	412	0.094
381	0.974	413	0.083
382	0.973	414	0.070
383	0.972	415	0.059
384	0.971	416	0.048
385	0.969	417	0.039
386	0.967	418	0.030
387	0.966	419	0.023
388	0.964	420	0.018
389	0.962	421	0.012
390	0.960	422	0.008
391	0.959	423	0.004
392	0.957	424	0.000

$NO_3 + h\nu \rightarrow NO + O_2$ (Φ_1)

$NO_3 + h\nu \rightarrow NO_2 + O$ (Φ_2)

The absorption cross sections of the nitrate free radical, NO_3, have been studied by (1) Johnston and Graham [142], (2) Graham and Johnston [109], (3) Mitchell et al. [198], (4) Marinelli et al. [179], (5) Ravishankara and Wine [251], (6) Cox et al. [69], (7) Burrows et al. [43], (8) Ravishankara and Mauldin [249], (9) Sander [267], (10) Cantrell et al. [51], (11) Canosa-Mas et al. [49], and (12) Yokelson et al. [333]. The 1st and 4th studies required calculation of the NO_3 concentration by modeling a complex kinetic system. The other studies are more direct, and the results in terms of integrated absorption coefficients are in good agreement. The recommended value at 298 K and 662 nm, (2.00 ± 0.25)x10-17 cm^2, is the average of the results of studies (4), (5), and (7) through (11). The values in the wavelength range 600-670 nm, shown in Figure 2 and listed in Table 15, were calculated using the spectra measured in studies (8), (9), and (11), and with the 662 nm value normalized to the above average. The spectra obtained in other studies are consulted for a more extended wavelength range. The temperature dependence of the 662 nm band has been studied by Ravishankara and Mauldin, Sander, Cantrell et al., and Yokelson et al. Except for Cantrell et al., these studies all showed that the cross section at 662 nm increases with decreasing temperature. The reason for this discrepancy is not clear.

The quantum yields Φ_1 and Φ_2 have been measured by Graham and Johnston [109], and under higher resolution by Magnotta and Johnston [168], who report the product of the cross section times the quantum yield in the 400 to 630 nm range. The total quantum yield value, $\Phi_1 + \Phi_2$, computed from the results of this latter study and the cross sections of Graham and Johnston [109], is above unity for λ <610 nm, which is, of course, impossible. Hence, there is some systematic error, and it is most likely in the primary quantum yield measurements. More recently, Orlando et al. [239] measured the photolysis quantum yields between 570 and 635 nm.

Johnston et al.[140] have recently re-analyzed the available laboratory data relevant to NO_3 photolysis, including quantum yield studies, chemiluminescence, LIF studies, and molecular beam scattering experiments. Their model reproduces the wavelength dependent quantum yield data reasonably well. The new recommendation is based on the J-values calculated by Johnston et al. for overhead sun in the stratosphere:

$$J_1(NO + O_2) = 0.0201\ s^{-1}$$

$$J_2(NO_2 + O) = 0.156\ s^{-1}$$

Wavelength-specific quantum yields over the temperature range 190-298 K may be found in the tabulation by Johnston et al.

The spectroscopy of NO_3 has been reviewed by Wayne et al. [326]. The reader is referred to this work for a more detailed discussion of the cross section and quantum yield data and for estimates of the photodissociation rates as a function of zenith angle.

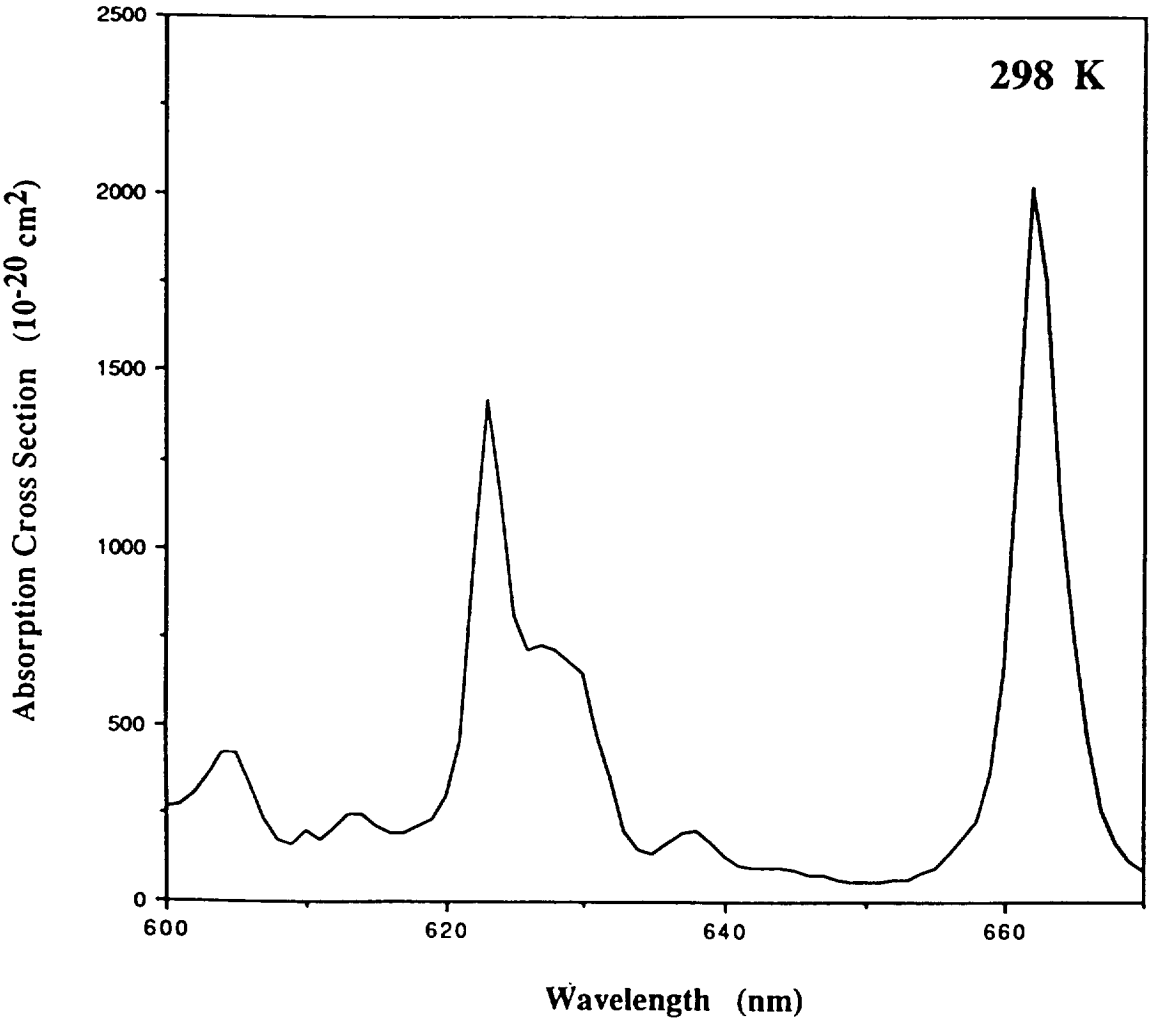

Figure 2. Absorption Spectrum of NO_3

Table 15. Absorption Cross Sections of NO_3 at 298 K

λ (nm)	$10^{20}\sigma$ (cm^2)	λ (nm)	$10^{20}\sigma$ (cm^2)	λ (nm)	$10^{20}\sigma$ (cm^2)
600	258	625	796	648	60
601	263	626	703	649	51
602	302	627	715	650	49
603	351	628	702	651	52
604	413	629	672	652	55
605	415	630	638	653	61
606	322	631	470	654	76
607	225	632	344	655	93
608	170	633	194	656	131
609	153	634	142	657	172
610	192	635	128	658	222
611	171	636	159	659	356
612	202	637	191	660	658
613	241	638	193	661	1308
614	242	639	162	662	2000
615	210	640	121	663	1742
616	190	641	99	664	1110
617	189	642	91	665	752
618	208	643	93	666	463
619	229	644	92	667	254
620	292	645	85	668	163
621	450	646	72	669	113
622	941	647	69	670	85
623	1407				
624	1139				

$N_2O + h\nu \rightarrow N_2 + O(^1D)$

The recommended values are taken from the work of Selwyn et al. [277], who measured the temperature dependence of the absorption cross sections in the atmospherically relevant wavelength region. They have fitted their data with the expression shown in Table 16; Table 17 presents the room temperature data. Hubrich and Stuhl [127] remeasured the N_2O cross sections at 298 K and 208 K and Merienne et al. [191] in the range from 220 K to 296 K. The results of these two sets of measurements are in very good agreement with those of Selwyn et al. The quantum yield for photodissociation is unity, and the products are N_2 and $O(^1D)$ (Zelikoff and Aschenbrand [343], Paraskevopoulos and Cvetanovic [240], Preston and Barr [244], Simonaitis et al. [285]). The yield of $N(^4s)$ and $NO(^2\Pi)$ is less than 1% (Greenblatt and Ravishankara [112]).

Table 16. Mathematical Expression for Absorption Cross Sections of N_2O as a Function of Temperature

$$\ln \sigma(\lambda,T) = \sum_{n=o}^{4} A_n \lambda^n + (T-300) \exp\left(\sum_{n=o}^{3} B_n \lambda^n\right)$$

Where T: temperature K; λ: nm;

$A_0 = 68.21023$	$B_0 = 123.4014$
$A_1 = -4.071805$	$B_1 = -2.116255$
$A_2 = 4.301146 \times 10^{-2}$	$B_2 = 1.111572 \times 10^{-2}$
$A_3 = -1.777846 \times 10^{-4}$	$B_3 = -1.881058 \times 10^{-5}$
$A_4 = 2.520672 \times 10^{-7}$	

Range 173 to 240 nm; 194 to 320 K

Table 17. Absorption Cross Sections of N_2O at 298 K

λ (nm)	$10^{20}\sigma$ (cm^2)	λ (nm)	$10^{20}\sigma$ (cm^2)	λ (nm)	$10^{20}\sigma$ (cm^2)
173	11.3	196	6.82	219	0.115
174	11.9	197	6.10	220	0.0922
175	12.6	198	5.35	221	0.0739
176	13.4	199	4.70	222	0.0588
177	14.0	200	4.09	223	0.0474
178	13.9	201	3.58	224	0.0375
179	14.4	202	3.09	225	0.0303
180	14.6	203	2.67	226	0.0239
181	14.6	204	2.30	227	0.0190
182	14.7	205	1.95	228	0.0151
183	14.6	206	1.65	229	0.0120
184	14.4	207	1.38	230	0.00955
185	14.3	208	1.16	231	0.00760
186	13.6	209	0.980	232	0.00605
187	13.1	210	0.755	233	0.00478
188	12.5	211	0.619	234	0.00360
189	11.7	212	0.518	235	0.00301
190	11.1	213	0.421	236	0.00240
191	10.4	214	0.342	237	0.00191
192	9.75	215	0.276	238	0.00152
193	8.95	216	0.223	239	0.00123
194	8.11	217	0.179	240	0.00101
195	7.57	218	0.142		

$N_2O_5 + h\nu \rightarrow$ Products

The absorption cross sections of dinitrogen pentoxide, N_2O_5 have been measured at room temperature by Jones and Wulf [146] between 285 and 380 nm, by Johnston and Graham [142] between 210 and 290 nm, by Graham [108] between 205 and 380 nm, and for temperatures in the 223 to 300 K range by Yao et al. [332], between 200 and 380 nm. The agreement is good, particularly considering the difficulties in handling N_2O_5. The recommended cross section values, listed in Table 18, are taken from Yao et al. [332]. For wavelengths shorter than 280 nm there is little or no temperature dependence, and between 285 and 380 nm the temperature effect is best computed with the expression listed at the bottom of Table 18. Recent measurements of the cross sections and their temperature dependence by Harwood et al. [116] yield values in excellent agreement with this recommendation except at the longest wavelengths (380 nm) and lowest temperatures (233 K), where the new values are about 30% lower. However, the contribution to solar photodissociation from these longer wavelengths is negligible, and the differences between the predicted photolysis rates from the two sets of data are smaller than 3% (Harwood et al. [116]).

There are several studies on the primary photolysis products of N_2O_5: Swanson et al. [297] have measured the quantum yield for NO_3 production at 249 and at 350 nm, obtaining a value close to unity, which is consistent with the observations of Burrows et al. [42] for photolysis at 254 nm. Barker et al. [15] report a quantum yield for $O(^3P)$ production at 290 nm of less than 0.1, and near unity for NO_3. For O-atom production Margitan (private communication, 1985) measured a quantum yield value of 0.35 at 266 nm, and Ravishankara et al. [252] report values of 0.72, 0.38, 0.21 and 0.15 at 248, 266, 287, and 289 nm, respectively, with a quantum yield near unity for NO_3 production at all these wavelengths. It appears, then, that NO_3 is produced with unit quantum yield while the O-atom, and hence the NO yield, increases at shorter wavelengths, with a consequent decrease in the NO_2 yield. The study of Oh et al. [233] indicates that, besides NO_3, the primary photolysis products are a wavelength-dependent mixture of NO_2, NO_2^* and NO + O, where NO_2^* represents one or more excited electronic states, most likely the $^2B_1$ state.

Table 18. Absorption Cross Sections of N_2O_5

λ (nm)	$10^{20}\sigma$ (cm^2)	λ (nm)	$10^{20}\sigma$ (cm^2)
200	920	245	52
205	820	250	40
210	560	255	32
215	370	260	26
220	220	265	20
225	144	270	16.1
230	99	275	13.0
235	77	280	11.7
240	62		

For 285 nm $< \lambda <$ 380 nm; 300 K $> T >$ 225 K:

$10^{20}\ \sigma = \exp[2.735 + ((4728.5 - 17.127\ \lambda)/T)]$

where σ is in cm^2/molecule; λ in nm; and T in K.

HONO + hν → OH + NO

The ultraviolet spectrum of HONO between 300 and 400 nm has been studied by Stockwell and Calvert [295] by examination of its equilibrium mixtures with NO, NO_2, H_2O, N_2O_3 and N_2O_4; the possible interferences by these compounds were taken into account. More recently, Vasudev [317] measured relative cross sections by monitoring the OH photodissociation product with laser-induced fluorescence; and Bongartz et al. [26] determined absolute cross section values at 0.1 nm resolution in a system containing a highly diluted mixture of NO, NO_2, H_2O, and HONO, by measuring total NO_x (NO and NO_2). There are some discrepancies between these two recent sets of results in terms of relative peak heights; however, both yield essentially the same photodissociation rate provided Vasudev's relative data are normalized to match the cross section value reported by Bongartz et al. at 354 nm. At this wavelength the value reported earlier by Stockwell and Calvert is about 20% smaller. The recommended values, listed in Table 19, are taken from Bongartz et al.

Table 19. Absorption Cross Sections of HONO

λ (nm)	$10^{20}\sigma$ (cm^2)	λ (nm)	$10^{20}\sigma$ (cm^2)	λ (nm)	$10^{20}\sigma$ (cm^2)
310	1.3	339	18.8	368	52.0
311	1.9	340	10.0	369	38.8
312	2.8	341	17.0	370	17.8
313	2.2	342	38.6	371	11.3
314	3.6	343	14.9	372	10.0
315	3.0	344	9.7	373	7.7
316	1.4	345	10.9	374	6.2
317	3.1	346	12.3	375	5.3
318	5.6	347	10.4	376	5.3
319	3.6	348	9.1	377	5.0
320	4.9	349	7.9	387	5.8
321	7.8	350	11.2	379	8.0
322	4.9	351	21.2	380	9.6
323	5.1	352	15.5	381	11.3
324	7.1	353	19.1	382	15.9
325	5.0	354	58.1	383	21.0
326	2.9	355	36.4	384	24.1
327	6.6	356	14.1	385	20.3
328	11.7	357	11.7	386	13.4
329	6.1	358	12.0	387	9.0
330	11.1	359	10.4	388	5.6
331	17.9	360	9.0	389	3.4
332	8.7	361	8.3	390	2.7
333	7.6	362	8.0	391	2.0
334	9.6	363	9.6	392	1.5
335	9.6	364	14.6	393	1.1
336	7.2	365	16.8	394	0.6
337	5.3	366	18.3	395	1.0
338	10.0	367	30.2	396	0.4

HNO_3 + hν → products

The recommended absorption cross sections and their temperature dependency, listed in Table 20, are taken from the work of Burkholder et al. [39]. The temperature effect is very important for estimates of atmospheric photodissociation; the results of Burkholder et al. agree well with those of Rattigan et al. [245, 246], except at 238 K, where these latter authors report significantly smaller values.

The new cross section values agree reasonably well at room temperature with the data of Molina and Molina [203], which provided the basis for the earlier recommendation. These data are also in good agreement throughout the 190-330 nm range with the values reported by Biaume [21]. They are also in very good agreement with the data of Johnston and Graham [141], except towards both ends of the wavelength range. Okabe [235] has measured the cross sections in the 110-190 nm range and his results are 20-30% lower than those of Biaume and of Johnston and Graham around 185-190 nm.

Johnston et al. [139] measured a quantum yield value of ~1 for the OH + NO_2 channel in the 200-315 nm range, using end product analysis. The quantum yield for O-atom production at 266 nm has been measured to be 0.03, and that for H-atom production less than 0.002, by Margitan and Watson [174], who looked directly for these products using atomic resonance fluorescence. Jolly et al. [145] measured a quantum yield for OH production of 0.89 ± 0.08 at 222 nm. Turnipseed et al. [308] have measured a quantum yield near unity for OH production at 248 and 222 nm. However, at 193 nm they report this quantum yield to be only ~0.33, and the quantum yield for production of O-atoms to be about 0.8. Thus, it appears that HONO is a major photolysis product at 193 nm. These results are qualitatively in agreement with those reported by Schiffman et al. [273], namely a quantum yield for OH production of 0.47 at 193 nm, and of 0.75 at 248 nm.

Table 20. Absorption Cross Sections and Temperature Coefficients of HNO_3 Vapor

λ (nm)	$10^{20}\sigma$ (cm^2)	10^3 B (K^{-1})	λ (nm)	$10^{20}\sigma$ (cm^2)	10^3 B (K^{-1})	λ (nm)	$10^{20}\sigma$ (cm^2)	10^3 B (K^{-1})
190	1360	0	244	2.16	1.75	298	0.316	2.92
192	1225	0	246	2.06	1.61	300	0.263	3.10
194	1095	0	248	2.00	1.44	302	0.208	3.24
196	940	1.70	250	1.97	1.34	304	0.167	3.52
198	770	1.65	252	1.96	1.23	306	0.133	3.77
200	588	1.66	254	1.95	1.18	308	0.105	3.91
202	447	1.69	256	1.95	1.14	310	0.0814	4.23
204	328	1.74	258	1.93	1.12	312	0.0628	4.70
206	231	1.77	260	1.91	1.14	314	0.0468	5.15
208	156	1.85	262	1.87	1.14	316	0.0362	5.25
210	104	1.97	264	1.83	1.18	318	0.0271	5.74
212	67.5	2.08	266	1.77	1.22	320	0.0197	6.45
214	43.9	2.17	268	1.70	1.25	322	0.0154	6.70
216	29.2	2.17	270	1.62	1.45	324	0.0108	7.16
218	20.0	2.21	272	1.53	1.49	326	0.00820	7.55
220	14.9	2.15	274	1.44	1.56	328	0.00613	8.16
222	11.8	2.06	276	1.33	1.64	330	0.00431	9.75
224	9.61	1.96	278	1.23	1.69	332	0.00319	9.93
226	8.02	1.84	280	1.12	1.78	334	0.00243	9.60
228	6.82	1.78	282	1.01	1.87	336	0.00196	10.5
230	5.75	1.80	284	0.909	1.94	338	0.00142	10.8
232	4.87	1.86	286	0.807	2.04	340	0.00103	11.8
234	4.14	1.90	288	0.709	2.15	342	0.00086	11.8
236	3.36	1.97	290	0.615	2.27	344	0.00069	9.30
238	2.93	1.97	292	0.532	2.38	346	0.00050	12.1
240	2.58	1.97	294	0.453	2.52	348	0.00042	11.9
242	2.34	1.88	296	0.381	2.70	350	0.00042	9.30

$\sigma(\lambda, T) = \sigma(\lambda, 298) \exp[B(\lambda)(T - 298)]$; T in K

$HO_2NO_2 + h\nu \rightarrow$ Products

There are five studies of the UV spectrum of HO_2NO_2 vapor: Cox and Patrick [72], Morel et al. [219], Graham et al. [110], Molina and Molina [203], and Singer et al. [286]. The latter three studies are the only ones covering the gas phase spectrum in the critical wavelength range for atmospheric photodissociation ($\lambda \geq$ 290 nm). The recommended values, listed in Table 21, are an average of the work of Molina and Molina [203] and of Singer et al. [286], which are the more direct studies. The cross sections appear to be temperature independent between 298 and 253 K (Singer et al. [286]). MacLeod et al. [167] report that photolysis at 248 nm yields one third OH and NO_3 and two thirds $HO_2 + NO_2$.

Table 21. Absorption Cross Sections of HO_2NO_2 Vapor

λ (nm)	$10^{20}\sigma$ (cm^2)	λ (nm)	$10^{20}\sigma$ (cm^2)
190	1010	260	28.5
195	816	265	23.0
200	563	270	18.1
205	367	275	13.4
210	239	280	9.3
215	161	285	6.2
220	118	290	3.9
225	93.5	295	2.4
230	79.2	300	1.4
235	68.2	305	0.9
240	58.1	310	0.5
245	48.9	315	0.3
250	41.2	320	0.2
255	35.0	325	0.1

$CH_2O + h\nu \rightarrow H + HCO \quad (\Phi_1)$

$CH_2O + h\nu \rightarrow H_2 + CO \quad (\Phi_2)$

The earlier recommendation for the formaldehyde absorption cross sections was based on the work carried out by Bass et al. [17] with a resolution of 0.05 nm at 296 K and 223 K, and by Moortgat et al. [214, 216] with a resolution of 0.5 nm in the 210-360 K temperature range. More recently, Cantrell et al. [50] measured the cross sections in the 300-360 nm range between 223 K and 293 K, and Rogers [260] measured the cross sections in the 235-365 nm range at 296 K, both groups using Fourier transform spectrometry at a resolution of up to 0.011 nm (1 cm^{-1}). The agreement between these two reports is very good. The recommended values are those given by Cantrell et al. as a function of temperature; the reader is referred to the original article to obtain the high-resolution data. Table 22 lists the low-resolution cross sections taken from that work, that are suitable for atmospheric photodissociation calculations.

The quantum yields have been reported with good agreement by Horowitz and Calvert [124], Clark et al. [60], Tang et al. [301], Moortgat and Warneck [218], and Moortgat et al. [214, 216]. The recommended values listed in Table 22 are based on the results of these investigators, as evaluated by S. Madronich (private communication, 1991). The quantum yield for the production of H_2 and CO is pressure- and temperature-dependent for wavelengths longer than about 330 nm (Moortgat et al. [216]). Table 22 gives the values at atmospheric pressure and room temperature; the reader is referred to the Moortgat et al. publication for information on values at lower pressures and temperatures.

Table 22. Absorption Cross Sections and Quantum Yields for Photolysis of CH_2O

λ (nm)	10^{20} σ(cm^2) 223 K	10^{20} σ(cm^2) 293 K	T-Parameters* A	T-Parameters* B	Φ_1 (H + HCO)	Φ_2 (H_2 + CO)
301.25	1.38	1.36	1.37	-0.21	0.749	0.251
303.75	4.67	4.33	4.43	-4.73	0.753	0.247
306.25	3.32	3.25	3.27	-1.06	0.753	0.247
308.75	2.27	2.22	2.24	-0.724	0.748	0.252
311.25	0.758	0.931	0.882	2.48	0.739	0.261
313.75	3.65	3.40	3.47	-3.64	0.724	0.276
316.25	4.05	3.89	3.94	-2.30	0.684	0.316
318.75	1.66	1.70	1.69	0.659	0.623	0.368
321.25	1.24	1.13	1.16	-1.52	0.559	0.423
323.75	0.465	0.473	0.471	0.118	0.492	0.480
326.25	5.06	4.44	4.61	-8.86	0.420	0.550
328.75	2.44	2.29	2.34	-2.15	0.343	0.634
331.25	1.39	1.28	1.31	-1.53	0.259	0.697
333.75	0.093	0.123	0.114	0.432	0.168	0.739
336.25	0.127	0.131	0.130	0.050	0.093	0.728
338.75	3.98	3.36	3.54	-8.96	0.033	0.667
341.25	0.805	0.936	0.898	1.86	0.003	0.602
343.75	1.44	1.26	1.31	-2.64	0.001	0.535
346.25	0.004	0.071	0.052	0.957	0	0.469
348.75	0.009	0.040	0.031	0.438	0	0.405
351.25	0.169	0.235	0.216	0.948	0	0.337
353.75	1.83	1.55	1.63	-4.05	0	0.265
356.25	0.035	0.125	0.099	1.27	0	0.197

Note: The values are averaged for 2.5 nm intervals centered on the indicated wavelength.

* Cross section for -50°C < T < 20°C calculated as $\sigma(T) = A + Bx10^{-3}$ T; T in °C, and σ in 10^{-20} cm^2.

CH_3O_2 + hν → Products

$C_2H_5O_2$ + hν → Products

The absorption cross sections have been reviewed by Wallington et al. [321] and by Lightfoot et al. [161]. Table 23 lists the recommended values, obtained as follows: the cross section value at 250 nm was set to 400 x 10^{-20} cm^2, which is the value we used previously in connection with rate constant recommendations; then, the average of the recommendations of Wallington et al. and Lightfoot et al. was used to determine the shape of the CH_3O_2 spectrum (these two sets of values agree very well with each other); finally, the cross section values at the other wavelengths were obtained by scaling the spectrum to the 250 nm value. The cross sections for $C_2H_5O_2$ were taken from Lightfoot et al., who included in their evaluation the data of Bauer et al. [19], that was not published in time to be included in the evaluation of Wallington et al. Recent studies of these spectra by Maricq and Wallington [177](CH_3O_2 and $C_2H_5O_2$), Fenter et al. [89] ($C_2H_5O_2$), and Roehl et al. [258] are in excellent agreement with the recommended values.

Table 23. Absorption Cross Sections of CH_3O_2 and $C_2H_5O_2$

λ (nm)	10^{20} σ (cm^2)	
	CH_3O_2	$C_2H_5O_2$
210.0	213	
215.0	273	251
220.0	335	310
225.0	392	361
230.0	438	402
235.0	452	428
240.0	450	436
245.0	432	427
250.0	400	400
255.0	366	361
260.0	322	315
265.0	278	265
270.0	231	214
275.0	170	167
280.0	141	126
285.0	98	91
290.0	63	65
295.0		43
300.0		

CH_3OOH + hν → Products

Vaghjiani and Ravishankara [310] measured the cross sections of CH_3OOH by monitoring the CH_3OOH concentration via trapping and titration. These results are recommended and are listed in Table 24. The earlier results of Molina and Arguello [210] are consistently 40% higher than the values shown in Table 24; this difference is believed to be due to difficulty in trapping CH_3OOH and measuring its concentration. CH_3OOH dissociates upon light absorption to give CH_3O with unit quantum yield (Vaghjiani and Ravishankara, [311]); these authors also observed some production of H and O atoms at shorter wavelengths (i.e., 193 nm). Thelen et al. [302] report unit quantum yield for OH production at 248 and 193 nm, in agreement with the results of Vaghjiani and Ravishankara.

Table 24. Absorption Cross Sections of CH_3OOH

λ (nm)	10^{20} σ (cm^2)	λ (nm)	10^{20} σ (cm^2)
210	31.2	290	0.69
220	15.4	300	0.41
230	9.62	310	0.24
240	6.05	320	0.14
250	3.98	330	0.079
260	2.56	340	0.047
270	1.70	350	0.027
280	1.09	360	0.016

HCN + hν → Products

Herzberg and Innes [122] have studied the spectroscopy of hydrogen cyanide, HCN, that starts absorbing weakly at $\lambda < 190$ nm.

The solar photodissociation rate for this molecule is rather small, even in the upper stratosphere; estimates of this rate would require additional studies of the absorption cross sections and quantum yields in the 200 nm region.

CH_3CN + hν → Products

McElcheran et al. [187] have reported the spectrum of acetonitrile or methyl cyanide, CH_3CN; the first absorption band appears at $\lambda < 220$ nm. More recently, Suto and Lee [296] and Zetzsch [344] have measured the cross sections around 200 nm; solar photodissociation is unimportant compared to reaction with OH radicals.

$CH_3C(O)O_2NO_2$ + hν → Products

Absorption spectra of $CH_3C(O)O_2NO_2$ (PAN) have been measured by Senum et al. [278] over the range 200-300 nm, Libuda and Zabel [160] over the range 220-325 nm, and Talukdar et al. [300] over the spectral range 195-345 nm and temperature range 250-298 K. The three studies are in excellent agreement over their range of overlap, with the values of Senum et al. being slightly smaller (15-20%) beyond 250 nm. Libuda and Zabel carried out simultaneous infrared absorption studies that showed that the measured cross sections need to be corrected for impurities that are transparent in the ultraviolet but contribute to the sample pressure in the absorption cell. These corrections are on the order of 20%. The recommended cross sections (Table 25) are based on the measurements of Talukdar et al. because of the good agreement with Libuda and Zabel and the wider spectral coverage and temperature range of this study. The uncertainties in the reported cross sections are probably quite large (on the order of a factor of 2), decreasing to about 30% at shorter wavelengths. The only PAN quantum yield studies are those of Mazely et al.[184, 185]. In these studies, PAN was photolyzed at 248 nm, with NO_2 and NO_3 products being observed by laser induced fluorescence at 298 K. Quantum yields of 0.83±0.09 were obtained for the $CH_3C(O)O_2 + NO_2$ channel and 0.3±0.1 for the $CH_3C(O)O + NO_3$ channel.

Table 25. Absorption Cross Sections of PAN

λ (nm)	10^{20} σ(298K) (cm^2)	10^3B (K^{-1})	λ (nm)	10^{20} σ(298K) (cm^2)	10^3B (K^{-1})
196	430	2.02	274	2.4	5.55
198	400	1.73	276	2.1	5.76
200	360	1.36	278	1.7	5.98
202	320	1.07	280	1.5	6.20
204	290	0.86	282	1.2	6.43
206	260	0.75	284	1.0	6.67
208	230	0.71	286	0.81	6.90
210	200	0.75	288	0.65	7.15
212	170	0.84	290	0.54	7.39
214	140	0.97	292	0.45	7.63
216	120	1.12	294	0.37	7.86
218	100	1.29	296	0.30	8.08
220	90	1.47	298	0.24	8.27
222	78	1.64	300	0.19	8.44
224	68	1.81	302	0.15	8.61
226	59	1.98	304	0.12	8.76
228	52	2.14	306	0.10	8.87
230	46	2.30	308	0.082	9.01
232	40	2.46	310	0.067	9.13
234	35	2.63	312	0.054	9.3
236	31	2.80	314	0.046	9.46
238	28	2.96	316	0.036	9.57
240	24	3.11	318	0.030	9.75
242	21	3.25	320	0.025	10.0
244	19	3.39	322	0.020	10.2
246	17	3.52	324	0.017	10.4
248	15	3.64	326	0.014	10.6
250	13	3.76	328	0.012	10.7
252	11	3.87	330	0.011	10.9
254	10	3.98	332	0.0086	11.2
256	8.9	4.10	334	0.0068	11.5
258	7.8	4.23	336	0.0061	11.7
260	6.8	4.38	338	0.0053	11.9
262	6.0	4.53	340	0.0050	12.2
264	5.2	4.68	342	0.0036	12.4
266	4.5	4.82	344	0.0024	12.5
268	3.9	4.97	346	0.0023	
270	3.4	5.14	348	0.0025	
272	2.9	5.34	350	0.0016	

Cross sections in the temperature range 250-298 K are calculated using the equation,

$$\ln[\sigma(T)/\sigma(298K)] = B(T-298).$$

$Cl_2 + h\nu \rightarrow Cl + Cl$

The recommended absorption cross sections are taken from the work of Maric et al. [175]; they can be calculated at various temperatures with the expression given at the bottom of Table 26. For convenience, some room temperature values are also listed in the table. Ganske et al. [96] have also measured the cross sections at room temperature, and the agreement with the recommended values is excellent. These two sets of data also agree well with the earlier recommendation, which was based on the work of Seery and Britton [276], which is in turn in good agreement with the results reported by Gibson and Bayliss [98], Fergusson et al. [90], and Burkholder and Bair [34]. The estimated atmospheric photodissociation rate is only weakly affected by the temperature dependency of the cross sections.

Table 26. Absorption Cross Sections of Cl_2

λ (nm)	10^{20} σ, 298K (cm^2)	λ (nm)	10^{20} σ, 298K (cm^2)
260	0.20	370	8.4
270	0.82	380	5.0
280	2.6	390	2.9
290	6.2	400	1.8
300	11.9	410	1.3
310	18.5	420	0.96
320	23.7	430	0.73
330	25.5	440	0.54
340	23.5	450	0.38
350	18.8	460	0.26
360	13.2	470	0.16

$$\sigma = 10^{-20}\,\alpha^{0.5}\,\{27.3\exp[-99.0\,\alpha\,(\ln\frac{329.5}{\lambda})^2] + 0.932\exp[-91.5\,\alpha\,(\ln\frac{406.5}{\lambda})^2]\}$$

where $\alpha = \tanh(402.7/T)$; λ in nm, and T in K; 300 K > T > 195 K.

$ClO + h\nu \rightarrow Cl + O$

The absorption cross sections of chlorine monoxide, ClO, have been reviewed by Watson [324]. There are more recent measurements yielding results in reasonable agreement with the earlier ones, (1) Mandelman and Nicholls [172] in the 250-310 nm region; (2) Wine et al. [329] around 283 nm; (3) Rigaud et al. [254], (4) Jourdain et al. [148], (5) Sander and Friedl [268], (6) Trolier et al. [303] in the 270-310 nm region, and (7) Simon et al. [282] between 240 and 310 nm. The peak cross section at the top of the continuum is 5.2×10^{-18}, based on the average of studies (4) - (7) and Johnston et al. [143]. Figure 3 shows a spectrum of ClO. It should be noted that the cross sections on the structured part are extremely dependent on instrument resolution, and the figure is only a guide to the line positions and approximate shapes. The cross sections of the continuum are independent of temperature (Trolier et al. [303]), while the structured part is extremely temperature dependent. The bands sharpen and grow with a decrease in temperature.

The calculations of Coxon et al. [74] and Langhoff et al. [154] indicate that photodecomposition of ClO accounts for at most 2 to 3 percent of the total destruction rate of ClO in the stratosphere, which occurs predominantly by reaction with oxygen atoms and nitric oxide.

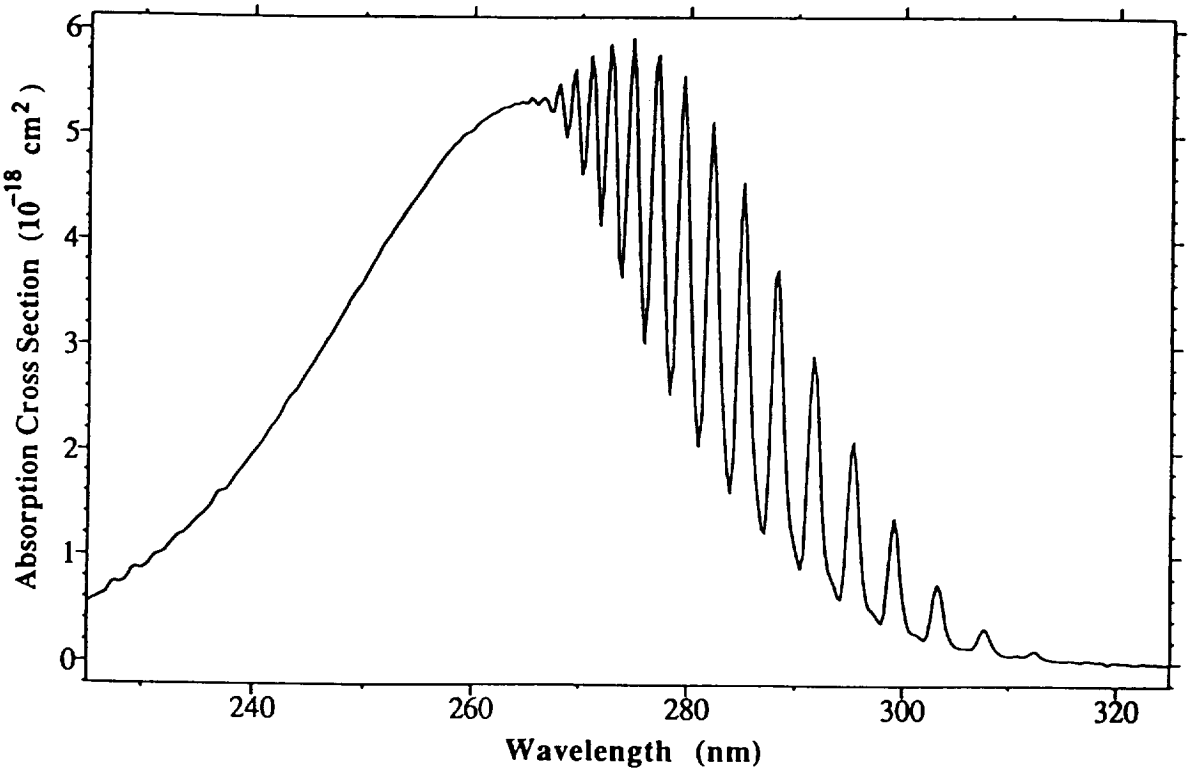

Figure 3. Absorption Spectrum of ClO

ClOO + hv → ClO + O

Johnston et al. [143] measured the absorption cross sections of the ClOO radical using a molecular modulation technique that required interpretation of a complex kinetic scheme. More recently, Mauldin et al. [183] reported cross section measurements in the range from 220 to 280 nm, and Baer et al. [11] from 240 to 300 nm. These two studies are in very good agreement, yielding cross section values that are more than twice as large as the older Johnston et al. values. The recommended cross sections are listed in Table 27, and are taken from the work of Mauldin et al.

Table 27. Absorption Cross Sections of ClOO

λ (nm)	$10^{20}\sigma$ (cm^2)	λ (nm)	$10^{20}\sigma$ (cm^2)
220	611	252	2630
222	670	254	2370
224	747	256	2120
226	951	258	1890
228	1100	260	1610
230	1400	262	1370
232	1650	264	1120
234	1960	266	905
236	2240	268	725
238	2520	270	596
240	2730	272	435
242	2910	274	344
244	2960	276	282
246	2980	278	210
248	2950	280	200
250	2800		

OClO + hv → O + ClO

The spectrum of OClO is characterized by a series of well-developed progressions of bands extending from ~280 to 480 nm. The spectroscopy of this molecule has been studied extensively, and the quantum yield for photodissociation appears to be unity throughout the above wavelength range. See for example, the review by Watson [324]. Birks et al. [23] have estimated a half-life against atmospheric photodissociation of OClO of a few seconds.

The recommended absorption cross section values are those reported by Wahner et al. [320], who measured the spectra with a resolution of 0.25 nm at 204, 296, and 378 K, in the wavelength range 240 to 480 nm. Table 28 lists the cross section values at the peak of the bands [a(0) to a(26)]. Figure 4, from Wahner et al., shows the OClO spectrum at 204 K and at room temperature. Hubinger and Nee [125] have extended the measurements of OClO cross sections over the spectral range 125-470 nm. Frost et al. [95] have studied the spectrum at very high spectral resolution (0.1 cm^{-1}) and at low temperature (200 K) in molecular beam expansion. In both of these studies, cross sections were measured relative to values obtained by Wahner et al.

The photochemistry of OClO is extremely complex, with several electronic excited states involved in the photodissociation dynamics. Several channels have been observed at wavelengths important in the stratosphere, including O + ClO, Cl + O_2 and isomerization to ClOO. Colussi [63] measured the quantum yield for chlorine atom production to be less than 0.01, and for oxygen atom production to be unity (within experimental error), both at 308 nm. Vaida et al. [313] and Ruhl et al. [265] reported chlorine atom production at 362 nm; and Bishenden et

al. [24, 25] measured the quantum yield for this process to be 0.15 ± 0.10 around that same wavelength. In contrast, Lawrence et al. [155] report a quantum yield for Cl-atom production in the 359-368 nm region of less than $5x10^{-4}$. This conclusion is supported by photofragment studies of Davis and Lee [82], who report Cl yields <0.2% below 370 nm, rising to a maximum of 4% near 404 nm. The recommendation is to use a quantum yield value of unity for the production of O-atoms. While accurate absorption cross section values are valuable for atmospheric measurements of OClO levels, the identity of the photodissociation products is only of minor importance in the context of atmospheric processes.

Table 28. Absorption Cross Sections of OClO at the Band Peaks

	$10^{20}\sigma(cm^2)$		
λ(nm)	204 K	296 K	378 K
475.53	-	13	-
461.15	17	17	16
446.41	94	69	57
432.81	220	166	134
420.58	393	304	250
408.83	578	479	378
397.76	821	670	547
387.37	1046	844	698
377.44	1212	992	808
368.30	1365	1136	920
359.73	1454	1219	984
351.30	1531	1275	989
343.44	1507	1230	938
336.08	1441	1139	864
329.22	1243	974	746
322.78	1009	791	628
317.21	771	618	516
311.53	542	435	390
305.99	393	312	291
300.87	256	219	216
296.42	190	160	167
291.77	138	114	130
287.80	105	86	105
283.51	089	72	90
279.64	073	60	79
275.74	059	46	-
272.93	053	33	-

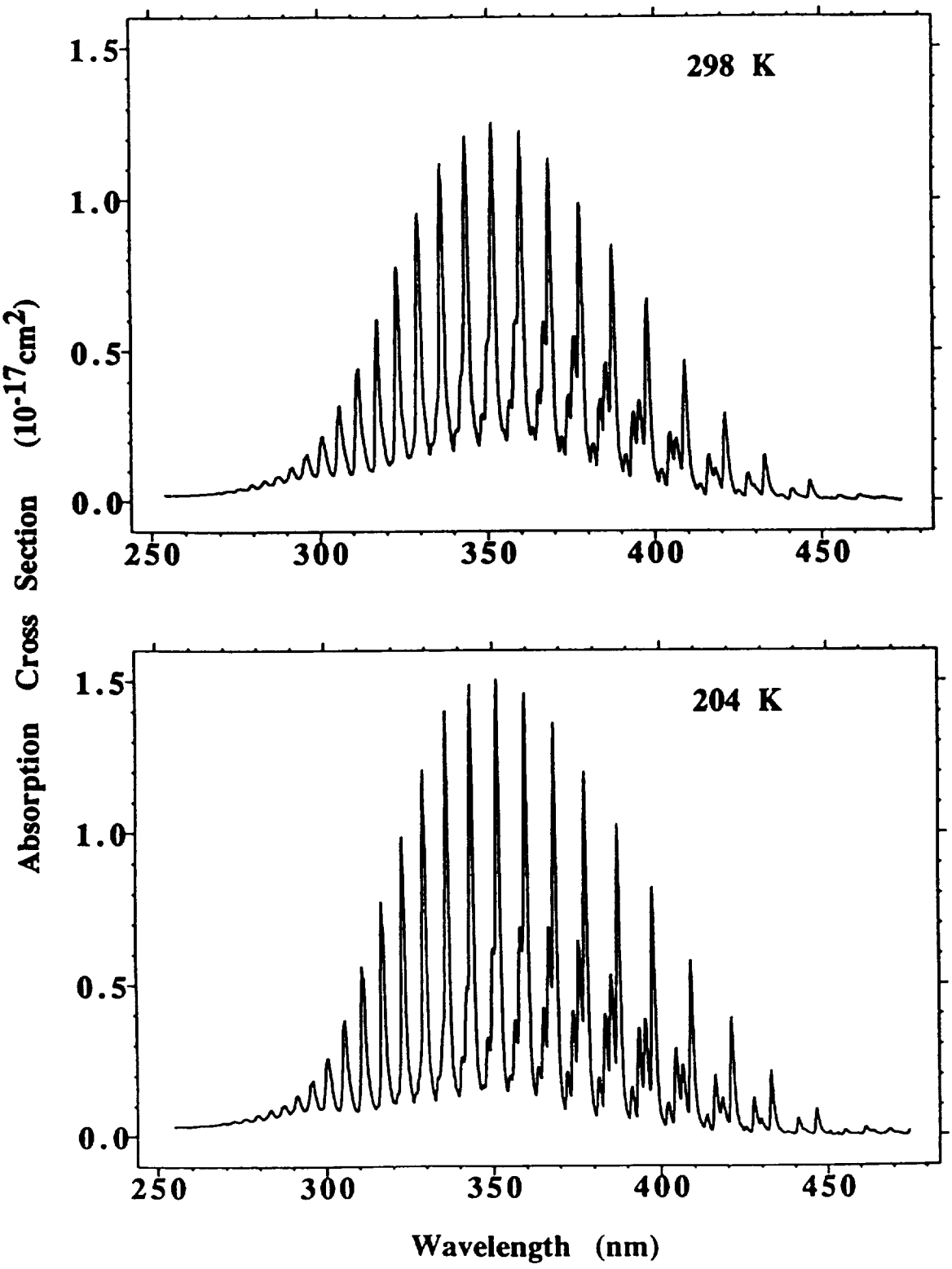

Figure 4. Absorption Spectrum of OClO

$ClO_3 + h\nu \rightarrow$ Products

The previous recommendation for absorption cross sections was based on the work of Goodeve and Richardson [107]. Lopez and Sicre [166] have shown that the spectrum reported by Goodeve and Richardson is most likely that of Cl_2O_6. Thermochemical estimates by Colussi et al. [64] further corroborate this assignment. No recommendation is given at present for the ClO_3 cross sections.

Grothe and Willner (1994; 1995) have reported UV and IR spectra of ClO_3 trapped in a neon matrix. By monitoring the amount of ClO formed as a photolysis product, they estimated UV absorption cross sections of the order of 2×10^{-18} cm^2 around 400-450 nm.

$Cl_2O + h\nu \rightarrow$ Products

The preferred absorption cross sections, listed in Table 29, are those reported by Knauth et al. [150] at 298 K. They are in very good agreement with the cross sections measured by Lin [163] and by Molina and Molina [201]; the discrepancy is largest at the longest wavelengths. Nee [223] has recently reported cross section measurements in the 150-200 nm wavelength region.

Sander and Friedl [268] have measured the quantum yield for production of O-atoms to be 0.25 ± 0.05, using a broadband photolysis source extending from 180 nm to beyond 400 nm. The main photolysis products are Cl and ClO. Using a molecular beam technique, Nelson et al. [224] found Cl + ClO to be the primary photodissociation channel at 193, 248, and 308 nm. More recently, Nickolaisen et al. [227] reported that broadband photolysis at wavelengths beyond 300 nm results in pressure-dependent ClO quantum yields. Furthermore, these authors detected a transient absorption spectrum, that they assigned to a metastable triplet state of Cl_2O; the implication is that the photodecomposition quantum yield is less than unity at atmospherically relevant wavelengths, in spite of the continuous nature of the absorption spectrum. Additional experimental work is needed to corroborate this interpretation.

Table 29. Absorption Cross Sections of Cl_2O

λ (nm)	$10^{20}\sigma$ (cm^2)	λ (nm)	$10^{20}\sigma$ (cm^2)
200	71.0	330	8.40
210	23.8	340	3.58
220	8.6	350	1.54
230	28.1	360	0.73
240	103	370	0.40
250	191	380	0.36
260	195	390	0.51
270	151	400	0.79
280	126	420	1.26
290	103	440	1.11
300	71.0	460	0.63
310	40.3	480	0.32
320	19.5	500	0.22

ClOOCl + hν → Cl + ClOO

Recommended absorption cross sections in the wavelength range 190-450 nm for ClOOCl are listed in Table 30. The values for the wavelength range 200 - 360 nm are the average of experimental results reported by Cox and Hayman [71], DeMore and Tschuikow-Roux [83], Permien et al.[243], and Burkholder et al. [36]. For the 190 – 200 nm range the data are from DeMore and Tschuikow-Roux, these being the only data available in that range. Data at wavelengths greater than 360 nm were obtained from a linear extrapolation of the logarithm of the cross sections, using the expression $\log[10^{20}\sigma(cm2)] = -0.01915 \times \lambda(nm) + 7.589$. For $\lambda > 360$ nm the extrapolated data are considered to be more reliable than the experimental measurements because of the very small dimer cross sections in this region. While the results of Cox and Hayman, DeMore and Tschuikow-Roux, Permien et al., and Burkholder et al. are in good agreement at wavelengths below 250 nm, there are significant discrepancies at longer wavelengths, which may be attributed to uncertainties in the spectral subtraction of impurities such as Cl_2O, Cl_2 and Cl_2O_3. Huder and DeMore [129] measured ClOOCl cross sections over the 190-310 nm range using a method that minimized the corrections required for impurities such as Cl_2O. The cross sections from this study are significantly smaller (up to a factor of 2) than the current recommendation, particularly when extrapolated beyond 400 nm Additional measurements are needed, particularly at the longer wavelengths, to validate the results of Huder and DeMore.

These studies also indicate that only one stable species is produced in the recombination reaction of ClO with itself, and that this species is dichlorine peroxide, ClOOCl, rather than ClOClO. Using submillimeter wave spectroscopy, Birk et al. [22] have further established the structure of the recombination product to be ClOOCl. These observations are in agreement with the results of quantum mechanical calculations (McGrath et al. [189, 190]; Jensen and Odershede [138]; Stanton et al. [292]). The experiments of Cox and Hayman [71] indicate that the main photodissociation products at 253.7 nm are Cl and ClOO. Molina et al. [211] measured the quantum yield ϕ for this channel to be unity at 308 nm, with no ClO detectable as a product, with an experimental uncertainty in ϕ of about ± 25%. These results are also supported by quantum mechanical calculations (Stanton et al. [292]; Stanton and Bartlett [291]). In contrast, Eberstein [85] suggested a quantum yield of unity for the production of two ClO radicals, based merely on an analogy with the photolysis of H_2O_2 at shorter wavelengths. For atmospheric photodissociation calculations the recommended quantum yield value is based on the work of Molina et al. [211], i.e., a quantum yield of unity for the Cl + ClOO channel.

Table 30. Absorption Cross Sections of ClOOCl at 200-250 K

λ (nm)	$10^{20}\sigma(cm^2)$	λ (nm)	$10^{20}\sigma(cm^2)$	λ (nm)	$10^{20}\sigma(cm^2)$	λ (nm)	$10^{20}\sigma(cm^2)$
190	565.0	256	505.4	322	23.4	388	1.4
192	526.0	258	463.1	324	21.4	390	1.3
194	489.0	260	422.0	326	19.2	392	1.2
196	450.0	262	381.4	328	17.8	394	1.1
198	413.0	264	344.6	330	16.7	396	1.0
200	383.5	266	311.6	332	15.6	398	0.92
202	352.9	268	283.3	334	14.4	400	0.85
204	325.3	270	258.4	336	13.3	402	0.78
206	298.6	272	237.3	338	13.1	404	0.71
208	274.6	274	218.3	340	12.1	406	0.65
210	251.3	276	201.6	342	11.5	408	0.60
212	231.7	278	186.4	344	10.9	410	0.54
214	217.0	280	172.5	346	10.1	412	0.50
216	207.6	282	159.6	348	9.0	414	0.46
218	206.1	284	147.3	350	8.2	416	0.42
220	212.1	286	136.1	352	7.9	418	0.38
222	227.1	288	125.2	354	6.8	420	0.35
224	249.4	290	114.6	356	6.1	422	0.32
226	280.2	292	104.6	358	5.8	424	0.29
228	319.5	294	95.4	360	5.5	426	0.27
230	365.0	296	87.1	362	4.5	428	0.25
232	415.4	298	79.0	364	4.1	430	0.23
234	467.5	300	72.2	366	3.8	432	0.21
236	517.5	302	65.8	368	3.5	434	0.19
238	563.0	304	59.9	370	3.2	436	0.17
240	600.3	306	54.1	372	2.9	438	0.16
242	625.7	308	48.6	374	2.7	440	0.15
244	639.4	310	43.3	376	2.4	442	0.13
246	642.6	312	38.5	378	2.2	444	0.12
248	631.5	314	34.6	380	2.1	446	0.11
250	609.3	316	30.7	382	1.9	448	0.10
252	580.1	318	28.0	384	1.7	450	0.09
254	544.5	320	25.6	386	1.6		

$Cl_2O_3 + h\nu \rightarrow$ Products

The absorption cross sections of Cl_2O_3 have been measured by Hayman and Cox [118], Burkholder et al. [35], and Harwood et al. [117]. The results from these studies are significantly different in the spectral regions below 240 nm and in the long-wavelength tail beyond 300 nm. Table 31 lists the recommended values. These are derived by averaging the spectra of Burkholder et al. and Harwood et al., which are obtained by the most direct methods. Additional work is needed, particularly in the spectral region beyond 300 nm.

Table 31. Absorption Cross Sections of Cl_2O_3

λ (nm)	10^{20} σ (cm^2)	λ (nm)	10^{20} σ (cm^2)
220	1200	275	1470
225	1130	280	1240
230	1060	285	990
235	1010	290	760
240	1020	295	560
245	1120	300	400
250	1270	305	290
255	1450	310	210
260	1610	315	160
265	1680	320	140
270	1630		

Cl_2O_4 + hν → Products

The absorption cross sections of Cl_2O_4 have been measured by Lopez and Sicre [165]; their results are given in Table 32.

Table 32. Absorption Cross Sections of Cl_2O_4

λ (nm)	10^{20} σ(cm^2)	λ (nm)	10^{20} σ(cm^2)
200	161	255	42
205	97	260	31
210	72	265	22
215	64	270	14
220	71	275	8.8
225	75	280	5.5
230	95	285	4.0
235	95	290	2.7
240	87	295	2.2
245	72	300	1.7
250	56	305	1.2
		310	0.7

Cl_2O_6 + hν → Products

The absorption cross sections for Cl_2O_6 are listed in Table 33 and are taken from the work of Lopez and Sicre [166]. These authors show that the spectrum originally attributed to ClO_3 by Goodeve and Richardson [107] was most likely that of Cl_2O_6. The cross section values measured by Lopez and Sicre are several times larger than those reported by Goodeve and Richardson, but the shape of the spectrum is similar.

Table 33. Absorption Cross Sections of Cl_2O_6

λ (nm)	$10^{20}\sigma$ (cm^2)	λ (nm)	$10^{20}\sigma$ (cm^2)
200	1230	300	980
210	1290	310	715
220	1230	320	450
230	1080	330	285
240	1010	340	180
250	1010	350	112
260	1290	360	59
270	1440	370	28
280	1440	380	12
290	1290		

$HF + h\nu \rightarrow H + F$

The ultraviolet absorption spectrum of HF has been studied by Safary et al. [266]. The onset of absorption occurs at $\lambda < 170$ nm, so that photodissociation of HF should be unimportant in the stratosphere.

$HCl + h\nu \rightarrow H + Cl$

The absorption cross sections of HCl, listed in Table 34, are taken from the work of Inn [134].

Table 34. Absorption Cross Sections of HCl Vapor

λ (nm)	$10^{20}\sigma$ (cm^2)	λ (nm)	$10^{20}\sigma$ (cm^2)
140	211	185	31.3
145	281	190	14.5
150	345	195	6.18
155	382	200	2.56
160	332	205	0.983
165	248	210	0.395
170	163	215	0.137
175	109	220	0.048
180	58.8		

$HOCl + h\nu \rightarrow OH + Cl$

The absorption cross sections of HOCl vapor have been measured by several groups. Molina and Molina [201] and Knauth et al. [150] produced this species using equilibrium mixtures with Cl_2O and H_2O; their results provided the basis for the earlier recommendation. More recently, Mishalanie et al. [197] and Permien et al. [243] used a dynamic source to generate the HOCl vapor. The cross section values reported by Molina and Molina [201], Mishalanie et al. [197], and Permien et al. [243] are in reasonable agreement between 250 and 330 nm. In this wavelength range, the values reported by Knauth et al. [150] are significantly smaller, e.g., a factor of 4 at 280 nm. Beyond 340 nm, the cross sections of Mishalanie et al. are much smaller than those obtained by the other three groups: at 365 nm, the discrepancy is about an order of magnitude.

The recent results by Burkholder [33] are in excellent agreement with the work of Knauth et al. [150], but in poor agreement with the more recent measurements of Mishalanie et al. [197] and Permien et al. [243]. The discrepancies can be attributed mostly to difficulties in correcting the measured absorptions for the presence of Cl_2 and Cl_2O. The recommended values, taken from the work of Burkholder [33], are listed in Table 35. In this work, several control experiments were carried out in order to check the internal consistency of the data. More recent work by Jungkamp et al. [149] yields cross section values in excellent agreement with this recommendation.

Molina et al. [212] observed production of OH radicals in the laser photolysis of HOCl around 310 nm, and Butler and Phillips [45] found no evidence for O-atom production at 308 nm, placing an upper limit of ~0.02 for the primary quantum yield for the HCl + O channel. Vogt and Schindler [318] used broadband photolysis in the 290 - 390 nm wavelength range, determining a quantum yield for OH production of >0.95.

Table 35. Absorption Cross Sections of HOCl

λ (nm)	$10^{20}\sigma$ (cm^2)	λ (nm)	$10^{20}\sigma$ (cm^2)	λ (nm)	$10^{20}\sigma$ (cm^2)
200	7.1	262	9.3	322	4.6
202	6.1	264	8.3	324	4.3
204	5.6	266	7.4	326	4.2
206	5.4	268	6.6	328	3.8
208	5.5	270	6.0	330	3.5
210	5.7	272	5.5	332	3.3
212	6.1	274	5.2	334	3.1
214	6.6	276	4.9	336	2.7
216	7.5	278	4.8	338	2.5
218	8.4	280	4.7	340	2.4
220	9.7	282	4.8	342	2.1
222	10.9	284	4.8	344	1.8
224	12.2	286	4.9	346	1.8
226	13.5	288	5.1	348	1.7
228	15.0	290	5.3	350	1.5
230	16.4	292	5.4	352	1.3
232	17.7	294	5.6	354	1.3
234	18.7	296	5.8	356	1.2
236	19.7	298	5.9	358	1.0
238	20.3	300	6.0	360	0.8
240	20.7	302	6.0	362	1.0
242	21.0	304	6.1	364	1.0
244	20.5	306	6.0	366	0.9
246	19.6	308	6.0	368	0.8
248	18.6	310	5.9	370	0.8
250	17.3	312	5.7	372	1.0
252	15.9	314	5.6	374	0.8
254	14.6	316	5.4	376	0.8
256	13.2	318	5.1	378	0.6
258	11.8	320	4.9	380	0.8
260	10.5				

FNO + hν → F + NO

The absorption cross sections have been measured by Burley et al. [41], who report their results in graphical form as well as in tabular form in 1 nm intervals, between 180 and 350 nm. The spectrum shows vibronic structure at wavelengths longer than 250 nm. The cross section values are listed in Table 36 in 2 nm intervals. The quantum yield for decomposition is expected to be unity (Brandon et al., [27]; Reid et al., [253]).

Table 36. Absorption Cross Sections of FNO

λ (nm)	$10^{20}\sigma$ (cm^2)	λ (nm)	$10^{20}\sigma$ (cm^2)	λ (nm)	$10^{20}\sigma$ (cm^2)
180	52.4	236	3.09	292	11.9
182	51.7	238	2.76	294	7.11
184	50.7	240	2.25	296	9.15
186	49.4	242	2.08	298	22.0
188	47.5	244	1.74	300	15.6
190	45.1	246	1.65	302	25.4
192	42.7	248	1.41	304	8.85
194	40.0	250	1.54	306	11.8
196	37.3	252	1.25	308	32.2
198	33.8	254	1.23	310	15.5
200	30.5	256	1.36	312	31.6
202	27.7	258	1.58	314	12.3
204	24.8	260	1.30	316	11.0
206	22.2	262	1.64	318	25.5
208	19.9	264	2.03	320	15.2
210	17.6	266	1.96	32.3	40.2
212	15.8	268	2.10	324	17.8
214	13.9	270	2.81	326	12.1
216	12.3	272	4.47	328	9.39
218	10.7	274	3.97	330	12.9
220	9.35	276	4.24	332	13.0
222	8.32	278	3.41	334	19.3
224	7.22	280	8.26	336	13.1
226	6.30	282	7.58	338	8.96
228	5.44	284	7.26	340	5.65
230	4.68	286	5.17	342	3.81
232	4.10	288	10.4	344	2.68
234	3.52	290	17.0	346	1.96
				348	1.48
				350	1.18

ClNO + hν → Cl + NO

Nitrosyl chloride has a continuous absorption extending beyond 650 nm. There is good agreement between the work of Martin and Gareis [180] for the 240 to 420 nm wavelength region, of Ballash and Armstrong [14] for the 185 to 540 nm region, of Illies and Takacs [133] for the 190 to 400 nm region, and of Tyndall et al. [309] for the 190 to 350 region except around 230 nm, where the values of Ballash and Armstrong are larger by almost a factor of two. Roehl et al. [259] measured the absorption cross sections between 350 and 650 nm at several temperatures between 223 and 343 K. Their room temperature results agree to within 15% with those of Martin and Gareis [180], Ballash and Amstrong [14], and Tyndall et al. [309]. Table 37 lists the recommended cross sections: these are taken from the work of Tyndall et al. [309] between 190 and 350 nm (unchanged from the previous recommendation), and from Roehl et al. [259] beyond 350 nm.

The quantum yield for the primary photolytic process has been reviewed by Calvert and Pitts [47]. It is unity over the entire visible and near-ultraviolet bands.

Table 37. Absorption Cross Sections of ClNO

λ (nm)	$10^{20}\sigma$ (cm^2)	λ (nm)	$10^{20}\sigma$ (cm^2)	λ (nm)	$10^{20}\sigma$ (cm^2)	λ (nm)	$10^{20}\sigma$ (cm^2)
190	4320	246	45.2	302	10.3	370	11.0
192	5340	248	37.7	304	10.5	375	9.95
194	6150	250	31.7	306	10.8	380	8.86
196	6480	252	27.4	308	11.1	385	7.82
198	6310	254	23.7	310	11.5	390	6.86
200	5860	256	21.3	312	11.9	395	5.97
202	5250	258	19.0	314	12.2	400	5.13
204	4540	260	17.5	316	12.5	405	4.40
206	3840	262	16.5	318	13.0	410	3.83
208	3210	264	15.3	320	13.4	415	3.38
210	2630	266	14.4	322	13.6	420	2.89
212	2180	268	13.6	324	14.0	425	2.45
214	1760	270	12.9	326	14.3	430	2.21
216	1400	272	12.3	328	14.6	435	2.20
218	1110	274	11.8	330	14.7	440	2.20
220	896	276	11.3	332	14.9	445	2.07
222	707	278	10.7	334	15.1	450	1.87
224	552	280	10.6	336	15.3	455	1.79
226	436	282	10.2	338	15.3	460	1.95
228	339	284	9.99	340	15.2	465	2.25
230	266	286	9.84	342	15.3	470	2.50
232	212	288	9.71	344	15.1	475	2.61
234	164	290	9.64	346	15.1	480	2.53
236	120	292	9.63	348	14.9	485	2.33
238	101	294	9.69	350	14.2	490	2.07
240	82.5	296	9.71	355	13.6	495	1.78
242	67.2	298	9.89	360	12.9	500	1.50
244	55.2	300	10.0	365	12.0		

$ClNO_2 + h\nu \rightarrow$ Products

The absorption cross sections of nitryl chloride, $ClNO_2$, have been measured between 230 and 330 nm by Martin and Gareis [180], between 185 and 400 nm by Illies and Takacs [133], and between 270 and 370 nm by Nelson and Johnston [226], and by Ganske et al. [96] between 200 and 370 nm. A major source of discrepancies in the data results from the presence of impurities. Table 38 lists the recommended values, which are taken from Ganske et al. Nelson and Johnston [226] report a value of one (within experimental error) for the quantum yield for production of chlorine atoms; they also report a negligible quantum yield for the production of oxygen atoms.

Table 38. Absorption Cross Sections of $ClNO_2$

λ (nm)	$10^{20}\sigma$ (cm^2)	λ (nm)	$10^{20}\sigma$ (cm^2)
190	2690	290	17.3
200	468	300	14.9
210	320	310	12.1
220	339	320	8.87
230	226	330	5.84
240	133	340	3.54
250	90.6	350	2.04
260	61.3	360	1.15
270	35.3	370	0.69
280	22.0		

ClONO + hν → Products

Measurements in the near-ultraviolet of the cross sections of chlorine nitrite (ClONO) have been made by Molina and Molina [200]. Their results are listed in Table 39. The characteristics of the spectrum and the instability of ClONO strongly suggest that the quantum yield for decomposition is unity. The Cl-O bond strength is only about 20 kilocalories, so that chlorine atoms are likely photolysis products.

Table 39. Absorption Cross Sections of ClONO at 231 K

λ (nm)	$10^{20}\sigma$ (cm^2)	λ (nm)	$10^{20}\sigma$ (cm^2)
235	215.0	320	80.3
240	176.0	325	75.4
245	137.0	330	58.7
250	106.0	335	57.7
255	65.0	340	43.7
260	64.6	345	35.7
265	69.3	350	26.9
270	90.3	355	22.9
275	110.0	360	16.1
280	132.0	365	11.3
285	144.0	370	9.0
290	144.0	375	6.9
295	142.0	380	4.1
300	129.0	385	3.3
305	114.0	390	2.2
310	105.0	395	1.5
315	98.1	400	0.6

$ClONO_2 + h\nu \rightarrow$ Products

The recommended cross sections are taken from the work of Burkholder et al. [38]; the values are listed in Table 40, together with the parameters needed to compute their temperature dependency. These values are in very good agreement with those reported by Molina and Molina [202], which provided the basis for the previous recommendation, and which supersedes the earlier work of Rowland, Spencer, and Molina [263].

The identity of the primary photolytic fragments has been investigated by several groups. Smith et al. [287] report O + ClONO as the most likely products, using end product analysis and steady-state photolysis. The results of Chang et al. [52], who employed the "Very Low Pressure Photolysis" (VLPPh) technique, indicate that the products are Cl + NO_3. Adler-Golden and Wiesenfeld [2], using a flash photolysis atomic absorption technique, find O-atoms to be the predominant photolysis product and report a quantum yield for Cl-atom production of less than 4%. Marinelli and Johnston [178] report a quantum yield for NO_3 production at 249 nm between 0.45 and 0.85, with a most likely value of 0.55; they monitored NO_3 by tunable dye-laser absorption at 662 nm. Margitan [173] used atomic resonance fluorescence detection of O- and Cl-atoms and found the quantum yield at 266 and at 355 nm to be 0.9 ± 0.1 for Cl-atom production and ~0.1 for O-atom production, with no discernible difference at the two wavelengths. These results were confirmed by Knauth and Schindler [151], who used end-product analysis to infer the quantum yields. Burrows et al. [44] report also Cl and NO_3 as the photolysis products at 254 nm, with a quantum yield of unity within experimental error. In contrast, Nikolaisen et al. [228] report relative branching ratios of 0.44 for production of ClO and NO_2 and 0.56 for production of Cl and NO_3 at wavelengths beyond 300 nm. Minton et al. [196], Nelson et al. [225], and Moore et al. [213] measured comparable yields for these two channels at 193, 248 and 308 nm, using a molecular beam technique.

The recommended quantum yield values for production of Cl + NO_3 (ϕ_1) and ClO + NO_2 (ϕ_2) are given at the bottom of Table 40 and are based on the work of Nelson et al. [225], Moore et al. [213], Nickolaisen et al. [228], and Ravishankara [248]. For wavelengths shorter than 308 nm the value of ϕ_1 is 0.6, and for ϕ_2 it is 0.4. For longer wavelengths ϕ_1 increases linearly to 0.9 at 350 nm, with the corresponding decrease in ϕ_2 to 0.1. There is no evidence for production of O + ClONO in the more recent work; the production of O-atoms reported in some of the earlier studies might have resulted from decomposition of excited NO_3.

Recent work by Nickolaisen et al. [228] indicates that the photodissociation quantum yield is less than unity at wavelengths longer than about 330 nm, because of the formation of a long-lived intermediate that might be quenched under atmospheric conditions (a situation analogous to that of Cl_2O). Additional work is needed to address these issues, which have potentially important atmospheric consequences.

Table 40. Absorption Cross Sections of $ClONO_2$

λ (nm)	$10^{20}\sigma(\lambda,296)$ (cm^2)	A1	A2	λ (nm)	$10^{20}\sigma(\lambda,296)$ (cm^2)	A1	A2
196	310	9.90 (-5)	-8.38 (-6)	316	1.07	5.07 (-3)	1.56 (-5)
198	294	6.72 (-5)	-8.03 (-6)	318	0.947	5.24 (-3)	1.69 (-5)
200	282	-5.34 (-6)	-7.64 (-6)	320	0.831	5.40 (-3)	1.84 (-5)
202	277	-1.19 (-4)	-7.45 (-6)	322	0.731	5.55 (-3)	2.00 (-5)
204	280	-2.60 (-4)	-7.50 (-6)	324	0.647	5.68 (-3)	2.18 (-5)
206	288	-4.12 (-4)	-7.73 (-6)	326	0.578	5.80 (-3)	2.36 (-5)
208	300	-5.62 (-4)	-8.05 (-6)	328	0.518	5.88 (-3)	2.54 (-5)
210	314	-6.96 (-4)	-8.41 (-6)	330	0.466	5.92 (-3)	2.70 (-5)
212	329	-8.04 (-4)	-8.75 (-6)	332	0.420	5.92 (-3)	2.84 (-5)
214	339	-8.74 (-4)	-9.04 (-6)	334	0.382	5.88 (-3)	2.96 (-5)
216	345	-9.03 (-4)	-9.24 (-6)	336	0.351	5.80 (-3)	3.05 (-5)
218	341	-8.86 (-4)	-9.35 (-6)	338	0.326	5.68 (-3)	3.10 (-5)
220	332	-8.28 (-4)	-9.38 (-6)	340	0.302	5.51 (-3)	3.11 (-5)
222	314	-7.31 (-4)	-9.34 (-6)	342	0.282	5.32 (-3)	3.08 (-5)
224	291	-6.04 (-4)	-9.24 (-6)	344	0.264	5.07 (-3)	2.96 (-5)
226	264	-4.53 (-4)	-9.06 (-6)	346	0.252	4.76 (-3)	2.74 (-5)
228	235	-2.88 (-4)	-8.77 (-6)	348	0.243	4.39 (-3)	2.42 (-5)
230	208	-1.13 (-4)	-8.33 (-6)	350	0.229	4.02 (-3)	2.07 (-5)
232	182	6.18 (-5)	-7.74 (-6)	352	0.218	3.68 (-3)	1.76 (-5)
234	158	2.27 (-4)	-7.10 (-6)	354	0.212	3.40 (-3)	1.50 (-5)
236	138	3.72 (-4)	-6.52 (-6)	356	0.205	3.15 (-3)	1.27 (-5)
238	120	4.91 (-4)	-6.14 (-6)	358	0.203	2.92 (-3)	1.06 (-5)
240	105	5.86 (-4)	-5.98 (-6)	360	0.200	2.70 (-3)	8.59 (-6)
242	91.9	6.64 (-4)	-6.04 (-6)	362	0.190	2.47 (-3)	6.38 (-6)
244	81.2	7.33 (-4)	-6.27 (-6)	364	0.184	2.22 (-3)	3.66 (-6)
246	71.6	8.03 (-4)	-6.51 (-6)	366	0.175	1.93 (-3)	2.42 (-7)
248	62.4	8.85 (-4)	-6.59 (-6)	368	0.166	1.62 (-3)	-3.62 (-6)
250	56.0	9.84 (-4)	-6.40 (-6)	370	0.159	1.33 (-3)	-7.40 (-6)
252	50.2	1.10 (-3)	-5.93 (-6)	372	0.151	1.07 (-3)	-1.07 (-5)
254	45.3	1.22 (-3)	-5.33 (-6)	374	0.144	8.60 (-4)	-1.33 (-5)
256	41.0	1.33 (-3)	-4.73 (-6)	376	0.138	6.73 (-4)	-1.54 (-5)
258	37.2	1.44 (-3)	-4.22 (-6)	378	0.129	5.01 (-4)	-1.74 (-5)
260	33.8	1.53 (-3)	-3.79 (-6)	380	0.121	3.53 (-4)	-1.91 (-5)
262	30.6	1.62 (-3)	-3.37 (-6)	382	0.115	2.54 (-4)	-2.05 (-5)
264	27.8	1.70 (-3)	-2.94 (-6)	384	0.108	2.25 (-4)	-2.11 (-5)
266	25.2	1.78 (-3)	-2.48 (-6)	386	0.103	2.62 (-4)	--2.11 (-5)
268	22.7	1.86 (-3)	-2.00 (-6)	388	0.0970	3.33 (-4)	-2.08 (-5)
270	20.5	1.94 (-3)	-1.50 (-6)	390	0.0909	4.10 (-4)	-2.05 (-5)
272	18.5	2.02 (-3)	-1.01 (-6)	392	0.0849	5.04 (-4)	-2.02 (-5)
274	16.6	2.11 (-3)	-4.84 (-7)	394	0.0780	6.62 (-4)	-1.94 (-5)
276	14.9	2.02 (-3)	9.02 (-8)	396	0.0740	8.95 (-4)	-1.79 (-5)
278	13.3	2.29 (-3)	6.72 (-7)	398	0.0710	1.14 (-3)	-1.61 (-5)
280	11.9	2.38 (-3)	1.21 (-6)	400	0.0638	1.38 (-3)	-1.42 (-5)
282	10.5	2.47 (-3)	1.72 (-6)	402	0.0599	1.63 (-3)	-1.20 (-5)
284	9.35	2.56 (-3)	2.21 (-6)	404	0.0568	1.96 (-3)	-8.97 (-6)
286	8.26	2.66 (-3)	2.68 (-6)	406	0.0513	2.36 (-3)	-5.15 (-6)
288	7.24	2.75 (-3)	3.09 (-6)	408	0.0481	2.84 (-3)	-6.64 (-7)
290	6.41	2.84 (-3)	3.41 (-6)	410	0.0444	3.38 (-3)	4.47 (-6)
292	5.50	2.95 (-3)	3.74 (-6)	412	0.0413	3.96 (-3)	1.00 (-5)
294	4.67	3.08 (-3)	4.27 (-6)	414	0.0373	4.56 (-3)	1.60 (-5)

Continued on next page

Table 40. (Continued)

λ (nm)	$10^{20}\sigma(\lambda,296)$ (cm^2)	A1	A2	λ (nm)	$10^{20}\sigma(\lambda,296)$ (cm^2)	A1	A2
296	4.09	3.25 (-3)	5.13 (-6)	416	0.0356	5.22 (-3)	2.28 (-5)
298	3.57	3.45 (-3)	6.23 (-6)	418	0.0317	5.96 (-3)	3.07 (-5)
300	3.13	3.64 (-3)	7.36 (-6)	420	0.0316	6.70 (-3)	3.87 (-5)
302	2.74	3.83 (-3)	8.38 (-6)	422	0.0275	7.30 (-3)	4.58 (-5)
304	2.39	4.01 (-3)	9.30 (-6)	424	0.0242	7.82 (-3)	5.22 (-5)
306	2.09	4.18 (-3)	1.02 (-5)	426	0.0222	8.41 (-3)	5.95 (-5)
308	1.83	4.36 (-3)	1.11 (-5)	428	0.0207	9.11 (-3)	6.79 (-5)
310	1.60	4.53 (-3)	1.20 (-5)	430	0.0189	9.72 (-3)	7.52 (-5)
312	1.40	4.71 (-3)	1.30 (-5)	432	0.0188	9.96 (-3)	7.81 (-5)
314	1.22	4.89 (-3)	1.42 (-5)				

$\sigma(\lambda, T) = \sigma(\lambda, 296)\,[1 + A_1 (T - 296) + A_2 (T - 296)^2]$; T in K

Quantum yields: $ClONO_2 + h\nu \rightarrow Cl + NO_3$

$\phi_1 = 0.6$ ($\lambda < 308$ nm)

$\phi_1 = 7.143 \times 10^{-3}\,\lambda$ (nm) - 1.60 (308 nm < λ < 364 nm)

$\phi_1 = 1.0$ ($\lambda > 364$ nm)

$ClONO_2 + h\nu \rightarrow ClO + NO_2$

$\phi_2 = 1 - \phi_1$

Halocarbon Absorption Cross Sections and Quantum Yields

The primary process in the photodissociation of chlorinated hydrocarbons is well established: absorption of ultraviolet radiation in the lowest frequency band is interpreted as an n-σ^* transition involving excitation to a repulsive electronic state (antibonding in C-Cl), which dissociates by breaking the carbon chlorine bond (Majer and Simons [169]). As expected, the chlorofluoromethanes, which are a particular type of chlorinated hydrocarbons, behave in this fashion (Sandorfy [270]). Hence, the quantum yield for photodissociation is expected to be unity for these compounds. There are several studies that show specifically that this is the case for CF_2Cl_2, $CFCl_3$, and CCl_4. These studies, which have been reviewed in CODATA [62], also indicate that at shorter wavelengths two halogen atoms can be released simultaneously in the primary process.

The absorption cross sections for various other halocarbons not listed in this evaluation have also been investigated: $CHCl_2F$ by Hubrich et al. [128]; $CClF_3$, $CHCl_3$, CH_2Cl_2, CH_2ClF, CF_3CH_2Cl, and CH_3CH_2Cl by Hubrich and Stuhl [127]; $CHCl_3$, $CHFCl_2$, C_2HCl_3, and $C_2H_3Cl_3$ by Robbins [256]; CH_2Cl_2 and $CHCl_3$ by Vanlaethem-Meuree et al. [314]; $CHCl_2F$, $CClF_2CH_2Cl$, and CF_3CH_2Cl by Green and Wayne [111]; and CH_2Br_2 and $CBrF_2CF_3$ by Molina et al. [208]. Simon and co-workers have reported absorption cross section measurements over the temperature range 295-210 K for various other halocarbons not listed here. These include the following: $CHCl_3$, CH_2Cl_2, $CHFCl_2$, and CF_3Cl by Simon et al. [283]. Orkin and Kasimovskaya [236] have measured cross sections at 295 K for CHF_2Br, $CHFBrCF_3$, CH_2BrCF_3, and $CHClBrCF_3$ in the wavelength range 190-320 nm.

As before, the recommendation for the photodissociation quantum yield value is unity for all these species. CF_4 and C_2F_6 do not have any absorptions at wavelengths longer than 105 and 120 nm, respectively (Sauvageau et al. [271, 272]; Inn, [135]); therefore, they are not expected to photodissociate until they reach the mesosphere.

$CCl_4 + h\nu \rightarrow$ Products

CCl_3F (CFC-11) + $h\nu \rightarrow$ Products

CCl_2F_2 (CFC-12) + $h\nu \rightarrow$ Products

Tables 41, 42, and 43 list the present recommendations for the cross sections of CCl_4, CCl_3F and CCl_2F_2, respectively. These data are given by the mean of the values reported by various groups, i.e., Hubrich et al. [128], Hubrich and Stuhl [127], Vanlaethem-Meuree et al. [314, 315], and Green and Wayne [111], as well as those referred to in earlier evaluations (CODATA [62]). Absorption cross sections for these species over the temperature range 295-210 K have also been reported by Simon et al. [283]. These results are in generally good agreement with the present recommendations. Expressions for the temperature dependence of the CCl_3F and CCl_2F_2 cross sections are given at the bottom of Tables 42 and 43, respectively. These expressions are valid in the wavelength range of maximum solar photodissociation, i.e., about 190-210 nm, but may not exactly reproduce the experimental temperature dependences outside this wavelength range. However, J-value calculations should not be affected.

Table 41. Absorption Cross Sections of CCl_4

λ (nm)	$10^{20}\sigma$ (cm^2)	λ (nm)	$10^{20}\sigma$ (cm^2)
174	995	218	21.8
176	1007	220	17.0
178	976	222	13.0
180	772	224	9.61
182	589	226	7.19
184	450	228	5.49
186	318	230	4.07
188	218	232	3.01
190	144	234	2.16
192	98.9	236	1.51
194	74.4	238	1.13
196	68.2	240	0.784
198	66.0	242	0.579
200	64.8	244	0.414
202	62.2	246	0.314
204	60.4	248	0.240
206	56.5	250	0.183
208	52.0	255	0.0661
210	46.6	260	0.0253
212	39.7	265	0.0126
214	33.3	270	0.0061
216	27.2	275	0.0024

Table 42. Absorption Cross Sections of CCl_3F

λ (nm)	$10^{20}\sigma$ (cm^2)	λ (nm)	$10^{20}\sigma$ (cm^2)
170	316	208	21.2
172	319	210	15.4
174	315	212	10.9
176	311	214	7.52
178	304	216	5.28
180	308	218	3.56
182	285	220	2.42
184	260	222	1.60
186	233	224	1.10
188	208	226	0.80
190	178	228	0.55
192	149	230	0.35
194	123	235	0.126
196	99	240	0.0464
198	80.1	245	0.0173
200	64.7	250	0.00661
202	50.8	255	0.00337
204	38.8	260	0.00147
206	29.3		

$\sigma_T = \sigma_{298} \exp[1.0 \times 10^{-4}(\lambda - 184.9)(T - 298)]$

Where σ_{298} = cross section at 298 K

λ : nm

T : temperature, K

Table 43. Absorption Cross Sections of CCl_2F_2

λ (nm)	$10^{20}\sigma$ (cm^2)	λ (nm)	$10^{20}\sigma$ (cm^2)
170	124	200	8.84
172	151	202	5.60
174	171	204	3.47
176	183	206	2.16
178	189	208	1.52
180	173	210	0.80
182	157	212	0.48
184	137	214	0.29
186	104	216	0.18
188	84.1	218	0.12
190	62.8	220	0.068
192	44.5	225	0.022
194	30.6	230	0.0055
196	20.8	235	0.0016
198	13.2	240	0.00029

$\sigma_T = \sigma_{298} \exp[4.1 \times 10^{-4}(\lambda - 184.9)(T - 298)]$

Where σ_{298} = cross section at 298 K

λ : nm

T : temperature, K

$CF_2ClCFCl_2$ (CFC-113) + hν → Products

CF_2ClCF_2Cl (CFC-114) + hν → Products

CF_3CF_2Cl (CFC-115) + hν → Products

The recommended absorption cross section values for these species at 295 K and at 210 K are presented in Table 44, and are taken from Simon et al. [284]. These values are in good agreement with those reported by Hubrich and Stuhl [127], who also carried out measurements at lower temperatures. They are also in good agreement with the data of Chou et al. [58], except that these authors report cross section values for CF_3CF_2Cl that are about 50% higher. Also, for this species the temperature dependency is unimportant in the wavelength range of interest.

Table 44. Absorption Cross Sections for $CF_2ClCFCl_2$, CF_2ClCF_2Cl and CF_3CF_2Cl

	$10^{20}\sigma(cm^2)$				
λ	$CF_2ClCFCl_2$		CF_2ClCF_2Cl		CF_3CF_2Cl
(nm)	295 K	210 K	295 K	210 K	295 K
172			69	69	5.65
174			55	55	4.05
176			43	43	2.85
178			34	34	2.05
180			26	26	1.45
182			19.8	19.8	1.05
184	118	118	15.0	15.0	0.75
186	104	104	11.0	11.0	0.53
188	83.5	83.5	7.80	7.72	0.38
190	64.5	64.5	5.35	5.03	0.27
192	48.8	48.8	3.70	3.28	0.19
194	36.0	36.0	2.56	2.13	0.13
196	26.0	24.3	1.75	1.39	0.090
198	18.3	15.9	1.20	0.88	0.063
200	12.5	10.1	0.80	0.55	0.044
202	8.60	6.54	0.54	0.34	0.031
204	5.80	4.09	0.37	0.22	0.021
206	4.00	2.66	0.24	0.13	
208	2.65	1.68	0.16	0.084	
210	1.8	1.12	0.104	0.051	
212	1.15	0.696	0.068	0.031	
214	0.760	0.452	0.044	0.020	
216	0.505	0.298	0.029	0.012	
218	0.318	0.184	0.019	0.007	
220	0.220	0.125	0.012	0.004	
222	0.145	0.081			
224	0.095	0.053			
226	0.063	0.034			
228	0.041	0.022			
230	0.027	0.014			

CCl_2O + hν → Products, CClFO + hν → Products, and CF_2O + hν → Products

The recommended absorption cross sections are listed in Table 45, as averages over the 500 cm^{-1} intervals commonly employed for atmospheric modeling (the wavelength given in the table is the center of the interval). The values for CCl_2O are based on the work of Gillotay et al. [105], who measured the cross sections between 170 and 320 nm at temperatures ranging from 210 to 295 K; the temperature effect is significant only at wavelengths longer than 250 nm. These cross section values are in good agreement with those recommended earlier, which were based on the data of Chou et al. [57]. For CClFO the recommended values are based on this latter work between 184 and 199 nm, and they are taken from the work of Nölle et al. [231] at the longer wavelengths. These workers measured the cross sections at temperatures ranging from 223 to 298 K; the temperature effect is not important for atmospheric photodissociation calculations, as is the case with CCl_2O. For CF_2O the cross section values are taken from Molina and Molina [204] between 184 and 199 nm, and from Nölle et al. [232] at the longer wavelengths. These authors measured the cross sections at 296 K between 200 and 230 nm.

The photodissociation quantum yield for CCl_2O is unity (Calvert and Pitts [47]); the spectrum is a continuum. Similarly, the quantum yield for CClFO is taken as unity; the spectrum shows little structure. In contrast, the CF_2O spectrum is highly structured.Nnevertheless, its photodissociation quantum yield is also taken as unity, as reported by Nölle et al. [232]. The self-reaction of the CFO photodissociation product regenerates CF_2O, and hence the apparent quantum yield is less than unity.

Table 45. Absorption Cross Sections of CCl_2O, CClFO and CF_2O at 298 K

λ (nm)	$10^{20}\sigma(cm^2)$		
	CCl_2O	CClFO	CF_2O
184.4	234	-	-
186.0	186	15.6	5.5
187.8	146	14.0	4.8
189.6	116	13.4	4.2
191.4	90.3	12.9	3.7
193.2	71.5	12.7	3.1
195.1	52.4	12.5	2.6
197.0	39.3	12.4	2.1
199.0	31.2	12.3	1.6
201.0	25.2	12.5	1.3
203.0	20.9	12.0	0.95
205.1	17.9	11.5	0.74
207.3	15.8	10.8	0.52
209.4	14.3	9.9	0.40
211.6	13.3	9.0	0.28
213.9	12.6	7.9	0.20
216.2	12.3	6.8	0.12
218.6	12.2	5.8	0.08
221.0	12.2	4.8	0.049
223.5	12.4	3.8	0.035
225.7	12.7	2.9	0.024
228.6	13.1	2.2	0.018

$CF_3OH + h\nu \rightarrow$ Products

An upper limit of 10^{-21} cm^2 has been determined experimentally by Molina and Molina [207] for the absorption cross sections of CF_3OH in the 190 - 300 nm wavelength range. This upper limit is in agreement with estimates based on similarities between CF_3OH and CH_3OH, as well as with quantum chemistry calculations, as reported by Schneider et al. [275].

$CH_3Cl + h\nu \rightarrow$ Products

The preferred absorption cross sections, listed in Table 46, are those given by Vanlaethem-Meuree et al. [314]. These values are in very good agreement with those reported by Robbins [255] at 298 K, as well as with those given by Hubrich et al. [128] at 298 K and 208 K, if the temperature trend is taken into consideration. The results recently reported by Simon et al. [283] over the temperature range 295-210 K are in excellent agreement with the present recommendation.

Table 46. Absorption Cross Sections of CH_3Cl

λ (nm)	10^{20} σ(cm^2) 296 K	279 K	255 K
186	24.7	24.7	24.7
188	17.5	17.5	17.5
190	12.7	12.7	12.7
192	8.86	8.86	8.86
194	6.03	6.03	6.03
196	4.01	4.01	4.01
198	2.66	2.66	2.66
200	1.76	1.76	1.76
202	1.09	1.09	1.09
204	0.691	0.691	0.691
206	0.483	0.475	0.469
208	0.321	0.301	0.286
210	0.206	0.189	0.172
212	0.132	0.121	0.102
214	0.088	0.074	0.059
216	0.060	0.048	0.033

$CH_3CCl_3 + h\nu \rightarrow$ Products

The absorption cross sections have been measured by Robbins [256], Vanlaethem-Meuree et al. [316], Hubrich and Stuhl [127], and Nayak et al. [222]. Hubrich and Stuhl corrected the results to account for the presence of a UV-absorbing stabilizer in their samples, a correction that might account for the rather large discrepancy with the other three sets of measurements, that are in good agreement with each other. The recommended values are taken from Vanlaethem-Meuree et al. [316], who report values at 210 K, 230 K, 250 K, 270 K and 295 K, every 2 nm, and in a separate table at wavelengths corresponding to the wavenumber intervals generally used in stratospheric photodissociation calculations. Table 47 lists the values at 210 K, 250 K and 295 K, every 5 nm; the odd wavelength values were computed by linear interpolation. These values agree within 10% with those reported by Nayak et al. at the atmospherically relevant 200-210 nm wavelength range; these authors carried out measurements between 160 and 260 nm, from 220 to 330 K.

Table 47. Absorption Cross Sections of CH_3CCl_3

λ (nm)	$10^{20}\sigma(cm^2)$ 295 K	250 K	210 K
185	265	265	265
190	192	192	192
200	81.0	81.0	81.0
205	46.0	44.0	42.3
210	24.0	21.6	19.8
215	10.3	8.67	7.47
220	4.15	3.42	2.90
225	1.76	1.28	0.97
230	0.700	0.470	0.330
235	0.282	0.152	0.088
240	0.102	0.048	0.024

$CHClF_2$ (HCFC-22) + hν → Products

The absorption cross sections of $CHClF_2$ (HCFC-22) have been measured at room temperature by Robbins and Stolarski [257] and by Chou et al. [59], at 208 K and 218 K by Hubrich et al. [128], and between 210 and 295 K by Simon et al. [283]. The agreement between these groups is reasonable. The preferred absorption cross sections, listed in Table 48, are taken from work of Simon et al. Photolysis of $CHClF_2$ is rather unimportant throughout the atmosphere: reaction with OH radicals is the dominant destruction process.

Table 48. Absorption Cross Sections of $CHClF_2$

λ (nm)	$10^{20}\sigma$ (cm^2) 295 K	270 K	250 K	230 K	210 K
174	5.72	5.72	5.72	5.72	5.72
176	4.04	4.04	4.04	4.04	4.04
178	2.76	2.76	2.76	2.76	2.76
180	1.91	1.91	1.91	1.91	1.91
182	1.28	1.28	1.28	1.28	1.28
184	0.842	0.842	0.842	0.842	0.842
186	0.576	0.576	0.576	0.576	0.576
188	0.372	0.372	0.372	0.372	0.372
190	0.245	0.245	0.245	0.245	0.242
192	0.156	0.156	0.156	0.152	0.148
194	0.103	0.102	0.099	0.096	0.093
196	0.072	0.069	0.067	0.064	0.062
298	0.048	0.045	0.043	0.041	0.039
200	0.032	0.029	0.029	0.0259	0.0159
202	0.0220	0.0192	0.0184	0.0169	0.0159
204	0.0142	0.0121	0.0114	0.0104	0.0096

CH_3CF_2Cl (HCFC-142b) + hν → Products

The preferred absorption cross sections at 298 K, listed in Table 49, are the mean of the values reported by Gillotay and Simon [103] and Orlando et al. [238] over the wavelength range where the agreement is better than a factor of 2. At lower wavelengths the agreement is much better; e.g., at 200 nm the agreement is within 5%. Green and Wayne [111] and Hubrich and Stuhl [127] have also measured the cross sections in the ranges 185-200 nm and 160-230 nm, respectively. The results of Green and Wayne are very different from the recommended value and were not considered for this evaluation. The results of Hubrich and Stuhl (reported at 5 nm intervals) are in reasonable agreement with the more recent studies of Gillotay and Simon and of Orlando et al. The temperature dependence of the cross sections has been measured by Orlando et al. and by Gillotay and Simon, but it has not been included in this evaluation.

CF_3CHCl_2 (HCFC-123) + hν → Products

The preferred absorption cross sections at 298 K, listed in Table 49, are the mean of the values reported by Gillotay and Simon [103] and Orlando et al. [238]. The agreement is quite good over the entire wavelength range. The measurements by Green and Wayne [111] over the range 185-205 nm are in reasonable agreement with the recommended values. The temperature dependence of the cross sections has been measured by Orlando et al. and by Gillotay and Simon, but it is not included here. Recent work by Nayak et al. ([221] yields values that are in good agreement (within 10%) with this recommendation.

CF_3CHFCl (HCFC-124) + hν → Products

The preferred values are the average of those reported by Orlando et al. [238] and Gillotay and Simon [102], these being the only available sets of measurements between 190 and 230 nm. The data are listed in Table 49. The temperature dependence of the cross section has been measured by both groups but has not been evaluated here. The quantum yield for the dissociation to give Cl atoms is expected to be unity.

CH_3CFCl_2 (HCFC-141b) + hν → Products

The preferred absorption cross sections listed in Table 49 are taken from the work of Fahr et al. [86], who investigated the spectrum at 298 K both for the gas and liquid phases. The agreement with the values reported by Gillotay and Simon [103] is very good; it is not as good with the results of Talkudar et al. [299]. These last two groups also report the temperature dependence of the cross sections down to 210 K.

$CF_3CF_2CHCl_2$ (HCFC-225ca) + hν → Products

CF_2ClCF_2CHFCl (HCFC-225cb) + hν → Products

Table 50 lists the absorption cross sections for these molecules at 298 K, taken from the work of Braun et al. [28]. These values have been fitted with a mathematical expression for the wavelength range from 170 to 250 nm, for each of the two molecules. The expressions are listed in the original publication. The authors also measured the cross sections in the liquid phase.

Table 49. Absorption Cross Sections of Hydrochlorofluoroethanes at 298 K

λ (nm)	10^{20} σ(cm^2) at 298 K			
	CH_3CFCl_2 (141b)	CH_3CF_2Cl (142b)	CF_3CHCl_2 (123)	CF_3CHFCl (124)
190	83.8	0.94	59.0	0.77
192	64.1	0.66	44.5	0.55
194	47.4	0.46	32.9	0.39
196	34.0	0.31	23.6	0.27
198	23.8	0.21	16.9	0.18
200	16.4	0.14	11.9	0.13
202	11.1	0.09	8.3	0.086
204	7.4	0.061	5.7	0.060
206	4.9	0.039	4.0	0.040
208	3.2	0.026	2.7	0.027
210	2.1	0.017	1.8	0.019
212	1.4	0.010	1.3	0.012
214	0.89	0.007	0.87	0.008
216	0.57	0.004	0.61	0.006
218	0.37	0.003	0.40	0.004
220	0.24	0.002	0.28	0.003

Table 50. Absorption Cross Sections of $CF_3CF_2CHCl_2$ and CF_2ClCF_2CHFCl

λ (nm)	10^{20} σ(cm^2)	
	$CF_3CF_2CHCl_2$ (225ca)	CF_2ClCF_2CHFCl (225cb)
160	269	188
165	197	145
170	183	91
175	191	47
180	177	21
185	129	9.1
190	74	3.5
195	37	1.4
200	16	0.63
205	6.9	0.33
210	2.9	0.25
215	1.2	
220	0.46	
225	0.17	
230	0.065	
235	0.025	
239	0.011	

$CH_3OCl + h\nu \rightarrow$ Products

The absorption cross sections of CH_3OCl have been determined by Crowley et al. [75] and by Jungkamp et al. [149]. The preferred cross sections, listed in Table 51, are the mean of the values reported by these two groups. The agreement between the two sets of measurements is excellent at wavelengths longer than 250 nm; at the maximum near 230 nm the results of Jungkamp et al. are about 15% smaller.

Table 51 Absorption Cross Sections of CH_3OCl

λ (nm)	$10^{20}\sigma$ (cm^2)	λ (nm)	$10^{20}\sigma$ (cm^2)	λ (nm)	$10^{20}\sigma$ (cm^2)
230	14.9	290	1.32	350	0.662
232	15.4	292	1.34	352	0.611
234	15.7	294	1.35	354	0.574
236	15.9	296	1.37	356	0.529
238	15.8	298	1.40	358	0.482
240	15.5	300	1.43	360	0.445
242	14.9	302	1.45	362	0.411
244	14.2	304	1.47	364	0.389
246	13.2	306	1.48	366	0.356
248	12.2	308	1.49	368	0.331
250	11.1	310	1.49	370	0.298
252	9.96	312	1.48	372	0.273
254	8.86	314	1.47	374	0.246
256	7.77	316	1.46	376	0.225
258	6.80	318	1.43	378	0.209
260	5.87	320	1.41	380	0.202
262	5.05	322	1.37	382	0.186
264	4.31	324	1.33	384	0.17
266	3.69	326	1.30	386	0.16
268	3.16	328	1.24	388	0.15
270	2.71	330	1.20	390	0.13
272	2.35	332	1.14	392	0.14
274	2.06	334	1.09	394	0.13
276	1.83	336	1.04		
278	1.64	338	0.980		
280	1.53	340	0.918		
282	1.42	342	0.875		
284	1.37	344	0.822		
286	1.33	346	0.760		
288	1.32	348	0.709		

$BrO + h\nu \rightarrow Br + O$

The BrO radical has a banded spectrum in the 290-380 nm range. The strongest absorption feature is around 338 nm. The measured cross sections are both temperature- and resolution-dependent. As an example, the spectrum measured by Wahner et al. [319] is shown in Figure 5. The bands are due to a vibrational progression in the $A \leftarrow X$ system, and the location of the bands, along with the assignments and cross sections measured using 0.4 nm resolution, are shown in Table 52. BrO is expected to dissociate upon light absorption. As a guide, the cross sections averaged over 5 nm wavelength intervals are taken from the work of Cox et al. [73], and are listed in Table 53. These authors estimate a BrO lifetime against atmospheric photodissociation of ~20 seconds at the earth's surface, for a solar zenith angle of 30°.

The earlier BrO cross section measurements were carried out mostly around 338 nm, and these have been reviewed by CODATA ([61, 62]).

Table 52. Absorption Cross Sections at the Peak of Various Bands in the A ← X Spectrum of BrO

v', v"	λ (nm)	10^{20} σ(cm^2) 298 K	10^{20} σ(cm^2) 223 K
13,0	313.5	712	938
12,0	317.0	1010	1360
11,0	320.8	1180	1570
10,0	325.0	1130	1430
9,0	329.1	1130	1390
8,0	333.5	1210	1470
7,0	338.3	1550	1950
6,0	343.7	935	1110
5,0	348.8	703	896
4,0	354.7	722	1050
3,0	360.4	264	344
2,0	367.7	145	154
1,0	374.5	90	96

Spectral resolution is 0.4 nm, fwhm.

Table 53. Absorption Cross Sections of BrO

λ (nm)	10^{20} σ(cm^2) average
300 - 305	200
305 - 310	259
310 - 315	454
315 - 320	391
320 - 325	600
325 - 330	753
330 - 335	628
335 - 340	589
340 - 345	515
345 - 350	399
350 - 355	228
355 - 360	172
360 - 365	161
365 - 370	92
370 - 375	51

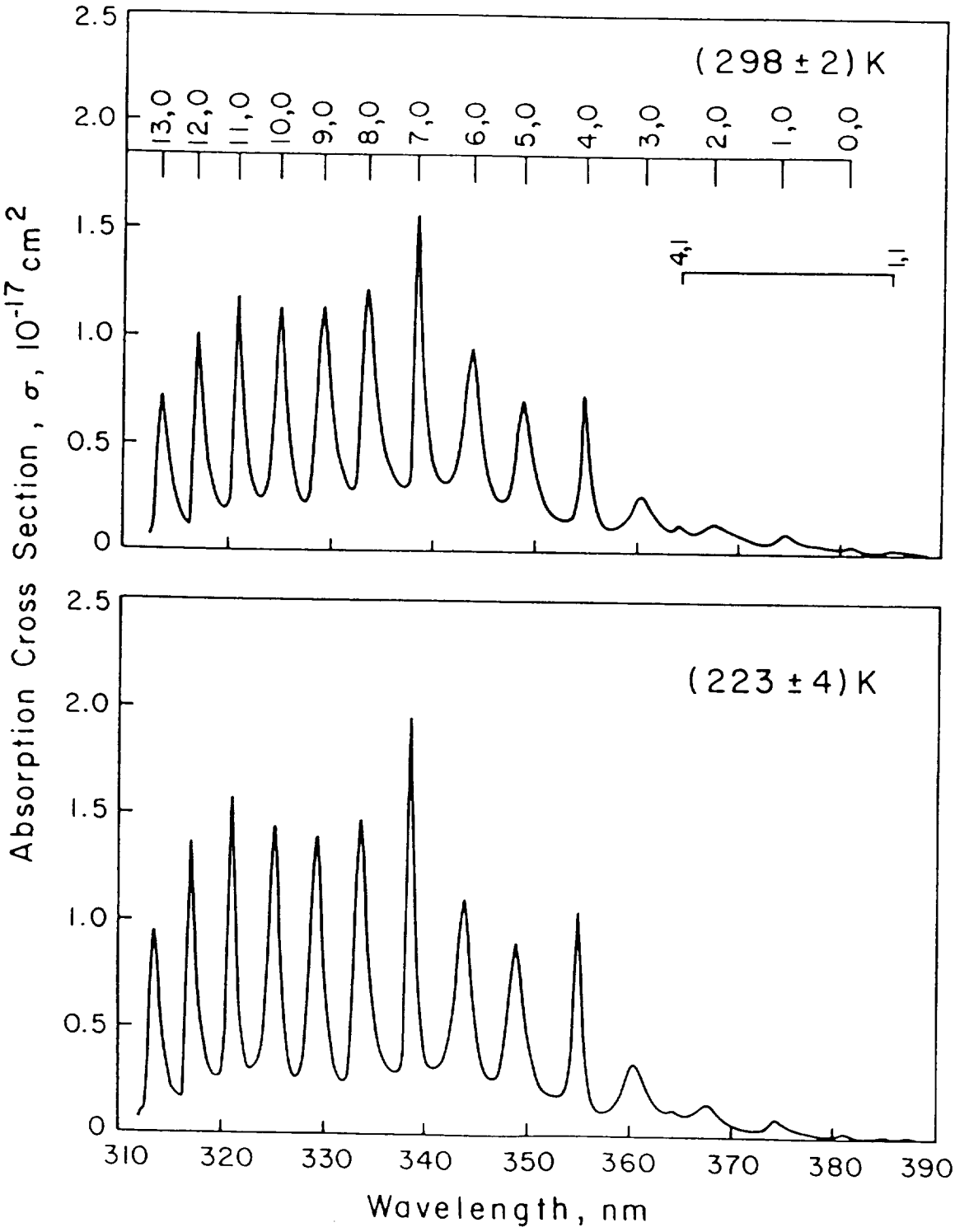

Figure 5. Absorption Spectrum of BrO

HOBr + hv → Products

The absorption spectrum of HOBr has been measured by Orlando and Burkholder [237], Deters et al. [84], Benter et al. [20], and Rattigan et al. [247]. The spectra cluster into two groups. Orlando and Burkholder, Deters et al., and Benter et al. agree reasonably well between 240 and 400 nm and show a sharp decrease in cross section above 400 nm. In contrast, the cross sections of Rattigan et al. are roughly 50% larger between 300 and 400 nm. Their spectrum also shows a pronounced absorption tail beyond 400 nm, leading to atmospheric photolysis rates for HOBr that are about a factor of 3 larger than those derived from the other studies. The long-wavelength tail observed by Rattigan et al. confirms the observations of Barnes et al. [16], who showed that laser photolysis of HOBr between 440-600 nm gives rise to OH fragments, implying the existence of weak HOBr absorption bands. The presence of a weak band beyond 400 nm is attributable to the presence of a forbidden transition from the ground electronic state to a triplet state predicted in *ab initio* calculations by Francisco et al. [91]. The differences in the spectral shapes are probably attributable to impurities such as Br_2O and Br_2. However, these cannot entirely explain the large differences in cross sections at the peaks of the absorption bands.

Because there is strong evidence in support of an absorption tail beyond 400 nm the recommendation (Table 54) is based on the study of Rattigan et al. The discrepancies in the measured cross sections between this work and the other studies throughout the measured spectral range require the assignment of large uncertainties (see Table 5). Additional work is required to resolve the significant discrepancies between the published spectra.

Benter et al. measured quantum yields for HOBr photolysis at 261 and 363 nm (the peaks of the strongest absorption bands). The observed quantum yield for Br formation at 363 nm was greater than 0.95. HBr was not detected as a photolysis product. As indicated above, the laser photofragment study of Barnes et al. also showed that OH was the major photolysis product at wavelengths beyond 400 nm.

Table 54. Absorption Cross Sections of HOBr

λ (nm)	10^{20} σ (cm^2)	λ (nm)	10^{20} σ (cm^2)	λ (nm)	10^{20} σ (cm^2)
240	6.7	330	11	420	1.3
245	5.2	335	11.5	425	1.1
250	6.7	340	12	430	0.9
255	9.9	345	12.3	435	0.8
260	14.1	350	12.5	440	0.7
265	18.9	355	12.2	445	0.7
270	23.9	360	11.6	450	0.7
275	28	365	10.7	455	0.7
280	30.4	370	9.6	460	0.6
285	30.8	375	8.4	465	0.5
290	28.7	380	7.4	470	0.5
295	25.2	385	6.2	475	0.4
300	20.9	390	5.1	480	0.3
305	16.8	395	4.1	485	0.3
310	13.8	400	3.3	490	0.2
315	11.8	405	2.6	495	0.1
320	10.8	410	2.0	500	0.1
325	10.6	415	1.6	505	.05

$BrONO_2 + h\nu \rightarrow$ Products

The bromine nitrate cross sections have been measured at room temperature by Spencer and Rowland [290] in the wavelength region 186-390 nm, and by Burkholder et al. [37] from 200-500 nm. The results from both studies are in excellent agreement over the range of spectral overlap. The recommended cross sections (Table 55) are taken from Burkholder et al.

The only study of photolysis products is that of Nickolaisen and Sander [227]. In that study, quantum yields for the Br + NO_3 and BrO + NO_2 channels were measured using broadband photolysis in quartz (λ>200 nm) and pyrex (λ>300 nm) reaction cells with the assumption that these were the only reaction pathways. The quantum yields were $\Phi_{BrO+NO2} = 0.71$ and $\Phi_{Br+NO3} = 0.29$.

Table 55. Absorption Cross Sections of $BrONO_2$

λ (nm)	$10^{20}\sigma$ (cm^2)	λ (nm)	$10^{20}\sigma$ (cm^2)	λ (nm)	$10^{20}\sigma$ (cm^2)
200	530	305	15	410	1.6
205	440	310	13	415	1.4
210	340	315	12	420	1.3
215	290	320	10	425	1.3
220	260	325	9.3	430	1.2
225	240	330	8.4	435	1.1
230	210	335	7.8	440	1.1
235	180	340	7.2	445	1.0
240	140	345	6.8	450	0.91
245	100	350	6.3	455	0.80
250	75	355	5.8	460	0.70
255	55	360	5.4	465	0.59
260	42	365	4.9	470	0.49
265	35	370	4.4	475	0.38
270	31	375	3.9	480	0.29
275	28	380	3.4	485	0.22
280	26	385	3.0	490	0.14
285	24	390	2.6	495	0.086
290	22	395	2.2	500	0.041
295	20	400	2.0		
300	17	405	1.7		

BrCl + hν → Br + Cl

The recommended absorption cross sections are given by the expression listed at the bottom of Table 56, which is take from the work of Maric et al. [176]. For convenience, some room temperature values are also listed in the table. Hubinger and Nee [126] have also measured the cross sections at room temperature. Their results are in excellent agreement with the recommended values.

Table 56. Absorption Cross Sections of BrCl at 298K

λ (nm)	$10^{20}\sigma$ (cm^2)	λ (nm)	$10^{20}\sigma$ (cm^2)
200	2.4	390	34.7
210	4.0	400	28.2
220	5.4	410	21.9
230	6.0	420	16.9
240	5.1	430	14.2
250	3.7	440	12.4
260	2.5	450	11.1
270	1.5	460	9.6
280	1.2	470	8.0
290	0.63	480	6.8
300	0.61	490	5.0
310	1.2	500	3.8
320	2.8	510	3.1
330	7.4	520	2.3
340	14.2	530	1.5
350	22.9	540	0.96
360	33.3	550	0.76
370	38.7	560	0.31
380	38.5		

$$\sigma = 10^{-20}\alpha^{0.5}\left\{7.34\exp\left[-68.6\alpha\left(\ln\frac{227.6}{\lambda}\right)^2\right] + 43.5\exp\left[-123.6\alpha\left(\ln\frac{372.5}{\lambda}\right)^2\right] + 11.2\exp\left[-84.8\alpha\left(\ln\frac{442.4}{\lambda}\right)^2\right]\right\}$$

where $\alpha = \tanh\left(\frac{318.8}{T}\right)$; λ in nm and T in K; 200 nm < λ < 600 nm; 300K > T > 195K.

$CH_3Br + h\nu \rightarrow$ Products

Table 57 lists the recommended absorption cross sections at 298 K, taken from Gillotay and Simon [100]. These authors measured the cross sections down to 210 K; for < 210 nm the temperature effect is negligible. Molina et al. [208] and Robbins [255] have also measured the absorption cross sections for this molecule at room temperature; the agreement among the three studies is very good.

Table 57. Absorption Cross Sections of CH_3Br

λ (nm)	$10^{20}\sigma$ (cm^2)	λ (nm)	$10^{20}\sigma$ (cm^2)
190	44	230	15
192	53	232	12
194	62	234	9.9
196	69	236	7.6
198	76	238	5.9
200	79	240	4.5
202	80	242	3.3
204	79	244	2.5
206	77	246	1.8
208	73	248	1.3
210	67	250	0.96
212	61	252	0.69
214	56	254	0.49
216	49	256	0.34
218	44	258	0.23
220	38	260	0.16
222	32		
224	28		
226	23		
228	19		

$CHBr_3 + h\nu \rightarrow$ Products

The absorption cross sections have been measured by Gillotay et al. [99] in the wavelength range from 190 to 310 nm, between 295 K and 240 K, and more recently by Moortgat et al. [215] in the 245 - 360 nm range at temperatures between 296 K and 256 K; the agreement in the overlap region is excellent. The recommended cross sections at room temperature are listed in Table 58. This new recommendation combines the two sets of values: between 190 and 285 nm they are taken from Gillotay et al. and at longer wavelengths from Moortgat et al. Table 58 also lists an expression, taken from Moortgat et al., that yields the cross sections as a function of temperature for wavelengths longer than 290 nm, the atmospherically important range. At these longer wavelengths the cross sections are relatively small; the presence of impurities as well as optical artifacts arising, e.g., from adsorption of $CHBr_3$ on the cell windows complicate the measurements. Hence, additional investigations of the spectra would be useful.

Table 58. Absorption Cross Sections of $CHBr_3$ at 296 K

λ (nm)	$10^{20}\sigma$ (cm^2)	λ (nm)	$10^{20}\sigma$ (cm^2)	λ (nm)	$10^{20}\sigma$ (cm^2)
190	399	248	194	306	0.298
192	360	250	174	308	0.226
194	351	252	158	310	0.171
196	366	254	136	312	0.127
198	393	256	116	314	0.0952
200	416	258	99	316	0.0712
202	433	260	83	318	0.0529
204	440	262	69	320	0.0390
206	445	264	57	322	0.0289
208	451	266	47	324	0.0215
210	468	268	38	326	0.0162
212	493	270	31	328	0.0121
214	524	272	25	330	0.0092
216	553	274	20	332	0.0069
218	574	276	16	334	0.0052
220	582	278	12	336	0.0040
222	578	280	9.9	338	0.0031
224	558	282	7.8	340	0.0024
226	527	284	6.1	342	0.0018
228	487	286	4.81	344	0.0013
230	441	288	3.75	346	0.0010
232	397	290	2.88	348	0.00080
234	362	292	2.22	350	0.00064
236	324	294	1.70	352	0.00054
238	295	296	1.28	354	0.00046
240	273	298	0.951	356	0.00032
242	253	300	0.719	358	0.00024
244	234	302	0.530	360	0.00017
246	214	304	0.394	362	0.00013

$\sigma(\lambda,T) = \exp[(0.06183 - 0.000241\,\lambda)(273 - T) - (2.376 + 0.14757\,\lambda)]$
λ: nm; T: K; σ: cm^2
290 nm < σ < 340 nm; 210 K < T < 300 K

CF_3Br (Halon-1301) + hν → Products

The preferred absorption cross sections at 298 K, listed in Table 59, are the mean of the values reported by Gillotay and Simon [101] at 2 nm intervals and Burkholder et al. [40] at 1 nm intervals over the wavelength range where the agreement is acceptable, i.e., better than 70%. At longer wavelengths Burkholder et al. [40] measure larger values than those reported by Gillotay and Simon. Molina et al. [208] have also measured these cross sections, which agree better with Gillotay and Simon. However, the agreement in the wavelength range 190-230 nm among the three studies is excellent. More recently, Orkin and Kasimovskaya [236] measured the cross sections at room temperature; their results are in good agreement with the recommended values over the wavelength region relevant for atmospheric photodissociation, i.e., ~ 200-220 nm. The temperature dependence of the cross sections has been measured by Gillotay and Simon as well as Burkholder et al. [40]. The agreement between these two studies is poor. We have not evaluated the temperature dependence of the cross sections, and the readers are referred to the original publications for this information. For all the bromofluoromethanes, photolysis is expected to cleave the C-Br bond with unit quantum efficiency. Orkin and Kasimovskaya measured the cross sections in the wavelength range 190-320 nm, at 295 K; their results agree with the recommendation.

CF_2Br_2 (Halon-1202) + hν → Products

The preferred absorption cross sections at 298 K, listed in Table 59, are the mean of the values reported by Gillotay and Simon [101] at 2 nm intervals and Burkholder et al. [40] at 1 nm intervals over the wavelength range where the agreement is no more than a factor of 2. At wavelengths longer than ~250 nm, Burkholder et al. [40] measured cross sections larger than those reported by Gillotay and Simon [101] and Molina et al. [208]. The discrepancy increases with wavelength and is more than a factor of 2 beyond 280 nm. However, the agreement between all three measurements is acceptable below 250 nm. The values of Molina et al. agree with those of Gillotay and Simon over the entire range of wavelengths. The temperature dependence of the cross sections has been measured by Gillotay and Simon as well as Burkholder et al. [40]. The agreement between these two studies is poor. Orkin and Kasimovskaya [236] measured the cross sections in the wavelength range 190-320 nm at 295 K; their results agree with the recommended values.

The quantum yield for the dissociation of CF_2Br_2 has been measured to be unity at 206, 248 and 308 nm by Molina and Molina [205], independent of pressure, in contrast to an earlier report by Walton [323] that the quantum yield at 265 nm decreases from unity when the system pressure is raised to 50 torr of CO_2. Orkin and Kasimovskaya [236] measured the cross sections in the wavelength range 190-320 nm, at 295 K; their results agree with the recommendation.

CF_2BrCF_2Br (Halon-2402) + hν → Products

The preferred absorption cross sections at 298 K, listed in Table 59, are the mean of the values reported by Gillotay et al. [104] at 2 nm intervals and Burkholder et al. [40] at 1 nm intervals over the wavelength range where the agreement is acceptable, i.e., ~70%. At longer wavelengths, Burkholder et al. [40] measured larger cross sections than those measured by Gillotay et al. Molina et al. [208] have also measured these cross sections, and they agree with the results of Gillotay et al. at longer wavelengths. The agreement between the three studies at wavelengths shorter than 250 nm is good. The results of Robbins [256] and of Orkin and Kasimovskaya [236] are in good agreement with the recommended values.

The temperature dependence of the cross sections has been measured by Gillotay et al. and Burkholder et al. The agreement between the two studies is poor at longer wavelengths. We have not evaluated the temperature dependence of the cross section, and the readers are referred to the investigators for the information. Orkin and Kasimovskaya measured the cross sections in the wavelength range 190-320 nm, at 295 K; their results agree with the recommendation.

Table 59. Absorption Cross Sections of CF_2ClBr, CF_2Br_2, CF_3Br, and CF_2BrCF_2Br at 298 K

λ (nm)	$10^{20}\ \sigma(cm^2)$			
	CF_2ClBr (1211)	CF_2Br_2 (1202)	CF_3Br (1301)	CF_2BrCF_2Br (2402)
190	47	114	6.4	109
192	58	109	7.5	114
194	70	100	8.5	119
196	83	91	9.5	122
198	96	82	10.4	124
200	112	75	11.2	124
202	118	72	11.8	124
204	121	74	12.2	120
206	122	81	12.4	117
208	121	93	12.4	112
210	117	110	12.0	106
212	112	136	11.4	100
214	106	155	10.7	92
216	98	180	9.8	85
218	90	203	8.8	77
220	81	224	7.7	69
222	72	242	6.7	61
224	64	251	5.7	54
226	56	253	4.7	47
228	49	250	3.8	40
230	42	241	3.1	35
232	36	227	2.4	29
234	31	209	1.9	24
236	26	189	1.4	20
238	22	168	1.1	16
240	18	147	0.81	13
242	15	126	0.59	11
244	12	106	0.43	8.4
246	10	88	0.31	6.7
248	8.0	73	0.22	5.2
250	6.5	59	0.16	4.1
252	5.1	47	0.11	3.1
254	4.0	37	0.076	2.3
256	3.2	29	0.053	1.8
258	2.4	23	0.037	1.3
260	1.9	18	0.026	0.95
262	1.4	13	0.018	0.71
264	1.1	10	0.012	0.53
266	0.84	7.6	0.009	0.39
268	0.63	5.7	0.006	0.28
270	0.48	4.2		0.21
272	0.36	3.1		0.16

Continued on next page. . .

Table 59. (Continued)

λ (nm)	10^{20} σ(cm^2)			
	CF_2ClBr (1211)	CF_2Br_2 (1202)	CF_3Br (1301)	CF_2BrCF_2Br (2402)
274	0.27	2.2		0.11
276	0.20	1.6		0.082
278	0.15	1.2		0.060
280	0.1	0.89		0.044
282	0.079	0.65		
284	0.058	0.48		
286	0.043	0.34		
288	0.031	0.24		
290		0.18		
292		0.13		
294		0.096		
296		0.068		
298		0.050		
300		0.036		

CF_2ClBr (Halon-1211) + hν → Products

The preferred absorption cross sections at 298 K, listed in Table 59, are the mean of the values reported by Gillotay and Simon [101] at 2 nm intervals and Burkholder et al. [40] at 1 nm intervals. Molina et al. [208], Giolando et al. [106], and Orkin and Kasimovskaya [236] have also measured the cross sections at 5 nm and 10 nm intervals, respectively. The agreement among all these studies is quite good.

The temperature dependence of the cross sections has been measured by Gillotay and Simon, as well as Burkholder et al. The agreement between the two studies is poor. We have not evaluated the temperature dependence of the cross section, and the readers are referred to the original publications for this information. Orkin and Kasimovskaya measured the cross sections in the wavelength range 190-320 nm, at 295 K; their results agree with the recommendation.

$CF_3I + h\nu \rightarrow CF_3 + I$

Table 60 lists the recommended absorption cross sections: The 298 K values are the average of the data from Solomon et al. [288] and Fahr et al. [87]. The fit of the temperature dependent data of Fahr et al. agrees with that of Solomon et al. to better than 15% at all temperatures and wavelengths. The B values in the table are from Solomon et al. The temperature effect is significant at the longer wavelengths: at 350 nm, the cross sections decrease by about 30% at 253 K and by about 40% at 233 K, compared to the room temperature value. Walters et al. [322] have also measured the cross sections as a function of temperature at the atmospherically important wavelengths beyond 300 nm. The Fahr et al. values are about 18% higher than those of Walters et al.; however, at the longer wavelengths and lower temperatures (253 K) the disagreement is larger.

Table 60. Absorption Cross Sections of CF_3I at 298 K and temperature coefficient B*

λ (nm)	$10^{20}\sigma(298)$ (cm^2)	$Bx10^3$ (K^{-1})	λ (nm)	$10^{20}\sigma(298)$ (cm^2)	$Bx10^3$ (K^{-1})
240	13.7	0.582	294	16.3	3.565
242	16.6	0.466	296	13.4	3.978
244	20.1	0.344	298	10.9	4.405
246	24.0	0.219	300	8.9	4.876
248	28.5	0.093	302	7.2	5.361
250	33.4	-0.042	304	5.8	5.806
252	38.8	-0.176	306	4.6	6.201
254	44.2	-0.304	308	3.7	6.542
256	49.6	-0.425	310	2.9	6.824
258	54.7	-0.530	312	2.3	7.045
260	59.5	-0.613	314	1.8	7.220
262	63.1	-0.670	316	1.5	7.355
264	65.9	-0.701	318	1.2	7.459
266	67.5	-0.696	320	0.93	7.531
268	67.6	-0.650	322	0.73	7.584
270	66.5	-0.568	324	0.56	7.670
272	64.4	-0.444	326	0.44	7.742
274	61.0	-0.271	328	0.34	7.777
276	56.9	-0.056	330	0.27	7.906
278	52.3	0.206	332	0.21	8.046
280	47.0	0.520	334	0.16	8.105
282	41.9	0.878	336	0.13	8.276
284	36.8	1.280	338	0.10	8.484
286	32.5	1.729	340	0.08	8.522
288	27.9	2.215	342	0.06	8.533
290	23.6	2.715	344	0.05	8.384
292	19.9	3.169			

* $\sigma(\lambda,T) = \sigma(\lambda,298) \exp [B(\lambda) (T-298)]$; T in K

$300 K > T > 210 K$

$SO_2 + h\nu \rightarrow$ Products

The UV absorption spectrum of SO_2 is highly structured, with a very weak absorption in the 340-390 nm region, a weak absorption in the 260-340 nm region, and a strong absorption extending from 180 to 235 nm; the threshold wavelength for photodissociation is ~220 nm. The atmospheric photochemistry of SO_2 has been reviewed by Heicklen et al. [120] and by Calvert and Stockwell [48]. Direct photo-oxidation at wavelengths longer than ~300 nm by way of the electronically excited states of SO_2 appears to be relatively unimportant.

The absorption cross sections have been measured by McGee and Burris [188] at 295 and 210 K, between 300 and 324 nm, which is the wavelength region commonly used for atmospheric monitoring of SO_2. Manatt and Lane [171] have recently compiled and evaluated the earlier cross section measurements between 106 and 403 nm.

$CS_2 + h\nu \rightarrow CS + S$

The CS_2 absorption spectrum is rather complex. Its photochemistry has been reviewed by Okabe [234]. There are two distinct regions in the near UV spectrum: a strong absorption extending from 185 to 230 nm, and a weaker one in the 290-380 nm range. The threshold wavelength for photodissociation is ~280 nm. Absorption cross section measurements have been reported recently by Xu and Joens [331] between 187 and 230 nm.

The photo-oxidation of CS_2 in the atmosphere has been discussed by Wine et al. [327], who report that electronically excited CS_2 may react with O_2 to yield eventually OCS.

$OCS + h\nu \rightarrow CO + S$

The absorption cross sections of OCS have been measured by Breckenridge and Taube [29], who presented their 298 K results in graphical form, between 200 and 260 nm; by Rudolph and Inn [264] between 200 and ~300 nm (see also Turco et al. [306]), at 297 and 195 K; by Leroy et al. [157] at 294 K, between 210 and 260 nm, using photographic plates; and by Molina et al. [199] between 195 and 260 nm, in the 195 K to 403 K temperature range. The results are in good agreement in the regions of overlap, except for $\lambda > 280$ nm, where the cross section values reported by Rudolph and Inn [264] are significantly larger than those reported by Molina et al. [199]. The latter authors concluded that solar photodissociation of OCS in the troposphere occurs only to a negligible extent.

The recommended cross sections, given in Table 61, are taken from Molina et al. [199]. (The original publication also lists a table with cross section values averaged over 1 nm intervals, between 185 and 300 nm.)

Rudolph and Inn [264] reported a quantum yield for photodissociation of 0.72, based on measurements of the quantum yield for CO production in the 220-254 nm range. Additional measurements would be useful.

Table 61. Absorption Cross Sections of OCS

λ (nm)	$10^{20}\sigma(cm^2)$ 295 K	225 K	λ (nm)	$10^{20}\sigma(cm^2)$ 295 K	225 K
186.1	18.9	13.0	228.6	26.8	23.7
187.8	8.33	5.63	231.2	22.1	18.8
189.6	3.75	2.50	233.9	17.1	14.0
191.4	2.21	1.61	236.7	12.5	9.72
193.2	1.79	1.53	239.5	8.54	6.24
195.1	1.94	1.84	242.5	5.61	3.89
197.0	2.48	2.44	245.4	3.51	2.29
199.0	3.30	3.30	248.5	2.11	1.29
201.0	4.48	4.50	251.6	1.21	0.679
203.1	6.12	6.17	254.6	0.674	0.353
205.1	8.19	8.27	258.1	0.361	0.178
207.3	10.8	10.9	261.4	0.193	0.0900
209.4	14.1	14.2	264.9	0.0941	0.0419
211.6	17.6	17.6	268.5	0.0486	0.0199
213.9	21.8	21.8	272.1	0.0248	0.0101
216.2	25.5	25.3	275.9	0.0119	0.0048
218.6	28.2	27.7	279.7	0.0584	0.0021
221.5	30.5	29.4	283.7	0.0264	0.0009
223.5	31.9	29.5	287.8	0.0012	0.0005
226.0	30.2	27.4	292.0	0.0005	0.0002
			296.3	0.0002	-

$SF_6 + h\nu \rightarrow$ Products

The species SF_6 does not absorb at wavelengths longer than 130 nm; it is expected to have an atmospheric residence time of thousands of years (Ravishankara et al. [250]; Ko et al. [152]).

NaOH + hν → Na + OH

The spectrum of NaOH vapor is poorly characterized. Rowland and Makide [261] inferred the absorption cross section values and the average solar photodissociation rate from the flame measurements of Daidoji [78]. Additional measurements are required.

NaCl + hν → Na + Cl

There are several studies of the UV absorption spectra of NaCl vapor. For a review of the earlier work, which was carried out at high temperatures, see Rowland and Rogers [262]. The recommended cross sections, listed in Table 62, are taken from the work of Silver et al. [281], who measured spectra of gas phase NaCl at room temperature in the range from ~190 to 360 nm by directly monitoring the product Na atoms.

Table 62. Absorption Cross Sections of NaCl Vapor at 300 K

λ(nm)	$10^{20}\sigma(cm^2)$
189.7	612
193.4	556
203.1	148
205.3	90.6
205.9	89.6
210.3	73.6
216.3	151
218.7	46.3
225.2	146
230.4	512
231.2	947
234.0	1300
237.6	638
241.4	674
248.4	129
251.6	251
254.8	424
260.2	433
268.3	174
277.0	40
291.8	0.8

References for Photochemistry Section

1. The Stratosphere 1981: Theory and Measurements, World Meteorological Organization Global Ozone Research and Monitoring Project, Report No. 11; see NASA-TM-84125, 1982, National Aeronautics and Space Administration.
2. Adler-Golden, S.M. and J.R. Wiesenfeld, 1981, Chem. Phys. Lett., **82**, 281.
3. Allen, M. and J.E. Frederick, 1982, J. Atmos. Sci., **39**, 2066-2075.
4. Amimoto, S.T., A.P. Force, J.R. Wiesenfeld, and R.H. Young, 1980, J. Chem. Phys., **73**, 1244-1247.
5. Amoruso, A., M. Cacciani, A. DiSarra, and G. Fiocco, 1990, J. Geophys. Res., **95**, 20565.
6. Amoruso, A., L. Crescentini, G. Fiocco, and M. Volpe, 1993, J. Geophys. Res., **98**, 16857-16863.
7. Amoruso, A., L. Crescentini, M. Silvia Cola, and G. Fiocco, 1996, J. Quant. Spectrosc. Radiat. Transfer, **56**, 145-152.
8. Anderson, G.P. and L.A. Hall, 1983, J. Geophys. Res., **88**, 6801-6806.
9. Anderson, G.P. and L.A. Hall, 1986, J. Geophys. Res., **91**, 14509-14514.
10. Arnold, I., F.J. Comes, and G.K. Moortgat, 1977, Chem. Phys., **24**, 211-217.
11. Baer, S., H. Hippler, R. Rahn, M. Siefke, N. Seitzinger, and J. Troe, 1991, J. Chem. Phys., **95**, 6463-6470.
12. Ball, S.M., G. Hancock, I.J. Murphy, and S.P. Rayner, 1993, Geophys. Res. Lett., **20**, 2063-2066.
13. Ball, S.M., G. Hancock, and F. Winterbottom, 1995, Faraday Discuss., **100**, 215.
14. Ballash, N.M. and D.A. Armstrong, 1974, Spectrochim Acta, **30A**, 941-944.
15. Barker, J.R., L. Brouwer, R. Patrick, M.J. Rossi, P.L. Trevor, and D.M. Golden, 1985, Int. J. Chem. Kinet., **17**, 991-1006.
16. Barnes, R.J., M. Lock, J. Coleman, and A. Sinha, 1996, J. Phys. Chem., **100**, 453-457.
17. Bass, A.M., L.C. Glasgow, C. Miller, J.P. Jesson, and S.L. Filken, 1980, Planet. Space Sci., **28**, 675.
18. Bass, A.M., A.E. Ledford, and A.H. Laufer, 1976, J. Res. NBS, **80A**, 143-166.
19. Bauer, D., J.N. Crowley, and G.K. Moortgat, 1992, J. Photochem. and Photobiol., **A65**, 3530-3538.
20. Benter, T., C. Feldmann, U. Kirchner, M. Schmidt, S. Schmidt, and R.N. Schindler, 1995, Ber. Bunsenges. Phys. Chem., **99**, 1144-1147.
21. Biaume, F., 1973, J. Photochem., **2**, 139.
22. Birk, M., R.R. Friedl, E.A. Cohen, H.M. Pickett, and S.P. Sander, 1989, J. Chem. Phys., **91**, 6588-6597.
23. Birks, J.W., B. Shoemaker, T.J. Leck, R.A. Borders, and L.J. Hart, 1977, J. Chem. Phys., **66**, 4591.
24. Bishenden, E., J. Haddock, and D.J. Donaldson, 1991, J. Phys. Chem., **95**, 2113.
25. Bishenden, E., J. Haddock, and D.J. Donaldson, 1992, J. Phys. Chem., **96**, 6513.
26. Bongartz, A., J. Kames, F. Welter, and U. Schurath, 1991, J. Phys. Chem., **95**, 1076-1082.
27. Brandon, J.T., S.A. Reid, D.C. Robie, and H. Reisler, 1992, J. Chem. Phys., **97**, 5246.
28. Braun, M., A. Fahr, R. Klein, M.J. Kurylo, and R.E. Huie, 1991, J. Geophys. Res., **96**, 13009.
29. Breckenridge, W. and H.H. Taube, 1970, J. Chem. Phys., **52**, 1713-1715.
30. Brion, J., A. Chakir, D. Daumont, J. Malicet, and C. Parisse, 1993, Chem. Phys. Lett., **213**, 610-612.
31. Brock, J.C. and R.T. Watson, 1980, Chem. Phys., **46**, 477-484.
32. Brock, J.C. and R.T. Watson, 1980, Chem. Phys. Lett., **71**, 371-375.
33. Burkholder, J.B., 1993, J. Geophys. Res., **98**, 2963-2974.
34. Burkholder, J.B. and E.J. Bair, 1983, J. Phys. Chem., **87**, 1859-1863.
35. Burkholder, J.B., R.L. Mauldin, R.J. Yokelson, S. Solomon, and A.R. Ravishankara, 1993, J. Phys. Chem., **97**, 7597-7605.
36. Burkholder, J.B., J.J. Orlando, and C.J. Howard, 1990, J. Phys. Chem., **94**, 687-695.
37. Burkholder, J.B., A.R. Ravishankara, and S. Solomon, 1995, J. Geophys. Res., **100**, 16793-16800.
38. Burkholder, J.B., R.K. Talukdar, and A.R. Ravishankara, 1994, Geophys. Res. Lett., **21**, 585-588.
39. Burkholder, J.B., R.K. Talukdar, A.R. Ravishankara, and S. Solomon, 1993, J. Geophys. Res., **98**, 22937-22948.
40. Burkholder, J.B., R.R. Wilson, T. Gierczak, R. Talukdar, S.A. McKeen, J.J. Orlando, G.L. Vaghjiani, and A.R. Ravishankara, 1991, J. Geophys. Res., **96**, 5025-5043.
41. Burley, J.D., C.E. Miller, and H.S. Johnston, 1993, J. Molec. Spec, **158**, 377-391.
42. Burrows, J.P., G.S. Tyndall, and G.K. Moortgat, paper presented at the 16th Informal Conf. on Photochemistry, 1984, Boston.
43. Burrows, J.P., G.S. Tyndall, and G.K. Moortgat, 1985, J. Phys. Chem., **89**, 4848-4856.
44. Burrows, J.P., G.S. Tyndall, and G.K. Moortgat, 1988, J. Phys. Chem., **92**, 4340-4348.
45. Butler, P.J.D. and L.F. Phillips, 1983, J. Phys. Chem., **87**, 183-184.

46. Cacciani, M., A.D. Sarra, G. Fiocco, and A. Amoruso, 1989, J. Geophys. Res., **94**, 8485-8490.
47. Calvert, J.G. and J.N. Pitts, Photochemistry, 1966, New York: John Wiley & Sons, Inc., pp. 230-231.
48. Calvert, J.G. and W.R. Stockwell, 1983, Acid Precipitation: SO_2, NO, NO_2 Oxidation Mechanisms: Atmospheric Considerations, Ann Arbor Sci. Publishers, Ann Arbor, Michigan.
49. Canosa-Mas, C.E., M. Fowles, P.J. Houghton, and R.P. Wayne, 1987, J. Chem. Soc. Faraday Trans. 2, **83**, 1465.
50. Cantrell, C.A., J.A. Davidson, A.H. McDaniel, R.E. Shetter, and J.G. Calvert, 1990, J. Phys. Chem., **94**, 3902-3908.
51. Cantrell, C.A., J.A. Davidson, R.E. Shetter, B.A. Anderson, and J.G. Calvert, 1987, J. Phys. Chem., **91**, 5858-5863.
52. Chang, J.S., J.R. Barker, J.E. Davenport, and D.M. Golden, 1979, Chem. Phys. Lett., **60**, 385-390.
53. Cheung, A.S.C., K. Yoshino, J.R. Esmond, S.S.L. Chiu, D.E. Freeman, and W.H. Parkinson, 1990, J. Chem. Phys., **92**, 842-849.
54. Cheung, A.S.C., K. Yoshino, W.H. Parkinson, and D.E. Freeman, 1984, Geophys. Res. Lett., **11**, 580-582.
55. Cheung, A.S.C., K. Yoshino, W.H. Parkinson, S.L. Guberman, and D.E. Freeman, 1986, Planet. Space Sci., **34**, 1007-1021.
56. Chiu, S.S.L., A.S.C. Cheung, K. Yoshino, J.R. Esmond, D.E. Freeman, and W.H. Parkinson, 1990, J. Chem. Phys., **93**, 5539-5543.
57. Chou, C.C., G. Crescentini, H. Vera-Ruiz, W.S. Smith, and F.S. Rowland, paper presented at the 173rd American Chemical Society Meeting, 1977, New Orleans, LA.
58. Chou, C.C., R.J. Milstein, W.S. Smith, H. Vera-Ruiz, M.J. Molina, and F.S. Rowland, 1978, J. Phys. Chem., **82**, 1.
59. Chou, C.C., H. Vera-Ruiz, K. Moe, and F.S. Rowland, 1976, unpublished results.
60. Clark, J.H., C.B. Moore, and N.S. Nogar, 1978, J. Chem. Phys., **68**, 1264-1271.
61. CODATA, 1980, J. Phys. Chem. Ref. Data, **9**, 295-471.
62. CODATA, 1982, J. Phys. Chem. Ref. Data, **11**, 327-496.
63. Colussi, A.J., 1990, J. Phys. Chem., **94**, 8922-8926.
64. Colussi, A.J., S.P. Sander, and R.R. Friedl, 1992, J. Phys.Chem., **96**, 4442-4445.
65. Cooper, I.A., P.J. Neill, and J.R. Wiesenfeld, 1993, J. Geophys. Res., **98**, 12795-12800.
66. Coquart, B., A. Jenouvier, and M.F. Merienne, 1995, J. Atm. Chem, **21**, 251-261.
67. Coquart, B., M.F. Merienne, and A. Jenouvrier, 1990, Planet. Space Sci., **38**, 287.
68. Corcoran, T.C., E.J. Beiting, and M.O. Mitchell, 1992, J. Molecular Spectroscopy, **154**, 119-128.
69. Cox, R.A., R.A. Barton, E. Ljungstrum, and D.W. Stocker, 1984, Chem. Phys. Lett., **108**, 228-232.
70. Cox, R.A. and J.P. Burrows, 1979, J. Phys. Chem., **83**, 2560-2568.
71. Cox, R.A. and G.D. Hayman, 1988, Nature, **332**, 796-800.
72. Cox, R.A. and R. Patrick, 1979, Int. J. Chem. Kinet., **11**, 635.
73. Cox, R.A., D.W. Sheppard, and M.P. Stevens, 1982, J. Photochem., **19**, 189-207.
74. Coxon, J.A., W.E. Jones, and D.A. Ramsey, paper presented at the 12th International Symposium on Free Radicals, 1976, Laguna Beach, California.
75. Crowley, J.N., R. Helleis, R. Muller, G.K. Moortgat, P.J. Crutzen, and J.J. Orlando, 1994, J. Geophys. Res., **99**, 20683-20688.
76. Crowley, J.N., F.G. Simon, J.P. Burrows, G.K. Moortgat, M.E. Jenkin, and R.A. Cox, 1991, J. Photochem. and Photobiol. A: Chem., **60**, 1-10.
77. Dagaut, P. and M.J. Kurylo, 1990, J. Photochem. and Photobiol. A:Chem., **51**, 133.
78. Daidoji, H., 1979, Bunseki Kagaku, **28**, 77.
79. Daumont, D., J. Brion, J. Charbonnier, and J. Malicet, 1992, J. Atmos. Chem., **15**, 145-155.
80. Davenport, J.E., 1978, Report No. FAA-EQ-78-14, Federal Aviation Administration, Washington, DC.
81. Davidson, J.A., C.A. Cantrell, A.H. McDaniel, R.E. Shetter, S. Madronich, and J.G. Calvert, 1988, J. Geophys. Res., **93**, 7105-7112.
82. Davis, H.F. and Y.T. Lee, 1992, J. Phys. Chem., **96**, 5681-5684.
83. DeMore, W.B. and E. Tschuikow-Roux, 1990, J. Phys. Chem., **94**, 5856-5860.
84. Deters, B., J.P. Burrows, S. Himmelmann, and C. Blindauer, 1996, Ann. Geophysicae, **14**, 468-475.
85. Eberstein, I.J., 1990, Geophys. Res. Lett., **17**, 721-724.
86. Fahr, A., W. Braun, and M.J. Kurylo, 1993, J. Geophys. Res., **98**, 20467-20472.
87. Fahr, A., A.K. Nayak, and R. Huie, 1995, Chem. Phys., **199**, 275-284.
88. Fairchild, C.E., E.J. Stone, and G.M. Lawrence, 1978, J. Chem. Phys., **69**, 3632-3638.

89. Fenter, F.F., V. Catoire, R. Lesclaux, and P.D. Lightfoot, 1993, J. Phys. Chem., **97**, 3530-3538.
90. Fergusson, W.C., L. Slotin, and W.G. Style, 1936, Trans. Far. Soc., **32**, 956.
91. Francisco, J.S., M.R. Hand, and I.H. Williams, 1996, J. Phys. Chem., **100**, 9250-9253.
92. Frederick, J.E. and R.D. Hudson, 1979, J. Atmos. Sci., **36**, 737-745.
93. Frederick, J.E. and J.E. Mentall, 1982, Geophys. Res. Lett., **9**, 461-464.
94. Frost, G.J., L.M. Goss, and V. Vaida, 1996, J. Geophys. Res, **101**, 3869-3877.
95. Frost, G.J., L.M. Goss, and V. Vaida, 1996, J. Geophys. Res., **101**, 3879-3884.
96. Ganske, J.A., H.N. Berko, and B.J. Finlayson-Pitts, 1992, J. Geophys. Res., **97**, 7651-7656.
97. Gardner, E.P., P.D. Sperry, and J.G. Calvert, 1987, J. Geophys. Res., **92**, 6642-6652.
98. Gibson, G.E. and N.S. Bayliss, 1933, Phys. Rev., **44**, 188.
99. Gillotay, D., A. Jenouvrier, B. Coquart, M.F. Merienne, and P.C. Simon, 1989, Planet. Space Sci., **37**, 1127-1140.
100. Gillotay, D. and P.C. Simon, 1988, Annales Geophysicae, **6**, 211-215.
101. Gillotay, D. and P.C. Simon, 1989, J. Atmos. Chem., **8**, 41-62.
102. Gillotay, D. and P.C. Simon, 1991, J. Atmos. Chem., **13**, 289-299.
103. Gillotay, D. and P.C. Simon, 1991, J. Atmos. Chem., **12**, 269-285.
104. Gillotay, D., P.C. Simon, and L. Dierickx, 1988, Aeronomica Acta, **A335**, 1-25.
105. Gillotay, D., P.C. Simon, and L. Dierickx, 1993, Aeronomica Acta, **A368**, 1-15.
106. Giolando, D.M., G.B. Fazekas, W.D. Taylor, and G.A. Takacs, 1980, J. Photochem., **14**, 335.
107. Goodeve, C.F. and F.D. Richardson, 1937, Trans. Faraday. Soc., **33**, 453-457.
108. Graham, R.A., 1975, Ph. D. Thesis, "Photochemistry of NO_3 and the Kinetics of the N_2O_5-O_3 System", University of California, Berkeley, CA.
109. Graham, R.A. and H.S. Johnston, 1978, J. Phys. Chem., **82**, 254-268.
110. Graham, R.A., A.M. Winer, and J.N. Pitts Jr., 1978, Geophys. Res. Lett., **5**, 909.
111. Green, R.G. and R.P. Wayne, 1976/77, J. Photochem., **6**, 375-377.
112. Greenblatt, G.D. and A.R. Ravishankara, 1990, J. Geophys. Res., **95**, 3539-3547.
113. Harder, J.W., J.W. Brault, P.V. Johnston, and G.H. Mount, 1996, J. Geophys. Res., submitted.
114. Harker, A.B., W. Ho, and J.J. Ratto, 1977, Chem. Phys. Lett., **50**, 394-397.
115. Harwood, M.H. and R.L. Jones, 1994, J. Geophys. Res., **99**, 22995-22964.
116. Harwood, M.H., R.L. Jones, R.A. Cox, E. Lutman, and O.V. Rattigan, 1993, J. Photochem. Photobiol. A: Chem., **73**, 167-175.
117. Harwood, M.H., D.M. Rowley, R.A. Freshwater, R.A. Cox, and R.L. Jones, 1995, J. Chem. Soc. Faraday Trans, **91**, 3027-3032.
118. Hayman, G.D. and R.A. Cox, 1989, Chem. Phys. Lett., **155**, 1-7.
119. Hearn, A.G., 1961, Proc. Phys. Soc. London, **78**, 932-940.
120. Heicklen, J., N. Kelly, and K. Partymiller, 1980, Rev. Chem. Intermediates, **3**, 315-404.
121. Herman, J.R. and J.E. Mentall, 1982, J. Geophys. Res., **87**, 8967-8975.
122. Herzberg, G. and K.K. Innes, 1957, Canad. J. Phys., **35**, 842.
123. Hochanadel, C.J., J.A. Ghormley, and P.J. Ogren, 1972, J. Chem. Phys., **56**, 4426-4432.
124. Horowitz, A. and J.G. Calvert, 1978, Int. J. Chem. Kinet., **10**, 805.
125. Hubinger, S. and J.B. Nee, 1994, Chem. Phys., **181**, 247-257.
126. Hubinger, S. and J.B. Nee, 1995, J. Photochem. and Photobiol. A: Chem., **85**, 1-7.
127. Hubrich, C. and F. Stuhl, 1980, J. Photochem., **12**, 93-107.
128. Hubrich, C., C. Zetzsch, and F. Stuhl, 1977, Ber. Bunsenges. Phys. Chem., **81**, 437-442.
129. Huder, K.J. and W.B. DeMore, 1995, J. Phys. Chem., **99**, 3905-3908.
130. Hudson, R.D., 1971, Reviews of Geophysics and Space Physics, **9**, 305-399.
131. Hudson, R.D., 1974, Canad. J. Chem., **52**, 1465-1478.
132. Hudson, R.D. and L.J. Kieffer, 1975, "Absorption Cross Sections of Stratospheric Molecules," The Natural Stratosphere of 1974, Monograph 1, CIAP, pp. (5-156)-(5-194).
133. Illies, A.J. and G.A. Takacs, 1976, J. Photochem., **6**, 35-42.
134. Inn, E.C.Y., 1975, J. Atmos. Sci., **32**, 2375.
135. Inn, E.C.Y., 1980, J. Geophys. Res., **85**, 7493.
136. Inn, E.C.Y. and Y. Tanaka, 1953, J. Opt. Soc. Am., **43**, 870-873.
137. Jenouvrier, A., B. Coquart, and M.F. Merienne, 1986, J. Quant. Spectros. Radiat. Transfer, **36**, 349-354.
138. Jensen, F. and J. Oddershede, 1990, J. Phys. Chem., **94**, 2235.
139. Johnston, H.S., S. Chang, and G. Whitten, 1974, J. Phys. Chem., **78**, 1-7.

140. Johnston, H.S., H.F. Davis, and Y.T. Lee, 1996, J. Phys. Chem., **100**, 4713-4723.
141. Johnston, H.S. and R. Graham, 1973, J. Chem. Phys., **77**, 62.
142. Johnston, H.S. and R. Graham, 1974, Canad. J. Chem., **52**, 1415-1423.
143. Johnston, H.S., E.D. Morris Jr., and J. Van den Bogaerde, 1969, J. Am. Chem. Soc., **91**, 7712.
144. Johnston, H.S., M. Paige, and F. Yao, 1984, J. Geophys. Res., **89**, 661.
145. Jolly, G.S., D.L. Singleton, D.J. McKenney, and G. Paraskevopoulos, 1986, J. Chem. Phys., **84**, 6662-6667.
146. Jones, E.L. and O.R. Wulf, 1937, J. Chem. Phys., **5**, 873.
147. Jones, I.T.N. and K. Bayes, 1973, J. Chem. Phys., **59**, 4836-4844.
148. Jourdain, J.L., G. Le Bras, G. Poulet, J. Combourieu, P. Rigaud, and B. LeRoy, 1978, Chem. Phys. Lett., **57**, 109.
149. Jungkamp, T.P.W., U. Kirchner, M. Schmidt, and R.N. Schindler, 1995, J. Photochem. Photobiol. A: Chemistry, **99**, 1-999.
150. Knauth, H.D., H. Alberti, and H. Clausen, 1979, J. Phys. Chem., **83**, 1604-1612.
151. Knauth, H.D. and R.N. Schindler, 1983, Z. Naturforsch., **38a**, 893.
152. Ko, M.K.W., D.S. Nien, W.C. Wang, G. Shia, A. Goldman, F.J. Murcray, D.G. Murcray, and C.P. Rinsland, 1993, J. Geophys. Res., **98**, 10499-10507.
153. Kurylo, M.J., T.J. Wallington, and P.A. Ouellette, 1987, J. Photochem., **39**, 201-215.
154. Langhoff, S.R., L. Jaffe, and J.O. Arnold, 1977, J. Quant. Spectrosc. Radiat. Transfer, **18**, 227.
155. Lawrence, W.G., K.C. Clemitshaw, and V.A. Apkarian, 1990, J. Geophys. Res., **95**, 18591.
156. Lee, L.C., 1982, J. Chem. Phys., **76**, 4909-4915.
157. Leroy, B., G. Le Bras, and P. Rigaud, 1981, Ann. Geophys., **37**, 297-302.
158. Lewis, B.R., L. Berzins, and J.H. Carver, 1986, J. Quant. Spectrosc. Radiat. Transfer, **36**, 209-232.
159. Lewis, B.R., L. Berzins, J.H. Carver, and S.T. Gibson, 1986, J. Quant. Spectrosc. Radiat. Transfer, **36**, 187-207.
160. Libuda, H.G. and F. Zabel, 1995, Ber. Bunsenges. Phys. Chem., **99**, 1205-1213.
161. Lightfoot, P.D., R.A. Cox, J.N. Crowley, M. Destriau, G.D. Hayman, M.E. Jenkin, G.K. Moortgat, and F. Zabel, 1992, Atmos. Environ., **26A**, 1805-1961.
162. Lightfoot, P.D. and A.A. Jemi-Alade, 1991, J.Photochem. and Photobiol. A: Chem., **59**, 1-10.
163. Lin, C.L., 1976, J. Chem. Eng. Data, **21**, 411.
164. Lin, C.L., N.K. Rohatgi, and W.B. DeMore, 1978, Geophys. Res. Lett., **5**, 113-115.
165. Lopez, M.I. and J.E. Sicre, 1988, J. Phys. Chem., **92**, 563-564.
166. Lopez, M.I. and J.E. Sicre, 1990, J. Phys. Chem., **94**, 3860-3863.
167. MacLeod, H., G.P. Smith, and D.M. Golden, 1988, J. Geophys. Res., **93**, 3813-3823.
168. Magnotta, F. and H.S. Johnston, 1980, Geophys. Res. Lett., **7**, 769-772.
169. Majer, J.R. and J.P. Simons, 1964, "Photochemical Processes in Halogenated Compounds," Advances in Photochemistry, 2, Interscience, pp. 137-181.
170. Malicet, J., D. Daumont, J. Charbonnier, C. Parisse, A. Chakir, and J. Brion, 1995, J. Atm. Chem, **21**, 263-273.
171. Manatt, S.L. and A.L. Lane, 1993, J. Quant. Spectrosc. Radiat. Transfer, **50**, 267-276.
172. Mandelman, M. and R.W. Nicholls, 1977, J. Quant. Spectrosc. Radiat. Trans., **17**, 483.
173. Margitan, J.J., 1983, J. Phys. Chem., **87**, 674-679.
174. Margitan, J.J. and R.T. Watson, 1982, J. Phys. Chem., **86**, 3819-3824.
175. Maric, D., J.P. Burrows, R. Meller, and G.K. Moortgat, 1993, J. Photochem. Photobiol. A Chem., **70**, 205-214.
176. Maric, D., J.P. Burrows, and G.K. Moortgat, 1994, J. Photochem. Photobiol A: Chem., **83**, 179-192.
177. Maricq, M.M. and T.J. Wallington, 1992, J. Phys. Chem., **96**, 982-986.
178. Marinelli, W.J. and H.S. Johnston, 1982, Chem. Phys. Lett., **93**, 127-132.
179. Marinelli, W.J., D.M. Swanson, and H.S. Johnston, 1982, J. Chem. Phys., **76**, 2864-2870.
180. Martin, H. and R. Gareis, 1956, Z. Elektrochemie, **60**, 959-964.
181. Mauersberger, K., J. Barnes, D. Hanson, and J. Morton, 1986, Geophys. Res. Lett., **13**, 671-673.
182. Mauersberger, K., D. Hanson, J. Barnes, and J. Morton, 1987, J. Geophys. Res., **92**, 8480-8482.
183. Mauldin, R.L., III, J.B. Burkholder, and A.R. Ravishankara, 1992, J. Phys. Chem., **96**, 2582-2588.
184. Mazely, T.L., R.R. Friedl, and S.P. Sander, 1995, J. Phys. Chem., **99**, 8162-8169.
185. Mazely, T.L., S.P. Sander, and R.R. Friedl, 1997, Manuscript in preparation.
186. McAdam, K., B. Veyret, and R. Lesclaux, 1987, Chem. Phys. Lett., **133**, 39-44.
187. McElcheran, D.E., M.H.J. Wijnen, and E.W.R. Steacie, 1958, Can. J. Chem., **36**, 321.
188. McGee, T.J. and J. Burris, 1987, J. Quant. Spectrosc. Radiat. Trans., **37**, 165-182.
189. McGrath, M.P., K.C. Clemitshaw, F.S. Rowland, and W.J. Hehre, 1988, Geophys. Res. Lett., **15**, 883-886.
190. McGrath, M.P., K.C. Clemitshaw, F.S. Rowland, and W.J. Hehre, 1990, J. Phys. Chem., **94**, 6126.

191. Merienne, M.F., B. Coquart, and A. Jenouvrier, 1990, Planet. Space Sci., **38**, 617-625.
192. Merienne, M.F., A. Jenouvrier, and B. Coquart, 1995, J. Atm. Chem, **20**, 281-297.
193. Michelsen, H.A., R.J. Salawitch, P.O. Wennberg, and J.G. Anderson, 1994, Geophys. Res. Lett., **21**, 2227-2230.
194. Minschwaner, K., G.P. Anderson, L.A. Hall, and K. Yoshino, 1992, J. Geophys. Res., **97**, 10103-10108.
195. Minschwaner, K. and D.E. Siskind, 1993, J. Geophys. Res., **98**, 20401-20412.
196. Minton, T.K., C.M. Nelson, T.A. Moore, and M. Okumura, 1992, Science, **258**, 1342-1345.
197. Mishalanie, E.A., J.C. Rutkowski, R.S. Hutte, and J.W. Birks, 1986, J. Phys. Chem., **90**, 5578-5584.
198. Mitchell, D.N., R.P. Wayne, P.J. Allen, R.P. Harrison, and R.J. Twin, 1980, J. Chem. Soc. Faraday Trans. 2, **76**, 785.
199. Molina, L.T., J.J. Lamb, and M.J. Molina, 1981, Geophys. Res. Lett., **8**, 1008.
200. Molina, L.T. and M.J. Molina, 1977, Geophys. Res. Lett., **4**, 83-86.
201. Molina, L.T. and M.J. Molina, 1978, J. Phys. Chem., **82**, 2410-2414.
202. Molina, L.T. and M.J. Molina, 1979, J. Photochem., **11**, 139-144.
203. Molina, L.T. and M.J. Molina, 1981, J. Photochem., **15**, 97.
204. Molina, L.T. and M.J. Molina, paper presented at the 182nd American Chemical Society National Meeting, 1982, New York.
205. Molina, L.T. and M.J. Molina, 1983, J. Phys. Chem., **87**, 1306.
206. Molina, L.T. and M.J. Molina, 1986, J. Geophys. Res., **91**, 14,501-14,508.
207. Molina, L.T. and M.J. Molina, 1996, Geophys. Res. Lett., **23**, 563-565.
208. Molina, L.T., M.J. Molina, and F.S. Rowland, 1982, J. Phys. Chem., **86**, 2672-2676.
209. Molina, L.T., S.D. Schinke, and M.J. Molina, 1977, Geophys. Res. Lett., **4**, 580-582.
210. Molina, M.J. and G. Arguello, 1979, Geophys. Res. Lett., **6**, 953-955.
211. Molina, M.J., A.J. Colussi, L.T. Molina, R.N. Schindler, and T.L. Tso, 1990, Chem. Phys. Lett., **173**, 310.
212. Molina, M.J., T. Ishiwata, and L.T. Molina, 1980, J. Phys. Chem., **84**, 821-826.
213. Moore, T.A., M. Okumura, M. Tagawa, and T.K. Minton, 1995, Faraday Discuss, **100**, 295-307.
214. Moortgat, G.K., W. Klippel, K.H. Mobius, W. Seiler, and P. Warneck, 1980, Report No. FAA-EE-80-47, Federal Aviation Administration, Washington, DC.
215. Moortgat, G.K., R. Meller, and W. Schneider, 1993, "Temperature dependence (256-296K) of the absorption cross-sections of bromoform in the wavelength range 285-360 nm," The Tropospheric Chemistry of Ozone in the Polar Regions, H. Niki and K.H. Becker, Editors, Springer-Verlag, Berlin, pp. 359-369.
216. Moortgat, G.K., W. Seiler, and P. Warneck, 1983, J. Chem. Phys., **78**, 1185-1190.
217. Moortgat, G.K., B. Veyret, and R. Lesclaux, 1989, J. Phys. Chem., **93**, 2362-2368.
218. Moortgat, G.K. and P. Warneck, 1979, J. Chem. Phys., **70**, 3639-3651.
219. Morel, O., R. Simonaitis, and J. Heicklen, 1980, Chem. Phys. Lett., **73**, 38.
220. Murtagh, D.P., 1988, Planet. Space Sci., **36**, 819-828.
221. Nayak, A.K., T.J. Buckley, M.J. Kurylo, and A. Fahr, 1996, J. Geophys. Res., **101**, 9055-9062.
222. Nayak, A.K., M.J. Kurylo, and A. Fahr, 1995, J. Geophys. Res, **100**, 11185-11189.
223. Nee, J.B., 1991, J. Quant. Spectrosc. Radiat. Transfer, **46**, 55.
224. Nelson, C.M., T.A. Moore, and M. Okumura, 1994, J. Chem. Phys., **100**, 8055-8064.
225. Nelson, C.M., T.A. Moore, M. Okumura, and T.K. Minton, 1996, Chem. Phys, **2248**, 287-307.
226. Nelson, H.H. and H.S. Johnston, 1981, J. Phys. Chem., **85**, 3891.
227. Nickolaisen, S.L. and S.P. Sander, 1996, Manuscript in preparation.
228. Nickolaisen, S.L., S.P. Sander, and R.R. Friedl, 1996, J. Phys. Chem., **100**, 10165.
229. Nicolet, M. and R. Kennes, 1989, Planet. Space Sci., **37**, 459-491.
230. Nicovich, J.M. and P.H. Wine, 1988, J. Geophys. Res., **93**, 2417.
231. Nolle, A., H. Heydtmann, R. Meller, and G.K. Moortgat, 1993, Geophys. Res. Lett., **20**, 707-710.
232. Nölle, A., H. Heydtmann, R. Meller, W. Schneider, and G.K. Moortgat, 1992, Geophys. Res. Lett., **19**, 281-284.
233. Oh, D., W. Sisk, A. Young, and H. Johnston, 1986, J. Chem. Phys., **85**, 7146-7158.
234. Okabe, H., 1978, Photochemistry of Small Molecules, John Wiley and Sons Inc., New York, pp. 217.
235. Okabe, H., 1980, J. Chem. Phys., **72**, 6642.
236. Orkin, V.L. and E.E. Kasimovskaya, 1995, J. Atm. Chem, **21**, 1-11.
237. Orlando, J.J. and J.B. Burkholder, 1995, J. Phys. Chem., **99**, 1143-1150.
238. Orlando, J.J., J.B. Burkholder, S.A. McKeen, and A.R. Ravishankara, 1991, J. Geophys. Res., **96**, 5013-5023.
239. Orlando, J.J., G.S. Tyndall, G.K. Moortgat, and J.G. Calvert, 1993, J. Phys. Chem., **97**, 10996-11000.
240. Paraskevopoulos, G. and R.J. Cvetanovic, 1969, J. Am. Chem. Soc., **91**, 7572.

241. Parrish, D.D., P.C. Murphy, D.L. Albritton, and F.C. Fehsenfeld, 1983, Atmos. Environ., **17**, 1365.
242. Paukert, T.T. and H.S. Johnston, 1972, J. Chem. Phys., **56**, 2824-2838.
243. Permien, T., R. Vogt, and R.N. Schindler, 1988, "Mechanisms of Gas Phase-Liquid Phase Chemical Transformations," Air Pollution Report #17, R.A. Cox, Editor, Environmental Research Program of the CEC., Brussels.
244. Preston, K.F. and R.F. Barr, 1971, J. Chem. Phys., **54**, 3347-3348.
245. Rattigan, O., E. Lutman, R.L. Jones, and R.A. Cox, 1992, J. Photochem. Photobiol. A: Chem., **66**, 313-326.
246. Rattigan, O., E. Lutman, R.L. Jones, R.A. Cox, K. Clemitshaw, and J. Williams, 1992, J. Photochem. Photobiol. A: Chem., **69**, 125-126.
247. Rattigan, O.V., D.J. Lary, R.L. Jones, and R.A. Cox, 1996, J. Geophys. Res., **101**, 23021-23033.
248. Ravishankara, A.R., 1995, Faraday Discuss, **100**, 335.
249. Ravishankara, A.R. and R.L. Mauldin, 1986, J. Geophys. Res., **91**, 8709-8712.
250. Ravishankara, A.R., S. Solomon, A.A. Turnipseed, and R.F. Warren, 1993, Science, **259**, 194-199.
251. Ravishankara, A.R. and P.H. Wine, 1983, Chem. Phys. Lett., **101**, 73.
252. Ravishankara, A.R., P.H. Wine, C.A. Smith, P.E. Barbone, and A. Torabi, 1986, J. Geophys. Res., **91**, 5355-5360.
253. Reid, S.A., J.T. Brandon, and H. Reisler, 1993, J. Phys. Chem., **97**, 540.
254. Rigaud, P., B. Leroy, G. Le Bras, G. Poulet, J.L. Jourdain, and J. Combourieu, 1977, Chem. Phys. Lett., **46**, 161.
255. Robbins, D.E., 1976, Geophys. Res. Lett., **3**, 213-216. See also Erratum, GRL, 1976, Vol. 3, p. 757.
256. Robbins, D.E., paper presented at the International Conference on Problems Related to the Stratosphere, 1977, Pasadena, California Jet Propulsion Laboratory, California Institute of Technology.
257. Robbins, D.E. and R.S. Stolarski, 1976, Geophys. Rev. Lett., **3**, 603-606.
258. Roehl, C.M., D. Bauer, and G.K. Moortgat, 1996, J. Phys. Chem., **100**, 4038-4047.
259. Roehl, C.M., J.J. Orlando, and J.G. Calvert, 1992, J. Photochem. Photobiol. A: Chem., **69**, 1-5.
260. Rogers, J.D., 1990, J. Phys. Chem., **94**, 4011-4015.
261. Rowland, F.S. and Y. Makide, 1982, Geophys. Res. Lett., **9**, 473.
262. Rowland, F.S. and P.J. Rogers, 1982, Proc. Natl. Acad. Sci. USA, **79**, 2737.
263. Rowland, F.S., J.E. Spencer, and M.J. Molina, 1976, J. Phys. Chem., **80**, 2711-2713.
264. Rudolph, R.N. and E.C.Y. Inn, 1981, J. Geophys. Res., **86**, 9891.
265. Ruhl, E., A. Jefferson, and V. Vaida, 1990, J. Phys. Chem., **94**, 2990.
266. Safary, E., J. Romand, and B. Vodar, 1951, J. Chem. Phys., **19**, 379.
267. Sander, S.P., 1986, J. Phys. Chem., **90**, 4135-4142.
268. Sander, S.P. and R.R. Friedl, 1989, J. Phys. Chem., **93**, 4764-4771.
269. Sander, S.P., M. Peterson, R.T. Watson, and R. Patrick, 1982, J. Phys. Chem., **86**, 1236-1240.
270. Sandorfy, C., 1976, Atmos. Environ., **10**, 343-351.
271. Sauvageau, P., J. Doucet, R. Gilbert, and C. Sandorfy, 1974, J. Chem. Phys., **61**, 391.
272. Sauvageau, P., R. Gilbert, P.P. Berlow, and C. Sandorfy, 1973, J. Chem. Phys., **59**, 762.
273. Schiffman, A., D.D. Nelson Jr., and D.J. Nesbitt, 1993, J. Chem. Phys., **98**, 6935-6946.
274. Schneider, W., G.K. Moortgat, J.P. Burrows, and G.S. Tyndall, 1987, J. Photochem. Photobiol., **40**, 195-217
275. Schneider, W.F., T.J. Wallington, K. Minschwaner, and E.A. Stahlberg, 1995, Environ. Sci. Technol., **29**, 247.
276. Seery, D.J. and D. Britton, 1964, J. Phys. Chem., **68**, 2263.
277. Selwyn, G., J. Podolske, and H.S. Johnston, 1977, Geophys. Res. Lett., **4**, 427-430.
278. Senum, G.I., Y.-N. Lee, and J.S. Gaffney, 1984, J. Phys. Chem., **88**, 1269-1270.
279. Shardanand and A.D.P. Rao, 1977, J. Quant. Spectrosc. Radiat. Transfer, **17**, 433-439.
280. Shetter, R.E., J.A. Davidson, C.A. Cantrell, N.J. Burzynski, and J.G. Calvert, 1988, J. Geophys. Res., **93**, 7113-7118.
281. Silver, J.A., D.R. Worsnop, A. Freedman, and C.E. Kolb, 1986, J. Chem. Phys., **84**, 4378-4384.
282. Simon, F.G., W. Schneider, G.K. Moortgat, and J.P. Burrows, 1990, J. Photochem. Photobiol., **A55**, 1-23.
283. Simon, P.C., D. Gillotay, N. Vanlaethem-Meuree, and J. Wisemberg, 1988, J. Atmos. Chem., **7**, 107-135.
284. Simon, P.C., D. Gillotay, N. Vanlaethem-Meuree, and J. Wisemberg, 1988, Annales Geophysicae, **6**, 239-248.
285. Simonaitis, R., R.I. Greenberg, and J. Heicklen, 1972, Int. J. Chem. Kinet., **4**, 497.
286. Singer, R.J., J.N. Crowley, J.P. Burrows, W. Schneider, and G.K. Moortgat, 1989, J. Photochem. Photobiol., **48**, 17-32.
287. Smith, W.S., C.C. Chou, and F.S. Rowland, 1977, Geophys. Res. Lett., **4**, 517-519.
288. Solomon, S., J.B. Burkholder, A.R. Ravishankara, and R.R. Garcia, 1994, J. Geophys. Res., **99**, 20929-20935.
289. Sparks, R.K., L.R. Carlson, K. Shobatake, M.L. Kowalczyk, and Y.T. Lee, 1980, J. Chem. Phys., **72**, 1401-1402.

290. Spencer, J.E. and F.S. Rowland, 1978, J. Phys. Chem., **82**, 7-10.
291. Stanton, J.F. and R.J. Bartlett, 1993, J. Phys. Chem., **98**, 9335-9339.
292. Stanton, J.F., C.M.L. Rittby, R.J. Bartlett, and D.W. Toohey, 1991, J. Phys. Chem., **95**, 2107-2110.
293. Steinfeld, J.I., S.M. Adler-Golden, and J.W. Gallagher, 1987, J. Phys. Chem. Ref. Data, **16**, 911-951.
294. Stief, L.J., W.A. Payne, and R.B. Klemm, 1975, J. Chem. Phys., **62**, 4000-4008.
295. Stockwell, W.R. and J.G. Calvert, 1978, J. Photochem., **8**, 193-203.
296. Suto, M. and L.C. Lee, 1985, J. Geophys. Res., **90**, 13037-13040.
297. Swanson, D., B. Kan, and H.S. Johnston, 1984, J. Phys. Chem., **88**, 3115.
298. Takahashi, K., Y. Matsumi, and M. Kawasaki, 1996, J. Phys. Chem., **100**, 4084-4089.
299. Talukdar, R., A. Mellouki, T. Gierczak, J.B. Burkholder, S.A. McKeen, and A.R. Ravishankara, 1991, J. Phys. Chem., **95**, 5815-5821.
300. Talukdar, R.K., J.B. Burkholder, A.-M. Schmoltner, J.M. Roberts, R. Wilson, and A.R. Ravishankara, 1995, J. Geophys. Res., **100**, 14163-14173.
301. Tang, K.Y., P.W. Fairchild, and E.K.C. Lee, 1979, J. Phys. Chem., **83**, 569.
302. Thelen, M.-A., P. Felder, and J.R. Huber, 1993, Chem. Phys. Lett., **213**, 275-281.
303. Trolier, M., R.L. Mauldin III, and A.R. Ravishankara, 1990, J. Phys. Chem., **94**, 4896-4907.
304. Trolier, M. and J.R. Wiesenfeld, 1988, J. Geophys. Res., **93**, 7119-7124.
305. Turco, R.P., 1975, Geophys. Surveys, **2**, 153-192.
306. Turco, R.P., R.J. Cicerone, E.C.Y. Inn, and L.A. Capone, 1981, J. Geophys. Res., **86**, 5373.
307. Turnipseed, A.A., G.L. Vaghjiani, T. Gierczak, J.E. Thompson, and A.R. Ravishankara, 1991, J. Chem. Phys., **95**, 3244-3251.
308. Turnipseed, A.A., G.L. Vaghjiani, J.E. Thompson, and A.R. Ravishankara, 1992, J. Chem. Phys., **96**, 5887.
309. Tyndall, G.S., K.M. Stedman, W. Schneider, J.P. Burrows, and G.K. Moortgat, 1987, J. Photochem., **36**, 133-139.
310. Vaghjiani, G.L. and A.R. Ravishankara, 1989, J. Geophys. Res., **94**, 3487-3492.
311. Vaghjiani, G.L. and A.R. Ravishankara, 1990, J. Chem. Phys., **92**, 996.
312. Vaghjiani, G.L., A.A. Turnipseed, R.F. Warren, and A.R. Ravishankara, 1992, J. Chem. Phys., **96**, 5878.
313. Vaida, V., S. Solomon, E.C. Richards, E. Ruhl, and A. Jefferson, 1989, Nature, **342**, 405.
314. Vanlaethem-Meuree, N., J. Wisemberg, and P.C. Simon, 1978, Bull. Acad. Roy. Belgique Cl. Sci., **64**, 31.
315. Vanlaethem-Meuree, N., J. Wisemberg, and P.C. Simon, 1978, Bull. Acad. Roy. Belgique Cl. Sci., **64**, 42.
316. Vanlaethem-Meuree, N., J. Wisemberg, and P.C. Simon, 1979, Geophys. Res. Lett., **6**, 451-454.
317. Vasudev, R., 1990, Geophys. Res. Lett., **17**, 2153-2155.
318. Vogt, R. and R.N. Schindler, 1992, J. Photochem. Photobiol. A: Chem., **66**, 133-140.
319. Wahner, A., A.R. Ravishankara, S.P. Sander, and R.R. Friedl, 1988, Chem. Phys. Lett., **152**, 507.
320. Wahner, A., G.S. Tyndall, and A.R. Ravishankara, 1987, J. Phys. Chem., **91**, 2734-2738.
321. Wallington, T.J., P. Dagaut, and M.J. Kurylo, 1992, Chem. Rev., **92**, 667-710.
322. Walters, E.A., M. Gupta, J.T. Clay, D.D. Baldyga, J.R. Smith, and K. Glidden, 1994, personal communication.
323. Walton, J.C., 1972, J. Chem. Soc. Farad. Trans., **68**, 1559.
324. Watson, R.T., 1977, J. Phys. Chem. Ref. Data, **6**, 871-917.
325. Wayne, R.P., 1987, Atm. Environ., **21**, 1683-1694.
326. Wayne, R.P., I. Barnes, J.P. Burrows, C.E. Canosa-Mas, J. Hjorth, G. Le Bras, G.K. Moortgat, D. Perner, G. Poulet, G. Restelli, and H. Sidebottom, 1991, Atmos. Environ., **25A**, 1-203.
327. Wine, P.H., W.L. Chameides, and A.R. Ravishankara, 1981, Geophys. Res. Lett., **8**, 543-546.
328. Wine, P.H. and A.R. Ravishankara, 1982, Chem. Phys., **69**, 365-373.
329. Wine, P.H., A.R. Ravishankara, D.L. Philen, D.D. Davis, and R.T. Watson, 1977, Chem. Phys. Lett., **50**, 101.
330. WMO, Atmospheric Ozone: 1985, World Meteorological Organization Global Ozone Research and Monitoring Project, Report No. 16, 1986, Geneva: National Aeronautics and Space Administration.
331. Xu, H. and J.A. Joens, 1993, Geophys. Res. Lett., **20**, 1035-1037.
332. Yao, F., I. Wilson, and H. Johnston, 1982, J. Phys. Chem., **86**, 3611.
333. Yokelson, R.J., J.B. Burkholder, R.W. Fox, R.K. Talukdar, and A.R. Ravishankara, 1994, J. Phys. Chem., **98**, 13144-13150.
334. Yoshino, K., A.S.C. Cheung, J.R. Esmond, W.H. Parkinson, D.E. Freeman, S.L. Guberman, A. Jenouvrier, B. Coquart, and M.F. Merienne, 1988, Planet. Space Sci., **36**, 1469-1475.
335. Yoshino, K., J.R. Esmond, A.S.-C. Cheung, D.E. Freeman, and W.H. Parkinson, 1992, Planet. Space Sci., **40**, 185-192.

336. Yoshino, K., J.R. Esmond, A.S.C. Cheung, D.E. Freeman, and W.H. Parkinson, 1990, J. Geophys. Res., **95**, 11743.
337. Yoshino, K., J.R. Esmond, D.E. Freeman, and W.H. Parkinson, 1993, J. Geophys. Res., **98**, 5205-5211.
338. Yoshino, K., D.E. Freeman, J.R. Esmond, R.S. Friedman, and W.H. Parkinson, 1988, Planet. Space Sci., **36**, 1201-1210.
339. Yoshino, K., D.E. Freeman, J.R. Esmond, R.S. Friedman, and W.H. Parkinson, 1989, Planet. Space Sci., **37**, 419-426.
340. Yoshino, K., D.E. Freeman, J.R. Esmond, and W.H. Parkinson, 1987, Planet. Space Sci., **35**, 1067-1075.
341. Yoshino, K., D.E. Freeman, and W.H. Parkinson, 1984, J. Phys. Chem. Ref. Data, **13**, 207-227.
342. Yoshino, K., D.F. Freeman, J.R. Esmond, and W.H. Parkinson, 1983, Planet. Space Sci., **31**, 339-353.
343. Zelikoff, M. and L.M. Aschenbrand, 1954, J. Chem. Phys., **22**, 1685-1687.
344. Zetzsch, C., 1989, Proceedings of the International Ozone Symposium 1988, R. Bojkov and P. Fabian, Editors, Deepak, Hampton, VA.

HETEROGENEOUS CHEMISTRY

We have evaluated and tabulated the currently available information on heterogeneous stratospheric processes. In addition, because of the increasing level of interest in tropospheric processes with a direct bearing on the fluxes of reactive species into the stratosphere, such as heterogeneous loss processes for partially oxidized degradation products of hydrohalocarbons and heterogeneous contrail and cloud processing of exhaust species from aircraft, we have included kinetic data for selected heterogeneous interactions relevant to modeling cloud droplet and aqueous aerosol chemistry in the free troposphere. However, both stratospheric and tropospheric heterogeneous chemistry are relatively new and rapidly developing fields, and further results can be expected to change our quantitative and even our qualitative understanding on a regular basis. The complexity is compounded by the difficulty of characterizing the chemical and physical properties of atmospheric heterogeneous surfaces and then reproducing suitable simulations in the laboratory [99].

Surface Types

To a first approximation there are three major types of surfaces believed to be present at significant levels in the stratosphere. They are: 1) Type I - polar stratospheric clouds (PSCs), nominally composed of nitric acid trihydrate ($HNO_3 \cdot 3H_2O$); 2) crystals of relatively pure water ice, designated as Type II PSCs because they form at lower temperatures than Type I and are believed to be nucleated by Type I (similar surfaces may form as contrails behind high-altitude aircraft under some stratospheric conditions); and 3) sulfuric acid aerosol, which is nominally a liquid phase surface generally composed of 60 - 80 weight percent H_2SO_4 and, concomitantly, 40-20 weight percent H_2O. While PSCs, as their name suggests, are formed primarily in the cold winter stratosphere at high latitudes, sulfuric acid aerosol is present year round at all latitudes and may influence stratospheric chemistry on a global basis, particularly after large injections of volcanic sulfur episodically increase their abundance and surface area. There is also increasing evidence that ternary $H_2SO_4/HNO_3/H_2O$ liquid solutions may play a significant role in PSC formation.

In addition to the major stratospheric surface types noted above, several other types of heterogeneous surfaces are found in the stratosphere and may play a significant role in some stratospheric processes. For instance, recent laboratory work has indicated that nitric acid dihydrate (NAD) may play an important role in the nucleation of Type I PSCs (Worsnop et al. [180]; Fox et al. [44]) and that mixtures of solid nitric acid hydrates and sulfuric acid tetrahydrate (SAT) (Molina et al. [122]; Zhang et al. [188]) and/or a more complex sulfuric acid/nitric acid hydrate (Fox et al. [44]) may also be key to understanding Type I PSC nucleation and evolution. Analyses of the range of atmospheric conditions possible in the polar stratosphere have also led to interest in solid SAT surfaces and possibly other forms of frozen sulfuric acid aerosols (Toon et al. [164]; Middlebrook et al. [117]), as well as liquid sulfuric acid aerosols significantly more dilute than the 60-80 weight percent normally present at lower latitudes (Wolff and Mulvaney [179]; Hofmann and Oltmans [77]; Toon et al. [164]). Some modeling studies also suggest that certain types of major volcanic eruptions transport significant levels of sodium chloride into the stratosphere (Michelangeli et al. [116]), so studies of stratospheric trace species interacting with solid NaCl or similar salts, as well as salt solutions, have also been included. Finally, aircraft and rocket exhausts contribute small but measurable amounts of carbonaceous soot (Pueschel et al. [133]) and aluminized solid propellant rocket exhausts and spacecraft debris produce increasing levels of alumina (Al_2O_3) and similar metal oxide particles (Zolensky et al. [189]) in the stratosphere. In the free troposphere the primary heterogeneous surfaces of interest are liquid or solid water (cloud droplets, contrails) or aqueous sulfate solutions representative of background aerosols.

The detailed composition and morphology of each surface type are uncertain and probably subject to a significant range of natural variability. Certain chemical and physical properties of these surfaces, such as their ability to absorb and/or solvate HCl and HNO_3, are known to be strongly dependent on their detailed chemical composition. Moreover, most heterogeneous processes studied under laboratory conditions (and in some cases proceeding under stratospheric conditions) can change the chemical composition of the surface in ways that significantly affect the kinetic or thermodynamic processes of interest. Thus, a careful analysis of the time-dependent nature of the active surface is required in the evaluation of measured uptake kinetics experiments. Experimental techniques which allow the measurement of mass accommodation or surface reaction kinetics with high time resolution and/or with low trace gas fluxes are often more credible in establishing that measured kinetic parameters are not seriously compromised by surface saturation or changing surface chemical composition.

The measured kinetic uptake parameters, mass accommodation coefficients, and surface reaction probabilities are separately documented for relevant atmospheric trace gas species for the major and, where available, the minor stratospheric surfaces noted above. Since these parameters can vary significantly with surface composition (e.g., the H_2SO_4/H_2O ratio for sulfate aerosol or the HNO_3/H_2O ratio for Type I PSC) the dependence of these parameters on surface composition is reviewed where sufficient data are available. Furthermore, data are also compiled for liquid water for several reasons. First, this surface is one asymptote of the H_2SO_4/H_2O aerosol con-

tinuum; second, the interactions of some trace species with liquid water and water ice (Type II PSC) surfaces are often similar; and third, the uptake of some trace species by water surfaces in the troposphere can play a key role in understanding their tropospheric chemical lifetimes and, thus, the fraction that may be transported into the stratosphere.

Surface Porosity

The experimental techniques utilized to measure mass accommodation, heterogeneous reaction, and other uptake coefficients generally require knowledge of the surface area under study. For solid surfaces, and most particularly for water and acid ice surfaces formed in situ, the determination of how the molecular scale ice surface differs from the geometrical surface of the supporting substrate is not easy. Keyser, Leu, and coworkers have investigated the structure of water and nitric acid ice films prepared under conditions similar to those used in their flow reactor for uptake studies (Keyser et al. [97]; Keyser and Leu [95]; Keyser and Leu [94]). They have demonstrated that ice films grown in situ from the vapor can have a considerably larger available surface than that represented by the geometry of the substrate; they have also developed a simple model to attempt to correct measured uptake rates for this effect (Keyser et al. [97]; Keyser et al. [96]). This model predicts that correction factors are largest for small uptake coefficients and thick films. The application of the model to experimental uptake data remains controversial (Keyser et al. [96]; Hanson and Ravishakara [71]; Kolb et al. [99]). Some experimenters prefer to attempt growing ice surfaces as smooth as possible and to demonstrate that their measured uptake coefficients are only weakly dependent on surface thickness (Hanson and Ravishankara, [68]). Similar issues arise for uptake experiments performed on powered, fused and single crystal salt or oxide surfaces (Fenter et al.[41]; Hanning-Lee et al. [57]). The degree to which measured uptake parameters must be corrected for porosity effects will remain in some doubt until a method is devised for accurately determining the effective surface area for the surfaces actually used in uptake studies. Most studies evaluated in this review assume that the effective ice or salt surface area is the geometrical area.

Temperature Dependence

A number of laboratory studies have shown that mass accommodation coefficients and, to some extent, surface reaction probabilities can be temperature dependent. While these dependencies have not been characterized for many systems of interest, temperature effects on kinetic data are noted where available. More work that fully separates heterogeneous kinetic temperature effects from temperature controlled surface composition is obviously needed.

Solubility Limitations

Experimental data on the uptake of some trace gases by various stratospherically relevant surfaces can be shown to be governed by solubility limitations rather than kinetic processes. In these cases properly analyzed data can yield measurements of trace gas solubility parameters relevant to stratospheric conditions. In general, such parameters can be strongly dependent on both condensed phase composition and temperature. Such parameters may be very important in stratospheric models, since they can govern the availability of a reactant for a bimolecular heterogeneous process (e.g., the concentration of HCl available for the HCl + $ClONO_2$ reaction on sulfuric acid aerosols) or the gas/condensed phase partitioning of a heterogeneous reaction product (e.g., the HNO_3 formed by the reaction of N_2O_5 on sulfuric acid aerosols).

Data Organization

Data for trace gas heterogenous interactions with relevant condensed phase surfaces are tabulated in Tables 63, 64, and 65. These are organized into:

Table 63 - Mass Accommodation Coefficients
Table 64 - Surface Reaction Probabilities
Table 65 - Solubility Data

Parameter Definitions

Mass accommodation coefficients (α), represent the probability of reversible uptake of a gaseous species colliding with the condensed surface of interest. For liquid surfaces this process is associated with interfacial (gas-to-liquid) transport and is generally followed by bulk liquid phase solvation. Examples include: simple surface absorption, absorption followed by ionic dissociation and solvation (e.g., $HCl + nH_2O \leftrightarrow H^+(aq) + Cl^-(aq)$), and absorption followed by a reversible chemical reaction with a condensed phase substituent (e.g., $SO_2 + H_2O \leftrightarrow H^+ + HSO_3^-$ or $CH_2O + H_2O \leftrightarrow CH_2(OH)_2$).

The term "sticking coefficient" is often used for mass accommodation on solid surfaces where physisorption or chemisorption takes the place of true interfacial mass transport.

Processes involving liquid surfaces are subject to Henry's law, which limits the fractional uptake of a gas phase species into a liquid. If the gas phase species is simply solvated, a physical Henry's law constraint holds; if the gas phase species reacts with a condensed phase substituent, as in the sulfur dioxide or formaldehyde hydrolysis cases noted above, a "chemically modified" or "effective" Henry's law constraint holds (Clegg and Brimblecombe [26]; Schwartz [149]; Watson et al. [174]). Henry's law constants relate the equilibrium concentration of a species in the gas phase to the concentration of the same species in a liquid phase, and they have, in this report, units of M atm^{-1}. These are tabulated for liquid surfaces in Table 65. Effective Henry's law constants are designated H*, while simple physical Henry's law constants are represented by H. Effective Henry's law constants are also employed to represent decreased trace gas solubilities in moderate ionic strength acid or salt solutions with the use of a Setchenow coefficient formulation which relates H* to the concentration of the acid or salt [81]. It is presently unclear whether "surface solubility" effects govern the uptake on nominally solid water ice or HNO_3/H_2O ice surfaces in a manner analogous to bulk solubility effects for liquid substrates.

For some trace species on some surfaces, experimental data suggest that mass accommodation coefficients untainted by experimental saturation limitations have been obtained. These are tabulated in Table 63. In other cases experimental data can be shown to be subject to Henry's law constraints, and Henry's law constants, or at least their upper limits, can be determined. Some experimental data sets are insufficient to determine if measured "uptake" coefficients are true accommodation coefficients or if the measurement values are lower limits compromised by saturation effects. These are currently tabulated, with suitable caveats, in Table 63.

Surface reaction probabilities (γ) are kinetic values for generally irreversible reactive uptake of trace gas species on condensed surfaces. Such processes may not be rate limited by Henry's law constraints; however, the fate of the uptake reaction products may be subject to saturation limitations. For example, N_2O_5 has been shown to react with sulfuric acid aerosol surfaces. However, if the H_2SO_4/H_2O ratio is too high, the product HNO_3 will be insoluble, and a large fraction will be expelled back into the gas phase. Surface reaction probabilities for substantially irreversible processes are presented in Table 64. Reaction products are identified where known. .

The total experimental uptake coefficient measured in laboratory heterogeneous kinetic experiments are also often symbolized by the symbol γ. In those cases where surface and/or bulk reaction dominate the uptake, the total uptake coefficient (γ_{total}) and reactive uptake coefficient (γ_{rxn}) may well be identical. More formally, for cases where bulk liquid phase reaction is facile and there are no gas phase diffusion constraints, the total uptake coefficient can be approximated in terms of γ_{rxn} and γ_{sol} as [99]:

$$\frac{1}{\gamma_{total}} = \frac{1}{\alpha} + \frac{1}{\gamma_{sol} + \gamma_{rxn}}$$

where

$$\gamma_{sol} = \frac{4HRT}{\pi^{1/2}\bar{c}}\left(\frac{D}{t}\right)^{1/2}$$

and

$$\gamma_{rxn} = \frac{4HRT}{\bar{c}} \left(Dk_{rxn}\right)^{1/2}$$

where t is the time the trace gas is exposed to the liquid surface, R is the gas constant, D is the liquid phase diffusion coefficient, and $\bar{c}$ is the mean trace gas molecular speed. In the limit of low solubility or long exposure time γ_{sol} becomes negligible and:

$$\frac{1}{\gamma_{total}} = \frac{1}{\alpha} + \frac{1}{\gamma_{rxn}} \quad .$$

Discussion of how to use this approach to model chemical reactions in liquid stratospheric aerosols can be found in Hanson et al. [74] and Kolb et al. [99]. Note that these formulations are approximate. In cases where separate terms are competitive, more rigorous solution of kinetic differential operations may be appropriate.

For solid surfaces, bulk diffusion is generally too slow to allow bulk solubility or bulk kinetic processes to dominate uptake. For solids, reactive uptake is driven by chemisorption/chemical reaction at the interface, a process that can also influence trace gas uptake on liquids. In these cases surface reaction (γ_{surf}) occurs in parallel, rather than in series with mass accommodation, thus:

$$\gamma_{total} = \gamma_{surf} + \left[\frac{1}{\alpha} + \frac{1}{\gamma_{sol} + \gamma_{rxn}}\right]^{-1}$$

Examples where this more complex situation holds for liquid surfaces can be found in Hu et al. [78] and Jayne et al.[88]. In such cases γ may be significantly larger than α.

The data in Tables 63 and 64 are organized by trace gas species, since some systematic variation may be expected for surface accommodation or reaction as the surface composition and/or phase is varied. Data presented for one surface may be judged for "reasonableness" by comparing with data for a "similar" surface. In some cases it is not yet clear if surface uptake is truly reversible (accommodation) or irreversibly reactive in nature. In such cases the available uptake coefficients are generally tabulated in Table 63 as accommodation coefficients, a judgment yhat will be subject to change if more definitive data become available.

Where a specific evaluated value for an accommodation coefficient or reaction probability has been obtained, an estimated uncertainty factor is also tabulated. However, when the data evaluation yielded only a lower or upper limit, no uncertainty factor can be reliably estimated and none is presented.

Description of and reference citations to many of the laboratory techniques used to obtain the data in the following three tables can be found in Kolb et al. [99].

Table 63. Mass Accommodation Coefficients (α)

Gaseous Species	Surface Type	Surface Composition	T(K)	α	Uncertainty Factor	Notes
O	Sulfuric Acid	$H_2SO_4 \cdot nH_2O(l)$ (97 wt.% H_2SO_4)	298	See Note		1
O_3	Water Ice	$H_2O(s)$	195-262	>0.04		2
	Liquid Water	$H_2O(l)$	292	>2 x 10^{-3}‡		3
	Nitric Acid Ice	$HNO_3 \cdot 3H_2O(s)$	195	2.5 x 10^{-4}‡	3	2
	Sulfuric Acid	$H_2SO_4 \cdot nH_2O(l)$ (50 wt.% H_2SO_4)	195	See Note		4
		(97 wt.% H_2SO_4)	196	See Note		4
OH	Water Ice	$H_2O(s)$	205-253	>0.1		5
	Liquid Water	$H_2O(l)$	275	>4 x 10^{-3}		6
	Sulfuric Acid	$H_2SO_4 \cdot nH_2O(l)$ (28 wt.% H_2SO_4)	275	>0.07		7
		(97 wt.% H_2SO_4)	298	>5 x 10^{-4}‡		7
	Alumina	$Al_2O_3(s)$	253-348	0.04	5	8
HO_2	Liquid Water	$H_2O(l)$	275	> 0.02		9
	Aqueous Salts	$NH_4HSO_4(aq)$ and $LiNO_3(aq)$	293	> 0.2		9
	Sodium Chloride	NaCl(s)	295	2 x 10^{-2}	5	10
	Potassium Chloride	KCl(s)	295	2 x 10^{-2}	5	10
H_2O	Water Ice	$H_2O(s)$	200	0.5	2	11
	Liquid Nitric Acid	$HNO_3 \cdot nH_2O(l)$	278	>0.3		12
	Nitric Acid Ice	$HNO_3 \cdot 3H_2O(s)$	197	See Note		13
	Sulfuric Acid	$H_2SO_4 \cdot nH_2O$ (96 wt.% H_2SO_4)	298	> 2 x 10^{-3}‡		14
	Sodium Chloride	NaCl(s)	~298	See Note		
		NaCl(aq)	~299	> 0.5		15
	Carbon/Soot	(C(s)	~298	>4 x 10^{-4}		16
H_2O_2	Liquid Water	$H_2O(l)$	273	0.18*	2	18
	Sulfuric Acid	$H_2SO_4 \cdot nH_2O(l)$ (96 wt.% H_2SO_4)	298	> 8 x 10^{-4}‡		19
NO	Water Ice	$H_2O(s)$	195	See Note		20
	Sulfuric Acid	$H_2SO_4 \cdot nH_2O$		See Note		
		(70 wt.% H_2SO_4)	193-243	See Note		21
		(97 wt.% H_2SO_4)	298	See Note		21

Table 63. (Continued)

Gaseous Species	Surface Type	Surface Composition	T(K)	α	Uncertainty Factor	Notes
NO_2	Water Ice	$H_2O(s)$	195	See Note		22
HONO	Water Ice	$H_2O(s)$	180-200	>1.0 x 10^{-3}		23
HNO_3	Water Ice	$H_2O(s)$	200	0.3	3	24
	Liquid Water	$H_2O(l)$	268	0.2*	2	25
	Nitric Acid Ice	$HNO_3 \cdot 3H_2O(s)$	191-200	0.4	2	26
	Liquid Nitric Acid	$HNO_3 \cdot nH_2O(l)$	278	0.6	2	27
	Sulfuric Acid	$H_2SO_4 \cdot nH_2O(l)$				
		(57.7 wt.% H_2SO_4)	191-200	>0.3		28
		(73 wt.% H_2SO_4)	283	0.1	2	28
		(75 wt.% H_2SO_4)	230	>2 x 10^{-3}		28
		(97 wt.% H_2SO_4)	295	>2.4 x 10^{-3}		28
	Sulfuric Acid Tetrahydrate	$H_2SO_4 \cdot 4\ H_2O(s)$	~192	>0.02*		28
HO_2NO_2	Water Ice	$H_2O(s)$	[a]200	0.1‡	3	29
	Sulfuric Acid	$H_2SO_4 \cdot nH_2O(l)$				
		(97 wt.% H_2SO_4)	298	See Note		30
NH_3	Liquid Water	$H_2O(l)$	~295	0.06*	3	31
CO_2	Liquid Water	$H_2O(l)$	293	See Note		32
CH_3OH	Liquid Water	$H_2O(l)$	260-291	0.12-0.02*	2	33
CH_3CH_2OH	Liquid Water	$H_2O(l)$	260-291	0.13-0.02*	2	34
$CH_3CH_2CH_2OH$	Liquid Water	$H_2O(l)$	260-291	0.08-0.02*	2	35
$CH_3CH(OH)CH_3$	Liquid Water	$H_2O(l)$	260-291	0.10-0.02*	2	35
$HOCH_2CH_2OH$	Liquid Water	$H_2O(l)$	260-291	0.13-0.04*	2	36
CH_2O	Liquid Water	$H_2O(l)$	260-270	0.04	3	37
	Sulfuric Acid	$H_2SO_4 \cdot nH_2O(l)$	235-300	0.04	3	37
CH_3O_2	Sodium Chloride	NaCl(s)	296	>4 x 10^{-3}		38
CH_3CHO	Liquid Water	$H_2O(l)$	267	>0.03*		39
$CH_3C(O)CH_3$	Liquid Water	$H_2O(l)$	260-285	0.07-0.01*	2	40
HC(O)OH	Liquid Water	$H_2O(l)$	260-291	0.10-0.02*	2	41
$CH_3C(O)OH$	Liquid Water	$H_2O(l)$	260-291	0.15-0.03*	2	42

Table 63. (Continued)

Gaseous Species	Surface Type	Surface Composition	T(K)	α	Uncertainty Factor	Notes
Cl_2	Water Ice	H_2O(s)	200	See Note		43
OClO	Water Ice	H_2O(s)	100,189, 200	See Note		44
HCl	Water Ice	H_2O(s)	191- 211	0.3	3	45
	Liquid Water	H_2O(l)	274	0.2*	2	46
	Nitric Acid Ice	$HNO_3 \cdot 3H_2O$(s)	191- 211	0.3	3	47
	Sulfuric Acid	$H_2SO_4 \cdot nH_2O$(l)	283	0.15*	2	48
		(n≥8, ≤40 wt.% H_2SO_4)	218	>0.005*		
		(n<8, >40 wt.% H_2SO_4)	(No data - all measurements limited by HCl solubility)			
	Sulfuric Acid Tetrahydrate	$H_2SO_4 \cdot 4H_2O$(s)	192-201	See Note		49
CCl_2O	Liquid Water	H_2O(l)	260-290	See Note		50
CCl_3CClO	Liquid Water	H_2O(l)	260-290	See Note		50
HBr	Water Ice	H_2O(s)	200	> 0.2		51
	Nitric Acid Ice	$HNO_3 \cdot 3H_2O$(s)	200	> 0.3		51
HOBr	Sulfuric Acid	H_2SO_4 in H_2O(l) (58 wt. % H_2SO_4)	-228	>0.05‡		52
$CHBr_3$	Water Ice	H_2O(l)	220	See Note		53
	Sulfuric Acid	$H_2SO_4 \cdot nH_2O$(l) (97 wt.% H_2SO_4)	220	>3 x 10^{-3}‡		53
HF	Water Ice	H_2O(s)	200	See Note		54
	Nitric Acid Ice	$HNO_3 \cdot 3H_2O$(s)	200	See Note		54
CF_2O	Water Ice	H_2O(s)	192	See Note		55
	Liquid Water	H_2O(l)	260-290	See Note		50
	Nitric Acid Ice	$HNO_3 \cdot 3H_2O$(s)	192	See Note		55
	Sulfuric Acid	$H_2SO_4 \cdot nH_2O$(l)	215-230			
		(40 wt.% H_2SO_4)		>3 x 10^{-6}‡		55
		(60 wt.% H_2SO_4)		>6 x 10^{-5}‡		55
CF_3CFO	Liquid Water	H_2O(l)	260-290	See Note		50
CF_3COOH	Liquid Water	H_2O(l)	263-288	0.2-0.1*	2	56
CF_3CClO	Liquid Water	H_2O(l)	260-290	See Note		50
SO_2	Liquid Water	H_2O(l)	260-292	0.11	2	57
	Sulfuric Acid	$H_2SO_4 \cdot nH_2O$(l) (97 wt.% H_2SO_4)	298	See Note		58
	Carbon/Soot	C(s)	298	3 x 10^{-3}	5	59

Table 63. (Continued)

Gaseous Species	Surface Type	Surface Composition	T(K)	α	Uncertainty Factor	Notes
$CH_3S(O)CH_3$	Liquid Water	$H_2O(l)$	262-281	0.16-0.08*	2	60
$CH_3S(O_2)CH_3$	Liquid Water	$H_2O(l)$	262-281	0.27-0.08*	2	60
$CH_3S(O_2)OH$	Liquid Water	$H_2O(l)$	264-278	0.17-0.11*	2	60

*Varies with T, see Notes
‡May be affected by surface saturation

Notes to Table 63

1. O on $H_2SO_4 \cdot nH_2O$ - Knudsen cell experiment of Baldwin and Golden [9] measured an uptake coefficient limit of $<10^{-6}$; this result probably cannot be equated with an accommodation coefficient due to surface saturation.

2. O_3 on $H_2O(s)$ and $HNO_3 \cdot nH_2O$ - Undoped ice surfaces saturate too quickly for reliable measurements. When ice is doped with Na_2SO_3 to chemically remove absorbed O_3 the apparent α increases to 1×10^{-2} (0.1M) or up to 4×10^{-2} (1M) (Dlugokencky and Ravishankara [34]). Limit of $\gamma < 10^{-6}$ for undoped ice is consistent with earlier measurement by Leu [103] of $\leq 1 \times 10^{-4}$ and with $< 6 \times 10^{-5}$ obtained by Kenner et al. [93]. Dlugokencky and Ravishankara also measured the tabulated value of an uptake coefficient for O_3 on a NAT "like" surface, but the data were difficult to reproduce and the surfaces were not well characterized. Kenner et al. also measured a lower limit for an uptake coefficient of 8×10^{-5} on NAT at 183 K, but this measurement is also certainly limited by surface saturation.

3. O_3 on $H_2O(l)$ - Utter et al. [165] used a wetted wall flow tube technique with various chemical scavengers to measure a lower limit for α of 2×10^{-3}. The stopped flow measurement technique using an $SO_3^=$ scavenger (Tang and Lee [157]) is subject to saturation effects, so their quoted α of 5.3×10^{-4} is also taken as a lower limit.

4. O_3 on $H_2SO_4 \cdot nH_2O$ - Recent flow tube measurements (Dlugokencky and Ravishankara [34]) of an uptake coefficient limit of $<10^{-6}$ on both 50 and 97 wt. % H_2SO_4 surfaces are consistent with earlier, but probably less quantitative, static systems measurements of Olszyna et al. [129] and aerosol chamber measurements of Harker and Ho [75], who report uptake coefficients of the order 10^{-8} or less for a variety of sulfuric acid concentrations and temperatures. In these earlier experiments, doping the H_2SO_4 with Ni^{2+}, Cr^{2+}, Al^{3+}, Fe^{3+} and NH_4^+ (Olszyna et al. [129]) or Al_2O_3 or Fe_2O_3 (Harker and Ho [75]) did not significantly increase measured O_3 loss. A lower limit of 1×10^{-6} was also reported by Baldwin and Golden [8] for 97 wt % H_2SO_4 at 295 K. All measurements are subject to solubility limitations and probably do not reflect true limits on mass accommodation.

5. OH on $H_2O(s)$ - Cooper and Abbatt[27] analyzed uptake rates in a wall-coated flow tube to determine an initial $\gamma \sim 0.1$ over the temperature range of 205 - 230 K. Uptake coefficients decreased at longer exposure times, indicating surface saturation. These data indicate that α is at least 0.1 and possibly much larger. This is confirmed by an earlier experiment using a coated insert/flow tube technique by Gerhenzon et al. [50], which yielded $\alpha > 0.4$ at 253 K.

6. OH on $H_2O(l)$ - see Note for HO_2 on $H_2O(l)$. The OH and HO_2 measurements of Hanson et al. [60] are subject to same analysis issues.

7. OH on $H_2SO_4 \cdot nH_2O$ - See Note for HO_2 on $H_2O(l)$ for measurement (28 wt.% H_2SO_4) by Hanson et al. [60] and Note for O on H_2SO_4 for measurement (97 wt. % H_2SO_4) by Baldwin and Golden [9].

8. OH on $Al_2O_3(s)$ - Measured value is from flow tube experiment with native oxide on aluminum as the active surface. An uptake coefficient of 0.4 ± 0.2 independent of temperature over the range of 253-348 K was measured (Gershenzon et al. [50]).

9. HO_2 on $H_2O(l)$ - Determination of α in liquid-wall flow tube (Hanson et al. [60]) is dependent on gas-phase diffusion corrections; measured limit ($\alpha > 0.02$) is consistent with $\alpha = 1$. In the aqueous salt aerosol measurements of Mozurkewich et al. [125], HO_2 was chemically scavenged by Cu^{++} from added $CuSO_4$ to avoid Henry's law constraints; the measured limit of >0.2 is also consistent with $\alpha = 1$.

10. HO_2 on NaCl(s) and KCl(s) - Measured values of $\gamma = 1.8 \times 10^{-2}$ for KCl and 1.6×10^{-2} for NaCl, both at 295 K by Gersherzon et al.[52] supplementing an earlier value of $\gamma - 8 \times 10^{-3}$ measured by Gersherzon and Purmal [51], results have not been calibrated with a competitive technique.

11. H_2O on $H_2O(s)$ - Measurements are available from Leu [104] giving 0.3 (+0.7, -0.1) at 200 K and Haynes et al. [76] (1.06 ± 0.1 to 0.65 ± 0.08) from 20 to 185 K. Brown et al.[18] used molecular beam reflection techniques to measure a value of $\alpha = 0.99 \pm 0.03$ between 85 and 150 K and optical interference methods to obtain $\alpha = 0.97 \pm 0.10$ between 97 and 145 K.

12. H_2O on $HNO_3/H_2O(l)$ - Rudolf and Wagner[147] used aerosol expansion chamber techniques to illustrate that on liquid water/nitric acid aerosols α is greater than 0.3 and is consistent with 1.0 at 278 K.

13. H_2O on $HNO_3 \cdot nH_2O(s)$ - Middlebrook et al. [118] measured an uptake coefficient of .002 for water vapor co-depositing with nitric acid over NAT at 197 K.

14. H_2O on $H_2SO_4 \cdot nH_2O$ - Baldwin and Golden [8] measured $\gamma \sim 2 \times 10^{-3}$, which is almost certainly affected by surface saturation. See Note 15 for H_2O_2 on $H_2SO_4 \cdot nH_2O$.

15. H_2O on NaCl(s) - Fenter et al.[40] used Knudsen cell/mass spectrometry methods to measure $\gamma < 2 \times 10^{4}$ for $H_2O(g)$ uptake on NaCl powders, an observation confirmed by Beichert and Finlayson-Pitts[13], who found $\gamma < 1 \times 10^{-5}$. However, Dai et al.[28] used FTIR spectroscopy on NaCl crystallite films at 240 and 296 K to determine that a water adlayer does adhere to dry salt and that a small fraction of surface sites (< 1%) cause H_2O dissociation. It is likely that the measurements of Fenter et al. and Beichert and Finlayson-Pitts were affected by surface saturation.

16. H_2O on NaCl(aq) - Fung et al.[46] used Mie resonance scattering techniques to quantify aqueous NaCl droplet growth (5.8 to 7.8 μm), yielding fitted values of $\alpha > 0.5$ and consistent with 1.0.

17. H_2O on C(s) - Rogaski et al.[142] used initial Knudsen cell uptake measurements to estimate $\alpha = (4 \pm 2) \times 10^{-4}$ for H_2O vapor on amorphous carbon at 298 K. Pretreatment of the carbon surface with gaseous O_3, NO_2, and SO_2 made little change in α. However, pretreatment with HNO_3 and H_2SO_4 increased uptake coefficients dramatically to $(11 \pm 1) \times 10^{-3}$ and $(27 \pm 1) \times 10^{-3}$, respectively.

18. H_2O_2 on $H_2O(l)$ - Measured accommodation coefficient (Worsnop et al. [181]) has a strong negative temperature dependence over the measured range of 260-292 K, with $\alpha = 0.3$ at 260 K decreasing to 0.1 at 292 K.

19. H_2O_2 on $H_2SO_4 \cdot nH_2O$ - Knudsen cell uptake measurements are subject to surface saturation, thus uptake coefficient value of 7.8×10^{-4} quoted by Baldwin and Golden [8] is almost certainly a lower limit for α. This effect is probably also responsible for the lack of measured uptake ($\gamma < 10^{-6}$) for NO, NO_2, SO_2, Cl_2, and other species reported in this reference and Baldwin and Golden [9].

20. NO on $H_2O(s)$ - NO data (Leu [103], Saastad et al. [148]) subject to same concerns as NO_2. See Note for NO_2 on $H_2O(s)$.

21. NO on $H_2SO_4 \cdot nH_2O$ - See Notes for H_2O_2 on $H_2SO_4 \cdot nH_2SO_4$ and NO_2 on $H_2SO_4 \cdot nH_2O$. NO is subject to the same concerns as NO_2 for both reported measurements (Saastad et al. [148]; Baldwin and Golden [8]).

22. NO_2 on H_2O(s) - In the absence of a chemical sink, Leu [103] measured no sustained uptake of NO_2 on ice yielding an apparent $\alpha \leq 1 \times 10^{-4}$. Saastad et al. [148] measured a lower limit of 5×10^{-5} for temperatures between 193 and 243 K. However these values are probably influenced by surface saturation.

23. HONO on H_2O(s) - Fenter and Rossi[42] measured reversible uptake on water ice between 180 and 200 K using a Knudsen cell technique. An initial uptake coefficient of 1×10^{-3} suggests that α equals or exceeds this value.

24. HNO_3 on H_2O(s) - Leu [104] reports 0.3 (+0.7, -0.1). Some additional uncertainty is introduced by effective ice surface area in fast-flow measurement (see Keyser et al. [97]). Hanson [58] measured an uptake coefficient of > 0.3 at 191.5 and 200 K.

25. HNO_3 on H_2O(l) - Measured α has a strong negative temperature dependence varying from 0.19 ± 0.02 at 268 K to 0.07 ± 0.02 at 293 K (Van Doren et al. [167]). Ponche et al. [132] measured an accommodation coefficient of 0.05 ± 0.01 at 297 K.

26. HNO_3 on $HNO_3 \cdot nH_2O$(s) - Hanson [58] measured uptake coefficients of > 0.3 and >0.2 on NAT surfaces at 191 K and 200 K, respectively. Middlebrook et al. [118] measured an uptake coefficient of 0.7 on NAT at 197 K under conditions where both nitric acid and water vapor were co-depositing.

27. HNO_3 on $HNO_3 \cdot nH_2O$(l) - Rudolf and Wagner used aerosol expansion chamber techniques to deduce that α for HNO_3 on 278 K H_2O/HNO_3 droplets is > 0.3 and probably close to 1. The consistency of this value with smaller (~0.2) values measured for uptake on pure water by Van Doren et al. [167] is unclear, since the mechanism of co-condensation is unknown and the composition of the surface in the aerosol expansion chamber experiments may be kinetically controlled and has not been well determined.

28. HNO_3 on $H_2SO_4 \cdot nH_2O$ and $H_2SO_4 \cdot 4H_2O$(s) - Initial uptake at 73 wt. % H_2SO_4 allows a measurement of $\alpha = 0.11 \pm 0.01$ at 283 K (Van Doren et al. [167]). This value is expected to increase at lower temperatures, in a manner similar to H_2O(l) uptake (Van Doren et al. [166]). Total HNO_3 uptake is subject to Henry's law solubility constraints, even at stratospheric temperatures (Reihs et al. [135]). Solubility limitations also affected the earlier "sticking coefficient" measurements of Tolbert et al. [161] for 75 wt % H_2SO_4 at 230 K. Hanson [58] measured an uptake coefficient of >0.3 for frozen 57.7 wt. % sulfuric acid at 191.5 and 200 K. Baldwin and Golden [8] reported a lower limit of 2.4×10^{-4} on 97 wt. % H_2SO_4 at 295 K, also reflecting solubility limits. Iraci et al. [83] monitored nitric acid trihydrate growth on sulfuric acid tetrahydrate with infrared techniques, measuring HNO_3 uptake coefficient limits of >0.03 at 192.5 K and >0.08 at 192 K. These measurements involved co-deposition of water vapor.

29. HO_2NO_2 on H_2O(s) - Li et al. [106] measured an uptake coefficient of 0.15 ± 0.10; uptake may be limited by surface saturation.

30. HO_2NO_2 on $H_2SO_4 \cdot nH_2O$(l) - Baldwin and Golden measured $\gamma = 2.7 \times 10^{-5}$, which is probably solubility limited; see Note 15 for H_2O_2 on $H_2SO_4 \cdot nH_2O$.

31. NH_3 on H_2O(l) - Ponche et al. [132] used a droplet train technique to obtain $\alpha = (9.7 \pm 0.9) \times 10^{-2}$ at 290 K, and Bongartz et al.[16] used a liquid jet technique to obtain $\alpha = 4.0\ (+3.0, -0.05) \times 10^{-2}$. Earlier levitated droplet evaporation experiments [158] on NH_4Cl obtained a larger evaporation coefficient of $\alpha = 0.29 \pm 0.03$, which is discounted because of the indirect nature of the experiment.

32. CO_2 on H_2O(l) - Noyes et al.[128] used a dynamic stirring technique to monitor pressure decreases in a closed cylinder. They inferred $\alpha = (5.5 \pm 0.5) \times 10^{-8}$ at 293 K. This technique is uncalibrated against more widely

used procedures and probably suffers from surface saturation effects. Measured α is probably many orders of magnitude too small.

33. CH_3OH on $H_2O(l)$ - Jayne et al. [86] measured uptake from 260-291 K and derived accommodation coefficients fitting $\alpha/(1-\alpha) = \exp(-\Delta G^{\ddagger}_{obs}/RT)$, where $\Delta G^{\ddagger}_{obs}$ = -8.0 kcal/mol + 34.9 cal mol^{-1} K^{-1} T(K).

34. CH_3CH_2OH on $H_2O(l)$ - Jayne et al. [86] measured uptake from 260-291 K and derived accommodation coefficients fitting $\alpha/(1-\alpha) = \exp(-\Delta G^{\ddagger}_{obs}/RT)$, where $\Delta G^{\ddagger}_{obs}$ = -11.0 kcal/mol + 46.2 cal mol^{-1} K^{-1} T(K). Similar, but somewhat larger values were reported for chloro-, bromo-, and iodo-ethanols.

35. $CH_3CH_2CH_2OH$ and $CH_3CH(OH)CH_3$ on $H_2O(l)$ - Jayne et al. [86] measured uptake coefficients between 260 and 291 K and derived accommodation coefficients fitting $\alpha/(1-\alpha) = \exp(-\Delta G^{\ddagger}_{obs}/RT)$, where $\Delta G^{\ddagger}_{obs}$ = -9.2 kcal mol^{-1} + 40.9 cal mol^{-1} K^{-1} T(K) for 1-propanol and -9.1 kcal mol^{-1} + 43.0 cal mol^{-1} K^{-1} T(K) for 2-propanol. Similar data for t-butanol were also reported.

36. $HOCH_2CH_2OH$ on $H_2O(l)$ - Jayne et al. [86] measured uptake coefficients for ethylene gycol between 260 and 291 K and derived accommodation coefficients fitting $\alpha/(1-\alpha) = \exp(-\Delta G^{\ddagger}_{obs}/RT)$, where $\Delta G^{\ddagger}_{obs}$ = -5.3 kcal mol^{-1} + 24.5 cal mol^{-1} K^{-1} T(K).

37. $CH_2O + H_2O(l)$, $H_2SO_4 \bullet mHNO_3 \bullet nH_2O(l)$ - Jayne et al.[88] report uptake measurements for 0 - 85 wt % H_2SO_4 and 0 - 54 wt% HNO_3 over a temperature range of 241 - 300 K. Measured uptake coefficients vary from 0.0027 - 0.027, increasing with H^+ activity (Jayne et al ([88]; Tolbert et al., [160]), and with increasing pH above 7 (Jayne et al., [87]). Reversible uptake is solubility limited through reactions to form $H_2C(OH)_2$ and $CH_3O.^+$ Model of uptake kinetics (Jayne et al., [88]) consistent with $\alpha = 0.04 \pm 0.01$ for all compositions. A chemisorbed surface complex dominates uptake at 10 - 20 wt % H_2SO_4, and CH_3O^+ formation dominates above 20 wt % (Tolbert et al., [94/1564]; Jayne et al.[88]). These chemical mechanisms allow γ to greatly exceed α for strong acid and basic solutions. A full uptake model for acid solutions is presented in Jayne et al. [88], and for basic solutions in Jayne et al. [87].

38. CH_3O_2 + NaCl(s) - Gershenzon et al.[52] measured the uptake of CH_3O_2 on crystalline NaCl(s) in a central rod flow apparatus. They determined a value of $\gamma = (4 \pm 1) \times 10^{-3}$ at 296 K, suggesting that $\alpha \geq 4 \times 10^{-3}$.

39. CH_3CHO on $H_2O(l)$ - Jayne et al. [87] measured a lower accommodation coefficient limit of > 0.03 at 267 K. Uptake can be limited by Henry's law and hydrolysis kinetics effects - see reference.

40. $CH_3C(O)CH_3$ on $H_2O(l)$ - Duan et al. [36] measured uptake between 260 and 285 K, deriving α = 0.066 at the lower temperature and 0.013 at the higher, with several values measured in between. Measured values fit $\alpha/(1-\alpha) = \exp(-\Delta G^{\ddagger}_{obs}/RT)$, where $\Delta G^{\ddagger}_{obs}$ = -12.7 kcal/mol + 53.6 cal mol^{-1} K^{-1} T(K).

41. $HC(O)OH$ on $H_2O(l)$ - Jayne et al. [86] measured uptake coefficients for formic acid between 260 and 291 K and derived accommodation coefficients fitting $\alpha/(1-\alpha) = \exp(-\Delta G^{\ddagger}_{obs}/RT)$, where $\Delta G^{\ddagger}_{obs}$ = -7.9 kcal mol^{-1} + 34.9 cal mol^{-1} K^{-1} T(K).

42. $CH_3C(O)OH$ on $H_2O(l)$ - Jayne et al. [86] measured uptake coefficients for acetic acid between 260 and 291 K and derived an accommodation coefficient fitting $\alpha/(1-\alpha) = \exp(-\Delta G^{\ddagger}_{obs}/RT)$, where $\Delta G^{\ddagger}_{obs}$ = -8.1 kcal mol^{-1} + 34.9 cal mol^{-1} K^{-1} T(K).

43. Cl_2 on $H_2O(s)$ - Measurement of Leu [104] yielded a limit of $< 1 \times 10^{-4}$ for Cl_2 and is subject to same concern as NO_2 (see note 18). A similar limit of $< 5 \times 10^{-5}$ has been measured by Kenner et al. [93], which is also probably limited by surface saturation.

44. $OClO + H_2O(s)$ - Brown et al.[19] and Graham et al.[56] used complementary ultra high-vacuum (UHV) and coated-wall flow tube techniques to show sub-monolayer reversible absorption of OClO on water ice at 100 K

(UVH) and 189 and 200 K (flow tube). No kinetic data are available at stratospheric temperatures but the mass accommodation coefficient for 100 K ice surfaces is near unity, with values of 0.8 ± 0.2 reported for amorphous ice and 0.6 ±0.2 for crystalline ice [56].

45. HCl on H_2O(s) - Leu [104] (0.4; +0.6, -0.2) and Hanson and Ravishankara, [66] ($\alpha \geq 0.3$) are in reasonable agreement at stratospheric ice temperatures. More recently, a great deal of experimental effort (Abbatt et al. [4], Koehler et al. [98], Chu et al. [25], Graham and Roberts [54], Graham and Roberts[55]; Rieley et al.[136]) has gone into understanding the uptake of HCl by ice surfaces. Rieley et al. measured α = 0.95±0.05 at 80 - 120 K. Water ice at stratospheric temperatures can take up a large fraction of a monolayer even at HCl partial pressures typical of the stratosphere. Both the thermodynamic and spectroscopic properties of this absorbed HCl indicate that it has dissociated to ions, forms ionic hydrates, and is highly reactive. These experimental results contrast with initial theoretical calculations that predicted undissociated HCl hydrogen bonded to the ice surface and a very small adsorption probability at stratospheric temperatures (Kroes and Clary [100]); more recent simulations result in higher adsorption energies and theoretical accommodation coefficients of one for 190 K surfaces [Wang and Clary [173]]. Recent molecular dynamics calculations by Gertner and Hynes[53] also show that ionic absorption is thermodynamically favorable by about 5 kcal/mole. At HCl partial pressures significantly above those typical of the stratosphere, a liquid surface layer forms on the ice, greatly enhancing the total amount of HCl that the surface can absorb.

46. HCl on H_2O(l) - Recommendation is based on Van Doren et al. [166]. Measured α's decrease from 0.18 ±0.02 at 274 K to 0.064 ±0.01 at 294 K, demonstrating a strong negative temperature dependence. Tang and Munkelwitz [158] have measured a larger (0.45 ±0.4) HCl evaporation coefficient for an aqueous NH_4Cl droplet at 299 K.

47. HCl on $HNO_3 \cdot nH_2O$ - There was previously severe disagreement between Hanson and Ravishankara [66] ($\alpha \geq 0.3$) for NAT (54 wt. % HNO_3), and Leu and coworkers (Moore et al. [123], Leu et al. [105]). However, subsequent experiments at lower HCl concentrations by Leu and coworkers (Chu et al. [25]) as well as Abbatt and Molina [5] are generally consistent with Hanson and Ravishankara. In particular, Abbatt and Molina [5] report a large uptake coefficient ($\alpha > 0.2$). The measurements of Hanson and Ravishankara are consistent with $\alpha = 1$. The experiments at stratospherically representative HCl concentrations show that HNO_3 rich NAT surfaces adsorb significantly less HCl than H_2O rich surfaces.

48. HCl on $H_2SO_4 \cdot nH_2O$ - Measurements by Watson et al. [174] at 284 K show $\alpha = 0.15 \pm 0.01$ independent of n for $n \geq 8$. Experimental uptake and, therefore, apparent α falls off for $n \leq 8$ (≥40 wt. % H_2SO_4). This behavior is also observed at stratospheric temperature (218 K) by Hanson and Ravishankara [66]. More recent measurements by Robinson et al. (to be published) extend mass accommodation measurements to lower temperatures, yielding significantly higher values. Solubility constraints also controlled earlier low temperature uptake measurements of Tolbert et al. [161]. A review of the most recent solubility data is presented in Table 60.

49. HCl on $H_2SO_4 \cdot 4H_2O$(s) - Uptake is a strong function of temperature and water vapor partial pressure (relative humidity) (Zhang et al. [188]), both of which affect adsorbed surface water.

50. Halocarbonyls on H_2O(l) - Uptake is limited by Henry's law solubility and hydrolysis rate constants (De Bruyn et al. [31, 33] and George et al. [47, 49]. See Table 60.

51. HBr on H_2O(s) and $HNO_3 \cdot nH_2O$ - Hanson and Ravishankara [67, 69] have reported large uptake coefficients for HBr on 200 K ice and NAT. Lower limits of >0.3 and >0.2 for ice are reported in the two referenced publications, respectively, and a limit of >0.3 is reported for NAT. No surface saturation was observed, leading to the supposition that HBr, like HCl, dissociates to ions on ice surfaces at stratospheric temperatures. Abbatt [1] measured an uptake coefficient lower limit of >0.03 on water ice at 228 K in agreement with Hanson and Ravishankara. Rieley et al. measured an α of 1.0 ± 0.05 for water ice at 80 - 120K and Chu and Heron[23] report equilibrium HBr coverages for ice at 188 and 195 K.

52. HOBr on $H_2SO_4 \bullet nH_2O(l)$ - Abbatt [1] measured an uptake coefficient of 0.06 ±(0.02) by measuring HOBr gas phase loss at 228 K. This result may well be a lower limit due to surface saturation effects.

53. $CHBr_3$ on $H_2O(s)$ and $H_2SO_4 \bullet nH_2O(l)$ - Hanson and Ravishankara [69] investigated the uptake of bromoform on ice and 58 wt.% sulfuric acid at 220 K. No uptake on ice was observed, with a measured uptake coefficient of $<6 \times 10^{-5}$. Reversible uptake by the sulfuric acid surface was observed with an initial uptake coefficient of $>3 \times 10^{-3}$; both measurements are probably limited by surface saturation.

54. HF on $H_2O(s)$ and $HNO_3 \bullet nH_2O(s)$ - Hanson and Ravishankara [67] attempted to measure the uptake of HF by 200 K water ice and NAT surfaces but were unable to observe measurable adsorption. They surmise that, unlike HCl and HBr, HF does not dissociate to ions on ice or NAT surfaces at 200 K. Lack of measurable uptake is probably due to surface saturation.

55. CF_2O on $H_2O(s)$, $HNO_3 \bullet nH_2O$ and $H_2SO_4 \bullet nH_2O$ - Uptake coefficient measurements by Hanson and Ravishankara [64] on stratospheric surfaces are probably subject to surface and/or bulk saturation effects and may not represent accommodation coefficient measurements, particularly the lower limits of $>3 \times 10^{-6}$ reported for water and nitric acid ices.

56. CF_3COOH on $H_2O(l)$ - Hu et al. [79] measured mass accommodation coefficients for five haloacetic acids, including trifluoroacetic acid (TFA); the others were mono-, di-, trichloro-, and chlorodifluoro-acetic acids. All displayed a negative temperature dependence and values for α of about 0.1 at 273 K.

57. SO_2 on $H_2O(l)$ - Measured α of 0.11 ± 0.02 has no significant temperature variation over a temperature range of 260 - 292 K (Worsnop et al. [181]). Ponche et al. [132] measured 0.13 ± 0.01 at 298 K, in agreement with the earlier measurement. Shimono and Koda[151] estimated an α of 0.2 at 293.5 K from analysis of pH-dependent uptake coefficients in a novel liquid impingement technique that has not been calibrated with other gases. Donaldson et al. ([35]) have used second harmonic generation spectroscopy to detect a chemisorbed SO_2 surface species which was predicted from earlier uptake measurements by Jayne et al.[85]; this surface complex may play a role in SO_2 heterogeneous reactions on aqueous surfaces.

58. SO_2 on $H_2SO_4 \bullet nH_2O$. See Note for H_2O_2 on $H_2SO_4 \bullet nH_2O$.

59. SO_2 on C(s) - Initial and longer-term uptake Knudsen cell values of Rogaski et al. yielded $\gamma = 3(\pm 1) \times 10^{-3}$ for room temperature amorphous carbon, suggesting $\alpha \sim 3 \times 10^{-3}$ since no reaction products were observable with gas phase mass spectrometry.

60. $CH_3S(O)CH_3$, $CH_3S(O_2)CH_3$ and $CH_3S(O_2)OH$ on $H_2O(l)$ - De Bruyn et al. [32] measured uptake over the temperature range ~262-281 K and derived accommodation coefficients fitting $\alpha / (1 - \alpha) = \exp(-\Delta G^{\ddagger}_{obs}/RT)$, where $\Delta G^{\ddagger}_{obs}$ = -0.12 kcal mol^{-1} + 23.1 cal mol^{-1} K^{-1} T(K) for dimethylsulfoxide, -10.7 kcal mol^{-1} + 43.0 cal mol^{-1} K^{-1} T(K) for dimethylsulfone and -3.50 kcal mol^{-1} + 16.7 cal mol^{-1} K^{-1} T(K) for methanesulfonic acid.

Table 64. Gas/Surface Reaction Probabilities (γ)

Gaseous Species	Surface Type	Surface Composition	T(K)	γ	Uncertainty Factor	Notes
O_3 + Surface → Products						
O_3	Alumina	Al_2O_3(s)	210-300	See Note		1
	Carbon/Soot	C(s)	≈300	3×10^{-3}	20	2
	Sodium Chloride	NaCl(s)	≈300	$>2 \times 15^{-10}$		1
OH + Surface → Products						
OH	**Water Ice**	**H_2O(s)**	**205-230**	**>0.01**		**3**
	Hydrochloric Acid	**HCl • nH_2O(l)**	**220**	**>0.2**		**4**
	Nitric Acid Ice	**HNO_3 • 3HzO(s)**	**200-228**	**>0.2**		**5**
	Sulfuric Acid	**H_2SO_4 • nH_2O(l)**	**200-298**	**>0.2**		**6**
	Sodium Chloride	**NaCl(s)**	**245-339**	**1.2×10^{-5} exp 1750/T**	**3**	**7**
HO_2 + Surface → Products						
	Water Ice	**H_2O(s)**	**223**	**0.025**	**3**	**8**
	Sulfuric Acid	**H_2SO4 • nH_2O(l)**				**8**
		(28 wt %)	**275**	**.0.07**		
		(55 wt %)	**223**	**>0.05**		
		(80-96 wt %)	**243**	**>0.2**		
$2NO_2 + H_2O(l) \rightarrow HONO + HNO_3$						
NO_2	**Liquid Water**	**H_2O(l)**		**See Note**		**9**
	Sulfuric Acid	**H_2SO_4 • nH_2O**		**See Note**		**10**
NO_2 + C(s) → Products						
NO_2	Carbon/Soot	C(s)		See Note		11
$2NO_2$ + NaCl(s) → ClNO + $NaNO_3$						
NO_2	Sodium Chloride	NaCl(s)	298	See Note		12
$NO_3 + H_2O(l) \rightarrow HNO_3 + OH$						
NO_3	**Liquid Water**	**H_2O(l)**	**273**	**2×10^{-4}**	**20**	13

Table 64. Continued

Gaseous Species	Surface Type	Surface Composition	T(K)	γ	Uncertainty Factor	Notes
$N_2O_5 + H_2O \rightarrow 2HNO_3$						
N_2O_5	Water Ice	$H_2O(s)$	195-200	0.01	3	14
	Liquid Water	$H_2O(l)$	260-295	0.05*	2	15
	Nitric Acid Ice	$HNO_3 \cdot 3H_2O(s)$	200	3×10^{-4}	3	16
	Sulfuric Acid	$H_2SO_4 \cdot nH_2O(l)$	195-300	≈0.1	See Note	17
	Sulfuric Acid Monohydrate	$H_2SO_4 \cdot H_2O(s)$	200-300	See Note	3	18
	Sulfuric Acid Tetrahydrate	$H_2SO_4 \cdot 4H_2O(s)$	195-207	0.006	2	19
	Ternary Acid	$H_2SO_4 \cdot nHNO_3 \cdot nH_2O(l)$	195-218	See Note		17
$N_2O_5 + HCl(s) \rightarrow ClNO_2 + HNO_3$						
N_2O_5	Water Ice	$H_2O(s) \cdot HCl(s)$	190-220	0.03	See Note	20
	Nitric Acid Ice	$HNO_3 \cdot 3H_2O(s) \cdot HCl(s)$	200	0.003	2	21
	Sulfuric Acid Monohydrate	$H_2SO_4 \cdot H_2O(s)$	195	$<1 \times 10^{-4}$		22
$N_2O_5 + NaCl(s) \rightarrow ClNO_2 + NaNO_3(s)$						
N_2O_5	Sodium Chloride	NaCl(s)	~300	5×10^{-4}	20	23
		NaCl(aq)		>0.02		23
$N_2O_5 + HBr(s) \rightarrow BrNO_2 + HNO_3$						
N_2O_5	Nitric Acid Ice	$HNO_3 \cdot 3H_2O(s)$	200	0.005	10	24
$N_2O_5 + MBr(s) \rightarrow$ Products						
N_2O_5	Sodium Bromide	NaBr(s)	~300		See Note	25
	Potassium Bromide	KBr(s)	~300	4×10^{-3}	10	25
$HONO + H_2O \rightarrow$ Products						
HONO	Liquid Water	$H_2O(l)$	247-297	0.04	5	26
$HONO + H_2SO_4 \rightarrow$ Products						
HONO	Sulfuric Acid	$H_2SO_4(l)$	180-200	See Note		27
$HONO + HCl \rightarrow ClNO + H_2O$						
HONO	Water Ice	$H_2O(s)$	180-200	0.05	3	28

Table 64. Continued

Gaseous Species	Surface Type	Surface Composition	T(K)	γ	Uncertainty Factor	Notes
HONO + NaCl → Products						
HONO	Sodium Chloride	NaCl(s)	~300	$<1 \times 10^{-4}$		29
$HNO_3 + C(s) \rightarrow$ Products						
HNO_3	Carbon/Soot	C(s)	190-440	0.04	5	30
$HNO_3 + NaX(s) \rightarrow HX + NaNO_3$						
HNO_3	Sodium Chloride	NaCl(s)	295-298	0.02	3	31
	Sodium Bromide	NaBr(s)	~290	0.02	10	31
	Potassium Chloride	KCl(s)	~290	0.02	10	31
	Potassium Bromide	KBr(s)	~290	0.02	10	31
$NH_3 + H_2SO_4 \rightarrow NH_4HSO_4$						
NH_3	Sulfuric Acid	$H_2SO4 \cdot nH_2O$	288-300	0.4	2.5	32
$CH_3C(O)O_2 + H_2O \rightarrow CH_3C(O)OH + HO_2$						
$CH_3C(O)O_2$	Liquid Water	$H_2O(l)$	225	4×10^{-3}	3	33
	Sulfuric Acid	$H_2SO_4 \cdot nH_2O$				33
		(84 wt % H_2SO_4)	246	3×10^{-3}	3	
		(51 wt % H_2SO_4)	223	1×10^{-3}	3	
		(71 wt % H_2SO_4)	298	1×10^{-3}	3	
Cl + Surface → Products						
Cl	Sulfuric Acid	$H_2SO_4 \cdot nH_2O(l)$	221-296	2×10^{-4}	10	34
$Cl_2 + HBr(s) \rightarrow BrCl + HCl$						
Cl_2	Water Ice • HBr(s)	$H_2O(s)$	200	>0.2		35
$Cl_2 + KBr(s) \rightarrow BrCl + KCl(s)$						
Cl_2	Potassium Bromide	KBr(s)	~295	>0.1		36
$Cl_2 + NaX$ (aq) → ClX + NaCl (aq)						
Cl_2	Aqueous Sodium Bromide	NaBr(aq)	See Note			37
	Aqueous Sodium Iodine	NaI(aq)	See Note			37

Table 64. Continued

Gaseous Species	Surface Type	Surface Composition	T(K)	γ	Uncertainty Factor	Notes
ClO + Surface → Products						
ClO	Water Ice	$H_2O(s)$	190	See Note		38
	Nitric Acid Ice	$HNO_3 \cdot 3H_2O(s)$	183	See Note		38
	Sulfuric Acid	$H_2SO_4 \cdot nH_2O(l)$ (60 to 95 wt.% H_2SO_4)	221-296	See Note		39
HOCl + HCl(s) → $Cl_2 + H_2O$						
HOCl	Water Ice	$H_2O(s) \cdot HCl(s)$	195-200	0.3	3	40
	Nitric Acid Ice	$HNO_3 \cdot 3H_2O(s) \cdot HCl(s)$	195-200	0.1	3	40
	Sulfuric Acid	$H_2SO_4 \cdot nH_2O(l)$	198-209	See Note		41
ClNO + NaCl(s) → Products						
ClNO	Sodium Chloride	NaCl(s)	298	$>1 \times 10^{-5}$		42
$ClNO_2$ + NaCl(s) → Products						
$ClNO_2$	Sodium Chloride	NaCl(s)	298	$<1 \times 10^{-5}$		42
$ClONO_2 + H_2O(s) \rightarrow HOCl + HNO_3$						
$ClNO_2$	Water Ice	$H_2O(s)$	180-200	0.3	3	43
	Nitric Acid Ice	$HNO_3 \cdot 3H_2O(s)$	200-202	0.001*	10	44
	Sulfuric Acid	$H_2SO_4 \cdot nH_2O(l)$	200-265	See Note		45
	Sulfuric Acid Monodydrate	$H_2SO_4 \cdot H_2O(s)$	195	$<1 \times 10^{-3}$		46
	Sulfuric Acid Tetrahydrate	$H_2SO_4 \cdot 4H_2O(s)$	196-206	See Note		46
$ClONO_2 + HCl(s) \rightarrow Cl_2 + HNO_3$						
$ClONO_2$	Water Ice	$H_2O(s)$	180-202	0.3	5	47
	Nitric Acid Ice	$HNO_3 \cdot 3H_2O \cdot HCl$	200-202	0.1	3	48
	Sulfuric Acid	$H_2SO_4 \cdot nH_2O(l) \cdot HCl(l)$		See Note		49
	Sulfuric Acid Monodydrate	$H_2SO_4 \cdot H_2O(s)$	195	$<1 \times 10^{-4}$		50
	Sulfuric Acid Tetrahydrate	$H_2SO_4 \cdot 4H_2O(s)$	195-206	See Note		50
	Alumina	Al_2O_3	180-200	0.3	3	51
$ClONO_2 + MX(s) \rightarrow XCl + MNO_3$						
$ClONO_2$	Sodium Chloride	NaCl(s)	200-300	5×10^{-2}	10	52
	Potassium Bromide	KBr(s)	~295	5×10^{-2}	10	52
	Sodium Bromide	NaBr(s)	~295	See Note		52

Table 64. Continued

Gaseous Species	Surface Type	Surface Composition	T(K)	γ	Uncertainty Factor	Notes
$ClONO_2 + HBr(s) \rightarrow BrCl + HNO_3$						
$ClONO_2$	Water Ice	$H_2O(s) \cdot HBr(s)$	200	>0.3		53
	Nitric Acid Ice	$HNO_3 \cdot 3H_2O(s) \cdot HBr(s)$	200	>0.3		53
$ClONO_2 + HF(s) \rightarrow$ Products						
$ClONO_2$	Water Ice	$H_2O(s) \cdot HF(s)$	200	See Note		54
	Nitric Acid Ice	$H_2O(s) \cdot HNO_3(s) \cdot HF(s)$	200	See Note		54
$CF_xCl_y + Al_2O_3(s) \rightarrow$ Products						
CCl_4	Alumina	$Al_2O_3(s)$	120-300	1×10^{-5}	10	55
$CFCl_3$	Alumina	$Al_2O_3(s)$	120-300	1×10^{-5}	10	55
CF_2Cl_2	Alumina	$Al_2O_3(s)$	120-300	1×10^{-5}	10	55
CF_3Cl	Alumina	$Al_2O_3(s)$	120-300	1×10^{-5}	10	55
$BrCl + KBr(s) \rightarrow Br_2 + KCl(s)$						
BrCl	Potassium Bromide	KBr(s)	~295	>0.1		36
$Br_2 + NaI(aq) \rightarrow BrI + NaBr(aq)$						
Br_2	Aqueous Sodium Iodine	NaI(aq)	See Note			37
$2BrO \rightarrow Br_2 + O_2$						
BrO	Water Ice	$H_2O(s)$	213	See Note		56
	Sulfuric Acid	$H_2SO_4 \cdot nH_2O$				
		(60 wt% H_2SO_4)	213	See Note		56
		(70 wt % H_2SO_4)	213	See Note		56
	Aqueous Sodium Chloride	NaCl(aq) (23 wt% NaCl)	253	See Note		56
$HOBr + HCl(s) \rightarrow BrCl + H_2O$						
HOBr	Water Ice	$H_2O(s) \cdot HBr(s)$	228	0.3	3	57
	Sulfuric Acid	$H_2SO_4 \cdot nH_2O$ (60-69 wt% H_2SO_4)	228	0.2	3	57
$HOBr + HBr(s) \rightarrow Br_2 + H_2O$						
HOBr	Water Ice	$H_2O(s) \cdot HBr(s)$	228	0.1	3	58
	Sulfuric Acid	$H_2SO_4 \cdot nH_2O$	228	See Note		58

Table 64. Continued

Gaseous Species	Surface Type	Surface Composition	T(K)	γ	Uncertainty Factor	Notes
$BrONO_2 + H_2O \rightarrow HOBr + HNO_3$						
$BrONO_2$	Water Ice	$H_2O(s)$	200	>0.3		59
	Sulfuric Acid	$H_2SO_4 \cdot nH_2O$	210-298	0.8	2	60
$BrONO_2 + HCl \rightarrow BrCl + HNO_3$						
$BrONO_2$/HCl	Water Ice	$H_2O(s)$	200	See Note		59
	Sulfuric Acid	$H_2SO_4 \cdot nH_2O$	229	0.9	2	60
$CF_2Br_2 + Al_2O_3(s) \rightarrow$ Products						
CF_2Br_2	Alumina	Al_2O_3	210, 315	2×10^{-5}	10	55
$CF_3OH + H_2O \rightarrow$ Products						
CF_3OH	Water Ice	$H_2O(l)$	274	>0.01		61
	Sulfuric Acid	$H_2SO_4 \cdot nH_2O$				
		(40 wt% H_2SO_4)	210-250	0.07	3	61
		(45 wt% H_2SO_4)	210-250	0.04	3	61
		(50 wt% H_2SO_4)	210-250	0.01	3	61
		(50 wt% H_2SO_4)	210-250	0.001	3	61

*γ is temperature dependent

Notes to Table 64

1. $O_3 + Al_2O_3(s)$ and NaCl(s) - Very low ozone decomposition efficiencies for reaction on coarse (3 μm dia.) and fine (0.1 μm dia., partially hydroxylated) γ-alumina and course (3 μm dia.) α-alumina were measured in flowing and static systems by Hanning-Lee et al.[57] at temperatures ranging between 212 and 473 K. Based on measured BET surface areas, γs ranged from 2×10^{-11} to 4×10^{-10} over the 212 to 298 K temperature range. γs for γ-alumina at lower temperatures exceeded those for α-alumina. Results are roughly consistent with earlier, unpublished flow tube data from L.F. Keyser and from fluidized bed reactor studies of Alebic'-Juretic' et al. [7]. Note that γs based on geometic surface particle surface areas would be significantly (10^4 - 10^7) larger. Alebic'-Juretic' et al. also studied ozone decomposition on small (<180 μm) NaCl crystals in their fluidized bed reactor and observed no effect, indicating γ for O_3 decomposition on NaCl(s) is much smaller than that for α-alumina.

2. $O_3 + C(s)$ - Fendel et al. [38] expand on earlier work reported by Fendel and Ott [39] showing large uptake coefficients for O_3 on small C(s) particles (<10 - 100 nm) formed from C(g) and added to an atmospheric pressure flow containing O_3. A γ of 3.3×10^{-3} was measured for the lowest O_3 concentration (160 ppbv) studied. Smaller values, ranging down to ~2×10^{-4}, were measured for higher O_3 concentrations. Rogaski et al. [142] used initial Knudsen cell uptake measurements to yield $\gamma = 1 (\pm 0.5) \times 10^{-3}$ for amorphous carbon at room temperature. Smith et al. [152] report that the ozone/soot reaction is first order in ozone, with CO, CO_2, and H_2O the only stable gaseous products. Stephens et al. [153] measured CO, CO_2, and O_2 as products, with an O_2 produced for each O_3 reacted; they measured uptake coefficients which varied from 10^{-3} to 10^{-5} depending on carbon sample and O_3 exposure. The O_3/C(s) reaction probability is clearly dependent on the C(s) surface history.

3. $OH + H_2O(s)$ - Cooper and Abbatt [27] measured initial irreversible OH uptake coefficients of ~ 0.1 for water ice between 205 - 230 K; these decayed to $\gamma = 0.03 \pm 0.02$ after repeated exposure to OH. Self

reaction to form H_2O or H_2O_2 was indicated by the lack of observable gas phase products despite observation of first order OH loss.

4. OH + HCl • nH_2O(l) - Cooper and Abbatt [27] demonstrated significant enhancement of OH uptake (to $\gamma > 0.2$) after HCl doping of 220 K ice surfaces sufficient to melt the surface layer. It is unclear whether OH is lost to self-reaction or reaction with hydrated Cl^- ions.

5. OH + HNO_3 • $3H_2O$ - Cooper and Abbatt [27] measured $\gamma > 0.2$ for nitric acid doped ice surfaces under conditions suitable for NAT formation at 200 and 228 K. Increase over pure ice uptake rates is probably due to $HNO_3 + OH \rightarrow H_2O + NO_3$ reaction.

6. OH + H_2SO_4 • nH_2O - Lower limits of 0.2 for uptake coefficients on 45-65 wt % H_2SO_4 between 220 and 230 K and for 96 wt % H_2SO_4 at 230 and 298 K by Cooper and Abbatt [27] are consistent with a lower limit of 0.07 on 28 wt % H_2SO_4 at 275 K in similar experiments by Hanson et al. [60] and a probable surface saturated value of $(4.9 \pm 0.5) \times 10^{-4}$ from Knudsen cell measurements by Baldwin and Golden [9] and an estimate of $\gamma = 1$ on ~96 wt % H_2SO_4 at 298 K by Gerhenzon et al. [50] using a coated insert flow tube technique. Uptake is probably reactive with $OH + HSO_4^- \rightarrow H_2O + SO_4^-$ the hypothesized process.

7. OH + NaCl(s) - Ivanov et al. [84] used a fast flow reactor with a central salt coated rod to measure heterogeneous loss of OH between 245 and 339 K. Their fit for NaCl(s) yielded $\gamma = (1.2 \pm 0.7) \times 10^{-5}$ exp[$(1750 \pm 200)/T$]. Similar data for NH_4NO_3 yielded γ - $(1.4 \pm 0.5) \times 10^{-4}$ exp [(1000 ± 100)]. Since uptake was irreversible, it is assumed that the loss was self-reaction.

8. HO_2 on H_2O(s) and H_2SO_4 • nH_2O(l) - Uptake of HO_2 on ice and super-cooled 55 wt % sulfuric acid at 223 K has been demonstrated to be limited by HO_2 surface saturation by Cooper and Abbatt [27]. They argue that self-reaction, presumably $2HO_2 \rightarrow H_2O_2 + O_2$ is limiting measured uptake coefficients of 0.025 ± 0.005 for ice and 0.055 ± 0.020 for 55 wt % H_2SO_4. However, Gersherzon et al. [52] measured $\gamma > 0.2$ for 80 and 96 wt % H_2SO_4 at 243 K and Hanson et al. [60] measured a lower limit for 28 wt % H_2SO_4 at 275 K of 0.07. However, large gas phase diffusion corrections mean this value is consistent with $\gamma = 1$.

9. $NO_2 + H_2O$(l) - Value for γ of $(6.3 \pm 0.7) \times 10^{-4}$ at 273 K (Tang and Lee, [157]) was achieved by chemical consumption of NO_2 by $SO_3^=$; their stopped-flow measurement was probably still affected by surface saturation, leading to the measurement of a lower limit. Ponche et al. [132] measured an uptake coefficient of $1.5 (\pm 0.6) \times 10^{-3}$ at 298 K, which was also probably subject to saturation limitations. Mertes and Wahner[115] used a liquid jet technique to measure a lower limit of $\gamma \geq 2 \times 10^{-4}$ at 278 K, and they observed partial conversion of the absorbed NO_2 to HONO. Msibi et al. [127] used a cylindrical/annular flow reactor to derive $g = (8.7 \pm 0.6) \times 10^{-5}$ on pH = 7 deionized water surfaces and $(4.2 \pm 0.9) \times 10^{-4}$ on pH = 9.3 wet ascorbate surfaces; it seems likely that these results are also subject to surface saturation given the gas/surface interaction times involved in the experiment. Data are consistent with an $\alpha \geq 1 \times 10^{-3}$ for 278 - 298 K and a liquid phase second-order hydrolysis of NO_2 to HONO and HNO_3 which depends on temperature and pH. However, the interplay between accommodation, possible surface reaction, and bulk reaction may be complex.

10. $NO_2 + H_2SO_4 \cdot nH_2O$ - Saastad et al. [148] measured a lower limit of 5×10^{-5} for an uptake coefficient on 70 wt % H_2SO_4 between 193 and 243 K. Baldwin and Golden [8] measured an uptake coefficient limit of $< 1.0 \times 10^{-6}$ on 96 wt. % H_2SO_4. See Note 15 for H_2O_2 on H_2SO_4 • nH_2O. Both measurements were probably limited by surface saturation.

11. NO_2 + C(S) - Tabor et al. [156] extended their previously published study (Tabor et al. [155]) to three types of amorphous carbon particles exposed to NO_2 in a low pressure Knudsen cell reactor. All three types of C(s) particles were reported to show initial γ values of (5.1 ± 1.7), (8.3 ± 2.7), and $(5.7 \pm 1.3) \times 10^{-2}$, compared with $(4.8 \pm 0.6) \times 10^{-2}$ reported in Tabor et al., all assuming a geometrical surface area for the bulk C(s) powder. NO was observed as a product from all samples, and some samples evolved CO, CO_2,

and a mass spectrometric peak consistent with NO_3 or N_2O_5 upon thermal desorption. The amount of NO evolved varied widely with the type of C(s) particle. Co-deposition of H_2O vapor had no major effect on NO_2 uptake. On the other hand, room temperature Knudsen cell studies of amorphous carbon by Rogaski et al. report an initial γ of 0.11 ±0.04, although γ for longer times agrees reasonably well with Tabor et al.[156]. However, $^{13}NO_2$ uptake studies with suspended small aerosol particles of graphitic or amorphous carbon by Kalberer et al. [90] measured uptake coefficients between (0.3 ±0.19) x 10^{-4} and (4.0 ±1.0) x 10^{-4}. NO was determined to be the principal gaseous product observed in these studies, and first-order absorbed NO_2 reaction rates of (4 to 9) x 10^{-4} s^{-1} were obtained. The large discrepancy between these measured uptake rates may be due to the difficulty of properly specifying the reactive surface area for bulk powders and the time-dependent nature of reactive uptake.

12. NO_2 + NaCl(s), NaBr(s) - Vogt and Finlayson-Pitts [170, 172] used diffuse reflectance infrared spectroscopy to study the reaction of NO_2 with NaCl(s) at 298 K, and Vogt et al.[169] used the same technique to study NO_2 + NaBr(s) at 298 K. Both reactions were shown to be approximately second order in NO_2. Assuming that adsorbed N_2O_4 is the reactant leads to γ = (1.3 ±0.6) x 10^{-4} for NaCl(s) and 2 (+4, -1.3) x 10^{-4} for NaBr(s). Peters and Ewing [131] measured reactive uptake for single-crystal NaCl(100) surfaces and observed both NO_3^-(c) and ClNO products. The value of $\gamma(N_2O_4)$ measured by Peters and Ewing at 298 K was only (1.3 ±0.3) x 10^{-6}. They noted that small amounts of water vapor (9.5 mbar) cause γ to increase by two orders of magnitude.

13. NO_3 + H_2O(l) - Rudich et al. [145, 146] used wetted-wall flow tube techniques to measure uptake coefficients for NO_3 on pure water and aqueous NaCl, NaBr, NaI, and $NaNO_2$ solutions. These studies were extended to other aqueous solutions by Imamura et al.[82]. Uptake on pure water was consistent with reaction of NO_3 to produce HNO_3 and OH. Uptake coefficients with solutions containing I^-, Cl^-, Br^-, NO_2^- and other anions were larger and scaled with anion concentration, indicating electon transfer reactions to produce NO_3^-. The γ of (2.0 ±1.0 x 10^{-4}) at 273 K determined for pure water by Rudich et al. is significantly lower than the lower limit of 2.5 x 10^{-3} quoted by Mihelcic et al. [119]. A detailed analysis of uptake coefficients for KI aqueous solutions indicated that the NO_3 mass accommodation coefficient is >0.04[146].

14. N_2O_5 + H_2O(s) - Leu [103] and Hanson and Ravishankara [63] have measured nearly identical values of 0.28 (±0.11) and 0.24 (±30%) near 200 K. Hanson and Ravishankara [68] presented new and re-analyzed data as a function of ice thickness, with a value of ~0.008 for the thinnest ice sample, rising to ~0.022 for the thickest. Quinlan et al. [134] have measured a lower limit for γ on fresh ice surfaces of 0.03 at 188 K.

15. N_2O_5 + H_2O(l) - Reaction on liquid water has a negative temperature dependence. Van Doren et al. [166] measured γ's of 0.057 ±0.003 at 271 K and 0.036 ±0.004 at 282 K. Mozurkewich and Calvert [124] studied γ on $NH_3/H_2SO_4/H_2O$ aerosols. For their most water-rich aerosols (RH = 76%) they measured γs of 0.10 ±0.02 at 274 and 0.039 ±0.012 at 293 K. George et al. [48] use droplet train/ion chromotography techniques to measure γs of (3.0 ±0.2) x 10^{-2} (262 K), (2.9 ±1.2) x 10^{-2} (267 K), 2.0 ±0.2) x 10^{-2} (273 K), (1.6 ±0.8) x 10^{-2} (276 K), and (1.3 ±0.8) x 10^{-2} (277 K). Msibi et al.[126]] measured a smaller γ of 2.5 x 10^{-3} for water adsorbed on a denuder flow tube well under 66-96% relative humidity conditions at room temperature.

16. N_2O_5 + $HNO_3 \cdot 3H_2O$(s) - Hanson and Ravishankara [63] have measured γ = 0.0006 (±30%) at 200 K. They presented re-analyzed and additional data as a function of ice thickness (Hanson and Ravishankara [68]), deriving a value of 3 x 10^{-4} for the thinnest NAT covered ice layer, with values up to three times higher for thicker NAT-covered ice layers. This is in very poor agreement with γ = 0.015 (±0.006) reported by Quinlan et al. [134]. This latter measurement may have been biased by a super-cooled nitric acid surface rather than NAT.

17. N_2O_5 + $H_2SO_4 \cdot nH_2O$(l) - This reaction has been intensively studied between 195 and 296 K for a wide range of H_2SO_4 wt % values using four complementary experimental techniques. Data are available from aerosol flow tube studies (Fried et al. [45], Hanson and Lovejoy [61], and Lovejoy and Hanson [108]), coated wall flow tube studies (Hanson and Ravishankara [66], Zhang et al. [186]), stirred Knudsen cell

studies (Williams et al. [178], Manion et al. [111]) and droplet train studies (Van Doren et al. [166], Robinson et al. [141]). All studies have yielded γs between ~0.05 and 0.20 with modest dependence on surface H_2SO_4 wt % and temperature. Aerosol flow tube studies at higher N_2O_5 exposure and the ternary $H_2SO_4/HNO_3/H_2O$ studies of Zhang et al. both illustrate that significant levels of HNO_3 in the H_2SO_4/H_2O solutions will reduce γ measurably; this fact explains some of the scatter in aerosol flow tube studies [45, 61, 108]. The effect of 5.0×10^{-7} torr HNO_3 for $\gamma(N_2O_5)$ as a function of temperature at two water vapor concentrations are plotted in Zhang et al.; the decrease in γ is greatest at low temperatures, approaching a factor of 2-5 between 200 and 195 K.

Robinson et al. have binned the data believed to be free of suspected HNO_3 dilution and surface saturation effects from the studies cited above into groups with similar H_2SO_4 concentration, and they have fit a temperature-dependent uptake model, taking into account temperature and composition dependence of the effective Henry's Law constant, liquid phase diffusion coefficient, and the liquid phase hydrolysis rate constant. The hydrolysis reaction was treated by modeling two reaction channels, a direct hydrolysis process dominating reaction at low H_2SO_4 concentrations with a reaction rate proportional to water activity, and a proton-catalyzed reaction with a rate proportional to H^+ activity, which dominates at higher acid concentrations. A parameterized fit for 30 to 80 wt % H_2SO_4 to the uptake model gives

$$\gamma = k_0 + k_1/T + k_2/T, \text{ where } k_i = \Sigma\, a_{ij}\, (\text{wt\% } H_2SO_4)^j,\ j = 0 \text{ to } 3$$

i = 0, j:	-11.548	0.65252	-0.013183	0.000081293
i = 1, j:	5521.6	-316.68	6.4268	-0.039527
i = 2, j:	-587410	34601	-712.3	4.3833

18. $N_2O_5 + H_2SO_4 \cdot H_2O(s)$ - Zhang et al. [185] used coated flow tube techniques to measure the uptake of N_2O_5 on solid sulfuric acid monohydrate over a temperature range of 200 to 225 K. The measurement values of γ were significantly higher at 200 K ($\gamma \sim 1 \times 10^{-3}$) than at 225 K ($\gamma \sim 10^{-4}$) and were well fit by $\log \gamma = [4.78 - 0.0386\, T(K)]$. Acid rich $H_2SO_4 \cdot H_2O$ surfaces had a lower γ than water rich surfaces ($\log \gamma = 0.162 - 0.789 \times \log \rho_{H2O}$] where ρ_{H2O} is their experimental water vapor partial pressure.

19. N_2O_5 on $H_2SO_4 \cdot 4H_2O(s)$ - Hanson and Ravishankara [71] studied N_2O_5 uptake by frozen 57.5 and 60 wt % H_2SO_4 as a function of temperature and relative humidity. The 57.5 wt % surface was not sensitive to relative humidity and was slightly more reactive ($\gamma = 0.008$ vs 0.005) at 205 K than at 195 K. Reaction probabilities on the 60 wt % surface dropped off with temperature and relative humidity.

20. N_2O_5 + HCl on $H_2O(s)$ - Leu [103] measured $\gamma = 0.028$ (± 0.011) at 195 K, while Tolbert et al. [162] measured a lower limit of 1×10^{-3} at 185 K. These experiments were done at high HCl levels probably leading to a liquid water/acid surface solution (Abbatt et al. [4]). The reaction probability may be much smaller on HCl/H_2O ice surfaces characteristic of the stratosphere.

21. N_2O_5 + HCl on $HNO_3 \cdot 3H_2O(s)$ - Hanson and Ravishankara [63] measured $\gamma = 0.0032$ ($\pm 30\%$) near 200 K.

22. N_2O_5 + HCl on $H_2SO_4 \cdot H_2O(s)$ - Zhang et al. [185] saw no increase in N_2O_5 uptake on sulfuric acid monohydrate at 195 K upon exposure to HCl, setting $\gamma < 10^{-4}$.

23. N_2O_5 + NaCl (s,aq) - Using FTIR analysis, Livingston and Finlayson-Pitts [107] have demonstrated that N_2O_5 reacts with crystalline NaCl to form $NaNO_3(s)$, and they report $\gamma > 2.5 \times 10^{-3}$ at 298 K. However, Leu et al.[102] used flow tube/mass spectrometric techniques to obtain $\gamma < 1 \times 10^{-4}$ for dry salt at 223 and 296 K; they also noted that exposing salt surfaces to small amounts of H_2O vapor increased γ significantly. Fenter et al.[41] measured $\gamma = (5.0 \pm 0.2) \times 10^{-4}$ on fused salt surfaces at room temperature, assuming the geometrical surface area is the only surface accessed. Msibi et al. [126] measured NO_3^- deposition on an annular flow reactor to determine $\gamma = 1 \times 10^{-3}$ for salt surfaces between 45 and 96% relative humidity at room temperature, rising to $\gamma = 1.5 \times 10^{-2}$ at 96/97% relative humidity, but they argue

that most of the uptake is due to reaction with H_2O. On aqeous NaCl solutions, Zetzsch, Behnke, and co-workers [11, 12, 182] have studied the reaction of N_2O_5 with aqueous NaCl aerosols in an aerosol chamber. The relative yields of $ClNO_2$ and HNO_3 rise with the NaCl concentration. A reaction probability of ~0.03 is measured with a 50% $ClNO_2$ yield at the deliquescence point (Zetsch and Behnke). This picture is confirmed by droplet uptake studies on 1 M NaCl solutions reported by George et al. [48] which confirm that uptake on salt solutions in the 263 - 278 K temperature range is larger than that on pure water droplets.

24. N_2O_5 + HBr on $HNO_3 \cdot 3H_2O$(s) - This reaction, yielding $\gamma \sim 0.005$, was investigated on NAT surfaces near 200 K by Hanson and Ravishankara [67]. Under some conditions a much higher reaction coefficient of ~0.04 was observed.

25. N_2O_5 + MBr - Finlayson-Pitts et al. [43] used FTIR techniques to demonstrate that $BrNO_2$(ads) is a major product of the N_2O_5(g) + NaBr(s) reaction. However, Fenter et al. [41] failed to measure gas phase evolution of $BrNO_2$ using Knudsen cell/mass spectrometry techniques, detecting Br_2(g) instead. They propose that $BrNO_2$ reacts with KBr(s) to yield KNO_2(s) + Br_2(g). A γ of $(4.0 \pm 2.0) \times 10^{-3}$ at room temperature was determined for fused KBr surfaces with well-defined surface areas.

26. HONO + H_2O(l) - Bongartz et al. [15] present uptake measurements by two independent techniques, the liquid jet technique of Schurath and co-workers and the droplet train/flow tube technique of Mirabel and co-workers (Ponche et al. [132]). With a surface temperature of ~245 K the droplet train techniques yielded $0.045 < \gamma < 0.09$, while the liquid jet operating with a surface temperature of 297 K obtained $0.03 < \gamma < 0.15$. Mertes and Wahner used a liquid jet technique to measure $4 \times 10^{-3} < \gamma < 4 \times 10^{-2}$ at 278 K. Since HONO uptake by liquid water probably involved hydrolysis, an increase in Henry's law solubility with decreasing temperature may be offset by a decreasing hydrolysis rate constant, leaving the uptake coefficient's temperature trend uncertain. Measured uptake coefficients will not correspond to the mass accommodation coefficient.

27. HONO + $H_2SO_4 \cdot nH_2O$(l) - Zhang et al.[187] measured uptake coefficients for HONO on sulfuric acid that increased from $(1.6 \pm 0.1) \times 10^{-2}$ for 65.3 wt % H_2SO_4 (214 K) to $(9.1 \pm 1.6) \times 10^{-2}$ for 73 wt % H_2SO_4 (226 K). Fenter and Rossi[42] measured uptake coefficients rising from 1.8×10^{-4} for 55 wt % H_2SO_4 (220 K) to 3.1×10^{-1} for 95 wt % H_2SO_4 (220 K and 273 K). In general, the values measured by Zhang et al. are a factor of 2 to 5 higher than those of Fenter et al. for comparable acid concentrations. Since the reaction probably depends on both temperature and acid concentration and since the data scatter is high in both experiments, further independent data will be required to define γ as a function of acid concentration and temperature. These data are generally consistent with the effective Henry's law constant measurements of Becker et al. [10] who illustrate that HONO solubility decreases exponentially with H_2SO_4 concentration until ~53 wt %, at which point reaction to form nitrosyl sulfuric acid increases H* dramatically as H_2SO_4 concentration increases.

28. HONO + HCl + H_2O(s) - Knudsen cell uptake studies for HONO/HCl co-deposited on ice (180-200 K) and for HONO on 0.1 to 10 m HCl frozen solutions (~190 K) by Fenter and Rossi showed HONO uptake coefficients in the 0.02 to 0.12 range as long as surface HCl concentrations significantly exceed HONO concentrations. ClNO was evolved quantitatively with HONO consumption.

29. HONO + NaCl(s) - Diffuse reflectance experiments by Vogt and Finlayson-Pitt [171] on room temperature NaCl(s) and Knudsen cell uptake experiments by Fenter and Rossi on room temperature NaCl(s) and frozen 0.1 M NaCl aqueous solutions, all failed to show HONO uptake. The latter results yield $\gamma < 1 \times 10^{-4}$.

30. HNO_3 + C(s) - Knudsen cell/mass spectrometry measurements by Rogaski et al. yielded $\gamma = 3.8 (\pm 0.8) \times 10^{-2}$ on one type of amorphous carbon over a temperature range of 190-440 K. Gas phase NO and NO_2 equivalent to ~2/3 of the HNO_3 uptake were observed as reaction products.

31. HNO_3 + NaX(s)/KX(s) - Vogt and Finlayson - Pitts [170, 172] used diffuse infrared reflectance spectroscopy to characterize the process. There was absorption of HNO_3, but no reaction was observed on completely dry NaCl(s); however, $NaNO_3$ forms in the presence of very low (well below the deliquescence

point) levels of H_2O(g). Using XPS spectroscopy to identify surface products and a dry HNO_3 source, Laux et al. [101] (also see Vogt et al.) measured $\gamma = (4 \pm 2) \times 10^{-4}$ at 298K. Fenter et al. [40] measured the room temperature uptake of HNO_3 on solid powders of NaCl, NaBr, KCl, KBr, and $NaNO_3$, using Knudsen cell/mass spectrometry techniques. They saw similar uptake for all surfaces, including unreactive $NaNO_3$, and recommend $\gamma = (2.8 \pm 0.3) \times 10^{-2}$ for all salts. HCl or HBr was produced with ~100% yield from the halide surfaces. There is some concern about the effective surface area of the powders used by Fenter et al. (see Leu et al.[102]). Fenter et al. report new HNO_3 data to support their argument that "sticky" gases such as HNO_3 cannot penetrate below the top surface layer of the powders used in their experiments. Leu et al. used flow tube/mass spectrometry techniques to measure $\gamma = (1.3 \pm 0.4) \times 10^{-2}$ at 296 K and $\gamma > 8 \times 10^{-3}$ at 223 K, both in the presence of low levels of H_2O(g). They determined that uptake at 296 K was reactive, producing HCl but that at 223 K reaction was suppressed and uptake was largely absorptive. Beichert and Finlayson-Pitts [13] measured $\gamma = (1.4 \pm 0.6) \times 10^{-2}$ at 298 K with a Knudsen cell technique, and, using D_2O, demonstrated that chemisorbed water, presumably retained on defect sites, was crucial for $NaNO_3$ formation. This suggests that low levels of defect-retained water are responsible for the small uptake values measured by Laux et al.

32. $NH_3 + H_2SO_4 \bullet nH_2O$ - Robbins and Cadle [137], Huntzicker et al. [80], McMurry et al. [114], and Daumer et al. [30] all studied NH_3 uptake by sulfuric acid aerosols in near room temperature flow reactors (T = 281 - 300 K). Uptake coefficients varied between 0.1 and 0.5. Rubel and Gentry [144] used levitated H_3PO_4 acid droplets to show that heterogeneous reaction does control the initial NH_3 uptake on strong acid solutions. Both Rubel and Gentry and Däumer et al. also explored the effect of organic surface coatings.

33 $CH_3C(O)O_2 + H_2O$(l) and $H_2SO_4 \bullet nH_2O$ - Villalta et al. [168] used wetted-wall flow tube techniques to measure $\gamma = 4.3\ (+2.4/-1.5) \times 10^{-3}$ for water at 274 ± 3K. They also measured uptake for 34 wt % H_2SO_4 at 246 K ($\gamma = (2.7 \pm 1.5) \times 10^{-3}$), 51 wt % at 273 K ($\gamma = (0.9 \pm 0.5) \times 10^{-3}$), and 71 wt % at 298 K ($\gamma = (1.4 \pm 0.7) \times 10^{-3}$). They suggest that products subsequent to hydrolysis are HO_2 and $CH_3C(O)OH$.

34. $Cl + H_2SO_4 \bullet nH_2O$ - Measured reaction probability (Martin et al. [113]) varies between 3×10^{-5} and 7×10^{-4} as H_2O and T co-vary. Reaction product is claimed to be HCl.

35. Cl_2+HBr + H_2O(s) - Hanson and Ravishankara [67] measured a reaction probability of >0.2 on water ice near 200 K. BrCl was not detected, presumably due to rapid reaction with excess HBr.

36. Cl_2 and BrCl + KBr(s) - Caloz et al. measured $\gamma > 0.1$ for reactive uptake of Cl_2 and BrCl on KBr(s) in a room temperature Knudsen cell experiment.

37. Cl_2 and Br_2 + NaBr(aq) and NaI(aq) - Hu et al.,[78] measured large uptake coefficients for Cl_2 on dilute aqueous droplets of NaBr and NaI solutions and Br_2 on NaI solutions using a droplet train technique. Reaction was demonstrated to proceed through both a chemisorbed surface complex and normal bulk solution second-order kinetics. Second-order bulk reaction rate constants near the diffusion limit and consistent with bulk-phase kinetic measurements were obtained between 263 and 293 K.

38. ClO + H_2O(s) and $HNO_3 \bullet nH_2O$ - Proposed reaction (Leu [103]) is $2\ ClO \rightarrow Cl_2 + O_2$; reactive uptake may depend on ClO surface coverage, which in turn may depend on gas phase ClO concentrations. Kenner et al. [93] measured reaction probabilities of $(8 \pm 2) \times 10^{-5}$ for ice at 183 K which is far lower than the limit of $>1 \times 10^{-3}$ obtained by Leu et al. [103]. Abbatt [3], using nearly the same low levels of ClO as Kenner et al., obtained $\gamma < 1 \times 10^{-5}$ at 213 K. The difference may lie in the level of ClO or other adsorbable reactive species present. The lower value of Abbatt is probably closer to the expected reactivity under stratospheric conditions. Kenner et al. also measured a reaction probability limit of $< (8 \pm 4) \times 10^{-5}$ for NAT at 183 K.

39. ClO + $H_2SO_4 \bullet nH_2O$ - Measured reaction probability (Martin et al. [113]) varies between 2×10^{-5} and 2×10^{-4} as H_2O content is varied by changing wall temperature. Reaction product is claimed to be HCl, not Cl_2. Abbatt[3] measured $\gamma < 1 \times 10^{-5}$ for 60 and 70 wt % H_2SO_4 at 213 K.

40. $HOCl + HCl + H_2O(s)$ and $HNO_3 \cdot 3H_2O(s)$ - Hanson and Ravishankara [66] and Abbatt and Molina [5] have investigated the HOCl + HCl reaction on water ice and NAT-like surfaces, and Chu et al. [24] studied water ice. Product yield measurements support the identification of Cl_2 and H_2O as the sole products. The high reaction probabilities measured indicate that this reaction may play a significant role in release of reactive chlorine from the HCl reservoir. The reaction probability on NAT-like surfaces falls off dramatically (a factor of 10) on water-poor (HNO_3-rich) surfaces (Abbatt and Molina). The measured yield of product Cl_2 is 0.87 ±0.20 (Abbatt and Molina [5]).

41. $HOCl + HCl + H_2SO_4 \cdot nH_2O$ - This process has been studied in coated flow tubes near 200 K by Zhang et al. [184] and Hanson and Ravishankara [70]. Both studies measured large γs for [HCl] > [HOCl]. Hanson and Ravishankara [70] deduced a second-order reaction rate constant of ~1 x 10^5 M^{-1} s^{-1} in 59.6 wt % H_2SO_4 at 201-205 K. A model of this and related sulfuric acid aerosol reactions tailored to stratospheric conditions has been published by Hanson et al. [74]. Zhang et al. held the water vapor partial pressure at 3.8 x 10^{-4} torr and showed γ increased by a factor of 50 as the temperature was lowered from 209 to 198 K, showing that the reaction rate is strongly dependent on water activity.

42. ClNO and $ClNO_2$ + NaCl(s) - Using a Knudsen cell technique Beichart and Finlayson-Pitts set upper limits of $\gamma < \sim 10^{-5}$ for reaction uptake of ClNO and $ClNO_2$ on NaCl(s) powders at 298 K.

43. $ClONO_2 + H_2O(s)$ - Measurement of $\gamma = 0.3$ (+0.7, -0.1) (Hanson and Ravishankara [65]) significantly exceeds previous measurements of Molina et al. [121], Tolbert et al. [163], Leu [104] and Moore et al. [123] and subsequent measurements by Chu et al. [24] and Zhang et al. [183]. Previous measurements were probably impeded by NAT formation on surface (Hanson and Ravishankara, [66], Chu et al.). Lower levels of $ClONO_2$(g) used by Hanson and Ravishankara [63] minimized this surface saturation problem. Also, using lower $ClONO_2$ concentrations, Zhang et al. obtained a reaction probability of 0.08 ± 0.02 at 195 K, in fair agreement with the range of 0.03 to 0.13 measured by Chu et al. More recent Knudsen cell measurements at 180 and 200 K by Oppliger et al.,[130] showed initial uptake gs in the 0.2 to 0.4 range. Reaction products are HNO_3 and HOCl. All of the HNO_3 and much of the HOCl is retained on the surface under polar stratospheric conditions (Hanson and Ravishankara). Hanson [59] deposited $ClONO_2$ on $H_2{}^{18}O$ enriched ice and detected $H^{18}OCl$ showing the Cl-ONO_2 bond is broken during reaction on ice at 191 K.

44. $ClONO_2 + HNO_3 \cdot nH_2O$ - Hanson and Ravishankara [63, 65] report a value of 0.006 for $ClONO_2$ reaction with the water on NAT ($HNO_3 \cdot 3H_2O$). However, these authors present re-analyzed and new data with $\gamma \approx 0.001$ in Hanson and Ravishankara [68]. Similar experiments (Moore et al. [123], Leu et al. [105]) report a larger value 0.02 ±0.01 which falls very rapidly as slight excesses of H_2O above the 3/1 H_2O/HNO_3 ratio for NAT are removed. They measure γ of less than 10^{-6} for slightly water poor "NAT" surfaces. The inconsistency between Hanson and Ravishankara [63, 65] and the JPL group (Moore et al. [123]; Leu et al., [105]) has not been resolved. Hanson and Ravishankara [66] report that γ for this reaction increases by a factor of 4 as the surface temperature increases from 191 to 211 K.

45. $ClONO_2 + H_2SO_4 \cdot nH_2O(l)$ - Results from wetted-wall flow tube (Hanson and Ravishankara, [72]) Knudsen cell reactor (Manion et al. [111], Williams et al., [178], aerosol flow tube (Hanson and Lovejoy [141]), and droplet train uptake experiments (Robinson et al., 96/63) supplement older wetted-wall flow tube (Hanson and Ravishankara [66]) and Knudsen cell measurements (Rossi et al. [143], Tolbert et al. [161]). Although earlier Knudsen cell measurements probably suffered from surface saturation, more recent results compare well with those from other techniques. Results are now available over a temperature range of 200-265 K and a H_2SO_4 concentration range of 39 to 75 wt.%. Measured γ values depend strongly on H_2SO_4 concentration and vary modestly with temperature, with a trend to somewhat higher values for the 210 - 220 temperature range, reflecting the temperature dependence of $Hk_{hyd}{}^{1/2}$ and the liquid phase diffusion coefficient for $ClONO_2$ and the rates of the direct- and proton-catalyzed hydrolysis reactions, which are proportional to the activity of H_2O and the activity of H^+, respectively. (Robinson et al., [141]).

Robinson et al. have binned the data believed to be free of suspected HNO_3 dilution and surface saturation effects from the studies cited above into groups with similar H_2SO_4 concentration and they have fit a temperature-dependent uptake model, taking into account temperature and composition dependence of the effective Henry's Law constant, liquid phase diffusion coefficient, and the liquid phase hydrolysis rate constant. The hydrolysis reaction was treated by modeling two reaction channels, a direct hydrolysis process dominating reaction at low H_2SO_4 concentrations with a reaction rate proportional to water activity, and a proton-catalyzed reaction with a rate proportional to H^+ activity, which dominates at higher acid concentrations. A parameterized fit to the uptake for 30-80 wt % H_2SO_4 model gives:

$$\gamma = k_0 + k_1/T + k_2/T, \text{ where } k_i = \Sigma\, a_{ij}\, (\text{wt\% } H_2SO_4)^j,\ j = 0 \text{ to } 3$$

i = 0, j:	-10.855	-0.12764	0.0087648	-0.00010047
i = 1, j:	4349.6	44.544	-3.8043	0.043465
i = 2, j:	-454140	-3061.2	376.53	-4.7098

46. $ClONO_2 + H_2SO_4 \cdot H_2O(s)$ and $H_2SO_4 \cdot 4H_2O(s)$ - Measurements by Hanson and Ravishankara [71] and Zhang et al. [183] demonstrate that the reaction probability on the tetrahydrate is a strong function of both temperature and relative humidity, both of which affect the level of adsorbed H_2O. Both groups covered the temperature range of 192-205 K. The reaction is slowest at higher temperatures and lower relative humidities. Zhang et al. [183] have parameterized their data in the form of $\log \gamma = a_1 + a_2 \log x + a_3 \log^2 x$; for 195 K and x = water partial pressure in torr: $a_1 = 10.12$, $a_2 = 5.75$ and $a_3 = 0.62$; for a water partial pressure of 3.4×10^{-4} torr and x = T(K) between 182 and 206: $a_1 = 318.67$, $a_2 = -3.13$ and $a_3 = 0.0076$. Zhang et al.[186] have also measured a low value of $\gamma \sim 2 \times 10^{-4}$ on sulfuric acid monohydrate at 195 K.

47. $ClONO_2 + HCl + H_2O(s)$ - Reaction probabilities of 0.27 (+0.73, -0.13) (Leu [104]) and 0.05 to 0.1 (Molina et al. [121]) have been reported near 200 K. Abbatt et al. [4], Abbatt and Molina [5], and Hanson and Ravishankara [65] report that a portion of the reaction may be due to $HOCl + HCl \rightarrow Cl_2 + H_2O$, with HOCl formed from $ClONO_2 + H_2O(s) \rightarrow HOCl + HNO_3(s)$. Hanson and Ravishankara [63] see no enhancement of the $ClONO_2$ reaction probability when $H_2O(s)$ is doped with HCl. Their preferred value is $\gamma = 0.3$, but this is consistent with $\gamma = 1$. Using a Knudsen cell technique and looking at initial uptake, Oppliger et al. [130] measured $\gamma = 0.7$ at 180 K and 0.2 at 200 K with HCl in excess.

48. $ClONO_2 + HCl + HNO_3 \cdot 3H_2O$ - Measurements by Hanson and Ravishankara [63, 66], Leu and co-workers (Moore et al. [123], Leu et al. [105]), and Abbatt and Molina [6] confirm a high γ. Work by Hanson and Ravishankara indicates that reaction probabilities on nitric acid dihydrate (NAD) are similar to those on NAT. The most recent NAT studies (Abbatt and Molina [6]) show a strong fall-off with relative humidity from $\gamma > 0.2$ at 90% RH to 0.002 at 20% RH, indicating the necessity of sufficient water to solvate reactants.

49. $ClONO_2 + HCl + H_2SO_4 \cdot nH_2O$ - Hanson and Ravishankara [65] estimated that low temperature solubility limits for HCl in $H_2SO_4 \cdot nH_2O$ (> 60 wt.% H_2SO_4) would restrict the $ClONO_2 + HCl$ reaction by demonstrating that HCl vapor has a minimal effect on $ClONO_2$ uptake on 60-75 wt.% H_2SO_4 surfaces. Tolbert et al. [161] also noted no measurable enhancement of $ClONO_2$ loss on a 65 wt.% H_2SO_4 surface at 210 K when the surface is exposed to HCl, but the reaction products do change to include Cl_2. However, subsequent work (Hanson and Ravishankara [72]) has led to a re-evaluation of the process as a second-order liquid phase reaction between Cl^- and $ClONO_2$, which they estimate to proceed at a diffusion limited rate of $1\text{-}3 \times 10^7\ M^{-1}\ s^{-1}$ near 200 K. Re-analysis of H^* for HCl in cold concentrated H_2SO_4 (see next table) may make this process important even for 60-70 wt% H_2SO_4. Additional measurements by Zhang et al.[184] and Elrod et al. [37] show substantial agreement with Hanson and Ravishankara [72] and illustrate the strong dependence of γ on HCl solubility, which, in turn, depends on water activity. Both Zhang et al. and Elrod et al. examined the effect of HNO_3 on the reaction and found no significant change. Hanson and Lovejoy used an aerosol flow tube method to measure a reacto-diffusive length, l, of 0.009 ± 0.005 for 60 wt % H_2SO_4 at 250 K. This is a factor of 4 smaller than l for $ClONO_2$ hydrolysis on the same aerosol, showing a significantly enhanced reaction rate for these conditions. Sulfuric acid surfaces with less than ~60 wt.% H_2SO_4 also have sufficient water to absorb significant levels of HCl. Wolff and

Mulvaney [179], Hofmann and Oltmans [77], and Toon et al. [164] have suggested that such water-rich H_2SO_4 aerosols may form under polar stratospheric conditions.

50. $ClONO_2$+HCl + H_2SO_4 • H_2O(s) and H_2SO_4 • $4H_2O$(s) - This reaction has been studied by Hanson and Ravishankara [71] and Zhang et al. [183]. The reaction probability is strongly dependent on the thermodynamic state of the SAT surface, which is controlled by the temperature and the water vapor partial pressure. At a water vapor pressure of 5.6 x 10^{-4} torr the measured γ drops by over two orders of magnitude as the SAT surface temperature rises from 195 to 206 K. The results from the two groups are in qualitative agreement, but sample different H_2O and HCl partial pressures. Zhang et al. have parameterized their data as a function of water partial pressure (at 195 K) and for temperature (both at an HCl partial pressure of 4 to 8 x 10^{-7} torr) in the form $\log \gamma = a_1 + a_2 \log x + a_3 (\log x)^2$. For H_2O partial pressure, $a_1 = 5.25$, $a_2 = 1.91$, and $a_3 = 0.0$; for T(K), $a_1 = 175.74$, $a_2 = -1.59$, and $a_3 = 0.0035$. Care must be taken in extrapolating either data set to lower HCl concentrations. Zhang et al. [186] measured no enhancement of $ClONO_2$ uptake on sulfuric acid monohydrate at 195 K with (2 - 8) x 10^{-7} torr of HCl present, implying $\gamma < 1 \times 10^{-4}$.

51. $ClONO_2$ + HCl + Al_2O_3(s) - Molina et al. [120] used flow tube techniques to measure $\gamma = 0.020 \pm 0.005$ on α–alumina at 195 - 230 K with stratospheric (5 ppmV) water vapor levels. Measured γ was independent of T and was affected very little by 5 ppbv HNO_3 vapor. The same γ was measured for a Pyrex surface, indicating the absorbed water and not the inorganic substrate hosted the reaction.

52. $ClONO_2$ + MX(s) - Finlayson-Pitts and co-workers have shown that $ClONO_2$ reacts with crystalline NaCl (Finlayson-Pitts et al. [43]) and NaBr (Berko et al. [14]) to produce Cl_2 and BrCl, respectively. Timonen et al. [159] have measured the reaction rate for $ClONO_2$ with dry and slightly wet (water vapor pressure 5 x 10^{-5} - 3 x 10^{-4} torr) NaCl at temperatures of 225 and 296 K. Reaction probabilities were analyzed as $\gamma = 4$ - 7 x 10^{-3} and were independent of temperature and water vapor pressure within experimental error. The Cl_2 yield on dry NaCl was 1.0 ±0.2. Caloz et al. [20] used a room temperature Knudsen cell technique to measure $\gamma = 0.23 \pm 0.06$ for NaCl(s) and $\gamma = 0.35 \pm 0.06$ for KBr(s). They argue that the surface corrections imposed by Timonen et al. were too large. Caloz et al. measured quantitative yields of Cl_2 and BrCl products.

53. $ClONO_2$+HBr + H_2O(s) and HNO_3 • nH_2O(s) - This reaction was studied by Hanson and Ravishankara [67] on water ice and NAT near 200 K. A diffusion-limited reaction probability of >0.3 was observed.

54. $ClONO_2$+HF + H_2O(s) and HNO_3 • nH2O(s) - Hanson and Ravishankara [67] were not able to observe this reaction on water ice and NAT surfaces near 200 K.

55. $CF_xCl_{(4-x)}$ (x=0-3) and CF_2Br_2 + Al_2O_3(s) - Robinson et al. [139] reported dissociative uptake of CF_2Cl_2 and CF_2Br_2 on α-alumina surfaces at 210 and 315 K. Reaction probabilities of about 1 x 10^{-3} at 210 K were measured by monitoring the amounts of surface species bonded to the Al_2O_3 substrate. A re-analysis (Robinson et al. [140]) lowered this value by about a factor of 50. Moderate surface dosage with water vapor did not quench the reaction. In addition, Dai et al. [29] and Robinson et al. [138] studied dissociative chemisorption of CF_3Cl, CF_2Cl_2, $CFCl_3$, and CCl_4 on dehydroxylated γ-alumina powders. The obtained reactive uptake probabilities ranging from 0.4 x 10^{-5} for $CFCl_3$ to 1.0 x 10^{-5} for $CFCl_3$ over a temperature range of 120 to 300 K. HCl and halomethyl radicals were observed as desorption products. Loss of these products may point to somewhat higher γs, since they were measured by integrating halogen bound to Al_2O_3 substrates.

56. BrO + H_2O(s) + H_2O(s) and H_2SO_4 • nH_2O(l) and NaCl(aq) - Abbatt [3] used a coated flow tube technique to measure heterogeneous uptake on water ice, 60 and 70 wt % H_2SO_4 at 213 K, and 23 wt % aqueous NaCl at 253 K. He obtained γ(ice) = (1.0 ±0.4) x 10^{-3}, γ (60 wt % H_2SO_4) = (7 ±2) x 10^{-4}, γ (70 wt % H_2SO_4) = (5 ±2) x 10^{-4} and γ (23 wt % NaCl) < 3 x 10^{-3}. He observed product Br_2, indicating BrO self-reaction on both water ice and sulfuric acid solutions. Since reaction rate will depend on BrO concentrations, no recommendation is made for an atmospheric rate.

57. $HOBr + HCl + H_2O(s)$ and $H_2SO_4 \cdot nH_2O$ - Abbatt [1] measured $\gamma = 0.25$ (+0.10/-0.05) for this reaction on ice at 228 K. The BrCl product was observed by mass spectrometry. Abbatt[2] measured γs of ~ 0.1 to 0.2 for [HCl] > 1 x 10^{12} cm^{-3} over 68.8 wt % H_2SO_4 at 228 K; yielding an estimated k_{II} = 1.4 x 10^5 M^{-1} s^{-1} with a factor of 2 uncertainty. Hanson and Ravishankara[73] also measured $\gamma = 0.2$ [+0.2, - 0.1] for 60 wt % H_2SO_4 at 210 K.

58. $HOBr + HBr + H_2O(s)$ and $H_2SO_4 \cdot nH_2O$ - Abbatt [1] measured $\gamma = 0.12 \pm (0.03)$ on ice at 228 K. The Br_2 product was observed by mass spectrometry. Abbatt [2] measured $\gamma = 0.25$ for [HBr] = 1 x 10^{12} cm^{-3} over 68.8 wt % H_2SO_4 at 228 K; yielding to an estimated $k_{II} > 5 \times 10^4$ M^{-1} s^{-1}.

59. $BrONO_2$ and $BrONO_2 + HCl + H_2O(s)$ - Hanson and Ravishankara [68] investigated these reactions in an ice-coated flow reactor at 200 (±10) K. The reaction of $BrONO_2$ with $H_2O(s)$ proceeded at a rate indistinguishable from the gas phase diffusion limit, implying that the reaction probability may be as high as one; the product BrNO(g) was observed. Depositing HCl and $BrONO_2$ on ice led to rapid production of BrCl. This may have been produced directly through reaction of $BrONO_2$ with adsorbed HCl or, indirectly, through production of HOBr in the $BrONO_2$/ice reaction, followed by reaction of HOBr + HCl. No kinetic parameters for BrCl production were given.

60. $BrONO_2$ and $BrONO_2 + HCl + H_2SO_4 \cdot nH_2O$ - Hanson and co-workers ([62, 73]) used both coated flow tube and aerosol flow tube techniques to show that the reaction of $BrONO_2$ with 45-70 wt % H_2SO_4 is extremely facile at temperatures from 210 to 298 K. Hanson and Ravishankara [73] measured γs of 0.5 (+ 0.5, - 0.25) (45 wt % H_2SO_4, 210 K, 0.4 (+0.6, -0.2) (60 wt %, 210 K) , and 0.3 (+ 0.7, -0.1 (70 wt %, 220 K) in a coated-wall flow tube experiment. Hanson et al. [62] measured γ ~ 0.8 (20 to 40% error) for submicron aerosols at temperatures between 249 and 298 K and H_2SO_4 concentrations of 45 to 70 wt %; they did observe a sharp fall off in γ for H_2SO_4 concentrations between 73 and 83 wt %. Addition of excess HCl to 229 K 40 and 60 wt % H_2SO_4 aerosols caused an increase in γ to 1.0 and 0.9, respectively.

61. $CF_3OH + H_2O + H_2O(l)$ and $H_2SO_4 \cdot nH_2O(l)$ - Lovejoy et al. [109] used both wetted-wall and aerosol flow tube techniques to measure reactive uptake of CF_3OH on water at 274 K and 39 - 60 wt % H_2SO_4 at various temperatures between 206 and 250 K. γs showed a strong dependence on water activity. Aerosol uptake studies yielded reacto-diffusive lengths, l, of > 0.4 μm for 40 wt % H_2SO_4 and 1.0 μm for 50 wt % H_2SO_4, both at 250 K. Recommended γs were estimated by averaging bulk uptake measurements at similar H_2SO_4 concentrations and ignoring temperature effects on water activity.

Table 65. Henry's Law Constants for Gas-Liquid Solubilities

T(K)	Wt. % H_2SO_4	H or H* (M/atm)	Notes
HONO in $H_2SO_4 \cdot nH_2O$(l)			
248-298	0.3 - 53	$H^* = (47.2 \pm 2.8) \exp(-0.044 \pm 0.002) X$ $X = (wt\ \%\ H_2SO_4)$	1
HNO_3 in $H_2SO_4 \cdot nH_2O$			
~195 - 300	0-80	See Note	2
HCl in $H_2SO_4 \cdot nH_2O \cdot H_2O$(l) and $H_2SO_4 \cdot nHNO_3 \cdot mH_2O$(l)			
~195 - 300	0 - 80	See Note	2
HBr in $H_2SO_4 \cdot nH_2O \cdot H_2O$(l) and $H_2SO_4 \cdot nHNO_3 \cdot mH_2O$(l)			
~195 - 300	0 - 80	See Note	2
HOCl in $H_2SO_4 \cdot nH_2O$(l)			
200 - 230	46 - 80	See Note	3
HC(O)OH in H_2O(l)			
298	0	1.1×10^4	4
$CH_3C(O)OH$ in H_2O(l)			
298	0	7×10^3	4
$CH_3C(O)O_2$ in H_2O(l)			
275	0	≤ 0.1	5
$CH_3C(O)OONO_2$ in H_2O(l)			
293	0	4.1	6
$CH_3CH_2C(O)OONO_2$ in H_2O(l)			
293	0	2.9	6
CCl_2O in H_2O(l)			
278	0	< 0.2	7
298	0	< 0.1	7
CCl_3CClO in H_2O(l)			
278	0	≤ 2	8
CF_2O in H_2O(l)			
278	0	< 1	9
CF_2O in $H_2SO_4 \cdot nH_2O$			
215-230	60	< 5	10
CF_3CFO in H_2O(l)			
278	0	< 1	9

Table 65. Henry's Law Constants for Gas-Liquid Solubilities

T(K)	Wt. % H_2SO_4	H or H* (M/atm)	Notes
CF_3CClO in H_2O(l)			
278	0	≤ 0.5	10
CF_3OH in $H_2SO_4 \cdot nH_2O$(l)			
250	40	>240	13
	50	210	
$CF_3C(O)OH$ in H_2O(l)			
278-308	0	See Note	14
NO_3 in H_2O(l)			
273	0	0.6 ±0.3	15

Notes to Table 65

1. Becker et al. [10] measured H^* for HONO between 248 and 298 K and 0.3 to 73.3 wt % H_2SO_4. H^* fell monotonically, with the expression tabulated up to 53 wt % H_2SO_4. Above that, H^* increased due to nitrosyl sulfuric acid formation (see previous table for reactive uptake γ).

2. Effective Henry's law coefficients, H^*, for HNO_3, HCl and HBr in binary H_2SO_4/H_2O and ternary $H_2SO_4/HNO_3/H_2O$ solutions over the temperature range 195 to 300 K are required to model the composition and heterogeneous chemistry of stratospheric and upper tropospheric aerosols. Solubility data can be obtained from analysis of heterogeneous uptake experiments with the liquid phase diffusion coefficient estimated from acid solution viscosity (Williams and Long [177]) or from vapor pressure data.

   Recent experimental solubility data for HNO_3 is provided by Van Doren et al. [167], Reihs et al. [135], and Zhang et al. [188]. Data for HCl solubility is provided by Watson et al. [174], Hanson and Ravishankara [66, 70], Zhang et al. [188], Williams and Golden [175], Abbatt [2] and Elrod et al. [37]. Data for HBr is provided by Williams et al. [176] and Abbatt [2].

   These studies all show that trace species solubility in H_2SO_4/H_2O and $H_2SO_4/HNO_3/H_2O$ solutions is a strong function of water activity, which, in turn, depends on both temperature and acid concentrations. Prediction of HNO_3, HCl, and HBr H^* values for atmospheric compositions requires a sophisticated model. Comprehensive thermodynamic models of acid solutions for a range of atmospheric conditions have been published by Carslaw et al. [21], Tabazadeh et al. [154] and Luo et al. [110] and reviewed by Carslaw and Peter [22]. These models do an excellent job of reproducing the available experimental data, even for ternary $H_2SO_4/HNO_3/H_2O$ solutions (Elrod et al. [37]). These models and the Carslaw review should be consulted for plots/predictions of H^* for HNO_3, HCl, and HBr in strong acid solutions over the atmospheric temperature range.

3. Huthwelker et al.[81] have extrapolated room temperature acqueous HOCl solubility data to stratospheric temperature and acid concentrations using a thermodynamic model of acid solutions. They obtain a Setchenow-type dependence on H_2SO_4 molality, mH_2SO_4, for HOCl activity and parameritize the physical Henry's law constant as:

$$\ln H^* = 6.4946 - mH_2SO_4\,(-0.04107 + 54.56/T) - 5862\,(1/T_o - 1/T)$$

   where $T = T(K)$, $T_o = 298.15$ K and $H = mHOCl/pHOCl$ in mol kg^{-1} atm^{-1}.

4. Johnson et al. [89] determined $H^* = (8.9 \pm 1.3) \times 10^3$ M atm^{-1} for formic acid and $H^* = (4.1 \pm 0.4) \times 10^3$ M atm^{-1} for acetic acid at 298 K in a packed column experiment. Earlier bubbler measurements by Servant et al. [150] measured $(13.4 \pm 1.6) \times 10^3$ at 297 K and $(9.3 \pm 1.1) \times 10^3$ at 296 K, respectively. Combining the measured values, "best" experimental values of $(11 \pm 2) \times 10^3$ and $(7 \pm 3) \times 10^3$ M atm^{-1} for 298 were recommended.

5. Villalta et al. [168] measured an upper limit for H of 0.1 M atm^{-1} in coated-wall flow tube uptake experiments on aqueous sodium ascorbate solutions.

6. Kames and Schurath[91] measured $H = 4.1 \pm 0.8$ M atm^{-1} for peroxyacetylnitrate (PAN) in distilled water at 293.2 K with a bubbler apparatus; a slightly lower value of 3.6 ± 0.2 was obtained for synthetic sea water of 0.61 ionic strength. They also measured 2.9 ± 0.06 (distilled water) and 2.5 ± 0.5 (synthetic sea water) for peroxypropionalnitrate. Their PAN value agrees with earlier measuremnts by Kames et al. [92] and unpublished work by Y.N. Lee.

7. De Bruyn et al. [33] reported limits of < 0.15 at 278 K and < 0.06 at 298 K from a bubble column uptake experiment. Uptake was controlled by $H(k_{hyd})^{1/2}$ in these experiments. Reported limits are consistent with values from a liquid jet experiment of 0.11 at 288 K, 0.07 at 298 K, 0.05 at 308 K and 0.03 at 319 K reported by Manogue and Pigford [112].

8. De Bruyn et al. report a limit of < 1.9 from a bubble column experiment where uptake was controlled by $H(k_{hyd})^{1/2}$. George et al. [47] report a value of 2 for the temperature range of 274-294 K from a droplet train experiment with uptake also controlled by $H(k_{hyd})^{1/2}$, although the k_{hyd} value used to deconvolute the data was not well determined.

9. De Bruyn et al. report a limit of < 1.0 at 278 K based on uptake controlled by $H(k_{hyd})^{1/2}$ in a bubble column experiment. This is consistent with the limit on the uptake coefficient measured by the same group with a droplet train experiment at 300 K (De Bruyn et al. [31]). George et al. [49] report much higher $(Hk_{hyd})^{1/2}$ values, implying H values > 20 for temperatures between 273 and 294 K. However, this analysis is suspect due to low signal strengths and large data scatter at all temperatures.

10. Hanson and Ravishankara [64] calculate an upper limit for H of CF_2O based on assumed solubility limit resulting in lack of measurable uptake into 60 wt% H_2SO_4.

11. De Bruyn et al. report a limit of < 0.9 at 278 K from a bubble column experiment where uptake was controlled by $H(k_{hyd})^{1/2}$. George et al. [49] report a value of 3 at 284 K from a droplet train experiment where uptake was also controlled by $H(k_{hyd})^{1/2}$; however, deconvolution of time-dependent uptake data to yield it and k_{hyd} is suspect due to low signals and high data scatter at each temperature.

12. De Bruyn et al. report a limit of < 0.3 at 278 K from a bubble column experiment where uptake was controlled by $H(k_{hyd})^{1/2}$. George et al. [49] report a value of 2 at 284 K from a droplet train experiment with uptake also controlled by $H(k_{hyd})^{1/2}$; however, deconvolution of time-dependent uptake data to yield H and k_{hyd} is suspect due to low signal strength and high data scatter at each temperature.

13. Lovejoy et al. [109] determined recto-diffusive lengths of > 0.4 μm and 1.0 μm for CF_3OH uptake at 250 K on 40 and 50 wt % H_2SO_4 aerosols, respectively. This leads to H^* estimates of > 240 and 210 M atm^{-1}, respectively.

14. Bowder et al. [17] measured $CF_3C(O)OH$ vapor pressures over water at 278.15, 298.15 and 308.15 K yielding a suggested parameterization of H (mol kg^{-1} atm^{-1}) = $9.009 - 9.328 \times 10^3 (1/T_o - 1/T)$ where T = T(K) and $T_o = 298.15$ K.

15. Wetted-wall flow tube measurements by Rudich et al. [145] yielded an $H(D_l)^{1/2}$ value of $(1.9 \pm 0.2) \times 10^{-3}$ M atm^{-1} cm s$^{-1/2}$. They assumed a liquid phase diffusion coefficient, $D_l = (1.0 \pm 0.5) \times 10^{-5}$ cm^2 s^{-1},

yielding a Henry's law constant of 0.6 ± 0.3 M atm-1 at 273 K. This is one third of an earlier measurement of 1.8 ±1.5 M atm-1 quoted in Michelcic et al. [119].

References for Heterogeneous Section

1. Abbatt, J.P.D., 1994, Geophys. Res. Lett., **21**, 665-668.
2. Abbatt, J.P.D., 1995, Geophys. Res. Lett., **100**, 14,009-14,017.
3. Abbatt, J.P.D., 1996, Geophys. Res. Lett., **23**, 1681-1684.
4. Abbatt, J.P.D., K.D. Beyer, A.F. Fucaloro, J.R. McMahon, P.J. Wooldridge, R. Zhong, and M.J. Molina, 1992, J. Geophys. Res., **97**, 15819-15826.
5. Abbatt, J.P.D. and M.J. Molina, 1992, Geophys. Res. Lett., **19**, 461-464.
6. Abbatt, J.P.D. and M.J. Molina, 1992, J. Phys. Chem., **96**, 7674-7679.
7. Alebic'-Juretic', A., T. Cuitas, and L. Klasine, 1992, Ber. Bunsenges Phys. Chem., **96**, 493-495.
8. Baldwin, A.C. and D.M. Golden, 1979, Science, **206**, 562.
9. Baldwin, A.C. and D.M. Golden, 1980, J. Geophys. Res., **85**, 2888-2889.
10. Becker, K.H., J. Kleffman, R. Kurtenbach, and P. Wiesen, 1996, J. Phys. Chem., **100**, 14,984-14,990.
11. Behnke, W., H.-U. Kruger, V. Scheer, and C. Zetzsch, 1992, J. Aerosol Sci., **23**, S923-S936.
12. Behnke, W., V. Scheer, and C. Zetzsch, 1993, J. Aerosol Sci., **24**, S115-S116.
13. Beichert, P. and B.J. Finlayson-Pitts, 1996, J. Phys. Chem., **100**, 15,218-15,228.
14. Berko, H.N., P.C. McCaslin, and B.J. Finlayson-Pitts, 1991, J. Phys. Chem., **95**, 6951-6958.
15. Bongartz, A., J. Kames, U. Schurath, C. George, P. Mirabel, and J.L. Ponche, 1994, J. Atm. Chem., **18**, 149-160.
16. Bongartz, A., S. Schweighoefer, C. Roose, and U. Schurath, 1995, J. Atmos. Chem., **20**, 35-58.
17. Bowder, D.J., S.L. Clegg, and P. Brimblecombe, 1996, Chemosphere, **32**, 405-420.
18. Brown, D.E., S.M. George, C. Huang, E.K.L. Wong, K.B. Rider, R.S. Smith, and B.D. Kay, 1996, J. Phys. Chem., **100**, 4988-4995.
19. Brown, L.A., V. Vaida, D.R. Hanson, J.D. Graham, and J.T. Roberts, 1996, J. Phys. Chem., **100**, 3121-3125.
20. Caloz, F., F.F. Fentner, and M.J. Rossi, 1996, J. Phys. Chem., **100**, 7494-7501.
21. Carslaw, K.S., S.L. Clegg, and P. Brimblecombe, 1995, J. Phys. Chem., **99**, 11,557-11,574.
22. Carslaw, K.S. and T. Peter, 1996, Rev. Geophys., submitted.
23. Chu, L.T. and J.W. Heron, 1995, Geophys. Res. Lett., **22**, 3211-3214.
24. Chu, L.T., M.-T. Leu, and L.F. Keyser, 1993, J. Phys. Chem., **97**, 12798-12804.
25. Chu, L.T., M.-T. Leu, and L.F. Keyser, 1993, J. Phys. Chem., **97**, 7779-7785.
26. Clegg, S.L. and P. Brimblecombe, 1986, Atmos. Environ., **20**, 2483.
27. Cooper, P.L. and J.P.D. Abbatt, 1996, J. Phys. Chem., **100**, 2249-2254.
28. Dai, D.J., S.J. Peters, and G.E. Ewing, 1995, J. Phys. Chem., **99**, 10,299-10,304.
29. Dai, Q., G.N. Robinson, and A. Freedman, 1996, J. Phys. Chem., submitted.
30. Daumer, R. Nissner, and D. Klockow, J. Aerosol Sci., **23**, 315-325.
31. De Bruyn, W.J., S.X. Duan, X.Q. Shi, P. Davidovits, D.R. Worsnop, M.S. Zahniser, and C.E. Kolb, 1992, Geophys. Res. Lett., **19**, 1939-1942.
32. De Bruyn, W.J., J.A. Shorter, P. Davidovits, D.R. Worsnop, M.S. Zahniser, and C.E. Kolb, 1994, J. Geophys. Res., **99**, 16927-16932.
33. DeBruyn, W.J., J.A. Shorter, P. Davidovits, D.R. Worsnop, M.S. Zahniser, and C.E. Kolb, 1995, Environ. Sci Technol., **29**, 1179-1185.
34. Dlugokencky, E.J. and A.R. Ravishankara, 1992, Geophys. Res. Lett., **19**, 41-44.
35. Donaldson, D.J., J.A. Guest, and M.C. Goh, 1995, J. Phys. Chem., **99**, 9313-9315.
36. Duan, S.X., J.T. Jayne, P. Davidovits, D.R. Worsnop, M.S. Zahniser, and C.E. Kolb, 1993, J. Phys. Chem., **97**, 2284-2288.
37. Elrod, M.J., R.E. Koch, J.E. Kim, and M.S. Molina, 1995, Faraday Discuss, **100**, 269-278.
38. Fendel, W., D. Matter, H. Burtscher, and A. Schimdt - Ott, 1995, Atmos. Environ, **29**, 967-973.
39. Fendel, W. and A.S. Ott, 1993, J. Aerosol Sci., **24**, S317-S318.
40. Fenter, F.F., F. Caloz, and M.J. Rossi, 1994, J. Phys. Chem., **98**, 9801-9810.
41 Fenter, F.F., F. Caloz, and M.J. Rossi, 1996, J. Phys. Chem., **100**, 1008-1019.
42. Fenter, F.F. and M.J. Rossi, 1996, J. Phys. Chem., **100**, 13765-13775.
43. Finlayson-Pitts, B.J., M.J. Ezell, and J.N. Pitts Jr., 1989, Nature, **337**, 241-244.

44. Fox, L.E., D.R. Worsnop, M.S. Zahniser, and S.C. Wofsy, 1994, Science, **267**, 351-355.
45. Fried, A., B.E. Henry, J.G. Calvert, and M. Mozukewich, 1994, J. Geophys. Res., **99**, 3517-3532.
46. Fung, K.N., I.N. Tang, and H.R. Munkelwitz, 1987, Appl. Optics, **26**, 1282-1287.
47. George, C., J. Lagrange, P. Lagrange, P. Mirabel, C. Pallares, and J.L. Ponche, 1994, J. Geophys. Res., **99**, 1255-1262.
48. George, C., J.L. Ponche, P. Mirabel, W. Behnke, V. Sheer, and C. Zetzsch, 1994, J. Phys. Chem., **98**, 8780-8784.
49. George, C., J.Y. Saison, J.L. Ponche, and P. Mirabel, 1994, J. Phys. Chem., **98**, 10857-10862.
50. Gershenzon, Y.M., A.V. Ivanov, S.I. Kucheryavyi, and V.B. Rozenshtein, 1986, Kinet. Katal., **27**, 1069-1074.
51. Gershenzon, Y.M. and A.P. Purmal, 1990, Russ. Chem. Rev., **59**, 1007-1023.
52. Gersherzon, V.M., V.M. Grigorieva, A.V. Ivanov, and R.G. Remorov, 1995, Faraday Discuss, **100**, 83-100.
53. Gertner, B.J. and J.T. Hynes, 1996, Science, **271**, 1563-1566.
54. Graham, J.D. and J.T. Roberts, 1994, J. Phys. Chem., **98**, 5974-5983.
55. Graham, J.D. and J.T. Roberts, 1995, Geophys. Res. Lett., **22**, 251-254.
56. Graham, J.D., J.T. Roberts, L.A. Brown, and V. Vaida, 1996, J. Phys. Chem., **100**, 3115-3120.
57. Hanning-Lee, M.A., B.B. Brady, L.R. Martin, and J.A. Syage, 1996, Geophys. Res. Lett., **23**, 1961-1964.
58. Hanson, D.R., 1992, Geophys. Res. Lett., **19**, 2063-2066.
59. Hanson, D.R., 1995, J. Phys. Chem., **99**, 13,059-13,061.
60. Hanson, D.R., J.B. Burkholder, C.J. Howard, and A.R. Ravishankara, 1992, J. Phys. Chem., **96**, 4979-4985.
61. Hanson, D.R. and E.R. Lovejoy, 1994, Geophys. Res. Lett., **21**, 2401-2404.
62. Hanson, D.R. and E.R. Lovejoy, 1995, Science, **267**, 1326-1329.
63. Hanson, D.R. and A.R. Ravishankara, 1991, J. Geophys. Res., **96**, 5081-5090.
64. Hanson, D.R. and A.R. Ravishankara, 1991, Geophys. Res. Lett., **18**, 1699-1701.
65. Hanson, D.R. and A.R. Ravishankara, 1991, J. Geophys. Res., **96**, 17307-17314.
66. Hanson, D.R. and A.R. Ravishankara, 1992, J. Phys. Chem., **96**, 2682-2691.
67. Hanson, D.R. and A.R. Ravishankara, 1992, J. Phys. Chem., **96**, 9441-9446.
68. Hanson, D.R. and A.R. Ravishankara, 1993, J. Phys. Chem., **97**, 2802-2803.
69. Hanson, D.R. and A.R. Ravishankara, 1993, The Tropospheric Chemistry of Ozone in the Polar Regions, H. Niki and K.H. Becker, Editors, NATO, pp. 17281-17290.
70. Hanson, D.R. and A.R. Ravishankara, 1993, J. Phys. Chem., **97**, 12309-12319.
71. Hanson, D.R. and A.R. Ravishankara, 1993, J. Geophys. Res., **98**, 22931-22936.
72. Hanson, D.R. and A.R. Ravishankara, 1994, J. Phys. Chem., **98**, 5728-5735.
73. Hanson, D.R. and A.R. Ravishankara, 1995, Geophys. Res. Lett., **22**, 385-388.
74. Hanson, D.R., A.R. Ravishankara, and S. Solomon, 1994, J. Geophys. Res., **99**, 3615-3629.
75. Harker, A.B. and W.W. Ho, 1979, Atmos. Environ., **13**, 1005-1010.
76. Haynes, D.R., N.J. Tro, and S.M. George, 1992, J. Phys. Chem., **96**, 8502-8509.
77. Hofmann, D.J. and S.J. Oltmans, 1992, Geophys. Res. Lett., **22**, 2211-2214.
78. Hu, J.H., Q. Shi, P. Davidovits, D.R. Worsnop, M.S. Zahniser, and C.E. Kolb, 1995, J. Phys. Chem., **99**, 8768-8776.
79. Hu, J.H., J.A. Shorter, P. Davidovits, D.R. Worsnop, M.S. Zahniser, and C.E. Kolb, 1993, J. Phys. Chem., **97**, 11037-11042.
80. Huntzicker, J.J., R.A. Cary, and C.-S. Ling, 1980, Environ. Sci. Technol., **14**, 819-824.
81. Huthwelker, T., T. Peter, B.P. Juo, S.L. Clegg, K.S. Carshlaw, and P. Brimblecombe, 1995, J. Atmos. Chem., **21**, 81-95.
82. Imamura, T., Y. Rudich, R.K. Talukdar, R.W. Fox, and A.R. Ravishankara, 1996, J. Phys. Chem., submitted.
83. Iraci, L.T., A.M. Middlebrook, M.A. Wilson, and M.A. Tolbert, 1994, Geophys. Res. Lett., **21**, 867-870.
84. Ivanov, A.V., Y.M. Gersherzon, F. Gratpanche, P. Devolder, and J.-P. Saverysyn, 1996, Am. Geophys., **14**, 659-664.
85. Jayne, J.T., P. Davidovits, D.R. Worsnop, M.S. Zahniser, and C.E. Kolb, 1990, J. Phys. Chem., **94**, 6041-6048.
86. Jayne, J.T., S.X. Duan, P. Davidovits, D.R. Worsnop, M.S. Zahniser, and C.E. Kolb, 1991, J. Phys. Chem., **95**, 6329-6336.
87. Jayne, J.T., S.X. Duan, P. Davidovits, D.R. Worsnop, M.S. Zahniser, and C.E. Kolb, 1992, J. Phys. Chem., **96**, 5452-5460.
88. Jayne, J.T., D.R. Worsnop, C.E. Kolb, E. Swartz, and P. Davidovits, 1996, J. Phys. Chem., **100**, 8015-8022.
89. Johnson, B.J., E.A. Betterton, and D. Craig, 1996, J. Atmos. Chem., **24**, 113-119.

90. Kalberer, M., K. Tubor, M. Ammann, Y. Parrat, E. Weingartner, D. Piguet, E. Rossler, D.T. Just, A. Jurles, H.W. Gaaggeler, and V. Baltersperger, 1996, J. Phys. Chem., **100**, 15,487-45,493.
91. Kames, J. and U. Schurath, 1995, J. Atmos. Chem., **21**, 151-164.
92. Kames, J., S. Schweighoefer, and U. Schurath, 1991, J. Atmos. Chem., **12**, 169-180.
93. Kenner, R.D., I.C. Plumb, and K.R. Ryan, 1993, Geophys. Res. Lett., **20**, 193-196.
94. Keyser, L.F. and M.-T. Leu, 1993, J. Colloid Interface Sci., **155**, 137-145.
95. Keyser, L.F. and M.-T. Leu, 1993, Micros. Res. Technol., **25**, 434-438.
96. Keyser, L.F., M.-T. Leu, and S.B. Moore, 1993, J. Phys. Chem., **97**, 2800-2801.
97. Keyser, L.F., S.B. Moore, and M.T. Leu, 1991, J. Phys. Chem., **95**, 5496-5502.
98. Koehler, B.G., L.S. McNeill, A.M. Middlebrook, and M.A. Tolbert, 1993, J. Geophys. Res., **98**, 10563-10571.
99. Kolb, C.E., D.R. Worsnop, M.S. Zahniser, P. Davidovits, L.F. Keyser, M.-T. Leu, M.J. Molina, D.R. Hanson, A.R. Ravishankara, L.R. Williams, and M.A. Tolbert, 1994, "Progress and Problems in Atmospheric Chemistry," Adv. Phys. Chem. Series, 3, J.R. Barker, Editor, , pp. 771-875.
100. Kroes, G.-J. and D.C. Clary, 1992, J. Phys. Chem., **96**, 7079-7088.
101. Laux, J.M., J.C. Hemminger, and B.J. Finlayson-Pitts, 1994, Geophys. Res. Lett., **21**, 1623-1626.
102. Leu, M.-T., R.S. Timonen, L.F. Keyser, and Y.L. Yung, 1995, J. Phys. Chem., **99**, 13,203-13,212.
103. Leu, M.T., 1988, Geophys. Res. Lett., **15**, 851-854.
104. Leu, M.T., 1988, Geophys. Res. Lett., **15**, 17-20.
105. Leu, M.T., S.B. Moore, and L.F. Keyser, 1991, J. Phys. Chem., **95**, 7763-7771.
106. Li, Z., R.R. Friedl, S.B. Moore, and S.P. Sander, 1996, J. Geophys. Res., **101**, 6795-6802.
107. Livingston, F.E. and B.J. Finlayson-Pitts, 1991, Geophys. Res. Lett., **18**, 17-20.
108. Lovejoy, E.R. and D.R. Hanson, 1995, J. Phys. Chem., **99**, 2080-2087.
109. Lovejoy, E.R., L.G. Huey, and D.R. Hanson, 1995, J. Geophys. Res., **100**, 18,775-18,780.
110. Luo, B., K.S. Carslaw, T. Peter, and S.L. Clegg, 1995, Geophys. Res. Lett., **22**, 247-250.
111. Manion, J.A., C.M. Fittschen, D.M. Golden, L.R. Williams, and M.A. Tolbert, 1994, Israel J. Chem., **34**, 355-363.
112. Manogue, W.H. and R.L. Pigford, 1960, A.I.Ch.E.J., **6**, 494-500.
113. Martin, L.R., H.S. Judeikis, and M. Wun, 1980, J. Geophys. Res., **85**, 5511-5518.
114. McMurry, P.H., H. Takano, and G.R. Anderson, 1983, Environ. Sci. Technol., **17**, 347-357.
115. Mertes, S. and A. Wahner, 1995, J. Phys. Chem., **99**, 14,000-14,006.
116. Michelangeli, D.V., M. Allen, and Y.L. Yung, 1991, Geophys. Res. Lett., **18**, 673-676.
117. Middlebrook, A.M., L.T. Iraci, L.S. McNeil, B.G. Koehler, M.A. Wilson, O.W. Saastad, and M.A. Tolbert, 1993, J. Geophys. Res., **98**, 20473-20481.
118. Middlebrook, A.M., B.G. Koehler, L.S. McNeill, and M.A. Tolbert, 1992, Geophys. Res. Lett., **19**, 2417-2420.
119. Mihelcic, D., D. Klemp, P. Msgen, H.W. Ptz, and A. Volz-Thomas, 1993, J. Atmos. Chem., **16**, 313-335.
120. Molina, M.J., R.F. Meads, D.D. Spencer, and L.T. Molina, 1996, Geophys. Res. Lett., submitted.
121. Molina, M.J., T.L. Tso, L.T. Molina, and F.C. Wang, 1987, Science, **238**, 1253-1259.
122. Molina, M.J., R. Zhang, P.J. Woolridge, J.R. McMahon, J.E. Kim, H.Y. Chang, and K.D. Beyer, 1993, Science, **261**, 1418-1423.
123. Moore, S.B., L.F. Keyser, M.T. Leu, R.P. Turco, and R.H. Smith, 1990, Nature, **345**, 333-335.
124. Mozurkewich, M. and J. Calvert, 1988, J. Geophys. Res., **93**, 889-896.
125. Mozurkewich, M., P.H. McMurray, A. Gupta, and J.G. Calvert, 1987, J. Geophys. Res., **92**, 4163-4170.
126. Msibi, I.M., Y. Li, J.P. Shi, and R.M. Harrison, 1994, J. Phys. Chem., **18**, 291-300.
127. Msibi, I.M., J.P. Shi, and R.M. Harrison, 1993, J. Atmos. Chem., 17,339-17,351.
128. Noyes, R.M., M.B. Rubin, and P.G. Bowers, 1996, J. Phys. Chem., **100**, 4167-4172.
129. Olszyna, K., R.D. Cadle, and R.G. dePena, 1979, J. Geophys. Res., **84**, 1771-1775.
130. Oppliger, R., A. Allanic, and M.J. Rossi, 1996, J. Phys. Chem., submitted.
131. Peters, S.J. and G.E. Ewing, 1996, J. Phys. Chem., **100**, 14,093-14,102.
132. Ponche, J.L., C. George, and P. Mirabel, 1993, J. Atmos. Chem., **16**, 1-21.
133. Pueschel, R.F., D.F. Blake, A.G. Suetsinger, A.D.A. Hansen, S. Verma, and K. Kato, 1992, Geophys. Res. Lett., **19**, 1659-1662.
134. Quinlan, M.A., C.M. Reihs, D.M. Golden, and M.A. Tolbert, 1990, J. Phys. Chem., **94**, 3255-3260.
135. Reihs, C.M., D.M. Golden, and M.A. Tolbert, 1990, J. Geophys. Res., **95**, 16,545-16,550.
136. Rieley, H., H.D. Aslin, and S. Haq, 1995, J. Chem. Soc. Faraday Trans., **91**, 2349-2351.
137. Robbins, R.C. and R.D. Cadle, 1958, J. Phys. Chem., **62**, 469-471.

138. Robinson, G.N., Q. Dai, and A. Freedman, 1996, J. Phys. Chem., submitted.
139. Robinson, G.N., A. Freedman, C.E. Kolb, and D.R. Worsnop, 1994, Geophys. Res. Lett., **21**, 377-380.
140. Robinson, G.N., A. Freedman, C.E. Kolb, and D.R. Worsnop, 1996, Geophys. Res. Lett., **23**, 317.
141. Robinson, G.N., D.R. Worsnop, J.T. Jayne, C.E. Kolb, and P. Davidovits, 1996, J. Geophys. Res., **102**, 3583-3601.
142. Rogaski, C.A., D.M. Golden, and L.R. Williams, 1996, Geophys. Res. Lett., **24**, 381-384.
143. Rossi, M.J., R. Malhotra, and D.M. Golden, 1987, Geophys. Res. Lett., **14**, 127-130.
144. Rubel, G.O. and J.W. Gentry, 1984, J. Aerosol Sci., **15**, 661-671.
145. Rudich, Y., R.K. Talukdar, R.W. Fox, and A.R. Ravishankara, 1996, J. Geophys. Res., **101**, 21,023-21,031.
146. Rudich, Y., R.K. Talukdar, T. Imamura, R.W. Fox, and A.R. Ravishankara, 1996, Chem. Phys. Lett., **261**, 467-473.
147. Rudolf, R. and P.E. Wagner, 1994, J. AerosolSci, **25**, 597-598.
148. Saastad, O.W., T. Ellerman, and C.J. Nielson, 1993, Geophys. Res. Lett., **20**, 1191-1193.
149. Schwartz, S.E., 1988, Atmos. Environ., **22**, 2331.
150. Servant, J., G. Koundio, B. Cross, and R. Delmas, 1991, J. Atmos. Chem., **12**, 367-380.
151. Shimono, A. and S. Koda, 1996, J. Phys. Chem., **100**, 10,269-10,276.
152. Smith, D.M., W.F. Welch, J.A. Jassim, A.R. Chughtai, and D.H. Stedman, 1988, Appl. Spectros., **42**, 1473-1482.
153. Stephens, S., M.J. Rossi, and D.M. Golden, 1986, Int. J. Chem. Kinetics, **18**, 1133-1149.
154. Tabazadeh, A., R.P. Turco, and M.Z. Jacobson, 1994, J. Geophys. Res., **99**, 12,897-12,914.
155. Tabor, K., L. Gutzwiller, and M.J. Rossi, 1993, Geophys. Res. Lett., **20**, 1431-1434.
156. Tabor, K., L. Gutzwiller, and M.J. Rossi, 1994, J. Phys. Chem., **98**, 6172-7186.
157. Tang, I.N. and J.H. Lee, 1987, The Chemistry of Acid Rain, G.E. Gordon and R.W. Johnson, Editors, Am. Chem. Soc. Symp. Series, pp. 109-117.
158. Tang, I.N. and H.R. Munkelwitz, 1989, J. Colloid Interface Sci., **128**, 289-295.
159. Timonen, R.S., L.T. Chu, M.-T. Leu, and L.F. Keyser, 1994, J. Phys. Chem., **98**, 9509-9517.
160. Tolbert, M.A., J. Praff, I. Jayaweera, and M.J. Prather, 1993, J. Geophys. Res., **98**, 2957-2962.
161. Tolbert, M.A., M.J. Rossi, and D.M. Golden, 1988, Geophys. Res. Lett., **15**, 847-850.
162. Tolbert, M.A., M.J. Rossi, and D.M. Golden, 1988, Science, **240**, 1018-1021.
163. Tolbert, M.A., M.J. Rossi, R. Malhotra, and D.M. Golden, 1987, Science, **238**, 1258-1260.
164. Toon, O., *et al.*, 1993, Science, **261**, 1136-1140.
165. Utter, R.G., J.B. Burkholder, C.J. Howard, and A.R. Ravishankara, 1992, J. Phys. Chem., **96**, 4973-4978.
166. Van Doren, J.M., L.R. Watson, P. Davidovits, D.R. Worsnop, M.S. Zahniser, and C.E. Kolb, 1990, J. Phys. Chem., **94**, 3265-3269.
167. Van Doren, J.M., L.R. Watson, P. Davidovits, D.R. Worsnop, M.S. Zahniser, and C.E. Kolb, 1991, J. Phys. Chem., **95**, 1684-1689.
168. Villalta, P.W., E.R. Lovejoy, and D.R. Hanson, 1996, Geophys. Res. Lett., **23**, 1765-1768.
169. Vogt, R., Elliott, C., Allen, H.C., Laux, J.M., J.C. Hemminger, and B.J. Finlayson-Pitts, 1996, Atmos. Environ, **30**, 1729-1737.
170. Vogt, R. and B. Finlayson-Pitts, 1994, J. Phys. Chem., **98**, 3747-3755.
171. Vogt, R. and B.F. Finlayson-Pitts, 1994, Geophys. Res. Lett., **21**, 2291-2294.
172. Vogt, R. and B.J. Finlayson-Pitts, 1995, J. Phys. Chem., **99**, 13,052.
173. Wang, L. and D.C. Clary, 1996, J. Chem. Phys., **104**, 5663-5673.
174. Watson, L.R., J.M.V. Doren, P. Davidovits, D.R. Worsnop, M.S. Zahniser, and C.E. Kolb, 1990, J. Geophys. Res., **95**, 5631-5638.
175. Williams, L.R. and D.M. Golden, 1993, Geophys. Res. Lett., **20**, 2227-2230.
176. Williams, L.R., D.M. Golden, and D.L. Huestis, 1995, J. Geophys. Res., **100**, 7329-7335.
177. Williams, L.R. and F.S. Long, 1995, J. Phys. Chem., **99**, 3748-3751.
178. Williams, L.R., J.A. Manion, D.M. Golden, and M.A. Tolbert, 1994, J. Appl. Meteor., **33**, 785-790.
179. Wolff, E.W. and R. Mulvaney, 1991, Geophys. Res. Lett., **18**, 1007-1010.
180. Worsnop, D.R., L.E. Fox, M.S. Zahniser, and S.C. Wofsy, 1993, Science, **259**, 71-74.
181. Worsnop, D.R., M.S. Zahniser, C.E. Kolb, J.A. Gardner, L.R. Watson, J.M.V. Doren, J.T. Jayne, and P. Davidovits, 1989, J. Phys. Chem., **93**, 1159-1172.
182. Zetzsch, C. and W. Behnke, 1992, Ber. Bunsenges. Phys. Chem., **96**, 488-493.
183. Zhang, R., J.T. Jayne, and M.J. Molina, 1994, J. Phys. Chem., **98**, 867-874.
184. Zhang, R., M.-T. Leu, and L.F. Keyser, 1994, J. Phys. Chem., **98**, 13,563-13,574.
185. Zhang, R., M.-T. Leu, and L.F. Keyser, 1995, Geophys. Res. Lett., **22**, 1493-1496.

186. Zhang, R., M.-T. Leu, and L.F. Keyser, 1995, J. Geophys. Res., **100**, 18,845-18,854.
187. Zhang, R., M.-T. Leu, and L.F. Keyser, 1996, J. Phys. Chem., **100**, 339-345.
188. Zhang, R., P.J. Wooldridge, and M.J. Molina, 1993, J. Phys. Chem., **97**, 8541-8548.
189. Zolensky, M.E., D.S. McKay, and L.A. Kaczor, 1989, J. Geophys. Res., **94**, 1047-1056.

APPENDIX 1: GAS PHASE ENTHALPY DATA

SPECIES	$\Delta H_f(298)$ (Kcal/mol)	SPECIES	$\Delta H_f(298)$ (Kcal/mol)	SPECIES	$\Delta H_f(298)$ (Kcal/mol)	SPECIES	$\Delta H_f(298)$ (Kcal/mol)
H	52.1	C_2H_4	12.45	CH_2FCH_2F	-107±1	CH_3CH_2Cl	-26.8
H_2	0.00	C_2H_5	28.4±0.5	CH2FCHF2	-159±2	CH_2CH_2Cl	22±2
O	59.57	C_2H_6	-20.0	CHF2CHF2	-210±1	CH_3CHCl	17.6±1
$O(^1D)$	104.9	CH_2CN	58.5±3	CH_2CF_3	-124±2	Br	26.7
O_2	0.00	CH_3CN	18±3	CH_3CF_3	-179±2	Br_2	7.39
$O_2(^1\Delta)$	22.5	CH_2CO	-11±3	CH_3CF_2	-71±2	HBr	-8.67
$O_2(^1\Sigma)$	37.5	CH_3CO	-2.4±0.5	CH_3CHF_2	-120±1	HOBr	-14±2
O_3	34.1	CH_3CHO	-39.7	CHFCF3	-163±2	BrO	30±2
HO	9.3	C_2H_5O	-4.1±1	CH2FCF3	-214±1	BrNO	19.7
HO_2	2.8±0.5	CH_2CH_2OH	-8±2	CF_2CF_3	-213±2	BrONO	25±7
H_2O	-57.81	C_2H_5OH	-56.2	CHF_2CF_3	-264±2	$BrNO_2$	17±2
H_2O_2	-32.60	CH_3CO_2	-49.6	Cl	28.9	$BrONO_2$	≤11
N	113.00	CH_3COOH	-103.3	Cl_2	0.00	BrCl	3.5
N_2	0.00	$C_2H_5O_2$	-6±2	HCl	-22.06	CH_2Br	40±2
NH	85.3	CH_3COO_2	-41±5	ClO	24.4	$CHBr_3$	6±2
NH_2	45.3±0.3	CH_3OOCH_3	-30.0	ClOO	23.3±1	$CHBr_2$	45±2
NH_3	-10.98	C_3H_5	39.4±2	OClO	22.6±1	CBr_3	48±2
NO	21.57	C_3H_6	4.8	$ClOO_2$	>16.7	CH_2Br_2	-2.6±2
NO_2	7.9	n-C_3H_7	22.6±2	ClO_3	52±4	CH_3Br	-8.5
NO_3	17.6±1	i-C_3H_7	19±3	Cl_2O	19.5±1	CH_3CH_2Br	-14.8
N_2O	19.61	C_3H_8	-24.8	Cl_2O_2	31±3	CH_2CH_2Br	32±2
N_2O_3	19.8	C_2H_5CHO	-44.8	Cl_2O_3	37±3	CH_3CHBr	30±2
N_2O_4	2.2	CH_3COCH_3	-51.9	HOCl	-18±3	I	25.52
N_2O_5	2.7±1	$CH_3COO_2NO_2$	-62±5	ClNO	12.4	I_2	14.92
HNO	25.6±1	F	19.0±0.1	$ClNO_2$	3.0	HI	6.3
HONO	-19.0	F_2	0.00	ClONO	13	CH_3I	3.5
HNO_3	-32.3	HF	-65.14±0.2	$ClONO_2$	5.5	CH_2I	52±2
HO_2NO_2	-12.5±2	HOF	-23.4±1	FCl	-12.1	IO	30.5±2
C	170.9	FO	26±3	CCl_2	57±5	INO	29.0
CH	142.0	F_2O	5.9±.4	CCl_3	17±1	INO_2	14.4
CH_2	93±1	FO_2	6±1	CCl_3O_2	-2.7±1	S	66.22
CH_3	35±0.2	F_2O_2	5±2	CCl_4	-22.9	S_2	30.72
CH_4	-17.88	FONO	13±7	$CHCl_3$	-24.6	HS	34.2±1
CN	104±3	FNO	-16±2	$CHCl_2$	23±2	H_2S	-4.9
HCN	32.3	FNO_2	-26±2	CH_2Cl	29±2	SO	1.3
CH_3NH_2	-5.5	$FONO_2$	3.1±2	CH_2Cl_2	-22.8	SO_2	-70.96
NCO	38±3	CF	61±2	CH_3Cl	-19.6	SO_3	-94.6
HNCO	-25±3	CF_2	-44±2	ClCO	-5±1	HSO	-1±2
CO	-26.42	CF_3	-112±1	$COCl_2$	-52.6	HSO_3	-92±2
CO_2	-94.07	CF_4	-223.0	CHFCl	-15±2	H_2SO_4	-176
HCO	10±1	CHF_3	-166.8	CH_2FCl	-63±2	CS	67±2
CH_2O	-26.0	CHF_2	-58±2	CFCl	7±6	CS_2	28.0
COOH	-53±2	CH_2F_2	-108.2	$CFCl_2$	-22±2	CS_2OH	26.4
HCOOH	-90.5	CH_2F	-8±2	$CFCl_3$	-68.1	CH_3S	29.8±1
CH_3O	4±1	CH_3F	-56±1	CF_2Cl_2	-117.9	CH_3SOO	18±2
CH_3O_2	4±2	FCO	-41±15	CF_3Cl	-169.2	CH_3SO_2	-57
CH_2OH	-3.6±1	F_2CO	-145±2	$CHFCl_2$	-68.1	CH_3SH	-5.5
CH_3OH	-48.2	CF_3O	-150±2	CHF_2Cl	-115.6	CH_2SCH_3	32.7±1
CH_3OOH	-31.3	CF_3O_2	-148±2	CF_2Cl	-67±3	CH_3SCH_3	-8.9
CH_3ONO	-15.6	CF_3OH	-218±3	COFCl	-102±2	CH_3SSCH_3	-5.8
CH_3ONO_2	-28.6	CF_3OOCF_3	-343±5	CH_3CF2Cl	-127±2	OCS	-34
$CH_3O_2NO_2$	-10.6±2	CF_3OOH	-191±5	CH_2CF_2Cl	-75±2		
C_2H	135±1	CF_3OF	-173±5	C_2Cl_4	-3.0		
C_2H_2	54.35	CH_3CHF	-17±2	C_2HCl_3	-1.9		
C_2H_2OH	30±3	CH_3CH_2F	-63±2	CH_2CCl_3	17±2		
C_2H_3	71±1			CH_3CCl_3	-34.0		

APPENDIX 2: GAS PHASE ENTROPY DATA

SPECIES	$S^o(298)$ (cal/mol/deg)	SPECIES	$S^o(298)$ (cal/mol/deg)	SPECIES	$S^o(298)$ (cal/mol/deg)	SPECIES	$S^o(298)$ (cal/mol/deg)
H	27.4	CH_3CN	58.2	CF_2CF_3	81.6	$BrONO_2$	(77)
H_2	31.2	CH_2CO	57.8	FCl	52.1	BrCl	57.3
O	38.5	CH_3CO	64.5	CH_2FCl	63.3	CH_3Br	58.7
O_2	49.0	CH_3CHO	63.2	CHFCl	(63)	CH_2Br	(61)
O_3	57.0	C_2H_5O	65.3	CFCl	62.0	CH_2Br_2	70.1
HO	43.9	C_2H_5OH	67.5	$CFCl_3$	74.0	$CHBr_2$	(72)
HO_2	54.4	CH_3CO_2	(68)	CF_2Cl_2	71.8	$CHBr_3$	79.1
H_2O	45.1	CH3COOH	67.5	CF_3Cl	68.3	CBr_3	80.0
H_2O_2	55.6	$C_2H_5O_2$	75.0	$CHFCl_2$	70.1	CH_3CH_2Br	68.6
N	36.6	CH_3COO_2	(80)	$CFCl_2$	71.5	CH_2CH_2Br	(70)
N_2	45.8	CH_3OOCH_3	74.1	CHF_2Cl	67.2	CH_3CHBr	(70)
NH	43.3	C_3H_5	62.1	CF_2Cl	68.7	I	43.2
NH_2	46.5	C_3H_6	63.8	COFCl	66.2	I_2	62.3
NH_3	46.0	n-C_3H_7	68.5	CH_3CF_2Cl	68.7	HI	49.3
NO	50.3	i-C_3H_7	66.7	CH_2CF_2Cl	(69)	CH_3I	60.6
NO_2	57.3	C_3H_8	64.5	Cl	39.5	CH_2I	(61)
NO_3	60.3	C_2H_5CHO	72.8	Cl_2	53.3	IO	58.8
N_2O	52.6	CH_3COCH_3	70.5	HCl	44.6	INO	67.6
N_2O_3	73.9	$CH_3COO_2NO_2$	(95)	ClO	54.1	INO_2	70.3
N_2O_4	72.7	F	37.9	ClOO	64.0	S	40.1
N_2O_5	82.8	F_2	48.5	OClO	61.5	S_2	54.5
HNO	52.7	HF	41.5	$ClOO_2$	73	H_2S	49.2
HONO	59.6	HOF	54.2	Cl_2O	64.0	HS	46.7
HNO_3	63.7	FO	51.8	Cl_2O_2	72.2	SO	53.0
HO_2NO_2	(72)	F_2O	59.1	HOCl	56.5	SO_2	59.3
C	37.8	FO_2	61.9	ClNO	62.6	SO_3	61.3
CH	43.7	F_2O_2	66.3	$ClNO_2$	65.1	H_2SO_4	69.1
CH_2	46.3	FONO	62.2	ClONO	(70)	CS	50.3
CH_3	46.4	FNO	59.3	$ClONO_2$	(74)	CS_2	56.9
CH_4	44.5	FNO_2	62.3	FCl	52.1	CH_3SH	61.0
CN	48.4	$FONO_2$	70.0	CCl_2	63.4	CH_3S	57.6
HCN	48.2	CF	50.9	CH_3Cl	56.1	CH_3SO_2	(62)
CH_3NH_2	58.0	CF_2	57.5	CH_2Cl	58.2	CH_3SCH_3	68.4
HNCO	56.9	CF_3	63.3	CH_2Cl_2	64.6	CH_2SCH_3	(69)
NCO	55.5	CF_4	62.4	$CHCl_2$	66.5	CH_3SSCH_3	80.5
CO	47.3	CH_3F	53.3	$CHCl_3$	70.7	OCS	55.3
CO_2	51.1	CH_2F	55.9	CCl_3	71.0		
HCO	53.7	CH_2F_2	58.9	CCl_4	74.0		
CH_2O	52.3	CHF_2	61.7	ClCO	63.5		
COOH	61.0	CHF_3	62.0	$COCl_2$	67.8		
HCOOH	59.4	FCO	59.4	C_2Cl_4	81.4		
CH_3O	55.0	COF_2	61.9	C_2HCl_3	77.5		
CH_3O_2	65.3	CF_3O	67.7	CH_2CCl_3	80.6		
CH_2OH	58.8	CF_3O_2	75.0	CH_3CCl_3	76.4		
CH_3OH	57.3	CF_3OH	69.3	CH_3CH_2Cl	65.9		
CH_3OOH	67.5	CF_3OOH	75.2	CH_2CH_2Cl	(66)		
CH_3ONO	68.0	CF_3OF	77.1	CH_3CHCl	(66)		
CH_3ONO_2	72.1	CH_3CH_2F	63.3	$CHCl_2CF_3$	84.0		
$CH_3O_2NO_2$	(82)	CH_3CHF	(64)	Br	41.8		
C_2H	49.6	CH_3CHF_2	67.6	Br_2	58.6		
C_2H_2	48.0	CH_3CF_2	69.9	HBr	47.4		
C_2H_3	56.3	CH_3CF_3	68.6	HOBr	59.2		
C_2H_4	52.5	CH_2CF_3	71.8	BrO	56.8		
C_2H_5	58.0	CH_2FCF3	75.8	BrNO	65.3		
C_2H_6	54.9	CHF_2CF_3	(80)	BrONO	(72)		
CH_2CN	58.0			$BrNO_2$	(67)		

Values in parentheses are estimates only.

APPENDIX 3: SOLAR FLUXES AND SPECIES PROFILES

Figures 6 and 7 show data for solar irradiances and fluxes. These were provided by Kenneth Minschwaner. The solar irradiances are from measurements by the Solar Ultraviolet Spectral Irradiance Monitor (SUSIM) for $\lambda \leq 400$ nm (VanHoosier et al. [6]), and by Neckel and Labs [5] for $400 < \lambda \leq 600$ nm. The SUSIM measurements are spectrally degraded to 2 nm full width half-maximum to correspond to the resolution of the Neckel and Labs data. Additionally, a normalization factor that varies linearly from 1.17 at 400 nm to 1.0 at 440 nm has been applied to the Neckel and Labs irradiances in order to match SUSIM values at 400 nm. Irradiances from 110 to 120 nm are based on measurements by Mount and Rottman [4] and Woods and Rottman [8]. Values below 110 nm are not plotted.

The solar fluxes are computed from the sum of the direct, attenuated solar beam plus angularly integrated scattered radiation. Fluxes at 0, 20, 30, 40, and 50 km are based on the solar irradiances, assuming a solar zenith angle of 30° and the U.S. Standard Atmosphere (1976). Molecular and aerosol scattering are taken into account; the latter process is appropriate for "moderate volcanic" conditions (Fenn et al. [2]). The surface albedo is 0.3. Ozone cross sections follow the recommendations herein; oxygen cross sections in the Herzberg continuum are taken from Yoshino et al. [9]; Schumann-Runge band absorption is determined using the high-resolution treatment of Minschwaner et al. [3], with fluxes spectrally degraded to 1.0 nm resolution.

The species and "J" value profiles presented in Figures 8-16 were provided by Peter Connell. They were generated by the LLNL 2-D model of the troposphere and stratosphere. The temperature profile is an interpolation to climatological values. Surface source gas boundary conditions are those for the year 1990, as reported in chapter 6 of the WMO/UNEP report [7]. The equatorial tropopause source gas mixing ratios are: total chlorine 3.4 ppb, total fluorine 1.6 ppb, total bromine 18 ppt, methane 1.67 ppm, and nitrous oxide 309 ppb. The kinetic parameters used were consistent, to the extent possible, with the current recommendations. Representations of sulfate aerosol and polar stratospheric heterogeneous processes which were included are hydrolysis of nitrogen pentoxide and chlorine and bromine nitrate and reaction of hydrogen chloride with chlorine nitrate and hypochlorous acid. The model run represents a periodic steady-state atmosphere with 1990 surface abundances of source gases.

The "J" values were calculated with a clear sky, two-stream radiative transfer model with wavelength binning of 5 nm above 310 nm and 500 cm^{-1} below. Surface reflectance includes the effect of average cloudiness on the albedo. Oxygen cross sections in the Schumann-Runge region were calculated by the method of Allen and Frederick [1], corrected for the Herzberg continuum values of Yoshino et al. [9].

The fluxes and profiles are given to provide "order of magnitude" values of important photochemical parameters. They are not intended to be standards or recommended values.

References

1. Allen, M. and J.E. Frederick, 1982, J. Atmos. Sci., **39**, 2066-2075.
2. Fenn, W.R., S.A. Clough, W.O. Gallery, R.E. Good, F.X. Kneizys, J.D. Mill, L.S. Rothman, E.P. Shettle, and F.E. Volz, 1985, "Optical and Infrared Properties of the Atmosphere," Handbook of Geophysics and the Space Environment, Chapter 18, A.S. Jursa, Editor, Air Force Geophysics Laboratory, Bedford, MA.
3. Minschwaner, K., G.P. Anderson, L.A. Hall, and K. Yoshino, 1992, J. Geophys. Res., **97**, 10103-10108.
4. Mount, G.H. and G.J. Rottman, 1985, J. Geophys. Res., **90**, 13031-13036.
5. Neckel, H. and D. Labs, 1984, Solar Physics, **90**, 205-258.
6. VanHoosier, M.E., J.-D.F. Bartoe, G.E. Brueckner, and D.K. Prinz, 1988, Astro. Lett. and Communications, **27**, 163-168.
7. WMO, Scientific Assessment of Ozone Depletion: 1994, World Meteorological Organization Global Ozone Research and Monitoring Project, Report No. 37, 1994, Geneva: National Aeronautics and Space Administration.
8. Woods, T.N. and G.J. Rottman, 1990, J. Geophys. Res., **95**, 6227-6236.
9. Yoshino, K., A.S.C. Cheung, J.R. Esmond, W.H. Parkinson, D.E. Freeman, S.L. Guberman, A. Jenouvrier, B. Coquart, and M.F. Merienne, 1988, Planet. Space Sci., **36**, 1469-1475.

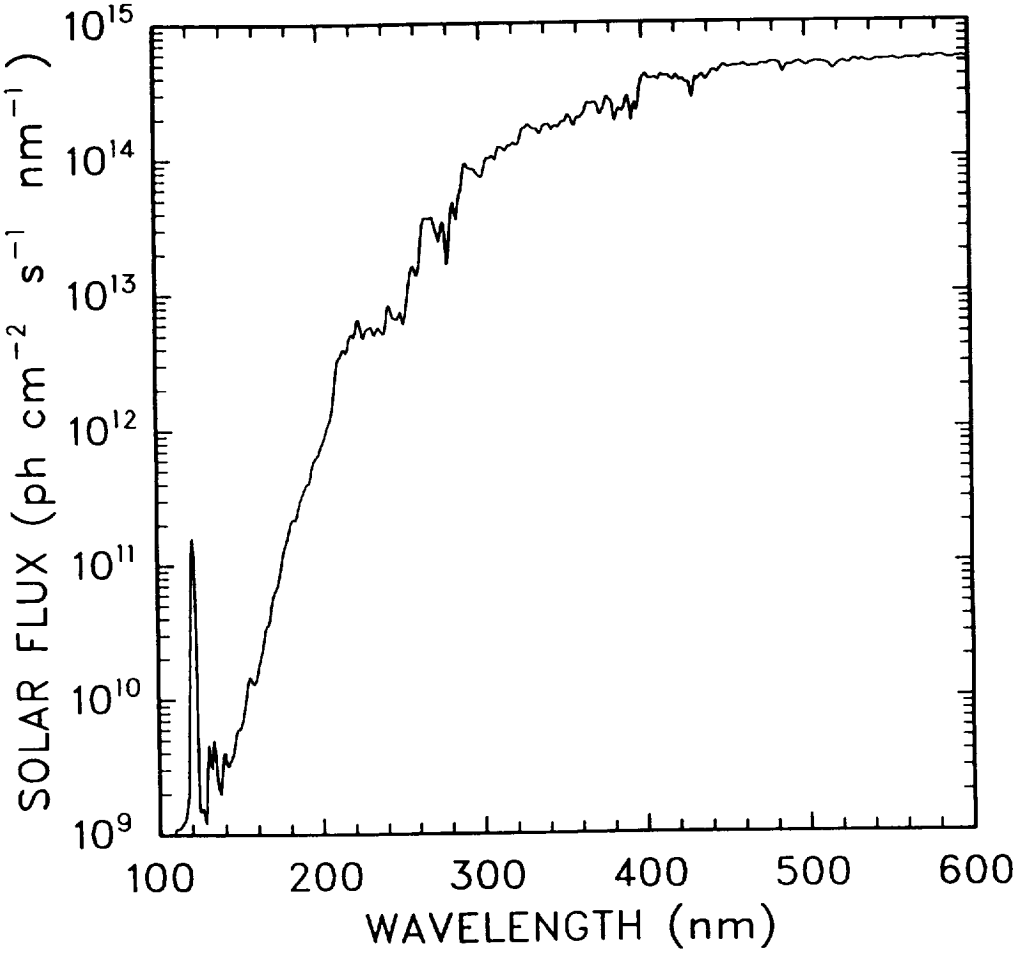

Figure 6. Solar Irradiance

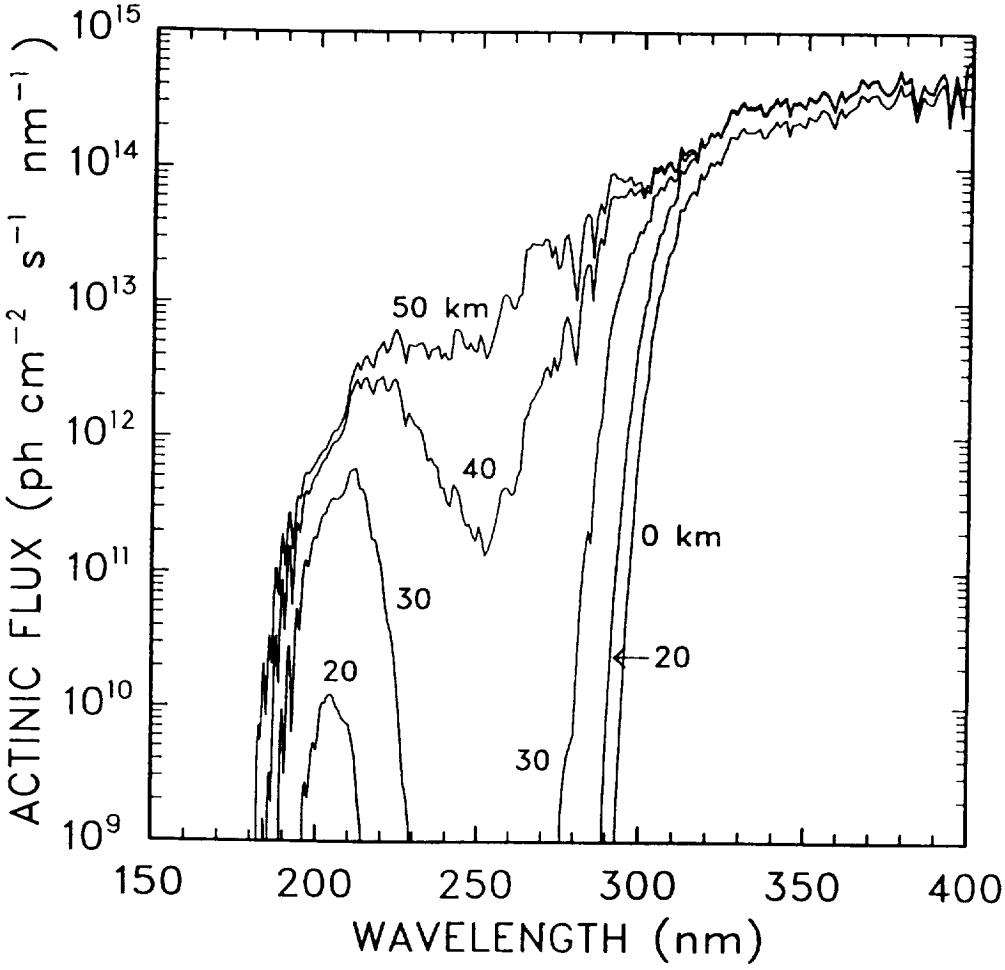

Figure 7. Actinic Flux at Several Altitudes

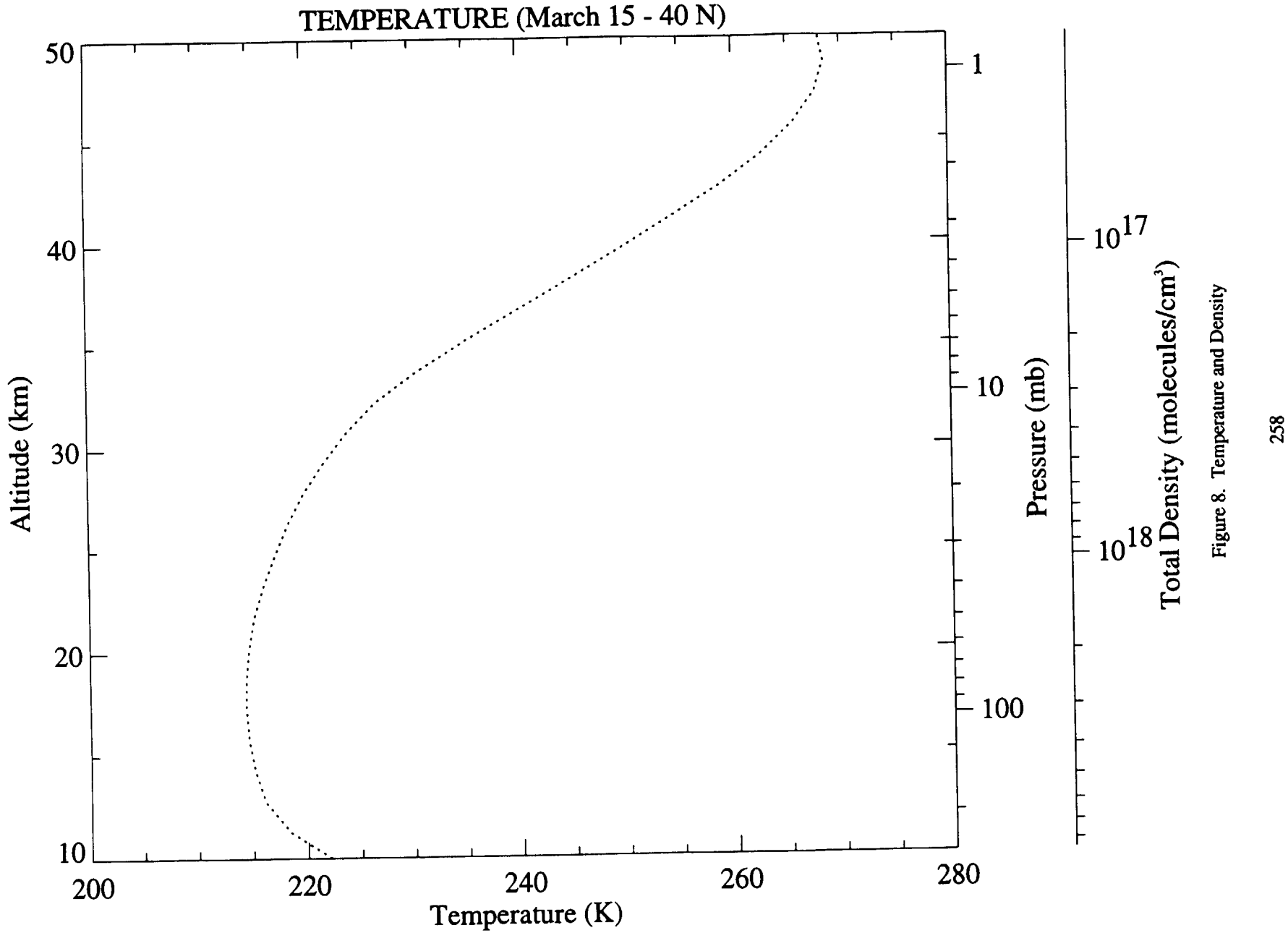

Figure 8. Temperature and Density

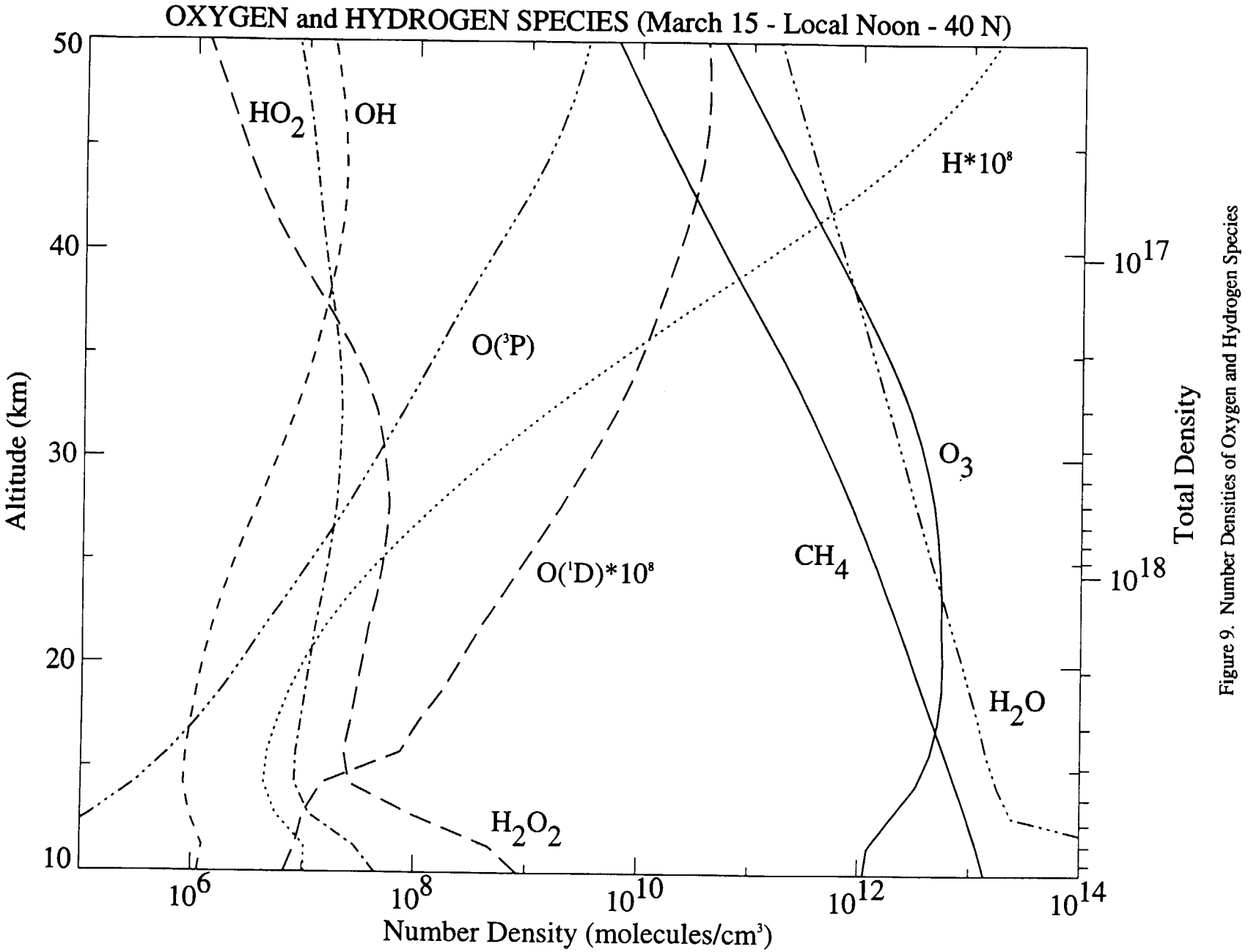

Figure 9. Number Densities of Oxygen and Hydrogen Species

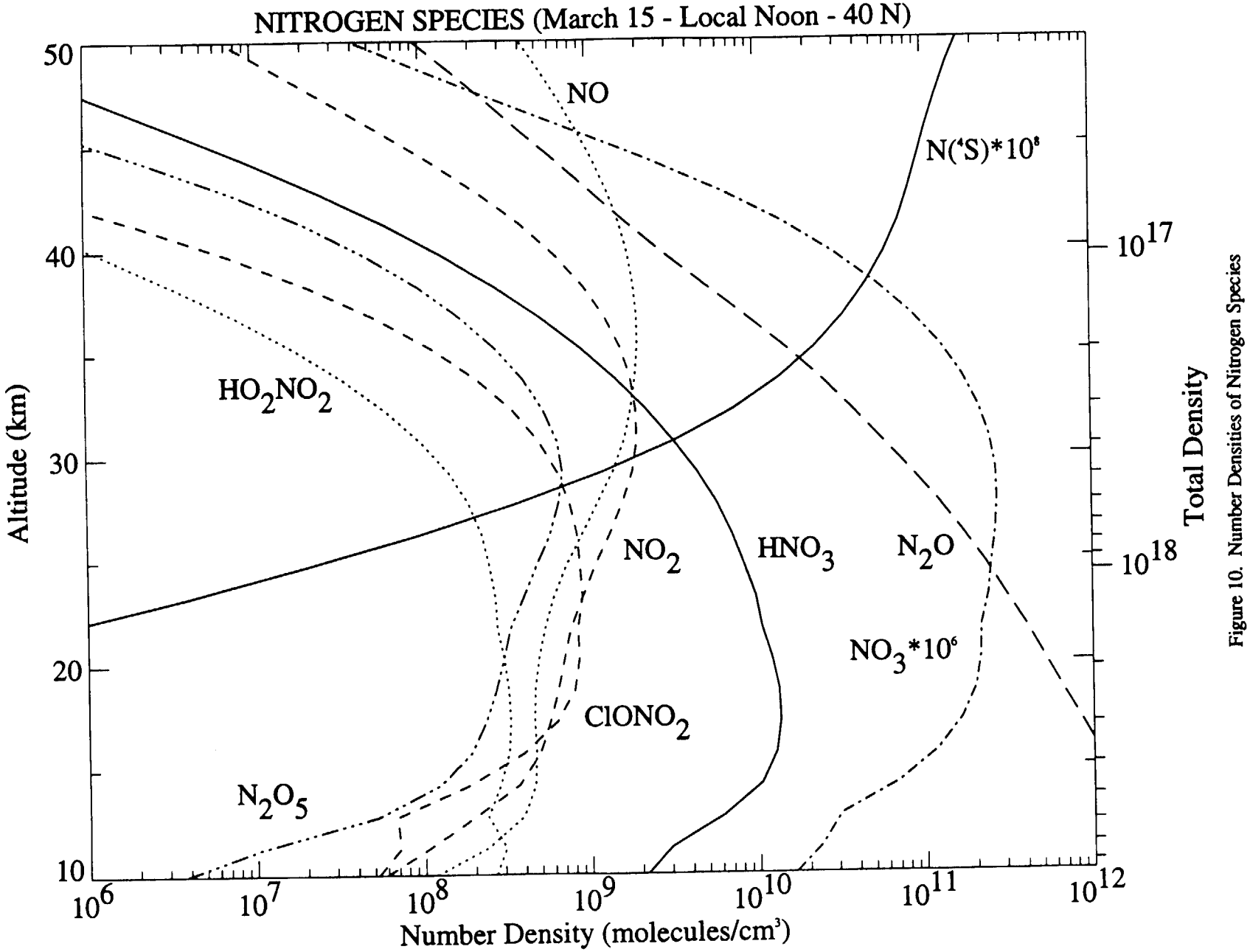

Figure 10. Number Densities of Nitrogen Species

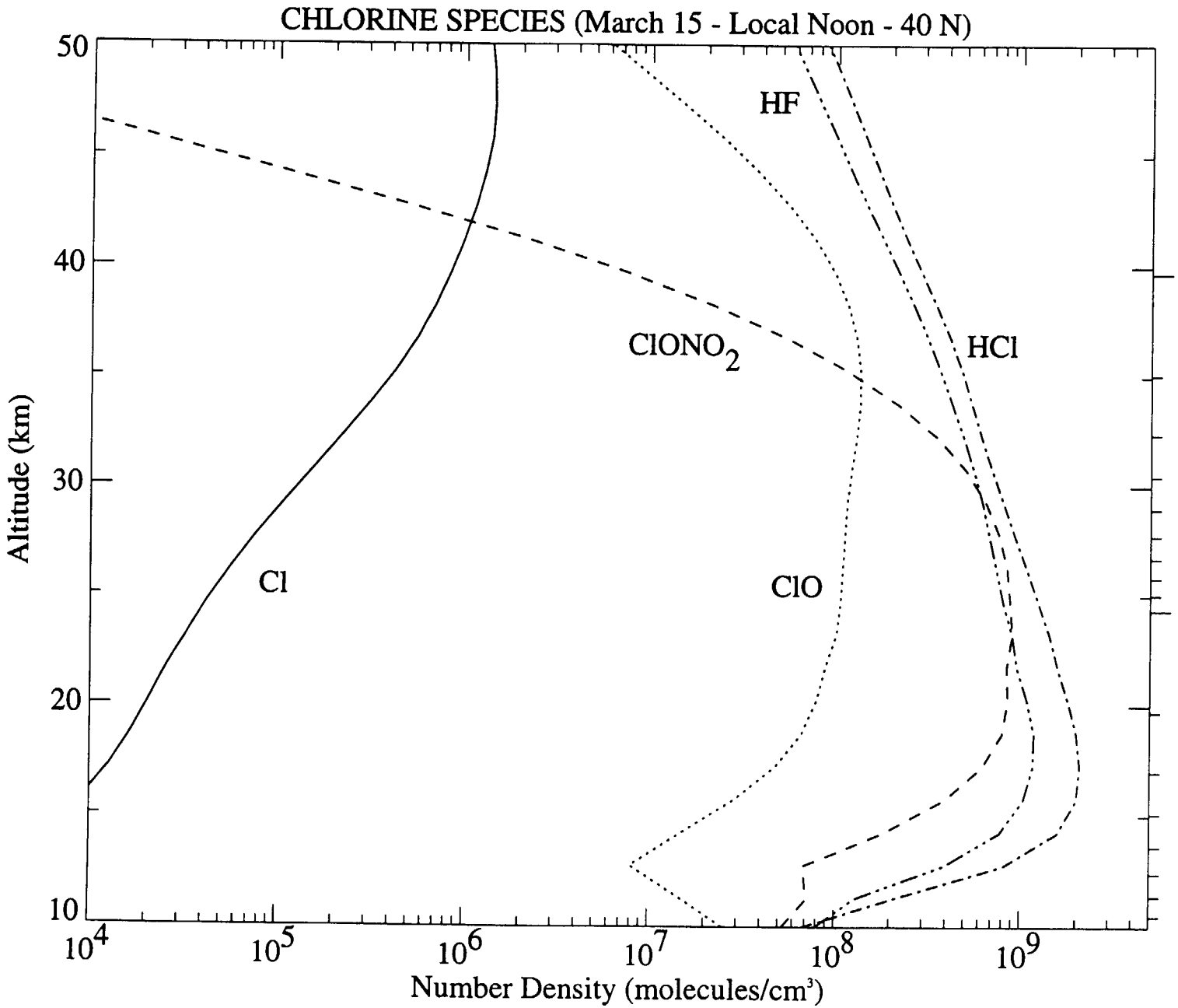

Figure 11. Number Densities of Chlorine Species

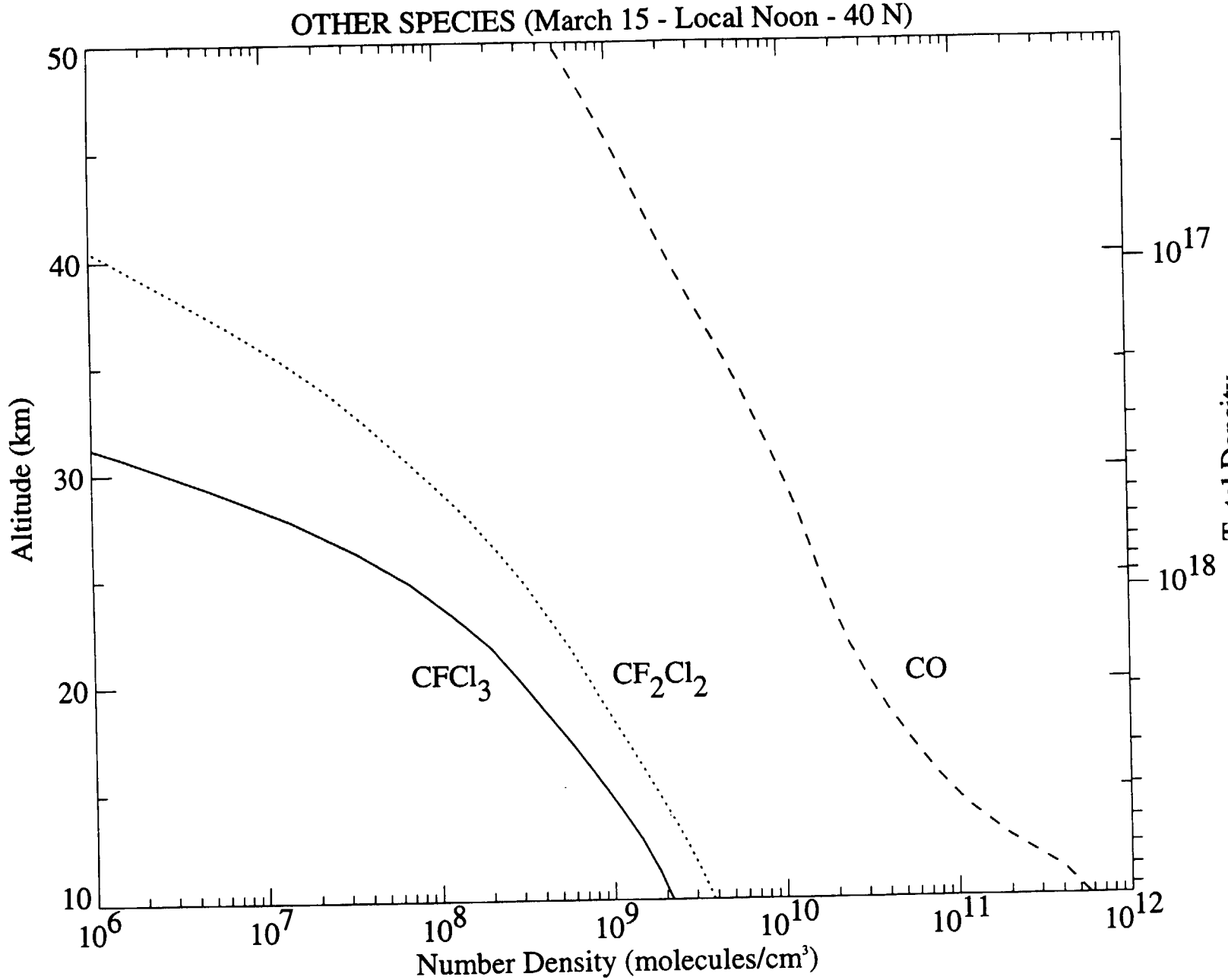

Figure 12. Number Densities of $CFCl_3$, CF_2Cl_2, and CO

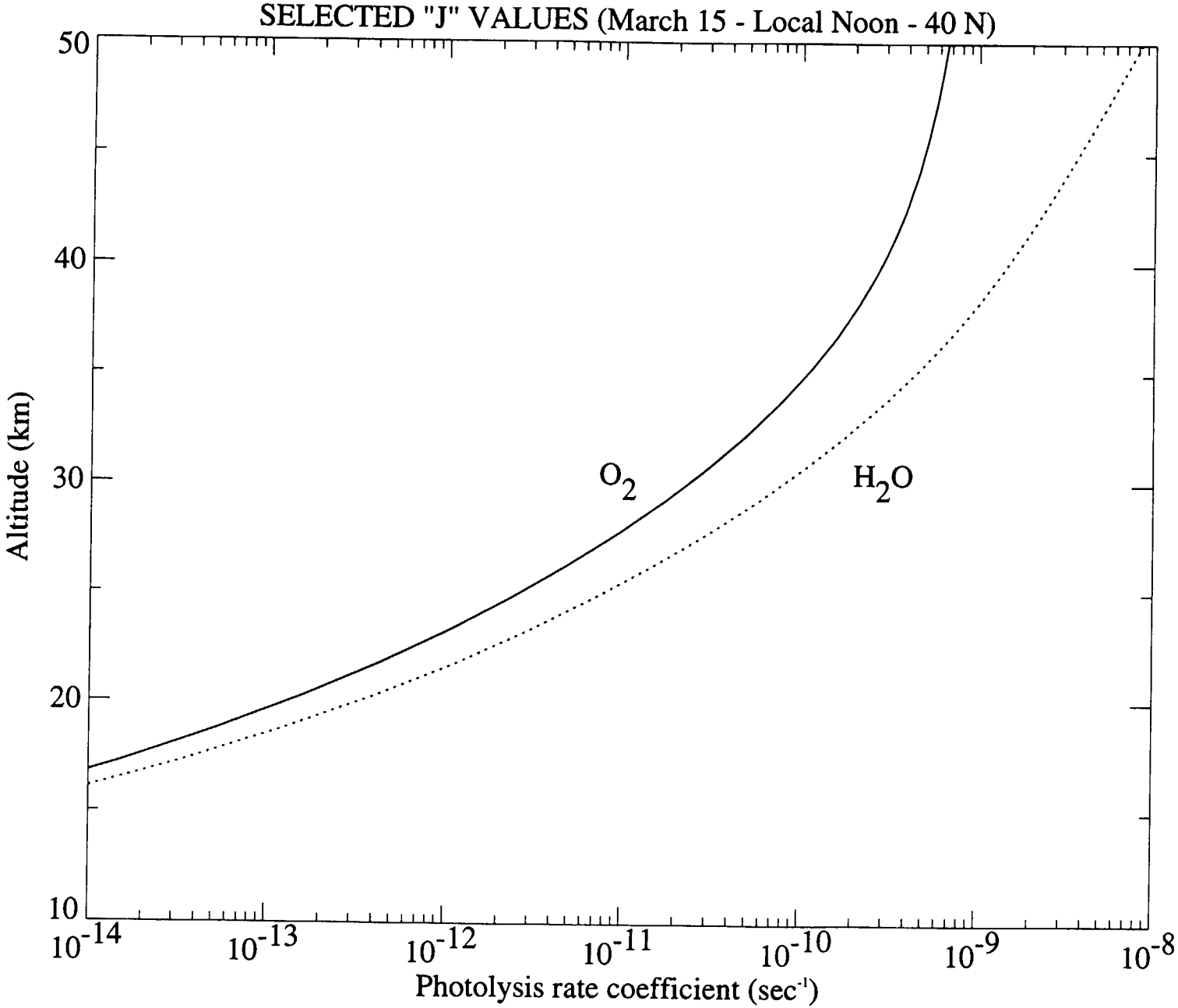

Figure 13. J-Values for O_2 and H_2O

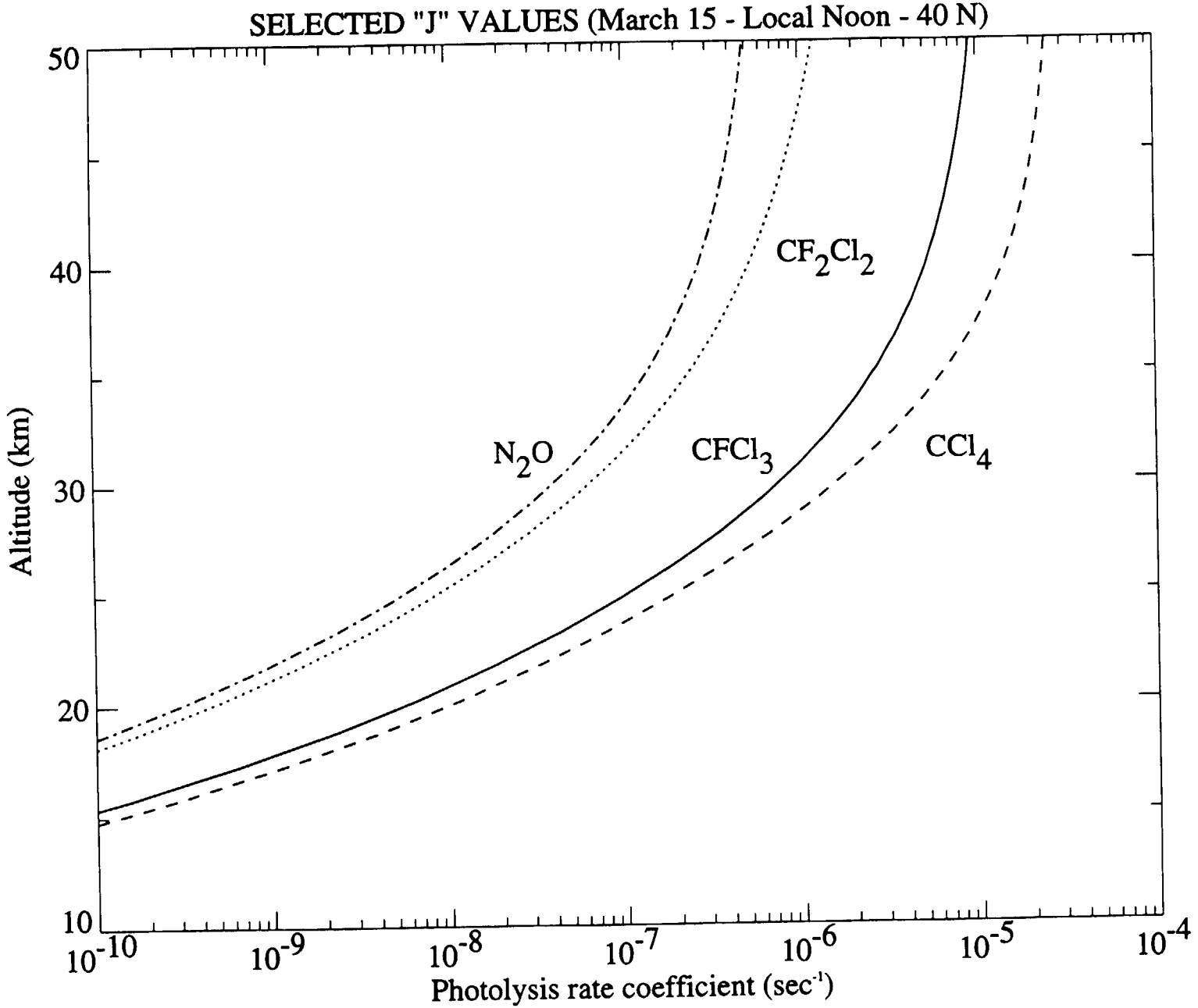

Figure 14. Selected J-Values

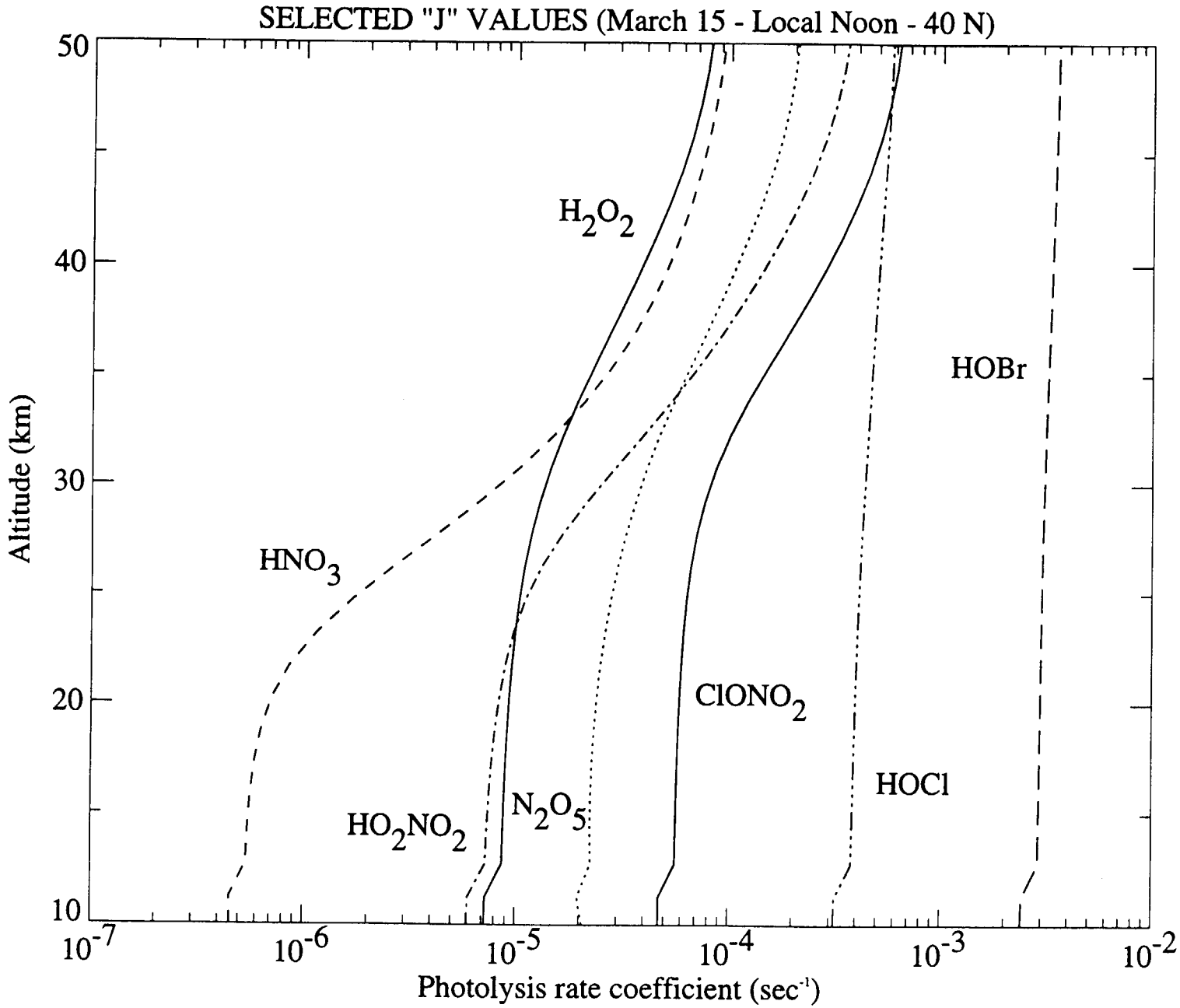

Figure 15. Selected J-Values

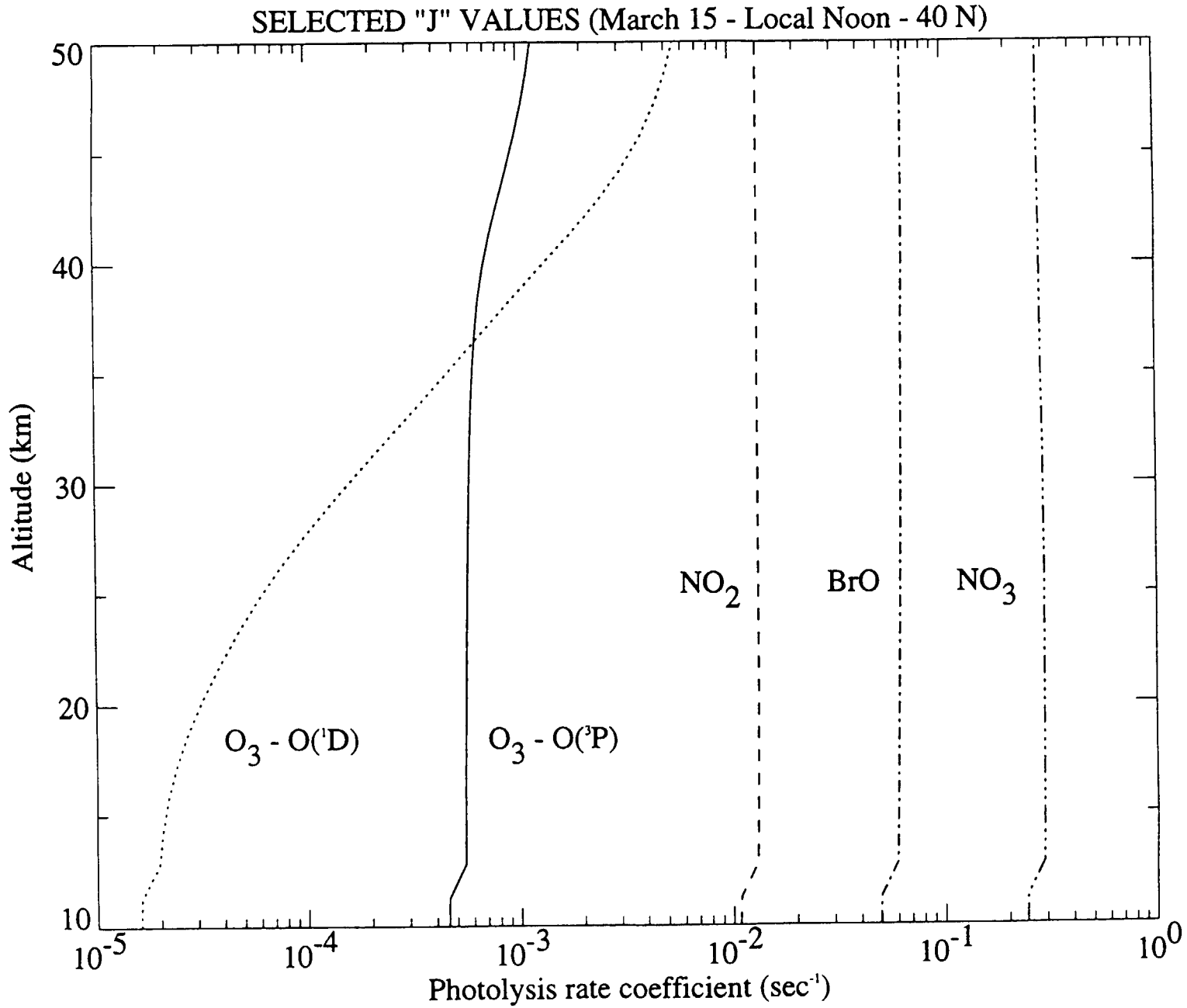

Figure 16. Selected J-Values